

# STUDIES IN SOME Mn-Cr-Cu MARTENSITIC AND AUSTENITIC WHITE CAST IRONS

A THESIS

Submitted in fulfilment of the  
requirements for the award of the degree  
of  
DOCTOR OF PHILOSOPHY  
in  
METALLURGICAL ENGINEERING

by

**NARESH CHAND JAIN**



DEPARTMENT OF METALLURGICAL ENGINEERING  
UNIVERSITY OF ROORKEE  
ROORKEE-247 667 (INDIA)

June, 1986

**DEDICATED TO**

**MY**

**PARENTS**

**TO MY BROTHER**

**J.P. JAIN**

**FOR HIS WHOLE HEARTED  
INSPIRATION AND SUPPORT**

**AND**

**TO MY BROTHER-IN-LAW**

**R.C. JAIN**

**FOR HIS ENCOURAGEMENT**

## CANDIDATE'S DECLARATION

I hereby certify that the work which is being presented in the thesis entitled **STUDIES IN SOME Mn-Cr-Cu MARTENSITIC AND AUSTENITIC WHITE CAST IRONS** in fulfilment of the requirement for the award of the Degree of Doctor of Philosophy, submitted in the Department of Metallurgical Engineering of the University, is an authentic record of my own work carried out during a period from January 1981 to May 1986 under the supervision of Professor Dr. A.K. Patwardhan.

The matter embodied in this thesis has not been submitted by me for the award of any other degree.

June 30, 1986



(Naresh Chand Jain)

This is to certify that the above statement made by the candidate is correct to the best of my knowledge.



(A.K. Patwardhan)  
Professor  
Department of Metallurgical Engineering,  
University of Roorkee  
Roorkee

## ACKNOWLEDGEMENT

The author wishes to record his indebtedness with sincere and heartfelt gratitude to Dr. A.K.Patwardhan, Professor, Department of Metallurgical Engineering, University of Roorkee for suggesting the problem, inspiration and expert guidance, active supervision, thought provoking discussions, illuminating criticism and suggestions given by him during the entire period and in all the phases of this investigation. Without his timely and untiring help it would not have been possible to present the thesis in its present form.

I am extremely thankful to :

-Dr. D.B.Goel, Professor and Head of Department of Metallurgical Engineering, Dr. M.L.Mehta, Professor, Ex-Head and Dr. M.L.Kapoor-Professor, Ex-Head for providing the laboratory facilities.

-Dr. P.Rama Rao, Director, Dr. V.S.Arunachalam, Ex-Director, Dr. N.C.Birla and Mr. A.Kailasam of the Defence Metallurgical Research Laboratory, Hyderabad for providing melting facilities.

-Dr. M.Vijay Kumar of DMRL, Hyderabad for helping with EPMA work.

-Mr. S.K.Khera, Mr. G.Kale and Mr. Bhanumurti of BARC, Trombay for providing facilities and the help with EPM analysis.

-Dr. S.R.Mediratta, Project coordinator, R & D Centre for Iron and Steel, Ranchi for permitting the use of quantimet and for providing facilities, Mr. Balbir Singh for helping with chemical analysis and Mr. U.N.Jha for the help rendered.

-Dr. K.C.Mittal, Professor and Director, USIC, University of Roorkee for providing facilities for X-ray diffractometry and scanning electron microscopy, Dr. N.K.Saini, Mr. B.P.Singh, Mr. K.N.R.Juyal

and Mrs. Rekha Sharma for the help rendered.

-Er. Boir, Mr. Eiser, Mr. A.K. Agarwal and Mr. Dinesh Mohan of the welding Research Laboratory, U.O.R for providing facilities and helping with compression testing.

-Dr. G.K. Tandon, Professor and Director, Computer Centre for providing facilities and Dr. Jialal for the help rendered.

I wish to record my sincerest thank to Dr. J.D. Sharma, Professor and Dr. Bhim Singh, Lecturer, Electrical Engineering Deptt., Dr. Surendra Kumar, Lecturer and Mr. B. Mohanty, Lecturer, Chemical Engineering Deptt., for suggesting modifications and for helping in the computational work and Mr. Vinod Kumar SRF Met. Engg. Deptt. for critical suggestions and helping in the experimental work.

Encouragement and help from my colleagues, Mr. Sharvan Kumar, Mr. Devendra Puri, Mr. Munish Sharma, Mr. D. Saxena, Mrs. Anju Julka and Dr. Km. Jyoti Lata Pandey is greatly appreciated.

The help rendered by Mr. M.C. Vaish, Mr. S.K. Seth, Mr. S.P. Kush, Mr. S.S. Gupta, Mr. S.C. Kaushik, Mr. R.M. Mangal, Mr. M.K. Singh, Mr. J.P. Sharma, Mr. Harichand (Retired Mechanic), Mr. S.N. Kaushik, Mr. Naresh Kumar Sharma and all technical staff of the laboratories is gratefully acknowledged. Thanks are also due to Mr. Ram Gopal, and **Mr. Sunil Juyal M/s Universal Systems Engineers Data Processing and Consultant** for meticulously typing the manuscript.

  
(N.C. JAIN)

## ABSTRACT

A comprehensive review of the literature revealed that corrosion resistant alloy cast irons can be broadly classified into three categories namely (a) ferritic (high silicon cast irons), (b) austenitic (Ni-resist cast irons) and (c) martensitic (high Cr cast irons with or without Mo). The first variety has useful applications where resistance to corrosion under oxidising conditions is the essential requirement. The poor mechanical strength and shock resistance associated with high silicon irons preclude their general engineering applications. Of the remaining two, the Ni-resist cast irons, although extensively used in a variety of conditions, have a low strength and are unsuitable at operating temperatures  $\geq 900^{\circ}\text{C}$  or more. The martensitic variety of cast irons exhibit a relatively higher strength and can be employed upto higher service temperatures. Their shock resistance can be improved by lowering the carbon content.

A critical analysis of the data on austenitic and martensitic cast irons revealed that little information is available on the structure-property relations in general. Furthermore, systematic information is lacking on the electro-chemical and the deformation behaviour of micro-structures commonly encountered in alloy white irons namely "martensite + carbide", (M + A), Austenite + Carbide (A + MC) and their allied counterparts. Detailed information on these aspects is likely to prove useful in ascertaining whether microstructures exhibiting good resistance to aqueous corrosion and useful mechanical properties could be attained through the 'white

iron' route. It would be equally pertinent to investigate whether these micro-structures could be generated by utilizing low cost alloying elements (Mn, Cu etc.) in preference to the conventionally employed alloying elements such as Ni, Mo etc.

The present investigation was undertaken in response to the above queries. It essentially comprised of conceiving/designing some new low cost Fe-Mn-Cr-Cu alloys based on fundamental considerations, assessing their heat-treatment response and characterizing them on the basis of corrosion behaviour and mechanical properties. The alloys, which were air induction melted and sand cast (25 mm round cylinders and 120x22x8 mm rectangular strips), were investigated by employing hardness measurements, optical and scanning electron microscopy, quantitative metallography, x-ray diffractometry, EPM analysis, compression testing and their electrochemical behaviour determined by the weight loss and potentiostatic methods. Computational techniques were extensively employed for data analysis.

The experimental work comprised of subjecting disc and rectangular specimens of the four alloys, containing  $\sim 6\%$  and  $\sim 8\%$  Mn\* and  $\sim 4\%$  Cr nominal alloy compositions at two different Cu\* levels namely  $\sim 1.5$  and  $\sim 3\%$ , to heat-treatments comprising of holding for 2,4,6,8, and 10 hrs at 800,850,900,950,1000 and 1050°C followed by oil quenching. This treatment was preferred over air cooling because a more uniform micro-structure was obtained. Optical metallography was extensively used to assess how the alloy content and heat-treating schedule influenced the micro-structure which



comprised of :

- (i) P/B + M + MC with and without RA in the as-cast state,
- (ii) M + MC + DC with and without retained austenite (RA) on heat-treating from upto 900°C,
- (iii) A + MC + DC or A + MC with and without M (in traces) on heat-treating from upto 1000°C, and
- (iv) A + MC + New phase (bridge type carbide) on heat-treating from 1050°C.

The volume fraction of massive carbides (MC) decreased with temperature or with soaking period at a given heat-treating temperature. The decrease was marked at temperatures > 1000°C. Simultaneously, massive carbides were rendered discontinuous from the early stages of heat-treatment. The 'rounding-off' tendency set in at 1000°C.

Dispersed carbides (DC) formed corresponding to the 800°C, 10 hr heat-treatment directly from austenite. They underwent coarsening with an increase in temperature and or soaking period. The extent of coarsening which was marked at 900 and 950°C, has been represented by the 'coarsening index' (CI). The dispersed carbides dissolved on heat-treating from 1000°C.

X-ray diffractometry was helpful in establishing that four types of carbides formed in the experimental alloys namely  $M_3C$ ,  $M_{23}C_6$ ,  $M_5C_2$  and  $M_7C_3$ . At heat-treating temperature > 1000°C only the  $M_5C_2$  and  $M_7C_3$  carbides existed.

The new phase [NP] formed on heat-treating from 1050°C was

formed by N & G type transformation. Its volume fraction initially increased with soaking period upto 4 hrs and decreased thereafter.

Hardness measurements provided a quick yet reliable indication of the mathematical modelling it was possible to establish that the hardness is related with the heat-treating temperature and time by an equation of the form :

$$H = C_1 e^{C_2/T} + (C_3 + C_4 T)t$$

where,

$$H = \text{VHN}_{30}$$

$$T = \text{temperature in } ^\circ\text{K}$$

$$t = \text{time in seconds}$$

the four constants were different for the four alloys.

From the point of view of mechanical properties the martensite bearing micro-structures were brittle and were characterized by low compressive strength (CS) and % strain. The austenite based micro-structures gave high values of compressive strength and % strain. The key parameter in influencing the deformation behaviour was the amount and stability of austenite. The effect of massive carbide (MC) on the deformation behaviour was a function of the compatibility, volume fraction and morphology. The behaviour was governed by their size, shape and distribution. The new phase (bridge carbide), formed on heat-treating from 1050°C, adversely affected the deformation behaviour.

Parameters controlling the deformation behaviour are also the key parameters in controlling the overall corrosion behaviour. Stress relieving in general proved to be detrimental due to enhan-

ced galvanic action. The presence of new phase was also found to be detrimental from the corrosion resistance point of view. It was further concluded that the austenite-carbide couple proved extremely satisfactory from the point of view of corrosion resistance because the experimental alloys did not undergo any localized attack.

Through mathematical modelling it was possible to establish that corrosion rate was related with the volume fraction of MC + DC and the number of particles (NOP) through the following equation :

$$CR = [C_1 + C_2 (VCb) + C_3 (VCb)^2] (NOP)^{C_4}$$

Where VCb = volume fraction of MC + DC

CR = corrosion rate in mdd

$C_1$  to  $C_4$  are constants which were different for different alloys.

The effect of dispersed carbides on the corrosion behaviour could be represented by an equation :

$$CR = [C_1 + C_2 (VMc) + C_3 (VMc)^2] (DF)^{C_4}$$

Where, VMc = volume fraction of Mc

DF = distribution factor which is defined as :

defined as

$$DF = \frac{\sum_{i=1}^n Ni Xi}{\sum_{i=1}^n Ni} \quad (\text{Ref. section 6.5})$$

Once again the constants  $C_1$  to  $C_4$  differed for the four alloys. Of the two models developed, the latter was found to be more satisfactory.

Based on a critical appraisal of the data, it was possible to draw conclusions regarding the most suitable alloys/micro-structure(s) from the point of view of corrosion resistance. It was further inferred that the CS and % strain were linearly interrelated with the corrosion rate in accordance with the equation :

$$Y = C_1 + C_2 (CR)$$

Where,  $Y$  = the property being measured

$CR$  = corrosion rate in mdd

$C_1$  and  $C_2$  are constants.

Based on a reappraisal of the preceding sections, it was evident that the data contained in this report is of considerable applied and theoretical significance.

## PREFACE

The first chapter deals with the microstructure-corrosion resistance interrelation in plain carbon and alloyed cast irons. This is followed by a discussion on the composition, properties and applications of the three types of corrosion resistant alloy cast-irons currently in use.

The second chapter, on fundamental considerations in the design of corrosion resistant microstructures, critically examines the different forms of corrosion, factors affecting corrosion and the effect of metallurgical factors (crystal structure, microstructure and defect structure) in controlling corrosion.

Major deductions arising from a critical appraisal of the information contained in the second chapter lead to the design of experimental alloys. This aspect along with a phase-wise planning of experiments have been included in chapter III.

Chapter IV deals with the experimental techniques and procedures employed.

Results summarized in chapter V include the effect of heat-treatment schedule(s) on hardness, microstructural examination by optical metallography, structural investigations by X-ray diffractometry, EPM analysis to assess the partitioning of Mn, Cr, Si and Cu into the massive carbide and the new phase formed on heat-treating from 1050°C, assessment of the deformation behaviour in the as-cast and heat-treated conditions by compression testing, corrosion characterization by the weight loss and potentiostatic methods and a

study of the corroded specimen surfaces by scanning electron microscopy. The data have been critically analysed and interpreted in chapter VI.

Based on the above findings, conclusions have been drawn with regard to the suitability of different micro-structures from the point of view of corrosion resistance and the deformation behaviour. They are enumerated in the chapter VII.

## ABBREVIATIONS

A	Austenite
AC	Aircooled
AVE	Average
B	Bainite
BHN	Brinell hardness number
B1, B2, B3, B4	Alloy designation
'C'	Carbon
Cb	Carbide
CI	Coarsening index
COND	Condition
COP	Cross over point
CR	Corrosion rate
CS	Compressive strength
DC	Dispersed carbide(s)
DF	Distribution factor
GB	Grain boundary
GMS	Grams
H	Hardness
HRS, h, hr, hrs	Hours; austenitizing period or test duration
HT, h/t	Heat-treatment
HV <sub>30</sub>	Vickers hardness at 30 kg. load
IPY, ipy	Inches per year
M	Martensite
MC	Massive carbide
Max	Maximum
Min	Minimum

MDD, mdd	Miligrams per decimeter square per day
MN/M <sup>2</sup> , MN/m <sup>2</sup>	Mega newton per square meter
MPa	Mega pascal
M3	M <sub>3</sub> C (Orthorhombic)
M5	M <sub>5</sub> C <sub>2</sub> (Monoclinic)
M7	M <sub>7</sub> C <sub>3</sub> (Hexagonal)
M23	M <sub>23</sub> C <sub>6</sub> (Cubic)
NOF	Number of particles
NP	New phase
NSR	Non stress relieved
OQ	Oil quenched
P	Pearlite
PC	Platy carbide
RA	Retained austenite
SP	Soaking period/austenitizing period
ST	Soaking temperature
S.AREA	Surface area
SQ.CM	Square centimeter
SR	Stress relieved at 600°C for 1/2 hr.
SD	Standard deviation
SG	Spheroidal graphite
SCC	Stress corrosion cracking
S.S.	Stainless steel
SFE	Stacking fault energy
TD	Test duration
TEMP	Temperature
TSI, tsi	Tonnes per square inch



T	Temperature
t	Time
$\mu$	Micron
UI	Unidentified
UA	Unaltered
VPN	Vickers pyramid number
vf	Volume fraction
Wt. %	Weight percent
Wt. Loss	Weight loss
$\alpha$	Ferrite
$\alpha'$	Martensite/shear transformatin product
$\gamma$	Austenite
$\gamma^*$	Austenite (low stability)

#### **Captions for optical micrographs**

Ist part	Specimen condition (h/t)
IIInd part	Magnification

#### **Captions for scanning micrographs**

Ist part	Specimen condition (h/t)
IIInd part	Test duration
IIIrd part	Magnification

#### **For mathematical modelling and otherwise**

#### **In weight loss studies:**

Ipy values rounded off to 4th place of decimal and mdd values rounded off to 1st place of decimal.

**For compression studies**

CS values rounded off to the nearest MPa

% strain values rounded off to the 1st place of decimal.

Unless otherwise stated, permissible experimental error for all measurements is + 2.5%.

**For compression studies**

CS values rounded off to the nearest MPa

% strain values rounded off to the 1st place of decimal.

Unless otherwise stated, permissible experimental error for all measurements is + 2.5%.

## CONTENTS

	Page	
CERTIFICATE	i	
ACKNOWLEDGEMENT	ii	
ABSTRACT	iv	
PREFACE	x	
ABBREVIATIONS	xii	
<b>CHAPTER I CORROSION RESISTANT ALLOY CAST IRONS</b>		
1.1	Introduction	1
1.2	Structural Parameters	2
1.2.1	Graphite Morphology and Matrix Microstructure	2
1.2.2	Size and Distribution of Carbides	4
1.2.3	Effect of Alloying	4
1.3	Alloy Cast Irons	5
1.3.1	High Si (Ferritic) Irons	5
1.3.1.1	Micro - structure	5
1.3.1.2	Mechanical Properties	6
1.3.1.3	General Corrosion Behaviour	6
1.3.1.4	Applications	7
1.3.2	High Cr Irons	7
1.3.2.1	Micro - structure	7
1.3.2.2	Mechanical Properties	8
1.3.2.3	General Corrosion Behaviour	8
1.3.2.4	Applications	9
1.3.3	Ni - resist (Austenitic) Irons	9
1.3.3.1	Micro - structure	9
1.3.3.2	Mechanical Properties	9
1.3.3.3	General Corrosion Behaviour	10

1.3.4	S. G. Ni - resist Irons	11
1.3.4.1	Mechanical Properties	11
1.3.4.2	Corrosion Behaviour	11
1.3.4.2	Applications	11
1.4	Conclusion	12

**CHAPTER II    FUNDAMENTAL CONSIDERATIONS IN THE DESIGN  
OF CORROSION RESISTANT ALLOYS.**

2.1	Introduction	13
2.2	Forms of Corrosion	14
2.3	Process Related Parameters	14
2.4	Metallurgical Factor	15
2.4.1	Introduction	15
2.4.2	Microstructure	15
2.4.2.1	Single Phase Microstructure	16
2.4.2.2	Two Phase Microstructure	17
2.4.2.2.1	Soft Matrix Containing a Soft Phase	17
2.4.2.2.2	Soft Matrix Containing a Phase Mixture	18
2.4.2.2.3	Second Phase as a Dispersoid in a Soft Matrix	18
2.4.2.3	Single Phase With High Hardness	20
2.4.2.3.1	Second Phase With a High Hardness in a Hard Matrix	22
2.4.2.3.2	Multi - phase Microstructure	23
2.4.2.4	Unintended Microconstituents	23
2.4.2.4.1	Grain Boundary Precipitation/Segregation	23
2.4.2.4.2	Formation of Sigma and Chi Phases	24
2.4.2.5	Minor Factors	25
2.4.2.5.1	Effect of Grain Structure	25
2.4.2.5.2	Effect of Grain Orientation	25

2.4.2.5.3	Inhomogeneity	26
2.4.2.6	Impurities	27
2.4.3	Defect Structures	28
2.4.3.1	Effect of Cold Work	29
2.4.4	Heat Treatment	30
2.4.5	Alloying	32
2.5	Passivity	32
2.6	Conclusion	35

### **CHAPTER III FORMULATION OF THE PROBLEM**

3.1	Introduction	37
3.2	The Approach	38
3.3	Design of Alloys	40
3.4	Planning of Experiments	41

### **CHAPTER IV EXPERIMENTAL TECHNIQUES AND PROCEDURES**

4.1	Alloy Preparation	43
4.2	Specimen Preparation	44
4.3	Heat - Treatment	45
4.4	Hardness Measurement	45
4.5	Compression Testing	46
4.6	Metallography	46
4.6.1	Optical Microscopy	46
4.6.2	Quantitative Metallography	46
4.6.3	Scanning Electron Microscopy	47
4.7	Electron Probe Micro - Analysis	47
4.8	X - Ray Diffractometry	48
4.9	Corrosion Studies	48
4.9.1	Weight Loss Method	48

4.9.2	Anodic Polarization Technique	49
4.10	Data Analysis	51

## **CHAPTER V      EXPERIMENTAL RESULTS**

5.1	General	52
5.2	Results	52
5.2.1	Effect of h/t on Hardness	52
5.2.2	Micro - structure	57
5.2.3	Quantitative Estimations	59
5.2.3.1	Massive Carbides	59
5.2.3.2	Dispersed Carbides	60
5.2.4	Structure Analysis by X - Ray Diffraction	62
5.2.5	Effect of Heat - Treatment on the Deformation Behaviour	65
5.2.6	Corrosion Behaviour	67
5.2.6.1	Weight Loss Studies	67
5.2.6.2	Potential - Static Studies	69
5.2.7	Scanning Metallography of Corroded Specimen Surfaces	70
5.2.8	EPMA Studies	71

## **CHAPTER VI      DISCUSSION OF THE RESULTS**

6.1	General	73
6.2	Structural Considerations	73
6.2.1	Change in the High Temperature Microstructure	74
6.2.2	Change During Cooling to Room Temperature	75
6.2.3	Strengthening Response of Different Transformations	78
6.3	Interrelation Between Microstructure and Hardness	78
6.3.1	As - cast State	79
6.3.2	Heat - treated Condition	79

6.3.2.1	Alloy B1	80
6.3.2.2	Alloy B2, B3 & B4	83
6.3.2.3	Comparative Hardness v/s Time Data	85
6.3.3	Correlation Between Hardness and Time	86
6.3.4	Effect of Temperature on Hardness	87
6.3.4.1	Nature of Variation	87
6.3.4.2	Effect of Temperature on Hardness and Microstructure	88
6.3.4.3	Comparative Hardness v/s Temperature Data	90
6.3.5	Effect of Temperature and Time on the Morphology and Volume Fraction of Massive Carbides	90
6.3.6	Effect of Time and Temperature on Dispersed Carbides	92
6.3.7	Mathematical Modelling of the Transformation Behaviour	96
6.3.8	Identity of the New Phase	100
6.3.9	Structural Analysis by X-ray Diffractometry	101
6.4	Effect of Microstructure on the Deformation Behaviour	103
6.5	Corrosion Behaviour	110
6.5.1	Weight Loss Data	110
6.5.2	Potential Static Data	119
6.5.3	Scanning Metallography Results	120
6.5.4	Mathematical Modelling of the Corrosion Behaviour	122
6.6	Interrelation Between Deformation and Corrosion Behaviour	126
6.7	General Discussion	127

## **CHAPTER VII CORRELATIONS AND SUGGESTIONS FOR FUTURE WORK**

7.1	Conclusions	132
7.2	Suggestions for Future Work	138

<b>REFERENCES</b>		139
-------------------	--	-----



## TABLES

1.1-1.6	Corrosion Resistant Irons	T-1 to T-5
2.1-2.3	Literature Review	T-6 to T-8
4.1-4.2	Chemical Analysis of Alloys	T-9
5.1-5.24	Hardness v/s Time Data	T-10 to T-21
5.25-5.44	Hardness v/s Temperature Data	T-22 to T-33
5.45-5.49	Massive Carbides	T-34 to T-36
5.50-5.59	Dispersed Carbides	T-37 to T-43
5.60-5.100	X-ray Diffractometric Data	T-44 to T-64
5.101-5.108	Compression Data	T-65 to T-71
5.109-5.130	Corrosion Rate Data	T-72 to T-81

## FIGURES

4.1-4.2	Experimental Set - up	F-1 to F-2
5.1-5.5	H v/s t Curves	F-3 to F-12
5.6-5.7	H v/s T Curves	F-13 to F-21
5.8-5.35	Micrographs (Optical)	F-22 to F-48
5.36-5.78	Histograms Showing Distribution of DC	F-49 to F-71
5.79-5.84	Compression Curves	F-72 to F-77
5.85-5.88	Temperature v/s Corrosion Rate Curves	F-78 to F-81
5.89-5.96	Potential v/s Current Density Curves	F-82 to F-89
5.97-5.105	Scanning Micrographs	F-90 to F-98
5.106-5.107	EPMA Data	F-99 to F-100
5.108-5.113	Comparative Histograms Between Electro- Chemical & Mechanical Properties	F-101 to F-106

APPENDIX 1-3	Experimental vs Calculated Curves.	A-1 to A-3
--------------	---------------------------------------	------------

## CHAPTER I

### CORROSION RESISTANT ALLOY CAST IRONS

#### 1.1 Introduction

Cast irons are extensively employed for diverse applications, including those where resistance to corrosion is an essential requirement. Both the types of cast irons namely grey and white irons are in use. The corrosion behaviour of cast irons in general is controlled by (i) the form and distribution of carbon, (ii) the nature of the matrix and (iii) the impurities present. Taking all possibilities into consideration, the phases most likely to be present are graphite,  $\text{Fe}_3\text{C}$  and its alloyed versions,  $\text{Fe}_3\text{P}$ ,  $\text{MnS}$ ,  $\text{FeS}$ , Ferrite, martensite and austenite. Alloy additions and the heat treatment employed are the controlling parameters in deciding which of the aforesaid microconstituents would be present in a given alloy (1,2).

Although information is available on the corrosion response of different matrices in the presence or absence of graphite, the main question is which region is attacked. This can be answered depending upon the (a) placing of the different phases in the electrochemical series, (b) possible effects of alloying, (c) nature of the corroding medium and (d) nature of the corrosion product (1,2).

The following sections are devoted to a discussion on the influence of micro-structure on the corrosion resistance of cast irons. Finally information on the three prominent grades of alloy cast irons has been discussed at length. Wherever data on the corrosion response of different constituents present in the cast

irons is not readily available, information on the corrosion resistant steels has been suitably included in the discussion.

## **1.2 Structural parameters**

### **1.2.1 Graphite morphology and matrix microstructure**

Corrosion of cast irons in any environment produces an attack on the iron matrix leaving behind a residue of corrosion resistant micro-constituents. Prominent amongst them is graphite. Graphite residue, due to being cathodic, may indirectly accelerate the attack. It (the attack) can however be stifled if the solid corrosion products are retained within the graphite skeleton. Fine interlocked flakes of graphite are most effective in this regard. Accordingly cast irons with (a) coarse graphite flakes (i.e. with more open and permeable structure) and (b) nodular graphite aggregates are less likely to show stifling of the attack (1).

Retention of the corrosion residue, besides being a function of the physical state of graphite, also depends upon the nature of the corrosion products. Pearlitic irons produce carbonaceous debris helpful in plugging and strengthening graphite skeleton. Ferritic irons produce no such residue. The graphite residue produced from a ferritic matrix is thus more permeable and therefore less effective than that produced from a pearlitic matrix with a similar graphite distribution (1).

Solubility of the corrosion products in a given environment is equally pertinent in assessing whether the attack will be stifled. In highly acidic environments, it is difficult to produce a corro-

sion product that will inhibit further corrosion irrespective of the nature of the graphite distribution and that of the matrix. Under neutral conditions, a protective layer would form independent of the graphite form or the type of matrix. These parameters (graphite morphology and the matrix) however assume significance under intermediate conditions (1-3). For example, in a 0.5%  $H_2SO_4$  solution, the flake graphite irons show an increase in the corrosion rate to start with because the graphite residue is unplugged. Thereafter, there is a decrease in the corrosion rate when the graphite residue is plugged with insoluble corrosion products and carbonaceous debris. Nodular irons however show a steady increase in the corrosion rate because the nodular graphite residue is in a form incapable of retaining the insoluble corrosion products or debris (1,2).

Graphite morphology and the nature of the matrix, besides being the key parameters in controlling the corrosion behaviour, are equally important in influencing the high temperature performance of cast irons. At temperatures  $\approx 425^\circ C$ , the combined carbon changes to graphite with a consequent increase in volume producing 'growth' of castings. The effect is principally observed in pearlitic irons and to a much lesser extent in the ferritic irons. These growth effects, although not strictly classified as corrosion, indirectly affect the results of high temperature oxidation tests. The graphite morphology has a more direct bearing on the oxidation of cast irons with the S.G. irons, showing much less oxide penetration than the flake graphite irons (1).

### 1.2.2 Size and distribution of carbides

The size and distribution of carbides also affect the corrosion rate. For a given volume fraction, it (corrosion rate) increases as the size of iron carbide particles decreases (3). The degree of dispersion of the carbides is quantitatively characterized by the total interfacial contact area between the cementite phase and the matrix. The relevance of this parameter in influencing the corrosion behaviour was first suggested by Uhlig (4).

### 1.2.3 Effect of alloying

Effect of alloying elements will depend upon their amount and nature. Alloying elements may be added (i) in small amounts to enhance resistance to corrosion in a specific environment e.g. additions of 0.25 to 1.0% Cu increase the corrosion resistance in dilute acetic, sulphuric and hydrochloric acids (5) and (ii) to alter the matrix microstructure e.g. converting pearlite into bainite, martensite or austenite. Their presence will also influence the relative stability of the micro-constituents and hence their electro-chemical behaviour e.g. element(s) which partition predominantly to  $Fe_3C$  will not only increase its hardness but render it more stable and thereby change its electro-chemical character. In addition to these effects, a film which inhibits corrosion may also form provided the amount of film forming element(s) exceeds a critical concentration e.g. the film formed in the presence of Cr, Si and Al (6).

The usefulness of the ferritic, austenitic and martensitic matrices in imparting corrosion resistance is now well established and has formed the basis of developing high alloyed cast irons discussed in the next section. Their usefulness, along with the

effect of alloying elements in general and that of the alloyed carbides, graphite and passivity in particular, in resisting corrosion has been discussed in detail in the next chapter.

### **1.3 Alloy cast irons**

Addition of alloying elements in smaller proportions has a limited effect on the corrosion resistance of cast irons. Therefore, larger additions have been made to develop cast irons with improved mechanical properties and corrosion resistance. They include (i) the high Si irons containing upto 18% Si, (ii) the high Cr irons with 12 to 35% Cr and (iii) the austenitic irons of the Ni-resist type essentially containing Ni from 14% to 36% (2).

#### **1.3.1 High Si (ferritic) irons**

##### **1.3.1.1 Micro-structure**

The micro-structure of the high Si irons containing less than 15.2% Si consists of a matrix of  $\alpha$ -silico-ferrite containing a distribution of fine graphite flakes (7). In irons containing more than 15.2% Si some  $\eta$  phase is also present (6). The high hardness and brittleness of the silicon irons is due to the nature of the silico-ferrite. An attempt has been made to produce high Si irons with a nodular graphite structure for improving the mechanical properties (8). However, since the low strength is due to the brittle matrix rather than the graphite form, the nodular graphite irons have not proved very popular. Composition of the high Si irons is given in the table 1.1 (9).

### 1.3.1.2 Mechanical properties

Representative mechanical properties are given in the table 1.2. As is evident, the alloys are characterized by a high hardness and a low resistance to impact. Machining is therefore limited to grinding. Fabrication by welding is very difficult, although simple shapes like pipes can be welded if proper precautions are taken (6, 9). Mechanical strength and shock resistance can be improved by lowering Si to ~ 12%. This however reduces resistance to corrosion.

### 1.3.1.3 General corrosion behaviour

The excellent corrosion resistance of high Si irons is due to the formation of an inert  $\text{SiO}_2$  surface film which forms during exposure to the environment. The full protective value of the film does not develop until at least 14.25% Si is present in the alloy (6,9). These irons are extremely resistant to  $\text{H}_2\text{SO}_4$ ,  $\text{HNO}_3$  and organic acids, and least resistant to hydrofluoric and sulphurous acids. High Si irons offer excellent resistance to attack by all concentrations of nitric-sulphuric acid mixtures. The additions of 3-3.5% Mo to an Fe-14.5 Si alloy results in the formation of extremely stable complex carbides with the consequent elimination of graphite (7). This is perhaps responsible for an improved resistance to HCl (7). Cr additions are similarly found to be useful. The high inherent hardness associated with high Si irons is responsible for their good corrosion-erosion behaviour.

High Si irons are inferior to the unalloyed grey when irons exposed to alkalies e.g. even to a weak base such as ammonium hydroxide, at liquid temperatures  $> 20^\circ\text{C}$  (6).

#### 1.3.1.4 Applications

These alloys are employed as castings for pumps, valves and other process equipments and have also found extensive use as anodes for impressed current cathodic protection. They are used for tubes and fittings for concentrated sulphuric and nitric acids. They are used for mixing nozzles, tanks, outlets and steam jets and for handling severe corrodants such as chromic acid, sulphuric acid, slurries, bleach solutions and acid chloride slurries which are frequently encountered in plants that manufacture paper pigments, dyestuffs or those using electroplating solutions (9).

#### 1.3.2 High Cr irons

##### 1.3.2.1 Micro-structure

As stated earlier the alloys contain Cr from 12 - 35% and C from 1.2 to 4% and some Mo. Accordingly the microstructure consists of a uniform dispersion of chromium-iron complex carbides in a matrix of chromium containing ferrite. The true nature of the matrix micro-structure would depend upon the Cr/C ratio; it may vary from  $\alpha$ -ferrite to martensite and austenite. The exact Cr content of the matrix is not known although it is assumed to be about 10 - 13%. The carbides are probably mixtures of the types  $\text{Cr}_7\text{C}_3$  and  $\text{Cr}_{23}\text{C}_6$  in which some of the Cr has been replaced by iron (10). Addition of Si refines the eutectic carbides in the iron and produces a more uniform structure (11). It also raises the temperature at which the matrix transforms from ferrite to austenite with consequent dimensional changes (11).



### 1.3.2.2 Mechanical properties

The high Cr irons are hard but not completely unmachinable. Shock resistances can be improved by lowering the carbon content to 0.12% (12). Table 1.2 gives the mechanical properties of high Cr irons.

### 1.3.2.3 General corrosion behaviour

The high Cr irons owe their excellent corrosion resistance to the presence of an impervious and highly tenacious surface film, probably consisting of a complex mixture of Cr and iron oxides. An increase in the Si content further increases the corrosion resistance of the iron by refining carbides (6,11). This leads to the development of a more continuous oxide film over the metal surface. It seems likely that the addition of Mo has a similar effect, although it may alternatively enhance corrosion resistance by displacing some Cr by combining with the carbon, thereby increasing the Cr content of ferrite (6).

The data available suggest that high Cr irons have no useful resistance to sulphuric acid at concentrations > 10% at any temperature (13). It is doubtful whether these irons have any useful resistance to HCl solutions at any concentration or temperature. Aqua-regia corrodes the alloys, although Kuttner has reported that an increase in the Cr content based on the formula % Cr = (% Cx5) + 36, may prove effective in inducing resistance to aqua-regia (11). Other acids are completely resisted by these irons at room temperature, although corrosion rate can at times increase at elevated temperatures.

Like the high Si irons, the high Cr irons are no better than the unalloyed grey irons in resisting alkalies (6). These alloys give good service in the presence of oxidising acids (both strong and weak) but are unsuitable under reducing conditions. They are also useful in salt solutions, organic acid solutions and in marine/industrial atmospheres (9).

#### **1.3.2.4 Applications**

These irons are most usefully employed in environments containing a plentiful supply of oxygen or oxidising agents. Anaerobic or reducing conditions would lead to rapid corrosion. Low 'C' versions are useful for annealing pots, Pb, Zn, or Al melting pots, conveyer links and other parts exposed to corrosion at high temperature (9). An important area of application is when high temperatures (upto 1000°C) are encountered.

#### **1.3.3 Ni-resist (austenitic) irons**

##### **1.3.3.1 Micro-structure**

The alloys contain Ni ranging from ~ 13.5 to 36%, Cr ranging from 1.6 to 6% and Mo upto 1%. Occasionally Cu may also be present [table 1.3] (9,14). The micro-structure consists of graphite flakes in a matrix of austenite and some carbide if Cr and/or Mo are present.

##### **1.3.3.2 Mechanical properties**

Flake graphite Ni-resist cast irons do not exhibit high strength. Machinability is satisfactory due to the presence of graphite. Toughness/shock resistance is the best amongst all the alloyed cast irons due to the austenitic matrix. Strength and toughness can be

improved upon by converting flakes into nodules. Representative mechanical properties are given in the table 1.4 (14).

#### 1.3.3.3 General corrosion behaviour

Ni-resist irons can withstand a wide range of corrosive media and give highly economical service in marine environment [Table 1.5](14). They can resist (i) all concentrations of sulphuric acid at room temperature and (ii) HCl and  $H_3PO_4$  even at elevated temperatures. Their resistance to nitric acid is similar to that of the unalloyed irons. Ni-resist irons are resistant to organic acids such as acetic, oleic and stearic. They are immune to the effects of strong and weak alkalies, although they are subjected to stress corrosion cracking (SCC) at stresses over 70 MPa in boiling alkali solutions (9).

The excellent corrosion resistance exhibited by Ni-resist cast irons is mainly due to the presence of an austenitic matrix (9,14). Unlike the high Si and high Cr alloys, the excellent corrosion resistance exhibited by Ni resist irons is not due to the formation of a passive film. Potentiodynamic studies have also revealed that these alloys exhibit active behaviour only under marine conditions (15).

Ni-resist irons do not remain rust free when exposed to the atmosphere although their corrosion resistance is considerably greater than that of the unalloyed and low alloy cast irons and steels. The rust film which develops over the first few years restricts further corrosion with the result that the corrosion rate becomes low (9).

The difference in electro-chemical potential between the graphite and the matrix in Ni-resist irons is less than in the ordinary grey irons. Therefore, in environment in which graphitic corrosion is a problem, Ni-resist iron will perform much better than the ordinary or low alloy cast irons (14).

#### **1.3.4 S.G. Ni-resist irons**

S.G. irons are commonly produced by adding Mg to liquid iron in sufficient quantity to enable graphite to separate as spheroids rather than as flakes.

##### **1.3.4.1 Mechanical properties**

Mechanical properties of the S.G. Ni-resist irons are better than the flake graphite irons [Table 1.6] (14).

To distinguish the spheroidal graphite irons from the flake ones, the prefix 'D' has been used. The composition ranges are given in table 1.3b(14).

##### **1.3.4.2 Corrosion behaviour**

It has been established that the corrosion resistance of any S.G. grade is similar to that of the corresponding flake graphite material.

##### **1.3.4.3 Applications**

They have very useful applications in all environments and also at elevated temperatures (700-800°C). Their most useful applications are in marine conditions, and also where cyclically-varying loads are experienced (9,14).

#### 1.4 Conclusion

A comprehensive review of the literature reveals that plain carbon cast irons are extensively employed for applications under mildly corrosive conditions because of their relatively low cost. However under strongly corrosive conditions only the alloyed cast irons are used. Of the three types of alloy cast irons discussed, the ferritic grades have most useful applications where resistance to corrosion under oxidising conditions is an essential requirement. Their poor mechanical strength and shock resistance preclude their general engineering applications. Of the remaining two, the Ni-resist cast irons, although extensively used in a variety of conditions, have a low strength and are unsuitable at operating temperature  $\sim 800^{\circ}\text{C}$  or more. The high Cr irons exhibit a relatively higher strength and can be employed upto higher service temperatures ( $\sim 1000^{\circ}\text{C}$ ). Their shock resistance can be improved by lowering the carbon content.

## CHAPTER - II

### FUNDAMENTAL CONSIDERATIONS IN THE DESIGN OF CORROSION RESISTANT ALLOYS

#### 2.1 Introduction

The term metallic corrosion embraces all interactions of a metal or an alloy (solid or liquid), with its environment (liquid or gas), at any temperature, irrespective of whether this is deliberate and beneficial or adventitious and deleterious (16-18). Corrosion has also been defined as 'the undesirable deterioration' of a metal or an alloy i.e. an interaction of the metal with its environment that adversely affects those properties of the metal that are to be preserved (19-21). The scope of the term corrosion is continually being extended and Fontana and Stachle (22) have defined corrosion as a process that would include the reaction of metals, glasses, ionic solids, polymeric solids and composites with environments that embrace liquid metals, gases, non-aqueous electrolytes and other non aqueous solutions. Evans (23) has considered corrosion as a branch of chemical thermodynamics or kinetics, as an outcome of electron affinities of metals and nonmetals, as short circuited electro-chemical cells or as the demolition of the crystal structure of a metal. Webster (24) defines corrosion as "the action or process of corrosive chemical change, ----- a gradual wearing away or alteration by a chemical or electro-chemical oxidising process as in the atmospheric rusting of iron". Thus in a way corrosion is a spontaneous process, electro-chemical in nature where electricity is generated.

Corrosion in its simplest form occurs by the formation of anode(s) and cathode(s). The manner in which anode(s) and cathode(s) are formed basically gives rise to different forms/types of corrosion. The extent to which it may occur is governed by (i) the process related, (ii) the materials related (metallurgical parameters) and (iii) the design related parameters.

Design is dictated by service requirements and incorporates features so as to ensure that corrosion in any form is at a minimum. Thus the important parameters needing consideration, for an optimum selection of materials, are the process related and the materials related parameters.

This chapter is accordingly devoted to a critical analysis of the (a) forms of corrosion, (b) process related parameters and (c) materials related or metallurgical parameters with the main emphasis on the last mentioned parameter. The discussion has been mainly confined to aqueous corrosion. Wherever data on the corrosion behaviour of cast irons is not available, data on corrosion aspects of plain carbon and alloyed steels has been appropriately incorporated to make the discussion more meaningful.

## **2.2 Forms of corrosion**

Important forms of corrosion, their appearance, causes and possible methods of prevention are listed in the table 2.1.

## **2.3 Process related parameters**

The different parameters along with their effect on corrosion have been summarized in the table 2.2.

## **2.4 Metallurgical factors**

### **2.4.1 Introduction**

The discussion so far has centred around an analysis of the different forms of corrosion and how the process related parameters may either enhance or stifle the attack. The present section deals with the effect of microstructure, crystal-structure and the defect-structure in controlling corrosion. Whereas the crystal structure is a fundamental entity, micro-structure depends upon the (i) composition (presence or absence of alloying, inhomogeneity), (ii) the heat treatment employed and (iii) whether or not a deformation (cold or hot) component is employed while treating. Although defects are inherently present in solids, their density would depend upon the processing history (i.e. on both the transformation and deformation components). Similarly, certain unintended micro-constituents may form during heat-treatment. Thus the term 'metallurgical factors' will encompass a discussion on the possible effects of the aforesaid parameters (42).

The following sections contain an account of how a combination of the above mentioned parameters may give rise to conditions responsible for inducing one or more of the different forms of corrosion already discussed (Table 2.1). It has also been shown how the problems thus created could be overcome by a skilful manipulation of alloying and heat-treatment.

### **2.4.2 Micro-structure**

Micro-structure has a marked effect on the corrosion rate. It has been established by Uhlig that the corrosion rate of any structure



may not depend on the total amount of second phase. However, its distribution may have an important bearing on the corrosion behaviour (4).

Thus a micro-structure exposes a very complex front to a corroding environment and an analysis of the possible interactions that may occur is of utmost importance in predicting the final outcome. Different parameters related with micro-structure have been discussed below.

#### **2.4.2.1 Single phase micro-structure**

A single phase micro-structure is most useful in resisting corrosion. Pure metals and solid solution type of alloys fall into this category. The preferred crystal structure is either fcc or hcp (c/a closest to the ideal value) because of their high packing factor. However, in the presence of a passive film, crystal structures with both higher (fcc and hcp) and lower (bcc) packing factors would prove equally effective ( $\gamma$  and  $\alpha$  stainless steels). From the point of view of formability and notch toughness, however, the former (fcc) would still be the preferred crystal structure (42).

Thus, while the lesser close packed crystal structures could be usefully employed only in the presence of a passive film, its presence would further enhance the usefulness of the more close packed crystal structures.

The main drawback with single phase micro-structures is that they exhibit limited strength. Therefore, in actual practice, either a two phase or multiphase micro-structure are employed. The following sections are devoted to a discussion on their relative

merits and demerits vis-a-vis resistance to corrosion.

#### 2.4.2.2 Two phase micro-structures

A large no. of possibilities arise and only the more relevant ones have been discussed.

##### 2.4.2.2.1 Soft matrix containing a soft phase

Such instances are not common and are likely to be adopted under special circumstances for a specific beneficial effect of the second phase e.g. utilization of controlled quantities of  $\delta$ -ferrite in an austenitic matrix for improving the susceptibility of the matrix to SCC (43). It is produced in 18-8 steel by cold-rolling (deformation induced transformation to the more stable phase) or by prolonged soaking at high temperatures. As long as the rolling temperature is low, ferrite and austenite are of the same composition and corrosion resistance is not appreciably altered. However, if for some reason a composition variation/gradient gets created, corrosion resistance will be adversely affected (44). Similarly, if the amount of  $\delta$ -ferrite exceeds a critical value, the notch toughness and formability are adversely affected (43).

A more common example is the presence of graphite in a ferrite matrix. As has been discussed earlier (section 1.2.1), this combination is most unfavourable from the corrosion stand point as the two constituents are farthest apart in the electro-chemical series [starting from the most noble graphite and followed by  $\text{Fe}_3\text{C}$ ,  $\text{Fe}_3\text{P}$ ,  $\text{MnS}$ ,  $\text{FeS}$ , to ferrite] (1). For optimum conditions (corrosion) graphite should be in the flake form (1).

Corrosion resistance can be improved by replacing ferrite matrix by pearlite (1). A costlier option which has also been used in practice (Ni-resist cast irons) is to convert ferrite into austenite. By doing so the matrix is made more noble (42).

Graphite bearing micro-structures suffer from graphitic corrosion, its adverse effect being maximum when the matrix is ferritic (1). The problem is however minimized in the presence of either a pearlitic or an austenitic matrix. Another option could be to convert flakes into nodules. However, by doing so the corrosion resistance is somewhat lowered (1).

#### **2.4.2.2.2 Soft matrix containing a phase mixture**

The most common example is the presence of pearlite in a ferrite matrix (a situation commonly encountered in steels). This combination is favourable from the point of view of corrosion particularly when the amount of the matrix phase is predominant e.g. the usefulness of mild steels in different environments. Although the relative proportion of ferrite and pearlite and the fineness of the micro-structure have an important bearing on the corrosion resistance (it decreases with an increase in the pearlite/carbide content), the morphology of cementite and the difference in electro-chemical potentials between ferrite and cementite are equally important. This difference is however smaller than the difference in electro-chemical potentials between ferrite and graphite (2).

#### **2.4.2.2.3 Second phase as dispersoid in a soft matrix**

Two possibilities arise (i) second phase is a soft constituent and (ii) second phase is a hard constituent. Presence of graphite

nodules in a ferrite/austenite matrix conforms to the first instance and that of the spheroidal dispersed carbides in a ferrite/austenite matrix corresponds to the second instance.

When a micro-structure of this type is present, the parameters governing the corrosion behaviour are (i) the difference in electro-chemical potential between the second phase and the matrix, (ii) size, shape and distribution of the second phase and (iii) the nature of the matrix-particle interface (4).

Coming to the electro-chemical aspects, their influence on the corrosion behaviour has already been discussed earlier (section 2.4.2.2.1). The overall corrosion behaviour will depend upon the electro-chemical potentials of the constituents and their volume fractions (2).

As regards the second factor, in addition to the electrochemical aspect, the optimum in terms of corrosion resistance would correspond to (i) a critical size and shape (most preferred being spherical) and (ii) a uniform dispersion. It would not be desirable to have a large number of very fine/coarse particles as their effect, based on interfacial surface area considerations, is likely to be analogous (4,45). If the particle size is below a threshold level (fine dispersion), the attack may tend to get localized e.g. as in pitting (44). It is infact suggested that the second phase particles may be graded, based on their effect on corrosion behaviour (42), on similar lines as the flake/nodular graphite classification in cast irons as proposed by AFS-ASTM (9).

The nature of the matrix-particle interface would depend upon

whether the second phase particles are coherent, semi-coherent or incoherent. Coherent shearable particles have a soft interface and should, therefore, be regarded as useful (46). To what extent they may improve corrosion resistance would, however be governed by the size, distribution and the heat-treatment [effect of stress relieving on the interface] (42). If the difference in hardness between the localized regions and the matrix is large, locally formed cells may accelerate corrosion. Under these conditions, the extent of acceleration/stifling would be decided by the crystal structure of the matrix.

Incoherent/semicoherent particles are by themselves hard and are not sheared (46). However, partial coherency is associated with strains and in this turn may set up local cells of the type mentioned above. This state would be altered by the heat-treatment (stress relieving) employed.

The discussion so far has been restricted to second phase particles in the form of spheres. All other factors being identical, the morphology of the second phase will have a bearing on the corrosion behaviour e.g. second phase in the form of platelets/plate or a massive region (with or without sharp edges) will mean a higher rate of corrosion in comparison to a sphere or a polygon because of a higher interfacial contact/surface area (45) and an unfavourable morphology from the point of view of crack propagation behaviour (42).

#### **2.4.2.3 Single phase with high hardness**

Martensites and bainites, which are formed partly or wholly by

shear transformations, fall into this category. Their effect on the corrosion behaviour would depend upon the (i) nature of the environment especially with regard to the possibility of inducing SCC, (ii) possibility of gas assisted cracking primarily due to the known susceptibility of shear microstructures to this type of attack e.g. susceptibility of twinned martensites to hydrogen embrittlement (47-49), (iii) the possible effect of surface stresses induced during transformation and (iv) the possible role of defect structure, (v) other features (if any) and a high hardness (42).

The role of a specific environment in bringing about SCC in a material has already been discussed and needs no further elaboration. This is a relevant parameter in the present context since micro-structures formed by shear transformations are metastable, contain deformation induced sub-structure and are in a state of high internal and surface stresses. The presence of twinning (as in high carbon and high carbon alloy martensites) helps in entrapping evolved hydrogen leading to hydrogen embrittlement (47). This tendency is further enhanced by the presence of micro-cracks along the (i) periphery of the plates, (ii) midribs and at the plate junctions-a feature associated with high carbon martensites (50).

The above analysis suggests that based on the mechanism of formation and because of certain features (discussed above) associated with its micro-structure, martensite may not prove useful in imparting good corrosion resistance. However, far from being so, the formation of martensite with a distorted tetragonal lattice results in 1/5 the corrosion rate of the same steel subsequently

tempered at 300-400°C [producing a second phase of finely dispersed iron carbides] (44). This observation clearly implies that the higher corrosion resistance of homogeneous single phase alloys holds even if the alloys are thermodynamically unstable and which can subsequently transform into an equilibrium multiphase micro-structure (44). Infact , the high hardness associated with martensite may lead to lesser rates of dissolution and hence to an improvement in corrosion resistance (50). Based on the above considerations, bainites (particularly lower bainite) may also prove useful due to (i) their high hardness and (ii) a crack resistant micro-structure (42).

#### 2.4.2.3.1 **Second phase with a high hardness in a hard matrix**

Second phases with a high hardness are usually compounds (carbides, nitrides, borides etc) which are inert and stable at high temperatures. Their stability both in the as-cast and in the heat-treated conditions is further improved by adding elements which primarily partition to them (e.g. addition of Cr, Mo, V, Ti etc in case of carbides). This would improve their inertness still further (42). The usefulness of martensites in improving corrosion resistance has already been discussed in the preceding section (2.4.2.3). The overall corrosion behaviour of the aforesaid combination (M + a compound) would depend upon the potential difference between these two, the state of stress and the crack propagation behaviour. Data on the behaviour of martensite + a hard phase couple, vis-a-vis their corrosion behaviour, is not readily available. However, based on fundamental considerations, the 'couple' is likely to perform satisfactorily, the high hardness of the matrix notwithstanding

(42).

#### 2.4.2.3.2 Multi-phase microstructures

In this category only those examples would be considered where a third phase has been deliberately introduced. Its presence would prove useful in resisting crack propagation if the phase is ductile and tough (e.g. the presence of  $\gamma$  along with M + C). The improved crack propagation behaviour will indirectly improve the corrosion and stress-corrosion resistance (42). In such micro-structures the location, amount and stability of the tough phase is equally important e.g. austenite around carbides would be the most useful configuration. Similarly a favourable carbide morphology would be an added advantage (51).

#### 2.4.2.4 Unintended microconstituents

##### 2.4.2.4.1 Grain boundary precipitation/segregation

While heat treating, it is possible that unintended micro - constituents may form either during soaking or during cooling after heat-treatment. Their location, electrochemical behaviour and the structural changes accompanying their formation will greatly influence the corrosion behaviour of the final microstructure. One such change is the grain boundary precipitation of a constituent e.g. precipitation of  $\text{Cr}_{23}\text{C}_6$  type carbide in austenitic stainless steels while cooling in the temperature range 550-950°C. It occurs when 'C' content in the austenitic steels exceeds  $\sim 0.03\%$ . The mechanism suggested is that carbon atoms rapidly diffuse to the grain boundary regions and react with the chromium to form the aforesaid carbide. The high proportion of Cr in the carbide



depletes the adjacent alloy of Cr to a point where its concentration falls below the 12% limit required for stable passivity. On exposure to a corrosive environment, the depleted zone sets up an active-passive zone with the larger area alloy grain acting as cathodes in contact with grain boundaries and the adjoining areas acting as anodes (44). Although creation of Cr depleted regions is the major cause of the accelerated attack, it has been suggested that setting up of pronounced compositional gradients may be equally damaging (23).

The problem created by the grain boundary precipitation can be overcome by elevated temperature heat-treatment (1050°C), which disperses carbon uniformly throughout the alloy, followed by fast cooling. Grain boundary corrosion can also be avoided by stabilization (adding Ti or Nb to the alloy). Their carbides have a lower free energy of formation i.e. are more stable than chromium carbides (6,44). An equally useful option is to keep the carbon low i.e. <0.03% (6).

#### 2.4.2.4.2 Formation of sigma and chi phases

The formation of the so-called 'sigma' and 'chi' phases (topologically close packed phases) is yet another example of unintended structural changes occurring while heat treating. They are usually formed in alloys with high alloy content e.g. stainless steels (44,52), 28Cr-4Mo (53), 28Cr-4Mo-4Ni and 48% Cr (atomic) iron based alloys (54). These phases have a complex structure and one of them namely the sigma phase has a structure related to the intermetallic compound FeCr (44).

There are conflicting opinions on the effect of sigma and chi phases on corrosion resistance and mechanical properties. Some workers find them to be harmful while others have not observed any adverse effect. An important observation is that the phases themselves exert no detrimental effect and that the concentration gradient set up in the proximity of the adjoining phase may cause a reduction in the corrosion resistance (52).

#### **2.4.2.5 Minor factors**

##### **2.4.2.5.1 Effect of grain structure**

The grain structure of alloys, like intergranular preprecipitation, can also influence the corrosion behaviour e.g. corrosion resistance of certain wrought micro-structures may be less on the surface perpendicular to the hot or cold working direction than on the surfaces parallel to this direction. There may be severe localized corrosion starting on the faces perpendicular to the working direction and proceeding into the metal in the working direction, while the surfaces parallel to the working direction remain relatively unattacked. Such end-grained attack, which is basically the result of the grain structure being elongated in the working direction, has been observed in austenitic stainless steels, Ti alloys and mild steels (6).

##### **2.4.2.5.2 Effect of grain orientation**

Grain orientation as a practical factor in aqueous corrosion is at best of minor importance. This is due to the fact that polycrystalline metals corrode more or less uniformly. Nevertheless there is a fundamental difference in tendency for one crystal face to corrode

compared to another. In general, however, the more reactive crystal planes corrode first, leaving a particular crystal face, which corrodes least in any given environment, as the residual face. For example the residual faces for iron in nitric acid and copper in copper sulphate are (100) and (111) respectively. The corrosion rate continues to vary slightly with crystal orientation. The preferred attack of all faces except the least corrodible one leads to roughening of the surface, depending upon the grain orientation, as has been shown by Gwathmey in the measurements of friction and wear. For example the (110) face of copper exposed to stearic acid at 185°C became very rough, whereas the (111) face remained smooth; it is least corroded (44).

For intermediate compounds or semi-conductors, the surface free energy of different crystal faces may differ more than for metal. Hence reactivities of different crystal faces may show large differences. Intermetallic compounds e.g. may form faces differing in composition with relatively a large potential difference. A 75 mv difference was found between (111) surfaces of indium antimonide which have indium atoms on one face and antimony atoms on the other. Conversely in another study a maximum difference of 5 mV was observed between the (111) face and either the (110), (100), and (210) faces of copper (44).

#### 2.4.2.5.3 Inhomogeneity

This refers to a variation in chemical composition within a grain e.g. as encountered during coring. This type of micro-structure can be considered as consisting of an inbuilt electro-chemical cell. Hence corrosion resistance will be adversely affected. Homogenise

anneal is recommended to overcome this problem (54).

#### 2.4.2.6 Impurities

Impurities generally found in iron and steel are S, P and inclusions. Both S and P have a detrimental effect and therefore have to be maintained at a low level. The level of impurities that can be tolerated in a material is a function of the strength level (6). S has been shown to accelerate corrosion in acidic environments (6). The detrimental influence of P increases as the purity of the alloy decreases (55). An important reason put forward to explain the adverse effect of S and P is that compounds between Fe and S or Fe and P are of low hydrogen overvoltage type (44). P also adversely affects the stress corrosion resistance in the range of lower applied stresses and markedly changes the polarization resistance of the alloys in the plastically deformed state (55).

Inclusions are also detrimental e.g. it has been observed that a relatively pure iron but containing sulphide inclusions has a marked tendency to react even in mildly corrosive environment (54). Inclusion size, shape, distribution and volume fraction will have an important bearing on the corrosion behaviour (56). Inclusions enhance corrosion by initiating pitting and in some instances even crevice corrosion (57). It has been shown that addition of chromium is useful in altering the electro-chemical behaviour of the sulphide inclusions by combining to form CrS. Consequently, the resistance to pitting and crevice corrosion improves (57). The adverse effect of inclusions is enhanced if the material is in the deformed state (54). This may in some way be related to directiona-

lity imparted to the inclusions due to deformation.

The adverse effect of impurities can be minimized by restricting them to a desired low level. Use of suitable melting and refining techniques e.g. vacuum melting and casting techniques would greatly help in achieving this objective. The other possible option is to resort to alloying.

#### 2.4.3 Defect structure

Mainly three types of defects are encountered in solids namely line defects, point defects and surface defects. Since defects are faulted regions, their presence is associated with a high energy and this will have a definite bearing on the corrosion behaviour. In the present context, the defects being considered are vacancies, interstitial atoms and dislocations, and more specifically the last mentioned. Each of these imperfections produce highly localized differences in the electro-chemical behaviour due to distortions associated with them. These areas act as anodic sites in comparison with the surrounding matrix (6). Pits are formed at the intersection of dislocations with the surface. Triangular etch pits around a dislocation are a result of selective chemical attack due to stress field around it (dislocation). The shape of the etch pit is related with the orientation of the grain to the etched surface (54).

Although the equilibrium concentration of defects in a solid is fixed, their density may be increased through heat-treatment/processing e.g. quenching from a high temperature will increase the concentration of vacancies; similarly cold working increases

the dislocation density. Therefore it is necessary to examine, in some detail, the possible effect of an increase in the defect density on the corrosion behaviour.

#### 2.4.3.1 Effect of cold work

When an annealed material ( $\rho = 10^5$  lines/cm<sup>2</sup>) is heavily cold worked, the stored energy of cold work increases the dislocation density to around  $10^{13}$  lines/cm<sup>2</sup>. It is therefore expected that this increased energy, together with the large distortion/state of stress that is generated, will enhance corrosion. However, there are differences of opinion about this observation as also the mechanism (s) by which corrosion resistance is adversely affected e.g. it has been suggested that the increase in the stored energy which is of the order of 8-80 kJ/kg mole is only equivalent to a potential difference of a few mV between the annealed and cold worked states (6). The difference in the driving force is not large enough to make any appreciable difference in the corrosion behaviour in the two states(6). However, since it has been experimentally established that corrosion is enhanced by cold working, a possible mechanism that has been suggested is that anodic and cathodic processes could be quite different on annealed and cold worked surfaces (6). Cold working increases the corrosion rate probably because of an increase in the dislocation density per second, possibly as a result of an increase in the no. of kink sites on the surface thereby increasing the anodic exchange current density. On the other hand Foroulis and Uhlig (58) suggest that the increased corrosion rate is due to the segregation of carbon and nitrogen atoms to dislocations, and that the cathodic

(hydrogen evolution) reaction is kinetically easier at these sites. This is supported by their observation that cold work does not increase the corrosion rate of high purity iron.

In addition to an increase in the dislocation density, grains get aligned in the direction of working and the boundaries may be fragmented as a consequence of cold working. Such areas are subjected to pitting (54). Impurities or alloying element atoms migrate to these imperfections thereby causing an even greater change in the electro-chemical character of these defects (54).

Another aspect of cold working is that it may create anodic and cathodic sites due to differential stress distribution from the periphery to the centre of a bar e.g. as in 'tor' steel (reinforcing material made by controlled cold torsion twisting mild steel bars). The increase in the corrosion rate is not so much a consequence of an increase in the dislocation density as much to a difference in stress distribution leading to galvanic action (41).

To overcome the problem associated with cold working, stored energy of cold work has to be effectively released. Heat treatment helps in doing so (54).

#### **2.4.4 Heat treatment**

Functionally, heat treatments are employed to bring about one or more of the following effects (i) strengthen, (ii) homogenise, (iii) soften, (iv) stress relieve, (v) removal of extraneous phase(s), (vi) other than those listed before (54).

Strengthening through heat treatment may involve either produ-

cing meta-stable micro-structures by inducing shear transformation or by affecting precipitation. Both the transformations are to be affected in the solid state. The effect of the resultant transformation products in influencing corrosion behaviour has already been discussed (section 2.4.2).

**Homogenising** is employed to bring about uniformity in composition and will therefore improve corrosion resistance.

Softening, which is brought about by annealing, leads to the attainment of micro-structures with low energy. Hence an improvement in corrosion resistance is expected provided no adverse micro-structural changes are taking place either during soaking or while cooling (42).

**Stress relieving** is useful in relieving residual stresses and is expected to lead to an improvement in corrosion and stress corrosion resistance.

An important function of a heat-treating schedule is to help eliminate/counteract the formation of extraneous phases/micro-constituents. Their effect on the corrosion behaviour has already been discussed in detail. Through carefully designed heat-treating cycles, it would be possible to overcome conditions leading to the formation of extraneous micro-constituents, e.g. cooling rapidly to suppress grain boundary precipitation or avoiding excessive soaking at high temperatures to prevent  $\delta$ -ferrite or sigma phase formation in stainless steels.

Lastly, heat-treatment may prove helpful in improving corro-



sion resistance by altering the surface characteristics e.g. heat-treatment of the surface to increase its hardness is useful in improving fretting and erosion-corrosion resistance (6,19-21).

#### 2.4.5 Alloying

Alloying elements form the basis of micro-structure control through heat-treatment. Accordingly, it is useful in controlling the corrosion behaviour. Alloy additions may also influence corrosion behaviour by forming solid solutions, by forming passive films (applicable when Cr, Si and Al are added in requisite amounts) and by altering the electro-chemical behaviour of the phases and the impurities present.

The effect of alloying elements, generally added to cast irons, has been summarized in the table 2.3.

#### 2.5 Passivity

Passivity refers to the useful corrosion resistance of many structural materials (metals and alloys). Some of them can be made passive by exposure to certain environments e.g. iron in chromate nitrite and concentrated nitric acid solutions (25,54).

A metal or an alloy active in the e.m.f. series is considered passive when its electro-chemical behaviour approaches that of a appreciably less active or noble metal i.e. as a consequence of passivity the electrode potential shifts in the noble direction. Alternatively a metal or an alloy is deemed as passive if it substantially resists corrosion in an environments where thermodynamically there is a large free energy decrease associated with its passage from the metallic state to appropriate corrosion product

(25).

A material can be rendered passive either chemically or mechanically. Chemical passivity involves treating metal surfaces with oxidising agents without physically altering their characteristics. It occurs either due to the formation of an invisible thin but tenacious and dense semi-conducting oxide film on the metal surface or by the formation of a chemisorbed layer of oxygen on to the metal surface, whose thickness, in principle, can be less than a monolayer. The mechanism of oxide film formation involves (a) formation of a salt layer (b) subsequent removal of the layer by evolution of oxygen and (c) evolved oxygen forming an adherent

Of the two possibilities indicated above, the former is more effective in imparting passivity because a chemisorbed layer will not be as effective as an oxide film in acting as a diffusion barrier in general and particularly when the thickness of the chemisorbed layer is small.

Mechanical passivity is produced by precipitation of a solid salt on the metal surface. Corrosion is resisted by the formation of a thick but more or less porous non-conducting layer.

Metals which can be passivated have been classified into three groups (25) (i) Ti, Cr and Sn which can be passivated even in the absence of oxidising agents (ii) iron which can be passivated by weak oxidising action between pH 9 and 13 and by strong oxidising action at all other pH values and (iii) Mn, Pb and Ag which can be passivated only by strong oxidising action. Transition elements

(Cr, Ni, Co, Fe, Mo) develop passivity due to a chemisorbed layer of oxygen. This has been attributed to the unfilled 3-d shell and to a high heat of sublimation (63).

The discussion regarding passivity has uptill now been confined to metals alone. However, several alloys such as Fe-Cr, Fe-Mo, Ni-Cu, Ni-Mo, Co-Cu also exhibit passivity. Certain general observation regarding passivity in alloys are (a) their major components are transition metals (b) a metal normally passive in air can often passivate another metal if the two form solid solutions over a range of composition (c) multiphase alloys can be made passive if the electrochemical potential of the participating phases is nearly similar and (d) a critical concentration is a must to induce passivity, the amount required being a function of the environment (63).

Elements which induce passivity in the Fe-base alloys are Cr, Si and Al. Critical concentrations of the elements required to induce passivity are indicated in the table 2.3. Although passivity ensures a high resistance to corrosion, not all the alloys employed in corrosive environments exhibit passivity in the classical sense. Under such circumstances the resistance to corrosion can only be attributed to a reduced galvanic action amongst the participating phases. Alloying and heat treatment would be the key elements in imparting corrosion resistance based on this principle.

The conditions under which passivity may be induced can be ascertained with the help of potential- pH diagrams. Chemical passivation can be studied by means of potential vs current density

curves also called as polarization curves. For metals and alloys exhibiting passivity, the diagram (S-shaped curve) consists of three regions; the active, the passive and the transpassive. For an easily passivable alloy the important attributes are (25) (i) a small primary passive potential ( $E_{pp}$ ) and (ii) a large passive voltage range (current density independent potential range).

## 2.6 Conclusion

The key parameters in corrosion control are (i) the material of construction, (ii) design, and (iii) forms of corrosion and the different parameters affecting the extent of corrosion. Incorporation of these parameters into a single unit is termed as integrated corrosion control (26).

The control involving materials of construction ensures that they are suitable for their function for the required length of time at a reasonable cost. Their resistance to corrosion in the given environment, the tendency to specific forms of corrosion, requirement of different treatments and joining methods and adjustability of material to a producible form that gives the best chance to the product (structure) to resist corrosion are appraised (26).

The objective of the control of design is to include in the product (structure), a selection of such shapes and component forms that will keep it free from destructive forms of corrosion during all the stages of fabrication, assembly and operation without excessive effort (26).

The relevance of information on forms of corrosion and the

parameters affecting it (corrosion) becomes evident from a critical appraisal of the preceding paragraphs.

Major conclusions arrived at from a critical analysis of the contents of this chapter are summarized in the chapter-III. They formed the basis of designing alloys investigated in the present study.

## CHAPTER - III

### FORMULATION OF THE PROBLEM

#### 3.1 Introduction

Certain factors of design interest emerge from a critical appraisal of the previous chapters (42):

(1) Corrosion control essentially centres around three parameters, the material of construction, process/design parameters, and forms of corrosion. Not much flexibility exists with regard to the latter two since they are primarily dictated by service conditions which can not be altered. The design would incorporate features so as to minimise corrosion damage. Thus the primary factor is the optimal selection of the material of construction.

(2) A single phase microstructure although exhibiting low strength is most useful in resisting corrosion. A more close packed crystal structure (e.g. fcc) is preferred. Its effectiveness is enhanced in the presence of a passive film.

(3) The effectiveness of a two phase/microconstituent microstructure in resisting corrosion depends upon (a) morphology, size, location and distribution of the 2nd phase (b) its volume fraction and (c) difference in the electrochemical potentials of the two constituents (i.e. between the matrix and the second phase).

(4) Presence of a hard metastable constituent (martensite) may prove helpful in reducing dissolution/corrosion rates.

(5) Alloying elements prove helpful in resisting corrosion firstly by being in the dissolved state, secondly by bringing about a change in the matrix microstructure (e.g. by converting pearlite into bainite, martensite or austenite) and thirdly by forming a

passive film.

(6) Impurities (inclusions) enhance corrosion rates by providing small anodic areas surrounded by large cathodic areas. Alloying is also effective in altering the behaviour of inclusions by altering their electrochemical character.

(7) Compositional/concentration gradients are more effective than micro-structural variations in enhancing the attack.

(8) Topologically close packed phases (sigma and chi phases), formed during prolonged soaking (while heat-treating), may either favourably or adversely affect corrosion behaviour. Another opinion is that the 'sigma phase' effect is more related with the concentration gradient it sets up.

(9) Thermal (heat treating) and processing (e.g. cold working vs hot working) histories and defect structure influence the corrosion rate.

(10) Corrosion resistant alloy cast irons have been based on austenitic (high Ni), ferritic (high Si) and martensitic/austenitic (high Cr + Mo) matrices. Second phase is graphite (both flake and nodular morphology) in the first two types and carbide in the third. Presence of a passive film resists corrosion in the ferritic and also in the martensitic/austenitic grades but not in the austenitic irons. Bulk of the literature on corrosion resistant cast irons is confined to the austenitic Ni-resist cast irons.

(11) Most graphite bearing corrosion resistant cast irons suffer from graphitic corrosion- a phenomenon considered as undesirable.

### 3.2 The approach

Based on the above, it clearly emerges that there are two possible

routes for developing corrosion resistant cast irons, namely the 'grey-iron' and the 'white-iron' routes. Considering the latter, little information is available on the electro-chemical behaviour of the different microstructures encountered in white irons namely the martensite + carbide (M + C). Martensite + austenite + carbide (M + A + C) and austenite + carbide (A+C) microstructures.

Patwardhan (42) opined that detailed information on this aspect will prove useful in deciding whether microstructures resistant to corrosion could be generated through the 'white iron' route. Further-more, such a study would become additionally meaningful if it were possible to attain the said microstructures at a minimum of cost i.e. by employing low cost indigenously available alloying elements (42).

The present investigation was accordingly undertaken in response to the above queries and consisted of conceiving certain low cost compositions incorporating Mn, Cr, and Cu as the main alloying elements. The compositions were to be so designed that the microstructures of interest could be attained with a minimum of alloying either in the as-cast condition or through simple heat treatment (s). It was decided to concentrate on (i) M + C (ii) M + A + C (iii) A + C microstructures and their allied counterparts. Thus the key element of alloy design was to ascertain the compositional limits for different elements so to obtain the (M + C) microstructure with relative ease. Once this was established, what was further required to be done was to raise the concentration of austenite stabilizing elements so as to retain austenite either completely or in large proportions at room temperature. Its propor-



tion and the morphology of carbides could then be further altered through suitably devised heat-treatments (42).

### 3.3 Design of alloys

The Fe-Cr-Mn-Cu system was chosen for the present investigation. Its selection can be justified as follows (42):

(i) Mn improves hardenability significantly at a low cost, helps in retaining  $\gamma$ , stabilizes carbide, and does not adversely affect fluidity.

(ii) Cu is a useful graphitizer (helpful in rendering carbides discontinuous and in altering carbide morphology during heat-treatment), solution hardens and improves resistance to corrosion in the presence of dilute acids (acetic, sulphuric, hydrochloric) and acid mine water (64,65).

(iii) Cr stabilizes carbide (not as strongly as Mo, V, W or Nb), is helpful in attaining a uniform microstructure (i.e. with a minimum of segregation) and may prove useful in attaining martensite/austenite even if present singly in large proportions.

The first stage in the planning was to decide upon the minimum Cr content to ensure that a base composition containing  $\sim 3\%$  C and 1.5-2% Si (normally acceptable limits in cast irons) is cast white during sand moulding over a range of section sizes. This amount is likely to be 3-4% (53). It was decided to restrict Cr to  $\sim 4-5\%$  and to depend upon Mn to make up for any deficiency in the carbide stabilizing tendency because (i) the carbide forming tendency of Cr and Mn is not much different and (ii) Singh (66) had shown that nearly  $\sim 55\%$  of the Mn added partitions to the carbide phase (42).

Two Mn levels namely  $\sim 6\%$  and  $\sim 8\%$  Mn were selected. The  $\sim 6\%$  Mn level was based on the study by Singh (66) in which it had been demonstrated that a Mn content  $\sim 5-6\%$  facilitated retention of austenite on heat-treating from temperature  $> 900^\circ\text{C}$  at  $\sim 6\%$  and  $\sim 9\%$  Cr contents (65). Since the Cr content in the present instance was intended to be  $\sim 4-5\%$ ,  $6\%$  Mn content was considered as a reasonable level for attaining the microstructures of interest. Presence of Cu, to be further incorporated in the composition, would additionally facilitate austenite retention thereby overcoming possible deficiency, if any, in the austenite retaining ability.

Cu was added in two distinct amounts  $\sim 1.5\%$  and  $3\%$ . Besides aiding the formation of austenite, its presence will also improve corrosion resistance. A silicon content  $1.5-2\%$  ensured that the alloys had good fluidity (67). Thus, in all 4 alloys were designed with the same base composition i.e.  $3\%$  C,  $\sim 4-5\%$  Cr and  $\sim 1.5-2\%$  Si but with different Mn and Cu contents (42):

<u>6Mn</u>	<u>8Mn</u>
B1 ( $\sim 1.5$ Cu)	B2 ( $\sim 1.5$ Cu)
B3 ( $\sim 3.0$ Cu)	B4 ( $\sim 3.0$ Cu)

### 3.4 Planning of experiments

The experiments were planned as follows:

#### Phase I

A study of the structure-property relation by subjecting the alloys to different heat-treatments, assessing their hardness and conducting structural investigations by optical metallography.

## Phase II

Electrochemical characterization of the alloys by the weight loss method and further detailed structural examination by x-ray diffractometry and by quantitative optical metallography.

## Phase III

Deformation behaviour of different microstructures by compression testing, structural investigation by EPMA and electrochemical characterization by the potentiostatic method.

## CHAPTER IV

### EXPERIMENTAL TECHNIQUES AND PROCEDURE

#### 4.1 Alloy preparation

Raw materials used for preparing different alloys were pig iron, low carbon ferro-alloys (ferro-chromium, ferro-manganese and ferro-silicon), graphite powder, electrolytic copper and mild steel scrap. Compositions of the pig iron and the ferro-alloys are reported in the table 4.1.

The charge consisted of the aforesaid raw materials in the requisite proportions so as to ensure that the desired compositions are attained. Due consideration was given to the metal content of the ferro-alloys and to the melt losses while making charge calculations. Alloys were air melted in clay bonded graphite crucibles in a medium frequency induction furnace.

Initially two base alloys, each weighing 65 kgs and containing 4-5% Cr and 1.5% Cu and 3% copper respectively, were prepared by first melting requisite proportions of pig iron, mild steel scrap and graphite to a super-heat followed by deslagging and subsequent addition of ferro-chromium, ferro-silicon and copper. After ensuring complete dissolution of alloy additions, small samples were taken out of the melt for estimation of carbon by the LECO analyser. In the intervening period the melt temperature was lowered to reduce losses. After ensuring that the carbon content had reached the desired level, the liquid metal temperature was raised to about 1400°C and slag removed. Each of the molten alloy was then cast

into two cylindrical blocks of approximately equal weight at the two Cu levels. Thus in all four castings were poured.

Finally, the Mn content was adjusted to the desired level (i.e. ~ 6% and 8%) by adding requisite amount of ferro-manganese to each of the four base alloy castings in the molten condition. Carbon content was rechecked even at this stage to ensure that it was maintained at the desired level. After deslagging, temperature of the molten metal was measured with an optical pyrometer. The alloys were poured at about 1425°C into ~ 25 mm diameter X 250 mm long cylindrical ingots and 8x22x120 mm rectangular strips in sand moulds.

Alloys were analysed for C, S, P and Si on a vacuum quantometer and for Mn, Cr, Cu, P and Si on x-Ray fluorescence spectrometer. Detailed chemical analysis is reported in table 4.2.

#### **4.2 Specimen preparation**

Alloys were very hard and could not be cut either with a power saw or with high speed steel tools. Disc samples (height 14 to 18 mm) were sliced off from the cylindrical ingots by making a 2 to 3 mm deep cut all along the circumference on a silicon carbide cut-off wheel followed by hammering. Heating of the specimens during slitting was kept to a minimum through water cooling. Specimens thus obtained were ground to have parallel faces and paper polished in the usual manner.

For corrosion studies by the weight loss method, specimens of the size ~ 8x6x4 mm were employed. They were cut from rectangular strips by a procedure outlined above. As before they were ground to

have parallel faces and paper polished to the 4/0 stage to obtain mirror finish.

#### 4.3 Heat-treatment

Heat-treatments primarily comprised of soaking at 800, 850, 900, 950, 1000 and 1050°C for 2, 4, 6, 8 and 10 hours followed by oil quenching. They were carried out in muffle furnaces whose temperature was measured with a Pt-Pt/Rh thermocouple and controlled to  $\pm 5^\circ\text{C}$ .

#### 4.4 Hardness measurement

Hardness testing was extensively employed because it provides a quick yet reliable indication of the effect of heat-treatment on properties.

Heat treated specimens were initially ground to a uniform depth of about 1 mm to remove any decarburized layer. Thereafter they were paper polished upto 3/0 stage in the usual manner. Hardness measurements were carried out on both the faces of a specimen on a Vickers hardness testing machine employing a 30 kg load. A minimum of 20 impressions were taken on each specimen. The permissible scatter in the hardness values was  $\pm 17$  VPN (68). In the event of the variation exceeding this limit, the hardness has been represented as a band denoting both the maximum and the minimum values.

As the alloy system under investigation is heterogeneous in character, both the representative hardness readings as well as the average values have been reported.

#### **4.5 Compression testing**

Deformation behaviour of the different microstructures was assessed by carrying out compression tests. They were carried out on cylindrical specimens (size approx. 10 mm dia x 10 mm height) on a 60 ton capacity West German made MFL microprocessor based universal testing machine, at a cross-head speed of 1.0 mm/min. Compressive strength and the percent deformation (height strain) were calculated from the stress-strain curves in the usual manner.

#### **4.6 Metallography**

##### **4.6.1 Optical microscopy**

This has been extensively employed to study how heat-treatment influenced microstructure. Specimens were paper polished in the usual manner (section 4.2). The final (wheel) polishing was carried out using 1 and 0.1 micron alumina as the abrasives. After proper cleaning, specimen surfaces were etched in freshly prepared 2% nital. Metallographic examination was carried out on a REICHERT METAVERT-368 microscope.

##### **4.6.2 Quantitative metallography**

It was carried out on LEITZ image analyser (Auto-scan) at a magnification of 2500X. Specimen size was the same as that employed during optical metallography. Ten different fields of view were examined on each specimen. Quantitative estimations including plotting of histograms were carried out with the help of computational techniques.

#### 4.6.3 Scanning electron microscopy

Scanning microscopy was also extensively employed on specimens, that had been subjected to corrosion studies in different environments, to ascertain the nature of the attack.

To ensure good electrical contact, specimens were glued to the specimen holder using a silver base paint. They were allowed to dry before being examined on a Phillips 501 scanning electron microscope at an operating voltage of 15 KV.

#### 4.7 Electron probe micro-analysis

This study was carried out for assessing the partitioning behaviour of different alloying elements, particularly Mn, Cr, Cu, C and Si, as influenced by heat-treatment. This was carried out on CAMEBAX EPMA/SEM at 15 KV and  $\approx 60 \mu\text{A}$  beam current using the crystals LiF (for Fe, Cr, Ni and Cu), TAP (for Mn and Si) and ODPb (for carbon).

The three different modes of analysis usually available are the fixed-probe technique, the line-scan technique and the area-scan technique. All the three methods were employed in the present investigation. Details concerning them have been reviewed elsewhere (66).

Specimens for electron probe micro-analysis were cut from rectangular strips, heat treated, and after removing approximately 1 mm thick layer from all the faces were cold mounted (mount size: 25 mm dia x 7 mm height). The samples, prepared for metallographic examination in the usual manner, were etched just enough to reveal the microstructure. This way it was ensured that the composition



of different phases/micro-constituents was practically unaltered.

#### **4.8 X-ray diffractometry**

As-cast and the heat-treated bulk specimens of the different alloys were subjected to structural investigations on a Phillips diffractometer PW 1140/90, employing an iron target and a manganese filter, at a voltage of 35 KV and a current of 12 mA.

Specimens, which were polished and lightly etched, were scanned from 35 to 135°. In most instances time constant and scanning speed were kept at 2 seconds and 2° per minute respectively. Diffractograms were analysed/indexed by adopting the following procedure:

- i) 'd' values were obtained discernable reflections/peaks;
- ii) assuming the height of the most prominent reflection as 100, the relative intensities of all the other peaks were calculated.
- iii) indices were assigned to different 'd' spacings based on the standard 'd' and I/I<sub>0</sub> values available from x-ray data/ASTM diffraction data cards. While doing so, peaks with relative intensities less than 3 were not considered.

#### **4.9 Corrosion studies**

Corrosion studies were carried out by the weight loss and the potentiostatic methods.

##### **4.9.1 Weight loss method**

These tests were carried out in accordance with the relevant ASTM standards (69). Specimens were prepared by adopting a procedure outlined in the section 4.2 and cleaned as per the standard procedure laid down(68). A specimen was tied on to a glass rod by a

nylon thread/cord. It was then suspended in a 100 ml capacity corning beaker containing 5% NaCl solution upto a preset level. Each specimen was weighed and its surface area determined prior to being subjected to the test. Tests were conducted for 7,15,30 and 45 days. After the completion of a test, the specimen was cleaned by scrubbing followed by washing in double distilled water, degreasing in acetone and finally air drying (70). It was then weighed again and the loss in weight calculated. Corrosion rates were calculated by using the formula (70):

$$\text{Corrosion rate} = \frac{K.W}{A.T.D}$$

K = Constant ( $3.45 \times 10^2$ ) for ipy

K = Constant ( $2.40 \times 10^6$ ) for mdd

T = exposure time in hrs. to the nearest 0.01h

A = Area in  $\text{cm}^2$  to the nearest 0.01  $\text{cm}^2$

W = weight loss in gms. nearest to 1 mg

D = Density in  $\text{g/cm}^3$

Corrosion rates have been reported in inches per year (ipy) and in mdd (milligrams per square decimeter per day). The latter unit is more reliable since density does not figure in the final calculations.

#### 4.9.2 Anodic polarization technique

This technique is useful in determining whether the alloy under investigation exhibits the active-passive transition.

The experimental set up, shown in Figure 4.1, consists of a polarization cell which is connected to a standard potentiostat

(WENKING ST 72), a voltage scan generator, and a recorder.

The polarization cell consisted of a one litre flat-bottom pyrex flask which was modified by the addition of various necks to introduce the test and the counter electrodes, thermometer, and a luggin capillary salt bridge which separated the bulk solution from the reference electrode. This cell and its components have been described in detail by Greene (71).

The test electrode, also known as the working electrode, was made of the test material of approximately  $0.5 \text{ cm}^2$  cross-sectional area. It was cold mounted in a manner that it was leak proof and was provided with a solderless electrical contact insulated from the electrolyte. The entire assembly is shown in Figure 4.2. The surface of the test electrode was prepared within one hour of the experimental measurements in accordance with the recommended practice (70). The specimens were cleaned in acetone five minutes before immersion, then rinsed in double distilled water and finally air dried.

The counter electrode was a  $2.5 \times 2.5 \text{ cm}$  platinum sheet connected with a thin platinum wire. The cleaning of this electrode was carried out in hot aqua-regia. The reference electrode was a saturated calomel electrode (SCE) and was throughout dipped in salt solution. The potential of the calomel electrode was checked at periodic intervals to ensure its stability.

The potentiostat has a range of 1 to  $10^4 \text{ mV}$  and a current output range from 1 to  $3 \times 10^6 \text{ } \mu\text{A}$ . It is also possible to maintain an electrode potential within 1 mV over a wide range of current

values.

The voltage scan generator has a scanning range from 0.01 to 10 mV/second in eight calibrated coarse positions with overlapping fine adjustments and a scan range that covers upto 10 volts from every potential to another within the limit  $\pm 10$ v.

A potential change of 50 mV was imposed after every 5 minutes and the current density noted at the end of each 5 minute interval. From the data it was possible to plot the potential vs current density curves and calculate the critical parameters.

#### 4.10 Data analysis

Analysis of the data obtained was carried out with the help of computational techniques using a DEC 2050 computer. Programmes were developed for analysing hardness, corrosion rate, x-ray diffraction and quantitative metallography data. Programmes were also developed for establishing structure property correlations (72-73).

**CHAPTER - V**  
**EXPERIMENTAL RESULTS**

**5.1 General**

The experimentation in the present study involved assessing (i) the heat-treatment response of the alloys B1 to B4 with the help of hardness measurements, optical metallography (including quantitative estimations), scanning microscopy, X-ray diffractometry and to a limited extent by the EPMA techniques, (ii) the deformation behaviour by compression testing and (iii) the corrosion behaviour by the weight loss and the potentiostatic methods. The data thus generated has been discussed in the following sections.

**5.2 Results**

**5.2.1 Effect of heat-treatment on hardness**

Disc specimens ( $\varnothing$ 25mm dia x 18 mm height) of the different alloys were heat-treated by austenitizing them at 800, 850, 900, 950, 1000 and 1050°C for periods ranging from 2 to 10 hrs followed by air cooling and oil quenching. Preliminary studies suggested that oil quenching lead to the attainment of a more uniform distribution of dispersed carbides. Hence, the alloys were primarily investigated in the oil quenched condition. Accordingly, the data contained in this report pertains to this state only.

The heat-treating experiments were primarily designed to assess the feasibility of attaining the microstructures of interest in the experimental alloys and to characterize them (microstructures) initially on the basis of hardness.

Effect of time and temperature on the hardness is summarized in the tables 5.1 to 5.44 and in the figures 5.1 to 5.4 (the base curves). The data points contained in the figures represent the experimentally determined values whereas the actual plots correspond to the best fit data. A perusal of the tables and the figures revealed that :

1. The overall transformation behaviour of the alloys could be classified into five parts :

(a) A general increase in the hardness with time on heat-treating from 800°C (valid for all the alloys).

(b) A general increase in the hardness with time on heat-treating from 850°C (valid for B1 and B3).

(c) Hardness remaining independent of the soaking period on heat-treating from 850°C (valid for B2 and B4).

(d) Hardness remaining independent of the soaking period on heat-treating from 900°C and 950°C (valid for all the alloys).

(e) Hardness decreasing with time on heat-treating from 1000 and 1050°C (valid for all the alloys).

(f) The hardness (H), in general, decreasing with heat treating temperature in the order

$$H_{800} > H_{850} > H_{900} > H_{950} > H_{1000} > H_{1050}$$

2. On heat treating from 800°C, the hardness of the alloys was higher than the corresponding as-cast hardness. (Figs. 5.1 to 5.4).

3. However, heat-treating from a temperature between 850 to 1050°C lead to a decrease in the hardness compared with as-cast

state; the exception being when B1 was oil quenched from 850°C (Figs. 5.1-5.4).

Although the data summarized in the figures 5.1 to 5.4 provided useful information, it was still not sufficient enough to arrive at a comprehensive understanding of the transformation behaviour of the alloys. The additional information sought for was obtained by replotting the data contained in the tables 5.1 to 5.44 in the following manner:

- (i) Effect of soaking period on the hardness for all the four alloys as influenced by each of the six heat-treating temperatures (Figs. 5.5 a-f).
- (ii) Effect of temperature on the hardness as influenced by the soaking period for each alloy (Figs 5.6 a-d).
- (iii) Effect of temperature on the hardness for all the four alloys at each of the five soaking periods (Figs.5.7 a-e).

The following deductions would reveal how the figures 5.5-5.7, along with the figs. 5.1-5.4, provided further useful information on the (a) individual and (b) comparative behaviour of the alloy(s).

4. The comparative hardness vs time curves for the four alloys, as influenced by temperature, further confirmed the similarity between B1 and B3 and that between B2 and B4 upon heat treating from upto 850°C (Figs. 5.5 a and b).
5. On oil quenching from 900°C, variation in the hardness with time was similar for all the alloys. However, B1 attained a

- higher level of hardness compared with the rest thereby revealing its ability to sustain hardness to a higher level (Fig. 5.5 c).
6. On oil quenching from 950°C, the differences in the hardness levels of the four alloys evened out and for all practical purposes their overall behaviour might be regarded as similar (Fig. 5.5 d).
  7. On oil quenching from 1000°C, once again the alloy B1 had the maximum overall hardness followed by B2, B3 and B4, except that the overall hardness of B4 was now appreciably lower than that of B1, B2 and B3 (Fig. 5.5 e).
  8. On oil quenching from 1050°C the trend in the hardness variation was similar to that observed on heat-treating from 1000°C (Fig. 5.5 f).
  9. (a) The hardness vs temperature curves as influenced by time (Figs. 5.6 a-d) represented how effectively each alloy sustained its hardness on heat-treating.  
(b) These curves had a horizontal S-shape.  
(c) The slope of the curves altered around a threshold temperature or over a narrow range of temperature termed as the cross over point (COP).  
(d) To its left, the higher the soaking period the higher was the level of hardness. To its right the situation was just the reverse. This was valid for all the alloys.
  10. The profiles of the hardness vs temperature curves for the



alloys B1 and B3 were steep (Figs. 5.6 a and c) whereas those of the alloys B2 and B4 tended to be flat (less steep; Figs. 5.6 b,d). Further, the hardness band (variation in the hardness as influenced by the soaking period) at 1050°C was the maximum for the alloy B1 followed by B3, B4 and B2 in that order.

Based on these observations the similarity in the behaviour of the alloys B1 and B3 and that of the alloys B2 and B4 was reaffirmed. Thus B1 and B3 and B2 and B4 could be grouped together.

11. The COP of the alloys B1 and B3 was approximately in the range of 915°C to 950°C (Figs. 5.6 a,c) whereas that for B2 and B4 was around 860°C (Figs. 5.6 b,d).
12. The maximum decrease in the hardness in the four alloys, as influenced by the soaking period, occurred on heat treating from 1050°C (Figs. 5.6 a-d).
13. The comparative hardness vs temperature curves for the four alloys, as influenced by the soaking period (Figs. 5.7 a-e), further reinforced the deduction regarding the similarity in behaviour between B1 and B3 and that between B2 and B4. At the lowest soaking period (2 hrs), the curves tended to be flat (Fig. 5.7a). The profiles of the curves became steeper with an increase in the soaking period (Figs. 5.7b-d), the steepest profile being attained at the 10 hr soaking period (Fig. 5.7e).
14. The aforesaid curves (Fig. 5.7a-e) might also be hardness sustainability of the different interpreted as indicating the

relative alloys sustained its hardness on heat-treating.

15. An important inference from the data summarized in the figures 5.1-5.7 was that it was easily possible to deduce (a) the heat treating temperature(s) at which the hardness was independent of the soaking period or (b) the different time and temperature combinations to arrive at any desired hardness value in all the four alloys.

### 5.2.2 Microstructure

Effect of heat-treatment on the hardness was substantiated by carrying out micro-structural examination. Initially the experiments were confined to assessing qualitative changes in the microstructure and these are summarized in the Figs. 5.8-5.35. Subsequently, quantitative estimations involving massive and dispersed carbides were also carried out. This data has been dealt with separately.

Considering the former to start with, the micro-structure of the four alloys in the as-cast condition consisted of :

1. (a) P/B + M + Carbide (B1) Fig. 5.8  
(b) B/M + Carbide + RA (B2) Fig. 5.9  
(c) B/M + Carbide + RA (?) (B3) Fig. 5.10  
(d) B/M + Carbide + RA (B4) Fig. 5.11
2. On heat treating from 800°C, the as-cast microstructure transformed to martensite + carbide in all the four alloys (Figs. 5.12-5.15). Additionally, the massive carbides were rendered discontinuous. The 800°C heat-treatment also lead to the forma-

tion of dispersed carbides, whose presence could be detected in the micro-structure clearly corresponding to the 800°C, 10 hrs heat treatment (Figs. 5.12C, 5.13C, 5.14C, 5.15C).

3. On heat-treating from 850°C, austenite was retained clearly in the micro-structure at 2 hrs soaking period although its amount differed from alloy to alloys (Figs. 5.16a, 5.17a, 5.18a, 5.19a) on raising the soaking period to 10 hrs, the amount of retained austenite had decreased. The size and volume fraction of the dispersed carbides increased with an increase in the soaking period. Massive carbides were mostly discontinuous and their volume fraction was comparable with that observed on heat-treating from 800°C (Figs. 5.16e and f, 5.17c and d, 5.18c and d, 5.19c and d).
4. On heat-treating from 900°C, the micro-structure was predominantly austenitic and containing both the massive as well as the dispersed carbides. The uneven nature of the matrix suggested that it was perhaps not totally free of martensite. The size of the dispersed carbides increased whereas its volume fraction decreased with time. Further, the volume fraction of the massive carbides also decreased somewhat with time (Figs. 5.20-5.23).
5. On heat-treating from 950°C, a similar situation as above existed (Figs. 5.24-5.27). The presence of obtuse plates was not fully understood but might indicate the possible presence of some martensite (Figs. 5.25e, 5.26e, 5.27c and e).
6. On heat-treating from 1000°C, the matrix was plane and completely austenitic (Figs. 5.28-5.31). The volume fraction of both

the massive and the dispersed carbides markedly reduced with time. Low magnification observations revealed possible interlinking or bridging together amongst different massive carbide regions (Figs. 5.28d, 5.29b and f, 5.30d and f, 5.31d). In some of the alloys massive carbides showed cracking (Fig. 5.30e). At the end of the 10 hrs. soaking period, the micro-structure was practically free of dispersed carbides. A general "rounding off" of the massive carbides was also observed.

7. On heat-treating from 1050°C, a new phase formed which resembled the sigma phase when observed at lower magnifications (Figs. 5.32-5.35; 5.32d and f, 5.33d, 5.34d, 5.35b and d). Higher magnification observations revealed that it resembled plate-like carbides. The volume fraction of the new phase initially increased upto 4-6hrs soaking period and decreased thereafter (Figs. 5.32-5.35). Volume fraction of the massive carbides steeply reduced with the time. At the end of the 10hrs soaking period, the new phase was still present (Figs. 5.32h, 5.33f, 5.34f, 5.35f) along with the massive carbide (now present as particles or platelets), although its amount was very small (Figs. 5.32j, 5.33f, 5.34f and 5.35f).

### 5.2.3 Quantitative estimations

#### 5.2.3.1 Massive carbides

Effect of heat-treatment on the volume fraction of the massive carbides was investigated by a LEITZ image analyser. The data thus obtained has been summarized in the tables 5.45-5.48. Table 5.49 gives an overall summary of the data contained in the tables 5.45-

5.48.

A perusal of the above tables revealed that :

1. Volume fraction in the as-cast state ranged from 22-27%.
2. An increase in temperature lead to a decrease in the amount of massive carbides.
3. For heat-treating temperatures upto 950°C, an increase in the soaking period resulted in a gradual decrease in the amount of massive carbides (valid for all the alloys).
4. On raising the temperature to 1000°C, there was a steep fall in the volume fraction with soaking period (valid for all the alloys). A similar response was qualitatively observed on heat treating from 1050°C (Figs. 5.32-5.35). The 1050°C,10hrs heat-treatment was characterized by the presence of lowest volume fractions of the massive carbides (Figs. 5.32j, 5.33f, 5.34f and 5.35f).
5. Taking an overall view, volume fraction of massive carbides was approximately of a similar order. However in absolute terms, B1 exhibited a slightly larger volume fraction compared with B3. A similar situation existed for the alloys B2 and B4, the latter exhibiting a slightly smaller volume fraction.

#### 5.2.3.2 Dispersed carbides

Dispersed carbides were characterized on the basis of the following parameters:

- (a) Average particle size

- (b) Total no. of particles
- (c) Total volume fraction of particles
- (d) Percentage no. of particles in different classes
- (e) Percent area occupied by the particles in different classes

In the present study there were a total of six classes separated from one another by  $\approx 0.58$  micron.

The data thus generated is summarized in the tables 5.50-5.59 and in the histograms 5.36-5.78. Each histogram is a composite of ten histograms representing ten different fields of observation for a given heat-treatment. The aforesaid data was analysed in two ways (a) by assessing whether any general trends existed and (b) by laying down a detailed account of how the heat-treating temperature and time affected the parameters employed to characterize dispersed carbides.

Considering to start with the former, the following general trends were observed for all the alloys:

1. Dispersed carbides predominantly belonged to class I and II (size upto 1.16 microns; Figs. 5.36-5.78 and Tables 5.57-5.58).
2. Maximum no. of particles were present corresponding to the  $800^{\circ}\text{C}$ , 10 hrs. heat-treatment (Table 5.55).
3. On increasing the heat-treating temperature upto  $950^{\circ}\text{C}$ , the average particle diameter increased (Table 5.54) whereas the carbide volume fraction decreased or remained unaltered (Table 5.56).

4. For a given heat-treating temperature, the volume fraction increased with an increase in the soaking period in a majority of instances (Table 5.56). A similar trend was observed for the average particle size (Table 5.54).
5. By and large the number of particles decreased on increasing the temperature at a given soaking period or by increasing the soaking period at a given heat treating temperature (Table 5.55).
6. At a given soaking period, the no. of particles and the percent area occupied by the particles in classes I and II decreased with an increase in temperature. A similar trend was observed on increasing the soaking period at a given heat-treating temperature (Tables 5.57 and 5.58 and Figs. 5.36-5.78).
7. The changes described in (6) above were simultaneously supplimented by changes in the classes III to VI, the nature of the changes being just the opposite of those described in (6) above.
8. The histograms (Figs. 5.36-5.78) proved extremely helpful in understanding how the distribution of the particles varied with temperature and time at the ten different locations that were scanned to arrive at the quantitative data.

#### 5.2.4 Structural analysis by x-ray diffraction

The as-cast and heat-treated specimens of the different alloys were extensively examined by x-ray diffractometry to help identify (i) the matrix microstructure in marginal cases (heat-treating temperature 900-950°C), (ii) the nature of the carbides as influenced by

heat-treating parameters and , (iii) any other phase/constituent if formed, during heat-treatment. In the event of a doubt or difficulty in identifying a reflection, a question mark has been put. With the help of the diffraction data, it was possible to interpret the structures more or less fully as would be evident from the following deductions (Tables 5.60-5.100):

1. Martensite was present as the matrix constituent along with P/B in the as-cast condition in all the alloys (Table 5.100 a).
2. Ambiguity concerning the identity of the matrix microstructure was satisfactorily resolved in most instances particularly in the marginal cases i.e. the possible presence of martensite is indicated in alloys B1, B2 and B3 upto 900-10 hrs heat-treatment and in the B4 possible upto possible 950°C-4hrs. heat-treatment.
3. Retention of  $\gamma$  was confirmed in the as-cast condition in the alloys B2, B3 and B4.
4.  $M_3C$  was the predominant carbide in the as-cast condition. While B1 additionally contained some  $M_{23}C_6$  and B2 and B3 contained only traces of  $M_{23}C_6$ , B4 did not contain any  $M_{23}C_6$  type carbide.  $M_5C_2$  carbide was present in traces in B1, B2 & B3 and in slightly higher proportion in B4.
5. On heat-treating, the  $M_3C$  and  $M_{23}C_6$  were successively replaced by  $M_5C_2$  and  $M_7C_3$  type carbides. The temperature upto which  $M_3$  and  $M_{23}$  type carbides persisted on heat-treating differed from alloy to alloy (was a function of the total concentration of Mn and Mn/Cu ratio, the Cr content being identical in all the



alloys).

6.  $M_5C_2$  and  $M_7C_3$  were the predominant carbides corresponding to the 1000°C, 10hrs. and other higher temperature heat-treatments.
7. On increasing the soaking period from 4 to 10 hrs at 1050°C, the  $M_5C_2$  carbide was replaced by  $M_7C_3$  in the alloys B1 and B2. At 1050°C, 10 hrs h/t,  $M_7C_3$  was the predominant carbide.
8. Under identical conditions the situation was somewhat different in B3 and B4. Whereas in B3, both  $M_5$  and  $M_7$  type of carbides were present corresponding to the 1050°C, 10 hrs. h/t, B4 consisted mostly of  $M_5C_2$  and some  $M_7C_3$  type carbides.
9. The combined effect of alloy content and heat-treatment on the nature of carbide transformation revealed that (Table 5.100 b):
  - (a) Based on the disappearance of  $M_{23}$  carbide,  
B2(better) > B4 > B1, B3
  - (b) Based on the disappearance of  $M_3C$ ,  
B2 > B3, B4 > B1
  - (c) Based on the extent of  $M_7C_3$   
B3 > B1, B2 > B4
  - (d) Based on the stability of  $M_7C_3$  at 1050°C,  
B1, B2, B3 (comparable) > B4
  - (e) Based on the stability/extent of  $M_5C_2$ ,  
B4, B3 > B2 > B1
  - (f) Taking an overall view, a high Mn content and a high Mn/Cu ratio appeared helpful in accelerating the carbide transformation (i.e. in converting the carbides present in the as-

cast state into  $M_5$  and  $M_7$  type carbides).

#### 5.2.5 Effect of heat-treatment on the deformation behaviour

Compression testing was employed for assessing the deformation behaviour in the as-cast and in the heat-treated conditions. The usual stress-strain curves were obtained from which the compressive strength and percent strain were calculated (Tables 5.101-5.106). Representative stress-strain curves are shown in the Figs. 5.79-5.83. The effect of heat-treatment on the deformation behaviour is further summarized in the fig. 5.84 and in the tables 5.107-5.108. On the basis of the above it can be inferred that:

1. The compressive strengths (CS) were 1972, 2116, 2253 and 2352  $MN/m^2$  and percent strain values were 7.34, 11.79, 7.47 and 12.01% in the as-cast state for the alloys B1, B2, B3 and B4 respectively (Tables 5.105-5.106).
2. Heat-treating in general lead to an improvement in the properties.
3. On heat-treating from 900 and 950°C, raising the soaking period from 4 to 10 hrs had no effect on the mechanical properties (valid for all the alloys).
4. At 1000°C, raising the soaking period from 4 to 10 hrs. lead to an increase in CS and % deformation in all the alloys.
5. At 1050°C, raising the soaking period from 4 to 10 hrs lead to an improvement in CS which was maximum in B2 followed by B3, B4 and B1.

For the same heat-treating temperature and at 4 hrs soaking period, the % deformation was maximum in B2, comparable in B3 and B4 and minimum in B1. On raising the soaking period to 10 hrs, the increase in % deformation was maximum in B1 followed by B2 and B3 and negligible in B4. However, at the end of 10 hrs soaking period, the situation with regard to the level of percent deformation was similar to that observed at 4 hrs soaking period (Tables 5.105-5.106).

6. At 4 hrs soaking period, raising the temperature from 900 to 1000°C lead to an increase in the CS followed by either a tapering off or a small decrease in it on further raising the temperature to 1050°C (Fig.5.84).
7. At 4 hrs soaking period, the % deformation in B1, B3 and B4 was practically unaltered or showed a slight increasing trend (except in B1) on raising the soaking temperature from 900 to 950°C. It increased thereafter on increasing the temperature upto 1050°C. The extent of increase was maximum in B3 followed by B4 and B1.

In B2, however, % deformation increased steeply with an increase in the soaking temperature from 900 to 950°C, remained unaltered/slightly increased upto 1000°C and increased steeply again on raising the temperature upto 1050°C.

8. At 10 hrs soaking period, raising the temperature from 900 to 950°C had little effect on the CS in B1, B3 and B4. This was followed by a sharp increase upto 1000°C and levelling off thereafter on raising the temperature to 1050°C. In B2, however,

CS increased steeply and continuously as the temperature was raised from 900 to 1050°C.

9. At 10 hrs soaking period, the % deformation was unchanged on raising the temperature from 900 to 950°C and increased steeply thereafter on raising the temperature upto 1050°C. The steepest rise was observed in B2 (Fig. 5.84).

Representative stress-strain curves (Figs. 5.79-5.83) in the as-cast and in the heat-treated conditions revealed that:

- (a) A linear behaviour between stress and strain existed in the as-cast state. The compressive strength and % deformation were low. However, in B2 and B4 some flattening of the curves was also observed.
- (b) Raising the temperature (from 900 to 1050°C) and time (from 4 to 10 hrs) lead to strengthening (strain-hardening) simultaneously accompanied by flattening of the curves (implying an improvement in the % strain).
- (c) An important feature is that there was a similarity in the deformation behaviour between B1 and B3 and between B2 and B4 (valid both in the as-cast and in the heat-treated conditions).

#### **5.2.6. Corrosion behaviour**

##### **5.2.6.1. Weight loss studies**

Corrosion behaviour was studied by the weight loss method. Experiments were conducted on the four experimental alloys in the as-cast and in the heat-treated conditions. The effect of stress relieving (600°C, 1/2 hrs followed by air cooling) was also critically exa-

mined. Although three test solutions namely 5% NaCl, 10% NH<sub>4</sub>Cl and 10% (NH<sub>4</sub>)<sub>2</sub>SO<sub>4</sub> were employed, bulk of the investigations were confined to the corrosion studies in 5% NaCl solution. Two standard (Ni-resist) irons were also examined for their corrosion response in the above mentioned solutions mainly for the purpose of comparison. The results thus obtained are summarized in the tables 5.109-5.130 and in the figures 5.85-5.88. It emerged that:

1. The corrosion rates (CR) for B1 to B4 in 5% NaCl solution were in the range of 30-32 mdd and 22-27 mdd, when tested for 168 and 720 hrs respectively.
2. Heat-treatment improved the corrosion resistance over that observed in the as-cast state.
3. The CR in general decreased with an increase in the test duration (valid for all the alloys, in the as-cast and in the heat-treated conditions).
4. Stress relieving in general was not found to be beneficial barring (i) a few instances in general and (ii) the 1050°C, 10 hrs heat-treatment in particular.
5. For a given heat-treating temperature, raising the soaking period from 4 to 10 hrs lead to a decrease in CR except on heat-treating from 950°C, wherein an increase in the CR was observed (valid for all the alloys; Tables 5.109 to 5.112).
6. At 4 hrs soaking period and a test duration of 168 hrs, the CR decreased with an increase in the soaking temperature from 900

to 950°C (valid for all the alloys in SR and NSR conditions). Thereafter it (CR) decreased gradually or remained unaltered on raising the temperature to 1050°C (valid for B1 to B3 in both SR and NSR conditions). However, the nature of the decrease in CR in B4, beyond 950°C, was sharp but less steep than that observed between 900 and 950°C (Fig. 5.85).

The above observation was also true for 720 hrs test duration (Fig. 5.87).

7. At 10 hrs soaking period and for a test duration of 168 hrs, the CR increased sharply with an increase in temperature from 900 to 950°C followed by a sharp decrease upto 1050°C (valid for all the alloys in both SR and NSR condition; Fig. 5.86).

The adverse effect of the 950°C heat-treating temperature was considerably minimized in B1, B2 and B4 on raising the test duration to 720 hrs (Fig. 5.88).

8. The most useful micro-structures from the point of view of corrosion resistance corresponded to the following heat-treatment(s) (valid for all the alloys):

(a) 1050,10,0Q, (b) 1050,4,0Q and (c) 1000,10,0Q

Similarly, micro-structures corresponding to 900,4,0Q and 950,10,0Q heat-treatment were most detrimental from the corrosion point of view.

#### 5.2.6.2 Potentiostatic studies

These studies were carried out to a limited extent for the higher

Cu ( $\approx 3\%$ ) alloys B3 and B4 to assess their corrosion behaviour in 10%  $(\text{NH}_4)_2\text{SO}_4$  solution. The potentiostatic behaviour of two standard Ni-resist alloys was also studied in 10%  $(\text{NH}_4)_2\text{SO}_4$  for the purpose of comparison. The data thus generated has been summarized in the Figs. 5.89-5.96. It was observed that:

1. The experimental and the standard alloys in general exhibited active passive behaviour.
2. In the as-cast condition, B4 appeared better than B3 based on the values of  $I_{pp}$  and  $I_{cr}$  (Figs. 5.89 and 5.92).
3. The  $900^\circ\text{C}$ , 4 hrs, 0Q heat-treatment lead to an improvement in the corrosion behaviour of B3 and B4 compared with the as-cast state. The value of  $I_{pp}$  reduced considerably while  $I_{cr}$  was more or less unaltered. Once again B4 was found to be better than B3 (Figs. 5.90 and 5.93).
4. Stress relieving lead to a small increase in the  $I_{pp}$  and to a substantial decrease in the  $I_{cr}$  (Figs. 5.91 and 5.94).
5. Comparing the behaviour of the two standard alloys, KC was found to be better than KCl, since  $I_{pp}$  and  $I_{cr}$  were lower (Figs. 5.95 and 5.96).

#### 5.2.7. Scanning metallography of corroded specimen surfaces

This study was carried out on those selected specimens of the experimental alloys and of the two standard Ni-resist compositions on whom weight loss studies had been carried out in 5% NaCl solution. The study was undertaken to ascertain the nature of corrosion in the experimental alloys and to find out whether it was different

from that observed in the standard alloys. Representative micrographs, summarized in the Figs. 5.97-5.105, revealed that:

1. In the standard Ni-resist compositions, the attack tended to be localized (Figs. 5.97a,d,e, and f). The matrix in general showed moderate cracking (Figs. 5.97c and f). In one of the instances extensive cracking was also observed (Fig. 5.97b).
2. The experimental alloys did not undergo localized attack (Figs. 5.98-5.105).
3. Matrix cracking was also observed in the experimental alloys, its extent varying with alloy composition and heat-treatment (Figs. 5.98 - 5.105)
4. Extensive cracking within the matrix as in the standard alloys, was also observed (Figs. 5.98b, 5.101, 5.103d, 5.104c.)

#### 5.2.8. EPMA studies

They were carried out on the four experimental alloys to ascertain the distribution of Mn, Cr, Si, Cu, C and Fe into the matrix and the carbide phases as influenced by heat-treatment and or alloy content. Additionally, concentration profiles (line scans) for the aforesaid elements were also determined within the massive carbides and the bridge type new phase. This data alongwith the corresponding x-ray images was recorded for the 1050°c heat-treatment. A careful analysis revealed that the concentration profiles were nearly similar. To avoid repetition only the representative data has been included in this report and is summarized in the figs. 5.106 and 5.107 respectively.



A perusal of these figures revealed that the element distribution within the massive carbides and in the new phase was similar.

## CHAPTER-VI

### DISCUSSION OF THE RESULTS

#### 6.1 General

The present investigation was aimed at establishing (i) the transformation behaviour of the newly designed Fe-Mn-Cu white irons and (ii) an interrelation between the microstructure and the properties. Data on the electrochemical behaviour would be of major interest as it would help optimize the microstructure from the corrosion resistance point of view. It would be equally pertinent to ascertain whether the microstructure thus optimized is also optimum from the point of view of mechanical properties i.e. whether an interrelation existed between the electrochemical and the deformation behaviour of the alloys. The possible clues to all this would be provided by the microstructure.

The nature of the microstructure would be governed by alloying, heat-treatment, and the basis on which the alloys have been designed. The following sections are devoted to a critical appraisal of the microstructures attained, through intensive structural examination (Chapter V). The volume fraction, size, shape and distribution of the second phase have been determined by quantitative metallography. Microstructures have been further characterized on the basis of their electrochemical response and the deformation behaviour so as to arrive at a comprehensive interrelation between structure and properties.

#### 6.2 Structural considerations

The general microstructure of white irons consists of pearlite + carbide. In the presence of Mn, Cr, and Cu, the structural changes

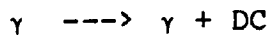
that may occur would be governed by the (i) partitioning of the elements into different microconstituents namely  $\gamma$  and carbide, (ii) effect of heat-treating parameters on the partitioning behaviour and the alterations in the high temperature microstructure there off, (iii) effect of the elements present in austenite on its transformation behaviour and (iv) possible retention of high temperature microstructure at room temperature.

The alloy design (Section 3.3) has been based on the (i) EPMA studies on Fe-Mn-Cr-Cu alloys containing Mn in the range of 3 to 6%, Cr 6 and 9% and Cu 1 and 1.5%, investigated in the aircooled condition by Singh (66), (ii) effect of Mn content on the transformation behaviour of austenite in general (74,75) (iii) amount of Mn required to render an Fe 0.8C austenite air hardening (74,76) and (iv) minimum Cr content required to render a given composition white (53,77). Assuming the trend of element distribution in the experimental alloys to be similar to the one observed in the afore-said study (66) namely that (a) nearly 45% of the Mn added partitions to  $\gamma$  and the balance to the carbide phase, (b) bulk of the Cr partitions to the carbide phase (c) bulk of the Cu partitions to  $\gamma$ , the likely structural changes that may occur on heat-treating may be summarized as follows.

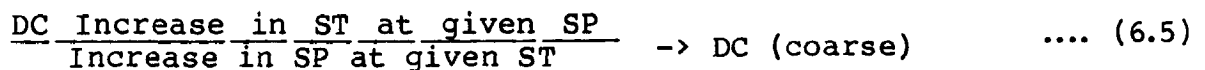
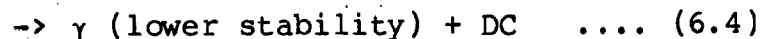
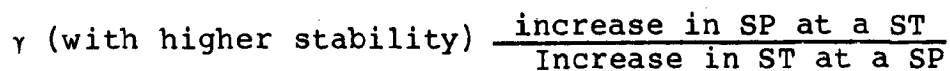
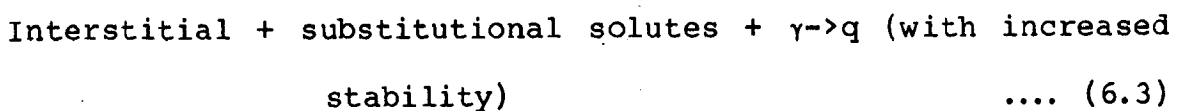
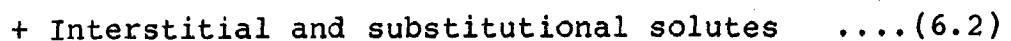
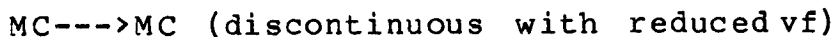
#### 6.2.1 Changes in the high temperature microstructure

They would comprise of the following (i) reduction in the volume fraction of the massive carbides due to the presence of Si and Cu (attributed to their graphitizing tendency) (ii) availability of an additional amount of interstitial and substitutional elements, as a

consequence of the above change, dissolving in the  $\gamma$  already present thereby leading to an increase in its stability (iii) massive carbides being rendered discontinuous due to (i) and, (iv) possible precipitation of carbides directly from  $\gamma$  on prolonged soaking, (78,79) represented by the reaction



As the carbides are formed by a diffusion controlled transformation, the temperature and time of soaking would be the controlling parameters. Their (carbides) nature would be different from  $M_3C$  since their formation would require possible participation of a relatively larger amount of substitutional elements. Evidently, a higher activation (temperature) is required for such a change to occur. The likely structural changes that may occur can thus be summarized with the help of the following equations:



### 6.2.2 Changes during cooling to room temperature

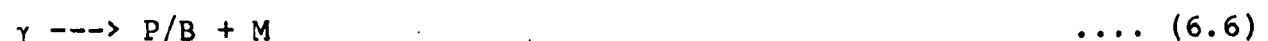
They will be governed by the cooling rate and the alloy content and would primarily be confined to  $\gamma$ . Some changes may also occur in the DC that have formed. The possible changes in  $\gamma$  would depend

upon the temperature and time as they govern the relative stability of  $\gamma$  in accordance with the equations (6.1), (6.3) and (6.4). If aircooling is done,  $\gamma$  may reject excess solute in the form of dispersed carbides and would subsequently transform to either B/M and or remain untransformed. Since the minimum Mn content in the alloys (6%) ensures that martensite can form on air cooling from 800 and 850°C and  $\gamma$  is partly retained on aircooling from 900°C(66), it is evident that the transformation product of  $\gamma$ , would be predominantly martensite on quenching from upto 850°C and predominantly  $\gamma$  on quenching from  $\sim$ 900°C. The relative proportions of  $\gamma$ /M will be governed by the extent to which the reactions (6.1) and (6.4) proceed.

Carbide precipitation during cooling mainly occurs because of a decrease in the solid solubility of 'C' in the  $\gamma$  iron with temperature. If  $\gamma$  is supersaturated after heat-treatment, it would reject out excess solute as carbides. However, if the  $\gamma$  is not supersaturated and is in a state wherein the solutes are fully dissolved (requiring a higher heat-treating temperature), it will be retained as such on cooling. Since oil quenching has been employed, the possibility of DC being rejected from  $\gamma$  during cooling is rather small.

Taking an overall view, the possible structural changes on cooling can be summarized with the help of the following equations:

Slow cooling (as during casting)



(relative proportion of P/B & M depending on alloy content)

Carbide ----> Unchanged ..... (6.7)

Retention of  $\gamma$  ----> [depends upon  $\gamma$  stabilizing tendency (Mn+Cu)]  
..... (6.8)

Final likely structure : P/B + M + MC + RA (?)

Heat-treated condition

(a) Lower temperatures 800 and 850°C

$\gamma$  ---->  $\gamma^*$  + DC ..... (6.4)

$\gamma^*$  ----> M ..... (6.9)

(extent of M depends upon soaking period i.e. less at lower SP and more at higher SP)

$\gamma^*$  ---->  $\gamma$  (depending upon alloy content) ..... (6.10)

Carbide ---->  $M_3C$  + other variants ..... (6.11)

DC ----> DC (Coarse) ..... (6.5)

Final likely structure : M +  $\gamma$  + MC + DC

(b) Temperatures 900 & 950°C

$\gamma^*$  ---->  $\gamma$  (most probable) ..... (6.12)

$\gamma^*$  ----> M (possible to a minor extent on h/t from 900°C)  
..... (6.13)

DC ----> DC (coarse) ..... (6.5)

MC ---->  $M_3C$  + other variants (vf reduced) ..... (6.11)

Likely final structure :  $\gamma$  + DC + MC + trace M (?)

(c) 1000 and 1050°C

$\gamma^*$  ---->  $\gamma$  (matrix completely  $\gamma$ ) ..... (6.14)

DC ----> DC (coarse) and possible dissolution at high SP/ST  
..... (6.5)

MC ---->  $M_3C$  + other variants (Vf low, possible rounding off  
may be observed). .... (6.11)

Final likely structure :  $\gamma$  + MC + some DC or  $\gamma$  + MC

### **6.2.3 Strengthening response of different transformations**

Before analysing the structure-property relations it would be appropriate to consider the strengthening response of the different transformations.

The austenite to martensite transformation leads to hardening and to simultaneous embrittlement. The attainment of austenitic matrices would lead to an improvement in the ease of deformation. In such instances, the stacking fault energy (SFE) of the matrix would determine the strength-ductility interrelation as it (SFE) controls the extent of work-hardening. It is relevant to record that Mn-austenites have a low SFE and hence exhibit a high rate of work-hardening (80).

Massive carbides have a high hardness and the strengthening response would be directly related to its volume fraction. Its morphology and compatibility with the matrix are equally important. The latter would also be governed by the crystal structure.

The effect of dispersed carbides would be governed by the volume fraction, compatibility with the matrix, size, shape and distribution (81,82).

### **6.3 Interrelation between microstructure and hardness**

The general microstructural changes that may occur in the experimental alloys, highlighted in the earlier section, facilitate interpretation of the structural changes that would occur in B1, B2, B3 and B4. As hardness is governed by the microstructure, the two have been discussed together.

### 6.3.1 As-cast state

The microstructure of the alloys in the as-cast condition namely, P/B + M + MC, B/M + RA + MC, B/M + RA (?) + MC and B/M + RA + MC respectively (Figs. 5.8-5.11), is in accordance with the analysis outlined in the section 6.2 (equations 6.6 to 6.8). In the as-cast condition Mn alone is controlling the matrix microstructure because Cu separates out on slow cooling and has a negligible effect on the transformation behaviour (83,84). This can be attributed to its solubility in  $\gamma$  and  $\alpha$  irons and to a further decrease in its solid solubility with temperature in ferrite (85,86). Accordingly, the matrix microstructures in the alloys B1 and B3 are not likely to be fully martensitic (Figs. 5.8, 5.10). Although this is clearly rejected in the microstructure of B1 (Figs. 5.8a,b), the same is not clearly evident from the microstructure of B3 (Fig. 5.10).

The matrix microstructures of the higher Mn alloys B2 and B4 would have an appreciably higher proportion of martensite (Figs. 5.9, 5.11) with some austenite retention a distinct possibility at least in B4 (Fig. 5.11). Accordingly, the hardness values of B1 and B3 and that of B2 and B4 are expected to be nearly similar. Furthermore, B4 is likely to be less harder than B2 due to possible retention of  $\gamma$ . However B3 is harder than B1 and B4 is harder than B2. This may be attributed to a higher P content in B3 and B4 (Table 4.2).

### 6.3.2 Heat-treated condition

As already stated, the alloys particularly those with lower Mn content, are so designed that they readily transform to martensite



and that the retention of  $\gamma$  is not ruled out on aircooling from 900°C. In the present context, since oil quenching alone has been employed, the  $\gamma$  retaining tendency is still further enhanced (retention will be possible even on heat-treating from temperatures lower than 900°C). This tendency would be further enhanced in the higher Mn/Cu alloys. When this is considered alongwith the general structural changes that have been outlined in section 6.2, it becomes easy to rationalize how micro-structure would vary on heat-treating.

#### 6.3.2.1. Alloy B1

The changes can be easily explained based on equations (6.1 to 6.14).

(a) 800°C : High hardness (Fig. 5.1) at 2 hrs soaking period is due to the formation of a martensitic matrix (Fig. 5.12. a and b). Hardness increased marginally with time (Fig. 5.1) only at 10 hrs soaking period due to the formation of some dispersed carbide (DC) (Fig.5.12 c and d).

(b) 850°C : The lower hardness at 2 hrs soaking period (Fig. 5.1) is due to the retention of  $\gamma$  in accordance with the equations 6.3 and 6.10 (Fig. 5.16 a and b). Increase in the hardness with soaking period (Fig. 5.1) is due to the formation of martensite and a higher volume fraction of dispersed carbide (Fig. 5.16 c,d,e and f) in accordance with equations 6.4 and 6.9. The lower overall hardness level at 850°C in comparison to that observed at 800°C is due to an increase in the  $\gamma$  stabilizing tendency and hence to the formation of a relatively smaller volume fraction of martensite.

An alternative interpretation of the hardness data on heat-treating from 850°C (shown in dotted line; Fig 5.1) is that the initial increase in hardness upto 4 hrs is due to the formation of some martensite. The hardness arrest upto 8 hrs, indicating practically no change in the microstructure, can be explained by stating that an increase in the martensite forming tendency is counterbalanced by an increase in the  $\gamma$  stabilizing tendency in accordance with the equations 6.3 and 6.10. However, on soaking for 10 hrs a higher activation not only results in a larger volume fraction of dispersed carbides but also improves the martensite forming tendency leading to an increase in hardness by about 50 VPN (Fig. 5.1). The decrease in the volume fraction of massive carbides with soaking period, which is small (Table 5.45) due to the temperature being relatively lower, is not expected to have a major effect on the overall hardness.

(c) 900°C: Low hardness (Fig. 5.1.) at 2/4 hrs soaking period is due to the matrix being predominantly austenitic (equation 6.12, Fig. 5.20 a & b). The unevenness and the dark etching characteristic of the matrix (Fig. 5.20 b) may indicate the possible presence of some martensite [equation 6.13]. Increasing the soaking period has practically no effect on the hardness because the microstructure is practically unaltered except for a limited coarsening of the dispersed carbides and some reduction in the volume fraction of the massive carbides (Fig. 5.20 c, d & e; Tables 5.45 and 5.54-5.56). The lower overall hardness at 900°C in comparison to that at 850°C is largely due to austenite replacing most of the martensite.

(d) 950°C: The basic structural changes at 950°C are similar to those at 900°C except that the coarsening of dispersed carbides is enhanced and reduction in the volume fraction of massive carbide is larger (Fig. 5.24 a-d; Tables 5.45 and 5.54-5.56). These changes, which promote the retention of relatively larger volume fraction of stable austenite, not only result in a lower overall hardness compared with that observed at 900°C but are also responsible for a slight decrease in hardness with soaking period (Fig.5.1). Volume fraction of the massive carbides has decreased to a level so as to contribute to the decreasing hardness trend.

(e) 1000°C: The low hardness at 2 hrs soaking is due to (i) a predominantly austenitic matrix rendered even more stable and (ii) a further decrease in the amount of massive and dispersed carbides (Fig. 5.28 a and b; Table 5.45). The decrease in hardness with soaking period (Fig. 5.1) is due to a marked decrease in volume fraction of the massive carbides and to a near complete dissolution of the dispersed carbides (Figs. 5.28 c and d; Table 5.45).

(f) 1050°C: Structural changes are similar to those observed at 1000°C but are still further accelerated due to the temperature being higher. This leads to a decrease in hardness with the soaking period. This decrease would have been steeper but for the formation of a new hard phase having a plate like appearance. Its volume fraction initially increased with soaking period (upto 4/6 hrs) and decreased thereafter on raising the soaking period to 10 hrs (Fig. 5.32 a-f). At the end of the 10 hrs soaking period this phase is still present alongwith massive carbides whose volume fraction is very small and which have attained a globular morphology (Figs.

5.32 g-j). The lowest overall hardness at 1050°C is due to the presence of a predominantly high stability austenitic matrix containing very small amounts of massive carbide and the new phase (NP).

#### 6.3.2.2 Alloys B2, B3 & B4

The structural changes occurring in B1 and the corresponding changes in hardness have been satisfactorily explained. Transformation in B2, B3 and B4 are also expected to proceed on similar lines. It would be reasonable to suggest that the changes taking place in these alloys may be classified as common with and different from those occurring in B1. The former shall comprise of transformations in which the final micro-structure is predominantly austenitic i.e. the structural changes occurring on heat treating from temperatures >900 C. Under these conditions, B2, B3 and B4 may differ from B1 in terms of the (a) volume fractions of massive carbides (Table 5.49), dispersed carbides (Table 5.56), and the new phase (Figs 5.32-5.35), (b) coarsening behaviour of dispersed carbides (Tables 5.54 & 5.55) and (c) the relative stability of austenite. All these parameters are a function of the alloy content and the heat-treating schedule.

The aforesaid differences in the microstructure would not only lead to differences in the overall hardness between B1 and B2, B3, B4 but also amongst B2, B3 and B4. The micro-structure and hardness on heat treating B2 (Figs. 5.2, 5.21, 5.25, 5.29, & 5.33), B3 (Figs. 5.3, 5.22, 5.26, 5.30, 5.34) and B4 (Figs. 5.4, 5.23, 5.27, 5.31, 5.35) from temperatures ranging from 900-1050°C are consis-

tent with the above reasoning.

B2, B3 and B4 would differ from B1 based on the transformations occurring at 800 and 850°C. At 800°C, the transformation behaviour of B3 will be similar to B1 in view of their similar Mn contents. The effect of a higher Cu content in B3, not experienced at 800°C due to the temperature being lower, is duly manifested at 850°C. In view of this the overall level of hardness and the rate of increase in hardness in B3 is lower than that in B1. This can be attributed to a higher  $\gamma$  stabilizing tendency which does not permit the reaction represented by equation 6.9 to go to completion (i.e. reactions corresponding to equations 6.9 and 6.10 occur only partly). The micro-structural and hardness changes in B3 at 800°C (Figs. 5.3 and 5.14 a-d) and 850°C (Figs. 5.3 and 5.18 a-d) are consistent with this reasoning.

In view of a higher Mn content (a higher  $\gamma$  stabilizing tendency), the nature of micro-structural and hardness changes in B2 at 800°C (Figs. 5.2 & 5.13 a-d) would be similar to those in B1 and at 850°C. A similar situation would exist in B4 on heat treating from 800°C (Figs. 5.4 and 5.15 a-d). On heat treating from 850°C, however, the aforesaid changes in B2 (Figs. 5.2 & 5.17 a-d) and in B4 (Figs. 5.4 & 5.19 a-d) would be similar to those generally observed on heat-treating from 900°C. This is attributed to an increased  $\gamma$  stabilizing tendency due to higher Mn/Cu contents and would lead to a decreasing trend in hardness with soaking period. The overall level of hardness in B4 would be lower than that in B2 (Figs. 5.2 & 5.4) in view of its higher  $\gamma$ -stabilizing tendency attributed to a higher Cu content.

### 6.3.2.3 Comparative hardness vs time data

The analysis put forth in the preceding sections very clearly explains the micro-structural and hardness changes in the experimental alloys. It would now be appropriate to compare the hardness levels in different alloys as influenced by time at different heat-treating temperatures. The derived curves (Figs. 5.5 a-f), drawn on the basis of the data already summarized in the base curves (Figs. 5.1-5.4), bring out this information unambiguously and at a glance. These curves can be interpreted on a similar basis as the base curves and reveal that:

(i) At 800°C the behaviour of B1 and B3 and that of the higher Mn alloys B2 and B4 are similar. As already explained, the transformation behaviour is controlled by the Mn content alone. The former combination attains a higher overall level of hardness (Fig. 5.5) due to a lower  $\gamma$  stabilizing tendency attributable to a lower Mn content (6%). Thus, the reaction corresponding to equation 6.9 goes to completion.

(ii) On heat-treating from 850°C the Cu effect comes into play. B1 and B3 show an increasing trend in hardness with soaking period (equations 6.3, 6.4 and 6.9), the overall level in B1 being higher than in B3 due to a lower  $\gamma$  stabilizing tendency. The hardness in B2 and B4 exhibits a decreasing trend with soaking period, because the reaction corresponding to equation 6.9 does not go to completion leading to  $\gamma$  retention. The overall level of hardness is higher in the former group of alloys (B1 and B3) for reasons already stated. Thus, from the overall hardness point of view

B1>B3>B2>B4 [hardness inversely proportional to  $\gamma$  stabilizing tendency which is directly proportional to the Mn+Cu contents] (Fig. 5.5b).

(iii) At 900°C, the bunching together of the H vs t curves is due to a similarity in the microstructure (Fig. 5.5 c). All the same, observation at (ii) regarding the relative hardness levels, holds as it is intrinsically related with the alloy content.

(iv) The situation at 950°C is nearly identical with that observed at 900°C due to a similarity in the micro-structure. However, the slight decrease in hardness with the soaking period is because the transformations inducing a reduction in the volume fraction of massive carbides and a coarsening of dispersed carbides are accelerated. A relatively higher (i) heat treating temperature and (ii) Mn as well as Cu contents are also contributing to the decreasing hardness trend (Figs. 5.5d).

(v) 1000°C : Reasons for a decrease in the hardness with soaking period have already been explained. The hardness levels associated with the alloys are (a) directly related to the vf of MC and (b) inversely proportional to the overall alloy content (Fig. 5.5e).

(vi) 1050°C : A situation similar to that at 1000°C exists, and the comparative hardness data can be explained essentially on a similar basis as in (v) (Fig. 5.5f).

### 6.3.3 Correlation between hardness and time

In order to arrive at a correlation between hardness and time, the data contained in the tables 5.1-5.24 was analysed with the help of

a computer programme. Constants for the first, second and third order variations were calculated using the least square technique (72,73) and are reported at the bottom of each of the tables 5.1-5.24. Although the variance decreased as the order of equations increased, plotting of the data revealed that the variation in hardness with time and its subsequent interpretation based on micro-structural changes can be best explained on the basis of a first order equation. The theoretical values of hardness calculated on this basis (also indicated at the bottom of each of the tables) were found to be in excellent agreement with the experimental values. Thus, the variation in hardness with time at each of the heat-treating temperatures can be most appropriately represented by an equation:

$$H = C_1 + C_2t \quad \dots (6.15)$$

The values of  $C_1$  and  $C_2$  for each of the alloys at different heat treating temperatures are indicated in the relevant tables (i.e. tables 5.1-5.24).

#### **6.3.4 Effect of temperature on hardness**

##### **6.3.4.1 Nature of variation**

In order to arrive at the aforesaid correlation, the hardness vs temperature data for each of the alloys (summarized in the tables 5.25-5.44) was analysed and the constants for first to 4th order variations were calculated (indicated at the bottom of the tables 5.25-5.44). In order to arrive at the optimal mode of variation, all the possibilities were considered. It emerged that it was not reasonable to assume the variation between hardness and temperature



to be a linear one especially when changes in the microstructure are being brought about by three different transformations. A fourth degree variation can similarly be ruled out. Of the three available options a third order variation appeared to be the most appropriate based on an analysis of the Figs. 5.1-5.4, which reveals a hardness plateau at 900 and 950°C, a decrease in hardness beyond 950°C and an increase in hardness below 900°C. A variation of this type also appeared to be consistent with the microstructural changes. Hence, the variation in hardness with temperature at each of the soaking periods can be most appropriately represented by a third order polynomial:

$$H = C_1 + C_2T + C_3T^2 + C_4T^3 \quad \dots (6.16)$$

The values of the constants  $C_1, C_2, C_3$  and  $C_4$  have been indicated in the tables 5.25-5.44. This analysis forms the basis of arriving at the hardness vs temperature curves (Figs. 5.6 and 5.7) which are in the form of a horizontal 'S'-shape.

#### 6.3.4.2 Effect of temperature on hardness and microstructure

The data summarized in the Figs. 5.6 and 5.7 can essentially be interpreted on a basis similar to the one employed for interpreting the data contained in the Figs. 5.1-5.4. However, in the present context, it is the shape of the hardness vs temperature curves that needs to be carefully analysed. As already stated (section 6.3.4.1), the hardness vs temperature plots should have an S-shaped configuration because the hardness, while decreasing, shows a plateau. It is nearly constant over a range of temperature 'X'. At temperatures lower than the aforesaid range (X), the hardness

increases because of an increase in the tendency to form martensite which is directly proportional to the soaking period and inversely related to Mn/Cu contents (sections 6.2, 6.3.1 and 6.3.2). At temperatures higher than the temperature range (x), the hardness decreases because of (i) an increase in the  $\gamma$  stability and (ii) the microstructures being predominantly austenitic (due to a reduction in the  $v_f$  of MC and DC). The two tendencies are directly proportional to the soaking period and the Mn/Cu contents (section 6.2). This analysis satisfactorily explains the general features of the hardness vs temperature curve (Figs. 5.6 a-d).

The higher Mn alloys B2 and B4 exhibit a flatter profile in comparison to the lower Mn alloys B1 and B3 due to a higher  $\gamma$  stabilizing tendency leading to an early (at relatively lower temperatures) formation of the  $\gamma$ -based microstructures (Figs. 5.6 b and d). The steeper profiles associated with B1 and B3, signifying a marked decrease in hardness with temperature in a unit of time, can be similarly explained based on a reduced  $\gamma$ -stabilizing tendency (Figs. 5.6 a,c). On the basis of a similar reasoning it is easy to deduce that the COP signifying the plateau region of the hardness vs temperature curves would set in at early (i.e. at lower temperatures) in B2 and B4 (Figs. 5.6 b,d) and later (at higher temperatures) in the alloys B1 and B3 (Fig. 5.6 a,c). The maximum decrease in hardness (hardness band) in the four alloys has occurred at 1050°C firstly because this is the highest heat-treating temperature employed and secondly because at this temperature the different structural changes leading to a decrease in hardness occur the fastest. At 1050°C, the higher the soaking period the smaller would

be the volume fraction of massive carbides and larger the volume fraction of  $\gamma$  i.e. lower will be the hardness (Figs. 5.6 a-d). This explains the existence of the hardness band (signifying hardness variation at 1050°C with soaking period) in each alloy. All other factors being identical, the width of the band would be mainly related to the  $\gamma$  stabilizing tendency (i.e. the soaking period and Mn+Cu content) and to the volume fraction of the massive carbides. Ideally the band width would be a maximum for B1 i.e. for the composition with the least alloy content to be followed by B2, B3 and B4. However, experimentally the order is found to be B1>B3>B4>B2. The deviation from the ideal behaviour may be attributed to the differing volume fractions of the new phase (NP).

#### **6.3.4.3 Comparative hardness vs temperature data**

The comparative curves indicating the effect of temperature on hardness (Figs. 5.7 a-f), essentially derived from the data summarized in the Figs. 5.6 a-d, indicate the effect of soaking period and can essentially be interpreted on a basis similar to the one employed for interpreting the Figs. 5.6 a-d. The usefulness of the figures 5.7 a-f is that they give the comparative data for the experimental alloys at a glance.

#### **6.3.5 Effect of temperature and time on the morphology and volume fraction of massive carbides**

Although the effect of massive carbides in controlling the overall hardness has been discussed at length in section 6.3.4.2, it would be appropriate to comment upon the effect of heat-treating parameters on their morphology and volume fraction. Massive carbides present in the as-cast structure (Figs. 5.8-5.11) are partly disco-

ntinuous and have been so rendered due to the graphitizing action of Cu (section 6.2). The same graphitizing action is also responsible for a reduction in their volume fraction on heat-treating. It will increase with an increase in the Cu content and the heat-treating temperature and time. Based on physical metallurgical considerations associated with malleabilizing (87), it is expected that the tendency to render the carbides discontinuous and their volume fraction to decrease would be pronounced only at temperature around 950°C. Another reason why volume fraction of massive carbides may not significantly decrease uptill 950°C is that other transformations (highlighted earlier) take precedence over those presently under consideration. This is because they require lesser activation. An equally important aspect needing consideration is that unlike in malleable irons the carbide phase in the experimental alloys has been rendered stable by Cr additions (section 3.3). Therefore as the heat-treating temperature and time are increased the massive carbides instead of decomposing into graphite will try to acquire a configuration/morphology which would help minimize the overall energy of the micro-structure. Such a morphology would either be near spherical or hexagonal. The precise nature would be governed by the crystal structures of the massive carbides as influenced by h/t temperature and time. This analysis explains the general rounding off observed in massive carbides on heat-treating from higher temperatures (Figs. 5.28-5.35).

Returning now to the decrease in the  $v_f$  of massive carbides, the Cr containing carbides are further rendered stable since nearly 50 to 55% of the Mn added also partitions to it (66). Therefore,

taking an overall view, the decrease in the volume fraction of massive carbides will be faster only at temperatures around 950°C or higher (i.e.  $\approx 1000^\circ\text{C}$ ) as has been observed in the present investigation. This process (involving a reduction of massive carbide) will be further aided by the presence of a fully austenitic matrix and this occurs only at temperatures around 950°C. This clearly explains why the volume fraction of massive carbides decreases rapidly with soaking period only at temperature  $> 950^\circ\text{C}$  i.e. at 1000°C (Figs. 5.24-5.31, and tables 5.45-5.49). The least volume fraction of massive carbides will accordingly be observed at 1050°C and that too at the highest soaking period since the austenitic matrix has maximum stability under these conditions (Table 5.49).

The volume fractions of massive carbides in the different alloys are directly related with the  $\gamma$  stabilizing tendency which is proportional to the Mn/Mn + Cu content as well as to the graphitizing tendency (a function of Cu content). The reasons for the least volume fraction of the massive carbide in B3 at 1050°C, 10 hr heat-treatment can be traced to the least Mn/Cu ratio and hence to the maximum graphitizing tendency in this alloy (Table 5.49).

#### **6.3.6 Effect of time and temperature on dispersed carbides**

Sections 6.2 and 6.2.2 highlight the mechanism of formation of dispersed carbides from austenite. The results summarized in the tables 5.50-5.59 and in the figures 5.36-5.78 prove helpful in characterizing them fully. As can be seen, particles constituting the dispersed carbides belong to classes I and II because they exclusively fall into these two classes at the formation stage.

This is valid for all the alloys. On heat-treating, their distribution is altered in a manner consistent with the attributes of a nucleation and growth type of transformation. Simultaneously, coarsening would also set in. This would involve a reduction in the number of particles in the first two classes and a simultaneous increase in the number of particles in the class III - VI. Additionally the mean diameter would also increase. This is what has been observed in a majority of the instances (Tables 5.54-5.58). The comparative data given in the table 5.59 reveals that it would be difficult to arrive at a general interrelation correlating the effect of alloy content and h/t schedule on the extent of coarsening. This parameter is, however, of interest as it would govern the overall properties of the alloys.

Studying the coarsening behaviour based on the equation representing Ostwald ripening (89) namely :

$$r_1^3 - r_0^3 = K (t_1 - t_0) \quad \dots (6.17)$$

Where  $r_1$  = Particle radius at time  $t_1$

$r_0$  = Particle radius at time  $t_0$

appeared difficult due to insufficient number of data points (data corresponding to only 3-4 soaking periods at a given heat-treating temperature are available). For ascertaining the validity of the above equation at least 10-12 data points are required. This difficulty was resolved by defining a new parameter called the DISTRIBUTION FACTOR (DF). The basis of its evolution and its mathematical

expression have been discussed latter (section 6.5.4) Distribution factors for the various alloys, as a function of heat treating schedules, are given below

Distribution factors for different alloys \*.

h/t	B1	B2	B3	B4
800°C, 10h	0.576	0.536	0.616	0.582
850°C, 2h	0.475	0.516	0.596	0.736
850°C, 6h	0.425	-	-	-
850°C, 10h	0.413	0.443	0.537	0.534
900°C, 2h	0.339	0.583	0.482	0.479
900°C, 4h	-	0.483	0.388	0.519
900°C, 6h	0.346	0.417	0.409	-
900°C, 10h	0.347	0.419	0.442	0.410
950°C, 2h	0.367	0.418	0.482	0.483
950°C, 4h	0.402	0.399	0.382	0.461
950°C, 6h	0.329	0.416	0.374	0.440
950°C, 10h	0.285	0.447	0.357	0.359

\* Calculated on the basis of particle distribution at each of ten fields of observation for a given heat-treatment and then averaged.

Using this parameter as the basis, the coarsening behaviour can be studied based on a parameter termed as the coarsening index (CI) which is given by

$$CI = \frac{\text{DF for a given heat treatment}}{\text{DF for the h/t with particles in class I\&II mainly}} \dots (6.18)$$

The smaller the CI the greater is the coarsening tendency. Based on this parameter the coarsening behaviour of the alloys can be compared and is summarized below:

## Relative coarsening behaviour of the alloys

### Coarsening index

h/t	B1	B2	B3	B4	Remarks
800°C, 10h	1.000	-	-	-	gradation based on increasing order of coarsening.
850°C, 2h	0.825	1.000	1.000	-	
850°C, 6h	0.738	-	-	-	
850°C, 10h	0.717	0.858	0.901	1.000	B3>B2>B1
900°C, 2h	0.588	1.130	0.809	0.899	B2>B4>B3>B1
900°C, 4h	-	0.936	0.651	0.972	B4>B2>B3
900°C, 6h	0.601	0.809	0.686	-	B2>B3>B1
900°C, 10h	0.603	0.812	0.740	0.769	B2>B4>B3>B1
950°C, 2h	0.638	0.811	0.808	0.903	B4>B2>B3>B1
950°C, 4h	0.698	0.773	0.640	0.863	B4>B2>B1>B3
950°C, 6h	0.571	0.807	0.627	0.825	B4>B2>B3>B1
950°C, 10h	0.495	0.867	0.599	0.672	B2>B4>B3>B1

From the table it is inferred that the higher Mn alloys undergo lesser coarsening i.e. an increase in the Mn content reduces coarsening. This appears logical since an increase in the Mn content retards the transformation of austenite (80). No comment is being made on the possible effect of Cu on the extent of coarsening because the both the higher Cu alloys B3 and B4 have a higher P content than in B1 and B2 (Table 4.2) thereby making any comparison untenable.

The data on the relative coarsening behaviour of the alloys is of considerable importance in understanding the deformation and the corrosion behaviour of the alloys. This aspect has been elaborated upon later in the sections 6.4 and 6.5.1).

A critical analysis reveals that distribution factor for the four alloys can be mathematically represented with the help of the



following equations:

$$B1: DF = 0.0097 e^{\frac{3358}{T}} - (0.058 - 5.8 \times 10^{-5})t \quad \dots (6.19)$$

$$B2: DF = 0.0357 e^{\frac{2378}{T}} - (0.103 - 10.6 \times 10^{-5}T)t \quad \dots (6.20)$$

$$B3: DF = 0.0306 e^{\frac{2503}{T}} - (0.008 - 0.03 \times 10^{-5}T)t \quad \dots (6.21)$$

$$B4: DF = 0.0156 e^{\frac{3279}{T}} - (0.147 - 14.3 \times 10^{-5}T)t \quad \dots (6.22)$$

The basis of arriving at these equations is the same as that on which the mathematical modelling of the transformation behaviour of the alloys was carried out. This has been elaborated upon in the next section. The theoretically calculated values of the DF agree well with the experimentally determined values i.e. in a majority of the instances the maximum difference between the experimental and the theoretical values is 10%.

Dispersed carbides in all the alloys dissolved at 1000°C on soaking for ~ 4 hrs (Figs. 5.28-5.31). The data on the relative stability of different carbides helps in deducing that the dispersed carbides are  $M_{23}C_6$  type (90).

### 6.3.7 Mathematical modelling of the transformation behaviour

Figs. 5.1-5.4 show that time and temperature control the transformation behaviour and therefore the hardness in the experimental alloys. It was concluded that hardness varies linearly with soaking period and can be represented by an equation.

$$H = C_1 + C_2t \quad (T^\circ K) \quad \dots (6.23)$$

The values of C1 and C2 were found to be different for different temperatures and can be expressed as

$$C1 = f(T) \quad \dots (6.24)$$

$$C2 = f(T) \quad \dots (6.25)$$

The plots of C1 vs T and C2 vs T revealed that the C2 vs T is linear and gives a relationship  $C2 = A3 + A4 T$ . However, the C1 vs T plots were exponential in nature. A plot between  $\ln C1$  vs  $1/T$  indicated a linear behaviour and hence the relation between C1 and T can be expressed as:

$$\ln C1 = \ln A1 + A2.1/t \quad \dots (6.26)$$

$$C1 = A1 e^{A2/T} \quad \dots (6.27)$$

Substituting for C1 and C2 in equation (6.17), the final relationship is

$$H = A1. e^{A2/T} + (A3+A4 T)t \quad \dots (6.28)$$

The constants A1, A2, A3 and A4 were calculated for different alloys using the multivariable nonlinear constraint optimization technique (72,73). The final equations along with the overall standard deviations are reported below:

$$\begin{aligned} B1: H &= 67.4 e^{2418.9/T} + (0.0318-2.7 \times 10^{-5} T)t \\ &\text{overall SD} = 25 \quad \dots (6.29) \end{aligned}$$

$$\begin{aligned} B2: H &= 61.8 e^{2442.5/T} + (0.0188-1.6 \times 10^{-5} T)t \\ &\text{overall SD} = 21 \quad \dots (6.30) \end{aligned}$$

$$\begin{aligned} B3: H &= 33.9 e^{3171.6/T} + (0.0239-2.1 \times 10^{-5} T)t \\ &\text{overall SD} = 27 \quad \dots (6.31) \end{aligned}$$

$$B4: H = 65.7 e^{2337.4/T} + (0.0217 - 1.9 \times 10^{-5} T)t$$

overall SD = 18

.... (6.32)

Where T = temperature in K

t = time in seconds

H = VHN<sub>30</sub>

The theoretical hardness values calculated from the above equations were plotted against the corresponding experimental values and are shown in Fig. A-1. The figure reveals that barring a few instances, the calculated values are well within the permissible error of 5%.

It is observed that the constants A1, A2, and A3 are positive for all the alloys. Hence their effect would be similar and additive. The constant A4 is negative for all the alloys. Therefore its effect needs to be analysed. This calls for an assessment of the contribution of second factor of the equation 6.28. At 800°C heat-treating temperature the contribution of this parameter to the hardness, as influenced by the soaking period is positive and given below:

Soaking period hrs.	Contribution of the factor (A3+A4T)t			
	B1	B2	B3	B4
2	20	12	10	10
4	41	24	20	19
6	61	35	30	28
8	82	47	39	38
10	102	59	49	47

The above table indicates the linear dependance of the contribution of this factor to the overall hardness on the soaking period

at a given h/t temperature. From the table it is further inferred that an increase in the Mn content appears to reduce the contribution of the said (second) factor. However a generalization to this effect can be made only after investigating a number of alloy compositions with varying Mn contents.

At 1050°C the contribution of the second factor is negative and the values for the different alloys as influenced by the soaking period are given below.

Soaking period hrs.	Contribution of the factor (A3+A4T)t			
	B1	B2	B3	B4
2	-28	-17	-28	-25
4	-57	-34	-56	-50
6	-85	-51	-84	-74
8	-113	-68	-112	-99
10	-141	-85	-140	-124

The above data also leads to a similar conclusion regarding the effect of Mn on the magnitude of the second factor.

Because of a difference in the nature of the contribution of the second factor as influenced by temperature, further calculations were made to find out the temperature at which the contribution of the aforesaid factor became. For B1 the changeover occurred at around 904°C which is infact the temperature representing the cross over point section (6.3.4.2). This deduction is valid for all the alloys, duly remembering that value of the COP differs from alloy to alloy.

The above discussion also reveals that the term (A3+A4T)t has a definite impact on the overall hardness.

### 6.3.8 Identity of the new phase

It now becomes necessary to ascertain the nature of the new phase formed. Although it has formed at 1050°C around massive carbides, eventually bridging the neighbouring massive carbide regions (Figs. 5.32-5.35), there are indications that its formation has been initiated to some extent even on prolonged soaking at 1000°C (Figs. 5.28-5.31). The new phase has evidently formed by a process of nucleation and growth because its volume fraction increases with soaking period upto ~4h/6h and decreases thereafter (88). Electron-probe micro analysis has revealed that the distribution of Mn, C, Cr and Fe in the new phase is similar to that observed in the massive carbide regions. This clearly identifies the new phase to be a carbide with a relatively higher concentration of Mn and Cr and a relatively lower concentration of Fe (Fig. 5.106, 5.107).

The precise nature of the 'bridge' carbide can be identified by either subjecting the extracted phase to X-ray diffraction studies or else by X-ray diffractometric technique. The latter was employed in the present study and the results obtained have been presented in the next section.

The formation of certain special type of carbides having a 'fibrous' morphology has been reported in certain high alloyed white irons (91). It has been further stated that the fibres are hexagonal and that the adjacent fibres are frequently joined together. This description agrees well with the nature of the 'bridge carbide' observed in the experimental alloys. It is therefore likely that aforesaid carbide is similar in nature to the

hexagonal 3-D carbides formed in the high alloyed white iron (91).

It may be significant to note that the amount of the bridge type carbide is different in different alloys, it being the maximum in B1, and comparable in B2, B3 and B4 (perhaps marginally lower in B3). An indirect inference from the observation is that perhaps a low Mn/Cu ratio, a relatively lower Mn content and a high Cu content may prove helpful in restricting/avoiding the formation of this type of carbide. Should this be so, the higher graphitizing tendency due to the presence of a higher Cu content, may be mainly responsible for the observed difference in the tendency to form the aforesaid type of carbide.

#### **6.3.9 Structural analysis by X-ray diffractometry**

This analysis has proved extremely useful in deciding (a) whether austenite was retained in the as-cast microstructures, (b) till what stage on heat-treating temperature and time martensite existed even in traces, (c) the nature of the carbides formed and (d) the effect of heat-treating parameters on the nature of the carbides (Tables 5.60 to 5.100).

X-ray analysis has proved useful in ascertaining that there is a distinct possibility of  $\gamma$  being retained in the as-cast structure in B3, a possibility that had been suggested while interpreting microstructures (section 6.3.1). Similarly, the possible presence of martensite in very small quantities has been confirmed corresponding to the 900°C, 4h, OQ and 900°C, 10h, OQ heat-treatments (section 6.3.2.1). It is equally pertinent to record that the X-ray analysis has further confirmed the absence of martensite on heat-

treating from 950°C except in one instance i.e in the alloy B4 [Table 5.100 (a)]. Interestingly enough this deduction, although unexpected, agrees well with the optical metallographic observations (observation 5 of section 5.2.2). This may be attributed to segregation within the austenitic matrix leading to the formation of regions depleted in alloying elements. They may transform to martensite on cooling.

Based on the diffractometric studies it is inferred that amongst the four carbides that are formed namely  $M_3C$ ,  $M_5C_2$ ,  $M_7C_3$  and  $M_{23}C_6$ , the  $M_3C$  is the predominant constituent. At high temperatures (1000 and 1050°C), mostly  $M_5C_2$  and  $M_7C_3$  are present. The  $M_{23}C_6$  and  $M_3C$  carbides were absent on heat-treating from upwards of 1000°C. The type of carbide that would form depends upon the effective Mn, Cr, C and Fe contents. They in turn would depend upon the (i) alloy content, (ii) heat-treating temperature and time and (iii) partitioning behaviour. In the absence of the quaternary Fe-Mn-Cr-C phase diagram, the basis for deciding the nature of the carbides would be the relevant ternary sections of the Fe-Cr-C and Fe-Mn-C phase diagrams. An analysis of the carbide transformation sequence in the experimental alloys [Table 5.100 (b)] reveals that the observed sequence is consistent with the information derived on the basis of the phase diagrams (92).

The presence of different types of carbides at different stages of heat-treatment would have an important bearing on the electrochemical as well as the deformation behaviour of the alloys since the compatibility of the carbide phase (be it dispersed or massive) with the matrix would influence these properties. Compati-

bility is a function of the crystal structure. The aforesaid aspect has been critically discussed in the following sections.

#### 6.4 Effect of microstructure on the deformation behaviour

Considering now the deformation behaviour, the as-cast state is typified by a brittle behaviour (low CS and % strain) consistent with a high hardness (Table 5.105 and figure 5.79). Differences in the compressive strengths and in the % strain in the as-cast state can be explained on the basis of the nature of the matrix microstructure and whether it is uniform or nonuniform, morphology and the volume fraction of massive carbides, possible retention of austenite and the location of  $\gamma$  in the microstructure. How these aspects differ from one alloy to another, has been clearly discussed in the sections 6.2 and 6.3. The similarity in the behaviour between B1 and B3 (lower CS and lower % strain and that between B2 and B4 (higher CS and higher % strain), highlighted earlier, (sections 6.2 and 6.3) is also reflected in their deformation behaviour. B2 and B4 have attained higher strength and percent strain due to a relatively uniform matrix microstructure, a lower volume fraction of  $M_c$  and retention of austenite (Figs. 5.8-5.11, 5.79).

Heat-treating has lead to an improvement in both the compressive strength (CS) and % strain because the volume fraction of massive carbides is reduced, they are rendered discontinuous and the matrix either comprises of  $\gamma+M$  or simply  $\gamma$  depending upon the temperature and time employed. Therefore the extent of improvement in properties would depend upon the heat-treating temperature and



time (Figs. 5.80-5.83).

On heat-treating from 900°C at 4hrs soaking period, the properties of the four alloys are different and consistent with their microstructures (Figs. 5.20-5.23, 5.80). On raising the soaking period to 10 hrs, the mechanical properties are practically unaltered because there are no major changes in the microstructures (5.20-5.23). The relatively inferior properties in B1 can be attributed to (i) the possible presence of a relatively larger proportion of 'M', (ii)  $\gamma$  with the least alloy content, (iii) a higher volume fraction of massive carbide and (iv) an unfavourable distribution of dispersed carbides. In spite of favourable microstructural changes occurring at 950°C (section 6.2), the mechanical properties are either unaltered or show a decreasing trend on raising the soaking period from 4 to 10 hours. This can be attributed to an unfavourable distribution of dispersed carbides (Figs. 5.24-5.27, 5.44, 5.46, 5.55, 5.57, 5.66, 5.68, 5.76, 5.78).

If properties corresponding to 900°C, 4 hrs. and 950°C, 4 hrs. heat-treatments are compared, it emerges that a definite improvement in compressive strength has occurred in all the alloys, although the extent of improvement varies. This can be attributed to (i) an improvement in the stability of austenite and (ii) a slightly lower volume fraction of massive carbide and (iii) the size and distribution of dispersed carbides being favourable. Similarly, barring B1, an improvement in % strain in B2, B3 and B4 can be explained on similar lines. It is important to note that no change in % strain is observed in B1. This can perhaps be attributed to an unfavourable distribution of dispersed carbides (Fig.

5.44 and Tables 5.57, 5.58) and to a slightly higher volume fraction of massive carbides (Table 5.49).

If the properties of the alloys corresponding to the 900°C, 10 hrs. and 950°C, 10 hrs. heat-treatments are compared, it is seen that inspite of decrease in hardness and the volume fraction of massive carbides, the expected improvement in properties due to an increase in the (i) volume fraction of  $\gamma$  and (ii) its stability, has not materialized. Infact improvement in compressive strength is maximum in B2, followed by B3 and negligible in B4; in B1 there is infact a marginal decrease. The same is valid for the  $\epsilon$  strain (Tables 5.105, 5.106). Quite clearly, therefore, the factors mentioned above are not the key parameters in controlling the deformation behaviour. The data can be best explained on the basis of the size and distribution of dispersed carbides of particular interest would be the coarsening behaviour namely the number of particles and volume fraction formed in class III - V. The tendency to form oversized fractions (III - V) is the maximum in B1 and minimum in B2 in the order B1>B3>B4>B2 (Tables 5.57, 5.58). The importance of the size and distribution of the dispersed carbides in controlling the deformation behaviour is thus unequivocally demonstrated.

Based on the above analysis it can be stated that from amongst the four heat-treatments namely 900°C-4hrs., 900°C-10hrs, 950°C-4hrs. and 950°C-10hrs., the overall situation vis-a-vis dispersed carbides, and hence properties are most favourable corresponding to the 4 hrs. soaking period and in particular corresponding to the 950°C-4hrs. heat-treatment (Figs. 5.44, 5.55, 5.66, 5.77 and Tables

5.57, 5.58). The situation is just the reverse corresponding to the 10hrs. soaking period and in particular corresponding to the 950°C, 10hrs. heat-treatment.

On heat-treating from 1000°C (4hrs. heat-treatment) there is a general improvement in properties due to (i) an increase in the stability of austenite, (ii) a reduction in the volume fraction of massive carbide and (iii) a gradual reduction in the volume fraction/dissolution of the dispersed carbides (Fig. 5.81 and tables 5.105, 5.106). An improvement in the properties on raising the soaking period from 4 to 10hrs can be similarly explained. It is noteworthy that the dispersed carbides are not present corresponding to 10hrs. heat-treatment.

The improvement in properties on raising the temperature from 950°C to 1000°C (10 hrs. soaking period) is more pronounced compared with that observed on moving from 4hrs. to 10hrs. at 1000°C (Tables 5.105, 5.106). The former can be attributed to the disappearance of the dispersed carbides (hence to the elimination of the adverse effect associated with them) and to other favourable changes already discussed. As regards the latter, the expected improvement in properties, inspite of favourable microstructural changes, has not materialized due to the possible (i) linking of massive carbide regions and (ii) formations of the new phase (Figs. 5.28-5.31). Its formation has already been reported on heat-treating from 1050°C at low soaking periods and the possibility of its forming on prolonged soaking at 1000°C can not be ruled out.

On heat-treating from 1050°C, the improvement in properties on

raising the soaking period from 4 to 10hrs. is once again due to the structure being predominantly austenitic, least volume fraction of massive carbide and a minimum of the new phase (Figs. 5.82, 5.83 and tables 5.105 and 5.106). At this soaking temperature the gradation of the alloys based on the overall properties namely  $B2 > B3, B4 > B1$  needs to be carefully analysed. Based on the stability of  $\gamma$  and the volume fraction of the massive carbide/new phase present as the main criterion, and assuming all other factors to be similar, the order should have been in direct proportion to the alloy content ( $\gamma$  stabilizing tendency) namely  $B4 > B3 > B2 > B1$ . In terms of microstructural features, the volume fraction of the new phase is higher in B1 and nearly similar in B2, B3 and B4. Similarly the volume fraction of the massive carbide differs slightly, it being the least in B3 (Figs. 5.34 e, f). An equally important factor to be considered is the compatibility of massive carbide with the austenite matrix. As has already been stated, this is governed by the crystal structure of the carbide; crystal structures having similarity with  $\gamma$  leading to better compatibility. This would be a major factor in controlling the deformation behaviour at 1050°C. Based on this parameter alone (governed by the relative proportions of the  $M_5$  and  $M_7$  carbides, tables 5.100 b), the deformation behaviour of the alloys would be in the order  $B1 > B2 > B4 > B3$ . Taking an overall view and remembering that the B3 and B4 have a higher 'P' content compared with B1 and B2, the overall behaviour sequence namely  $B2 > B3, B4 > B1$  appears reasonable.

Based on the above discussion, the variation in properties as a function of the heat-treating time and temperature (Figure 5.84),

is easy to comprehend on the basis of the following table. It also brings out the adverse effect of the bridge carbide (NP) on the deformation behaviour.

4hrs. soaking period		
Property	Reasons for changes	Remarks
CS		
1. Increase continuous upto 950°C.	more stable $\gamma$ , less MC, DC distribution favourable.	Increase least in B1 due to higher 'M' and high vf MC.
2. Increase continuous upto 1000°C	more $\gamma$ (high stability), less MC, negligible DC.	increase in CS is directly related to the proportion and stability of
3. Slight increase or tapering off in B1 up to 1050°C	Fine nature of NP.	Decrease in CS was possible due to largest vf of platy carbide (M)
4. Decrease in B2, B3 and B4.	(a) Coarse nature of NP.	Decrease in CS nearly identical in B2, B3 and B4 due to similar vf of platy carbide

#### % Strain

1. 900°C-max <sup>m</sup> in B4 followed by B2, B1, B1 and B3 (comparable)	Least particles in B4 class III followed by B2, B3 and B1	High % strain due to more stable favourable distribution of DC.
2. Increase upto to 950°C marginal in B1, B3, B4 and Steep in B2	B4-900°C 4hrs-already high, no further increase expected; DC situation favourable. Particles (DC) B1→Max in class III & IV B3→No. in class III & IV, B2→most favourable distribution in class III&IV.	order is B4>B2>B1>B3 consistent with coarsening behaviour (max <sup>m</sup> coarsening in B1 and B3) lesser.
3. Increase upto 1050°C continuous in B2, B3&B4	Larger amount of stable $\gamma$ , low MC and least NP	Reason for a tapering off in % strain in B2 between 950-1000°C is clear.

4. Increase in B1 negligible. Large vf of NP

10 hrs. soaking period

CS

(a) Upto to 950°C

1. Small increase in B1, B3 and B4 most adverse distribution of DC (particles present) upto class V)

2. Increase in B2 steep. particles mostly in class I-III

(b) Increase upto 1000°C steep and nearly similar NO DC, minimum MC, structure predominantly  $\gamma$

(c) Increase upto 1050°C

1. Minimum in B1  $\gamma$  stability least,  $\max^m$  vf of NP amongst alloys. More increase expected due to good MC compatibility

2. Comparable in B3, B4 and  $\gamma$  stability  $\max^m$ , vf of NP low, reduced compatibility between MC and the matrix

3.  $\max^m$  in B2 large  $\gamma$  stability, low vf of new phase, MC compatibility good. precise reason for steepest increase in B2 is not clear

% Strain

Upto 950°C

1. Negligible increase or no change in B1, B3, B4. same as those for negligible change in CS.

2. Increase in B2 large same as for CS

data consistent

3. Increase upto 1050°C continuous, minimum in B1. relatively lesser-stable  $\gamma$ ,  $\max^m$  platy carbide (NP) amongst all the alloys.

with the coarsening behaviour  $\min^m$  in B2 &  $\max$  in B1 in the order B2 > B4 > B3 > B1 MC compatible; should have lead to higher increase (not actually observed)

<p>4. Increase in B2, more stable <math>\gamma</math>, less          B3, B4 in the order MC and new phase          B2 &gt; B3, B4</p>	<p>Difference between          B2 and B3, B4 due          to better compa-          tibility of MC.</p>
---	---

## 6.5 Corrosion behaviour

### 6.5.1 Weight loss data

The experimental alloys were characterized for their corrosion behaviour in the as-cast and in the heat-treated conditions in order to assess the electrochemical response of the different microstructures observed in the present study. The weight loss technique was employed as it is accepted as a reliable and a standard technique (69,70) and also because bulk of the corrosion data on commercial alloys is based on this technique. Of the two units employed to represent corrosion rate namely ipy and mdd, the latter is more accurate because density of the material does not figure in the final calculations (section 4.9.1). Using the weight loss method is further justified because the experimental alloys undergo uniform corrosion.

A perusal of the data contained in the tables 5.109-5.124 and summarized in the figures 5.85-5.88 (pertaining to 5% NaCl solution) reveals that there are certain general trends clearly discernable namely (i) a decrease in CR with test duration (valid for all the test solutions) (ii) a decrease in CR with soaking period (for a given test duration) on heat-treating from all the temperatures between 900-1050°C except 950°C (iii) stress relieving proving detrimental barring some instances and the 1050, 10hr, OQ h/t. An equally important observation to be discussed later is that any heat-treatment which improved mechanical properties also improved

the corrosion resistance. As such it would be reasonable to infer that the corrosion data can in general be interpreted on the same basis as the mechanical properties. Therefore to avoid repetition only the general trends will be discussed.

1. The decrease in CR with test duration is consistent with the self passivating nature of the Fe-base alloys (93). The maximum decrease in CR with test duration is observed in the as-cast state due to the faster initial corrosion of the martensite-associated microstructures attributed to their highly stress state and a steep decrease in CR thereafter due to the high hardness associated with martensite (50).
2. Heat-treatment has in general improved the corrosion resistance due to the formation of austenitic microstructures. Presence of martensite even in small amounts is proving detrimental for reasons already stated. This is one of the reasons why higher than expected CRs are observed in all the alloys in general and B1 in particular corresponding to the 900°C,4hr,OQ h/t.

The higher the stability and proportion of austenite the larger would be the improvement in corrosion resistance. The higher the heat treating temperature the larger would be the proportion and stability of austenite. A similar change would also be brought about by increasing the soaking period at a given heat treating temperature. Transformations bringing about an increase in the proportion and stability of austenite also reduce the vf of MC. CR would additionally decrease due to this (section 6.3.2.1). For a given volume fraction of MC, a rounded morphology is prefer-



red over the plate morphology (section 6.3.2.1). The transformations, bringing about changes in  $\gamma$  and MC, favourable to corrosion resistance, would occur only at high temperature i.e. at  $> 950^{\circ}\text{C}$ . Therefore, a marked improvement in corrosion resistance can be expected only on heat treating from temperatures higher than  $950^{\circ}\text{C}$ . This is what has been observed (Table 5.109-5.124 and figures 5.85-5.88). The  $950^{\circ}\text{C}$ -10hr. h/t has not proved useful from the corrosion resistance point of view because favourable microstructural changes are counteracted by the adverse effect associated with dispersed carbides.

3. The effect of dispersed carbides would depend upon their size, shape and distribution. For a given temperature, they are altered by increasing the soaking period. For a given soaking period, a similar change would be brought about by increasing the heat-treating temperature. The beneficial effect of increasing the ST or SP would be experienced so long as the size, shape and distribution are not unfavourable. This adverse effect, which would be mainly characterized by a marked coarsening tendency, is experienced in all the alloys corresponding to the  $950^{\circ}\text{C}$ -10hr heat treatment thereby leading to an increase in the corrosion rate (42).

Although there is no clear cut yardstick to conclude whether a given particle size or distribution of particles is adverse, the relative inferiority/superiority of the alloys based on their coarsening behaviour can perhaps be judged on the basis of the distribution of particles in classes III to VI (section 6.3.6). Quantitatively, the coarsening index can provide us the required informa-

tion. Based on it (section 6.3.6), B2 should be superior to the others in the order.

B2 > B4 > B3 > B1

The corrosion data corresponding to the 950°C, 10hr, OQ heat treatment agrees reasonably well with this deduction. Based on similar reasoning it would be possible to deduce why the adverse effect related with the size, shape and distribution of DC is not experienced in all the alloys at the 950°C-4hr h/t.

The above reasoning proves useful in examining the role of stress-relieving on the CR in the experimental alloys. It is postulated that stress relieving brings about softening at the matrix second phase interface. This would lead to enhanced galvanic action and hence to an increase in CR. In the present context the term second phase signifies both the massive as well as the dispersed carbides. The extent of softening due to dispersed carbides will be governed by the volume fraction, size, shape, distribution and compatibility with  $\gamma$ . Similarly, the extent of softening attributed to massive carbides will depend upon their volume fraction, morphology and compatibility.

The enhanced galvanic action at 900 and 950°C is due to the combined effect of MC and DC. At 1000°C both coarse DC & MC contribute at 4 hrs soaking period whereas MC alone is contributing at 1 hrs. At 1050°C, the enhanced galvanic action is due to the combined effect of MC and NP (platy carbide). In order to understand and evaluate the relative contribution of different parameters, percent

deterioration in CR due to stress relieving was calculated at different heat-treatments. This data is summarized below :

percent deterioration (168 hrs test duration)

h/t	B1	B2	B3	B4
900,4, OQ -	5.3	5.2 (33)	4.5 (33)	5.7 (28)
900,10, OQ -	3.4 (40)	2.9 (26)	1.7*(32)	5.3 (27)
950,4, OQ -	4.6 (37)	4.0 (30)	4.7 (30)	1.1**(29)
950,10, OQ -	2.5 (38)	1.3 (26)	2.7 (29)	1.7 (31)
1000,4, OQ -	13.7**(17)	13.6**(14)	3.9 (15)	3.9 (18)
1000,10, OQ -	2.9 (14)	5.8 (12)	6.0 (11)	3.3 (15)
1050,4, OQ -	12.4	12.8	15.7**	1.3
1050,6, OQ -	7.6*	4.8*	15.8**	1.2
1050,10, OQ -	2.7*	4.9*	7.5	3.9

\* indicates improvement

\*\* needs further confirmation

( ) values represent MC + DC

The above table reveals that the extent of deterioration in general decreases with soaking period at a given heat-treating temperature. However, for a given soaking period (SP), the extent of deterioration as influenced by an increase in heat-treating temperature does not conform to a consistent pattern. This reflects upon the varied and complex nature of the structural changes that occur on increasing the temperature. Notwithstanding certain data needing confirmation, an effort has been made to interpret the overall data qualitatively, as would be evident from the following table. To facilitate interpretation simple rationalizations have been made.

4 hrs. soaking period

Nature of changes	Reasons	Remarks
<u>B1</u>		
(1) 900 to 950°C	(a) stable $\gamma$	
(a) No change/marginal improvement	(b) less MC (c) DC not unfavourable	
(2) 950 to 1000°C deterioration(marked)	coarse DC, interlinking of MC	
(3) 1000 to 1050°C No change/marginal improvement	larger proportion of stable $\gamma$ , decrease in MC	Improvement counterbalanced by larger vf of NP
<u>B2</u>		
(1) 900 to 950°C same as in B1	same as in B1	- -
(2) 950 to 1000°C, same as in B1	same as in B1 +MC elongated plate like and often interconnected.	- -
(3) 1000 to 1050°C	same as in B1	i) vf of NP is less than in B1; but NP coarse and platy, hence harmful  ii) benefit due to less vf of NP not experienced
<u>B3</u>		
(1) 900-950°C No change; as in B1	same as in B1	

- |                                      |  |     |
|--------------------------------------|--|-----|
| (2) 950-1000°C<br>improvement        | No DC, no interlinkin<br>of MC, more stable $\gamma$<br>and rounding 'off' of<br>MC (discontinuous). | - - |
| (3) 1000 to 1500°C,<br>deterioration | NP coarse and interli-<br>nking through elon-<br>gated thread like con-<br>stituent(s)               | - - |

B4

- |   |  |  |
|---|--|--|
| (1) 900-950°C<br>improvement  | same as in B1  | - -  |
| (2) 950-1000°C,<br>expected trend should<br>have been as in B3<br>(some improvement/pract-<br>ically no change) | same as in B3  | - -  |
| (3) 1000 to 1050°C,<br>improvement  | highest alloy con-<br>tent, maximum stable<br>$\gamma$ , low NP, low MC. | expected<br>trend, no<br>change of<br>minor im-<br>provement |

10 hrs soaking period

Nature of change	Reasons	Remarks
(1) 900 to 950°C, minor imporvement/ no change	larger proportions of more stable $\gamma$ & lessor MC	Expected improvement offset by adverse di- stribution of DC
(2) 950-1000°C no change	-do-	Expected improvement due to still hig- her propor- tion of stabel $\gamma$ and reduced MC offest by forma- tion of NP small+inte- rlinking

(3) 1000 to 1050°C No deterioration but improvement in corrosion resistance	Rounded MC with low vf, MC compatible with the matrix	Improvement could have been more if vf NP was smaller
--	---	---

B2

(1) 900 to 950°C, improvement more than in B1	same as in B1	DC distri- buton al- though adverse but better than in B1
---	---------------	--

(2) 950 to 1000°C, deterioration	Platy MC, bridging/ interlinking of MC, formation of NP	- -
-------------------------------------	---	-----

(3) 1000 to 1050°C, same as in B1	same as in B1	Improvement marginally more than in B1 due to lesser vf of NP
--------------------------------------	---------------	--

B3

(1) 900 to 950°C, No change (minor improve- ment expected)	same as in B1	DC adverse as in B1
--	---------------	------------------------

(2) 950-1000°C, minor deterioration	cracking of MC, inter- linking and gruping together of MC, forma- tion of NP	- -
--	---	-----

(3) 1000-1050°C, minor deterioration or no change	Fibering, nonuniform structure	Improvement expected due to lar- ge vf of $\gamma$ and least MC perhaps offest by fibering / non uniform structure
---	-----------------------------------	---

B4

(1) 950-950°C, improvement	same as in B2	DC distri- bution bet- ter than B1, B3 but inferrior B2
-------------------------------	---------------	--

(2) 950-1000°C, minor deterioration/ no change	not apparent; poss- ibly due to like plate MC morphology and some bridging tendency	NP neglig- ible
(3) 1000 to 1050°C, no change	Maximum stable $\gamma$ , low MC, low NP	Improvement no occurring due to low compatibil- ity between MC and the matrix.

The above inferences have been arrived at after duly considering the accompanying microstructural changes (Figs.5.20-5.35).

This discussion further reflects upon the large number of variables that have to be considered while arriving at a reasonable understanding of the corrosion behaviour of the experimental alloys.

The above discussion proves helpful in assessing the effect of NEW PHASE on the corrosion resistance. A possible method to arrive at the required information is to compare the corrosion rates corresponding to 1000°C,10,OQ and 1050°C,4,OQ heat-treatments. The latter has been selected because the volume fraction of the NP is maximum corresponding to this heat-treatment. On doing so it emerges that the CR has decreased. The possible inference is that the new phase has a favourable effect. However, it would be erroneous to arrive at such a conclusion because the observed improvement in corrosion resistance is small and may have resulted due to favourable microstructural changes (reduction in vf of MC and a further increase in the proportion of high stability austenite). A better

method to arrive at the required result would be to compare the extent of deterioration in corrosion resistance on stress relieving corresponding to the 1000°C, 10h, OQ and 1050°C, 4h, OQ heat-treatments. On doing so a marked deterioration in the corrosion resistance is observed in B1, B2 and B3. In B4 the extent of deterioration is reduced. Thus it can be categorically stated that NP has an adverse effect on corrosion resistance in B1, B2 and B3 but apparently not in B4. It is likely that the adverse effect from the presence of NP is effectively counteracted by the favourable microstructural changes (i.e.  $\gamma$  with the highest stability amongst all the alloys and very small  $v_f$  of MC). However, based on the evidence of its effect on the deformation behaviour, it may not be incorrect to state that the presence of NP will also have an adverse effect in B4.

#### 6.5.2 Potentiostatic data

The potentiostatic data has proved helpful in reaffirming the inferences drawn on the basis of weight loss studies namely in confirming that (i) 900, 4, OQ heat-treatment improves the corrosion resistance compared with that observed in as-cast state (ii) stress-relieving has a detrimental effect on the corrosion resistance corresponding to the aforesaid heat-treatment and (iii) B3 is better than B4 both in the 900, 4, OQ and 900, 4, OQ+SR conditions (Figs. 5.89-5.94).

However, there are certain areas of disagreement which need mentioning. The observation that B4 is better than B3 in the as-cast state is based on the logic that  $I_{CR}$  is lower and a passive



potential range exists. However, on the basis of  $I_{pp}$ , B3 appears marginally better than B4 (Figs. 5.89,5.92). Taking an overall view, it may perhaps be more appropriate to classify B3 and B4 to be comparable. The observations based on the weight loss studies suggest B3 to be better than B4 (Table 5.123,5.124) and hence are at variance.

The behaviour of B3 and B4 in the heat-treated (900,4,00) condition is comparable with that of the alloy KC (nodular Ni-resist). This agrees well with the findings based on the weight loss studies and reflect upon the usefulness of  $\gamma$ -carbide couple in resisting corrosion.

The reasons why KCl is inferior to KC (deduction on the basis of weight loss studies being just the opposite) are not clearly understood (Figs. 5.95-5.96). The matter is under investigation.

### 6.5.3 Scanning metallography results

The main utility of this study has been in ascertaining the nature of corrosion in the experimental and the standard Ni-resist alloys. The absence of any localized attack (pitting) in B1,B2,B3 and B4 (Figs. 5.98-5.105), unlike in the standard Ni-resist compositions (Figs. 5.97) is a definite plus point in favour of the experimental alloys. This may be attributed to the absence of graphite. This also reflects upon the superiority of the micro-structures (more particularly of the  $\gamma/Fe_3C$  couple) formed in alloyed white irons in resisting localized attack (pitting). Matrix cracking observed in the experimental alloys can not be regarded as an adverse feature since the same is also observed in the Ni-resist compositions.

Based on the observation that the extent of cracking varies with the alloys compositions and heat-treatment, it is postulated that the magnitude of cracking can be minimized by further increasing the stability of the austenitic matrix. This inference needs to be duly considered while designing alloys in the future.

A careful analysis reveals that the cracking might be mainly confined to a surface film formed as a result of exposure to the environment (5% NaCl). This possibility occurred because difficulty was experienced while focusing the specimen surface during the scanning microscopic examination. This difficulty was resolved by gold plating the specimen surfaces. On doing so they could be properly focused without any difficulty. This confirms the existence of a non-conducting surface film.

A critical examination revealed that the micrographs (Figs. 5.97-5.105) are also useful in corroborating the corrosion data summarized in the tables 5.109-5.112. e.g. based on an appraisal of the scanning micrographs, the following deductions may be arrived at regarding the relative corrosion behaviour of B1 and B2 :

- (a) In the as-cast and 900°C, 4h, NSR condition, the corrosion rates are comparable.
- (b) For the 950°C, 10h, SR heat-treatment, B2 is better than B1.
- (c) For the 1000°C, 10h, SR heat-treatment, corrosion rates appear comparable.
- (d) For the 1050°C, 4h, NSR, heat treatment B1 is better than B2.
- (e) For the 1050°C, 4h, SR heat treatment, corrosion rates are comparable, and

(f) For the 1050°C, 10h, SR, heat treatment, corrosion rates are either comparable or B2 is better than B1.

Except for the inference at (c) [experimentally, B2 was found to be better than B1], all the other inferences are in agreement with the deductions, relating to the corrosion behaviour, based on the weight loss data. Similar inferences can also be drawn regarding the relative corrosion behaviour of B3 and B4.

#### 6.5.4 Mathematical modelling of the corrosion behaviour

An analysis of the preceding sections reveals how different microstructural parameters influence the corrosion behaviour during the different stages of heat-treatment e.g. the massive and the dispersed carbides have an important bearing on the corrosion behaviour when the alloys are heat treated from 900 and 950°C. It was, therefore, felt appropriate to examine the possibility of establishing a mathematical correlation between corrosion rate and the different parameters employed to characterize dispersed and massive carbides.

For these heat-treatments, corrosion rate (CR) can be expressed by an equation of the form :

$$\text{CR} = f(\gamma \text{ vf/stability}) + f(\text{vf of MC}) + f(\text{vf of DC}) + f(\text{distribution of the DC}) \dots (6.33)$$

Excluding the last term to start with, as a first approximation the contribution of the volume fraction and the stability of  $\gamma$  may be treated as nearly a constant because the hardness values of the four alloys at 900 and 950°C are approximately constant. From a plot of corrosion rate vs the total volume fraction of carbides

(massive+dispersed), it was clear that the functional relationship can be represented by a second order polynomial :

$$CR = A + B (VCb) + C (VCb)^2 \quad \dots (6.34)$$

Where VCb = Total volume fraction of the carbides

The constants A,B and C were calculated by using the least square method (72,73). The contribution of the 'second-phase' particles was additionally included in this expression by incorporating a factor based on the number of particles (NOP). This leads to the expression.

$$CR = [ A + B(VCb) + C(VCb)^2 ] (NOP)^D \quad \dots (6.35)$$

The constants A,B,C and D were finally calculated and computed to minimum error by using a non-linear multivariable constraint optimization technique (72,73).

The final equation for the different alloys are

$$B1: CR = [1516.9-79.6(VCb)+1.13(VCb)^2] (NOP)^{-0.48} \quad \dots (6.36)$$

$$B2: CR = [7999.8-541.2(VCb)+9.45(VCb)^2] (NOP)^{-0.73} \quad \dots (6.37)$$

$$B3: CR = [9.94-0.624(VCb)+0.0099(VCb)^2] (NOP)^{1.4} \quad \dots (6.38)$$

$$B4: CR = [44.3-3.07(VCb)+0.0545(VCb)^2] (NOP)^{0.83} \quad \dots (6.39)$$

The calculated values of CR, based on the above equations, were plotted against the experimentally determined corrosion rates (Figs. A-2 of appendix-2). It is observed that the calculated values agree well with the experimentally determined values.

In order to understand the physical implication of the model, the values of the constants A,B,C and D were carefully scrutinized. It emerged that whereas the constants A,B and C are consistent

(either all +ve or all -ve), D is negative for B1 and B2 and positive for B3 and B4. To understand its possible implications, the factor (NOP)<sup>D</sup> was calculated for all the alloys and the values are given below :

Heat-treatment	B1	B2	B3	B4
900°C, 4hr, OQ	-	0.056	203.68	23.59
900°C, 10hr, OQ	0.163	0.068	211.05	19.27
950°C, 4hr, OQ	0.183	0.082	168.02	19.71
950°C, 10hr, OQ	0.216	0.073	154.36	17.93

It is observed that the factor (NOP)<sup>D</sup> is varying widely for the four alloys. This gives an indication that NOP can not be regarded as a satisfactory parameter for representing the distribution of dispersed carbides and this model needs further investigation (94).

In order to overcome this problem a new parameter, representing the effect of dispersed carbides, was defined. This has been named as the distribution factor (DF). To incorporate this parameter, the effects of massive and dispersed carbides have to be considered separately.

A plot of corrosion rate vs the volume fraction of massive carbides revealed that the functional relationship can be represented by a second order polynomial

$$CR = A' + B'(VMc) + C'(VMc)^2 \quad \dots (6.40)$$

Where VMc = Volume fraction of massive carbide

The constants A', B' and C' were calculated by a method discussed earlier (72,73). The distribution factor (DF), included in the final equation, is given by the expression:

$$DF = \frac{\sum_{i=1}^n Ni Xi}{\sum_{i=1}^n}$$

Where n = the no. of classes

Ni = the number of particles in ith class (i=1,2,3,...n)

Xi = volume fraction in class 'i'/VDC

and VDC = total volume fraction of dispersed carbides.

Accordingly, the final expression is

$$CR = [C1 + C2 (VMc) + C3 (VMc)^2] (DF)^{C4} \quad \dots (6.42)$$

The constants C1, C2, C3 and C4 were evaluated and the final equations are :

$$B1: CR = [14.35 - 0.48(VMc) + 0.0128(VMc)^2] (DF)^{-0.8} \quad \dots (6.43)$$

$$B2: CR = [-999.9 + 118.7(VMc) - 3.128(VMc)^2] (DF)^{1.76} \quad \dots (6.44)$$

$$B3: CR = [456.2 - 45.92(VMc) + 1.199(VMc)^2] (DF)^{-0.31} \quad \dots (6.45)$$

$$B4: CR = [-186.68 + 22.92(VMc) - 0.619(VMc)^2] (DF)^{-0.02} \quad \dots (6.46)$$

The magnitude of the constant C4 is -ve for B1, B3 and B4 and +ve for B2. To understand its implications, the factor (DF)<sup>C4</sup> was calculated and the corresponding values are given below :

Heat treatment	B1	B2	B3	B4
900, 4, OQ	-	0.28	1.34	1.01
900, 10, OQ	2.23	0.22	1.28	1.02
950, 4, OQ	2.07	0.20	1.34	1.01
950, 10, OQ	2.72	0.24	1.37	1.02

The magnitude of the factor  $(DF)^{C4}$  does not vary widely. As such it can be concluded that the model is reasonable (94,95).

Based on the equations 6.43-6.46, values of the corrosion rates were calculated and plotted against the experimentally determined values (Fig. A-3 of appendix-3). It is observed that the calculated values agree well with the experimentally determined values.

### **6.6. Interrelation between deformation and corrosion behaviour**

Since one of the main objectives of the present investigation was ultimately to examine whether an interrelation as above existed, the compressive properties (CS and % strain) and the corrosion rates for the four alloys were plotted. This data is summarized in the form of histograms given in the Figs. 5.108-5.113. It is clearly observed that as the CS and % strain reduce, corrosion rate increases and vice versa. This inference appears logical since both the deformation and the corrosion behaviour in general reflect upon the state of a material. An embrittled state characterized by a low CS and % strain would naturally result in enhanced corrosion.

An attempt has been made to establish an interrelation between the aforesaid properties for each alloy. Through a plotting of the relevant data, it emerges that the interrelation between CS & CR and between % strain and CR be represented by an expression

$$Y = C1 + C2X \quad \dots (6.47)$$

where Y = the concerned property (CS in MPa or % strain)

X = CR in mdd

and C1 and C2 = constants :

These constants were evaluated for the different alloys using the least square method and final equations are :

$$B1 : \quad CS = 3582 - 58.9(CR) \quad \dots (6.48)$$

$$B2 : \quad CS = 4997 - 109.4(CR) \quad \dots (6.49)$$

$$B3 : \quad CS = 3721 - 54.5(CR) \quad \dots (6.50)$$

$$B4 : \quad CS = 2154 + 0.16(CR) \quad \dots (6.51)$$

$$B1 : \quad \% \text{ Strain} = 37.2 - 0.61(CR) \quad \dots (6.52)$$

$$B2 : \quad \% \text{ Strain} = 76.1 - 2.05(CR) \quad \dots (6.53)$$

$$B3 : \quad \% \text{ Strain} = 70.1 - 1.89(CR) \quad \dots (6.54)$$

$$B4 : \quad \% \text{ Strain} = 54.3 - 1.05(CR) \quad \dots (6.55)$$

## 6.7 General discussion

Through this investigation it has been possible to demonstrate microstructures with useful mechanical properties and good corrosion resistance could be generated through the 'white-iron route' by utilizing low cost elements Mn, Cu and Cr. Heat treatments for generating different microstructures have been established. Structural changes in the experimental alloys follow a logical pattern, namely the as-cast microstructure initially transforming itself into a microstructure consisting of M + discontinuous MC +  $\gamma$  through low temperature heat-treatments to be subsequently followed by the formation of dispersed carbides directly from  $\gamma$  during soaking. On heat treating from 900°C upwards, the microstructures are predominantly austenitic containing lesser and lesser volume



fractions of MC and DC as the temperature and or time are raised. Coarsening of dispersed carbides has been assessed on the basis of a parameter defined as the 'coarsening index'. Dispersed carbides dissolve at 1000°C after soaking for more than 4 hrs. Thereafter, the microstructure is predominantly austenitic with some massive carbides. The 1050°C heat-treatment is characterized by the formation of a bridge type platy carbide initially described as the new phase (NP). Its volume fraction initially increases with time upto ~ 4 hrs and decreases thereafter.

The hardness changes are consistent with the changes in the microstructure. This has enabled mathematical modelling of the transformation behaviour to be carried out. Plots between the experimental and the theoretically calculated hardness values reveal that the model is able to predict hardness data with an accuracy of  $\pm 5\%$ .

A further interpretation of the microstructure was made possible with the help of x-ray diffractometric technique. It has proved extremely useful in deciding upon the nature of the matrix microstructures in marginal cases (as-cast for retained  $\gamma$  and 900°C heat treatments for the possible presence of martensite) and in identifying the various carbides formed over the entire range of heat treating temperatures. There are difficulties in identifying the nature of carbides precisely based on this technique since many of prominent reflections are common to them (different carbides). There is, therefore, a need to employ another technique for identifying different carbides. Subjecting the extracted carbides to x-ray diffraction studies could be one such technique.

A key aspect of the present investigation has been the quantification of the microstructures. The precisely determined voluminous quantitative data, affectively employed to characterize both the MC and DC, has been effectively utilized in establishing qualitative and quantitative interrelations between the microstructure and properties.

The extensive data on the deformation behaviour of the alloys, under high speed compression, proves very useful in characterizing the different microstructures. It clearly brings into focus how brittleness in general leads to lower CS and % strain values and how these two parameters improve as the extent of brittleness reduces. It has been possible to establish qualitatively authentic correlation between the volume fraction, size and distribution of the dispersed carbides and the deformation behaviour. The superiority of the predominantly austenitic matrices in attaining high CS and % strain is clearly in evidence. The bridge type carbide has an adverse effect on the deformation behaviour. This has been attributed to its plate like morphology.

Weight loss method is still one of the most effective and reliable methods for characterizing the corrosion behaviour. The method is applicable to the experimental alloys since they undergo uniform corrosion. Even then there are definite problems to be overcome/precautions to be taken in ensuring that this technique gives reproducible results e.g. the state of stress and the extent of surface finish of all the specimens has to be the same. So also, it has to be ensured that the specimens are free from cracks (sur-

face/sub-surface) and inclusions. The weight loss data gives an excellent comparative idea of the corrosion behaviour of different microstructures in three different environments with the main emphasis on 5% NaCl. The limited corrosion data in other solutions namely 10%  $\text{NH}_4\text{Cl}$  and 10%  $(\text{NH}_4)_2\text{SO}_4$  has not been separately discussed as the overall behaviour of the alloys in these solutions is similar to that observed in 5% NaCl. It also clearly reflects how the size, shape, volume fraction and distribution of the second phase particles (DC) are the controlling parameters in influencing corrosion behaviour. Based on the data generated, two mathematical models have been developed corresponding to heat-treating temperatures of 900 and 950°C. The former incorporates the volume fractions of MC + DC and the NOP. The later incorporates the vf of MC and the distribution factor representing DCs.

Although the experimental alloys were characterized on the basis of weight loss studies extensively, it would be appropriate to characterize them further on the basis of potentiostatic studies. This has been done only to a limited extent and accordingly the data contained in the thesis is only a representative one. However, enough evidence exists to suggest that the potentiostatic data is in good agreement with the weight loss data. Experiments are in progress to characterize the alloys in detail on the basis of their potentiostatic behaviour. Similarly it would be of interest to assess the corrosion behaviour of a microstructure with a fully martensitic matrix.

The adverse effect of stress relieving clearly brings out the

role of DC, MC, NP and the compatibility factor in affecting corrosion behaviour. This is an important inference and has been explained on the basis of enhanced galvanic action. While making this postulate it has been ensured that no structural change(s) occurred during stress relieving.

EPMA has been pursued only to a limited extent mainly to identify the new phase. A more detailed analysis will prove useful in arriving at the partitioning data which will eventually be of considerable interest in alloy design.

Amongst the alloys investigated, the alloy B2 has been found to be most suitable from the point of view of overall properties. It would be appropriate to base alterations in the alloy compositions around this composition. Not barring the higher 'P' content of the alloys B3 and B4, the present study none the less provides for a very critical appraisal of the structure-property correlations in high alloyed white cast irons. An inference of major dimension is that there is a definite interrelation between the deformation and the corrosion behaviour. The fundamental and the applied significance of the data is thus evident.

## CHAPTER VII

### CONCLUSIONS AND SUGGESTIONS FOR FUTURE WORK

#### 7.1 Conclusions

Under the existing experimental conditions, the following conclusions may be arrived at:

1. Low cost elements Mn, Cu along with Cr can be advantageously employed in designing alloy white irons with useful mechanical properties and corrosion behaviour. The microstructures that were characterized for their deformation and electrochemical behaviour (mostly in 5% NaCl solution) are P/B + M + MC, M +  $\gamma$  + MC, M +  $\gamma$  + MC + DC,  $\gamma$  + MC + DC and  $\gamma$  + MC. Most of the aforesaid microstructures were generated through heat-treatments. The temperature ranges over which different microstructures exist are given below:

As-cast : P/B + M + MC with and without RA

Upto 900°C : M + MC + DC with and without RA depending upon ST and SP.

Upto 1000°C : A + MC + DC or A + MC with and without M (in traces) depending upon ST and SP.

1050°C : A + MC + NP (bridge type carbide)

2. The vf of MC decreased with temperature or with soaking period at a given heat-treating temperature. The decrease was marked at temperatures >1000°C. MC were rendered discontinuous from the early stages of heat-treatment. The 'rounding-off' tendency set in at 1000°C.

3. Dispersed carbides formed during soaking, corresponding to the 800°C, 10hr heat-treatment, by a mechanism involving direct precipitation from austenite. Particles constituting them belonged to classes I and II (size upto 1.16 micron). On heat-treating the overall spread of the particles extended up to class VI (size upto 3.48 micron).

4. Dispersed carbides underwent coarsening which was characterized by the 'spilling over' of the particles into the classes III to VI. Coarsening was marked at 900 and 950°C and was assessed on the basis of the coarsening index CI which is given by the expression

$$CI = \frac{\text{DF for a given heat-treatment}}{\text{DF for h/t for which particles are in classes I\&II mainly}}$$

Where DF = Distribution factor

$$= \frac{\sum_{i=1}^n Ni Xi}{\sum_{i=1}^n Ni}$$

i = 1, 2, 3 ..... n

Ni = No. of particles in the ith class

$$Xi = \frac{\text{Vf in the ith class}}{\text{Total Vf}}$$

5. Dispersed carbides get dissolved on heat-treating from 1000°C. Accordingly they are of the type M<sub>23</sub>C<sub>6</sub>.

6. The carbides to form in the experimental alloys are M<sub>3</sub>C, M<sub>23</sub>C<sub>6</sub>, M<sub>5</sub>C<sub>2</sub>, M<sub>7</sub>C<sub>3</sub>. M<sub>3</sub>C and M<sub>23</sub>C<sub>6</sub> carbides dissolved/transformed or were replaced by the higher temperature carbides M<sub>5</sub>C<sub>2</sub> and M<sub>7</sub>C<sub>3</sub>. The

latter are predominant in B1 and B2 whereas the former are predominant in B3 and B4 on prolonged soaking at 1050°C.

7. The new phase (NP), formed on heat-treating from 1050°C in the form of plates and hexagons, is basically a carbide as confirmed by EPMA. Its morphology is harmful from the point of view of overall properties because it is in the form of plates bridging massive carbide regions. There are definite indications suggest that this phase begins to form even on prolonged soaking at 1000°C (soaking period >10 hrs. or more).

8. Hardness in general decreased with an increase in the soaking temperature in the order

$$H_{800} > H_{850} > H_{900} > H_{950} > H_{1000} > H_{1050}$$

9. For a given heat-treating temperature, hardness varied linearly with the soaking period. It increased with an increase in soaking period on heat-treating from 800 and 850°C, remained practically unaltered on heat-treating from 900 and 950°C and decreased on heat-treating from 1000 and 1050°C. Exceptions are B2 and B4 when heat-treated from 850°C (hardness was independent of the soaking period).

10. For a given soaking period, the variation in hardness with temperature was in the form of a horizontal 'S' shape.

11. Transformation behaviour of the experimental alloys, over the entire range of temperature and soaking period, can be represented by the equations:

$$B1: H = 67.5 e^{2418.9/T} + (0.0318 - 2.7 \times 10^{-5} T)t$$

$$B2: H = 61.8 e^{2442.5/T} + (0.0188 - 1.6 \times 10^{-5} T)t$$

$$B3: H = 33.9 e^{3171.6/T} + (0.0239 - 2.1 \times 10^{-5} T)t$$

$$B4: H = 65.7 e^{2337.4/T} + (0.0217 - 1.9 \times 10^{-5} T)t$$

Where H = Vicker's hardness at 30 kg load

T = Temperature in °K

t = Time in seconds.

12. From the point of view of mechanical properties, martensite bearing microstructures are brittle whereas the austenite based microstructures give high value of CS and % strain. The effect of DC on the deformation behaviour depends upon their size, shape and distribution. Similarly, the effect of MC is governed by their vf, morphology and compatibility with the matrix.
13. Bridge type carbide has (NP) a detrimental effect on the deformation behaviour.
14. From the point of view of overall mechanical properties, the alloy B2 has been found to be most useful followed by B4, B3 and B1. It is possible that the presence of a higher P content in B3 and B4 may have lead to some what inferior properties in them.
15. From the corrosion resistance point of view the austenite based microstructures were found to be superior to the martensite based micro-structures. With regard to the former, the stability and proportion of  $\gamma$  are the key parameters.
16. The compatibility, volume fraction and morphology of MC are



equally important in governing the corrosion behaviour of the austenitic matrices.

17. The effect of dispersed carbides on the corrosion behaviour is governed by their size shape and distribution.
18. Corrosion rate in general decreased with an increase in the (i) test duration, (ii) soaking period at a given heat treating temperature except 950°C and (iii) the soaking temperature for a given soaking period except on moving from 900-950°C at 10 hrs soaking period. The observations at (ii) and (iii) are attributed to the unfavourable distribution of the dispersed carbides.
19. Stress relieving in general has proved to be detrimental. This has been attributed to enhanced galvanic action whose nature would depend upon the temperature and time of heat-treating.
20. The austenite-carbide couple has proved to be extremely satisfactory from the point of view of corrosion resistance. Unlike the austenite-graphite couple, the austenite-carbide couple does not undergo pitting.
21. On heat-treating from 900 and 950°C, the corrosion rate is related with the volume fractions of MC+DC and NOP through the following equations:  
B1:  $CR = [1516.9 - 79.6 (VCb) + 1.13 (VCb)^2] (NOP)^{-0.48}$   
B2:  $CR = [7999.8 - 541.2 (VCb) + 9.45 (VCb)^2] (NOP)^{-0.73}$   
B3:  $CR = [9.94 - 0.624 (VCb) + 0.0099 (VCb)^2] (NOP)^{1.4}$   
B4:  $CR = [44.3 - 3.07 (VCb) + 0.0545 (VCb)^2] (NOP)^{0.83}$

Where VCb = Total volume fraction of massive and dispersed carbides.

NOP = Number of particles (dispersed carbides).

CR = Corrosion rate in mdd.

22. On incorporating the effect of dispersed carbides, the above equations are modified as:

$$B1: CR = [14.35 - 0.48 (VMc) + 0.0128 (VMc)^2] (DF)^{-0.8}$$

$$B2: CR = [-999.9 + 118.7 (VMc) - 3.128 (VMc)^2] (DF)^{1.76}$$

$$B3: CR = [456.2 - 45.92 (VMc) + 1.199 (VMc)^2] (DF)^{-0.31}$$

$$B4: CR = [-186.68 + 22.92 (VMc) - 0.619 (VMc)^2] (DF)^{-0.02}$$

Where VMc = Volume fraction of massive carbides

DF = Distribution factor

23. From the corrosion resistance point of view the alloy B2 has once again been found to be most useful followed by B4, B3 and B1.

24. The compressive strength and % strain are linearly interrelated with the corrosion rate in accordance with the equation

$$Y = C1 + C2(CR)$$

Where Y = Property being measured (CS in MPa or % strain)

CR = Corrosion rate in mdd.

C1, C2 are constants

25. In view of 23 and 24 it is recommended that the future modifications in the alloy chemistry should incorporate the beneficial features of the compositions B2. Further, the alloying elements should be so adjusted that the microstructures(s) of form on heat-treating from lower temperatures.

## 7.2 Suggestions for future work

The future work should be carried out on the following lines:

1. Detailed corrosion characterization by potentiostatic method.
2. Evolution of a standardized procedure for preparing specimens for weight loss studies
3. Detailed characterization of corrosion behaviour in 10%  $\text{NH}_4\text{Cl}$  and 10%  $(\text{NH}_4)_2\text{SO}_4$  and other solutions.
4. Arriving at the most useful composition based on the optimization technique.

## REFERENCES

1. Campbell, H.S., 'Metallurgical factors' , Hand-book of corrosion testing and evaluation, Corrosion monograph series, Ed. Ailor, W.H., etal., Reynold metals co., Virginia (USA), 1971, p.5.
2. Butlef and Ison, 'Corrosion and its prevention in water', Leonard hill, London.
3. Collins, H.H., 'Graphitic corrosion of cast iron', BCIRA Jour., 10, No. 5, 543 (1962).
4. Cleary, H.J. and Greene, N.D., 'Corrosion properties of iron and steel', Corrosion science, vol. 7, 1967 pp. 821-831.
5. Yang, W. and Pourbaix, A., 'Effect of Cr and Mo on the propagation of localized corrosion of steels', Met. Abs., 8212 - 72 -0550, Metallic corrosion, vol. 1.
6. 'Corrosion', edited by L.L.Shreir, Newnes-Butterworths, London, vol. 1, 1976, p 3:86, 8:123.
7. Hurst, J.E., and Piley, R.V., JISI, 155, 172, (1947).
8. Dumitsescu, T., Medeleanu, V., Nicolaid, M. and Dinu, I., Rev. Metall. (Roumania),3 No. 2, 19 (1958).
9. Metals Hand-book vol. 1, 9th edition, ASM, Metals park, Ohio, 'Properties and selection; Irons and steels', 1978, pp. 76.
10. Jackson, R.S., JISI, 208, 163 - 167 (1970).
11. Kutner, C., Tech. Mitt. Krup., No. 1, March 17 (1933).
12. Metals Hand-book, vol. 1, 8th edition (1964), 402.

13. Corrodur Bergit, Bergischer, Stahl Industries, Remscheid, Germany (1957), pp. 19-34.
14. Ni-resist austenitic cast irons : Properties and applications, International Nickel co. In corp., 1965, pp. 1-21.
15. Craig, B.D. and McCLYMONDS, L.A., 'A potentiometric study of the corrosion of Ni-resist in sea water', Corrosion, vol. 37, No. 8 August, 1981, p-485.
16. Hoar, T.P., J. Appl. Chemistry, 11, 121 (1961).
17. Vernon, W.H.J., 'The conservation of natural resources', Instn. of Civil Engineers, London, 105 (1957).
18. Potter, E.C., Electrochemistry, Cleaver Hume, London, 231 (1956).
19. Uhlig, H.H. (Ed.), The corrosion Hand-book, wiley, New York and chapman and Hall, London (1948).
20. Uhlig, H.H., Corrosion and corrosion control, wiley, New York (1971).
21. Fontana, M.G. and Greene, N.D., Corrosion Engineering, McGraw-Hill (1967).
22. Fontana, M.G. and Stachle, R.W., 'Advances in corrosion science and technology', Plenum Press, New York (1970).
23. Evans, U.R., 'The corrosion and oxidation of metals : Scientific principles and practical applications', Edward arnold (publishers) Ltd., London, 12 (1960).

24. Webster's third new international dictionary, G and C Merriam Co., Springfield, Mass., 1966, p-512.
25. Narain, S. and Sharan, R., 'An introduction to electrometallurgy', March 1969, pp. 117 - 144.
26. Pludek, V.R., 'Design and corrosion control', 1977, pp. 16 - 33.
27. Levin, I.A., 'Intercrystalline corrosion and corrosion of metals under stress', Leonard hill (Boods) Ltd. London, 1963.
28. Kolotyrkin, JA.M., 'Pitting corrosion of metals', 2nd international congress on metallic corrosion, New York, N.Y., March 11 - 15, 1963, pp. 23 - 30.
29. Kotaro Ogura and Noriyaki Takesue, 'Pit formation in the cathodic polarization of passive iron', corrosion, Sept. 1980, vol. 36, NO. 9, p-487.
30. Symposium on stress corrosion cracking, ASTM publication (1945).
31. Pickering, H.W., Beak, F.H., Fontana, M.G., Corrosion 1962, 18, 230.
32. NACE Basic corrosion course, official publication, 4 - 11, K.G. compton university of Miami, FLA.
33. Rosenfeld, I.L. and Marshakov, I.K., 'Mechanism of crevice corrosion', 2nd international congress on metallic corrosion, New York, N.Y., March 11 - 15, 1963, pp. 244 - 255.

34. Roy JOHNSEN and EINAR BARADAL, 'Cathodic properties of different stainless steels in natural sea water', corr., May 1985, Vol.41, No. 5, page 296.
35. Van LOO, M., Laiderman, D.D., Brukin, R.R., Corrosion 1953, 9 (8) 277.
36. Slabaugh, W.H., Morris Grother, Industrial engineering chemistry, 1954, 46 (5), 1014.
37. Uhlig, H.H., Proceedings of conference-fundamental aspects of stress corrosion cracking - Published by NACE, 1969, 86.
38. Chemistry and Industry, September, 1957, 1190.
39. Fitzgerald Lee, G., Corrosion technology, Nov. 1959, 330.
40. Speller, F., Corrosion, McGraw-Hill, London, (1951).
41. Antondes, Brasunas and Norman Hammer.
42. Patwardhan, A.K., Personal communication.
43. Pickering, F.B., 'Physical metallurgy and design of steels', 1978.
44. Uhlig, H.H., 'Effect of metal composition and structure on corrosion and oxidation', 2nd international conference on metallic corrosion, New York, 1963. pp. 1-7.
45. Uhlig, H.H., 'In relation of properties of microstructure' ASM Transactions, pp. 189 - 208, clevelend, ohio (1954).

46. Rohrig, K., 'Gejuge and Bestanligkeit gogen mineralverschluss cor. carbide schem gusseisen', Gisserei, 58, 1971, pp. 697-705.
47. Boniszewski, T., Wathinson, F., 'Metals and materials', 7(2), 7(3), 90, 145 (1973).
48. Benson, R.B., Jr., Dann, R.K. and Roberts, L.W., 'Hydrogen embrittlement of stainless steels', Trans. Met. Soc. AIME, vol 242, p. 2199 - 2205 (1966).
49. Steigerwald, R.f., 'The effect of metallic second phase in stainless steels', corr., vol. 33, No. 9, 1977, pp. 338-342.
50. Krauss, G. and Marder, A.R., 'The morphology of martensite in iron alloys', Met. Trans., 2. 2345 (1971).
51. Snape, E., Schaller, F.W. and Forbesjones, R.M., 'A method of improving hydrogen sulfide accelerated cracking resistance of low alloy steels', Corr., vol. 25, No. 9, Sept. 1969, p-380.
52. Lena, A., Metals progress, 66, pp. 97-99 (1954).
53. Michael, L. Streicherg, 'Micro-structure and some properties of Fe- 28%Cr- 4%Mo alloys', corrosion, vol. 30, No. 4, April 1974.
54. Hochman, R.F., NACE Basic corrosion course, official publica- tion, Chapter 11, pp. 3-18, Univ. of miami, FLA.
55. 'Influence of Mo and P on the stress corrosion resistance of austenitic stain less steels', Met. Abs., vol. 16, April 1985.



56. Gainer, L.J. and Wallwork, G.R., 'The effect of nonmetallic inclusions on the pitting of mild steel, Corr., Oct. 1979, vol. 35, No. 10, p-435.
57. Biom, K.J. and Degerbeck, J., 'Low Mn stainless steels of the 316 type', vol. 16, Oct. 1983, Metals abstracts, Pulp and paper Industry corrosion problems, vol. 4.
58. Firivkusm, Z.P., and Uhlig, H.H., J. Electrochem. SOC., 111, 522 (1964).
59. Bain, E.C., and Paxton, H.W., Alloying elements in steels', ASM, Metals Park, Ohio, 1962.
60. Metals Handbook volume 10, 8th edition, 'Failure analysis and prevention', ASM, Metals Park Ohio, 1975.
61. Lakhtin, Y., Physical metallurgy for engineers, MIR Publication, Moscow.
62. Dundas, H.T. and Bond, A.P., 'Effect of variation of Cu, Mo and Cr on corrosion of austenitic stainless steels', vol. 15, Metals abstracts, Jan. 1982.
63. Wranglen, G., 'An introduction to corrosion and protection of metals', Institute for Metallskydd, Fack 10041., Stockholm, 26, 1972, 13.
64. Yang, W. and pourbaix, A., 'Effect of Cr and Mo on the propagation of localised corrosion of steels', Met. Abstracts, 8212 - 72 - 0550, Metallic corrosion, 8th international congress on metallic corrosion, vol. 1.

65. Pearce, J.G., and Bromage, K., 'Copper in cast iron', C.D.A. Publication, No. 65, Hutchinson of London for the copper Development Association, 1964, pp. 61 - 64.
66. Singh, S.S., Ph.D. Thesis, university of Roorkee, 1982.
67. Higgin, R.A., 'Engineering metallurgy, Part 1,' the english university press Ltd., London, pp. 246 - 262.
68. Angus, H.T., 'Cast iron', Butterworths, London, 1976, p-53.
69. G-1-72, Standard Recommended practice for preparation, cleaning and evaluating corrosion test specimens, Annual book of ASTM standards, Part 10, Philadelphia, 1978.
70. G.31, Standard Recommended practice for preparation, cleaning and evaluating corrosion test specimens, Annual book of ASTM standards, Part 10, Philadelphia, 1978.
71. Greene, N.D., Experimental electrode kinetics, Ressenlaer polytechnic institute, Troy, New York (1965).
72. Himmelblau, D.M., 'Applied nonlinear programming', McGraw-Hill book company, 1972.
73. Nonlinear programming 2, edited by Mangasarian, O.L., Meyer, R.R., and Robinson, S.M., Academic Press, Inc., New York, San Francisco, London, 1975.
74. Bolten, J.D., Petty, E.R., and Allen, G.B., Met. Trans. 2 (10), 2915 (1971), 'The mechanical properties of  $\alpha$ -phase low-carbon Fe-Mn alloys'.

75. Patwardhan, A.K., 'Development and mechanical properties of as-rolled extra low-carbon Fe-4Mn-1.0 Si HSLA "MAR" steels' Int. conf. on technology and applications of HSLA steels, 1, Philadelphia, Pennsylvania, October 1983.
76. WHITE, C.H., and Honeycombe, R.W.K., 'Structural changes during the deformation of high purity Fe-Mn-C alloys', JISI, 200, 1962, p. 457.
77. 'Nickel as an alloy in cast irons', A.F.S. Current information Report, 1977, pp. 1-16.
78. Copley, S.M. and Kear, B.H., 'Temperature and orientation dependence of the flow stress in off-stoichiometric Ni<sub>3</sub>Al ( $\gamma$  phase)', Trans. AIME, 1967, V. 239, 977.
79. Copley, S.M. and Kear, B.H., 'A dynamic theory of coherent precipitation hardening with application to Nickel base super alloys', Trans. AIME, 1967, V. 239, 984.
80. Bolton, J.D., Petty, E.R., and Allen, G.B., JISI, 209, 1314 (1969).
81. Orowan, E., 'Symposium on internal stresses in metals and alloys', 451 (1948).
82. Smallman, R.E., 'Modern physical metallurgy', Third edition, Butterworths London, 1970, pp. 405-459.
83. Reiss, M., Rosenthal, P.C., Loper, C.R., and Heine, R.W., 'Sn and Cu in malleable iron', AFS Transactions, 79, 1971, p-565.

84. Burgess, P.B., AFS Transactions, 71, 1963, p-477.
85. Pearce, J.G. and Bromage, K., 'Copper in Cast iron', Copper development association, London, 1964, pp. 41-43.
86. Ref. 85, pp. 41-43.
87. Heine, R.W., and Rosenthal, P.C., 'Principles of metal casting', McGraw-Hill, New York, 1967.
88. Burke, J., 'The kinetics of phase transformation in metals,' Pergamon Press, 1965, pp. 93-98.
89. Wagner, C., Z. Electrochem. 65(61) 581.
90. Goldschmidt, H.J., 'interstitial alloys', London, Butterworths, 1967, p-96.
91. Powell, G.L.F. and Heard, L.S., 'Misinterpretation of microstructure in wear resistant alloy white irons', BCIRA, Jan 1983, 31/111.
92. Metals Hand Book, 'Metallography, structures and phase diagrams', vol. 8, 8th edition, 1973, pp. 402-408.
93. Tomashov, N.D., and Chernova, G.P., 'Passivity and protection of metals against corrosion', PLENUM Press, New York, 1967, pp. 71-74.
94. Kumar, S.; Personal Communication.
95. Sharma, J.D.; Personal Communication.

**TABLE - 1.1 RANGES OF ALLOY CONTENT FOR VARIOUS TYPES OF ALLOY CAST IRONS**

Description	TC(b)	Mn	P	S	Composition, wt % (a)			Cr	Mo	Cu	Matrix structure, as-cast(c)
					Si	Ni	Cu				
<b>Corrosion-Resistant Irons</b>											
High silicon iron(Ω)	0.4 to 1.1	1.5	0.15	0.15	14 to 17	...	5.0	1.0	0.5	F	
High chromium iron	1.2 to 4.0	0.3 to 1.5	0.15	0.15	0.5 to 3.0	5.0	12 to 35	4.0	3.0	M, A	
Nickel-chromium gray iron(g)	3.0	0.5 to 1.5	0.08	0.12	1.0 to 2.8	13.5 to 36	1.5 to 6.0	1.0	7.0	A	
Nickel-chromium ductile iron(h)	3.0	0.7 to 4.5	0.08	0.12	1.0 to 3.0	18 to 36	1.0 to 5.5	1.0	...	A	

**TABLE - 1.2 TYPICAL MECHANICAL PROPERTIES OF CORROSION-RESISTANT CAST IRONS**

Type of iron(a)	Hardness, HB	Tensile strength		Compressive strength		Impact energy	Transverse breaking load(b)		Transverse deflection(b)		
		MPa	ksi	MPa	ksi		J	ft · lb	kg	lb	mm
High-silicon iron	480 to 520	90 to 180	13 to 26	690	100	2.7 to 5.4(c)	2 to 4(c)	545 to 1000	1200 to 2200	0.65	0.026
High-chromium iron	250 to 740	205 to 830	30 to 120	690	100	0.1 to 3(d)	0.1 to 2(d)	910 to 2000	2000 to 3500	1.5 to 3.8	0.06 to 0.15
High-nickel gray iron	120 to 250	170 to 310	25 to 45	690 to 1100	100 to 160	27 to 47(c)	20 to 35(c)	1590	820 to 1800	5 to 25	0.20 to 1.00
High-nickel ductile iron	130 to 240	380 to 480	55 to 70	1240 to 1380	180 to 200	80 to 200(c)	60 to 150(c)	1590	3500	25	1.00

(a) For composition ranges, see Table 1. (b) For as-cast 30.5-mm (1.2-in.) diam bar broken over a 457-mm (18-in.) span. (c) Unnotched 30.5-mm diam test bar broken over a 152-mm (6-in.) span in a Charpy testing machine. (d) Standard Charpy.

TABLE -1.3(a) CHEMICAL COMPOSITION OF NI-RESIST IRONS, PERCENT

	Type 1' Aus 101a	Type 1B Aus 101b	Type 2' Aus 102a	Type 2B Aus 102b	Type 3 Aus 105	Type 4	Type 5
C	3.00 max	3.00 max	3.00 max	3.00 max	2.60 max	2.60 max	2.40 max
Si	1.00-2.80	1.00-2.80	1.00-2.80	1.00-2.80	1.00-2.00	5.00-6.00	1.00-2.00
Mn	1.00-1.50	1.00-1.50	0.80-1.50	0.80-1.50	0.40-0.80	0.40-0.80	0.40-0.80
Ni	13.50-17.50	13.50-17.50	18.00-22.00	18.00-22.00	28.00-32.00	29.00-32.00	34.00-36.00
Cu	5.50-7.50	5.50-7.50	0.50 max	0.50 max	0.50 max	0.50 max	0.50 max
Cr	1.75-2.50	2.75-3.50	1.75-2.50	3.00-6.00 <sup>3</sup>	2.50-3.50	4.50-5.50	0.10 max <sup>4</sup>

<sup>1</sup> Where the presence of copper offers corrosion-resistance advantages, Type 1 is recommended.

<sup>2</sup> For handling caustics, food, etc., where copper contamination cannot be tolerated, Type 2 is recommended.

<sup>3</sup> Where some machining is required, the 3.0-4.0 chromium level is recommended.

<sup>4</sup> Where higher hardness, greater strength and added heat resistance are desired, the chromium may be 2.5-3.0% at the expense of increased expansivity.

TABLE - 1.3 (b) CHEMICAL COMPOSITION OF SG NI-RESIST IRONS, PERCENT

	Type D-2 Aus 202a	Type D-2B Aus 202b	Type D-2C Aus 203	Type D-2M Aus 205	Type D-3 Aus 205	Type D-3A	Type D-4	Type D-5	Type D-5B
C	3.00 max	3.00 max	2.90 max	2.7 max	2.60 max	2.60 max	2.60 max	2.40 max	2.40 max
Si	1.75-3.00	1.75-3.00	2.0-3.0	1.5-2.6	1.50-2.80	1.50-2.80	5.0-6.0	1.50-2.75	1.50-2.75
Mn	0.70-1.0	0.70-1.0	1.80-2.40	3.75-4.50	0.50 max	0.50 max	0.50 max	0.50 max	0.50 max
P	0.08 max	0.08 max	0.08 max	0.08 max	0.08 max	0.08 max	0.08 max	0.08 max	0.08 max
Ni	18.0-22.0	18.0-22.0	21.0-24.0	21.5-24.0	28.0-32.0	28.0-32.0	29.0-32.0	34.0-36.0	34.0-36.0
Cr	1.75-2.50	2.75-4.0	0.50 max	0.2 max	2.50-3.50	1.00-1.50	4.50-5.50	0.10 max	2.0-3.0

TABLE - 1.4 MECHANICAL PROPERTIES OF NI-RESIST IRONS

	Type 1 Aus 101a	Type 1B Aus 101b	Type 2 Aus 102a	Type 2B Aus 102b	Type 3 Aus 105	Type 4	Type 5
Tensile Strength $\text{ton/in}^2$ ( $\text{kg/mm}^2$ )	11-13.5 (17-21)	11-15.5 (17-24)	11-13.5 (17-21)	11-15.5 (17-24)	11-15.5 (17-24)	11-15.5 (17-24)	9-11 (14-17)
Compressive Strength $\text{ton/in}^2$ ( $\text{kg/mm}^2$ )	44-53 (69-84)	44-53 (69-84)	44-53 (69-84)	58-71 (91-112)	44-50 (69-79)	36 (57)	36-44 (57-69)
Torsional Strength $\text{lb/in}^2 \times 10^3$ ( $\text{kg/mm}^2$ )	35-40 (25-28)	35-40 (25-28)	35-40 (25-28)	45-60 (32-42)	35-45 (25-32)	29 (20)	30-35 (21-25)
Torsional Modulus $\text{lb/in}^2 \times 10^4$ ( $\text{kg/mm}^2 \times 10^3$ )	4.5 (3.2)	4.5 (3.2)	4.5 (3.2)	5.5 (3.9)	5.0 (3.5)	4.0 (2.8)	4.5 (3.2)
Modulus of Elasticity $\text{lb/in}^2 \times 10^4$ ( $\text{kg/mm}^2 \times 10^3$ )	12-14 (8.4-9.8)	14-16 (9.8-11.2)	15-16.2 (10.5-11.4)	15-16.5 (10.5-11.6)	15-15.5 (10.5-10.9)	15 (10.5)	10.5 (7.4)
Permanent Set Point $\text{lb/in}^2$ ( $\text{kg/mm}^2$ )	3,000 (2.1)	3,000 (2.1)	3,000 (2.1)	3,000 (2.1)	3,000 (2.1)		
Transverse Properties (18 in) load— $\text{lb} \times 10^3$ ( $\text{kg} \times 10^3$ ) deflection— $\text{inch}$ ( $\text{cm}$ )	2.0-2.2 (0.9-1.0) 0.3-0.6 (0.8-1.5)	2.0-2.2 (0.9-1.0) 0.3-0.6 (0.8-1.5)	2.0-2.2 (0.9-1.0) 0.3-0.6 (0.8-1.5)	2.4-2.8 (1.1-1.3) 0.2-0.4 (0.5-1.0)	2.0-2.4 (0.9-1.1) 0.5-0.6 (1.3-1.5)	1.8 (0.8) 0.3-0.6 (0.8-1.5)	1.8-2.0 (0.8-0.9) 0.5-1.0 (1.3-2.5)
Vibration Damping	High	Medium	High	Medium	High	Medium	High
Capacity	12,000	12,000	12,000	18,000	13,500	9,000	9,900
Endurance Limit $\text{lb/in}^2$ ( $\text{kg/mm}^2$ )	(8.4)	(8.4)	(8.4)	(12.6)	(9.5)	(6.3)	(7.0)
Hardness Brinell	130-170	125-170	125-170	170-250	120-160	150-210	100-125
Toughness by Impact (Izod) $\text{ft. lbf} (\text{kgm})^*$	100 (14)	80 (11)	100 (14)	60 (8)	150 (21)	80 (11)	150 (21)

\* 1.2 inch (3 cm) diameter bar unnotched - struc. \ 3 inches (7.6 cm) above supports (Grey iron shows 25-35 ft-lbf (3.46-4.48 kgm))

TABLE - 1.5 CORROSION RESISTANCE OF NI-RESIST IRONS EXPRESSED  
IN INCHES PENETRATION PER YEAR (mm per year)

Corrosive Media	SG Ni-Resist Iron Type D-2C	SG Ni-Resist Iron Type D-2	Flake Graphite Type 2 Ni-Resist Iron
Ammonium chloride solution : 10% NH <sub>4</sub> Cl, pH 5.15, 13 days at 30°C 6.25 ft/min (1.9 m/min)	0.0280 (0.711)	0.0168 (0.427)	0.0095 (0.2413)
Ammonium sulphate solution : 10% (NH <sub>4</sub> ) <sub>2</sub> SO <sub>4</sub> , pH 5.7, 15 days at 30°C 6.25 ft/min (1.9 m/min)	0.0128 (0.325)	0.0111 (0.282)	
Ethylene Yapours & splash : 38% ethylene glycol, 50% diethylene glycol, 4.5% H <sub>2</sub> O, 4% Na <sub>2</sub> SO <sub>4</sub> , 2.7% NaCl, 0.8% Na <sub>2</sub> CO <sub>3</sub> + trace NaOH, pH 8 to 9, 85 days at 135-150°C	0.0023 (0.057)	0.0019* (0.048)	0.0013 (0.033)
Fertilizer : commercial 5-10-5*, damp, 290 days at atmospheric temperature	0.0062 (0.157)	0.0012 (0.030)	0.0025 (0.064)
Nickel chloride solution : 15% NiCl <sub>2</sub> , pH 5.3, 7 days at 30°C 6.25 ft/min (1.9 m/min)	0.213 (5.410)	0.0040 (0.102)	0.0040 (0.102)
Phosphoric acid : 85%, aerated at 30°C, Velocity 16 ft/min (4.9 m/min), 12 days	0.0023 (0.057)	0.235 (5.969)	0.087 (2.210)
Raw sodium chloride brine : 300 gpi of chlorides, 2.7 g/l CaO, 0.06 g/l NaOH, traces of NH <sub>3</sub> & H <sub>2</sub> S, pH 6-6.5, 61 days at 10°C, 0.1 to 0.2 ft/s (30-60 mm/s)	0.0023 (0.058)	0.0020* (0.051)	0.0020 (0.051)
Sea water at 26.6°C : 27°C, Velocity 27 ft/s (8.2 m/s), 60 days test	0.039 (0.991)	0.018 (0.457)	0.016 (0.406)
Soda & brine : 15.5% NaCl, 9.0% NaOH, 1.0% Na <sub>2</sub> SO <sub>4</sub> , 32 days at 80°C	0.0028 (0.071)	0.0015 (0.038)	0.0025 (0.064)
Sodium bisulphate solution : 10% NaHSO <sub>4</sub> , pH 1.3, 13 days at 30°C 6.25 ft/min (1.9 m/min)	0.0431 (1.095)	0.0444 (1.128)	0.0612 (1.545)
Sodium chloride solution : 5% NaCl, pH 5.6, 7 days at 30°C 6.25 ft/min (1.9 m/min)	0.0028 (0.071)	0.0019 (0.048)	0.0021 (0.053)
Sodium hydroxide : 50% NaOH + heavy conc. of suspended NaCl, 173 days at 55°C 40 gal/min (181.81 l/min)	0.0002 (0.005)	0.0002 (0.005)	0.00018 (0.0046)
Sodium hydroxide : 50% NaOH saturated with salt, 67 days at 95°C, 40 gal/min (181.81 l/min)	0.0009 (0.023)	0.0006 (0.015)	0.0006 (0.015)
Sodium hydroxide : 50% NaOH, 10 days at 128°C, 4 days at 21°C	0.0048 (0.122)	0.0049 (0.124)	0.0046 (0.117)
Sodium hydroxide : 30% NaOH + heavy conc. of suspended NaCl, 82 days at 85°C	0.0004 (0.010)	0.0005 (0.013)	0.0004 (0.010)
Sodium hydroxide : 74% NaOH, 193 days at 128°C	0.005 (0.127)	0.0056 (0.142)	0.006 (0.15)
Sodium sulphate solution : 10% Na <sub>2</sub> SO <sub>4</sub> , pH 4.0, 7 days at 30°C, 6.25 ft/min (1.9 m/min)	0.0136 (0.345)	0.0130 (0.330)	0.0132 (0.335)
Sulphuric acid : 5% at 30°C aerated, Velocity 14 ft/min (4.3 m/min), 4 days	0.120 (3.048)	0.104 (2.642)	0.112 (2.845)
Synthesis of sodium bicarbonate by Solvay process : 44% solid NaHCO <sub>3</sub> , slurry plus 200 g/l NH <sub>4</sub> Cl, 100 g/l NH <sub>4</sub> HCO <sub>3</sub> , 80 g/l NaCl, 8 g/l NaHCO <sub>3</sub> , 40 g/l CO <sub>2</sub> , 64 days at 30°C	0.0009 (0.023)	0.0003 (0.008)	0.0006 (0.015)
Tap water : aerated, Velocity 16 ft/min (4.9 m/min), 28 days	0.0015 (0.038)	0.0023 (0.058)	0.0045 (0.114)
Vapour above ammonia liquor : 40% NH <sub>3</sub> , 9% CO <sub>2</sub> , 51% H <sub>2</sub> O, 109 days at 85°C, low velocity	0.011 (0.279)	0.025 (0.635)	0.017 (0.432)
Zinc chloride solution : 20% ZnCl <sub>2</sub> , pH 5.25, 13 days at 30°C, 6.25 ft/min (1.9 m/min)	0.0125 (0.318)	0.0064 (0.163)	

\* Contains 1% chromium



TABLE-1.6 MECHANICA PROPERTIES OF SG NI-RESIST IRONS

	Type D-2 Aus 202a	Type D-2B Aus 202b	Type D-2C Aus 203	Type D-3 Aus 205	Type D-3A	Type D-4	Type D-5	Type D-5B
Tensile Strength <i>ton/in<sup>2</sup> (kg/mm<sup>2</sup>)</i>	24-30 (38-47)	26-31 (41-49)	24-29 (38-46)	24-30 (38-47)	24-29 (38-46)	27-32 (43-50)	24-27 (38-43)	24-29 (38-46)
Yield Strength (2% Offset) <i>ton/in<sup>2</sup> (kg/mm<sup>2</sup>)</i>	14-16 (22-25)	14.5-16.5 (23-26)	13.5-15.5 (21-24)	14.5-16.5 (23-26)	14-17 (22-27)	17-20 (27-32)	13.5-16.5 (21-26)	16.5-19 (26-30)
Elongation, % on 2 in (5.1 cm)	8-20	7-15	20-40	7-18	13-18	1.5-4.0	20-40	5-10
Proportional Limit <i>ton/in<sup>2</sup> (kg/mm<sup>2</sup>)</i>	7.3-8.3 (11.6-13.0)	7.1-8.5 (11.2-13.4)	5.4-7.1 (8.4-11.2)	7.1-8.5 (11.2-13.4)	6.7-8.5 (10.5-13.4)	5.4-7.1 (8.4-11.2)	4.2-4.9 (6.7-7.7)	4.7-5.8 (7.4-9.1)
Modulus of Elasticity <i>lb/in<sup>2</sup> x 10<sup>6</sup> (kg/mm<sup>2</sup> x 10<sup>3</sup>)</i>	16.5-18.5 (11.6-13.0)	16.5-19 (11.6-13.4)	15 (10.5)	13.5-14.5 (9.5-10.2)	16-18.5 (11.2-13.0)	13 (9.1)	16-20 (11.2-14.1)	16-17.5 (11.2-12.3)
Hardness Brinell	140-200	150-210	130-170	140-200	130-190	170-240	130-180	140-190
Impact ft-lb/(kgm/cm <sup>2</sup> ) Charpy V-notch Room Temperature	12 (2.075)	10 (1.73)	28 (4.84)	7 (1.21)	14 (2.42)		17 (2.94)	6 (1.04)

Table 2.1 FORMS OF CORROSION (1, 6, 25, 26)

Sl. No.	Form of corrosion	Appearance/characteristics	Cause(s)	General Remarks
1.	Uniform	Smooth exposed surface, occurs on a wider scale	Highly heterogeneous active surface presented to the environment.	Coating and cathodic protection may prevent the corrosion in steel tanks.
2.	Galvanic (21) (i) two metal (ii) differential concentration (iii) differential stress (iv) differential temperature (v) differential aeration	Localised attack	(i) Potential difference between two dissimilar metals or two different phases in a material (ii) Regions with different stress concentration (b) temperature and concentration of solution lead to the formation of anode and cathode.	Depending on the conductivity of solution, attack is max <sup>m</sup> at the junction and decreases with increasing distance from the junction.
3.	Intergranular (21, 27)	Intergranular	(i) Presence of impurities at grain boundaries and (ii) absorption of element to grain boundaries leading to precipitation and to simultaneous depletion of corrosion preventing elements from areas adjacent to G.B.	Occurs in austenitic and martensitic stainless steels and can be minimized by rapid cooling through critical range.

4. Selective dissolution  
 (a) Dezincification (21)  
 (b) Graphitization
- Observable with naked eye  
 No Characteristic appearance; superficial rusting observed
- Dezincified portion is weak porous and permeable Ferritic matrix attacked leaving iron; porous and weak graphite mass/residue
- Occurs in brasses; mechanical strength reduced  
 Occurs in flake type cast mechanical strength reduced
5. Pitting
- Dotted, Saucershaped honeycombed surface, intergranular pits.
- (i) Concentration of aggressive anions more than a critical value. (ii) adsorptive anions on the surface of the passive film which penetrate through the film (28,29).
- may be prevented by reducing the absolute and relative concn of aggressive anions, and by increasing the strength of the metal bond with the passivating oxygen (28).
6. Stress corrosion Cracking (21,30,31)
- Combination of intergranular and transgranular cracking, fine cracks propagation through the material may nucleate at grain or twin boundaries, surface inclusions and slip steps.
- (i) Presence of tensile stresses at the surface or sub surface. (ii) Environment specific to a material.
- Remove tensile stress or maintain stress level below the threshold value (KISCC).
7. Layer corrosion or exfoliation
- Ruptured surface
- Pressure developed by intergranular product in the banded region causing bursting of the skin.
- Slight overaging of artificially aged alloy will eliminate susceptibility to exfoliation (32).
8. Cavitation (19-21)
- Closed spaced pitted areas.
- Wearing away of metal due to repeated impacted blows by the formation and collapse of voids/bubbles within a fluid.
- metal is severely deformed and in some areas, the metal is torn away from the matrix and any corrosion resistant film previously formed is rapidly removed.

9. Erosion (19-21)  
 Like grooves, gullies, waves, rounded holes and usually exhibits a directional pattern.  
 Relative movement between fluid and metal surface, turbulent flow and galvanic effect under moving cond.n.  
 Rate of attack accelerates due to relative movement and metal is removed from the surface as dissolved ions or as solid corrosion products.
10. Crevice (21)  
 Localised form of attack  
 Insignificant differences in potentials of metal in the crevice and that of metal outside the crevice; another des are the metals in the crevice (33).  
 May be reduced by cathodic protection in stainless steels (34), by removing solid in suspension alloys which are corrosion resistant due to oxide film formation are susceptible
11. Filiform (21,35,36)  
 Thread like (filamental)  
 High oxygen concentration difference between head and tail of filament at the surface and high humidity (65-95%)  
 Occurs in Cr plated automobile hardware and tool coated with a film of oil.
12. Hydrogen damage (i) Blistering (21,37)  
 Complete destruction of vessel walls; local deformation  
 Formation of molecular hydrogen which can not diffuse leading to a pressure build up within voids at grain boundaries.  
 Occurs in Ni base alloys due to very low hydrogen diffusion rate.
- (ii) H<sub>2</sub> embrittlement (21,37)  
 Like brittle fracture  
 H<sub>2</sub> penetration in a metal results in a loss of ductility and tensile strength; slip interference by dissolved hydrogen.  
 Occurs in Ti and strong hydride forming metals, dissolved H<sub>2</sub> forms brittle hydride compounds.

Table 2.2 PROCESS RELATED PARAMETER AFFECTING CORROSION RATE

PARAMETERS	EFFECT ON CORROSION RATE
1. Increase in the rate of formation of corrosion cell.	Increases
2. Increase in the efficiency of corrosion cell.	Increases
3. Corrosive media	
(i) dissolved oxygen, salt and acid in water.	Increases
(ii) Moisture and solid particles in air.	Increases
4. Increase in temp. of corrosive environment (40).	Increased due to increased mobility of ions.
5. Pressure	depends on how the activity of elements affected.
6. Volume of corrosive media.	constt. upto a critical value and then decreases.
7. Agitation (2).	(i) Increases due to rupture of passive film.  (ii) Decreases as the mobility of metal ions hindered.
8. pH value	<4, decreases (acidity decreases). <9.5, >4, nearly constant. >9.5, <12, decreases again. >12, increases.
9. Shape of the specimen.	Increases when sharp corners, edges, and notches present.
10. Increase in size and surface area (32).	Decreases because anode area increases.
11. Test duration (32).	Decreases (linear behaviour, $Y = Kt$ ) upto a critical value and then increases (parabolic $Y = K \sqrt{t}$ ).
12. Radiation (41).	Increases slightly.

Table 2.3 Effect of alloying elements

Element	6.58 Ferrite stabilization	58 Austenite stabilization	59 Graphitization	58 Carbide forming tendency	Eutectoid carbon	Eutectoid temperature	59 Chill depth	59 Hardenability	58 Partitioning	59 Corrosion resistance	60 Heat resistance	Remarks
Al	↑↑	-	↑	-	-	-	<18Si	if dissolved	Al <sub>2</sub> O <sub>3</sub> , Al <sub>2</sub> N <sub>3</sub>	-	-	Modifies corrosion behaviour, much better sealing resistance than Fe & Si alloys, limited use due to brittleness and castability
B	↑	-	↑	↑	-	↑	<48Si	-	-	-	-	Provides resistance to inter-granular corrosion in Austenitic S.S., pitting resistance improves slightly.
C	-	↑	-	-	-	-	>48Si	-	-	-	-	Helpful in retaining high hardness at high temperatures by maintaining coherency
Co	-	↑↑	-	(Fe)	↑	-	<18Si	Mn	>Cb, Cr <sub>2</sub> O <sub>3</sub>	>12%Cr	-	CRS inclusions -> resistance to pitting and crevice corrosion improves.
Cr	↑	-	↑	↑ W<Cr<Wn	↑ S1	↑ S1	<48Si	When in solution pronounced (0.5-2.8%)	>0.8%Cr elemental	(3-10%Cr) (atmospheric CR)	-	Atmospheric corrosion resistance is improved.
Cu	-	↑ S1, 2%	↑	-	↑ S1	↑ S1	>48Si	>Cr	>Cb, MnS MnO, SiO <sub>2</sub>	helpful in reducing Ni	-	Mn<0.03% - pitting corrosion resistance improves, better C.R. to Austenitic Stainless Steel but poorer to high Si Irons.
Mn	-	↑↑	-	Cr<Wn>Fe	↑ CR	↑ CR	in presence of sulphur	-	-	-	-	Helpful in reducing temper-embrittlement, at high temperature applications (oxidising atmosphere)
Mo	↑↑	-	↑	↑↑>Cr	↑ S1	↑ S1	1/3 Cr	-	-	0.25-0.75 Mo for pitting I-4 (Cl ions)	-	Extremely helpful in preventing stress corrosion cracking in Austenitic Stainless Steels.
Nb	↑↑	-	↑	↑↑	↑ V	↑ V	-	-	-	-	-	Improves corrosion resistance and high temp. oxidation resistance by forming austenitic matrix.
Si	-	↑↑	↑	-	↑ S1	↑ S1	1/4 Si	-	.NiSi(7)Mn <sub>3</sub> Al	(14-36%)	-	Ni increases the ability of phosphorous to enhance corrosion.
P	↑↑	-	↑ mild	-	-	-	in presence of Mn	-	(Mn Fe) <sub>2</sub> S <sub>2</sub> S	-	-	Improves machinability but produces hot shortness.
S	↑	-	-	-	-	-	-	-	-	-	-	Helpful in designing corrosion resistant and oxidation resistant irons, only useful in presence of other alloying elements like Ni, Mn, Cr, Si, etc.
S1	↑↑	-	↑↑	-	↑ Wn	↑ Wn	-	>Ni	.SiO <sub>2</sub> W <sub>2</sub> O <sub>3</sub>	-	-	Phosphorous-induced embrittlement is reduced, useful in attaining secondary hardening (61).
Ti	↑↑	-	-	↑↑	↑ S1	↑ S1	-	-	.Cb, Ti <sub>2</sub> O <sub>3</sub>	-	-	Useful in attaining secondary hardening.
V	↑↑	-	↑↑	↑↑	↑ S1	↑ S1	-	Ti <sub>2</sub> O <sub>3</sub> , Ti <sub>2</sub> N <sub>3</sub>	-	-	-	Same as V but less effective.
W	↑	-	-	↑↑	↑ S1	↑ S1	-	.Cb, V <sub>2</sub> O <sub>5</sub> , V <sub>4</sub> N <sub>3</sub>	-	-	-	

TABLE-4.1 CHEMICAL ANALYSIS OF RAW MATERIALS

RAW MATERIAL	C	SI	P	S	MN	CR	CU
PIG IRON	3.55	2.15	0.40	0.050	1.12	.....	.....
FERRO CHROMIUM (LOW CARBON)	0.10 MAX	0.70 MAX	0.03 MAX	0.010 MAX	.....	67.0- 75.0	.....
FERRO MANGANESE (LOW CARBON)	0.03 MAX	.....	0.03 MAX	0.008	97.0	.....	.....
FERRO SILLICON (LOW CARBON)	0.03 MAX	75.0	.....	.....	.....	.....	.....
COPPER (ELECTROLYTIC)	.....	.....	.....	.....	.....	.....	99.99

TABLE-4.2 CHEMICAL ANALYSIS OF THE ALLOYS

ALLOY	C	S	P	SI	MN	CR	CU
B1	3.05	0.070	0.183	2.24	6.1	4.8	1.46
B2	2.90	0.065	0.173	2.14	7.5	4.8	1.48
B3	2.90	0.068	0.280	1.80	6.2	4.7	2.84
B4	2.85	0.072	0.305	1.80	7.3	4.5	2.86

## EFFECT OF SOAKING PERIOD ON HARDNESS IN O.O. CONDITION

ALLOY B1 AS CAST HARDNESS(HV30)= 594

TABLE-5.1 TEMP.(DEG.C) = 800

TIME (HRS)	HARDNESS (HV30)										SD	AVERAGE (HV30)
2	715	710	710	710	705	700	700	700	700	700	13.21	695
	695	695	695	690	690	685	685	685	680	657		
4	730	730	720	720	720	720	715	715	715	710	12.38	709
	710	710	700	700	700	700	695	695	690	690		
6	730	730	725	725	715	715	715	715	710	710	14.40	708
	705	705	705	705	700	700	700	700	685	671		
8	736	730	730	730	730	725	725	725	725	725	14.05	718
	725	720	720	720	715	710	700	695	695	685		
10	730	730	730	730	725	725	725	725	715	715	11.95	715
	715	715	710	710	710	710	705	705	700	685		

FOR DEGREE OF 1 COEFFICIENTS ARE

694.3000 2.4500  
 BEST FIT VALUES 699.2 704.1 709.0 713.9 718.8  
 STANDARD DEVIATION IS 4.9631975

FOR DEGREE OF 2 COEFFICIENTS ARE

682.8000 7.3786 -0.4107  
 BEST FIT VALUES 695.9 705.7 712.3 715.5 715.5  
 STANDARD DEVIATION IS 4.2493718

FOR DEGREE OF 3 COEFFICIENTS ARE

679.9995 9.3456 -0.7858 0.0208  
 BEST FIT VALUES 695.7 706.1 712.3 715.1 715.7  
 STANDARD DEVIATION IS 5.9761403

TABLE-5.2 TEMP.(DEG.C) = 850

2	568	564	557	557	557	554	550	550	550	547	8.94	548
	547	547	543	543	543	543	540	540	537	533		
4	644	639	631	631	631	626	626	626	626	622	10.68	622
	622	622	622	618	614	614	610	610	606	602		
6	635	631	631	626	626	626	626	626	622	618	14.18	616
	618	618	614	614	614	606	606	590	590	586		
8	631	626	626	626	626	626	626	626	626	622	10.19	617
	622	618	610	610	610	610	610	606	598	598		
10	695	685	680	680	675	675	671	671	666	666	14.06	665
	666	661	661	661	657	652	652	652	644	639		

FOR DEGREE OF 1 COEFFICIENTS ARE

544.9000 11.4500  
 BEST FIT VALUES 567.8 590.7 613.6 636.5 659.4  
 STANDARD DEVIATION IS 24.4206180

FOR DEGREE OF 2 COEFFICIENTS ARE

522.4000 21.0929 -0.8036  
 BEST FIT VALUES 561.4 593.9 620.0 639.7 653.0  
 STANDARD DEVIATION IS 28.6745260

FOR DEGREE OF 3 COEFFICIENTS ARE

344.5983 145.9774 -24.6163 1.3229  
 BEST FIT VALUES 548.7 619.3 620.0 614.3 665.7  
 STANDARD DEVIATION IS 5.6175753



## EFFECT OF SOAKING PERIOD ON HARDNESS IN O.O. CONDITION

ALLOY B1 AS CAST HARDNESS(HV30)= 594

TABLE-5.3 TEMP.(DEG.C) = 900

TIME (HRS)	HARDNESS (HV30)										SD	AVERAGE (HV30)
2	508	505	505	502	502	499	499	499	496	496	9.80	492
	493	490	487	484	484	484	481	481	478	478		
4	508	508	505	502	496	493	493	490	490	487	12.97	486
	487	484	481	478	478	476	470	470	470	467		
6	520	511	511	511	511	505	505	505	499	496	14.14	495
	493	490	490	490	484	484	484	478	473	470		
8	517	514	514	511	511	508	508	502	502	499	10.84	499
	496	496	496	496	496	493	493	484	484	478		
10	543	543	540	533	533	533	533	533	533	533	6.70	530
	530	530	530	530	530	523	523	523	523	517		

FOR DEGREE OF 1 COEFFICIENTS ARE

473.7000 4.4500  
 BEST FIT VALUES 482.6 491.5 500.4 509.3 518.2  
 STANDARD DEVIATION IS 11.4469770

FOR DEGREE OF 2 COEFFICIENTS ARE

508.2000 -10.3357 1.2321  
 BEST FIT VALUES 492.5 486.6 490.5 504.4 528.1  
 STANDARD DEVIATION IS 5.1492022

FOR DEGREE OF 3 COEFFICIENTS ARE

491.3994 1.4647 -1.0179 0.1250  
 BEST FIT VALUES 491.3 489.0 490.5 502.0 529.3  
 STANDARD DEVIATION IS 6.2151887

TABLE-5.4 TEMP.(DEG.C) = 950

2	508	508	502	502	502	499	496	493	490	490	11.02	489
	490	484	484	484	484	481	476	476	476	473		
4	502	496	493	490	487	487	484	484	484	484	9.83	481
	481	478	478	478	476	473	470	470	470	462		
6	487	487	484	481	478	476	476	473	473	473	8.33	471
	470	467	467	467	467	465	465	462	462	459		
8	496	490	487	487	487	487	484	484	484	484	6.73	481
	478	478	478	476	476	476	476	473	473	470		
10	496	493	490	487	487	484	484	481	481	473	11.12	476
	473	473	467	467	467	465	465	465	465	459		

FOR DEGREE OF 1 COEFFICIENTS ARE

487.4000 -1.3000  
 BEST FIT VALUES 484.8 482.2 479.6 477.0 474.4  
 STANDARD DEVIATION IS 6.0991805

FOR DEGREE OF 2 COEFFICIENTS ARE

500.4000 -6.8714 0.4643  
 BEST FIT VALUES 488.5 480.3 475.9 475.1 478.1  
 STANDARD DEVIATION IS 5.6264673

FOR DEGREE OF 3 COEFFICIENTS ARE

518.5997 -19.6545 2.9017 -0.1354  
 BEST FIT VALUES 489.8 477.7 475.9 477.7 476.8  
 STANDARD DEVIATION IS 6.8128008

## EFFECT OF SOAKING PERIOD ON HARDNESS IN O.O. CONDITION

ALLOY B1 AS CAST HARDNESS(HV30)= 594

TABLE-5.5 TEMP.(DEG.C) = 1000

TIME (HRS)	HARDNESS (HV30)										SD	AVERAGE (HV30)
2	473	473	462	459	451	451	451	449	449	449	9.92	449
	449	446	446	444	444	444	441	441	441	436		
4	446	446	441	439	439	439	439	436	434	432	7.32	433
	432	429	429	429	429	427	427	427	425	418		
6	409	406	406	404	402	402	398	393	391	391	7.19	394
	391	391	389	389	389	389	389	389	389	389		
8	398	398	398	393	393	391	391	387	387	387	7.51	386
	383	383	383	383	381	381	377	377	375	375		
10	379	368	368	368	364	362	349	349	346	346	13.87	349
	346	344	344	344	344	336	336	336	331	331		

FOR DEGREE OF 1 COEFFICIENTS ARE

476.3000 -12.3500  
 BEST FIT VALUES 451.6 426.9 402.2 377.5 352.8  
 STANDARD DEVIATION IS 8.1219870

FOR DEGREE OF 2 COEFFICIENTS ARE

470.8000 -9.9929 -0.1964  
 BEST FIT VALUES 450.0 427.7 403.8 378.3 351.2  
 STANDARD DEVIATION IS 9.7277212

FOR DEGREE OF 3 COEFFICIENTS ARE

479.2003 -15.8931 0.9286 -0.0625  
 BEST FIT VALUES 450.6 426.5 403.8 379.5 350.6  
 STANDARD DEVIATION IS 13.6256070

TABLE-5.6 TEMP.(DEG.C) = 1050

2	434	434	429	418	418	415	411	411	411	411	9.13	413
	411	409	409	409	409	406	406	406	404	404		
4	377	373	373	371	370	368	364	364	364	362	6.76	363
	362	362	360	360	360	360	358	355	355	351		
6	318	317	317	317	315	315	311	311	309	307	7.25	307
	307	307	305	305	305	304	299	297	297	295		
8	304	302	301	298	297	297	294	294	291	289	10.81	287
	289	285	282	277	277	277	276	274	272	272		
10	293	289	282	277	277	275	275	272	271	271	7.77	272
	271	271	271	269	268	266	266	266	264	264		

FOR DEGREE OF 1 COEFFICIENTS ARE

435.8000 -17.9000  
 BEST FIT VALUES 400.0 364.2 328.4 292.6 256.8  
 STANDARD DEVIATION IS 17.2317530

FOR DEGREE OF 2 COEFFICIENTS ARE

488.8000 -40.6143 1.8929  
 BEST FIT VALUES 415.1 356.6 313.3 285.0 271.9  
 STANDARD DEVIATION IS 6.6418585

FOR DEGREE OF 3 COEFFICIENTS ARE

473.3997 -29.7974 -0.1697 0.1146  
 BEST FIT VALUES 414.0 358.8 313.3 282.8 273.0  
 STANDARD DEVIATION IS 8.7251680

## EFFECT OF SOAKING PERIOD ON HARDNESS IN O.O. CONDITION

ALLOY B2 AS CAST HARDNESS (HV30) = 590

TABLE-5.7 TEMP. (DEG.C) = 800

TIME (HRS)	HARDNESS (HV30)										SD	AVERAGE (HV30)
2	626	622	622	618	618	618	618	618	618	618	10.75	612
	614	614	614	610	610	610	606	594	594	583		
4	652	648	648	648	648	639	639	639	639	635	12.22	632
	631	626	626	626	622	622	618	618	618	614		
6	652	648	648	648	648	644	644	644	644	644	8.75	639
	644	644	635	635	635	635	631	631	626	618		
8	671	671	671	666	666	666	661	661	661	661	10.42	657
	661	661	657	648	648	648	648	644	639	639		
10	680	680	680	680	675	675	671	671	671	671	8.48	668
	666	666	666	666	661	661	661	661	661	648		

FOR DEGREE OF 1 COEFFICIENTS ARE

600.5000 6.8500  
 BEST FIT VALUES 614.2 627.9 641.6 655.3 669.0  
 STANDARD DEVIATION IS 3.2812576

FOR DEGREE OF 2 COEFFICIENTS ARE

597.0000 8.3500 -0.1250  
 BEST FIT VALUES 613.2 628.4 642.6 655.8 668.0  
 STANDARD DEVIATION IS 3.7947308

FOR DEGREE OF 3 COEFFICIENTS ARE

588.6009 14.2494 -1.2499 0.0625  
 BEST FIT VALUES 612.6 629.6 642.6 654.6 668.6  
 STANDARD DEVIATION IS 5.0199602

TABLE-5.8 TEMP. (DEG.C) = 850

2	550	550	550	550	547	547	547	547	547	540	9.63	539
	537	537	533	533	533	533	533	523	523	523		
4	543	540	533	530	527	527	527	527	527	527	9.82	523
	523	523	520	520	517	517	517	508	508	505		
6	540	540	537	537	533	533	533	533	530	527	6.90	529
	527	527	527	527	527	527	523	523	517	514		
8	533	523	523	523	523	520	517	517	517	517	5.56	517
	517	517	514	514	514	514	511	511	511	511		
10	527	527	527	527	527	523	523	523	523	520	4.35	521
	520	520	517	517	517	517	517	517	517	514		

FOR DEGREE OF 1 COEFFICIENTS ARE

538.4000 -2.1000  
 BEST FIT VALUES 534.2 530.0 525.8 521.6 517.4  
 STANDARD DEVIATION IS 6.2289655

FOR DEGREE OF 2 COEFFICIENTS ARE

549.4001 -6.8143 0.3929  
 BEST FIT VALUES 537.3 528.4 522.7 520.0 520.5  
 STANDARD DEVIATION IS 6.3964291

FOR DEGREE OF 3 COEFFICIENTS ARE

557.8016 -12.7153 1.5181 -0.0625  
 BEST FIT VALUES 537.9 527.2 522.7 521.2 519.9  
 STANDARD DEVIATION IS 8.8446879

EFFECT OF SOAKING PERIOD ON HARDNESS IN O.O. CONDITION  
 -----  
 ALLOY B2 AS CAST HARDNESS(HV30)= 590

TABLE-5.9 TEMP.(DEG.C) = 900

TIME (HRS)	HARDNESS (HV30)										SD	AVERAGE (HV30)
2	508 496	505 496	502 496	502 496	502 493	499 493	499 490	499 490	499 490	496 484	5.75	496
4	511 499	508 499	508 499	505 496	505 496	505 496	502 493	499 487	499 487	499 487	6.95	499
6	511 499	508 499	505 496	505 496	502 496	502 493	499 490	499 484	499 484	499 484	7.57	497
8	508 496	508 496	508 496	505 496	502 493	499 493	499 493	499 490	496 487	496 481	6.97	497
10	508 496	508 496	502 493	502 490	502 490	499 490	499 490	499 487	499 487	499 487	6.64	496

FOR DEGREE OF 1 COEFFICIENTS ARE

497.6000 -0.1000  
 BEST FIT VALUES 497.4 497.2 497.0 496.8 496.6  
 STANDARD DEVIATION IS 1.3662605

FOR DEGREE OF 2 COEFFICIENTS ARE

494.6000 1.1857 -0.1071  
 BEST FIT VALUES 496.5 497.6 497.9 497.2 495.7  
 STANDARD DEVIATION IS 1.2305619

FOR DEGREE OF 3 COEFFICIENTS ARE

489.0002 5.1189 -0.8571 0.0417  
 BEST FIT VALUES 496.1 498.4 497.9 496.4 496.1  
 STANDARD DEVIATION IS 1.1952272

TABLE-5.10 TEMP.(DEG.C) = 950

2	493 481	487 481	487 481	487 478	484 478	484 478	484 476	481 476	481 476	481 470	5.14	481
4	470 457	467 454	467 454	465 454	465 451	465 451	462 449	462 449	459 449	457 444	7.50	457
6	467 449	465 449	462 449	462 449	457 449	457 446	454 446	454 446	454 441	451 441	7.43	452
8	467 449	465 449	465 449	459 446	459 439	457 436	454 436	451 434	451 434	451 434	10.90	449
10	470 444	465 441	459 441	457 441	457 439	454 439	446 439	446 439	446 436	446 434	10.03	446

FOR DEGREE OF 1 COEFFICIENTS ARE

480.4000 -3.9000  
 BEST FIT VALUES 472.6 464.8 457.0 449.2 441.4  
 STANDARD DEVIATION IS 7.6941535

FOR DEGREE OF 2 COEFFICIENTS ARE

502.4000 -13.3286 0.7857  
 BEST FIT VALUES 478.9 461.7 450.7 446.1 447.7  
 STANDARD DEVIATION IS 4.4336367

FOR DEGREE OF 3 COEFFICIENTS ARE

529.0000 -32.0119 4.3482 -0.1979  
 BEST FIT VALUES 480.8 457.9 450.7 449.9 445.8  
 STANDARD DEVIATION IS 1.7928438

EFFECT OF SOAKING PERIOD ON HARDNESS IN O.Q. CONDITION  
 -----  
 ALLOY B2 AS CAST HARDNESS(HV30)= 590

TABLE-5.11 TEMP.(DEG.C) = 1000

TIME (HRS)	HARDNESS (HV30)										SD	AVERAGE (HV30)
2	411	404	402	402	400	398	398	398	398	396	8.49	393
	393	391	389	387	387	387	385	385	383	377		
4	398	396	393	393	391	391	389	389	389	387	6.34	386
	385	385	385	383	381	379	379	379	377	377		
6	406	406	402	402	402	400	400	400	400	400	8.48	396
	400	400	398	398	393	391	387	387	385	371		
8	371	371	366	364	355	353	349	349	348	344	15.12	345
	344	344	343	343	333	331	331	331	328	314		
10	377	373	366	364	362	357	355	353	349	349	26.06	339
	346	336	336	331	321	308	305	305	299	293		

FOR DEGREE OF 1 COEFFICIENTS ARE  
 416.5000 -7.4500  
 BEST FIT VALUES 401.6 386.7 371.8 356.9 342.0  
 STANDARD DEVIATION IS 16.4387760

FOR DEGREE OF 2 COEFFICIENTS ARE  
 387.0000 5.1929 -1.0536  
 BEST FIT VALUES 393.2 390.9 380.2 361.1 333.6  
 STANDARD DEVIATION IS 16.7639060

FOR DEGREE OF 3 COEFFICIENTS ARE  
 347.8002 32.7261 -6.3035 0.2917  
 BEST FIT VALUES 390.4 396.5 380.2 355.5 336.4  
 STANDARD DEVIATION IS 21.9922070

TABLE-5.12 TEMP.(DEG.C) = 1050

2	371	368	366	366	364	364	360	358	358	358	4.91	359
	358	357	357	357	357	357	357	355	355	353		
4	355	355	344	339	334	333	333	333	333	331	9.28	332
	331	331	329	329	329	326	326	325	321	321		
6	362	353	351	351	351	346	346	346	344	343	9.14	342
	343	341	341	339	336	333	333	329	328	328		
8	314	314	308	307	307	304	304	304	304	302	5.76	302
	302	302	299	299	299	299	299	298	294	291		
10	299	298	297	295	295	295	295	293	291	291	7.63	289
	291	291	289	289	286	285	285	277	277	270		

FOR DEGREE OF 1 COEFFICIENTS ARE  
 375.8000 -8.5000  
 BEST FIT VALUES 358.8 341.8 324.8 307.8 290.8  
 STANDARD DEVIATION IS 11.9554730

FOR DEGREE OF 2 COEFFICIENTS ARE  
 364.8000 -3.7857 -0.3929  
 BEST FIT VALUES 355.7 343.4 327.9 309.4 287.7  
 STANDARD DEVIATION IS 14.0397410

FOR DEGREE OF 3 COEFFICIENTS ARE  
 378.8001 -13.6191 1.4822 -0.1042  
 BEST FIT VALUES 356.7 341.4 327.9 311.4 286.7  
 STANDARD DEVIATION IS 19.6017490

## EFFECT OF SOAKING PERIOD ON HARDNESS IN O.Q. CONDITION

ALLOY B3 AS CAST HARDNESS(HV30)= 652

TABLE-5.13 TEMP.(DEG.C) = 800

TIME (HRS)	HARDNESS (HV30)										SD	AVERAGE (HV30)
2	710 695	705 695	705 695	700 695	700 690	700 690	700 690	700 685	700 685	695 671	8.66	695
4	715 700	715 700	715 695	705 695	705 695	705 690	705 690	700 685	700 685	700 680	9.95	699
6	752 730	741 730	741 730	741 725	741 725	741 725	736 725	736 725	736 720	736 720	8.59	732
8	725 700	725 700	720 700	720 695	715 695	710 695	710 695	710 695	705 690	700 690	11.41	704
10	725 700	720 700	720 695	720 695	720 695	720 690	705 690	705 690	705 690	705 685	12.86	703

FOR DEGREE OF 1 COEFFICIENTS ARE

700.3000 1.0500  
 BEST FIT VALUES 702.4 704.5 706.6 708.7 710.8  
 STANDARD DEVIATION IS 16.4630880

FOR DEGREE OF 2 COEFFICIENTS ARE

664.8000 16.2643 -1.2679  
 BEST FIT VALUES 692.3 709.6 716.7 713.8 700.7  
 STANDARD DEVIATION IS 15.0503920

FOR DEGREE OF 3 COEFFICIENTS ARE

667.6005 14.2973 -0.8928 -0.0208  
 BEST FIT VALUES 692.5 709.2 716.7 714.2 700.5  
 STANDARD DEVIATION IS 21.2750700

TABLE-5.14 TEMP.(DEG.C) = 850

2	571 561	571 561	568 561	568 561	568 557	564 554	564 550	564 550	564 550	564 550	7.04	561
4	550 537	543 533	543 533	543 530	543 530	540 530	540 530	540 527	540 527	537 523	7.07	535
6	568 557	564 554	564 554	564 550	561 550	561 550	561 547	561 540	557 527	557 527	11.40	553
8	575 568	575 564	575 564	571 564	571 557	571 557	571 557	571 557	568 554	568 554	7.26	565
10	661 635	648 631	648 631	648 631	648 631	644 631	635 631	635 626	635 626	635 622	9.76	636

FOR DEGREE OF 1 COEFFICIENTS ARE

516.0000 9.0000  
 BEST FIT VALUES 534.0 552.0 570.0 588.0 606.0  
 STANDARD DEVIATION IS 30.1993370

FOR DEGREE OF 2 COEFFICIENTS ARE

610.0000 -31.2857 3.3571  
 BEST FIT VALUES 560.9 538.6 543.1 574.6 632.9  
 STANDARD DEVIATION IS 10.2817460

FOR DEGREE OF 3 COEFFICIENTS ARE

588.9999 -16.5356 0.5446 0.1563  
 BEST FIT VALUES 559.4 541.6 543.1 571.6 634.4  
 STANDARD DEVIATION IS 13.7451300

EFFECT OF SOAKING PERIOD ON HARDNESS IN O.O. CONDITION  
 -----  
 ALLOY B3 AS CAST HARDNESS(HV30)= 652

TABLE-5.15 TEMP.(DEG.C) = 900

TIME (HRS)	HARDNESS (HV30)										SD	AVERAGE (HV30)
2	511	499	499	499	496	493	493	493	490	487	8.03	490
	487	487	487	487	484	484	484	484	478	478		
4	496	496	496	496	493	493	493	490	487	487	8.26	486
	487	487	484	484	484	481	476	473	473	470		
6	499	493	493	490	490	487	487	484	481	481	9.70	480
	478	478	478	478	473	473	473	467	465	465		
8	502	499	499	496	496	493	490	490	484	484	9.37	485
	484	484	484	481	481	478	478	473	473	470		
10	499	496	496	496	496	493	493	490	490	487	8.80	487
	487	487	487	487	484	481	478	478	478	462		

FOR DEGREE OF 1 COEFFICIENTS ARE

487.7000 -0.3500  
 BEST FIT VALUES 487.0 486.3 485.6 484.9 484.2  
 STANDARD DEVIATION IS 4.0124814

FOR DEGREE OF 2 COEFFICIENTS ARE

499.2000 -5.2786 0.4107  
 BEST FIT VALUES 490.3 484.7 482.3 483.3 487.5  
 STANDARD DEVIATION IS 2.2928450

FOR DEGREE OF 3 COEFFICIENTS ARE

500.6002 -6.2621 0.5982 -0.0104  
 BEST FIT VALUES 490.4 484.5 482.3 483.5 487.4  
 STANDARD DEVIATION IS 3.2271163

TABLE-5.16 TEMP.(DEG.C) = 950

2	481	481	478	478	476	476	476	473	473	473	8.51	469
	470	470	467	465	462	462	459	457	457	454		
4	473	467	465	459	459	459	459	457	454	454	6.59	455
	454	454	454	454	451	451	451	449	449	446		
6	459	457	457	454	451	451	451	451	449	449	7.83	446
	449	446	441	439	439	439	439	436	436	434		
8	473	473	473	470	467	467	467	467	465	459	13.49	457
	459	459	459	457	457	446	441	434	434	432		
10	481	481	481	478	476	470	470	470	467	467	13.24	463
	467	457	457	454	454	454	449	446	441	441		

FOR DEGREE OF 1 COEFFICIENTS ARE

461.0000 -0.5000  
 BEST FIT VALUES 460.0 459.0 458.0 457.0 456.0  
 STANDARD DEVIATION IS 9.8319206

FOR DEGREE OF 2 COEFFICIENTS ARE

491.0000 -13.3571 1.0714  
 BEST FIT VALUES 468.6 454.7 449.4 452.7 464.6  
 STANDARD DEVIATION IS 4.0532179

FOR DEGREE OF 3 COEFFICIENTS ARE

505.0001 -23.1905 2.9464 -0.1042  
 BEST FIT VALUES 469.6 452.7 449.4 454.7 463.6  
 STANDARD DEVIATION IS 4.7809148

## EFFECT OF SOAKING PERIOD ON HARDNESS IN O.O. CONDITION

ALLOY B3 AS CAST HARDNESS(HV30)= 652

TABLE-5.17 TEMP.(DEG.C) = 1000

TIME (HRS)	HARDNESS (HV30)										SD	AVERAGE (HV30)
2	429	429	429	427	427	425	425	420	420	418	9.88	417
	418	418	418	413	411	411	409	406	398	396		
4	398	396	393	393	393	393	387	385	383	383	8.49	383
	381	381	379	377	377	375	375	375	373	370		
6	375	375	370	368	366	366	364	364	362	362	7.39	361
	362	360	360	357	355	353	353	353	351	351		
8	366	364	362	362	362	362	358	358	358	358	6.03	356
	358	358	357	355	353	353	349	348	348	343		
10	364	362	362	362	358	357	353	353	353	351	9.60	349
	349	349	349	346	341	341	339	337	334	334		

FOR DEGREE OF 1 COEFFICIENTS ARE

422.1000 -8.1500  
 BEST FIT VALUES 405.8 389.5 373.2 356.9 340.6  
 STANDARD DEVIATION IS 11.3710150

FOR DEGREE OF 2 COEFFICIENTS ARE

457.6000 -23.3643 1.2679  
 BEST FIT VALUES 415.9 384.4 363.1 351.8 350.7  
 STANDARD DEVIATION IS 3.7301866

FOR DEGREE OF 3 COEFFICIENTS ARE

477.1999 -37.1309 3.8928 -0.1458  
 BEST FIT VALUES 417.3 381.6 363.1 354.6 349.3  
 STANDARD DEVIATION IS 2.8685459

TABLE-5.18 TEMP.(DEG.C) = 1050

2	381	381	379	377	377	377	375	375	370	370	7.91	369
	368	366	366	366	362	362	362	358	358	358		
4	334	326	326	325	311	311	305	305	305	305	11.08	307
	305	304	301	301	301	301	299	297	297	297		
6	287	287	286	285	283	282	274	274	272	272	10.00	272
	272	272	265	265	264	263	263	263	257	257		
8	265	265	265	263	263	263	262	262	262	261	9.66	255
	256	255	252	251	251	243	250	244	243	230		
10	256	255	254	252	251	251	249	249	246	246	7.02	245
	246	246	245	244	244	242	239	238	231	231		

FOR DEGREE OF 1 COEFFICIENTS ARE

379.6000 -15.0000  
 BEST FIT VALUES 349.6 319.6 289.6 259.6 229.6  
 STANDARD DEVIATION IS 19.1763740

FOR DEGREE OF 2 COEFFICIENTS ARE

440.6001 -41.1429 2.1786  
 BEST FIT VALUES 367.0 310.9 272.2 250.9 247.0  
 STANDARD DEVIATION IS 4.4753292

FOR DEGREE OF 3 COEFFICIENTS ARE

468.6008 -60.8101 5.9287 -0.2083  
 BEST FIT VALUES 369.0 306.9 272.2 254.9 245.0  
 STANDARD DEVIATION IS 0.2390442



## EFFECT OF SOAKING PERIOD ON HARDNESS IN O.O. CONDITION

ALLOY B4 AS CAST HARDNESS(HV30)= 621

TABLE-5.19 TEMP.(DEG.C) = 800

TIME (HRS)	HARDNESS (HV30)										SD	AVERAGE (HV30)
2	594	594	594	590	590	590	590	590	586	586	6.98	585
	586	586	586	583	583	583	579	579	579	564		
4	626	626	626	626	626	622	622	622	622	622	8.92	616
	618	618	614	614	610	606	606	602	602	602		
6	657	657	652	652	652	652	648	648	644	644	6.41	645
	644	644	644	644	639	639	639	639	639	635		
8	652	648	648	644	644	644	639	639	635	631	11.17	632
	631	626	626	626	626	622	622	618	618	618		
10	661	661	661	657	657	657	652	652	648	648	12.13	645
	648	644	639	639	639	639	636	626	626	622		

FOR DEGREE OF 1 COEFFICIENTS ARE

583.8000 6.8000  
 BEST FIT VALUES 597.4 611.0 624.6 638.2 651.8  
 STANDARD DEVIATION IS 15.0510230

FOR DEGREE OF 2 COEFFICIENTS ARE

544.8000 23.5143 -1.3929  
 BEST FIT VALUES 586.3 616.6 635.7 643.8 640.7  
 STANDARD DEVIATION IS 11.0686170

FOR DEGREE OF 3 COEFFICIENTS ARE

505.6002 51.0475 -6.6428 0.2917  
 BEST FIT VALUES 583.5 622.2 635.7 638.2 643.5  
 STANDARD DEVIATION IS 12.9084680

TABLE-5.20 TEMP.(DEG.C) = 850

2	543	540	540	533	533	533	530	530	530	527	11.19	525
	527	523	523	520	520	517	514	508	505	505		
4	540	540	533	530	530	527	523	523	523	523	8.26	522
	520	520	520	517	517	514	514	514	514	514		
6	530	530	530	530	530	530	527	527	523	523	9.35	520
	523	520	517	514	514	514	508	505	505	505		
8	547	547	547	543	543	540	537	533	530	530	8.31	533
	530	530	530	530	527	527	527	523	523	523		
10	527	527	523	523	520	520	517	517	514	511	8.74	512
	511	508	508	505	505	505	502	502	502	502		

FOR DEGREE OF 1 COEFFICIENTS ARE

526.9000 -0.7500  
 BEST FIT VALUES 525.4 523.9 522.4 520.9 519.4  
 STANDARD DEVIATION IS 8.3805331

FOR DEGREE OF 2 COEFFICIENTS ARE

516.4000 3.7500 -0.3750  
 BEST FIT VALUES 522.4 525.4 525.4 522.4 516.4  
 STANDARD DEVIATION IS 9.4657274

FOR DEGREE OF 3 COEFFICIENTS ARE

565.4003 -30.6669 6.1875 -0.3646  
 BEST FIT VALUES 525.9 518.4 525.4 529.4 512.9  
 STANDARD DEVIATION IS 7.5299383

## EFFECT OF SOAKING PERIOD ON HARDNESS IN D.Q. CONDITION

ALLOY B4 AS CAST HARDNESS(HV30)= 621

TABLE-5.21 TEMP.(DEG.C) = 900

TIME (HRS)	HARDNESS (HV30)										SD	AVERAGE (HV30)
2	499	499	490	490	487	487	487	484	484	484	8.25	482
	478	478	478	478	478	476	473	473	473	470		
4	490	490	487	487	484	484	484	481	481	476	9.10	476
	476	476	473	473	473	470	465	465	465	459		
6	478	476	476	476	473	473	470	470	467	467	9.40	466
	467	465	465	465	465	465	454	457	454	439		
8	478	478	478	478	476	476	476	473	470	470	8.54	468
	470	467	467	467	465	465	462	462	454	446		
10	496	484	484	481	481	481	481	481	481	478	8.04	476
	476	476	470	470	470	470	467	467	465	465		

FOR DEGREE OF 1 COEFFICIENTS ARE

479.6000 -1.0000  
 BEST FIT VALUES 477.6 475.6 473.6 471.6 469.6  
 STANDARD DEVIATION IS 6.6131182

FOR DEGREE OF 2 COEFFICIENTS ARE

499.6000 -9.5714 0.7143  
 BEST FIT VALUES 483.3 472.7 467.9 468.7 475.3  
 STANDARD DEVIATION IS 2.9081167

FOR DEGREE OF 3 COEFFICIENTS ARE

485.5999 0.2620 -1.1607 0.1042  
 BEST FIT VALUES 482.3 474.7 467.9 466.7 476.3  
 STANDARD DEVIATION IS 2.6295024

TABLE-5.22 TEMP.(DEG.C) = 950

2	465	457	457	457	454	454	454	454	454	451	9.71	447
	449	446	446	444	439	439	439	439	429	429		
4	451	449	446	446	446	446	446	446	444	444	7.84	441
	444	444	444	441	439	439	439	432	422	422		
6	451	449	449	446	446	441	441	441	441	439	5.50	440
	439	439	439	436	436	434	434	434	434	434		
8	459	451	449	449	449	446	446	446	446	446	6.56	443
	444	444	444	444	439	439	434	434	434	434		
10	459	459	457	457	457	451	451	451	446	446	10.22	444
	444	441	441	439	436	434	434	432	432	427		

FOR DEGREE OF 1 COEFFICIENTS ARE

444.2000 -0.2000  
 BEST FIT VALUES 443.8 443.4 443.0 442.6 442.2  
 STANDARD DEVIATION IS 3.0767952

FOR DEGREE OF 2 COEFFICIENTS ARE

453.2000 -4.0571 0.3214  
 BEST FIT VALUES 446.4 442.1 440.4 441.3 444.8  
 STANDARD DEVIATION IS 1.6212888

FOR DEGREE OF 3 COEFFICIENTS ARE

463.0005 -10.9408 1.6340 -0.0729  
 BEST FIT VALUES 447.1 440.7 440.4 442.7 444.1  
 STANDARD DEVIATION IS 0.5976148

## EFFECT OF SOAKING PERIOD ON HARDNESS IN O.O. CONDITION

ALLOY B4 AS CAST HARDNESS(HV30)= 621

TABLE-5.23 TEMP.(DEG.C) = 1000

TIME (HRS)	HARDNESS (HV30)										SD	AVERAGE (HV30)
2	418	418	418	418	413	413	411	411	411	409	6.54	408
	409	406	404	404	404	404	402	402	398	398		
4	400	389	387	385	383	381	379	377	377	377	9.78	375
	373	373	370	368	368	368	366	366	364	362		
6	383	377	377	377	377	375	375	375	368	366	7.78	368
	366	364	364	364	362	362	360	360	358	358		
8	366	366	366	362	358	358	358	357	357	357	10.63	352
	355	355	349	349	349	348	339	339	331	331		
10	366	364	358	357	357	357	349	349	348	346	10.00	347
	344	344	344	343	341	339	339	337	331	331		

FOR DEGREE OF 1 COEFFICIENTS ARE

413.5000 -7.2500  
 BEST FIT VALUES 399.0 384.5 370.0 355.5 341.0  
 STANDARD DEVIATION IS 8.6313381

FOR DEGREE OF 2 COEFFICIENTS ARE

437.0000 -17.3214 0.8393  
 BEST FIT VALUES 405.7 381.1 363.3 352.1 347.7  
 STANDARD DEVIATION IS 5.7321148

FOR DEGREE OF 3 COEFFICIENTS ARE

458.0001 -32.0715 3.6518 -0.1563  
 BEST FIT VALUES 407.2 378.1 363.3 355.1 346.2  
 STANDARD DEVIATION IS 6.5737560

TABLE-5.24 TEMP.(DEG.C) = 1050

2	377	377	373	373	373	373	371	371	370	368	9.25	364
	366	366	358	358	355	355	353	353	351	351		
4	336	334	333	333	331	331	329	328	328	323	9.48	322
	321	321	320	318	318	315	315	311	308	302		
6	315	315	314	314	312	312	312	311	311	309	7.57	306
	308	308	305	305	298	298	298	298	294	291		
8	289	287	287	286	286	286	285	283	283	283	7.27	280
	282	281	281	280	277	276	269	269	266	266		
10	282	277	276	275	272	272	269	266	266	264	6.67	266
	263	263	263	263	263	261	260	260	260	260		

FOR DEGREE OF 1 COEFFICIENTS ARE

379.0000 -11.9000  
 BEST FIT VALUES 355.2 331.4 307.6 283.8 260.0  
 STANDARD DEVIATION IS 8.5401019

FOR DEGREE OF 2 COEFFICIENTS ARE

402.0000 -21.7571 0.8214  
 BEST FIT VALUES 361.8 328.1 301.0 280.5 266.6  
 STANDARD DEVIATION IS 5.8162326

FOR DEGREE OF 3 COEFFICIENTS ARE

421.5999 -35.5237 3.4464 -0.1458  
 BEST FIT VALUES 363.2 325.3 301.0 283.3 265.2  
 STANDARD DEVIATION IS 6.9323264

EFFECT OF SOAKING TEMPERATURE ON HARDNESS IN O.O. CONDITION  
 -----  
 ALLOY B1 AS CAST HARDNESS(HV30)= 594

TABLE-5.25 TIME(HRS) = 2

TEMP (DEG.C)	HARDNESS (HV30)										SD	AVERAGE (HV30)
800	715	710	710	710	705	700	700	700	700	700		
	695	695	695	690	690	685	685	685	680	657	13.21	695
850	568	564	557	557	557	554	550	550	550	547		
	547	547	543	543	543	543	540	540	537	533	8.94	548
900	508	505	505	502	502	499	499	499	496	496		
	493	490	487	484	484	484	481	481	478	478	9.80	492
950	508	508	502	502	502	499	496	493	490	490		
	490	484	484	484	484	481	476	476	476	473	11.02	489
1000	473	473	462	459	451	451	451	449	449	449		
	449	446	446	446	446	444	444	444	441	441	9.22	450
1050	434	434	429	418	418	415	411	411	411	411		
	411	409	409	409	409	406	406	406	404	404	9.13	413

FOR DEGREE OF 1 COEFFICIENTS ARE  
 141.6772 -0.9754  
 BEST FIT VALUES 636.4 587.7 538.9 490.1 441.3 392.6  
 STANDARD DEVIATION IS 43.8608190  
 FOR DEGREE OF 2 COEFFICIENTS ARE  
 516.1243 -9.1412 0.0441  
 BEST FIT VALUES 673.2 580.3 509.5 460.7 434.0 429.4  
 STANDARD DEVIATION IS 32.3953180  
 FOR DEGREE OF 3 COEFFICIENTS ARE  
 3517.6767 -107.4759 1.1126 -0.0039  
 BEST FIT VALUES 687.5 560.1 498.0 472.3 454.2 414.8  
 STANDARD DEVIATION IS 16.3879710  
 FOR DEGREE OF 4 COEFFICIENTS ARE  
 2860.6672 -63.7151 0.1519 0.0049 -0.0000  
 BEST FIT VALUES 694.1 551.7 491.9 476.8 464.3 408.1  
 STANDARD DEVIATION IS 19.8104540

TABLE-5.26 TIME(HRS) = 4

800	730	730	720	720	720	720	715	715	715	710		
	710	710	700	700	700	700	695	695	690	690	12.38	709
850	644	639	631	631	631	626	626	626	626	622		
	622	622	622	618	614	614	610	610	606	602	10.68	622
900	508	508	505	502	496	493	493	490	490	487		
	487	484	481	478	478	476	470	470	470	467	12.97	486
950	502	496	493	490	487	487	484	484	484	484		
	481	478	478	478	476	473	470	470	470	462	9.83	481
1000	446	446	441	439	439	439	439	436	434	432		
	432	429	429	429	429	427	427	427	425	418	7.32	433
1050	377	373	373	371	370	368	364	364	364	362		
	362	362	360	360	360	360	358	355	355	351	6.76	363

FOR DEGREE OF 1 COEFFICIENTS ARE  
 173.2439 -1.3154  
 BEST FIT VALUES 680.1 614.3 548.6 482.8 417.0 351.2  
 STANDARD DEVIATION IS 36.0708310  
 FOR DEGREE OF 2 COEFFICIENTS ARE  
 438.0186 -7.0895 0.0312  
 BEST FIT VALUES 706.1 609.1 527.7 462.0 411.8 377.2  
 STANDARD DEVIATION IS 31.2568710  
 FOR DEGREE OF 3 COEFFICIENTS ARE  
 2063.3876 -60.3387 0.6098 -0.0021  
 BEST FIT VALUES 713.9 598.2 521.5 468.3 422.8 369.4  
 STANDARD DEVIATION IS 32.8690520  
 FOR DEGREE OF 4 COEFFICIENTS ARE  
 1661.5880 -33.5764 0.0223 0.0032 -0.0000  
 BEST FIT VALUES 717.9 593.1 517.8 471.0 429.0 365.3  
 STANDARD DEVIATION IS 45.2742040

EFFECT OF SOAKING TEMPERATURE ON HARDNESS IN O.O. CONDITION  
 -----  
 ALLOY B1 AS CAST HARDNESS(HV30)= 594

TABLE-5027 TIME(HRS) = 6

TEMP (DEG. C)	HARDNESS (HV30)										SD	AVERAGE (HV30)
800	730	730	725	725	715	715	715	715	710	710	14.40	708
850	705	705	705	705	700	700	700	700	685	671	14.18	616
900	635	631	631	626	626	626	626	626	622	618	14.14	495
950	618	618	614	614	614	606	606	590	590	586	8.33	471
1000	520	511	511	511	511	505	505	505	499	496	7.19	394
1050	493	490	490	490	484	484	484	478	473	470	7.25	307
	487	487	484	481	478	476	476	473	473	473		
	470	467	467	467	467	465	465	462	462	459		
	409	406	406	404	402	402	398	393	391	391		
	391	391	389	389	389	389	389	389	389	389		
	318	317	317	317	315	315	311	311	309	307		
	307	307	305	305	305	304	299	297	297	295		

FOR DEGREE OF 1 COEFFICIENTS ARE  
 192.3001 -1.5400  
 BEST FIT VALUES 691.0 614.0 537.0 460.0 383.0 306.0  
 STANDARD DEVIATION IS 23.9791580  
 FOR DEGREE OF 2 COEFFICIENTS ARE  
 314.0826 -4.1958 0.0144  
 BEST FIT VALUES 703.0 611.6 527.4 450.4 380.6 318.0  
 STANDARD DEVIATION IS 24.6240870  
 FOR DEGREE OF 3 COEFFICIENTS ARE  
 1812.5934 -53.2889 0.5478 -0.0019  
 BEST FIT VALUES 710.1 601.5 521.7 456.3 390.7 310.7  
 STANDARD DEVIATION IS 24.1818410  
 FOR DEGREE OF 4 COEFFICIENTS ARE  
 1462.2205 -29.9519 0.0354 0.0027 -0.0000  
 BEST FIT VALUES 713.6 597.1 518.5 458.6 396.1 307.1  
 STANDARD DEVIATION IS 33.1399480

TABLE-5028 TIME(HRS) = 8

TEMP	HARDNESS										SD	AVERAGE
800	736	730	730	730	725	725	725	725	725	725	14.05	718
850	725	720	720	720	715	710	700	695	695	685	10.19	617
900	631	626	626	626	626	626	626	626	626	622	10.84	499
950	622	618	610	610	610	610	610	606	598	598	6.73	481
1000	517	514	514	511	511	508	508	502	502	499	7.51	386
1050	496	496	496	496	496	493	493	484	484	478	10.81	287
	496	490	487	487	487	487	484	484	484	484		
	478	478	478	476	476	476	476	473	473	470		
	398	398	398	393	393	391	391	387	387	387		
	383	383	383	383	381	381	377	377	375	375		
	304	302	301	298	297	297	294	294	291	289		
	289	285	282	277	277	277	276	274	272	272		

FOR DEGREE OF 1 COEFFICIENTS ARE  
 201.2885 -1.6377  
 BEST FIT VALUES 702.7 620.8 538.9 457.1 375.2 293.3  
 STANDARD DEVIATION IS 25.3661760  
 FOR DEGREE OF 2 COEFFICIENTS ARE  
 263.0772 -2.9852 0.0073  
 BEST FIT VALUES 708.8 619.6 534.1 452.2 374.0 299.4  
 STANDARD DEVIATION IS 28.5768770  
 FOR DEGREE OF 3 COEFFICIENTS ARE  
 2237.3058 -67.6634 0.7101 -0.0025  
 BEST FIT VALUES 718.2 606.3 526.6 459.9 387.3 289.8  
 STANDARD DEVIATION IS 25.7779700  
 FOR DEGREE OF 4 COEFFICIENTS ARE  
 1797.5373 -38.3722 0.0670 0.0033 -0.0000  
 BEST FIT VALUES 722.6 600.7 522.5 462.9 394.0 285.3  
 STANDARD DEVIATION IS 35.1237390

-----  
**EFFECT OF SOAKING TEMPERATURE ON HARDNESS IN O.Q. CONDITION**  
 -----

ALLOY B1 AS CAST HARDNESS(HV30)= 594

TABLE-5029 TIME(HRS) = 10

TEMP (DEG.C)	HARDNESS (HV30)										SD	AVERAGE (HV30)
800	730	730	730	730	725	725	725	725	715	715		
	715	715	710	710	710	710	705	705	700	685	11.95	715
850	695	685	680	680	675	675	671	671	666	666		
	666	661	661	661	657	652	652	652	644	639	14.06	665
900	543	543	540	533	533	533	533	533	533	533		
	530	530	530	530	530	523	523	523	523	517	6.70	530
950	496	493	490	487	487	484	484	481	481	473		
	473	473	467	467	467	465	465	465	465	459	11.12	476
1000	379	368	368	368	364	362	349	349	346	346		
	346	344	344	344	344	336	336	336	331	331	13.87	349
1050	293	289	282	277	277	275	275	272	271	271		
	271	271	271	269	268	266	266	266	264	264	7.77	272

FOR DEGREE OF 1 COEFFICIENTS ARE

220.1581 -1.8383

BEST FIT VALUES 731.0 639.0 547.1 455.2 363.3 271.4

STANDARD DEVIATION IS 21.5963470

FOR DEGREE OF 2 COEFFICIENTS ARE

157.7446 -0.4772 -0.0074

BEST FIT VALUES 724.8 640.3 552.0 460.1 364.5 265.2

STANDARD DEVIATION IS 24.0305860

FOR DEGREE OF 3 COEFFICIENTS ARE

-746.1192 29.1345 -0.3291 0.0012

BEST FIT VALUES 720.5 646.3 555.5 456.6 358.4 269.6

STANDARD DEVIATION IS 27.3684220

FOR DEGREE OF 4 COEFFICIENTS ARE

-558.1962 16.6177 -0.0543 -0.0013 0.0000

BEST FIT VALUES 718.6 648.7 557.2 455.3 355.5 271.6

STANDARD DEVIATION IS 38.5847900

-----

EFFECT OF SOAKING TEMPERATURE ON HARDNESS IN O.O. CONDITION  
 -----  
 ALLOY B2 AS CAST HARDNESS(HV30)= 590

TABLE-5.30 TIME(HRS) = 2

TEMP (DEG.C)	HARDNESS (HV30)										SD	AVERAGE (HV30)
800	626	622	622	618	618	618	618	618	618	618	10.75	612
850	550	550	550	550	547	547	547	547	547	540	9.63	539
900	508	505	502	502	496	493	493	490	490	496	5.75	496
950	496	487	487	487	478	478	478	476	476	470	5.14	481
1000	411	404	402	402	400	398	398	398	398	396	8.49	393
1050	393	391	389	387	387	387	385	385	383	377	4.91	359

FOR DEGREE OF 1 COEFFICIENTS ARE  
 138.8086 -0.9817  
 BEST FIT VALUES 602.7 553.6 504.5 455.5 406.4 357.3  
 STANDARD DEVIATION IS 17.3736230  
 FOR DEGREE OF 2 COEFFICIENTS ARE  
 147.8969 -1.1799 0.0011  
 BEST FIT VALUES 603.6 553.5 503.8 454.7 406.2 358.2  
 STANDARD DEVIATION IS 20.0390690  
 FOR DEGREE OF 3 COEFFICIENTS ARE  
 921.5045 -26.5243 0.2765 -0.0010  
 BEST FIT VALUES 607.3 548.2 500.9 457.7 411.4 354.4  
 STANDARD DEVIATION IS 22.7156490  
 FOR DEGREE OF 4 COEFFICIENTS ARE  
 776.3569 -16.8566 0.0642 0.0009 -0.0000  
 BEST FIT VALUES 608.7 546.4 499.5 458.7 413.6 352.9  
 STANDARD DEVIATION IS 32.1892420

TABLE-5.31 TIME(HRS) = 4

800	652	648	648	648	648	639	639	639	639	635	12.22	632
850	631	626	626	626	622	622	618	618	618	614	9.82	523
900	543	540	533	530	527	527	527	527	527	527	6.95	499
950	523	523	520	520	517	517	517	508	508	505	7.50	457
1000	511	508	508	505	505	505	502	499	499	499	6.34	386
1050	499	499	499	496	496	496	493	487	487	487	9.28	332

FOR DEGREE OF 1 COEFFICIENTS ARE  
 150.3800 -1.1160  
 BEST FIT VALUES 611.0 555.2 499.4 443.6 387.8 332.0  
 STANDARD DEVIATION IS 20.3764550  
 FOR DEGREE OF 2 COEFFICIENTS ARE  
 203.0918 -2.2655 0.0062  
 BEST FIT VALUES 616.2 554.2 495.3 439.5 386.8 337.2  
 STANDARD DEVIATION IS 22.8815250  
 FOR DEGREE OF 3 COEFFICIENTS ARE  
 1784.2870 -54.0675 0.5691 -0.0020  
 BEST FIT VALUES 623.7 543.5 489.2 445.6 397.4 329.5  
 STANDARD DEVIATION IS 20.6442060  
 FOR DEGREE OF 4 COEFFICIENTS ARE  
 1468.9994 -33.0674 0.1080 0.0022 -0.0000  
 BEST FIT VALUES 626.9 539.5 486.3 447.8 402.3 326.3  
 STANDARD DEVIATION IS 29.0351210

EFFECT OF SOAKING TEMPERATURE ON HARDNESS IN O.Q. CONDITION  
 ALLOY B2 AS CAST HARDNESS(HV30)= 590

TABLE-5032 TIME(HRS) = 6

TEMP (DEG.C)	HARDNESS (HV30)										SD	AVERAGE (HV30)
800	652	648	648	648	648	644	644	644	644	644		
	644	644	635	635	635	635	631	631	626	618	8.75	639
850	540	540	537	537	533	533	533	533	530	527		
	527	527	527	527	527	527	523	523	517	514	6.90	529
900	511	508	505	505	502	502	499	499	499	499		
	499	499	496	496	496	493	490	484	484	484	7.57	497
950	467	465	462	462	457	457	454	454	454	451		
	449	449	449	449	449	446	446	446	441	441	7.43	452
1000	406	406	402	402	402	400	400	400	400	400		
	400	400	398	398	393	391	387	387	385	371	8.48	396
1050	362	353	351	351	351	346	346	346	344	343		
	343	341	341	339	336	333	333	329	328	328	9.14	342

FOR DEGREE OF 1 COEFFICIENTS ARE  
 149.5448 -1.1023  
 BEST FIT VALUES 613.6 558.5 503.4 448.3 393.2 338.0  
 STANDARD DEVIATION IS 19.9568610  
 FOR DEGREE OF 2 COEFFICIENTS ARE  
 261.0235 -3.5534 0.0131  
 BEST FIT VALUES 624.6 556.3 494.6 439.5 391.0 349.0  
 STANDARD DEVIATION IS 19.9169570  
 FOR DEGREE OF 3 COEFFICIENTS ARE  
 1839.9532 -55.2611 0.5752 -0.0020  
 BEST FIT VALUES 632.1 545.7 488.6 445.6 401.6 341.3  
 STANDARD DEVIATION IS 15.3152070  
 FOR DEGREE OF 4 COEFFICIENTS ARE  
 1509.7664 -33.2687 0.0924 0.0024 -0.0000  
 BEST FIT VALUES 635.4 541.5 485.6 447.9 406.7 338.0  
 STANDARD DEVIATION IS 21.1516530

TABLE-5033 TIME(HRS) = 8

800	671	671	671	666	666	666	661	661	661	661		
	661	661	657	648	648	648	648	644	639	639	10.42	657
850	533	523	523	523	523	520	517	517	517	517		
	517	517	514	514	514	514	511	511	511	511	5.56	517
900	508	508	508	505	502	499	499	499	496	496		
	496	496	496	496	493	493	493	490	487	481	6.97	497
950	467	465	465	459	459	457	454	451	451	451		
	449	449	449	446	439	436	436	434	434	434	10.90	449
1000	371	371	366	364	355	353	349	349	348	344		
	344	344	343	343	333	331	331	331	328	314	15.12	345
1050	314	314	308	307	307	304	304	304	304	302		
	302	302	299	299	299	299	299	298	294	291	5.76	302

FOR DEGREE OF 1 COEFFICIENTS ARE  
 169.7495 -1.3366  
 BEST FIT VALUES 628.2 561.4 494.6 427.8 360.9 294.1  
 STANDARD DEVIATION IS 29.8865330  
 FOR DEGREE OF 2 COEFFICIENTS ARE  
 260.0185 -3.3051 0.0106  
 BEST FIT VALUES 637.1 559.6 487.5 420.7 359.2 303.0  
 STANDARD DEVIATION IS 33.2090400  
 FOR DEGREE OF 3 COEFFICIENTS ARE  
 1860.4689 -55.7379 0.5804 -0.0021  
 BEST FIT VALUES 644.7 548.9 481.4 426.9 369.9 295.2  
 STANDARD DEVIATION IS 35.8337800  
 FOR DEGREE OF 4 COEFFICIENTS ARE  
 1558.6385 -35.6342 0.1390 0.0020 -0.0000  
 BEST FIT VALUES 647.7 545.0 478.6 428.9 374.6 292.1  
 STANDARD DEVIATION IS 50.8460230



EFFECT OF SOAKING TEMPERATURE ON HARDNESS IN O.Q. CONDITION

-----

ALLOY B2 AS CAST HARDNESS(HV30)= 590

TABLE-5.34 TIME(HRS) = 10

TEMP (DEG.C)	HARDNESS (HV30)										SD	AVERAGE (HV30)
800	680	680	680	680	675	675	671	671	671	671		
	666	666	666	666	661	661	661	661	661	648	8.48	668
850	527	527	527	527	527	523	523	523	523	520		
	520	520	517	517	517	517	517	517	517	514	4.35	521
900	508	508	502	502	502	499	499	499	499	499		
	496	496	493	490	490	490	490	487	487	487	6.64	496
950	470	465	459	457	457	454	446	446	446	446		
	444	441	441	441	439	439	439	439	436	434	10.03	446
1000	377	373	366	364	362	357	355	353	349	349		
	346	336	336	331	321	308	305	305	299	293	26.06	339
1050	299	298	297	295	295	295	295	293	291	291		
	291	291	289	289	286	285	285	277	277	270	7.63	289

-----

FOR DEGREE OF 1 COEFFICIENTS ARE

177.6505 -1.4234

BEST FIT VALUES 637.8 566.6 495.4 424.2 353.1 281.9

STANDARD DEVIATION IS 30.4746590

FOR DEGREE OF 2 COEFFICIENTS ARE

272.7818 -3.4980 0.0112

BEST FIT VALUES 647.1 564.7 487.9 416.8 351.2 291.2

STANDARD DEVIATION IS 33.7706830

FOR DEGREE OF 3 COEFFICIENTS ARE

2055.5906 -61.9051 0.6459 -0.0023

BEST FIT VALUES 655.6 552.7 481.1 423.7 363.2 282.6

STANDARD DEVIATION IS 35.4025240

FOR DEGREE OF 4 COEFFICIENTS ARE

1716.2719 -39.3044 0.1497 0.0022 -0.0000

BEST FIT VALUES 659.0 548.4 478.0 426.0 368.5 279.1

STANDARD DEVIATION IS 50.1984450

-----

EFFECT OF SOAKING TEMPERATURE ON HARDNESS IN O.O. CONDITION  
 -----  
 ALLOY B3 AS CAST HARDNESS(HV30)= 652

TABLE-5.35 TIME(HRS) = 2

TEMP (DEG.C)	HARDNESS (HV30)										SD	AVERAGE (HV30)
800	710	705	705	700	700	700	700	700	700	695		
	695	695	695	695	690	690	690	685	685	671	8.66	695
850	571	571	561	561	557	554	550	550	550	550		
	561	561	561	561	557	554	550	550	550	550	7.04	561
900	511	499	499	499	496	493	493	493	490	487		
	487	487	487	487	484	484	484	484	478	478	8.03	490
950	481	481	478	478	476	476	476	473	473	473		
	470	470	467	465	462	462	459	457	457	454	8.51	469
1000	429	429	429	427	427	425	425	420	420	418		
	418	418	418	413	411	411	409	406	398	396	9.88	417
1050	381	381	379	377	377	377	375	375	370	370		
	368	366	366	366	362	362	362	358	358	358	7.91	369

FOR DEGREE OF 1 COEFFICIENTS ARE  
 160.1181 -1.1903  
 BEST FIT VALUES 649.0 589.4 529.9 470.4 410.9 351.4  
 STANDARD DEVIATION IS 34.9023830  
 FOR DEGREE OF 2 COEFFICIENTS ARE  
 466.6988 -7.8760 0.0361  
 BEST FIT VALUES 679.1 583.4 505.8 446.3 404.9 381.5  
 STANDARD DEVIATION IS 24.6620930  
 FOR DEGREE OF 3 COEFFICIENTS ARE  
 2730.8888 -82.0538 0.8421 -0.0029  
 BEST FIT VALUES 689.9 568.2 497.2 455.1 420.1 370.5  
 STANDARD DEVIATION IS 12.9387160  
 FOR DEGREE OF 4 COEFFICIENTS ARE  
 2230.5618 -48.7290 0.1105 0.0037 -0.0000  
 BEST FIT VALUES 694.8 561.8 492.6 458.5 427.8 365.4  
 STANDARD DEVIATION IS 15.7256700

TABLE-5.36 TIME(HRS) = 4

800	715	715	715	705	705	705	705	700	700	700		
	700	700	695	695	695	690	690	685	685	680	9.95	699
850	550	543	543	543	543	540	540	540	540	537		
	537	533	533	530	530	530	530	527	527	523	7.07	535
900	496	496	496	496	493	493	493	490	487	487		
	487	487	484	484	484	481	476	473	473	470	8.26	486
950	473	467	465	459	459	459	459	457	454	454		
	454	454	454	454	451	451	451	449	449	446	6.59	455
1000	398	396	393	393	393	393	387	385	383	383		
	381	381	379	377	377	375	375	375	373	370	8.49	383
1050	334	326	326	325	311	311	305	305	305	305		
	305	304	301	301	301	301	299	297	297	297	11.08	307

FOR DEGREE OF 1 COEFFICIENTS ARE  
 177.0914 -1.3983  
 BEST FIT VALUES 652.3 582.4 512.5 442.5 372.6 302.7  
 STANDARD DEVIATION IS 36.7674150  
 FOR DEGREE OF 2 COEFFICIENTS ARE  
 387.9388 -5.9963 0.0249  
 BEST FIT VALUES 673.0 578.2 495.9 426.0 368.5 323.4  
 STANDARD DEVIATION IS 36.3577420  
 FOR DEGREE OF 3 COEFFICIENTS ARE  
 3653.4013 -112.9771 1.1873 -0.0042  
 BEST FIT VALUES 688.6 556.3 483.4 438.7 390.5 307.6  
 STANDARD DEVIATION IS 21.1112030  
 FOR DEGREE OF 4 COEFFICIENTS ARE  
 2959.8644 -66.7833 0.1731 0.0050 -0.0000  
 BEST FIT VALUES 695.5 547.4 477.0 443.4 401.2 300.5  
 STANDARD DEVIATION IS 27.4697170

EFFECT OF SOAKING TEMPERATURE ON HARDNESS IN O.Q. CONDITION  
 -----  
 ALLOY R3 AS CAST HARDNESS(HV30)= 652

TABLE-5.37 TIME(HRS) = 6

TEMP (DEG.C)	HARDNESS (HV30)										SD	AVERAGE (HV30)
800	752	741	741	741	741	741	736	736	736	736	8.59	732
	730	730	730	725	725	725	725	725	720	720		
850	568	564	564	564	561	561	561	561	561	557	11.40	553
	557	554	554	550	550	550	547	540	527	527		
900	499	493	493	490	490	487	487	484	481	481	9.70	480
	478	478	478	478	473	473	473	467	465	465		
950	459	457	457	454	451	451	451	451	449	449	7.83	446
	449	446	441	439	439	439	439	436	436	434		
1000	375	375	370	368	366	366	364	364	362	362	6.56	362
	362	360	360	360	360	357	355	355	353	351		
1050	287	287	286	285	283	282	274	274	272	272	10.00	272
	272	272	265	265	264	263	263	263	257	257		

FOR DEGREE OF 1 COEFFICIENTS ARE  
 201.0724 -1.6611  
 BEST FIT VALUES 681.8 598.8 515.7 432.6 349.6 266.5  
 STANDARD DEVIATION IS 39.5261760  
 FOR DEGREE OF 2 COEFFICIENTS ARE  
 444.0353 -6.9595 0.0286  
 BEST FIT VALUES 705.7 594.0 496.6 413.5 344.8 290.4  
 STANDARD DEVIATION IS 38.0130680  
 FOR DEGREE OF 3 COEFFICIENTS ARE  
 3941.6935 -121.5473 1.2737 -0.0045  
 BEST FIT VALUES 722.3 570.5 483.3 427.1 368.4 273.4  
 STANDARD DEVIATION IS 20.0903090  
 FOR DEGREE OF 4 COEFFICIENTS ARE  
 3191.4434 -71.5761 0.1766 0.0055 -0.0000  
 BEST FIT VALUES 729.8 560.9 476.3 432.3 380.0 265.8  
 STANDARD DEVIATION IS 25.0982820

TABLE-5.38 TIME(HRS) = 6

TEMP (DEG.C)	HARDNESS (HV30)										SD	AVERAGE (HV30)
800	725	725	720	720	715	710	710	710	705	700	11.41	704
	700	700	700	695	695	695	695	695	690	690		
850	575	575	575	571	571	571	571	571	568	568	7.26	565
	568	564	564	564	557	557	557	557	554	554		
900	502	499	499	496	496	493	490	490	484	484	9.37	485
	484	484	484	481	481	478	478	473	473	470		
950	473	473	473	470	467	467	467	467	465	459	13.49	457
	459	459	459	457	457	446	441	434	434	432		
1000	366	364	362	362	362	362	358	358	358	358	6.03	356
	358	358	357	355	353	353	349	348	348	343		
1050	265	265	265	263	263	263	262	262	262	261	9.66	255
	256	255	252	251	251	243	250	244	243	230		

FOR DEGREE OF 1 COEFFICIENTS ARE  
 200.3190 -1.6571  
 BEST FIT VALUES 677.5 594.6 511.8 428.9 346.0 263.2  
 STANDARD DEVIATION IS 28.5152370  
 FOR DEGREE OF 2 COEFFICIENTS ARE  
 264.5389 -3.0576 0.0076  
 BEST FIT VALUES 683.8 593.4 506.7 423.9 344.8 269.5  
 STANDARD DEVIATION IS 32.2423740  
 FOR DEGREE OF 3 COEFFICIENTS ARE  
 3104.1206 -96.0860 1.0184 -0.0036  
 BEST FIT VALUES 697.3 574.3 495.9 434.9 363.9 255.7  
 STANDARD DEVIATION IS 20.0154330  
 FOR DEGREE OF 4 COEFFICIENTS ARE  
 2499.4991 -55.8145 0.1343 0.0044 -0.0000  
 BEST FIT VALUES 703.3 566.5 490.3 439.0 373.2 249.6  
 STANDARD DEVIATION IS 26.0957580

EFFECT OF SOAKING TEMPERATURE ON HARDNESS IN O.Q. CONDITION

ALLOY B3 AS CAST HARDNESS(HV30)= 652

TABLE-5.39 TIME(HRS) = 10

TEMP (DEG.C)	HARDNESS (HV30)										SD	AVERAGE (HV30)
800	725	720	720	720	720	720	705	705	705	705		
	700	700	695	695	695	690	690	690	690	685	12.86	703
850	661	648	648	648	648	644	635	635	635	635		
	635	631	631	631	631	631	631	626	626	622	9.76	636
900	499	496	496	496	496	493	493	490	490	487		
	487	487	487	487	484	481	478	478	478	462	8.80	487
950	481	481	481	478	476	470	470	470	467	467		
	467	457	457	454	454	454	449	446	441	441	13.24	463
1000	364	362	362	362	358	357	353	353	353	351		
	349	349	349	346	341	341	339	337	334	334	9.60	349
1050	256	255	254	252	251	251	249	249	246	246		
	246	246	245	244	244	242	239	238	231	231	7.02	245

FOR DEGREE OF 1 COEFFICIENTS ARE

215.8715      -1.8143

BEST FIT VALUES    707.3    616.6    525.9    435.1    344.4    253.7

STANDARD DEVIATION IS      26.3560800

FOR DEGREE OF 2 COEFFICIENTS ARE

188.6295      -1.2202      -0.0032

BEST FIT VALUES    704.6    617.1    528.0    437.3    345.0    251.0

STANDARD DEVIATION IS      30.3010770

FOR DEGREE OF 3 COEFFICIENTS ARE

982.6250      -27.2325      0.2794      -0.0010

BEST FIT VALUES    708.4    611.8    525.0    440.4    350.3    247.2

STANDARD DEVIATION IS      35.8945630

FOR DEGREE OF 4 COEFFICIENTS ARE

794.2215      -14.6837      0.0039      0.0015      -0.0000

BEST FIT VALUES    710.3    609.4    523.2    441.7    353.2    245.3

STANDARD DEVIATION IS      50.4807200

EFFECT OF SOAKING TEMPERATURE ON HARDNESS IN O.O. CONDITION  
 -----  
 ALLOY B4 AS CAST HARDNESS(HV30)= 621

TABLE-5.40 TIME(HRS) = 2

TEMP (DEG.C)	HARDNESS (HV30)										SD	AVERAGE (HV30)
800	594	594	594	590	590	590	590	590	586	586		
	586	586	586	583	583	583	579	579	579	564	6.98	585
850	543	540	540	533	533	533	530	530	530	527		
	527	523	523	520	520	517	514	508	505	505	11.19	525
900	499	499	490	490	487	487	487	484	484	484		
	478	478	478	478	478	476	473	473	473	470	8.25	482
950	465	457	457	457	454	454	454	454	454	451		
	449	446	446	444	439	439	439	439	429	429	9.71	447
1000	418	418	418	418	413	413	411	411	411	409		
	409	406	404	404	404	404	402	402	398	398	6.54	408
1050	377	377	373	373	373	373	371	371	370	368		
	366	366	358	358	355	355	353	353	351	351	9.25	364

FOR DEGREE OF 1 COEFFICIENTS ARE  
 125.6601 -0.8520  
 BEST FIT VALUES 575.0 532.4 489.8 447.2 404.6 362.0  
 STANDARD DEVIATION IS 7.6026320  
 FOR DEGREE OF 2 COEFFICIENTS ARE  
 183.8248 -2.1204 0.0069  
 BEST FIT VALUES 580.7 531.3 485.2 442.6 403.5 367.7  
 STANDARD DEVIATION IS 6.3635868  
 FOR DEGREE OF 3 COEFFICIENTS ARE  
 797.7273 -22.2327 0.2254 -0.0008  
 BEST FIT VALUES 583.6 527.1 482.9 445.0 407.6 364.7  
 STANDARD DEVIATION IS 2.4298206  
 FOR DEGREE OF 4 COEFFICIENTS ARE  
 659.7889 -13.0451 0.0237 0.0010 -0.0000  
 BEST FIT VALUES 585.0 525.4 481.6 446.0 409.7 363.3  
 STANDARD DEVIATION IS 2.1878490

TABLE-5.41 TIME(HRS) = 4

800	626	626	626	626	626	622	622	622	622	622		
	618	618	614	614	610	606	606	602	602	602	8.92	616
850	540	540	533	530	530	527	523	523	523	523		
	520	520	520	517	517	514	514	514	514	514	8.26	522
900	490	490	487	487	484	484	484	481	481	476		
	476	476	473	473	473	470	465	465	465	459	9.10	476
950	451	449	446	446	446	446	446	446	444	444		
	444	444	444	441	439	439	439	432	422	422	7.84	441
1000	400	389	387	385	383	381	379	377	377	377		
	373	373	370	368	368	368	366	366	364	362	9.78	375
1050	336	334	333	333	331	331	329	328	328	323		
	321	321	320	318	318	315	315	311	308	302	9.48	322

FOR DEGREE OF 1 COEFFICIENTS ARE  
 148.7267 -1.1120  
 BEST FIT VALUES 597.7 542.1 486.5 430.9 375.3 319.7  
 STANDARD DEVIATION IS 15.4639360  
 FOR DEGREE OF 2 COEFFICIENTS ARE  
 224.4545 -2.7634 0.0089  
 BEST FIT VALUES 605.1 540.6 480.5 424.9 373.8 327.1  
 STANDARD DEVIATION IS 16.0262460  
 FOR DEGREE OF 3 COEFFICIENTS ARE  
 1495.3005 -44.3980 0.4613 -0.0016  
 BEST FIT VALUES 611.2 532.0 475.7 429.9 382.4 320.9  
 STANDARD DEVIATION IS 12.3195150  
 FOR DEGREE OF 4 COEFFICIENTS ARE  
 1229.5168 -26.6952 0.0727 0.0019 -0.0000  
 BEST FIT VALUES 613.8 528.6 473.2 431.7 386.4 318.2  
 STANDARD DEVIATION IS 16.9947250

EFFECT OF SOAKING TEMPERATURE ON HARDNESS IN O.O. CONDITION  
 -----  
 ALLOY B4 AS CAST HARDNESS(HV30)= 621

TABLE-5.42 TIME(HRS) = 6

TEMP (DEG.C)	HARDNESS (HV30)										SD	AVERAGE (HV30)
800	657	657	652	652	652	652	648	648	644	644		
	644	644	644	644	639	639	639	639	639	635	6.41	645
850	530	530	530	530	530	530	527	527	523	523		
	523	520	517	514	514	514	508	505	505	505	9.35	520
900	478	476	476	476	473	473	470	470	467	467		
	467	465	465	465	465	465	454	457	454	439	9.40	466
950	451	449	449	446	446	441	441	441	441	439		
	439	439	439	436	436	434	434	434	434	434	5.50	440
1000	383	377	377	377	377	375	375	375	368	366		
	366	364	364	364	362	362	360	360	358	358	7.78	368
1050	315	315	314	314	312	312	312	311	311	309		
	308	308	305	305	298	298	298	298	294	291	7.57	306

FOR DEGREE OF 1 COEFFICIENTS ARE  
 160.8200 -1.2440  
 BEST FIT VALUES 613.0 550.8 488.6 426.4 364.2 302.0  
 STANDARD DEVIATION IS 25.9749910  
 FOR DEGREE OF 2 COEFFICIENTS ARE  
 308.0496 -4.4547 0.0174  
 BEST FIT VALUES 627.5 547.9 477.0 414.8 361.3 316.5  
 STANDARD DEVIATION IS 25.7930050  
 FOR DEGREE OF 3 COEFFICIENTS ARE  
 2535.9945 -77.4450 0.8105 -0.0029  
 BEST FIT VALUES 638.1 532.9 468.5 423.5 376.3 305.6  
 STANDARD DEVIATION IS 16.7857760  
 FOR DEGREE OF 4 COEFFICIENTS ARE  
 2063.0629 -45.9449 0.1189 0.0034 -0.0000  
 BEST FIT VALUES 642.8 526.9 464.2 426.7 383.6 300.8  
 STANDARD DEVIATION IS 22.4182310

TABLE-5.43 TIME(HRS) = 8

800	652	648	648	644	644	644	639	639	635	631		
	631	626	626	626	626	622	622	618	618	618	11.17	632
850	547	547	547	543	543	540	537	533	530	530		
	530	530	530	530	527	527	527	523	523	523	8.31	533
900	478	478	478	478	476	476	476	473	470	470		
	470	467	467	467	465	465	462	462	454	446	8.54	468
950	459	451	449	449	449	446	446	446	446	446		
	444	444	444	444	439	439	434	434	434	434	6.56	443
1000	366	366	366	362	358	358	358	357	357	357		
	355	355	349	349	349	348	339	339	331	331	10.63	352
1050	289	287	287	286	286	286	285	283	283	283		
	282	281	281	280	277	276	269	269	266	266	7.27	280

FOR DEGREE OF 1 COEFFICIENTS ARE  
 168.1848 -1.3303  
 BEST FIT VALUES 617.6 551.1 484.6 418.1 351.6 285.0  
 STANDARD DEVIATION IS 19.0833980  
 FOR DEGREE OF 2 COEFFICIENTS ARE  
 186.9748 -1.7400 0.0022  
 BEST FIT VALUES 619.5 550.7 483.1 416.6 351.2 286.9  
 STANDARD DEVIATION IS 21.9489170  
 FOR DEGREE OF 3 COEFFICIENTS ARE  
 1855.3849 -56.3993 0.5961 -0.0021  
 BEST FIT VALUES 627.4 539.5 476.8 423.1 362.4 278.8  
 STANDARD DEVIATION IS 17.9908990  
 FOR DEGREE OF 4 COEFFICIENTS ARE  
 1508.3762 -33.2864 0.0887 0.0025 -0.0000  
 BEST FIT VALUES 630.9 535.1 473.5 425.5 367.8 275.3  
 STANDARD DEVIATION IS 24.8170670

EFFECT OF SOAKING TEMPERATURE ON HARDNESS IN O.Q. CONDITION

ALLOY B4 AS CAST HARDNESS(HV30)= 621

TABLE-544 TIME(HRS) = 10

TEMP (DEG.C)	HARDNESS (HV30)										SD	AVERAGE (HV30)
800	661	661	661	657	657	657	652	652	648	648		
	648	644	639	639	639	639	636	626	626	622	12.13	645
850	527	527	523	523	520	520	517	517	514	511		
	511	508	508	505	505	505	502	502	502	502	8.74	512
900	496	484	484	481	481	481	481	481	481	478		
	476	476	470	470	470	470	467	467	465	465	8.04	476
950	459	459	457	457	457	451	451	451	446	446		
	444	441	441	439	436	434	434	432	432	427	10.22	444
1000	366	364	358	357	357	357	349	349	348	346		
	344	344	344	343	341	339	339	337	331	331	10.00	347
1050	282	277	276	275	272	272	269	266	266	264		
	263	263	263	263	263	261	260	260	260	260	6.67	266

FOR DEGREE OF 1 COEFFICIENTS ARE

172.8533 -1.3840

BEST FIT VALUES 621.3 552.1 482.9 413.7 344.5 275.3

STANDARD DEVIATION IS 28.4083310

FOR DEGREE OF 2 COEFFICIENTS ARE

182.5437 -1.5953 0.0011

BEST FIT VALUES 622.3 551.9 482.2 413.0 344.3 276.3

STANDARD DEVIATION IS 32.7876330

FOR DEGREE OF 3 COEFFICIENTS ARE

2779.7358 -86.6827 0.9257 -0.0033

BEST FIT VALUES 634.7 534.5 472.3 423.1 361.9 263.7

STANDARD DEVIATION IS 25.4008370

FOR DEGREE OF 4 COEFFICIENTS ARE

2251.0525 -51.4691 0.1526 0.0037 -0.0000

BEST FIT VALUES 639.9 527.7 467.4 426.7 370.0 258.3

STANDARD DEVIATION IS 35.1536960

EFFECT OF HEAT-TREATMENT(OQ) ON VOLUME FRACTION OF MASSIVE CARBIDE

TABLE-5.45 (ALLOY B1)

TEMP DEG.C	TIME HRS	MASSIVE CARBIDE (%)										AVE (%)
AS CAST		32.1	29.7	27.6	27.3	27.1	27.0	24.5	24.0	23.1	22.0	26.4
800	2	27.4	27.2	27.2	26.7	26.4	26.4	26.3	25.6	25.6	25.4	26.4
800	10	26.7	26.5	24.9	24.3	23.7	23.6	22.9	22.8	22.8	22.3	24.0
850	2	29.5	29.1	28.2	28.0	26.8	26.7	26.4	25.7	24.7	24.7	27.0
850	4	27.8	27.6	27.3	26.9	26.7	26.4	26.0	25.7	25.4	24.9	26.5
850	6	26.9	26.4	25.3	24.1	24.1	23.9	23.6	22.9	22.4	21.8	24.1
850	10	26.7	26.7	25.9	24.7	23.7	23.7	22.9	22.1	22.1	21.5	24.0
900	2	33.3	28.9	28.4	28.4	27.9	27.9	26.4	27.3	26.4	26.3	28.1
900	4	27.3	26.6	26.1	26.0	26.0	25.1	24.6	23.4	23.4	22.9	25.1
900	6	27.2	25.3	25.1	24.1	22.2	21.9	21.9	21.1	21.1	21.0	23.1
900	10	27.9	25.7	23.7	23.3	22.6	22.2	22.0	21.7	20.9	19.6	23.0
950	2	33.0	32.6	32.0	32.0	29.0	28.7	27.3	27.3	27.1	25.8	29.5
950	4	30.7	28.4	28.4	28.0	28.0	28.0	26.7	25.8	23.2	23.2	27.0
950	6	25.2	23.4	22.1	22.1	21.5	21.1	21.1	20.5	20.5	20.2	21.8
950	10	23.6	23.2	22.0	21.7	21.5	21.5	20.7	18.1	18.1	17.9	20.8
1000	2	21.3	20.3	20.3	20.1	18.3	18.2	16.0	16.1	16.0	15.4	18.2
1000	10	16.5	15.3	14.5	14.5	14.5	14.4	12.5	13.8	12.5	12.3	14.1

TABLE-5.46 (ALLOY B2)

TEMP DEG.C	TIME HRS	MASSIVE CARBIDE (%)										AVE (%)
AS CAST		28.2	27.9	27.5	27.3	25.2	25.2	24.3	23.1	22.9	22.3	25.4
800	2	21.2	20.8	20.4	20.2	19.4	19.3	19.3	18.9	18.5	18.5	19.7
800	10	19.2	18.2	17.7	17.5	17.2	17.1	16.6	16.6	16.3	16.3	17.3
850	2	21.5	21.5	21.2	21.0	20.8	20.5	20.1	19.0	18.4	18.4	20.2
850	4	21.1	21.0	20.2	19.9	19.6	19.6	18.6	18.6	17.9	17.9	19.4
850	6	21.3	20.9	20.2	20.1	19.9	19.5	18.0	17.6	17.6	17.4	19.3
850	10	20.7	20.1	19.9	19.1	19.0	19.0	17.3	17.3	16.8	16.6	18.6
900	2	28.5	28.1	28.1	25.6	23.8	23.8	22.9	22.7	22.7	22.7	24.9
900	4	26.4	25.7	23.3	21.5	21.5	21.4	20.9	20.3	20.3	20.2	22.2
900	6	21.8	21.6	20.8	20.5	20.5	19.5	19.3	19.3	16.3	15.5	19.5
900	10	20.3	17.9	17.5	17.5	17.4	16.6	16.3	15.6	15.6	14.7	16.9
950	2	25.1	23.7	23.0	22.9	22.1	20.7	20.3	18.8	18.7	18.5	21.4
950	4	24.8	21.9	21.6	20.6	20.6	20.6	20.5	20.5	20.2	18.4	21.0
950	6	19.7	19.3	19.0	18.3	18.3	18.2	18.2	18.2	18.0	16.2	18.3
950	10	19.6	18.1	16.8	16.6	16.4	15.4	14.6	14.9	14.6	14.5	16.2
1000	2	17.6	17.6	16.0	14.6	14.4	14.4	12.6	12.9	12.6	12.5	14.5
1000	10	16.5	15.7	14.0	13.2	12.2	10.8	10.8	10.1	10.1	8.9	12.2



EFFECT OF HEAT-TREATMENT(OO) ON VOLUME FRACTION OF MASSIVE CARBIDE

TABLE-5-47 (ALLOY B3)

TEMP DEG. C	TIME HRS	MASSIVE CARBIDE (%)										AVE (%)
AS CAST		27.7	25.5	25.4	24.4	22.0	21.9	21.9	21.5	20.6	20.4	23.1
800	2	26.8	26.1	24.6	24.1	23.8	23.5	23.5	23.5	23.1	21.2	24.0
800	10	20.9	19.1	17.7	17.6	17.0	16.6	15.5	15.0	15.0	14.8	16.9
850	2	27.0	26.1	26.0	25.9	24.5	23.8	23.4	23.1	22.9	22.6	24.5
850	4	26.7	26.4	26.3	25.5	25.3	24.2	22.1	22.0	21.3	20.7	24.1
850	6	28.0	26.8	25.9	24.6	23.5	22.5	22.4	22.1	21.7	19.3	23.7
850	10	25.9	25.4	24.0	23.1	23.0	22.8	22.3	22.5	22.3	22.0	23.3
900	2	23.8	23.1	22.5	22.3	22.1	22.0	21.9	20.5	20.4	20.3	21.9
900	4	22.0	21.5	21.3	21.1	21.0	19.5	20.8	19.5	19.3	19.3	20.5
900	6	22.1	21.6	20.1	19.1	19.0	18.8	18.8	18.3	18.3	18.0	19.4
900	10	20.1	19.8	19.2	19.2	18.3	17.9	17.9	17.2	16.9	14.9	18.1
950	2	23.4	22.4	20.4	20.3	18.3	17.9	17.5	17.0	17.0	16.7	19.1
950	4	23.0	22.1	20.0	20.0	17.9	16.8	17.2	16.9	16.8	16.5	18.7
950	6	20.9	20.9	20.8	19.8	19.8	18.4	16.3	16.1	15.6	14.9	18.4
950	10	20.6	19.0	17.7	17.7	17.7	17.1	16.9	16.6	16.5	15.6	17.5
1000	2	21.5	18.1	18.1	17.9	17.9	16.8	14.8	15.2	14.8	12.0	16.7
1000	10	16.7	12.5	12.4	11.6	11.2	10.6	10.6	8.6	8.6	7.7	11.1

TABLE-5-48 (ALLOY B4)

TEMP DEG. C	TIME HRS	MASSIVE CARBIDE (%)										AVE (%)
AS CAST		24.5	24.5	23.3	23.0	22.8	22.3	21.2	21.0	20.7	20.3	22.4
800	2	21.6	21.6	20.9	20.6	20.1	19.0	18.4	18.4	15.9	15.6	19.2
800	10	24.1	23.1	19.2	19.0	18.8	18.0	17.7	16.7	16.3	16.3	18.9
850	2	23.9	22.4	21.9	21.4	21.1	19.5	19.5	19.1	19.1	15.5	20.3
850	4	23.3	23.3	21.8	21.2	20.8	20.5	18.9	18.9	18.5	14.7	20.2
850	6	22.6	22.6	21.5	21.5	20.1	19.8	18.2	18.2	17.8	14.0	19.6
850	10	20.4	19.4	18.9	18.6	18.6	18.0	17.8	17.7	16.3	14.5	18.0
900	2	24.5	24.5	24.3	21.5	21.3	20.7	19.9	19.1	18.6	17.2	21.2
900	4	20.1	20.0	19.7	19.3	18.8	18.7	18.6	18.6	17.9	17.9	19.0
900	6	20.3	20.3	19.1	18.0	17.8	17.6	17.3	17.3	15.8	15.8	17.9
900	10	19.3	18.1	17.0	16.8	16.5	15.2	16.2	14.7	14.7	14.4	16.4
950	2	30.5	26.8	26.4	24.8	23.1	20.4	15.4	14.5	14.5	14.1	21.0
950	4	25.8	23.9	20.5	20.3	20.1	19.7	19.7	19.4	18.7	17.5	20.6
950	6	28.4	28.4	24.7	24.5	22.8	21.1	18.4	17.4	12.5	12.5	21.1
950	10	20.6	20.6	19.0	18.3	18.1	18.1	18.0	18.0	18.0	16.2	18.5
1000	2	20.1	19.4	19.4	18.7	18.3	18.3	18.2	18.0	17.8	17.8	18.6
1000	10	18.2	18.2	16.2	15.5	15.0	15.0	14.8	14.1	12.5	10.3	15.0

TABLE-5.49 EFFECT OF HT ON VOLUME PERCENT OF MASSIVE CARBIDE

ALLOY NO.	TEMP. DEG. C	S O A K I N G P E R I O D (HRS)			
		2	4	6	10
B1	800	26.4	.....	.....	24.0
	850	27.0	26.5	24.1	24.0
	900	28.1	25.1	23.1	23.0
	950	29.5	27.0	21.8	20.8
	1000	18.2	.....	.....	14.1
B2	800	19.7	.....	.....	17.3
	850	20.2	19.4	19.3	18.6
	900	24.9	22.2	19.5	16.0
	950	21.4	21.0	18.3	16.2
	1000	14.5	.....	.....	12.2
B3	800	24.0	.....	.....	16.9
	850	24.5	24.1	23.7	23.3
	900	21.9	20.5	19.4	18.1
	950	19.1	18.7	18.4	17.5
	1000	16.7	.....	.....	11.1
B4	800	19.2	.....	.....	18.9
	850	20.3	20.2	19.6	18.0
	900	21.2	19.0	17.9	16.4
	950	21.0	20.6	21.1	18.5
	1000	18.6	.....	.....	15.0

EFFECT OF HEAT TREATMENT(OO) ON SIZE AND DISPERSION OF 2ND PHASE PARTICLES

TABLE-5.50 (ALLOY B1) AS CAST HARDNESS(HV30)=594

TEMP DEG.C	TIME HRS	HV30 MD U	1ST CLASS %AREA NOP	2ND CLASS %AREA NOP	3RD CLASS %AREA NOP	4TH CLASS %AREA NOP	5TH CLASS %AREA NOP	6TH CLASS %AREA NOP							
800	10	715	.48	6.69	68	3.06	31	0.06	1	0.00	0	0.00	0	0.00	0
850	2	548	.59	9.19	54	6.39	37	1.47	9	0.08	0	0.00	0	0.00	0
850	6	616	.71	8.00	37	10.42	49	2.74	13	0.18	1	0.00	0	0.00	0
850	10	665	.80	6.42	30	11.66	54	3.15	15	0.34	2	0.00	0	0.00	0
900	2	492	.95	4.07	23	7.23	42	5.05	29	1.05	6	0.00	0	0.00	0
900	6	495	1.12	1.93	13	5.89	39	6.02	40	1.18	8	0.13	1	0.00	0
900	10	530	1.01	3.17	19	6.86	41	5.82	34	0.95	6	0.00	0	0.00	0
950	2	489	.95	3.09	20	7.40	47	4.33	28	0.91	6	0.00	0	0.00	0
950	4	481	.70	4.70	48	3.37	34	1.66	17	0.07	1	0.00	0	0.00	0
950	6	481	.86	5.73	38	4.54	30	3.85	25	0.98	6	0.06	0	0.00	0
950	10	476	1.43	1.60	9	3.71	22	6.25	37	3.96	24	0.93	6	0.38	2

TABLE-5.51 (ALLOY B2) AS CAST HARDNESS(HV30)=590

TEMP DEG.C	TIME HRS	HV30 MD U	1ST CLASS %AREA NOP	2ND CLASS %AREA NOP	3RD CLASS %AREA NOP	4TH CLASS %AREA NOP	5TH CLASS %AREA NOP	6TH CLASS %AREA NOP							
800	10	668	.51	9.45	62	5.51	36	0.19	1	0.00	0	0.00	0	0.00	0
850	2	539	.53	8.85	59	5.92	40	0.29	2	0.00	0	0.00	0	0.00	0
850	10	521	.62	6.01	53	4.03	36	1.08	10	0.12	1	0.00	0	0.00	0
900	2	496	.47	4.53	70	1.91	29	0.06	1	0.00	0	0.00	0	0.00	0
900	4	499	.58	5.91	53	4.74	42	0.58	15	0.03	0	0.00	0	0.00	0
900	6	497	.68	4.50	46	3.94	40	1.23	13	0.08	1	0.00	0	0.00	0
900	10	496	.65	4.93	49	3.73	37	1.28	13	0.04	0	0.00	0	0.00	0
950	2	481	.67	4.05	47	3.22	37	1.31	15	0.12	1	0.00	0	0.00	0
950	4	457	.71	4.51	48	3.18	34	1.53	16	0.13	1	0.00	0	0.00	0
950	6	452	.66	4.05	49	3.22	39	0.94	11	0.12	1	0.00	0	0.00	0
950	10	446	.63	5.08	54	2.92	31	1.18	13	0.16	2	0.00	0	0.00	0

EFFECT OF HEAT TREATMENT(OQ) ON SIZE AND DISPERSION OF 2ND PHASE PARTICLES

TABLE-5.52 (ALLOY B3) AS CAST HARDNESS(HV30)=652

TEMP DEG.C	TIME HRS	HV30 MD	1ST CLASS %AREA	2ND CLASS %AREA	3RD CLASS %AREA	4TH CLASS %AREA	5TH CLASS %AREA	6TH CLASS %AREA							
800	10	703	.45	7.36	70	3.10	30	0.04	0	0.00	0	0.00	0	0.00	0
850	2	561	.46	6.19	69	2.72	30	0.05	1	0.00	0	0.00	0	0.00	0
850	10	636	.51	4.49	64	2.27	32	0.25	4	0.00	0	0.00	0	0.00	0
900	2	490	.58	4.86	55	3.28	37	0.74	8	0.00	0	0.00	0	0.00	0
900	4	486	.73	5.01	41	5.26	43	1.45	12	0.32	3	0.14	1	0.00	0
900	6	480	.70	5.88	44	5.23	39	1.87	14	0.27	2	0.00	0	0.00	0
900	10	487	.62	7.01	53	4.78	36	1.17	19	0.18	1	0.00	0	0.00	0
950	2	469	.58	3.98	53	3.06	41	0.51	7	0.00	0	0.00	0	0.00	0
950	4	455	.72	5.00	45	3.97	36	2.04	18	0.16	1	0.00	0	0.00	0
950	6	446	.75	4.63	44	3.81	36	1.77	17	0.34	3	0.08	1	0.00	0
950	10	463	.78	4.78	42	4.09	36	2.10	18	0.41	4	0.03	0	0.00	0

TABLE-5.53 (ALLOY B4) AS CAST HARDNESS(HV30)=621

TEMP DEG.C	TIME HRS	HV30 MD	1ST CLASS %AREA	2ND CLASS %AREA	3RD CLASS %AREA	4TH CLASS %AREA	5TH CLASS %AREA	6TH CLASS %AREA							
800	10	645	.47	8.47	70	3.60	30	0.08	1	0.00	0	0.00	0	0.00	0
850	2	525	.38	6.06	82	1.29	17	0.02	0	0.00	0	0.00	0	0.00	0
850	10	512	.51	5.58	61	3.41	37	0.15	2	0.00	0	0.00	0	0.00	0
900	2	482	.58	5.29	53	4.01	40	0.62	6	0.00	0	0.00	0	0.00	0
900	4	476	.53	5.51	60	3.41	37	0.31	3	0.00	0	0.00	0	0.00	0
900	10	476	.70	4.27	41	4.65	45	1.32	13	0.08	1	0.00	0	0.00	0
950	2	447	.57	5.79	56	3.82	37	0.67	7	0.00	0	0.00	0	0.00	0
950	4	441	.60	4.53	51	3.66	42	0.59	7	0.03	0	0.00	0	0.00	0
950	6	447	.62	5.92	50	5.03	42	0.92	8	0.02	0	0.00	0	0.00	0
950	10	444	.77	5.57	46	3.79	31	1.92	16	0.86	7	0.06	0	0.00	0

TABLE-5.54 EFFECT OF HT ON MEAN DIAMETER OF DISPERSED CARBIDES

ALLOY NO.	TEMP. DEG. C	SOAKING PERIOD(HRS)				ALLOY	SOAKING PERIOD(HRS)			
		2	4	6	10		2	4	6	10
B1	800	....	....	....	0.48	B3	....	....	....	0.45
	850	0.59	....	0.71	0.80		0.46	....	....	0.51
	900	0.95	....	1.12	1.01		0.58	0.73	0.70	0.62
	950	0.95	0.70	0.86	1.43		0.58	0.72	0.75	0.78
B2	800	....	....	....	0.51	B4	....	....	....	0.47
	850	0.53	....	....	0.62		0.38	....	....	0.51
	900	0.47	0.58	0.68	0.65		0.58	0.53	....	0.70
	950	0.67	0.71	0.66	0.63		0.57	0.60	....	0.77

TABLE-5.55 EFFECT OF HT ON THE AVERAGE NO. OF DISPERSED CARBIDES

ALLOY NO.	TEMP. DEG. C	SOAKING PERIOD(HRS)				ALLOY	SOAKING PERIOD(HRS)			
		2	4	6	10		2	4	6	10
B1	800	..	..	..	70	B3	..	..	..	65
	850	87	..	76	65		55	..	..	40
	900	47	..	29	43		38	40	43	41
	950	39	34	37	24		37	35	32	33
B2	800	..	..	..	73	B4	..	..	..	66
	850	71	..	..	40		55	..	..	49
	900	39	52	34	40		42	46	..	36
	950	31	31	31	36		47	37	..	33

\* FRAME AREA = 359.75 SQ. MICRON

TABLE-5.56 EFFECT OF HT ON VOLUME PERCENT OF DISPERSED CARBIDES

ALLOY NO.	TEMP. DEG. C	SOAKING PERIOD(HRS)			
		2	4	6	10
B1	800	....	....	....	9.8
	850	17.1	....	21.3	21.6
	900	17.4	....	15.2	16.9
	950	15.7	9.8	15.2	16.8
B2	800	....	....	....	15.2
	850	15.0	....	....	11.3
	900	6.5	11.2	9.8	10.0
	950	8.7	9.3	8.4	9.4
B3	800	....	....	....	10.5
	850	9.0	....	....	7.0
	900	8.9	12.2	13.3	13.4
	950	7.6	11.2	10.6	11.4
B4	800	....	....	....	12.2
	850	7.4	....	....	9.1
	900	9.9	9.2	....	10.3
	950	10.3	8.8	....	12.2

\* FRAME AREA = 359.75 SQ. MICRON

TABLE-5.57 EFFECT OF HT ON PERCENT NO. OF DISPERSED CARBIDES IN DIFFERENT CLASSES

ALLOY NO.	TEMP. DEG. C	S O A K I N G P E R I O D (HRS)																							
		CLASS 1			CLASS 2			CLASS 3			CLASS 4			CLASS 5			CLASS 6								
		2	4	6	10	2	4	6	10	2	4	6	10	2	4	6	10	2	4	6	10	2	4	6	10
B1	800	..	..	..	68	..	..	..	31	..	..	..	1	..	..	..	0	..	..	..	0	..	..	..	0
	850	54	..	37	30	37	..	49	54	9	..	13	15	0	..	1	2	0	..	0	0	0	0	0	
	900	23	..	13	19	42	..	39	41	29	..	40	34	6	..	8	6	0	..	1	0	0	0	0	
	950	20	48	38	9	47	34	30	22	28	17	25	37	6	1	6	24	0	0	0	6	0	0	0	2
B2	800	..	..	..	62	..	..	..	36	..	..	..	1	..	..	..	0	..	..	..	0	..	..	0	
	850	59	..	..	53	40	..	..	36	2	..	..	10	0	..	..	1	0	..	..	0	0	..	0	
	900	70	53	46	49	29	42	40	37	1	5	13	13	0	0	1	0	0	0	0	0	0	0	0	
	950	47	48	49	54	37	34	39	31	15	16	11	13	1	1	1	2	0	0	0	0	0	0	0	
B3	800	..	..	..	70	..	..	..	30	..	..	..	0	..	..	..	0	..	..	..	0	..	..	0	
	850	69	..	..	64	30	..	..	32	1	..	..	4	0	..	..	0	0	..	..	0	0	..	0	
	900	55	41	44	53	37	43	39	37	8	12	14	10	0	3	2	1	0	1	0	0	0	0	0	
	950	53	45	44	42	41	36	36	36	7	18	17	18	0	1	3	4	0	0	1	0	0	0	0	
B4	800	..	..	..	70	..	..	..	30	..	..	..	1	..	..	..	0	..	..	..	0	..	..	0	
	850	82	..	..	61	17	..	..	37	0	..	..	2	0	..	..	0	0	..	..	0	0	..	0	
	900	53	60	..	41	40	37	..	45	6	3	..	13	0	0	..	1	0	0	..	0	0	0	0	
	950	50	51	..	46	42	42	..	31	8	7	..	16	0	0	..	7	0	0	..	0	0	0	0	

\* FRAME AREA = 359.75 SQ. MICRON & CLASS WIDTH = 0.5781 MICRON

TABLE-5.58 EFFECT OF HEAT-TREATMENT ON THE PERCENT AREA OF DISPERSED CARRIDESIN DIFFERENT CLASSES

ALLOY NO.	TEMP DEG.C	S O A K I N G P E R I O D (HRS)																							
		CLASS I		CLASS II		CLASS III		CLASS IV		CLASS V		CLASS VI													
		2	4	6	10	2	4	6	10	2	4	6	10	2	4	6	10								
B1	800	...	...	6.7	...	...	3.1	...	...	...	0.1	...	...	...	...	...	...	...	...	...	...	...	...	...	
B1	850	9.2	...	8.0	6.4	6.4	...	10.4	11.7	1.5	...	2.7	3.2	0.08	...	0.18	0.34	NIL	...	NIL	NIL	NIL	...	NIL	NIL
B1	900	4.1	...	1.9	3.2	7.2	...	5.9	6.9	5.1	...	6.0	5.8	1.05	...	1.18	0.95	NIL	...	0.13	NIL	NIL	...	NIL	NIL
B1	950	3.1	4.7	5.7	1.6	7.4	3.4	4.5	3.7	4.3	1.7	3.9	6.3	0.91	0.07	0.98	3.96	NIL	NIL	0.06	0.93	NIL	NIL	NIL	...
B2	800	...	...	9.5	...	...	...	...	5.5	...	...	...	0.2	...	...	...	...	...	...	...	...	...	...	...	...
B2	850	8.9	...	6.0	5.9	...	...	...	4.0	0.3	...	...	1.1	NIL	...	...	0.12	NIL	...	...	...	...	...	...	...
B2	900	4.5	5.9	4.5	4.9	1.9	4.7	3.9	3.7	0.1	0.6	1.2	1.3	NIL	0.03	0.08	0.04	NIL	NIL	NIL	NIL	NIL	NIL	NIL	NIL
B2	950	4.1	4.5	4.0	5.1	3.2	3.2	3.2	2.9	1.3	1.5	0.9	1.2	0.12	0.13	0.12	0.16	NIL	NIL	NIL	NIL	NIL	NIL	NIL	NIL
B3	800	...	...	7.4	...	...	...	...	3.1	...	...	...	0.04	...	...	...	...	...	...	...	...	...	...	...	...
B3	850	6.2	...	4.5	2.7	...	...	...	2.3	0.05	...	...	0.25	NIL	...	...	...	...	...	...	...	...	...	...	...
B3	900	4.9	5.0	5.9	7.0	3.3	5.3	5.2	4.9	0.7	1.45	1.87	1.30	NIL	0.32	0.27	0.18	NIL	0.14	NIL	NIL	NIL	NIL	NIL	NIL
B3	950	4.0	5.0	4.6	4.8	3.1	4.0	3.8	4.1	0.5	2.04	1.77	2.10	NIL	0.16	0.34	0.41	NIL	NIL	0.08	0.03	NIL	NIL	NIL	NIL
B4	800	...	...	8.5	...	...	...	...	3.6	...	...	...	0.08	...	...	...	...	...	...	...	...	...	...	...	...
B4	850	6.1	...	5.6	1.3	...	...	...	3.4	0.02	...	...	0.15	NIL	...	...	...	...	...	...	...	...	...	...	...
B4	900	5.3	5.5	...	4.3	4.0	3.4	...	4.7	0.62	0.31	...	0.32	NIL	NIL	...	0.08	NIL	NIL	...	...	...	...	...	
B4	950	5.8	4.5	...	5.6	3.8	3.7	...	3.8	0.67	0.6	...	1.92	NIL	0.03	...	0.96	NIL	NIL	...	0.06	NIL	NIL	...	...

FRAME AREA S 350.75 SQ.MICRON & CLASS WIDTH S 0.5781 MICRON



TABLE 5.59 INFLUENCE OF HEAT-TREATMENT ON DISPERSED CARBIDES - A COMPARATIVE SUMMARY

Temp.	Parameter	B1	B2	B3	B4
800	(a) NOP at 10 hrs soaking	70	73 B1, B2 > B3, B4	65	66
	(b) Size at 10 hrs soaking ( $\mu$ )	0.48	0.51 B2 > B1, B3, B4	0.45	0.47
850	(a) Maximum Size ( $\mu$ ) at 10 hrs. soaking	0.80	<B1, (0.62) B1 > B2 > B3, B4	(0.51)	(0.51)
	(b) % increase in size with time		B1 > B4 > B2 > B3		
	(c) % decrease in NOP with time		B2 > B1 > B3 > B4		
	(d) Volume fraction at 2 hrs soaking		B1 > B2 > B3 > B4		
	(e) Volume fraction at 10 hrs soaking		B1 > B2 > B3, B4		
900	(a) Size at 10 hrs soaking ( $\mu$ )	max., (1.01)	<B4, (0.65) B1 > B4 > B2, B3	<B2, (0.62)	<B1, (0.70)
	(b) % decrease in NOP with time (2 to 10 hrs)	47-43	UA, UA		(42-36)
	(c) Volume fraction at 2 hrs soaking	max.	least B1 > B4 > B3, B2	<B1, B4	<B1

(d) Volume fraction at 10 hrs	max.	B1 > B3 > B2, B4	least	<B1	=B2
950 (a) Size at 10 hrs soaking	max.		<B1	=B4	least
(b) Size at 2 hrs soaking	max. (1.43)		least, (0.63)	=B4	least
(c) NOP at 10 hrs soaking	min. (24)		max., (36)	<B2, (33)	=B3
(d) Volume fraction at 2 hrs	max.		> B3, (8.7)	least	=B3
(e) Volume fraction at 10 hrs	max.	B1 > B4, B3 > B2	least	=B4	=B1
<b>GENERAL REMARKS</b>					
Class I (i) NOP at 800 10 hrs	>B2	B4, B3, B1 < B2	min.	=B1,	=B1
(ii) % decrease in NOP with temp. (800-950) at 10 hrs.	max.		min.	<< B1	=B3
Class II (i) NOP at 800, 10 hrs	<B2, (31)		max. (36)	=B1, (30)	=B3, (30)
(ii) % decrease in NOP with temp. (850-950) at 10 hrs	max.		=UA	=UA	=UA
Class III (i) NOP at 800, 10hrs	nil		nil	nil	nil
(ii) % increase in NOP with temp. (800-900) at 10 hrs	max.		least	<B1	=B3

(iii) Overall NOP	max.	< B1,	=B2	=B3
Class IV (i) NOP at 800, 10 hrs	nil	nil	nil	nil
(ii) % increase in NOP with temp. (800-950) at 10 hrs.	max.	least	<B4	<B1
Class V (i) NOP at 800, 10 hrs	nil	nil	nil	nil
(ii) NOP at 950, 10 hrs.	max., (2)	nil	nil	nil
Class VI (i) NOP at 950, 10hrs (overall)	max.	nil	nil	nil

TABLE-5060 X-RAY DIFFRACTOMETRIC DATA OF ALLOY B1

## AS CAST

SL NO	2 $\theta$	D(A)	I/I <sub>0</sub>	POSSIBLE MATRIX	CONSTITUENTS	CARBIDE(S)
1	48.0	2.382	8.3		M23	M3 M7
2	56.0	2.064	13.3	M		M3 M5
3	57.3	2.021	100.0	ALPHA	M	M3 M5 M7
4	57.5	2.014	35.8	M		M3 M5 M7
5	58.8	1.974	10.0			M3
6	62.4	1.870	10.8			M3
7	85.1	1.433	7.5	ALPHA		
8	93.7	1.328	5.8		M23	
9	97.2	1.292	5.0		M23	
10	111.9	1.169	15.8	ALPHA	M23	M7
11	118.2	1.129	5.8			M5

STRUCTURE : PEARLITE/BAINITE

+ MARTENSITE

+ M3C [ISOMORPHOUS WITH FE3C (23-1113)]

+ SOME M23C6 [ISOMORPHOUS WITH M23C6 (11-0545)]

+ TRACE M5C2 [ISOMORPHOUS WITH FE5C2(20-0508)]

TABLE-5.61 X-RAY DIFFRACTOMETRIC DATA OF ALLOY B1

HEAT TREATMENT : 900,4,00

SL NO	2θ	D(A)	I/I0	POSSIBLE MATRIX	CONSTITUENTS CARBIDE(S)
1	48.0	2.382	7.0		M23 M3 M7
2	52.1	2.206	14.0		M3 M5
3	53.0	2.172	7.0		M23 M3
4	55.7	2.074	100.0	A	M3 M5
5	56.2	2.057	18.0	M	M23 M3 M5
6	57.7	2.008	36.5	M*	M3 M5
7	59.0	1.968	11.0		M3
8	62.5	1.868	11.0		M3
9	65.1	1.801	29.0	A	M23 M5
10	70.3	1.683	7.0		M23 M3
11	99.3	1.271	13.0	A	
12	126.0	1.087	16.0		M23

STRUCTURE : AUSTENITE  
 + TRACE/SOME MARTENSITE  
 + M3C [ISOMORPHOUS WITH FE3C (23-1113)]  
 + M23C6 [ISOMORPHOUS WITH M23C6 (11-0545)]  
 + TRACE M5C2 [ISOMORPHOUS WITH FE5C2 (20-0508)]

TABLE-5.62 X-RAY DIFFRACTOMETRIC DATA OF ALLOY B1

HEAT TREATMENT : 900,10,00

SL NO	2θ	D(A)	I/I0	POSSIBLE MATRIX	CONSTITUENTS CARBIDE(S)
1	48.3	2.368	13.0		M23
2	51.0	2.251	10.0		M7
3	55.6	2.078	100.0	A	M3 M5
4	56.2	2.057	32.0	M	M23 M3 M5
5	56.8	2.037	10.0		M5 M7
6	57.7	2.008	37.0	M*	M3 M5
7	58.4	1.986	6.0		M7
8	59.1	1.965	13.0		M3 M7
9	62.6	1.865	12.0		M3 M7
10	65.3	1.796	27.0	A	M23 M5
11	65.8	1.784	11.0		M23 M7
12	93.7	1.328	10.0		M23 M5
13	99.3	1.271	25.0	A	
14	126.0	1.087	67.0		M23
15	126.8	1.083	27.0	A	

STRUCTURE : AUSTENITE  
 + TRACE/SOME MARTENSITE  
 + M3C [ISOMORPHOUS WITH FE3C (23-1113)]  
 + M23C6 [ISOMORPHOUS WITH M23C6 (11-0545)]  
 + TRACE M5C2 [ISOMORPHOUS WITH FE5C2 (20-0508)]  
 + TRACE M7C3 [ISOMORPHOUS WITH FE7C3 (17-0333)]

\* PROBABLE

TABLE-5.63 X-RAY DIFFRACTOMETRIC DATA OF ALLOY B1

HEAT TREATMENT : 950,4,00

SL NO	2θ	D(A)	I/I <sub>0</sub>	POSSIBLE MATRIX	CONSTITUENTS	CARBIDE(S)
1	48.2	2.373	4.0		M23	M3 M7
2	50.3	2.280	4.0			M5 M7
3	51.0	2.251	6.0			M7
4	55.1	2.074	100.0	A		M3 M5
5	57.8	2.005	35.0	M*		M3 M5
6	58.3	1.989	5.0			M5 M7
7	59.1	1.965	8.0			M3 M7
8	62.7	1.862	8.0			M7
9	65.1	1.801	22.0	A	M23	M5
10	70.3	1.683	7.0		M23	M3
11	98.5	1.279	8.0			M7
12	99.3	1.271	14.0	A		
14	125.9	1.088	24.0		M23	

STRUCTURE : AUSTENITE

- + M3C [ISOMORPHOUS WITH FE3C (23-1113)]
- + SOME M23C6 [ISOMORPHOUS WITH M23C6 (11-0545)]
- + TRACE M5C2 [ISOMORPHOUS WITH FE5C2 (20-0508)]
- + TRACE M7C3 [ISOMORPHOUS WITH FE7C3 (17-0333)]

TABLE-5.64 X-RAY DIFFRACTOMETRIC DATA OF ALLOY B1

HEAT TREATMENT : 950,10,00

SL NO	2θ	D(A)	I/I <sub>0</sub>	POSSIBLE MATRIX	CONSTITUENTS	CARBIDE(S)
1	48.2	2.373	5.8		M23	M3 M7
2	51.0	2.251	3.9			M7
3	55.7	2.074	100.0	A		M3 M5
4	57.6	2.011	25.2	M*		M3 M5
5	59.1	1.965	9.7			M3 M7
6	62.6	1.865	5.8			M3 M7
7	65.0	1.803	22.3	A	M23	M5 M7
8	67.0	1.756	5.8			M3
9	125.9	1.088	13.1		M23	

STRUCTURE : AUSTENITE

- + M3C [ISOMORPHOUS WITH FE3C (23-1113)]
- + SOME M23C6 [ISOMORPHOUS WITH M23C6 (11-0545)]
- + TRACE M5C2 [ISOMORPHOUS WITH FE5C2 (20-0508)]
- + TRACE M7C3 [ISOMORPHOUS WITH FE7C3 (17-0333)]

\* PROBABLE

TABLE-5.65 X-RAY DIFFRACTOMETRIC DATA OF ALLOY B1

HEAT TREATMENT : 1000,4,00

SL NO	2θ	D(A)	I/I <sub>0</sub>	POSSIBLE MATRIX	CONSTITUENTS CARBIDE(S)
1	48.2	2.373	5.0		M23 M3 M7
2	51.0	2.251	3.5		M7
3	55.5	2.081	100.0	A	M3 M5
4	56.7	2.041	7.0		M7
5	57.7	2.008	16.0		M3 M5 M7
6	58.3	1.989	6.0		M5 M7
7	62.6	1.865	6.0		M3 M7
8	65.0	1.803	24.0	A	M23 M5 M7
9	98.5	1.279	7.0		M7
10	125.1	1.092	13.0	UI	
11	126.2	1.086	6.0		M23

STRUCTURE :AUSTENITE

- + SOME M3C [ISOMORPHOUS WITH FE3C (23-1113)]
- + SOME M5C2 [ISOMORPHOUS WITH FE5C2 (20-0508)]
- + SOME M7C3 [ISOMORPHOUS WITH CR7C3+MN7C3 (03-075), FE7C3 (17-0333)]
- + TRACE M23C6 [ISOMORPHOUS WITH M23C6 (11-0545)]

TABLE-5.66 X-RAY DIFFRACTOMETRIC DATA OF ALLOY B1

HEAT TREATMENT : 1000,10,00

SL NO	2θ	D(A)	I/I <sub>0</sub>	POSSIBLE MATRIX	CONSTITUENTS CARBIDE(S)
1	50.8	2.259	3.0		M3 M5 M7
2	55.5	2.081	100.0	A	M3 M5
3	56.3	2.054	7.1		M23 M3 M5
4	57.6	2.011	20.2		M3 M5
5	64.1	1.826	4.2		M5 M7
6	64.7	1.811	28.0		M5 M7
7	65.1	1.801	4.2	A	M23 M5 M7
8	98.4	1.280	12.2		M7
9	125.1	1.092	16.0	UI	

STRUCTURE :AUSTENITE

- + SOME M3C [ISOMORPHOUS WITH FE3C (23-1113)]
- + M5C2 [ISOMORPHOUS WITH FE5C2 (20-0508)]
- + SOME M7C3 [ISOMORPHOUS WITH CR7C3 (11-0550), (CR,FE)7C3 (05-0720)]

TABLE-5.67 X-RAY DIFFRACTOMETRIC DATA OF ALLOY B1

HEAT TREATMENT : 1050,4,00

SL NO	2θ	D(A)	I/I0	POSSIBLE MATRIX	CONSTITUENTS CARBIDE(S)
1	54.6	2.113	9.8		M5
2	55.4	2.084	100.0	A	M3 M5
3	56.3	2.054	12.5		M23 M3 M5
4	57.2	2.024	6.3	M	M3 M5 M7
5	64.8	1.808	32.1		M7
6	65.3	1.796	14.3	A	M23 M5
7	98.4	1.280	8.5		M7
8	125.2	1.091	10.0	UI	

STRUCTURE : AUSTENITE  
 + M5C2 [ISOMORPHOUS WITH FE5C2 (20-0508)]  
 + M7C3 [ISOMORPHOUS WITH CR7C3 (11-0550),  
 FE7C3 (17-0333)]  
 + TRACE M3C [ISOMORPHOUS WITH FE3C (23-1113)]

TABLE-5.68 X-RAY DIFFRACTOMETRIC DATA OF ALLOY B1

HEAT TREATMENT : 1050,6,00

SL NO	2θ	D(A)	I/I0	POSSIBLE MATRIX	CONSTITUENTS CARBIDE(S)
1	49.7	2.306	3.8		M7
2	55.4	2.084	100.0	A	M3 M5
3	57.2	2.024	4.3	M	M3 M5 M7
4	59.4	1.956	3.9		M5 M7
5	64.6	1.813	40.9		M5 M7
6	65.0	1.803	5.8	A	M23 M5 M7
7	98.2	1.282	14.4		M7
8	124.8	1.093	30.0	UI	

STRUCTURE : AUSTENITE  
 + M7C3 [ISOMORPHOUS WITH CR7C3 (11-0550),  
 (CR, FE)7C3 (05-0720)]  
 + M5C2 [ISOMORPHOUS WITH FE5C2 (20-0508)]

TABLE-5.69 X-RAY DIFFRACTOMETRIC DATA OF ALLOY B1

HEAT TREATMENT : 1050,10,00

SL NO	2θ	D(A)	I/I0	POSSIBLE MATRIX	CONSTITUENTS CARBIDE(S)
1	49.7	2.306	3.7		M7
2	54.5	2.116	4.5		M5 M7
3	55.4	2.084	100.0	A	M3 M5
4	57.2	2.024	7.1	M	M3 M5 M7
5	65.1	1.801	49.1	A	
6	98.2	1.282	12.5		M7
7	125.0	1.092	13.0	UI	
8	126.1	1.087	4.5		M23

STRUCTURE : AUSTENITE  
 + M7C3 [ISOMORPHOUS WITH (CR, FE)7C3 (05-0720)]  
 + SOME M5C2 [ISOMORPHOUS WITH FE5C2 (20-0508)]



TABLE-5.70 X-RAY DIFFRACTOMETRIC DATA OF ALLOY B2

AS CAST							
SL NO	2 $\theta$	D(A)	I/I <sub>0</sub>	POSSIBLE MATRIX	CONSTITUENTS	CARBIDE(S)	
1	47.9	2.387	22.5		M23	M3	M7
2	50.8	2.259	30.0			M3	M5 M7
3	54.8	2.106	10.0			M3	M5
4	55.9	2.067	39.0	A*M			
5	57.2	2.024	70.5	ALPHA	M	M3	M5 M7
6	57.5	2.014	100.0		M	M3	M5 M7
7	58.8	1.974	25.0			M3	
8	62.3	1.873	17.5			M3	
9	63.1	1.852	7.5			M3	M7
10	66.8	1.760	15.5			M3	
11	85.1	1.433	8.8	ALPHA			
12	93.6	1.329	10.0			M23	
13	105.7	1.216	10.0	UI			
14	111.8	1.170	20.0	ALPHA	M23		M7
15	118.2	1.129	10.0				M5
16	119.0	1.124	10.0	UI			

STRUCTURE : PEARLITE/BAINITE

+ MARTENSITE

+ M3C [ISOMORPHOUS WITH FE3C (23-1113)]

+ TRACE M23C6 [ISOMORPHOUS WITH M23C6 (11-0545)]

+ TRACE M5C2 [ISOMORPHOUS WITH FE5C2 (20-508)]

\* PROBABLE

TABLE-5071 X-RAY DIFFRACTOMETRIC DATA OF ALLOY B2

HEAT TREATMENT : 900,4,00

SL NO	2θ	D(A)	I/I0	POSSIBLE MATRIX	CONSTITUENTS	CARBIDE(S)
1	47.9	2.387	14.1		M23	M3 M7
2	50.6	2.267	9.4			M3 M5
3	54.8	2.106	15.6			M3 M5
4	55.5	2.081	100.0	A		M3 M5
5	55.9	2.067	25.0	A		
6	57.0	2.031	21.9	ALPHA		M5
7	57.4	2.018	56.3		M	M3 M5 M7
8	58.8	1.974	25.0			M3
9	62.3	1.873	18.8			M3
10	63.1	1.852	14.1			M3 M7
11	64.9	1.806	20.3	A		M7
12	66.9	1.758	9.4			M3
13	93.4	1.331	9.4		M23	
14	98.4	1.280	15.6			M7
15	98.9	1.275	38.0	UI		
16	105.2	1.220	7.8			M7
17	113.1	1.161	10.9			M3 M7
18	117.6	1.133	9.0	UI		
19	118.4	1.128	8.0	UI		
20	126.7	1.084	71.9		A	

STRUCTURE : AUSTENITE  
 + TRACE MARTENSITE OR/AND PEARLITE/BAINITE  
 + M3C [ISOMORPHOUS WITH FE3C (23-1113)]  
 + TRACE M23C6 [ISOMORPHOUS WITH M23C6 (11-0545)]  
 + M5C2 [ISOMORPHOUS WITH FE5C2 (20-0508)]

TABLE-5072 X-RAY DIFFRACTOMETRIC DATA OF ALLOY B2

HEAT TREATMENT : 900,10,00

SL NO	2θ	D(A)	I/I0	POSSIBLE MATRIX	CONSTITUENTS	CARBIDE(S)
1	50.6	2.267	3.4			M3 M5
2	55.7	2.074	100.0	A		M3 M5
3	57.4	2.018	3.4		M	M3 M5 M7
4	57.8	2.005	6.7			M3 M5
5	58.0	1.999	6.7			M5
6	59.3	1.959	2.9			M7
7	65.2	1.798	4.8		A	M23 M5
8	118.8	1.126	5.0	UI		
9	126.1	1.087	7.7			M23

STRUCTURE : AUSTENITE  
 + TRACE MARTENSITE  
 + SOME M3C [ISOMORPHOUS WITH FE3C (23-1113)]  
 + SOME M5C2 [ISOMORPHOUS WITH FE5C2 (20-508)]  
 + TRACE M7C3 [ISOMORPHOUS WITH CR7C3 (11-0550)]

TABLE-5.73 X-RAY DIFFRACTOMETRIC DATA OF ALLOY B2

HEAT TREATMENT : 950,4,00

SL NO	2θ	D(A)	I/I0	POSSIBLE MATRIX	CONSTITUENTS	CARBIDE(S)
1	48.0	2.382	2.7		M23	M3 M7
2	55.7	2.074	100.0	A	M3	M5
3	56.2	2.057	8.0	M	M23	M3 M5
4	57.8	2.005	8.0		M3	M5
5	58.9	1.971	3.0		M3	
6	63.3	1.847	2.0		M3	M7
7	64.9	1.806	5.3			M7
8	65.1	1.801	5.3	A	M23	M5
9	125.5	1.090	57.0	UI		

STRUCTURE : AUSTENITE  
 + M3C [ISOMORPHOUS WITH FE3C (23-1113)]  
 + M5C2 [ISOMORPHOUS WITH FE5C2 (20-508)]  
 + TRACE M7C3 [ISOMORPHOUS WITH CR7C3+MN7C3 (03-075)]

TABLE-5.74 X-RAY DIFFRACTOMETRIC DATA OF ALLOY B2

HEAT TREATMENT : 950,10,00

SL NO	2θ	D(A)	I/I0	POSSIBLE MATRIX	CONSTITUENTS	CARBIDE(S)
1	48.1	2.378	6.0		M23	M3 M7
2	55.7	2.074	100.0	A	M3	M5
3	57.8	2.005	24.8	M*	M3	M5 M7
4	58.0	1.999	26.3			M5
5	59.1	1.965	7.5		M3	M7
6	59.7	1.947	4.5			M5
7	59.9	1.941	3.0	UI		
8	62.7	1.862	6.0			M7
9	65.0	1.803	30.8	A	M23	M5 M7
10	66.3	1.772	4.0	UI		
11	67.3	1.749	4.5			M7
12	91.8	1.349	3.4			M7
13	99.3	1.271	6.0	A		
14	109.0	1.190	12.0		M23	
15	118.2	1.129	6.0			M5
16	119.1	1.124	9.0	UI		
17	125.6	1.089	16.5	UI		

STRUCTURE : AUSTENITE  
 + M5C2 [ISOMORPHOUS WITH FE5C2 (20-508)]  
 + SOME M7C3 [ISOMORPHOUS WITH CR7C3 (11-0550),  
 CR7C3+MN7C3 (03-075)]  
 + SOME M3C [ISOMORPHOUS WITH FE3C (23-1113)]

\* PROBABLE

TABLE-5.75 X-RAY DIFFRACTOMETRIC DATA OF ALLOY B2

HEAT TREATMENT : 1000,4,00

SL NO	2θ	D(A)	I/I <sub>0</sub>	POSSIBLE MATRIX	POSSIBLE CARBIDE(S)
1	48.2	2.373	4.6		M23 M3 M7
2	49.8	2.301	4.6		M7
3	55.6	2.078	100.0	A	M3 M5
4	57.6	2.011	16.1		M3 M5
5	58.1	1.995	5.0		M5
6	58.5	1.983	4.6		M7
7	58.9	1.971	4.1		M3
8	64.6	1.813	19.7		M5 M7
9	65.2	1.798	11.0	A	M23 M5
10	67.2	1.751	3.3		M7
11	98.4	1.280	6.0		M7
12	124.7	1.094	11.0	UI	

STRUCTURE : AUSTENITE

- + M5C2 [ISOMORPHOUS WITH FE5C2 (20-0508)]
- + SOME M7C3 [ISOMORPHOUS WITH CR7C3 (11-0550), (CR,FE)7C3 (05-0720)]
- + TRACE M3C [ISOMORPHOUS WITH FE3C (23-1113)]

TABLE-5.76 X-RAY DIFFRACTOMETRIC DATA OF ALLOY B2

HEAT TREATMENT : 1000,10,00

SL NO	2θ	D(A)	I/I <sub>0</sub>	POSSIBLE MATRIX	POSSIBLE CARBIDE(S)
1	55.7	2.074	100.0	A	M3 M5
2	56.1	2.061	97.2	M	M3 M5
3	59.1	1.965	8.3		M3 M7
4	62.6	1.865	8.3		M3 M7
5	65.2	1.798	38.9	A	M23 M5
6	98.9	1.275	19.0	UI	
7	99.6	1.268	6.9	A	
8	109.6	1.186	7.0	UI	
9	125.6	1.089	31.0	UI	
10	126.0	1.087	16.7		M23

STRUCTURE : AUSTENITE

- + M5C2 [ISOMORPHOUS WITH FE5C2 (20-508)]
- + TRACE/SOME M7C3 [ISOMORPHOUS WITH CR7C3 (11-0550)]
- + TRACE M3C [ISOMORPHOUS WITH FE3C (23-1113)]

TABLE-5.77 X-RAY DIFFRACTOMETRIC DATA OF ALLOY B2

HEAT TREATMENT : 1050,4,00

SL NO	2θ	D(A)	I/I <sub>0</sub>	POSSIBLE MATRIX	CONSTITUENTS	CARBIDE(S)
1	49.7	2.306	2.8			M7
2	54.3	2.123	7.4			M5 M7
3	55.4	2.084	100.0		A	M3 M5
4	57.3	2.021	4.6	ALPHA	M	M3 M5 M7
5	64.6	1.813	17.6			M5 M7
6	65.0	1.803	10.2		A	M23 M5 M7
7	98.5	1.279	3.7			M7
8	124.4	1.095	10.0	UI		
9	126.3	1.086	4.0	UI		

STRUCTURE : AUSTENITE  
 + M5C2 [ISOMORPHOUS WITH FE5C2 (20-0508)]  
 + M7C3 [ISOMORPHOUS WITH CR7C3 (11-0550), (CR,FE)7C3 (05-0720)]

TABLE-5.78 X-RAY DIFFRACTOMETRIC DATA OF ALLOY B2

HEAT TREATMENT : 1050,6,00

SL NO	2θ	D(A)	I/I <sub>0</sub>	POSSIBLE MATRIX	CONSTITUENTS	CARBIDE(S)
1	54.5	2.116	5.1			M5 M7
2	55.4	2.084	100.0		A	M3 M5
3	57.5	2.014	4.2		M	M3 M5 M7
4	64.6	1.813	17.8			M5 M7
5	65.3	1.796	4.2		A	M23 M5
6	98.3	1.281	11.9			M7
7	124.8	1.093	25.0	UI		
8	126.7	1.084	3.4		A	

STRUCTURE : AUSTENITE  
 + M5C2 [ISOMORPHOUS WITH FE5C2 (20-0508)]  
 + M7C3 [ISOMORPHOUS WITH CR7C3 (11-0550)]

TABLE-5.79 X-RAY DIFFRACTOMETRIC DATA OF ALLOY B2

HEAT TREATMENT : 1050,10,00

SL NO	2θ	D(A)	I/I <sub>0</sub>	POSSIBLE MATRIX	CONSTITUENTS	CARBIDE(S)
1	49.7	2.306	2.9			M7
2	55.4	2.084	100.0		A	M3 M5
3	57.2	2.024	2.5	ALPHA		M23 M3 M5 M7
4	64.9	1.806	18.0			M7
5	65.3	1.796	22.5		A	M23 M5
6	98.5	1.279	9.8			M7
7	124.8	1.093	10.0	UI		
8	125.02	1.091	10.0	UI		

STRUCTURE : AUSTENITE  
 + M7C3 [ISOMORPHOUS WITH CR7C3 (11-0550), (CR,FE)7C3 (05-0720)]  
 + SOME M5C2 [ISOMORPHOUS WITH FE5C2 (20-508)]

TABLE-5080 X-RAY DIFFRACTOMETRIC DATA OF ALLOY B3

AS CAST

SL NO	2θ	D(A)	I/I0	POSSIBLE MATRIX	CONSTITUENTS	CARBIDE(S)
1	47.9	2.387	8.0		M23	M3 M7
2	50.7	2.263	5.7			M3 M5
3	54.9	2.102	9.1			M3
4	55.5	2.081	11.4	A		M3 M5
5	55.9	2.067	20.5	M		M7
6	57.2	2.024	100.0	ALPHA	M	M3 M5
7	58.8	1.974	12.5			M3
8	62.3	1.873	9.1			M3
9	63.2	1.849	5.7			M3 M7
10	66.8	1.760	3.4			M3
11	70.3	1.683	3.4		M23	M3
12	85.0	1.434	8.0	ALPHA		
13	111.2	1.174	6.8		M	M7
14	111.8	1.170	14.8	ALPHA	M23	M7
15	119.2	1.123	6.0	UI		
16	126.0	1.087	5.0	A	M23	

STRUCTURE : PEARLITE/BAINITE

- + MARTENSITE+AUSTENITE(γ)
- + M3C [ISOMORPHOUS WITH FE3C (23-1113)]
- + TRACE M23C6 [ISOMORPHOUS WITH M23C6 (11-0545)]
- + M5C2(δ) [ISOMORPHOUS WITH FE5C2 (20-0508)]

TABLE-5081 X-RAY DIFFRACTOMETRIC DATA OF ALLOY B3

HEAT TREATMENT : 900,4,00

SL NO	2θ	D(A)	I/I <sub>0</sub>	POSSIBLE CONSTITUENTS MATRIX	CARBIDE(S)
1	48.1	2.378	12.5		M23 M3 M7
2	50.9	2.255	10.9		M3 M5 M7
3	54.6	2.113	9.4		M5
4	55.4	2.098	12.5		M3
5	55.5	2.081	50.0	A M	M3 M5
6	55.9	2.067	100.0		
7	57.1	2.027	18.8	ALPHA	M5
8	57.7	2.008	37.5		M3 M5
9	59.0	1.968	21.0		M3
10	62.5	1.868	25.0		M3
11	64.8	1.808	28.1		M7
12	65.2	1.798	37.5	A	M23 M5
13	70.3	1.683	9.4		M23 M3
14	99.3	1.274	41.0	UI	
15	99.5	1.269	18.8	A	
16	119.1	1.124	14.0	UI	
17	125.9	1.088	34.4		M23
18	126.7	1.084	15.6	A	

STRUCTURE : AUSTENITE  
 + SOME MARTENSITE  
 + M3C [ISOMORPHOUS WITH FE3C (23-1113)]  
 + SOME M23C6 [ISOMORPHOUS WITH M23C6 (11-0545)]  
 + TRACE M5C2 [ISOMORPHOUS WITH FE5C2 (20-508)]  
 + TRACE M7C3 [ISOMORPHOUS WITH FE7C3 (17-0333)]

TABLE-5082 X-RAY DIFFRACTOMETRIC DATA OF ALLOY B3

HEAT TREATMENT : 900,10,00

SL NO	2θ	D(A)	I/I <sub>0</sub>	POSSIBLE CONSTITUENTS MATRIX	CARBIDE(S)
1	48.1	2.378	24.0		M23 M3 M7
2	50.9	2.255	10.0		M3 M5 M7
3	55.1	2.095	22.0		M3
4	55.7	2.074	100.0	A	M3 M5
5	57.6	2.011	80.0		M3 M5
6	59.9	1.941	54.0	UI M*	
7	62.5	1.868	24.0		M3
8	63.3	1.847	22.0		M3 M7
9	65.1	1.801	42.0	A	M23 M5
10	80.0	1.507	17.1		M7
11	99.1	1.273	22.0	UI A*	
12	105.8	1.215	29.0	UI	M5* M7*
13	113.4	1.159	24.4		M3 M7
14	114.8	1.150	16.0	UI	
15	117.9	1.131	24.4		M5
16	119.0	1.124	24.0	UI	
17	122.8	1.103	20.0	UI	
18	126.0	1.087	39.0		M23

STRUCTURE : AUSTENITE  
 + M3C [ISOMORPHOUS WITH FE3C (23-1113)]  
 + M5C2 [ISOMORPHOUS WITH FE5C2 (20-0508)]  
 + SOME M7C3 [ISOMORPHOUS WITH CR7C3+MN7C3 (03-075)]  
 + SOME M23C6 [ISOMORPHOUS WITH M23C6 (11-0545)]  
 \* PROBABLE CONSTITUENT

TABLE-5.83 X-RAY DIFFRACTOMETRIC DATA OF ALLOY B3

HEAT TREATMENT : 950,4,00

SL NO	2θ	D(A)	I/I0	POSSIBLE MATRIX	CONSTITUENTS	CARBIDE(S)
1	48.4	2.364	2.9			M23
2	50.4	2.276	2.9			M7
3	51.3	2.238	3.0	UI		
4	54.8	2.106	6.0			M3 M5
5	55.1	2.095	13.4			M3 M5
6	55.7	2.074	100.0	A		
7	57.2	2.024	2.9	ALPHA	M	M3 M5 M7
8	57.6	2.011	4.0		M*	M3 M5
9	58.0	1.999	13.5			M5
10	59.2	1.962	4.8			M7
11	63.0	1.854	2.9			M3
12	65.3	1.796	9.6	A		M23 M5
13	98.4	1.280	4.8			M7
14	117.0	1.136	4.0	UI		M5*
15	125.0	1.092	32.0	UI		M23*

STRUCTURE : AUSTENITE  
 + M3C [ISOMORPHOUS WITH FE3C (23-1113)]  
 + M5C2 [ISOMORPHOUS WITH FE5C2 (20-0508)]  
 + SOME M7C3 [ISOMORPHOUS WITH CR7C3 (11-0550)]  
 + TRACE M23C6 [ISOMORPHOUS WITH M23C6 (11-0545)]

TABLE-5.84 X-RAY DIFFRACTOMETRIC DATA OF ALLOY B3

HEAT TREATMENT : 950,10,00

SL NO	2θ	D(A)	I/I0	POSSIBLE MATRIX	CONSTITUENTS	CARBIDE(S)
1	48.2	2.373	5.0			M23 M3 M7
2	54.8	2.106	3.3			M3 M5
3	55.7	2.074	100.0	A		M3 M5
4	56.6	2.044	4.4			M23 M7
5	57.8	2.005	21.1		M*	M3 M5
6	59.1	1.965	8.9			M3 M7
7	62.7	1.862	6.7			M7
8	65.2	1.798	7.2	A		M23 M5
9	66.9	1.758	3.3			M3
10	70.6	1.677	4.4			M3
11	98.9	1.275	7.0	UI		M7*
12	99.4	1.270	4.4	A		
13	105.9	1.214	3.0	UI		M5* M7*
14	119.1	1.124	8.0	UI		M5*
15	125.6	1.089	32.0	UI		M23*
16	125.9	1.088	33.3			M23
17	126.9	1.083	6.1	A		

STRUCTURE : AUSTENITE  
 + M3C [ISOMORPHOUS WITH FE3C (23-1113)]  
 + M5C2 [ISOMORPHOUS WITH FE5C2 (20-0508)]  
 + SOME M7C3 [ISOMORPHOUS WITH CR7C3+MN7C3 (03-075)]  
 + SOME M23C6 [ISOMORPHOUS WITH M23C6 (11-0545)]

\* PROBABLE



TABLE-5.85 X-RAY DIFFRACTOMETRIC DATA OF ALLOY B3

HEAT TREATMENT : 1000,4,00

SL NO	2 $\theta$	D(A)	I/I <sub>0</sub>	POSSIBLE MATRIX	CONSTITUENTS	CARBIDE(S)
1	48.3	2.368	3.9			M23
2	55.7	2.074	100.0	A		M3 M5
3	57.2	2.024	7.8	ALPHA	M	M3 M5 M7
4	58.1	1.995	17.2			M5
5	58.8	1.974	7.0			M3
6	59.2	1.962	9.4			M7
7	63.0	1.854	7.8			M3 M7
8	65.0	1.803	28.1			M23 M5 M7
9	65.8	1.784	15.6			M23 M7
10	98.4	1.280	6.3			M7
11	98.6	1.278	11.0	UI		M7*
12	99.3	1.271	7.8	A		
13	119.1	1.124	5.0	UI		M5*
14	124.8	1.093	19.0	UI		

STRUCTURE : AUSTENITE  
 + M5C2 [ISOMORPHOUS WITH FE5C2 (20-508)]  
 + M7C3 [ISOMORPHOUS WITH CR7C3 (11-0550)],  
 FE7C3 (17-0333), CR7C3+MN7C3 (03-075)]  
 + SOME M3C [ISOMORPHOUS WITH FE3C (23-1113)]  
 + TRACE M23C6 [ISOMORPHOUS WITH M23C6 (11-0545)]

TABLE-5.86 X-RAY DIFFRACTOMETRIC DATA OF ALLOY B3

HEAT TREATMENT : 1000,10,00

SL NO	2 $\theta$	D(A)	I/I <sub>0</sub>	POSSIBLE MATRIX	CONSTITUENTS	CARBIDE(S)
1	49.9	2.297	2.0			M7
2	54.5	2.116	2.7			M5 M7
3	55.4	2.084	100.0	A		M3 M5
4	57.6	2.011	9.5			M3 M5
5	58.2	1.992	1.8			M5 M7
6	59.1	1.965	2.3			M3 M7
7	65.0	1.803	15.0	A		M23 M5 M7
8	98.4	1.280	4.0			M7
9	124.8	1.093	6.0	UI		
10	125.1	1.092	8.0	UI		
11	126.0	1.087	2.7			M23

STRUCTURE : AUSTENITE  
 + M5C2 [ISOMORPHOUS WITH FE5C2 (20-508)]  
 + M7C3 [ISOMORPHOUS WITH CR7C3 (11-0550)],  
 FE7C3 (17-0333), CR7C3+MN7C3 (03-075)]  
 + TRACE M23C6 [ISOMORPHOUS WITH M23C6 (11-0545)]

\* PROBABLE

TABLE-5387 X-RAY DIFFRACTOMETRIC DATA OF ALLOY B3

HEAT TREATMENT : 1050,4,00

SL NO	2θ	D(A)	I/I <sub>0</sub>	POSSIBLE MATRIX	CONSTITUENTS CARBIDE(S)
1	49.8	2.301	2.1		M3 M7
2	54.2	2.127	2.1		M5 M7
3	55.4	2.084	100.0	A	M3 M5
4	64.0	1.828	2.9		M5 M7
5	64.7	1.811	13.9		M5 M7
6	65.1	1.801	2.9	A	M23 M5
7	98.2	1.282	2.3		M7
8	124.5	1.095	12.0	UI	

STRUCTURE : AUSTENITE  
 + M5C2 [ISOMORPHOUS WITH MN5C2 (14-0176)]  
 + SOME M7C3 [ISOMORPHOUS WITH CR7C3 (11-0550), (CR,FE)7C3 (05-0720)]

TABLE-5388 X-RAY DIFFRACTOMETRIC DATA OF ALLOY B3

HEAT TREATMENT : 1050,6,00

SL NO	2θ	D(A)	I/I <sub>0</sub>	POSSIBLE MATRIX	CONSTITUENTS CARBIDE(S)
1	49.7	2.306	5.3		M7
2	54.4	2.120	4.4		M7
3	55.4	2.084	100.0	A	M3 M5
4	63.8	1.834	1.9		M5 M7
5	64.6	1.813	23.9		M5 M7
6	65.1	1.801	2.5	A	M23 M5
7	98.3	1.281	10.1		M7
8	98.7	1.277	5.0	UI	
9	124.7	1.094	12.0	UI	
10	126.0	1.087	2.5		M23

STRUCTURE : AUSTENITE  
 + M5C2 [ISOMORPHOUS WITH MN5C2 (14-0176)]  
 + M7C3 [ISOMORPHOUS WITH CR7C3 (11-0550), (CR,FE)7C3 (05-0720)]

TABLE-5389 X-RAY DIFFRACTOMETRIC DATA OF ALLOY B3

HEAT TREATMENT : 1050,10,00

SL NO	2θ	D(A)	I/I <sub>0</sub>	POSSIBLE MATRIX	CONSTITUENTS CARBIDE(S)
1	49.7	2.306	1.7		M7
2	54.4	2.120	1.6		M5 M7
3	55.6	2.078	100.0	A	M3 M5
4	56.6	2.044	3.0		M23 M5
5	63.3	1.847	3.0		M3 M7
6	64.7	1.811	7.6		M5 M7
7	65.3	1.796	3.0	A	M23 M5
8	98.3	1.281	3.6		M7
9	125.1	1.092	22.0	UI	
10	125.4	1.090	15.0	UI	

STRUCTURE : AUSTENITE  
 + M5C2 [ISOMORPHOUS WITH MN5C2 (14-0176)]  
 + M7C3 [ISOMORPHOUS WITH CR7C3 (11-0550), (CR,FE)7C3 (05-0720)]

TABLE-5090 X-RAY DIFFRACTOMETRIC DATA OF ALLOY B4

AS CAST

SL NO	2 $\theta$	D(A)	I/I <sub>0</sub>	POSSIBLE MATRIX	CONSTITUENTS	CARBIDE(S)
1	48.0	2.382	3.3		M23	M3 M7
2	55.9	2.067	100.0	M		M5
3	57.2	2.024	44.2	A		M3 M5
4	57.5	2.014	40.0	ALPHA	M	M3 M5 M7
5	58.8	1.974	4.5		M	M3 M5 M7
6	62.3	1.873	4.8			M3
7	64.1	1.826	4.2			M3 M7
8	65.0	1.803	26.1	A*		M5
9	111.9	1.169	4.8	ALPHA		
10	112.5	1.165	3.0	ALPHA	M23	M7
11	118.2	1.161	3.0			M5
12	126.4	1.085	3.0	UI		

STRUCTURE : PEARLITE/BAINITE

+ MARTENSITE+AUSTENITE (P)

+ M3C [ISOMORPHOUS WITH FE3C (23-1113)]

+ M5C2 [ISOMORPHOUS WITH FE5C2 (20-508)]

\* PROBABLE

TABLE-5.91 X-RAY DIFFRACTOMETRIC DATA OF ALLOY B4

HEAT TREATMENT : 900,4,00

SL NO	2θ	D(Å)	I/I0	POSSIBLE MATRIX	POSSIBLE CARBIDE(S)
1	48.0	2.382	9.3		M23 M3 M7
2	50.9	2.255	6.5		M3 M5 M7
3	55.7	2.074	100.0	A	M3 M5
4	56.0	2.037	7.4	ALPHA	M3 M5 M7
5	57.3	2.021	16.7	M*	M3 M5
6	57.6	2.011	50.0		M3 M5
7	58.9	1.971	13.0		M3
8	62.6	1.865	9.3		M3 M7
9	63.3	1.847	8.3		M3 M7
10	65.0	1.803	40.7	A	M23 M5 M7
11	66.8	1.760	7.4		M3
12	70.3	1.683	3.7		M23 M3
13	99.0	1.274	11.0	UI	
14	99.6	1.268	5.6	A	
15	105.7	1.216	6.0	UI	
16	108.6	1.193	7.4		M23
17	125.6	1.089	14.0	UI	
18	126.0	1.087	14.8		M23

STRUCTURE : AUSTENITE  
 + TRACE MARTENSITE  
 + M3C [ISOMORPHOUS WITH FE3C (23-1113)]  
 + M5C2 [ISOMORPHOUS WITH FE5C2 (20-508)]  
 + TRACE M23C6 [ISOMORPHOUS WITH M23C6 (11-0545)]  
 + TRACE M7C3 [ISOMORPHOUS WITH FE7C3 (17-0333), CR7C3+MN7C3 (03-075)]

TABLE-5.92 X-RAY DIFFRACTOMETRIC DATA OF ALLOY B4

HEAT TREATMENT : 900,10,00

SL NO	2θ	D(Å)	I/I0	POSSIBLE MATRIX	POSSIBLE CARBIDE(S)
1	48.0	2.382	3.4		M23 M3 M7
2	50.8	2.259	2.5		M3 M5 M7
3	55.7	2.074	100.0	A	M3 M5
4	57.0	2.031	8.5	ALPHA	M5 M7
5	57.5	2.014	14.4	M	M3 M5 M7
6	58.8	1.974	6.8		M3
7	62.3	1.873	5.9		M3
8	63.0	1.854	4.7		M3 M7
9	64.4	1.818	3.4		M5 M7
10	65.0	1.803	7.6	A	M23 M5 M7
11	66.7	1.762	2.5		M3
12	70.3	1.683	3.0		M23 M3
13	108.6	1.193	3.4		M23
14	113.2	1.160	3.0		M3 M7
15	118.8	1.126	5.0	UI	
16	125.5	1.090	5.0	UI	
17	126.1	1.087	4.2		M23
18	126.8	1.083	3.0	A	

STRUCTURE : AUSTENITE  
 + MARTENSITE (\*)  
 + M3C [ISOMORPHOUS WITH FE3C (23-1113)]  
 + M5C2 [ISOMORPHOUS WITH FE5C2 (20-0508)]  
 + TRACE M23C6 [ISOMORPHOUS WITH M23C6 (11-0545)]  
 + TRACE M7C3 [ISOMORPHOUS WITH FE7C3 (17-0333), CR7C3+MN7C3 (03-075)]

\* PROBABLE

TABLE-5-93 X-RAY DIFFRACTOMETRIC DATA OF ALLOY B4

HEAT TREATMENT : 950,4,00

SL NO	2θ	D(A)	I/I0	POSSIBLE CONSTITUENTS MATRIX	CARBIDE(S)
1	48.0	2.382	10.6		M23 M3 M7
2	50.9	2.255	6.7		M3 M5 M7
3	55.0	2.098	11.5		M3 M5 M7
4	55.6	2.078	100.0	A	M3 M5 M7
5	56.1	2.061	28.8	M	M3 M5 M7
6	57.7	2.008	39.4		M3 M5 M7
7	58.9	1.971	14.4		M3 M5 M7
8	62.4	1.870	15.4		M3 M5 M7
9	64.9	1.806	51.0		M3 M5 M7
10	65.0	1.803	46.2		M23 M3 M5 M7
11	66.7	1.762	9.6	A	M3 M5 M7
12	93.7	1.328	5.8	M	M23 M3 M5 M7
13	98.3	1.281	5.8		M23 M3 M5 M7
14	98.8	1.276	17.0	UI	
15	99.6	1.268	15.8	A	
16	105.7	1.216	11.0	UI	
17	117.9	1.131	7.7		M5
18	119.2	1.123	10.0	UI	
19	124.1	1.097	8.0	UI	
20	125.6	1.089	69.0	UI	

STRUCTURE : AUSTENITE  
 + TRACE MARTENSITE(M)  
 + M3C [ISOMORPHOUS WITH FE3C (23-1113)]  
 + M5C2 [ISOMORPHOUS WITH FE5C2 (20-508)]  
 + SOME M7C3 [ISOMORPHOUS WITH CR7C3 (11-0550),  
 FE7C3 (17-0333)]  
 + TRACE M23C6 [ISOMORPHOUS WITH M23C6 (11-0545)]

TABLE-5-94 X-RAY DIFFRACTOMETRIC DATA OF ALLOY B4

HEAT TREATMENT : 950,10,00

SL NO	2θ	D(A)	I/I0	POSSIBLE CONSTITUENTS MATRIX	CARBIDE(S)
1	48.1	2.378	28.1		M23 M3 M7
2	51.1	2.247	19.0	UI	
3	55.7	2.074	100.0	A	M23 M3 M5 M7
4	56.2	2.057	67.2	M	M23 M3 M5 M7
5	56.7	2.041	17.2		M23 M3 M5 M7
6	57.3	2.021	21.9	ALPHA	M3 M5 M7
7	57.8	2.005	92.2	M	M3 M5 M7
8	59.1	1.965	48.4		M23 M3 M5 M7
9	60.6	1.920	7.8		M3 M5 M7
10	61.5	1.895	9.4		M3 M5 M7
11	62.0	1.881	9.4		M23 M3 M5 M7
12	62.6	1.865	35.9		M3 M5 M7
13	63.5	1.841	19.0	UI	
14	64.6	1.813	39.1		M3 M5 M7
15	65.1	1.801	67.2	A	M23 M3 M5 M7
16	67.0	1.756	9.4		M23 M3 M5 M7
17	70.3	1.683	7.8		M23 M3 M5 M7
18	93.5	1.330	4.7		M23 M3 M5 M7
19	93.8	1.327	6.0	UI	
20	100.5	1.260	15.6		M23 M3 M5 M7
21	118.5	1.127	13.0	UI	
22	122.4	1.106	13.0	UI	
23	126.0	1.087	37.5		M23

STRUCTURE : AUSTENITE  
 + M3C [ISOMORPHOUS WITH FE3C (23-1113)]  
 + M5C2 [ISOMORPHOUS WITH FE5C2 (20-508)]  
 + SOME M7C3 [ISOMORPHOUS WITH CR7C3 (11-0550),  
 CR7C3+MN7C3 (03-075)]  
 + TRACE M23C6 [ISOMORPHOUS WITH M23C6 (11-0545)]

TABLE-5.95 X-RAY DIFFRACTOMETRIC DATA OF ALLOY B4

HEAT TREATMENT : 1000,4,00

SL NO	2θ	D(A)	I/I0	POSSIBLE MATRIX	CONSTITUENTS	CARBIDE(S)
1	50.0	2.293	3.9			M5 M7
2	55.4	2.084	100.0	A M		M3 M5
3	56.2	2.057	9.1		M	M23 M3 M5
4	56.7	2.041	3.0			M7
5	57.7	2.008	14.4			M3 M5
6	58.9	1.971	7.7			M3
7	62.6	1.865	5.8			M3 M7
8	64.8	1.808	7.7			M7
9	65.0	1.803	32.7	UI A		M23 M5 M7
10	124.7	1.014	4.0	UI		
11	125.0	1.092	19.2	UI		

STRUCTURE : AUSTENITE

- + M5C2 [ISOMORPHOUS WITH FE5C2 (20-0508)]
- + SOME M3C [ISOMORPHOUS WITH FE3C (23-1113)]
- + SOME M7C3 [ISOMORPHOUS WITH CR7C3 (11-0550), (CR,FE)7C3 (05-0720)]

TABLE-5.96 X-RAY DIFFRACTOMETRIC DATA OF ALLOY B4

HEAT TREATMENT : 1000,10,00

SL NO	2θ	D(A)	I/I0	POSSIBLE MATRIX	CONSTITUENTS	CARBIDE(S)
1	48.2	2.373	12.5			M23 M3 M7
2	52.3	2.199	16.1			M3 M5
3	55.6	2.078	100.0	A		M3 M5 M7
4	57.2	2.024	12.5			M3 M5 M7
5	58.2	1.992	6.4			M5 M7
6	59.1	1.965	25.0			M3 M7
7	63.0	1.854	14.3			M3 M7
8	65.0	1.803	28.6	A		M23 M3 M5 M7
9	98.5	1.279	17.9			M7
10	104.9	1.222	9.0	UI		
11	105.9	1.214	18.0	UI		
12	124.6	1.094	41.0	UI		

STRUCTURE : AUSTENITE

- + M3C [ISOMORPHOUS WITH FE3C (23-1113)]
- + M5C2 [ISOMORPHOUS WITH FE5C2 (20-508)]
- + M7C3 [ISOMORPHOUS WITH CR7C3 (11-0550), CR7C3+MN7C3 (03-075)]

TABLE-5.97 X-RAY DIFFRACTOMETRIC DATA OF ALLOY B4

HEAT TREATMENT : 1050,4,00

SL NO	2θ	D(A)	I/I0	POSSIBLE MATRIX	CONSTITUENTS CARBIDE(S)		
1	50.0	2.293	2.8			M5	M7
2	51.0	2.251	2.4				M7
3	55.7	2.074	100.0	A	M23	M3	M5
4	57.6	2.011	3.2			M3	M5
5	64.7	1.811	15.7				M5
6	65.0	1.803	15.7	A	M23	M3	M5
7	98.3	1.281	3.2				M7
8	124.9	1.094	10.0	UI			
9	125.9	1.088	5.2		M23		

STRUCTURE : AUSTENITE  
 + MSC2 [ISOMORPHOUS WITH FE5C2 (20-0508)]  
 + SOME M7C3 [ISOMORPHOUS WITH FE7C3 (17-0333), (CR,FE)7C3 (05-0720), CR7C3 (11-0550)]

TABLE-5.98 X-RAY DIFFRACTOMETRIC DATA OF ALLOY B4

HEAT TREATMENT : 1050,6,00

SL NO	2θ	D(A)	I/I0	POSSIBLE MATRIX	CONSTITUENTS CARBIDE(S)		
1	50.6	2.267	7.3			M3	M5
2	55.4	2.084	100.0	A		M3	M5
3	64.4	1.818	7.9				M5
4	64.6	1.813	6.7				M5
5	65.0	1.803	5.0	A	M23		M5
6	98.2	1.282	6.7				M7
7	124.6	1.094	10.0	UI			
8	125.0	1.092	8.0	UI			
9	125.5	1.090	7.0	UI			

+ AUSTENITE + MARTENSITE  
 + MSC2 [ISOMORPHOUS WITH MN5C2 (14-0176)]  
 + TRACE M7C3 [ISOMORPHOUS WITH CR7C3 (11-0550)]

TABLE-5.99 X-RAY DIFFRACTOMETRIC DATA OF ALLOY B4

HEAT TREATMENT : 1050,10,00

SL NO	2θ	D(A)	I/I0	POSSIBLE MATRIX	CONSTITUENTS CARBIDE(S)		
1	54.6	2.113	10.0				M5
2	55.6	2.078	32.9	A		M3	M5
3	64.3	1.821	7.6				M5
4	65.0	1.803	100.0	A	M23		M5
5	98.2	1.283	6.0				M7
6	124.6	1.094	7.0	UI			
7	125.2	1.091	10.0	UI			

STRUCTURE : AUSTENITE  
 + MSC2 [ISOMORPHOUS WITH MN5C2 (14-0176)]  
 + SOME M7C3 [ISOMORPHOUS WITH CR7C3 (11-0550), FE7C3 (17-0333)]

TABLE-5.100(A) SUMMARY OF X-RAY DIFFRACTOMETRIC DATA

HT COND	ALLOY	MATRIX			CARBIDE(S)			
		P/B	M	A	M23	M3	M5	M7
AS CAST	B1	P	P		S	P	T	
	B2	P	P		T	P	T	
	B3	P	P	T*	T	P	T*	
	B4	P	P	T		P	P	
900 4 00	B1		S/T	P	P	P	T	
	B2		S/T	P	T	P	T	T
	B3		S	P	S	P	T	T
	B4		T	P	T	P	T	T*
900 10 00	B1		T/S	P	P	P	T	T*
	B2		T	P		S	S	T*
	B3		T*	P	S	P	P	S*
	B4		T*	P	T	P	P	P*
950 4 00	B1			P	S	P	T	T
	B2			P		S	S	T
	B3			P	T*	P	P	S
	B4		T*	P	T	P	P	S
950 10 00	B1			P	P*	P	T	T
	B2			P		S	T	S
	B3			P	S	P	P	S
	B4			P	T	P	P	S
1000 4 00	B1			P	T	S	S	S
	B2			P		T	S	S
	B3			P	T	S	P	P
	B4			P		S	P	S
1000 10 00	B1			P		S	P	S
	B2			P		T	P	S
	B3			P	T		P	P
	B4			P		S	P	P*
1050 4 00	B1			P		T	P	P
	B2			P			P	P
	B3			P			P	S*
	B4			P			P	S*
1050 6 00	B1			P			P	P
	B2			P			P	P
	B3			P			P	P
	B4			P			P	S
1050 10 00	B1			P			S	P
	B2			P			S	P
	B3			P			P	P
	B4			P			P	S

P=PRESENT ; S=SOME ; T=TRACE ; \*\*PROBABLE



## SUMMARY OF THE CARBIDE TRANSFORMATION IN EXPERIMENTAL ALLOYS

TABLE 5:100(B)

CARBIDE	COND/HEAT-TREATMENT		B1	B2	B3	B4
M3	AS-CAST		P	P	P	P
	900	4 00	P	P	P	P
	900	10 00	P	S	P	P
	950	4 00	P	S	P	P
	950	10 00	P	S	P	P
	1000	4 00	S	T	S	S
	1000	10 00	S	T	S	S
	1050	4 00	T	-	-	-
	1050	6 00	-	-	-	-
	1050	10 00	-	-	-	-
M5	AS-CAST		T	T	T*	P
	900	4 00	T	T	T*	T
	900	10 00	T	S	T*	T
	950	4 00	T	S	P	P
	950	10 00	T	S	P	P
	1000	4 00	S	P	P	P
	1000	10 00	S	P	P	P
	1050	4 00	P	P	P	P
	1050	6 00	P	P	P	P
	1050	10 00	S	S	P	P
M23	AS-CAST		S	T	T	-
	900	4 00	P	T	S	T
	900	10 00	P	-	S	T
	950	4 00	S	-	T*	T
	950	10 00	P	-	S*	T
	1000	4 00	T	-	T	-
	1000	10 00	T	-	T	-
	1050	4 00	-	-	-	-
	1050	6 00	-	-	-	-
	1050	10 00	-	-	-	-
M7	AS-CAST		-	-	-	-
	900	4 00	T*	T	T	T*
	900	10 00	T*	T	S	T*
	950	4 00	T	T	S	S
	950	10 00	T	T	S	S
	1000	4 00	S	S	P	S
	1000	10 00	S	S	P	S
	1050	4 00	P	P	S*	S
	1050	6 00	P	P	S*	S
	1050	10 00	P	P	S*	S

P=PRESENT ; S=SOME ; T=TRACE ; \*=PROBABLE

TABLE-5.101 EFFECT OF HT ON COMPRESSION BEHAVIOUR OF ALLOY B1

HT CONDITION	DEFORMATION	COMPRESSIVE STRENGTH MN/M2	TSI
AS CAST	7.34	1972.08	127.23
900 4 00	21.96	2008.08	129.55
900 10 00	20.56	2091.73	134.95
950 4 00	21.00	2094.34	141.57
950 10 00	21.18	2022.91	130.51
1000 4 00	23.47	2305.35	148.73
1000 10 00	24.60	2444.66	157.72
1050 4 00	23.87	2350.58	151.65
1050 6 00	25.98	2337.40	150.80
1050 10 00	28.66	2450.40	158.09

TABLE-5.102 EFFECT OF HT ON COMPRESSION BEHAVIOUR OF ALLOY B2

HT CONDITION	DEFORMATION %	COMPRESSIVE STRENGTH MN/M2	TSI
AS CAST	11.79	2116.22	136.53
900 4 00	22.43	2083.67	134.43
900 10 00	23.58	2132.18	137.56
950 4 00	28.38	2400.95	154.90
950 10 00	28.63	2464.66	159.01
1000 4 00	29.22	2747.53	177.26
1000 10 00	32.07	2886.49	186.41
1050 4 00	38.67	2647.93	167.72
1050 6 00	35.97	2756.52	177.84
1050 10 00	42.68	3218.40	207.64

TABLE-5.103 EFFECT OF HT ON COMPRESSION BEHAVIOUR OF ALLOY B3

HT CONDITION	DEFORMATION %	COMPRESSIVE STRENGTH MN/M2	TSI
AS CAST	7.47	2253.03	145.36
900 4 00	20.41	2175.03	140.33
900 10 00	21.25	2228.90	143.80
950 4 00	22.58	2434.43	157.06
950 10 00	22.17	2353.39	151.83
1000 4 00	28.07	2533.79	163.47
1000 10 00	31.28	2779.35	179.31
1050 4 00	33.91	2416.63	155.91
1050 6 00	31.54	2559.21	165.11
1050 10 00	35.14	2863.30	184.36

TABLE-5.104 EFFECT OF HT ON COMPRESSION BEHAVIOUR OF ALLOY B4

HT CONDITION	DEFORMATION	COMPRESSIVE STRENGTH MN/M2	TSI
AS CAST	12.01	2352.37	151.77
900 4 00	27.25	2219.33	143.18
900 10 00	28.31	2287.96	147.61
950 4 00	28.10	2340.50	151.00
950 10 00	28.43	2297.35	148.22
1000 4 00	30.90	2682.59	173.07
1000 10 00	31.79	2845.30	183.57
1050 4 00	35.80	2552.70	164.69
1050 6 00	35.40	2772.33	178.86
1050 10 00	34.81	2909.22	187.69

TABLE-5.105 RELATIVE COMPRESSIVE BEHAVIOUR OF THE ALLOYS

HT CONDITION	COMPRESSION STRENGTH MN/M2			
	B1	B2	B3	B4
AS CAST	1972.08	2116.22	2253.03	2352.37
900 4 00	2008.08	2083.67	2175.03	2219.33
900 10 00	2091.73	2132.18	2228.90	2287.96
950 4 00	2094.34	2400.95	2434.43	2340.50
950 10 00	2022.91	2464.66	2353.39	2297.35
1000 4 00	2305.35	2747.53	2533.79	2682.59
1000 10 00	2444.66	2886.49	2779.35	2845.30
1050 4 00	2350.58	2647.93	2416.63	2552.70
1050 6 00	2337.40	2756.52	2559.21	2772.33
1050 10 00	2450.40	3218.40	2863.30	2909.22

TABLE-5.106 RELATIVE PERCENT DEFORMATION OF THE ALLOYS

HT CONDITION	DEFORMATION (%)			
	B1	B2	B3	B4
AS CAST	17.34	11.79	7.47	12.01
900 4 00	21.96	22.43	20.41	27.25
900 10 00	20.56	23.58	21.25	28.31
950 4 00	21.00	28.38	22.58	28.10
950 10 00	21.18	28.63	22.17	28.43
1000 4 00	23.47	29.22	28.07	30.90
1000 10 00	24.60	32.07	31.28	31.79
1050 4 00	23.87	38.67	33.91	35.80
1050 6 00	25.98	35.97	31.54	35.40
1050 10 00	28.66	42.68	35.14	34.81

TABLE - 5.107 SUMMARY OF COMPRESSIVE STRENGTH DATA

PARAMETER	B1	B2	B3	B4
CS in As cast cond. (MPa)	1972	2116	2253	2352
		B4 > B3 > B2 > B1		
Effect of SP (4 to 10 hrs)				
(a) At 900°C (% improvement in CS)	max., (4.2)	2.3	2.5	3.1
		B1 > B4 > B3, B2		
(b) At 950°C (% deterioration in CS)	max., (3.4)	UA	≈, (3.3)	min., (1.8)
		B1, B3 > B4 > B2		
(c) At 1000°C (% improvement in CS)	≈B4, (6.0)	min., (5.1)	mix., (9.7)	≈B1, (6.1)
		B3 > B1, B4 > B2		
(d) At 1050°C (% improvement in CS)	min., (4.3)	max., (21.5)	<B2, (18.5)	<B3, (14.0)
		B2 > B3 > B4 > B1		
Effect of ST (900-950)				
(a) At 4 hrs. (% improvement in CS)	min., (4.3)	max., (15.2)	<B2, (11.9)	<B3, (5.5)
		B2 > B3 > B4 > B1		
(b) At 10 hrs.	-	(15.6%)	(5.6%)	(0.4%)
		B2 > B3 > B4 > B1		

Effect of ST (950-1000°C)

(a) At 4 hrs. (% improvement in CS)  $\leq B2, (10.1)$

(b) At 10 hrs. (% improvement in CS)  $=B4, (14.4)$

$B2, B4 > B1 > B3$  min., (4.1)

$=B2, (14.6)$

Effect of ST (1000-1050°C)

(a) At 4 hrs. (% deterioration in CS)

$=B3, (17.1)$

$B4 > B1 > B3, B2$

$=B2, (18.1)$  max., (23.9)

(b) At 10 hrs (% improvement in CS)

(3.6)

(4.6)

(4.8)

CS at 1050, 10 hrs.00 min.

min., (0.2)

max., (11.5)

$B2 > B3 > B4 > B1$

$\leq B2, (3.0)$

$\leq B3, (2.3)$

$B2 > B4 > B3 > B1$

$=B4$

$=B3$



TABLE 5-108 PERCENT DEFORMATION AT A GLANCE

PARAMETER	B1	B2	B3	B4
% deformation in as-cast cond.				
% deformation at 1050°C, 10 hrs in min., =B3				
Effect of SP (4 to 10 hrs)				
(a) at 900 and 950°C				
(b) at 1000°C (increased)	UA			
(c) at 1050°C (increased) max.				

max, =B4  
B2, B4 > B1, B3

max.  
B2 > B3 > B4 > B1

UA

UA

=B3  
B2, B3 > B1 > B4

=B2

=B1

B1, B2 > B3 > B4

<B1

UA

=B1

Effect of ST (900-1050 °C)

(a) at 4 hrs ( increased) min.

<B3

<B2

max.  
B2 > B3 > B4 > B1

(b) at 10 hrs (increased) <B3

min

<B2

max.  
B2 > B3 > B1 > B4

Effect of ST (1000-1050 °C)

(a) at 4 hrs (increased) Min

=B3

=B4

max.  
B2 > B3, B4 > B1

(b) at 10 hrs (increased) =B3

min.

=B1

max.  
B2 > B1, B3 > B4

Effect of ST (900-950 °C)

(a) at 4 hrs (increased) -

<B3

<B2

max.  
B2 > B3 > B4 > B1

(b) at 10 hrs (increased) =B3

min.

=B1

max.  
B2 > B1, B3 > B4

TABLE-5.109 EFFECT OF HT AND TD ON CORROSION BEHAVIOUR

CORROSIVE ENVIRONMENT : 5% NaCl AS CAST, 168HRS = 30.354 MDD  
 ALLOY DESIGNATION : B1 720HRS = 21.439 MDD

H.T. CONDITION		S.R. CONDITION			CORROSION DATA					
TEMP. DEG. C	TIME HRS	HT	TEMP. DEG. C	TIME HRS	HT	S. AREA SQ. CM	WT. LOSS GMS	T D HRS	CORROSION RATE IPY	MDD
900	4	00	---	---	--	2.8309	.00527	168	.00486	26.595
900	4	00	---	---	--	2.8841	.01897	720	.00401	21.925
900	4	00	600	0.5	AC	2.5146	.00493	168	.00512	28.008
900	4	00	600	0.5	AC	2.5737	.01865	720	.00471	22.810
900	10	00	---	---	--	2.9329	.00477	168	.00425	23.234
900	10	00	---	---	--	2.8578	.01707	720	.00364	19.911
900	10	00	600	0.5	AC	2.9732	.00500	168	.00439	24.024
900	10	00	600	0.5	AC	2.9531	.01826	720	.00377	20.611
950	4	00	---	---	--	5.3959	.00829	168	.00401	21.948
950	4	00	---	---	--	5.4205	.02898	720	.00326	17.821
950	4	00	600	0.5	AC	5.7621	.00926	168	.00420	22.958
950	4	00	600	0.5	AC	5.7147	.03096	720	.00330	18.059
950	10	00	---	---	--	4.4679	.00836	168	.00489	26.730
950	10	00	---	---	--	4.3465	.02727	720	.00382	20.913
950	10	00	600	0.5	AC	3.7959	.00728	168	.00501	27.398
950	10	00	600	0.5	AC	3.7543	.02440	720	.00396	21.664
1000	4	00	---	---	--	5.9483	.00885	168	.00389	21.255
1000	4	00	---	---	--	5.9162	.03092	720	.00319	17.421
1000	4	00	600	0.5	AC	5.5517	.00939	168	.00442	24.162
1000	4	00	600	0.5	AC	5.5087	.02955	720	.00327	17.881
1000	10	00	---	---	--	4.3555	.00702	168	.00421	23.025
1000	10	00	---	---	--	4.5088	.02467	720	.00334	18.238
1000	10	00	600	0.5	AC	5.1837	.00860	168	.00433	23.701
1000	10	00	600	0.5	AC	4.8857	.02807	720	.00350	19.151
1050	4	00	---	---	--	4.6415	.00684	168	.00385	21.052
1050	4	00	---	---	--	4.6115	.02236	720	.00296	16.162
1050	4	00	600	0.5	AC	4.7739	.00791	168	.00433	23.670
1050	4	00	600	0.5	AC	4.4475	.02380	720	.00326	17.838
1050	6	00	---	---	--	4.5630	.00668	168	.00382	20.913
1050	6	00	---	---	--	4.0697	.02555	720	.00383	20.927
1050	6	00	600	0.5	AC	4.6218	.00625	168	.00353	19.319
1050	6	00	600	0.5	AC	4.5015	.02484	720	.00336	18.394
1050	10	00	---	---	--	4.9467	.00724	168	.00382	20.909
1050	10	00	---	---	--	4.4262	.02261	720	.00311	17.027
1050	10	00	600	0.5	AC	4.3047	.00613	168	.00372	20.343
1050	10	00	600	0.5	AC	4.1276	.02013	720	.00308	16.823

TABLE-56110 EFFECT OF HT AND TD ON CORROSION BEHAVIOUR

CORROSIVE ENVIRONMENT : 5% NaCl AS CAST, 168HRS = 29.576 MDD  
 ALLOY DESIGNATION : B2 720HRS = 27.243 MDD

H.T. CONDITION		S.R. CONDITION		CORROSION DATA						
TEMP DEG.C	TIME HRS	HT	TEMP DEG.C	TIME HRS	HT	S. AREA SQ. CM	WT. LOSS GMS	T D HRS	CORROSION RATE IPY	MDD
900	4	00	---	---	--	3.6373	.00663	168	.00476	26.040
900	4	00	---	---	--	3.7582	.02359	720	.00383	20.923
900	4	00	600	0.5	AC	3.9288	.00753	168	.00501	27.381
900	4	00	600	0.5	AC	3.6831	.02533	720	.00419	22.925
900	10	00	---	---	--	3.9850	.00583	168	.00382	20.900
900	10	00	---	---	--	3.9452	.02211	720	.00342	18.681
900	10	00	600	0.5	AC	5.4447	.00820	168	.00393	21.515
900	10	00	600	0.5	AC	5.3604	.03109	720	.00354	19.333
950	4	00	---	---	--	4.8411	.00767	168	.00414	22.634
950	4	00	---	---	--	4.8424	.02532	720	.00319	17.429
950	4	00	600	0.5	AC	5.1450	.00848	168	.00431	23.546
950	4	00	600	0.5	AC	5.1337	.02754	720	.00327	17.882
950	10	00	---	---	--	4.5257	.00799	168	.00461	25.221
950	10	00	---	---	--	4.4302	.02685	720	.00369	20.202
950	10	00	600	0.5	AC	4.5504	.00814	168	.00467	25.555
950	10	00	600	0.5	AC	4.4780	.02759	720	.00376	20.538
1000	4	00	---	---	--	4.6032	.00692	168	.00393	21.476
1000	4	00	---	---	--	4.5820	.02284	720	.00304	16.616
1000	4	00	600	0.5	AC	4.9644	.00848	168	.00446	24.402
1000	4	00	600	0.5	AC	4.9233	.02749	720	.00340	18.612
1000	10	00	---	---	--	4.7971	.00712	168	.00388	21.203
1000	10	00	---	---	--	4.6738	.02496	720	.00326	17.801
1000	10	00	600	0.5	AC	4.8505	.00762	168	.00410	22.442
1000	10	00	600	0.5	AC	4.5145	.02493	720	.00337	18.407
1050	4	00	---	---	--	4.6405	.00673	168	.00379	20.718
1050	4	00	---	---	--	4.5812	.02484	720	.00331	18.074
1050	4	00	600	0.5	AC	4.8715	.00797	168	.00427	23.372
1050	4	00	600	0.5	AC	4.8863	.02600	720	.00324	17.736
1050	6	00	---	---	--	5.0109	.00708	168	.00369	20.184
1050	6	00	---	---	--	4.8280	.02172	720	.00274	14.996
1050	6	00	600	0.5	AC	5.1243	.00689	168	.00351	19.208
1050	6	00	600	0.5	AC	4.9068	.02840	720	.00353	19.293
1050	10	00	---	---	--	4.3903	.00587	168	.00349	19.101
1050	10	00	---	---	--	4.7074	.02388	720	.00309	16.909
1050	10	00	600	0.5	AC	4.6339	.00589	168	.00332	18.158
1050	10	00	600	0.5	AC	4.5291	.02157	720	.00290	15.875

TABLE-5.111 EFFECT OF HT AND TD ON CORROSION BEHAVIOUR

CORROSIVE ENVIRONMENT : 5% NaCl AS CAST, 168HRS = 30.097 MDD  
 ALLOY DESIGNATION : B3 720HRS = 21.793 MDD

H.T. CONDITION		S.R. CONDITION		CORROSION DATA						
TEMP DEG.C	TIME HRS	HT	TEMP DEG.C	TIME HRS	HT	S. AREA SQ. CM	WT. LOSS GMS	T D HRS	CORROSION RATE IPY	MDD
900	4	OQ	---	---	--	2.9198	.00495	168	.00457	25.002
900	4	OQ	---	---	--	3.1006	.01968	720	.00387	21.157
900	4	OQ	600	0.5	AC	2.2572	.00413	168	.00478	26.138
900	4	OQ	600	0.5	AC	2.5742	.01689	720	.00400	21.871
900	10	OQ	---	---	--	6.9460	.01114	168	.00419	22.912
900	10	OQ	---	---	--	6.8346	.04177	720	.00373	20.372
900	10	OQ	600	0.5	AC	6.7468	.01100	168	.00426	23.291
900	10	OQ	600	0.5	AC	6.6459	.04231	720	.00388	21.221
950	4	OQ	---	---	--	4.8610	.00765	168	.00411	22.482
950	4	OQ	---	---	--	4.8360	.02641	720	.00333	18.204
950	4	OQ	600	0.5	AC	5.1929	.00856	168	.00431	23.548
950	4	OQ	600	0.5	AC	5.1833	.02939	720	.00346	18.900
950	10	OQ	---	---	--	3.2324	.00613	168	.00495	27.092
950	10	OQ	---	---	--	4.0442	.02896	720	.00437	23.870
950	10	OQ	600	0.5	AC	3.6498	.00711	168	.00509	27.829
950	10	OQ	600	0.5	AC	3.5175	.02551	720	.00442	24.174
1000	4	OQ	---	---	--	4.7968	.00747	168	.00407	22.247
1000	4	OQ	---	---	--	4.7795	.02534	720	.00323	17.673
1000	4	OQ	600	0.5	AC	5.0020	.00809	168	.00423	23.105
1000	4	OQ	600	0.5	AC	5.0125	.02768	720	.00337	18.407
1000	10	OQ	---	---	--	3.3958	.00556	168	.00428	23.390
1000	10	OQ	---	---	--	3.3174	.02067	720	.00380	20.770
1000	10	OQ	600	0.5	AC	3.1452	.00574	168	.00453	24.791
1000	10	OQ	600	0.5	AC	3.2393	.02138	720	.00402	22.001
1050	4	OQ	---	---	--	3.2910	.00471	168	.00374	20.445
1050	4	OQ	---	---	--	3.2425	.01880	720	.00353	19.327
1050	4	OQ	600	0.5	AC	3.6548	.00605	168	.00432	23.648
1050	4	OQ	600	0.5	AC	3.6218	.02133	720	.00357	19.631
1050	6	OQ	---	---	--	3.3290	.00544	168	.00427	23.345
1050	6	OQ	---	---	--	3.2579	.01943	720	.00364	19.880
1050	6	OQ	600	0.5	AC	3.4129	.00646	168	.00495	27.041
1050	6	OQ	600	0.5	AC	3.3483	.02217	720	.00404	22.071
1050	10	OQ	---	---	--	3.3649	.00461	168	.00358	19.572
1050	10	OQ	---	---	--	3.0582	.01755	720	.00350	19.129
1050	10	OQ	600	0.5	AC	3.4238	.00504	168	.00385	21.030
1050	10	OQ	600	0.5	AC	3.1874	.01914	720	.00366	20.016

TABLE-5.112 EFFECT OF HT AND TD ON CORROSION BEHAVIOUR

CORROSIVE ENVIRONMENT : 5% NaCl AS CAST, 168HRS = 31.550 MDD  
 ALLOY DESIGNATION : B4 720HRS = 24.851 MDD

H.T. CONDITION		S.R. CONDITION		CORROSION DATA						
TEMP DEG.C	TIME HRS	HT	TEMP DEG.C	TIME HRS	HT	S. AREA SQ. CM	WT. LOSS GMS	T D HRS	CORROSION IPY	RATE MDD
900	4	00	---	---	--	3.9895	.00720	168	.00472	25.782
900	4	00	---	---	--	3.9165	.02788	720	.00434	23.728
900	4	00	600	0.5	AC	3.0499	.00582	168	.00499	27.261
900	4	00	600	0.5	AC	3.4588	.02660	720	.00469	25.635
900	10	00	---	---	--	5.0548	.00820	168	.00424	23.175
900	10	00	---	---	--	5.0470	.03041	720	.00367	20.085
900	10	00	600	0.5	AC	4.3612	.00745	168	.00446	24.404
900	10	00	600	0.5	AC	4.2591	.02585	720	.00370	20.231
950	4	00	---	---	--	4.5852	.00748	168	.00426	23.305
950	4	00	---	---	--	4.5938	.02541	720	.00337	18.438
950	4	00	600	0.5	AC	4.8151	.00794	168	.00431	23.557
950	4	00	600	0.5	AC	4.7572	.02941	720	.00377	20.607
950	10	00	---	---	--	3.4461	.00629	168	.00477	26.075
950	10	00	---	---	--	3.6821	.02274	720	.00376	20.586
950	10	00	600	0.5	AC	4.2004	.00780	168	.00485	26.528
950	10	00	600	0.5	AC	4.0530	.02581	720	.00388	21.227
1000	4	00	---	---	--	5.5972	.00841	168	.00393	21.465
1000	4	00	---	---	--	5.5930	.03056	720	.00333	18.213
1000	4	00	600	0.5	AC	5.2444	.00819	168	.00408	22.310
1000	4	00	600	0.5	AC	5.2615	.03126	720	.00362	19.804
1000	10	00	---	---	--	3.9187	.00576	168	.00384	20.998
1000	10	00	---	---	--	3.7376	.02032	720	.00331	18.122
1000	10	00	600	0.5	AC	4.3541	.00661	168	.00397	21.687
1000	10	00	600	0.5	AC	4.2771	.02476	720	.00353	19.296
1050	4	00	---	---	--	4.8761	.00708	168	.00379	20.743
1050	4	00	---	---	--	4.8628	.02380	720	.00298	16.314
1050	4	00	600	0.5	AC	5.5732	.00820	168	.00384	21.019
1050	4	00	600	0.5	AC	5.5770	.02866	720	.00313	17.130
1050	6	00	---	---	--	4.0503	.00550	168	.00355	19.399
1050	6	00	---	---	--	3.9456	.02083	720	.00322	17.597
1050	6	00	600	0.5	AC	4.5017	.00682	168	.00396	21.643
1050	6	00	600	0.5	AC	4.3308	.02516	720	.00354	19.365
1050	10	00	---	---	--	3.8560	.00494	168	.00335	18.302
1050	10	00	---	---	--	3.5707	.01895	720	.00324	17.690
1050	10	00	600	0.5	AC	3.6893	.00491	168	.00348	19.013
1050	10	00	600	0.5	AC	3.7569	.02075	720	.00337	18.410

**EFFECT OF TEST DURATION ON CORROSION BEHAVIOUR**

**TABLE-5.113 CORROSIVE ENVIRONMENT : 5% NaCl ; ALLOY B1**

H.T.CONDITION			S.R.CONDITION			CORROSION DATA				
TEMP DEG.C	TIME HRS	HT	TEMP DEG.C	TIME HRS	HT	S.AREA SQ.CM	WT.LOSS GMS	T D HRS	CORROSION RATE IPY	MDD
	A S		C A S T			1.9390	.00412	168	.00555	30.354
	A S		C A S T			2.2363	.00891	360	.00486	26.561
	A S		C A S T			2.2436	.01443	720	.00392	21.439
	A S		C A S T			2.3696	.02051	1080	.00352	19.234
900	4	00	---	---	---	2.8309	.00527	168	.00486	26.595
900	4	00	---	---	---	2.7609	.01043	360	.00461	25.185
900	4	00	---	---	---	2.8841	.01897	720	.00401	21.925
900	4	00	---	---	---	3.0687	.02613	1080	.00346	18.923
900	4	00	600	0.5	AC	2.5146	.00493	168	.00512	28.008
900	4	00	600	0.5	AC	2.5844	.00946	360	.00446	24.403
900	4	00	600	0.5	AC	2.5737	.01865	720	.00417	22.810
900	4	00	600	0.5	AC	2.6545	.02460	1080	.00377	20.594

**TABLE-5.114 CORROSIVE ENVIRONMENT : 10% NH4CL ; ALLOY B1**

H.T.CONDITION			S.R.CONDITION			CORROSION DATA				
TEMP DEG.C	TIME HRS	HT	TEMP DEG.C	TIME HRS	HT	S.AREA SQ.CM	WT.LOSS GMS	T D HRS	CORROSION RATE IPY	MDD
	A S		C A S T			2.0967	.01870	168	.02330	127.411
	A S		C A S T			1.9306	.03147	360	.01987	108.673
	A S		C A S T			1.7431	.05090	720	.01780	97.334
	A S		C A S T			2.2314	.08712	1080	.01587	86.762
900	4	00	---	---	---	2.8229	.02383	168	.02206	120.595
900	4	00	---	---	---	3.0147	.04825	360	.01951	106.699
900	4	00	---	---	---	2.9869	.05516	720	.01126	61.557
900	4	00	---	---	---	2.7340	.06090	1080	.00905	49.501
900	4	00	600	0.5	AC	2.1646	.01548	168	.01868	102.165
900	4	00	600	0.5	AC	2.2753	.03982	360	.02134	116.675
900	4	00	600	0.5	AC	2.6437	.07327	720	.01690	92.383
900	4	00	600	0.5	AC	2.4445	.06880	1080	.01144	62.544

**TABLE-5.115 CORROSIVE ENVIRONMENT : 10% (NH4)2SO4 ; ALLOY B1**

H.T.CONDITION			S.R.CONDITION			CORROSION DATA				
TEMP DEG.C	TIME HRS	HT	TEMP DEG.C	TIME HRS	HT	S.AREA SQ.CM	WT.LOSS GMS	T D HRS	CORROSION RATE IPY	MDD
	A S		C A S T			1.6171	.01535	168	.02480	135.605
	A S		C A S T			1.5771	.02944	360	.02276	124.449
	A S		C A S T			1.9055	.06050	720	.01936	105.836
	A S		C A S T			2.0552	.08563	1080	.01693	92.589
900	4	00	---	---	---	2.5845	.02098	168	.02121	115.966
900	4	00	---	---	---	2.8600	.04208	360	.01794	98.087
900	4	00	---	---	---	2.6869	.06719	720	.01524	83.354
900	4	00	---	---	---	2.9262	.07576	1080	.01052	57.534
900	4	00	600	0.5	AC	2.2412	.02193	168	.02556	139.784
900	4	00	600	0.5	AC	1.9862	.03200	360	.01964	107.407
900	4	00	600	0.5	AC	2.6082	.07724	720	.01805	98.713
900	4	00	600	0.5	AC	2.3287	.08015	1080	.01399	76.484

**EFFECT OF TEST DURATION ON CORROSION BEHAVIOUR**

**TABLE-5-116 CORROSIVE ENVIRONMENT : 5% NaCl / ALLOY B2**

H.T. CONDITION		S.R. CONDITION		CORROSION DATA						
TEMP DEG.C	TIME HRS	HT	TEMP DEG.C	TIME HRS	HT	S. AREA SQ. CM	WT. LOSS GMS	T D HRS	CORROSION RATE IPY	MDD
A S			C A S T			2.8643	.00593	168	.00541	29.576
A S			C A S T			4.3204	.01861	360	.00525	28.717
A S			C A S T			3.0736	.02512	720	.00498	27.243
A S			C A S T			3.0440	.03323	1080	.00444	24.259
900	4	OQ	---	---	---	3.6373	.00663	168	.00476	26.040
900	4	OQ	---	---	---	3.5626	.01261	360	.00432	23.597
900	4	OQ	---	---	---	3.7582	.02359	720	.00383	20.923
900	4	OQ	---	---	---	3.8566	.03546	1080	.00374	20.432
900	4	OQ	600	0.5	AC	3.9288	.00753	168	.00501	27.381
900	4	OQ	600	0.5	AC	3.9931	.01453	360	.00444	24.258
900	4	OQ	600	0.5	AC	3.6831	.02533	720	.00419	22.925
900	4	OQ	600	0.5	AC	4.0363	.03824	1080	.00385	21.053

**TABLE-5-117 CORROSIVE ENVIRONMENT : 10% NH4CL / ALLOY B2**

H.T. CONDITION		S.R. CONDITION		CORROSION DATA						
TEMP DEG.C	TIME HRS	HT	TEMP DEG.C	TIME HRS	HT	S. AREA SQ. CM	WT. LOSS GMS	T D HRS	CORROSION RATE IPY	MDD
A S			C A S T			2.3460	.01805	168	.02010	109.913
A S			C A S T			2.4715	.04560	360	.02250	123.004
A S			C A S T			2.5967	.08291	720	.01946	106.428
A S			C A S T			2.9971	.13476	1080	.01827	99.920
900	4	OQ	---	---	---	3.9794	.02257	168	.01482	81.025
900	4	OQ	---	---	---	4.0413	.05735	360	.01730	94.606
900	4	OQ	---	---	---	3.5827	.09449	720	.01608	87.913
900	4	OQ	---	---	---	3.7161	.12964	1080	.01418	77.524
900	4	OQ	600	0.5	AC	3.5302	.02288	168	.01693	92.589
900	4	OQ	600	0.5	AC	4.0937	.07110	360	.02118	115.789
900	4	OQ	600	0.5	AC	4.1767	.13550	720	.01978	108.140
900	4	OQ	600	0.5	AC	3.8134	.18037	1080	.01922	105.109

**TABLE-5-118 CORROSIVE ENVIRONMENT : 10% (NH4)2SO4 / ALLOY B2**

H.T. CONDITION		S.R. CONDITION		CORROSION DATA						
TEMP DEG.C	TIME HRS	HT	TEMP DEG.C	TIME HRS	HT	S. AREA SQ. CM	WT. LOSS GMS	T D HRS	CORROSION RATE IPY	MDD
A S			C A S T			2.3694	.01866	168	.02058	112.506
A S			C A S T			3.2214	.05173	360	.01958	107.054
A S			C A S T			3.4444	.10462	720	.01852	101.246
A S			C A S T			2.6543	.10499	1080	.01608	87.901
900	4	OQ	---	---	---	3.4632	.02190	168	.01652	90.338
900	4	OQ	---	---	---	3.6740	.05500	360	.01825	99.802
900	4	OQ	---	---	---	3.7804	.09902	720	.01597	87.309
900	4	OQ	---	---	---	3.8787	.11995	1080	.01257	68.724
900	4	OQ	600	0.5	AC	3.5798	.02866	168	.02092	114.372
900	4	OQ	600	0.5	AC	3.4752	.05562	360	.01951	106.698
900	4	OQ	600	0.5	AC	4.0836	.13698	720	.02045	111.812
900	4	OQ	600	0.5	AC	4.0730	.18723	1080	.01868	102.152



**EFFECT OF TEST DURATION ON CORROSION BEHAVIOUR**
**TABLE-5.119 CORROSIVE ENVIRONMENT : 5% NaCl ; ALLOY B3**

H.T. CONDITION		S.R. CONDITION			CORROSION DATA					
TEMP DEG.C	TIME HRS	HT	TEMP DEG.C	TIME HRS	HT	S. AREA SQ. CM	WT. LOSS GMS	T D HRS	CORROSION RATE IPY	MDD
	A S		C A S T			2.7530	.00580	168	.00550	30.097
	A S		C A S T			2.3021	.00935	360	.00495	27.077
	A S		C A S T			2.7149	.01775	720	.00399	21.793
	A S		C A S T			2.7453	.02537	1080	.00376	20.536
900	4	00	---	---	---	2.9198	.00495	168	.00457	25.002
900	4	00	---	---	---	2.9517	.01171	360	.00484	26.448
900	4	00	---	---	---	3.1006	.01968	720	.00387	21.157
900	4	00	---	---	---	3.2132	.02549	1080	.00322	17.629
900	4	00	600	0.5	AC	2.2572	.00413	168	.00478	26.138
900	4	00	600	0.5	AC	2.2267	.00800	360	.00438	23.952
900	4	00	600	0.5	AC	2.5742	.01689	720	.00400	21.871
900	4	00	600	0.5	AC	2.5085	.02306	1080	.00374	20.428

**TABLE-5.120 CORROSIVE ENVIRONMENT : 10% NH4CL ; ALLOY B3**

H.T. CONDITION		S.R. CONDITION			CORROSION DATA					
TEMP DEG.C	TIME HRS	HT	TEMP DEG.C	TIME HRS	HT	S. AREA SQ. CM	WT. LOSS GMS	T D HRS	CORROSION RATE IPY	MDD
	A S		C A S T			1.8630	.01576	168	.02210	120.847
	A S		C A S T			1.6378	.02963	360	.02206	120.612
	A S		C A S T			1.8581	.05807	720	.01905	104.176
	A S		C A S T			2.1460	.07702	1080	.01459	79.754
900	4	00	---	---	---	2.5003	.02208	168	.02307	126.157
900	4	00	---	---	---	3.2310	.05193	360	.01960	107.150
900	4	00	---	---	---	3.0001	.05845	720	.01188	64.941
900	4	00	---	---	---	2.7448	.05925	1080	.00877	47.969
900	4	00	600	0.5	AC	2.0604	.01793	168	.02274	124.318
900	4	00	600	0.5	AC	1.8115	.03500	360	.02356	128.804
900	4	00	600	0.5	AC	2.1596	.06282	720	.01773	96.964
900	4	00	600	0.5	AC	2.0124	.05895	1080	.01191	65.097

**TABLE-5.121 CORROSIVE ENVIRONMENT : 10% (NH4)2SO4 ; ALLOY B3**

H.T. CONDITION		S.R. CONDITION			CORROSION DATA					
TEMP DEG.C	TIME HRS	HT	TEMP DEG.C	TIME HRS	HT	S. AREA SQ. CM	WT. LOSS GMS	T D HRS	CORROSION RATE IPY	MDD
	A S		C A S T			1.4431	.01340	168	.02426	132.655
	A S		C A S T			1.9704	.03617	360	.02238	122.378
	A S		C A S T			2.0329	.06707	720	.02011	109.974
	A S		C A S T			2.2705	.09349	1080	.01673	91.501
900	4	00	---	---	---	3.1252	.02218	168	.01854	101.389
900	4	00	---	---	---	3.2490	.03834	360	.01439	78.672
900	4	00	---	---	---	2.7588	.06783	720	.01499	81.957
900	4	00	---	---	---	3.0522	.07526	1080	.01002	54.795
900	4	00	600	0.5	AC	2.0051	.01989	168	.02592	141.711
900	4	00	600	0.5	AC	1.7780	.02849	360	.01954	106.827
900	4	00	600	0.5	AC	2.2115	.06761	720	.01864	101.906
900	4	00	600	0.5	AC	2.0269	.07113	1080	.01426	77.983

## EFFECT OF TEST DURATION ON CORROSION BEHAVIOUR

TABLE-5.122 CORROSIVE ENVIRONMENT : 5% NaCl ; ALLOY B4

H.T.CONDITION		S.R.CONDITION			CORROSION DATA					
TEMP DEG.C	TIME HRS	HT	TEMP DEG.C	TIME HRS	HT	S.AREA SQ.CM	WT.LOSS GMS	T D HRS	CORROSION RATE IPY	MDD
	A S		C A S T			3.4322	.00758	168	.00577	31.550
	A S		C A S T			3.3321	.01535	360	.00562	30.712
	A S		C A S T			3.4097	.02542	720	.00454	24.851
	A S		C A S T			3.4916	.03605	1080	.00420	22.944
900	4	00	---	---	---	3.9895	.00720	168	.00472	25.782
900	4	00	---	---	---	4.1276	.01639	360	.00484	26.472
900	4	00	---	---	---	3.9165	.02788	720	.00434	23.728
900	4	00	---	---	---	3.4683	.02666	1080	.00312	17.082
900	4	00	600	0.5	AC	3.0499	.00582	168	.00499	27.261
900	4	00	600	0.5	AC	4.1954	.01605	360	.00466	25.504
900	4	00	600	0.5	AC	3.4588	.02660	720	.00469	25.635
900	4	00	600	0.5	AC	3.9473	.04040	1080	.00416	22.744

TABLE-5.123 CORROSIVE ENVIRONMENT : 10% NH4CL ; ALLOY B4

H.T.CONDITION		S.R.CONDITION			CORROSION DATA					
TEMP DEG.C	TIME HRS	HT	TEMP DEG.C	TIME HRS	HT	S.AREA SQ.CM	WT.LOSS GMS	T D HRS	CORROSION RATE IPY	MDD
	A S		C A S T			2.0944	.01908	168	.02380	130.142
	A S		C A S T			2.9858	.05035	360	.02056	112.421
	A S		C A S T			3.4537	.10419	720	.01839	100.558
	A S		C A S T			3.6661	.15497	1080	.01718	93.937
900	4	00	---	---	---	2.9334	.02184	168	.01945	106.363
900	4	00	---	---	---	3.1409	.04669	360	.01812	99.101
900	4	00	---	---	---	2.7841	.05999	720	.01314	71.825
900	4	00	---	---	---	4.1657	.13228	1080	.01291	70.565
900	4	00	600	0.5	AC	3.5038	.02524	168	.01882	102.909
900	4	00	600	0.5	AC	4.4754	.07713	360	.02101	114.896
900	4	00	600	0.5	AC	3.5666	.09555	720	.01633	89.301
900	4	00	600	0.5	AC	4.1702	.19067	1080	.01858	101.603

TABLE-5.124 CORROSIVE ENVIRONMENT : 10% (NH4)2SO4 ; ALLOY B4

H.T.CONDITION		S.R.CONDITION			CORROSION DATA					
TEMP DEG.C	TIME HRS	HT	TEMP DEG.C	TIME HRS	HT	S.AREA SQ.CM	WT.LOSS GMS	T D HRS	CORROSION RATE IPY	MDD
	A S		C A S T			3.2739	.02904	168	.02317	126.717
	A S		C A S T			3.4852	.06367	360	.02227	121.789
	A S		C A S T			3.1852	.10082	720	.01930	105.508
	A S		C A S T			3.6233	.15012	1080	.01684	92.071
900	4	00	---	---	---	3.0017	.02104	168	.01831	100.135
900	4	00	---	---	---	2.2492	.03403	360	.01845	100.865
900	4	00	---	---	---	3.3620	.10455	720	.01896	103.658
900	4	00	---	---	---	3.3469	.12505	1080	.01518	83.029
900	4	00	600	0.5	AC	3.2767	.02708	168	.02159	118.062
900	4	00	600	0.5	AC	3.1604	.04723	360	.01822	99.628
900	4	00	600	0.5	AC	3.9238	.11155	720	.01733	94.760
900	4	00	600	0.5	AC	3.8556	.17970	1080	.01894	103.573

**CORROSION BEHAVIOUR OF NODULAR GRAPHITE NI-RESIST CAST IRON**

**TABLE-5.125 CORROSIVE ENVIRONMENT : 5% NaCl**

H.T.CONDITION		S.R.CONDITION		C O R R O S I O N D A T A				
TEMP DEG.C	TIME HT HRS	TEMP DEG.C	TIME HT HRS	S.AREA SQ.CM	WT.LOSS GMS	T D HRS	CORROSION RATE IPY	MDD
A S	C A S T			1.6951	.00155	168	.00239	13.063
A S	C A S T			3.6200	.00533	360	.00180	9.816
A S	C A S T			2.0374	.00470	720	.00141	7.690
A S	C A S T			3.6012	.00914	1080	.00103	5.640

**TABLE-5.126 CORROSIVE ENVIRONMENT : 10% NH4CL**

H.T.CONDITION		S.R.CONDITION		C O R R O S I O N D A T A				
TEMP DEG.C	TIME HT HRS	TEMP DEG.C	TIME HT HRS	S.AREA SQ.CM	WT.LOSS GMS	T D HRS	CORROSION RATE IPY	MDD
A S	C A S T			1.8205	.01614	168	.02316	126.654
A S	C A S T			1.6922	.02886	360	.02079	113.696
A S	C A S T			1.8866	.03651	720	.01180	64.509
A S	C A S T			2.8318	.03586	1080	.00515	28.140

**TABLE-5.127 CORROSIVE ENVIRONMENT : 10% (NH4)2SO4**

H.T.CONDITION		S.R.CONDITION		C O R R O S I O N D A T A				
TEMP DEG.C	TIME HT HRS	TEMP DEG.C	TIME HT HRS	S.AREA SQ.CM	WT.LOSS GMS	T D HRS	CORROSION RATE IPY	MDD
A S	C A S T			1.3669	.01102	168	.02106	115.168
A S	C A S T			1.4241	.01368	360	.01171	64.042
A S	C A S T			2.1465	.03253	720	.00924	50.517
A S	C A S T			1.8683	.02203	1080	.00479	26.203

**CORROSION BEHAVIOUR OF FLAKE GRAPHITE NI-RESIST CAST IRON**

**TABLE-5.128 CORROSIVE ENVIRONMENT : 5% NaCl**

H.T. CONDITION		S.R. CONDITION		C O R R O S I O N D A T A						
TEMP DEG.C	TIME HRS	HT	TEMP DEG.C	TIME HRS	HT	S.AREA SQ.CM	WT.LOSS GMS	T D HRS	CORROSION RATE IPY	MDD
A	S	C	A	S	T	1.7212	.00128	168	.00194	10.624
A	S	C	A	S	T	2.0835	.00287	360	.00168	9.183
A	S	C	A	S	T	2.0269	.00412	720	.00124	6.775
A	S	C	A	S	T	2.9803	.00720	1080	.00098	5.369

**TABLE-5.129 CORROSIVE ENVIRONMENT : 10% NH4Cl**

H.T. CONDITION		S.R. CONDITION		C O R R O S I O N D A T A						
TEMP DEG.C	TIME HRS	HT	TEMP DEG.C	TIME HRS	HT	S.AREA SQ.CM	WT.LOSS GMS	T D HRS	CORROSION RATE IPY	MDD
A	S	C	A	S	T	2.3158	.00998	168	.01126	61.564
A	S	C	A	S	T	1.9748	.01479	360	.00913	49.928
A	S	C	A	S	T	2.1571	.02196	720	.00621	33.934
A	S	C	A	S	T	3.8452	.02308	1080	.00508	27.796

**TABLE-5.130 CORROSIVE ENVIRONMENT : 10% (NH4)2SO4**

H.T. CONDITION		S.R. CONDITION		C O R R O S I O N D A T A						
TEMP DEG.C	TIME HRS	HT	TEMP DEG.C	TIME HRS	HT	S.AREA SQ.CM	WT.LOSS GMS	T D HRS	CORROSION RATE IPY	MDD
A	S	C	A	S	T	1.7600	.00617	168	.00916	50.082
A	S	C	A	S	T	1.7524	.01050	360	.00731	39.946
A	S	C	A	S	T	1.9282	.01626	720	.00514	28.109
A	S	C	A	S	T	4.2048	.05141	1080	.00497	27.170

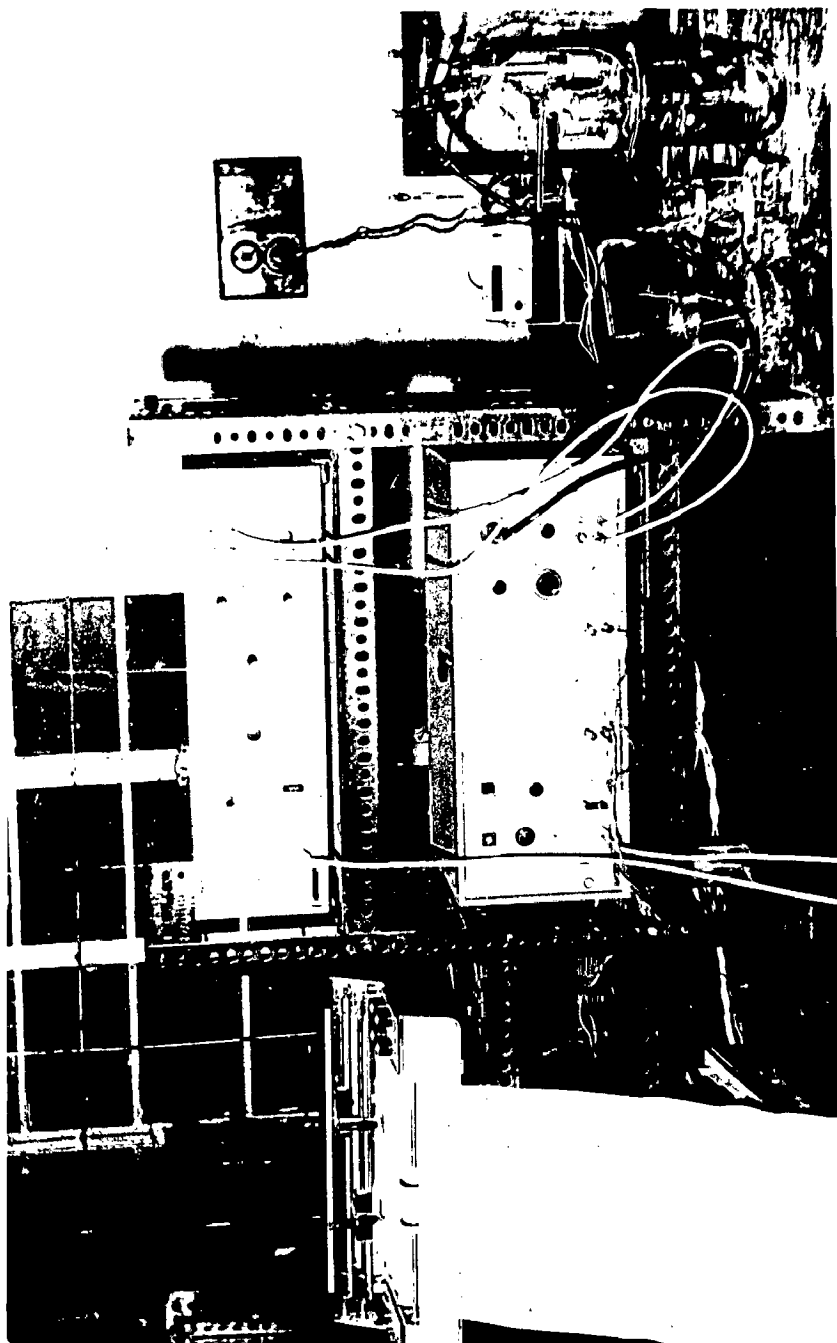
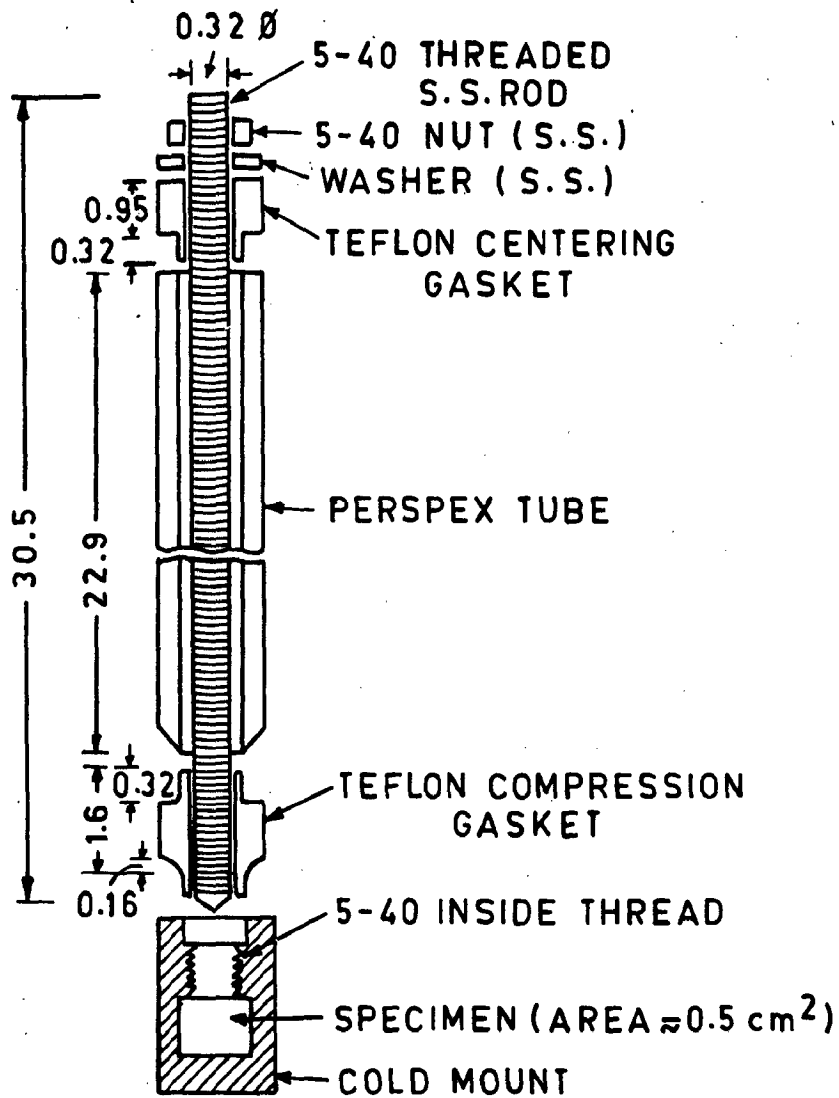


FIG. 4.1 EXPERIMENTAL SET-UP FOR CORROSION STUDIES.



S.S. = 304 AUSTENITIC STAINLESS STEEL

DIMENSIONS IN cm

FIG. 4.2 ELECTRODE HOLDER ALONG WITH SPECIMEN FOR CORROSION STUDIES.

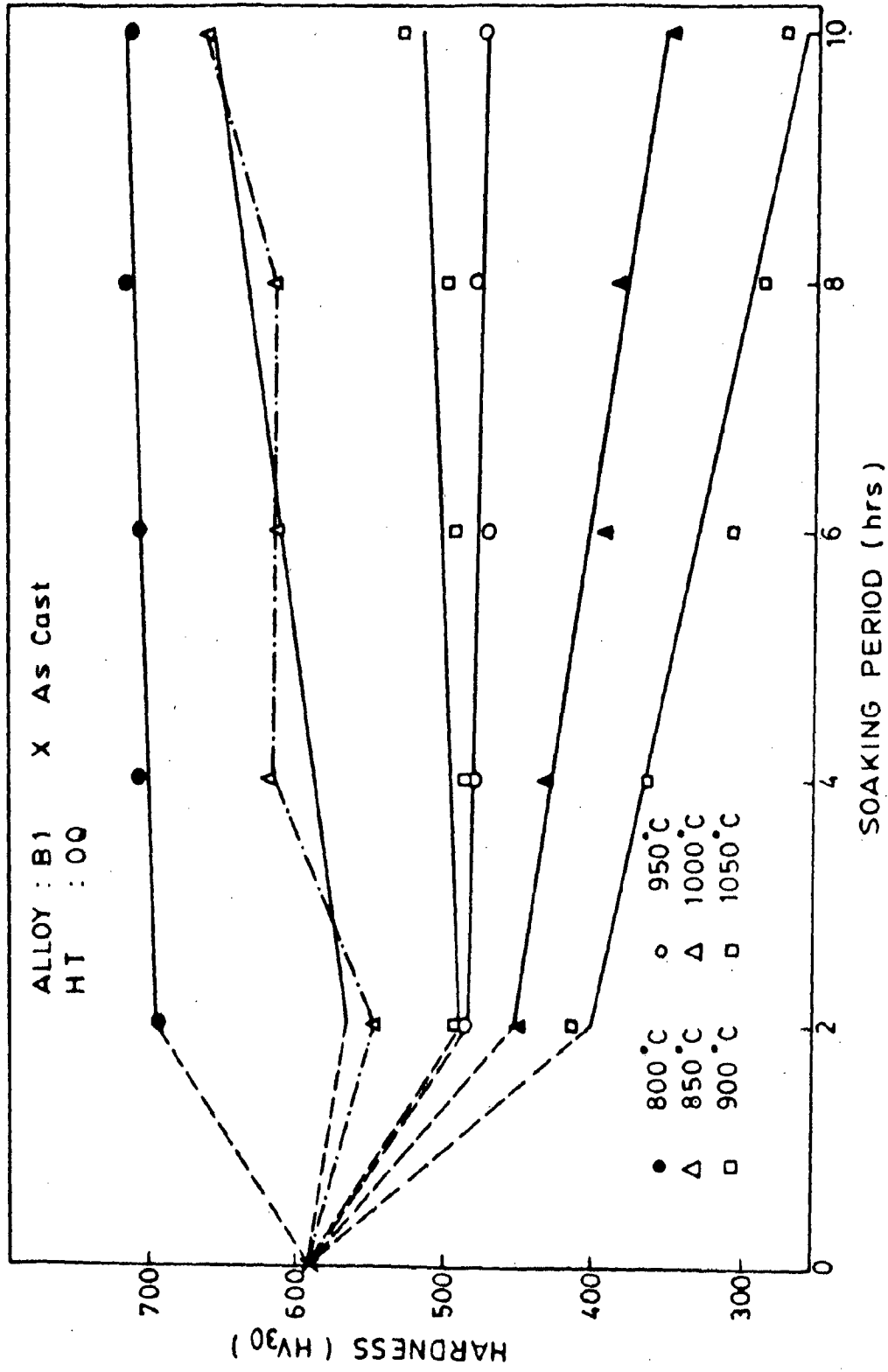


FIG. 5.1 EFFECT OF SOAKING PERIOD ON HARDNESS.

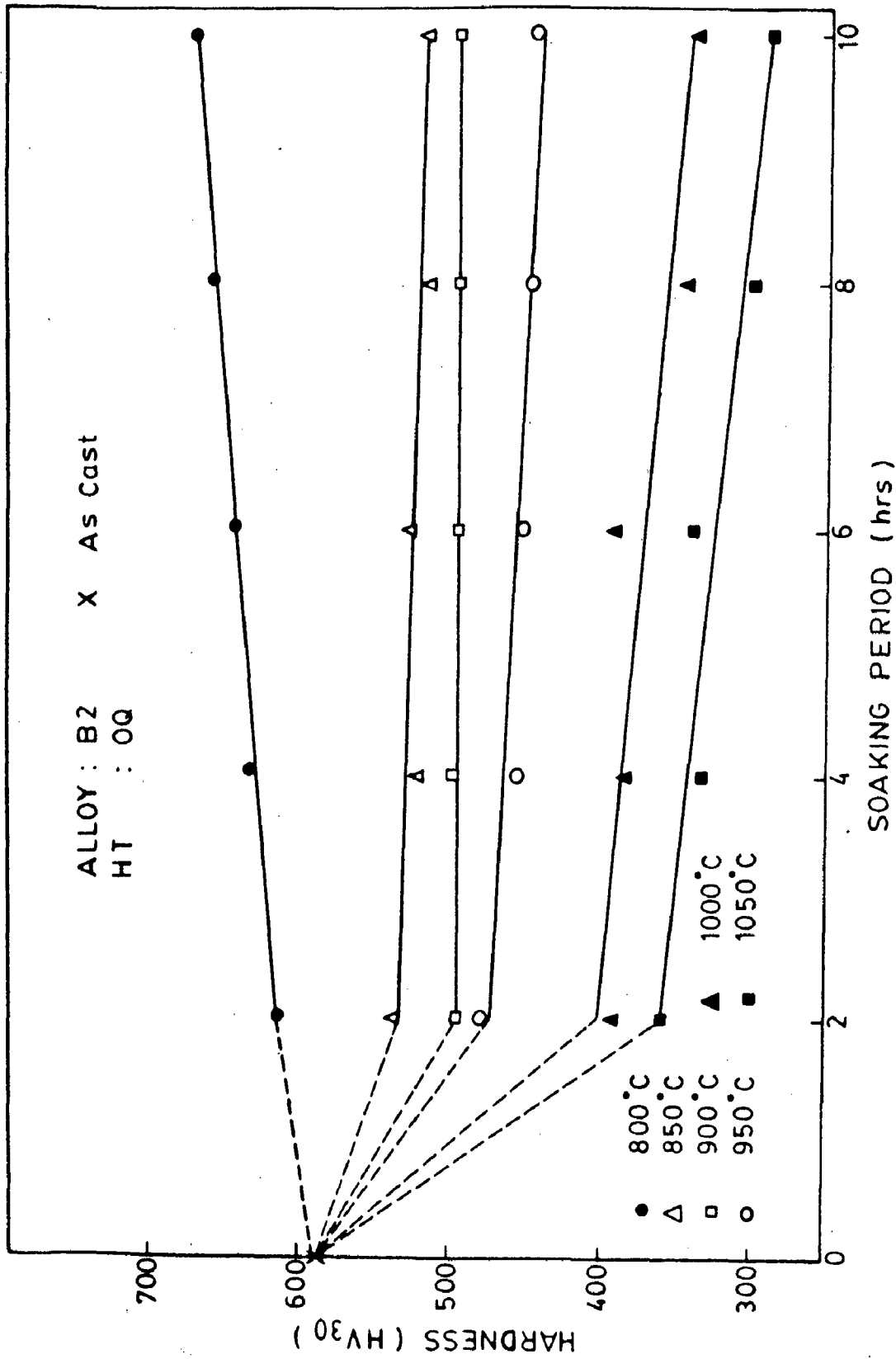


FIG. 5.2 EFFECT OF SOAKING PERIOD ON HARDNESS.



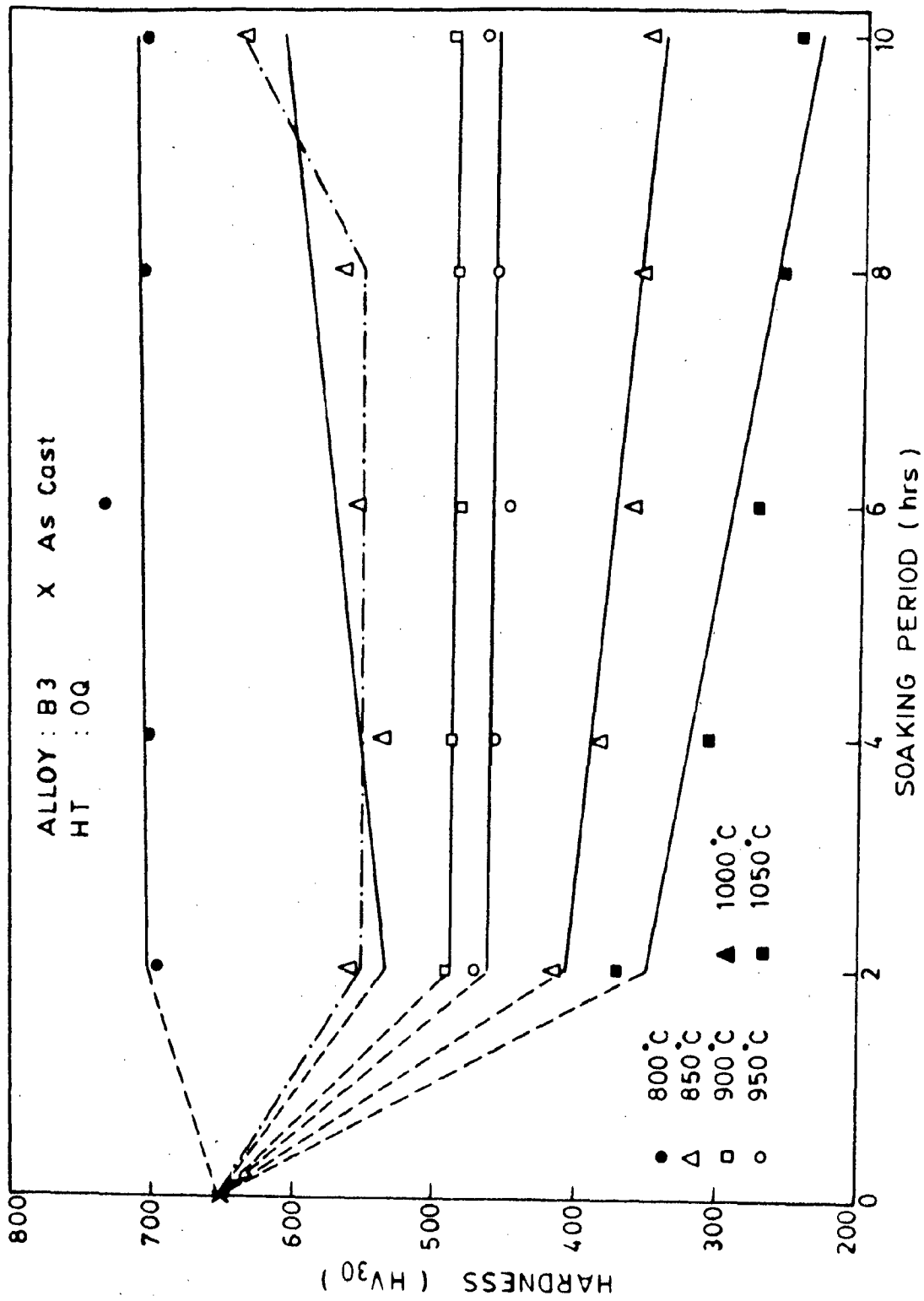


FIG. 5.3 EFFECT OF SOAKING PERIOD ON HARDNESS.

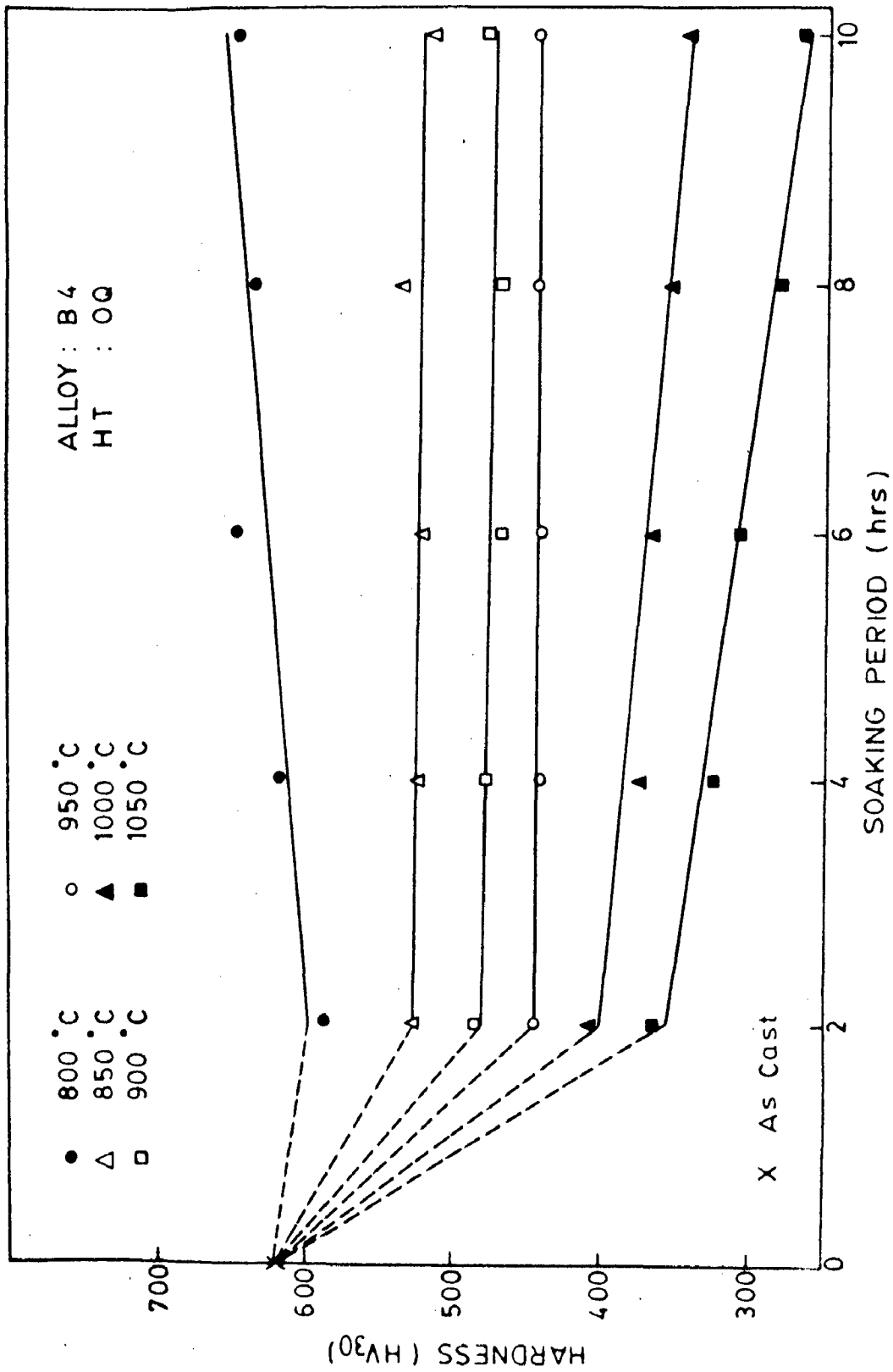


FIG. 5.4 EFFECT OF SOAKING PERIOD ON HARDNESS.

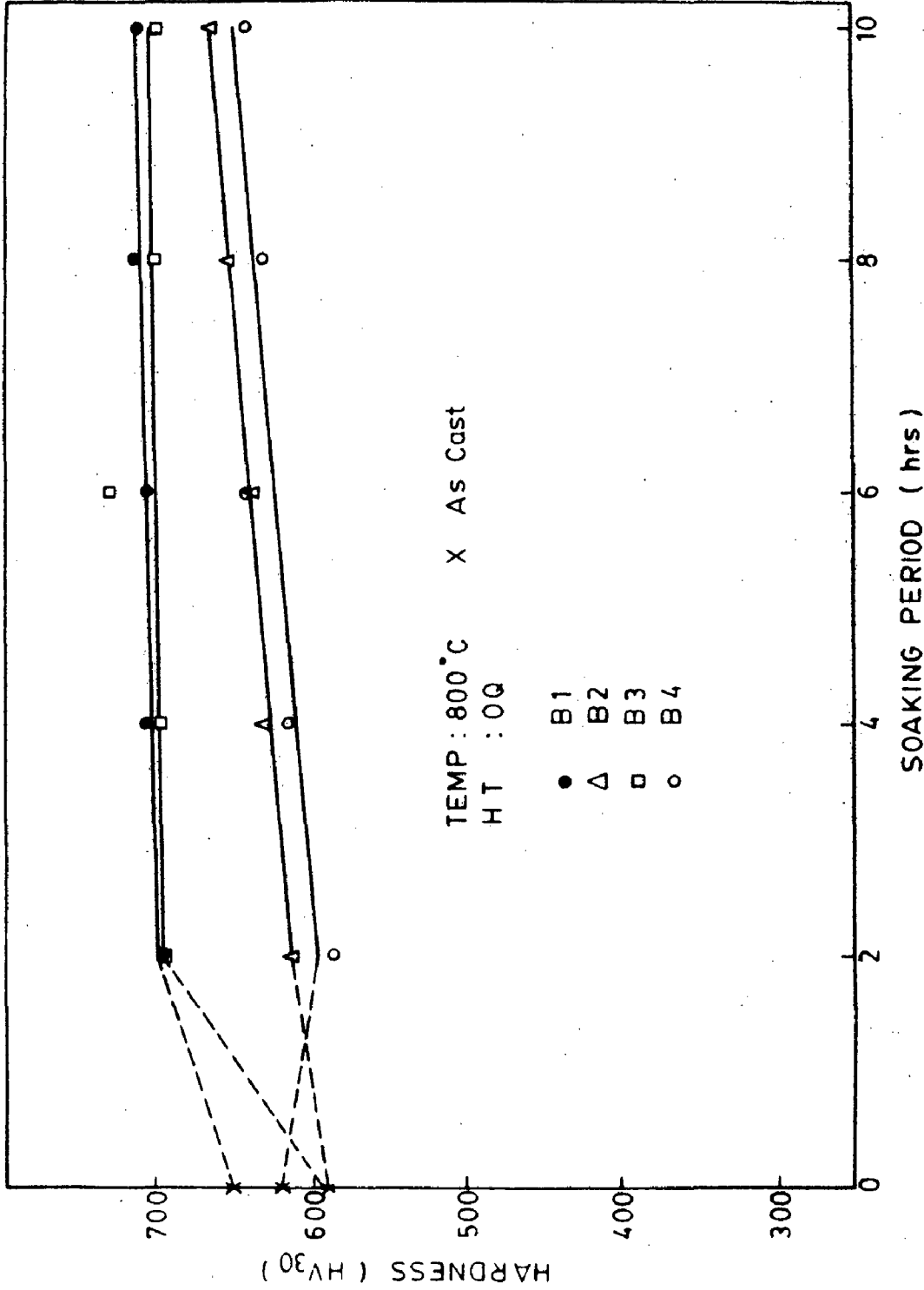


FIG. 5.5(a) EFFECT OF SOAKING PERIOD ON HARDNESS.

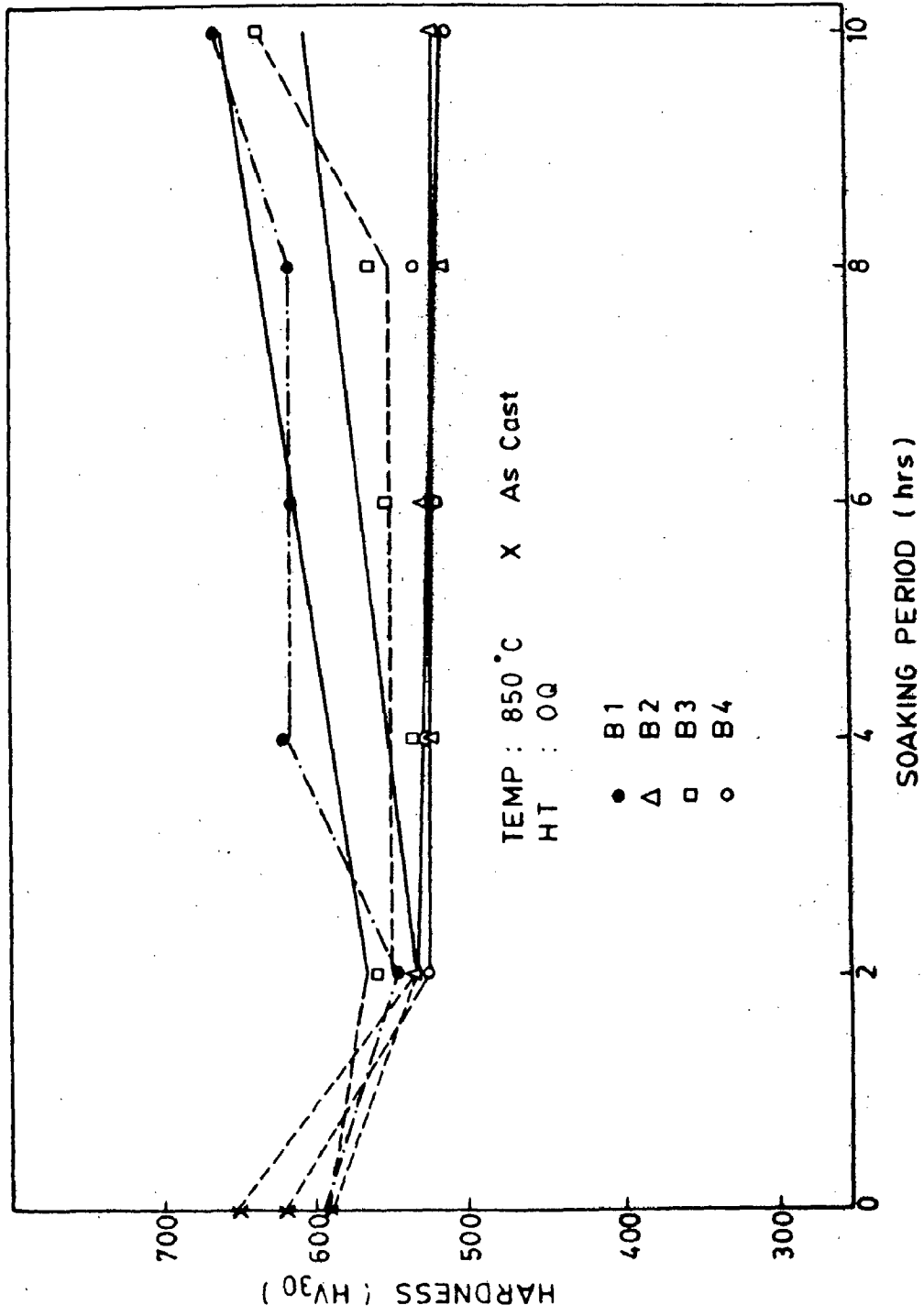
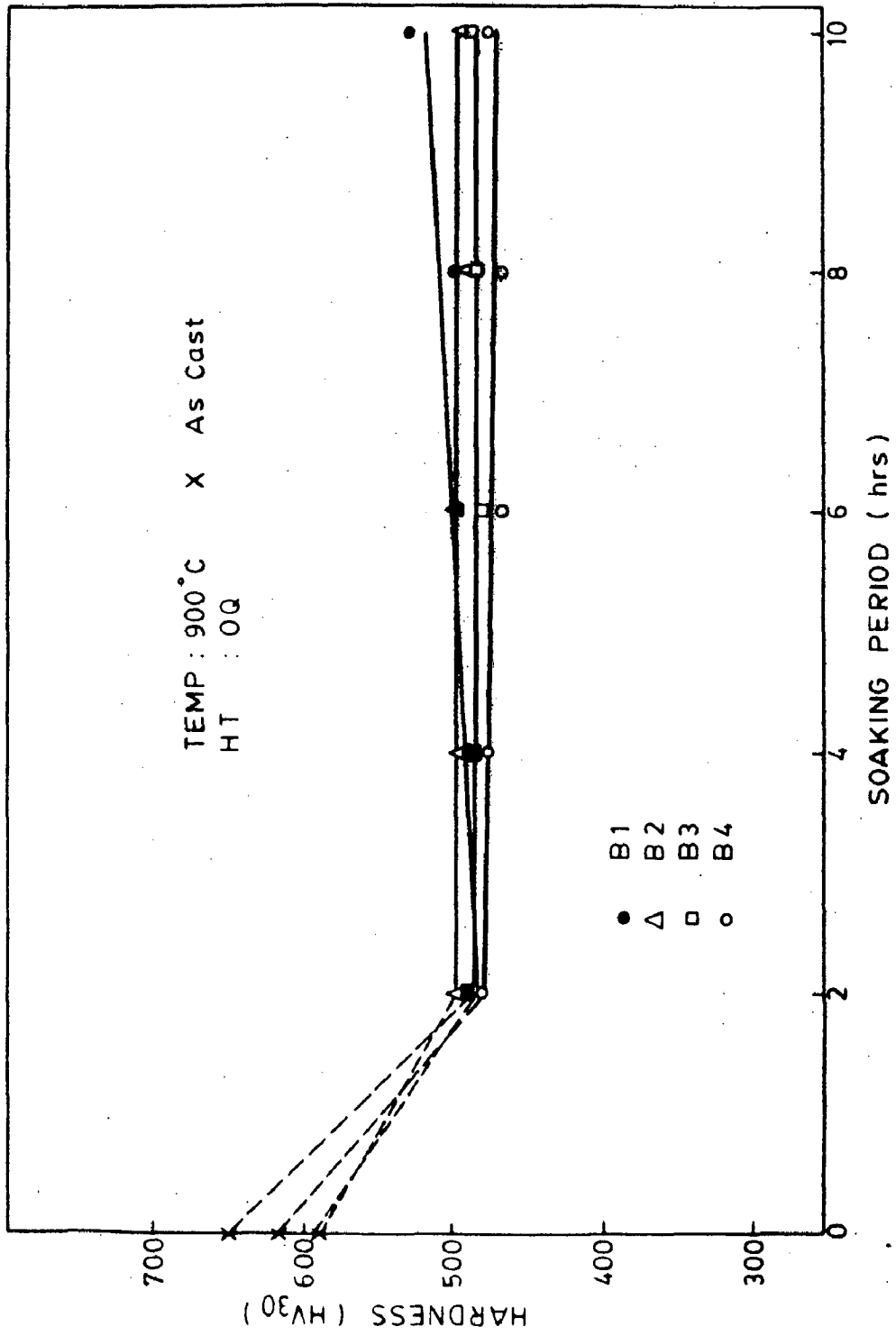


FIG. 5.5(b) EFFECT OF SOAKING PERIOD ON HARDNESS.



T-9

FIG. 5.5(c) EFFECT OF SOAKING PERIOD ON HARDNESS.

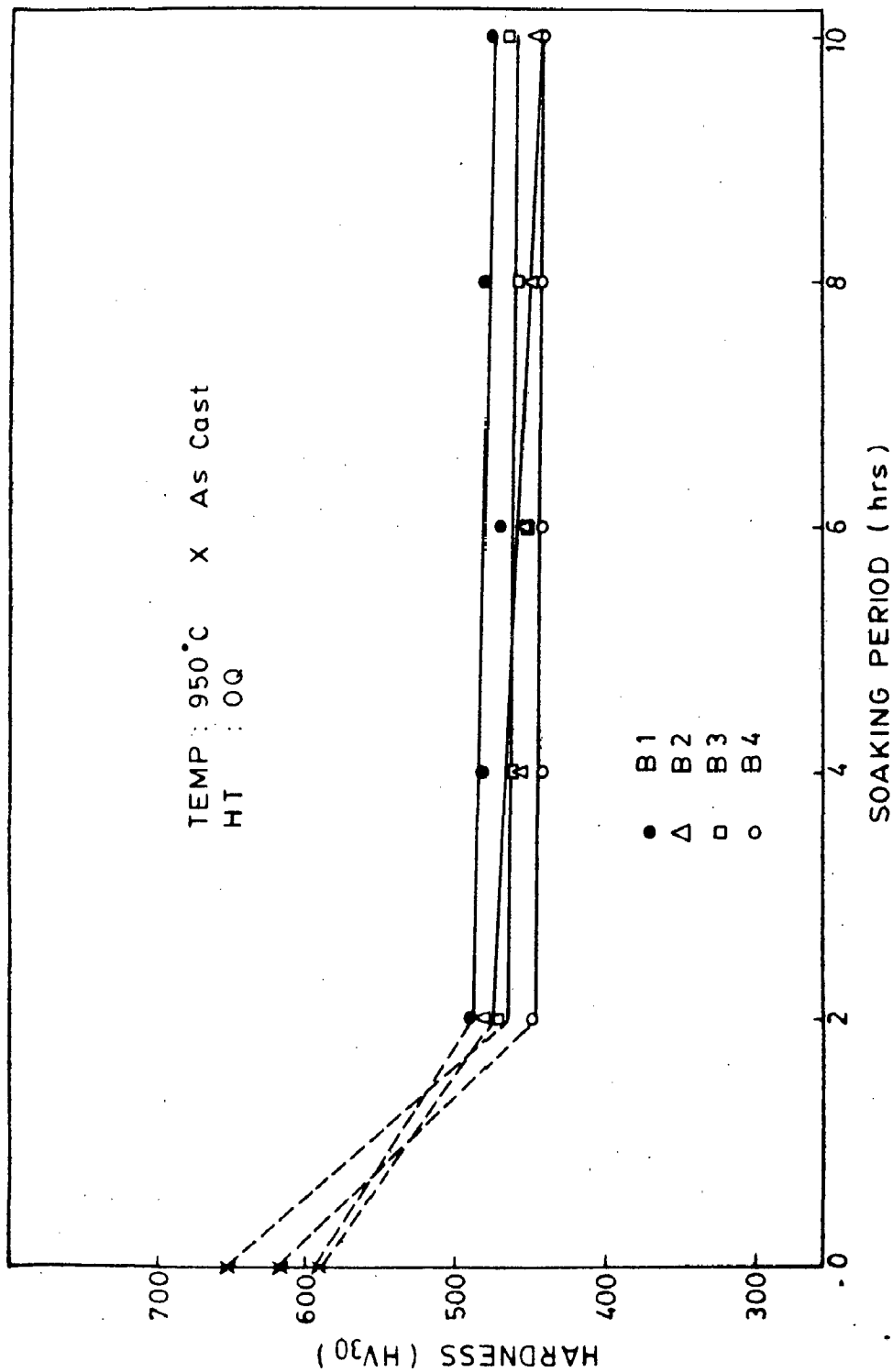


FIG. 5.5(d) EFFECT OF SOAKING PERIOD ON HARDNESS.

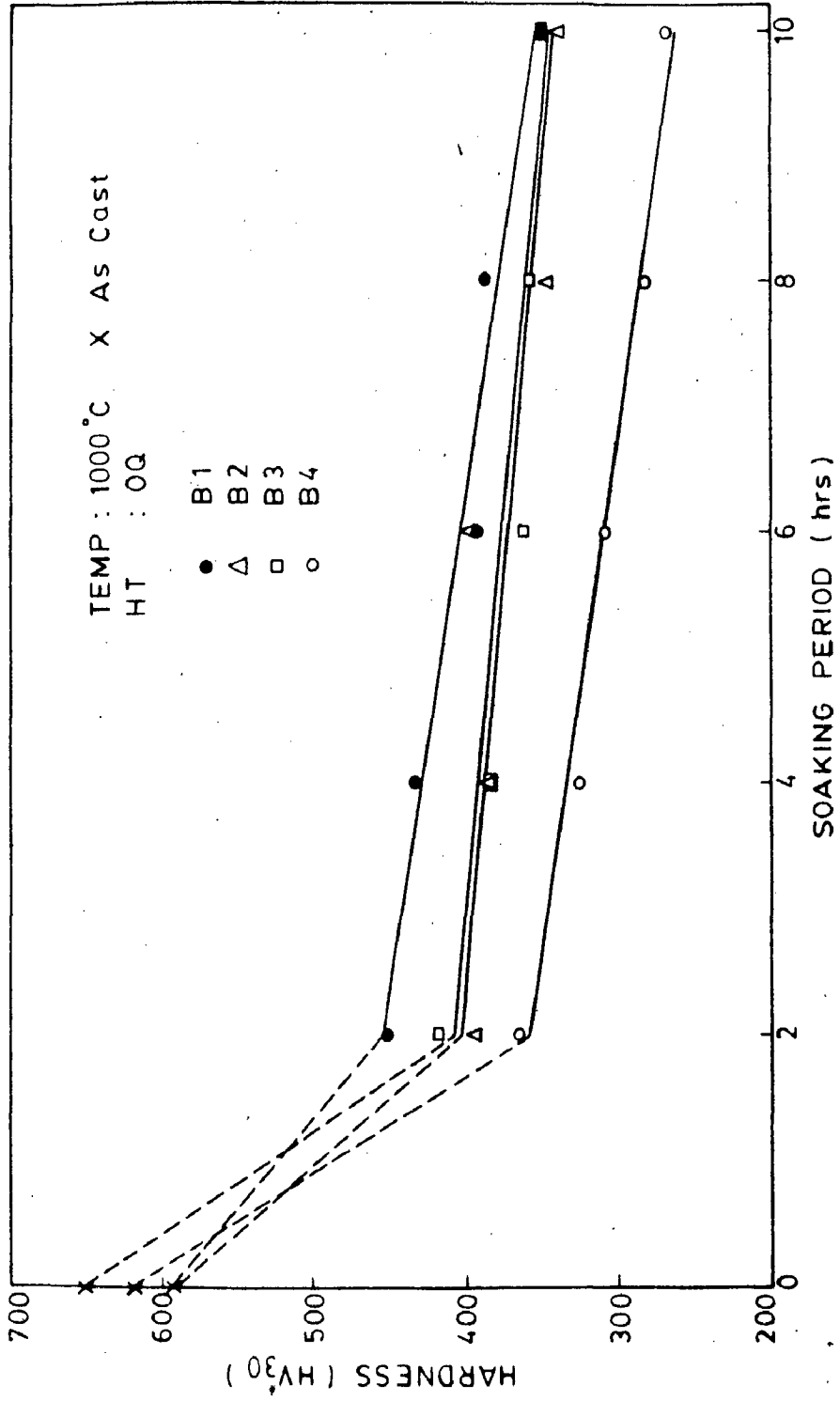


FIG. 5.5(e) EFFECT OF SOAKING PERIOD ON HARDNESS.

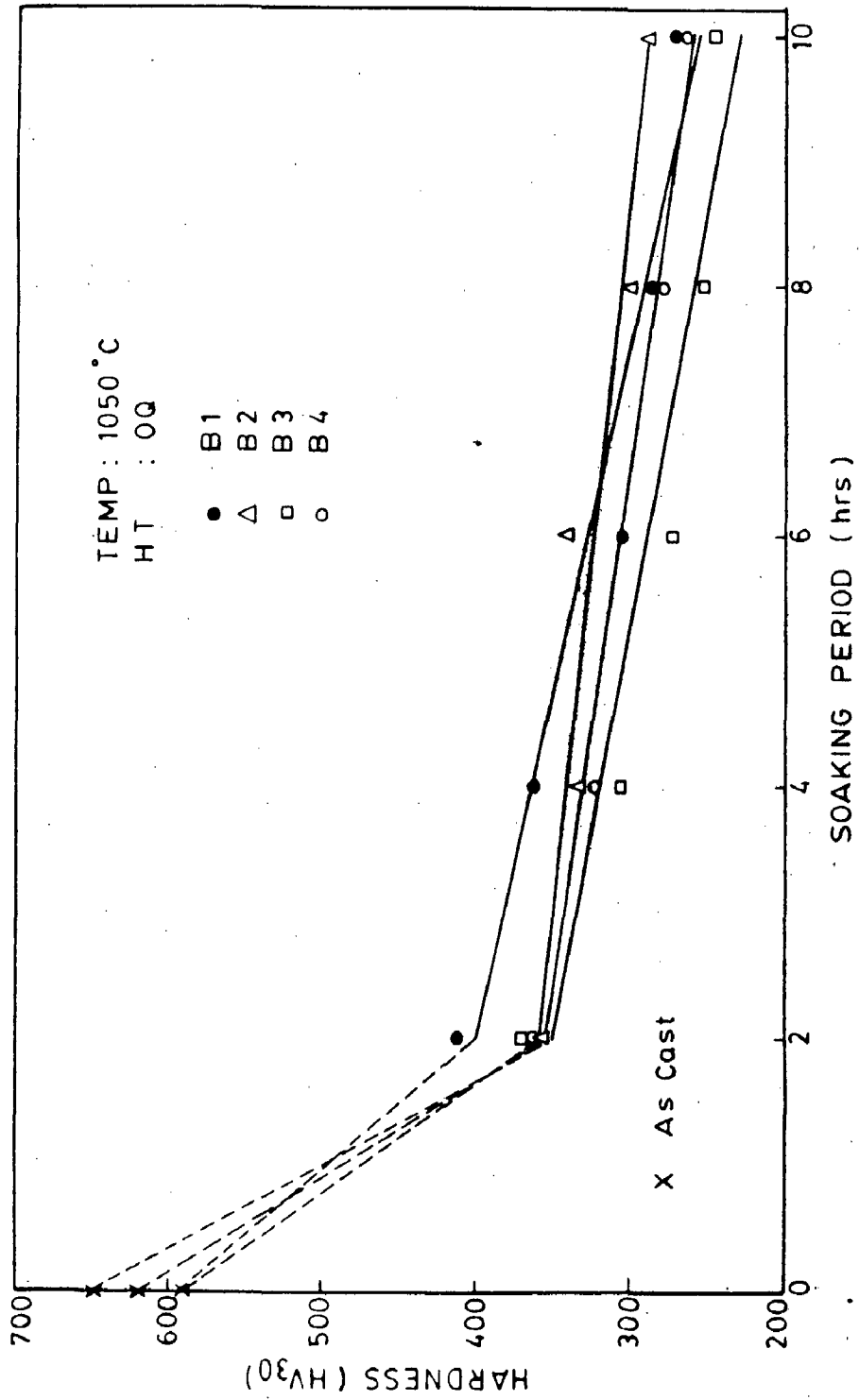


FIG. 5.5(f) EFFECT OF SOAKING PERIOD ON HARDNESS.



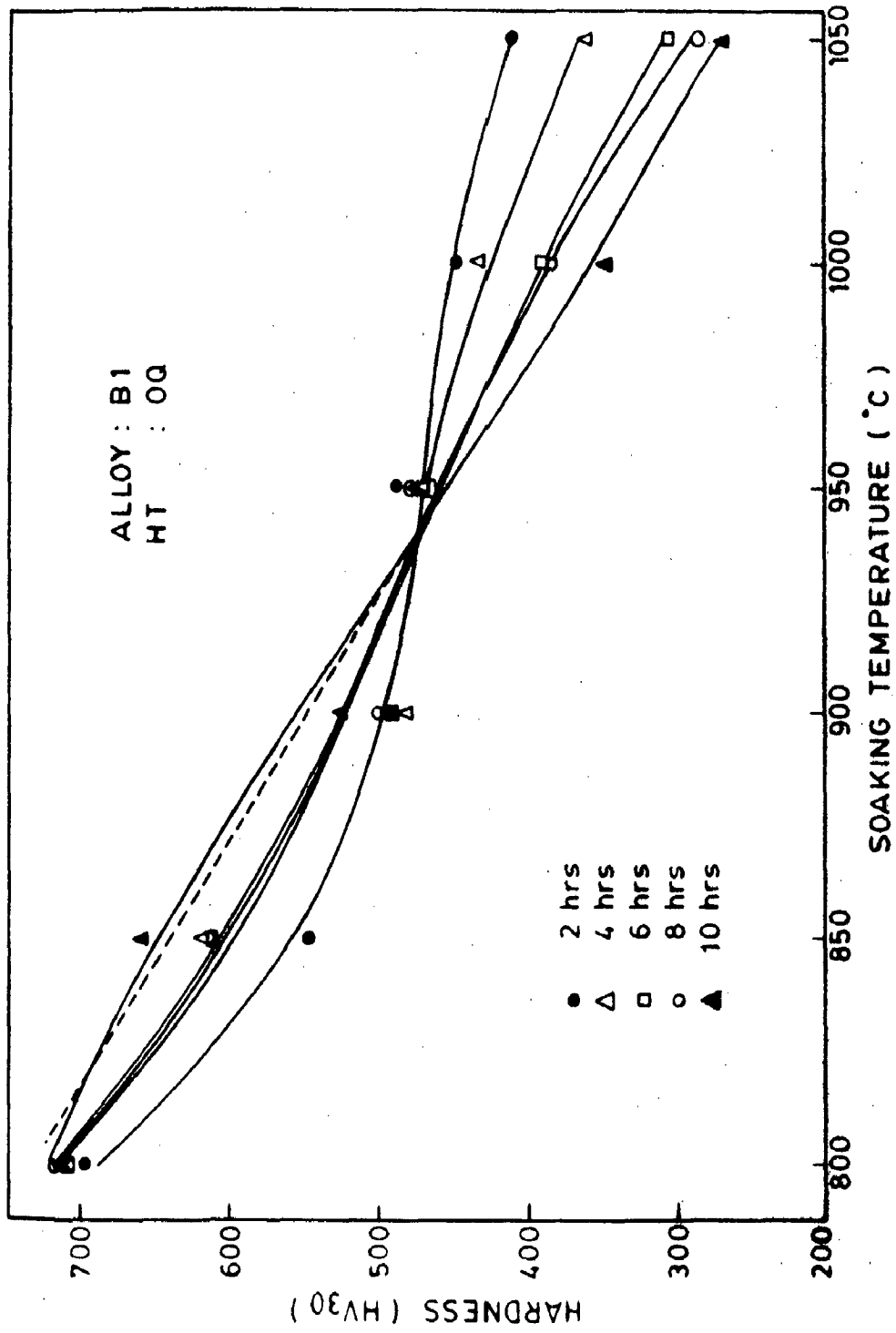


FIG. 5.6(a) EFFECT OF SOAKING TEMPERATURE ON HARDNESS. F-3

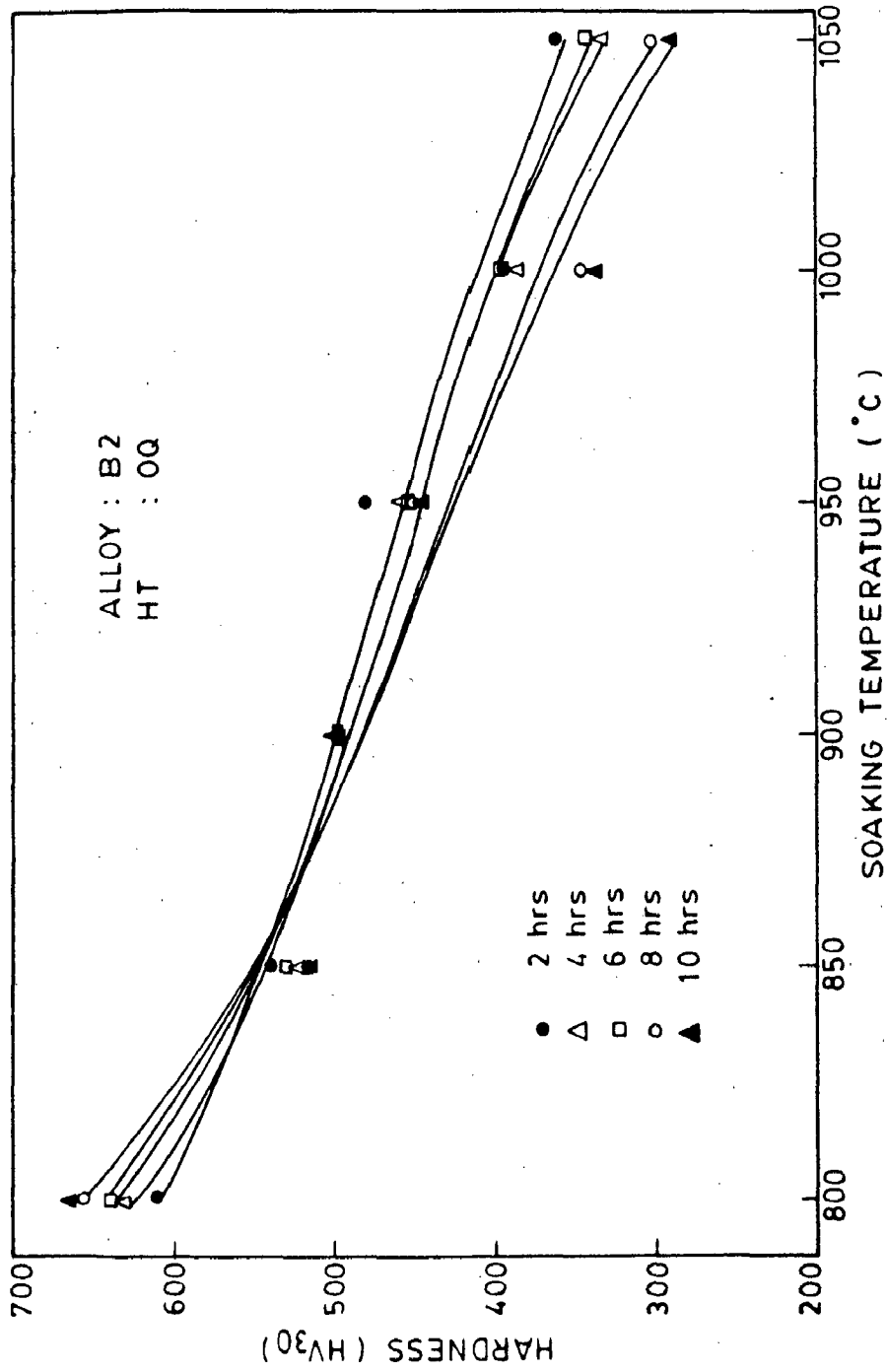


FIG.5.6(b) EFFECT OF SOAKING TEMPERATURE ON HARDNESS.

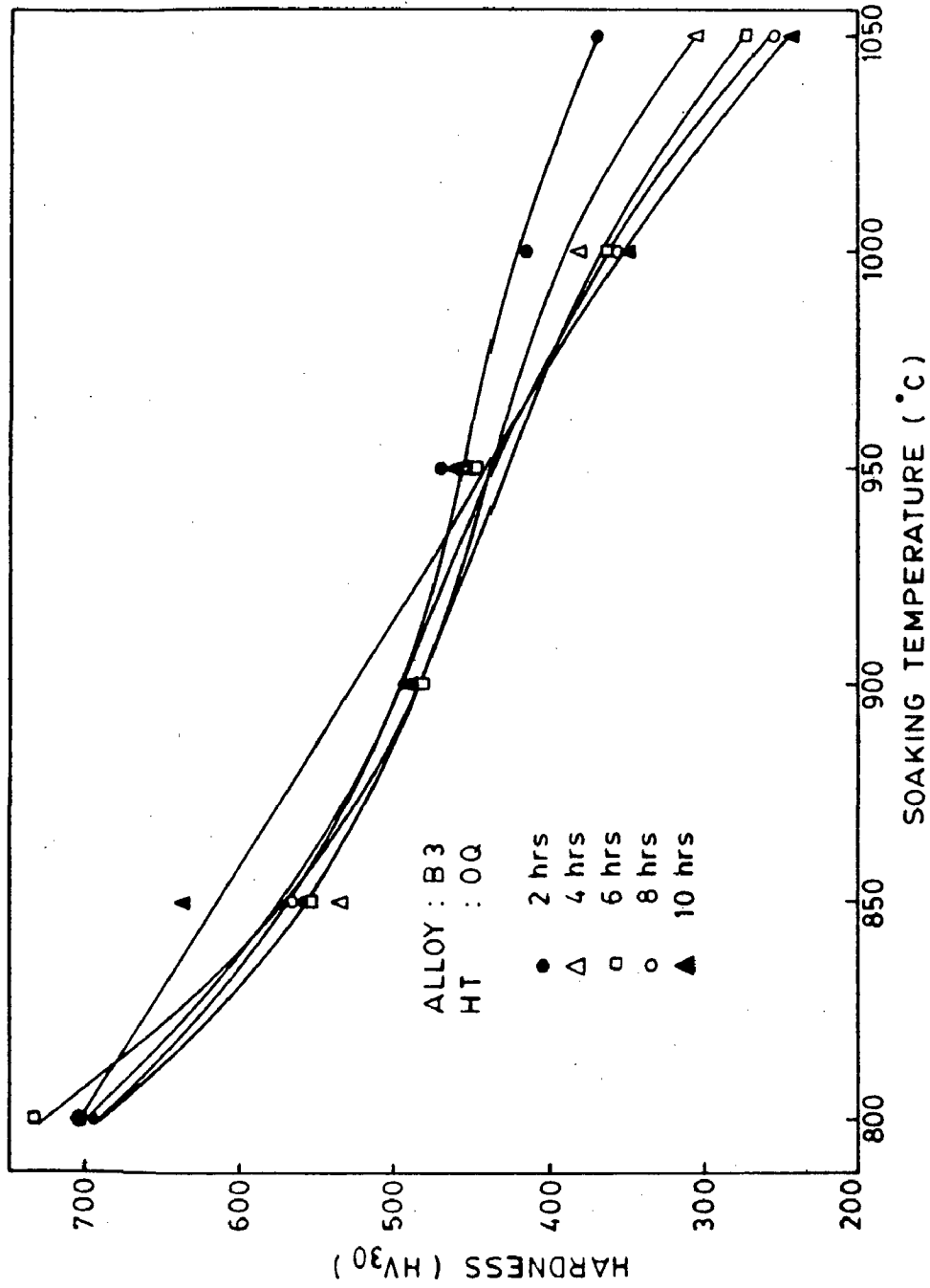


FIG. 5.6(c) EFFECT OF SOAKING TEMPERATURE ON HARDNESS.

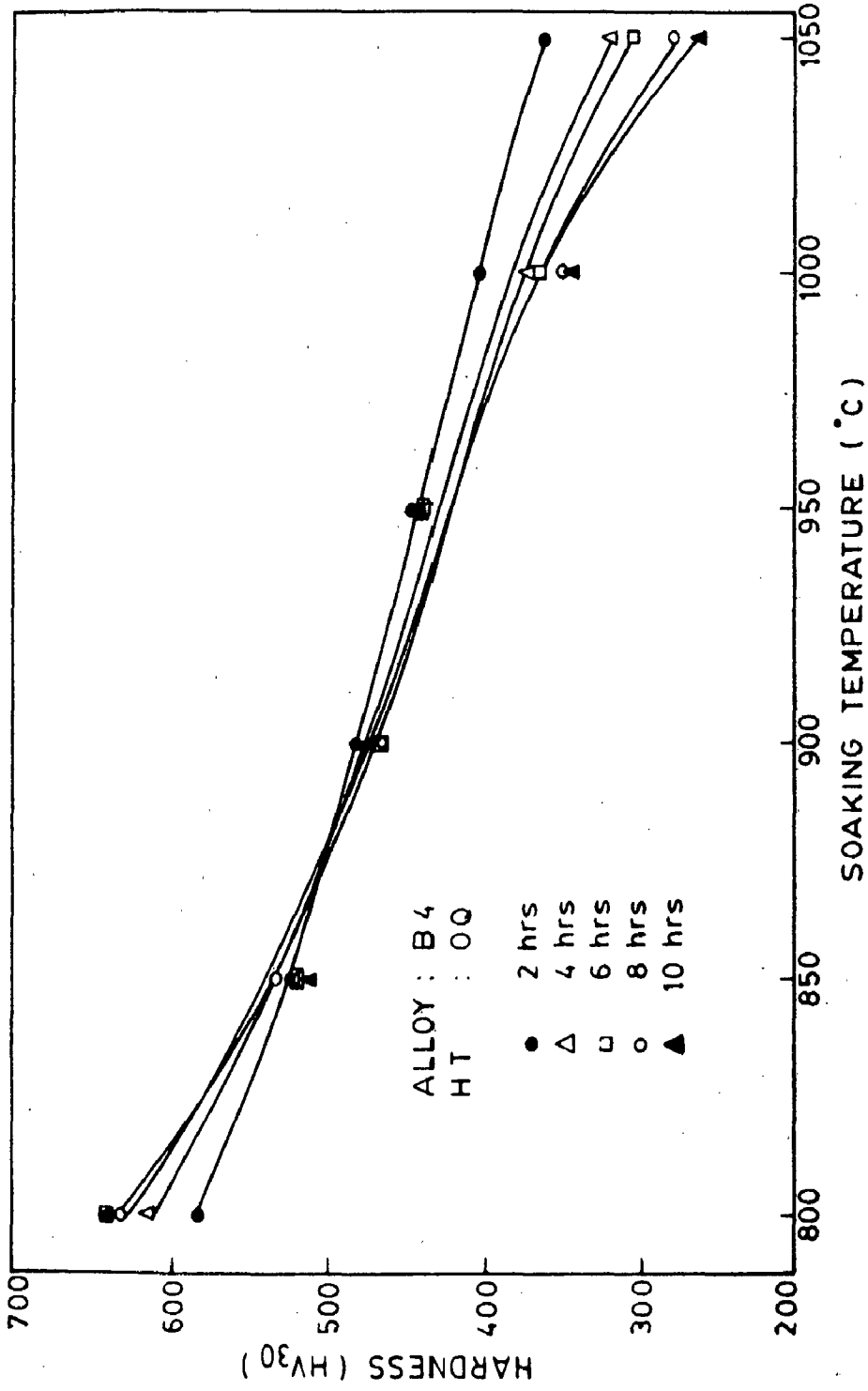


FIG. 5.6(d) EFFECT OF SOAKING TEMPERATURE ON HARDNESS.

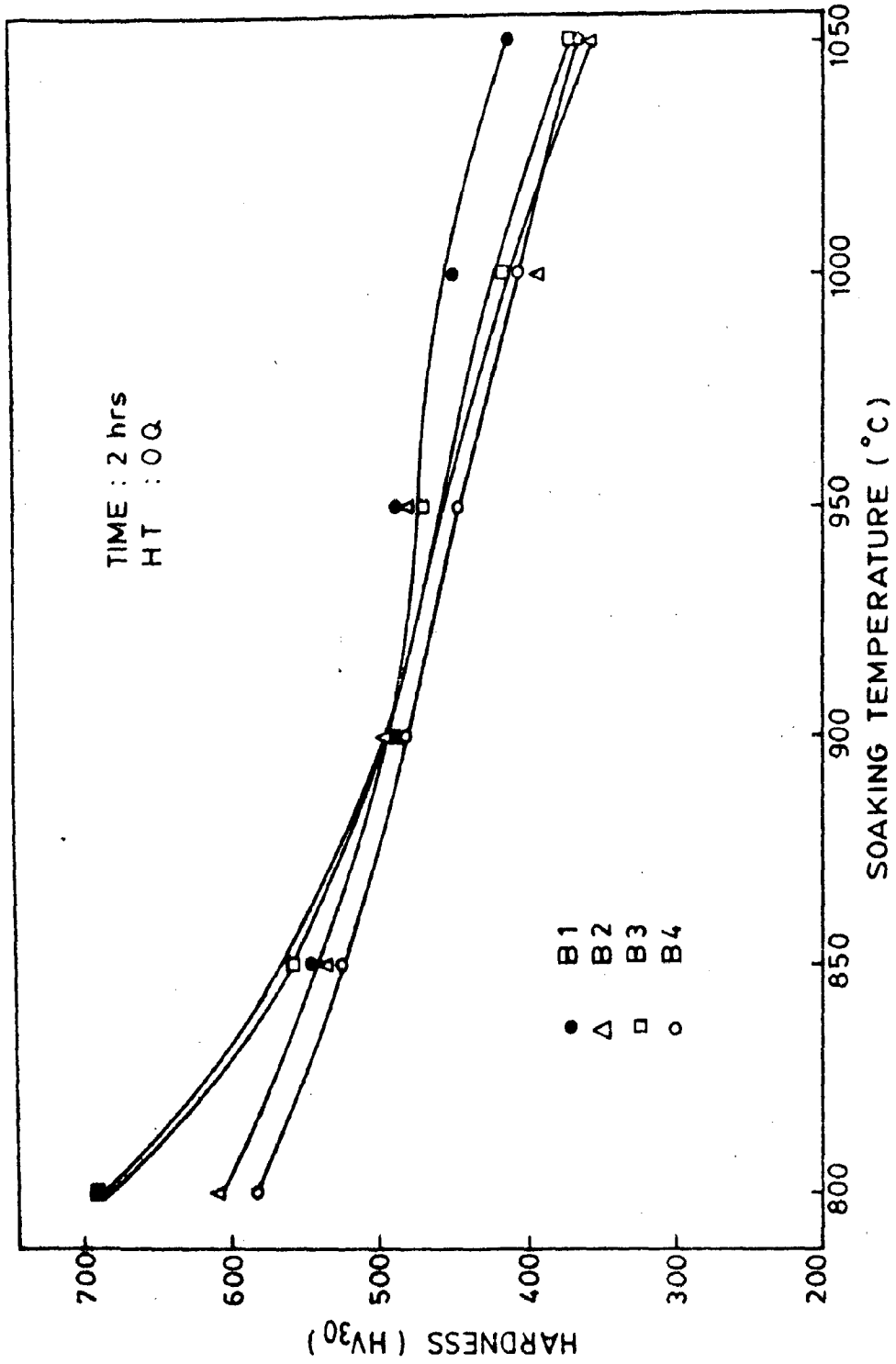


FIG. 5.7(a) EFFECT OF SOAKING TEMPERATURE ON HARDNESS.

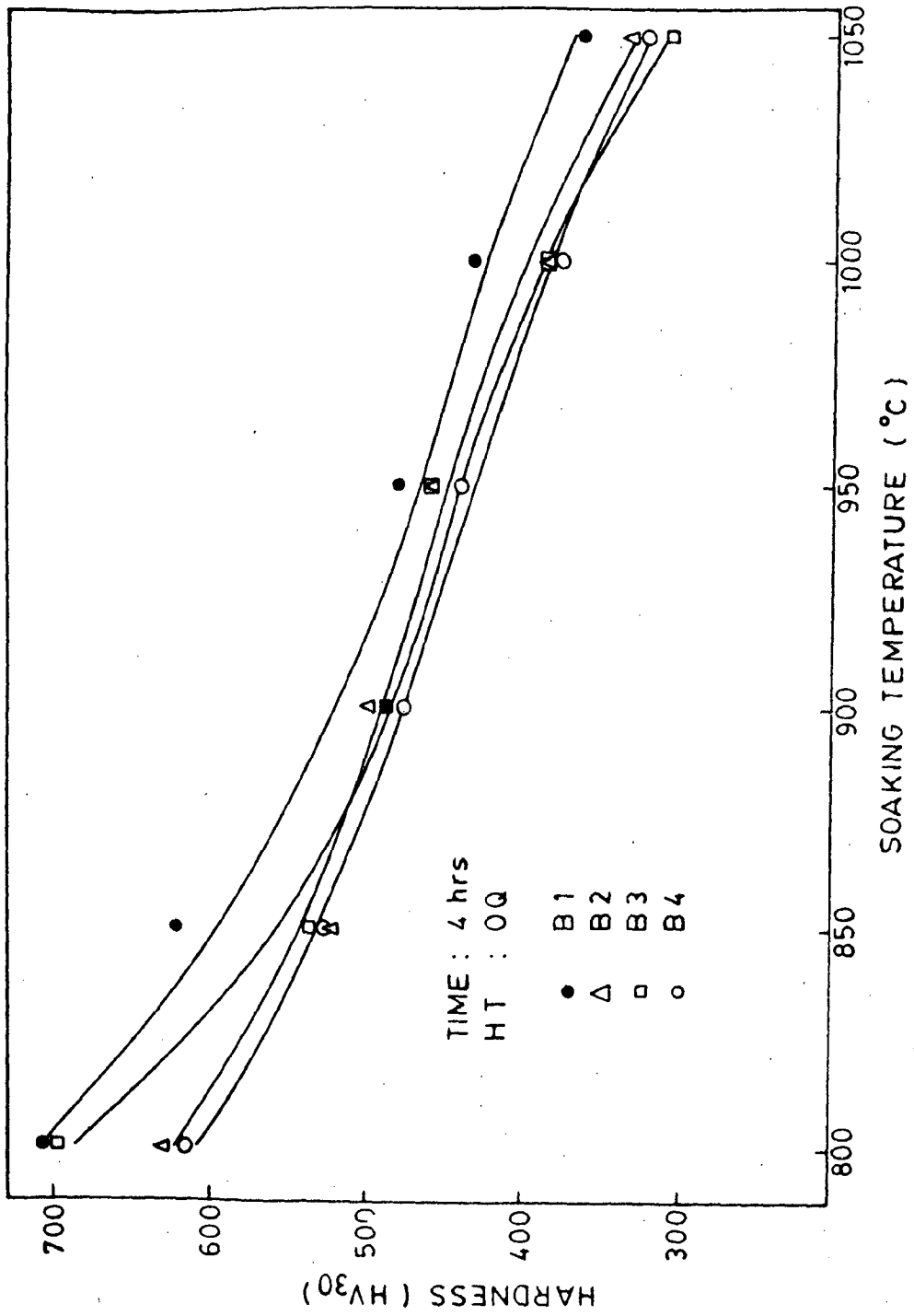


FIG. 5.7(b) EFFECT OF SOAKING TEMPERATURE ON HARDNESS.

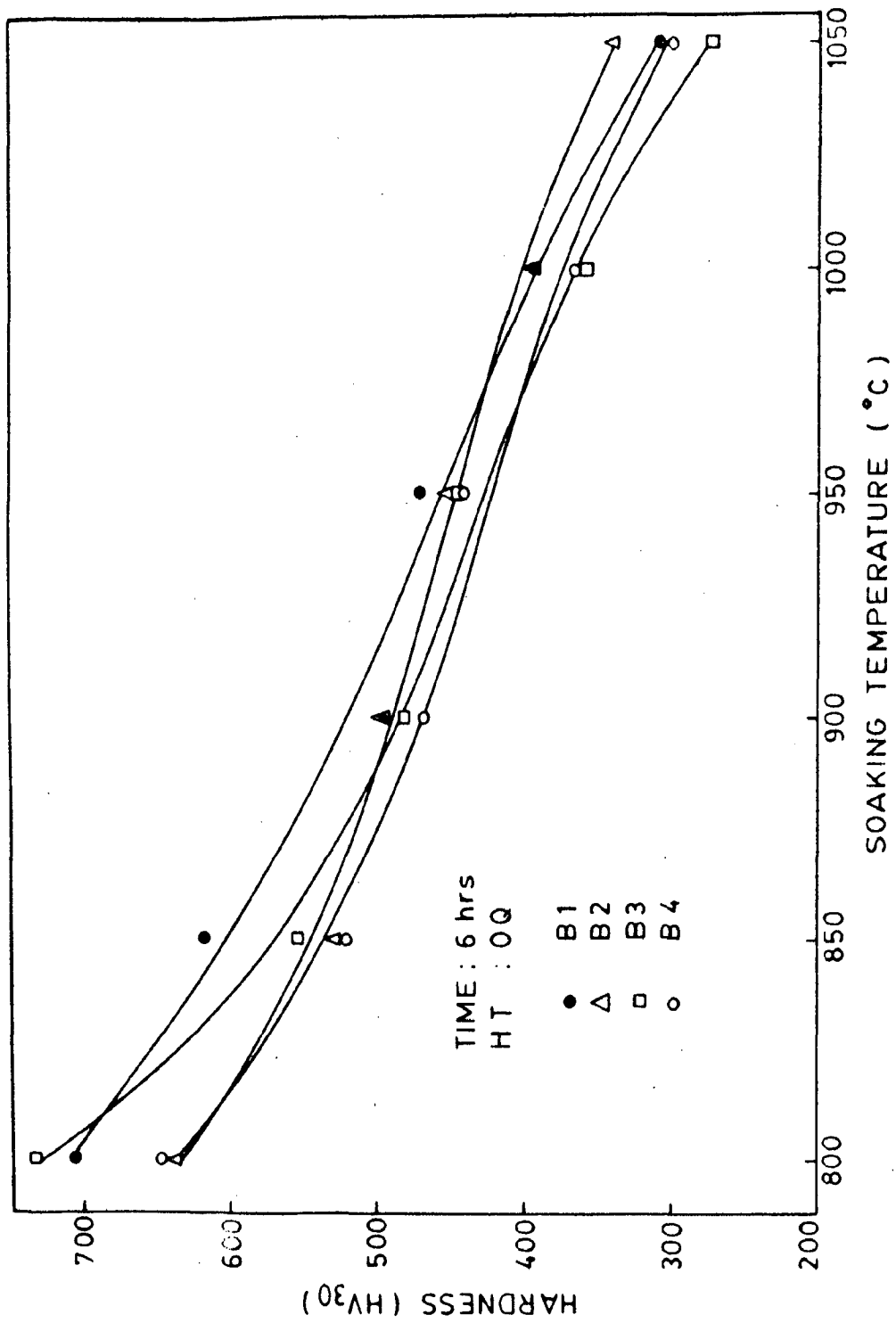


FIG. 5.7(c) EFFECT OF SOAKING TEMPERATURE ON HARDNESS.

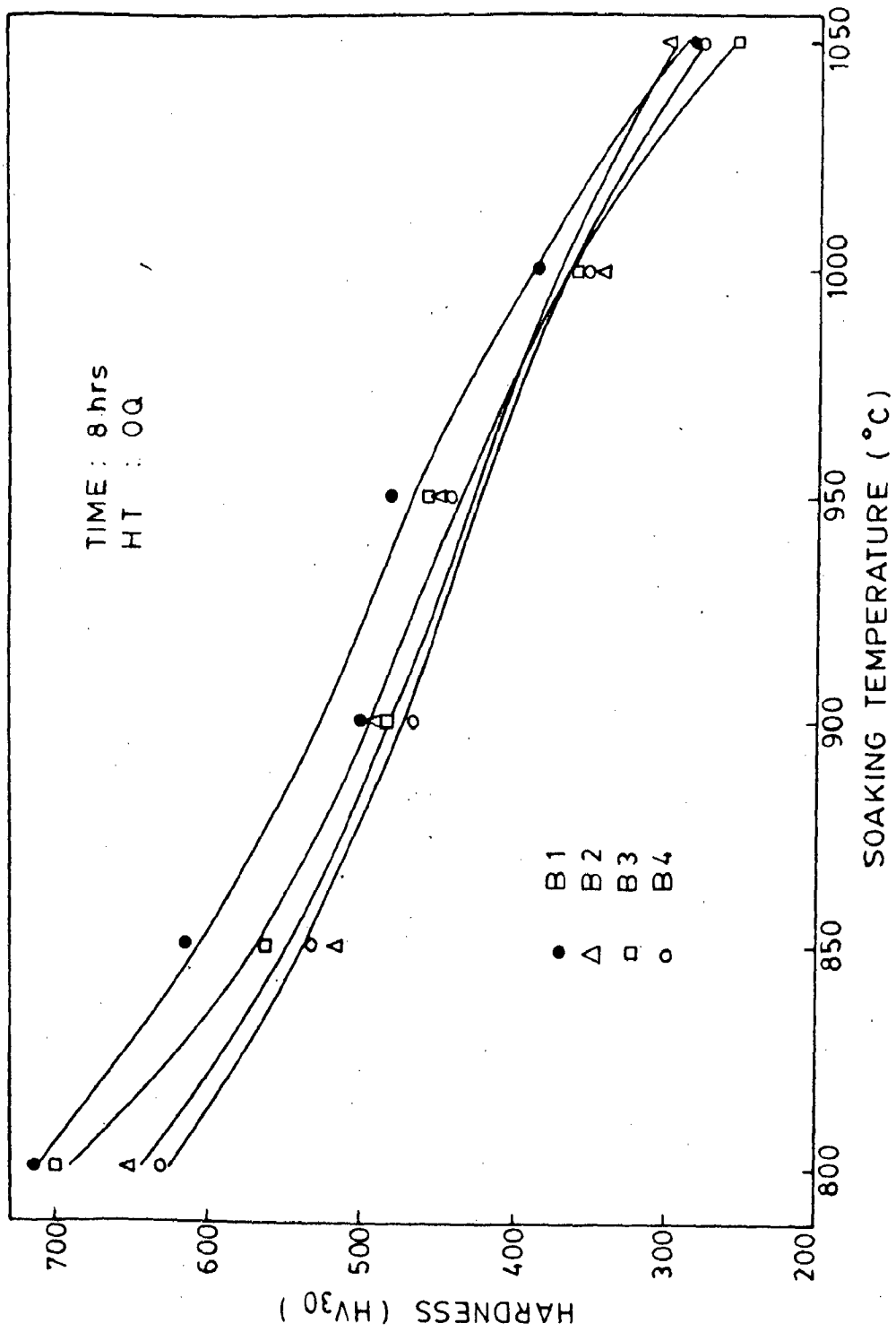


FIG. 5.7(d) EFFECT OF SOAKING TEMPERATURE ON HARDNESS.



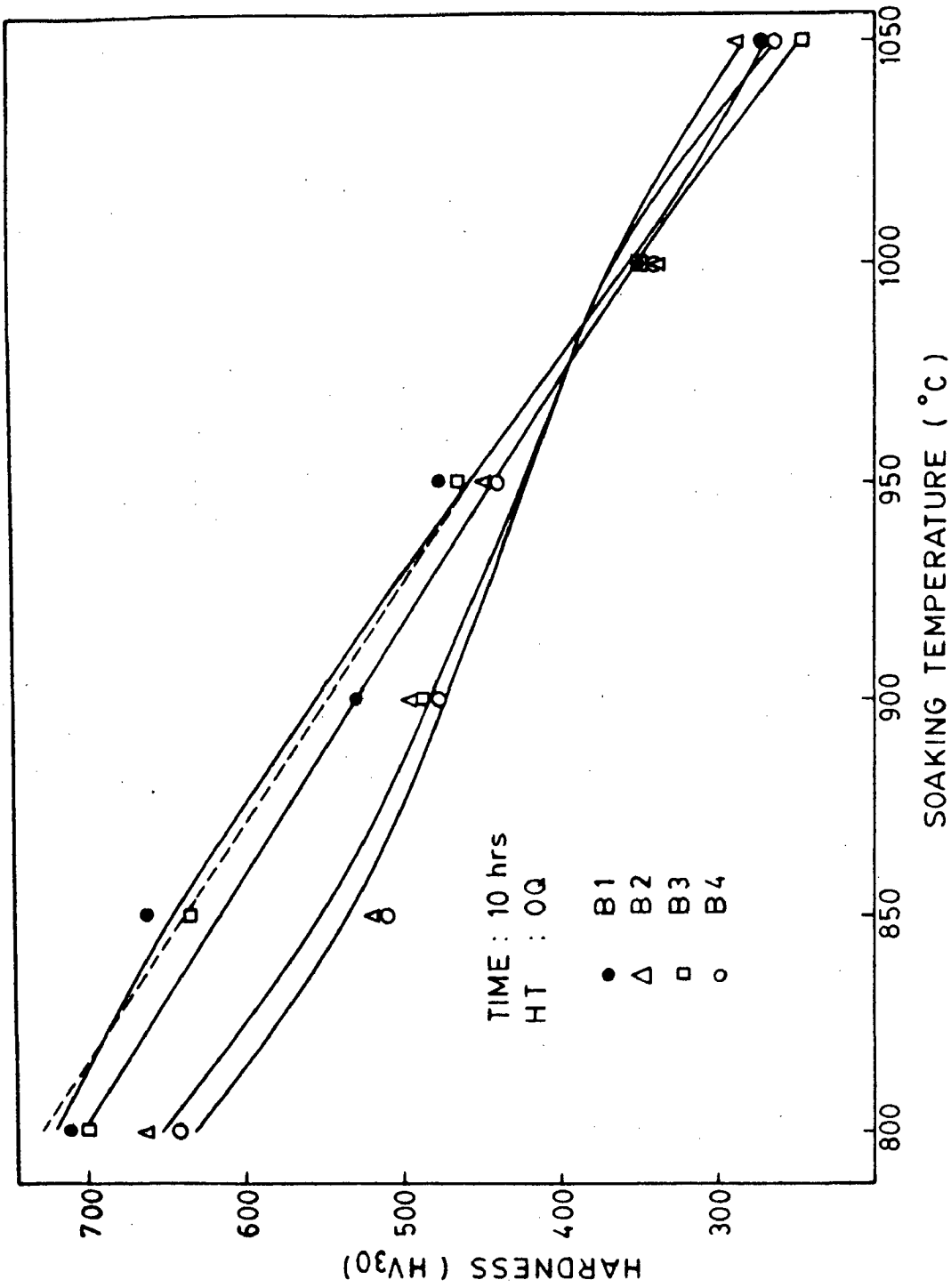


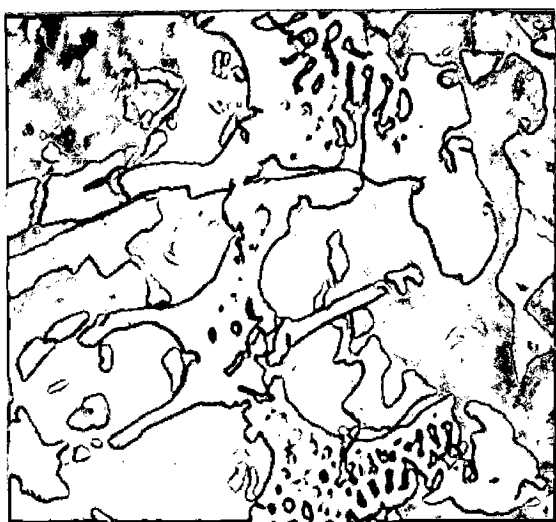
FIG. 5.7(e) EFFECT ON SOAKING TEMPERATURE ON HARDNESS.



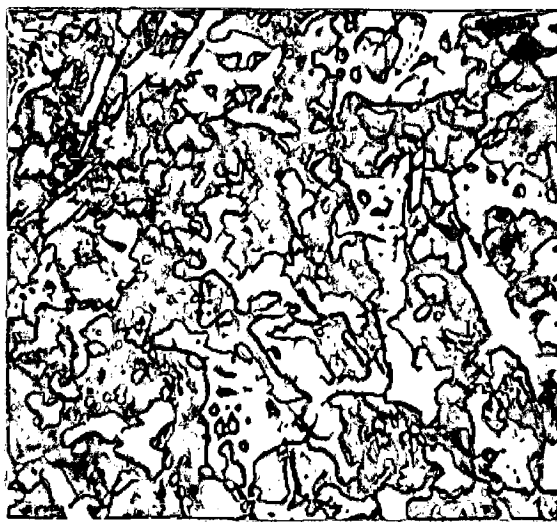
(a)



(b)



(c)



(d)

FIG. 5.8



(a)



(b)

FIG. 5.9

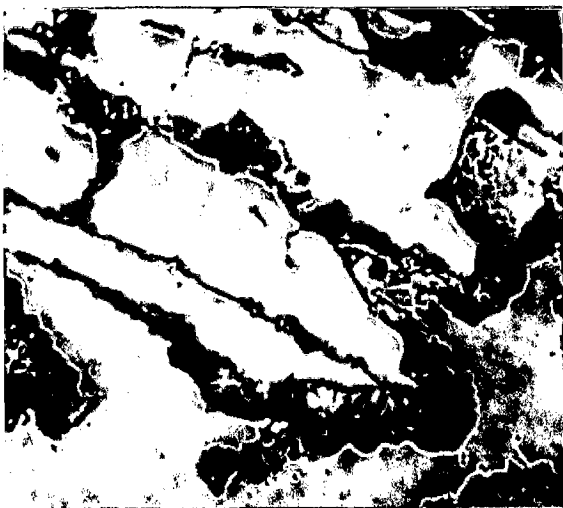


(a)



(b)

FIG. 5.10



(a)



(b)

FIG. 5.11

Fig. 5.12

(a) B<sub>I</sub>, 800°C, 2h, 00  
(x1000)

(b) B<sub>I</sub>, 800°C, 2h, 00  
(x200)

(c) B<sub>I</sub>, 800°C, 10h, 00  
(x1000)

(d) B<sub>I</sub>, 800°C, 10h, 00  
(x200)

(c)  $B_I$ , As-Cast  
(x500)

(d)  $B_I$ , As-Cast  
(x200)

(a)  $B_I$ , As-Cast  
(x1000)

(b)  $B_I$ , As-cast  
(x1000)

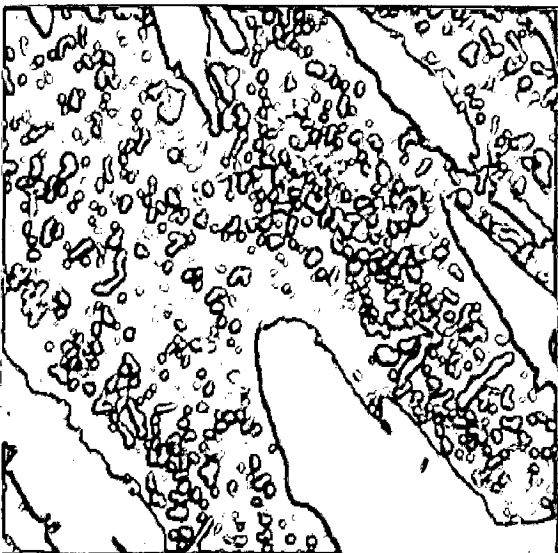
Fig. 5.8



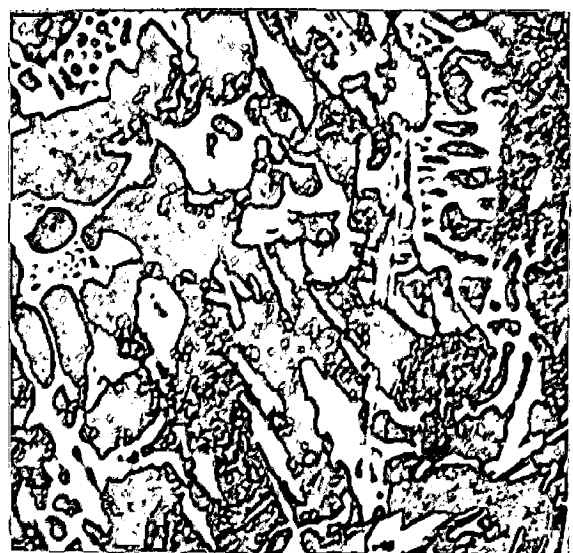
(a)



(b)



(c)



(d)

FIG. 5.12

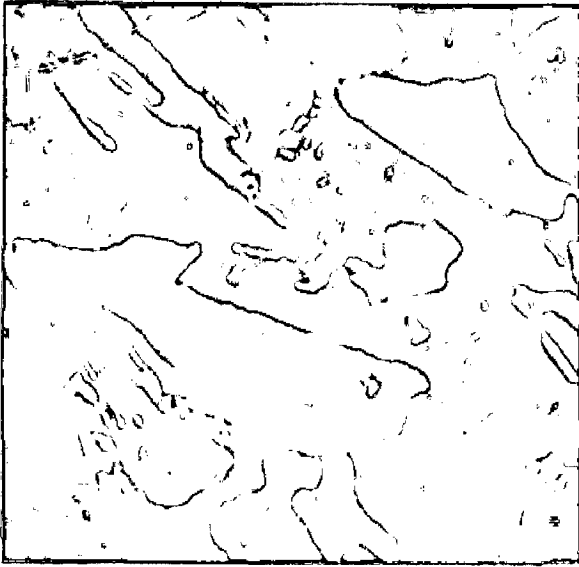
Fig. 5.13

(a) B<sub>2</sub>, 800°C, 2h, OQ  
(x1000)

(b) B<sub>2</sub>, 800°C, 2h, OQ  
(x200)

(c) B<sub>2</sub>, 800°C, 10h, OQ  
(x1000)

(b) B<sub>2</sub>, 800°C, 10h, OQ  
(x200)



(a)



(b)



(c)



(d)

FIG. 5.13



Fig. 5.14

(a) B<sub>3</sub>, 800°C, 2h, 00  
(x1000)

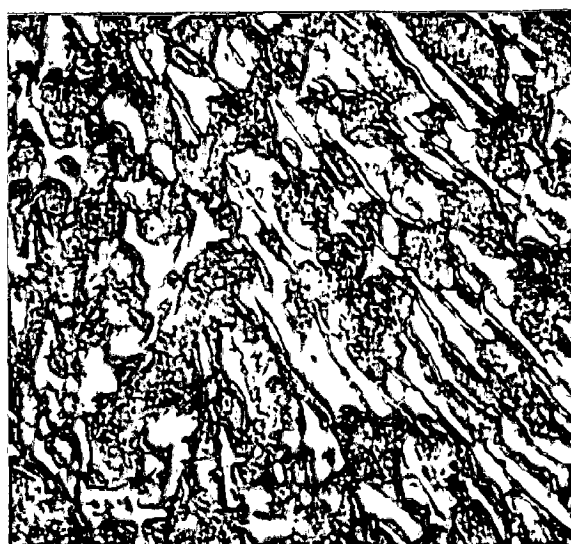
(b) B<sub>3</sub>, 800°C, 2h, 00  
(x200)

(c) B<sub>3</sub>, 800°C, 10h, 00  
(x1000)

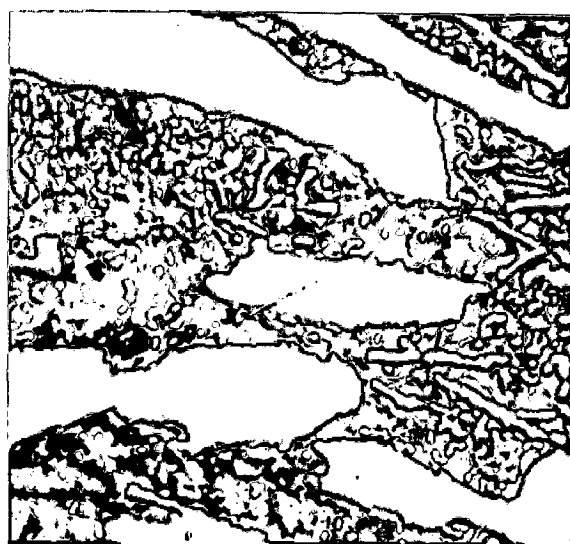
(d) B<sub>3</sub>, 800°C, 10h, 00  
(x200)



(a)



(b)



(c)



(d)

FIG. 5.14

Fig. 5.15

(a)  $B_4, 800^\circ\text{C}, 2\text{h}, 00$

(x1000)

(b)  $B_4, 800^\circ\text{C}, 2\text{h}, 00$

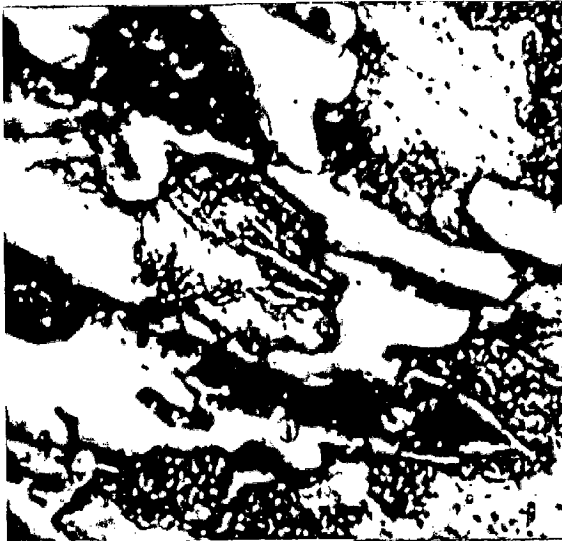
(x200)

(c)  $B_4, 800^\circ\text{C}, 10\text{h}, 00$

(x1000)

(d)  $B_4, 800^\circ\text{C}, 10\text{h}, 00$

(x200)



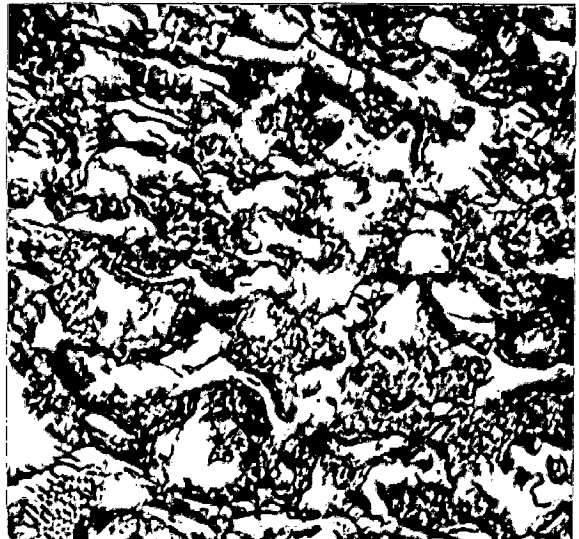
(a)



(b)



(c)



(d)

FIG.5.15

Fig. 5.16

- (a)  $B_I$ , 850°C, 2h, 00 (x1000)
- (b)  $B_I$ , 850°C, 2h, 00 (x200)
- (c)  $B_I$ , 850°C, 4h, 00 (x1000)
- (d)  $B_I$ , 850°C, 6h, 00 (x200)
- (e)  $B_I$ , 850°C, 10h, 00 (x1000)
- (f)  $B_I$ , 850°C, 10h, 00 (x200)



(a)



(b)



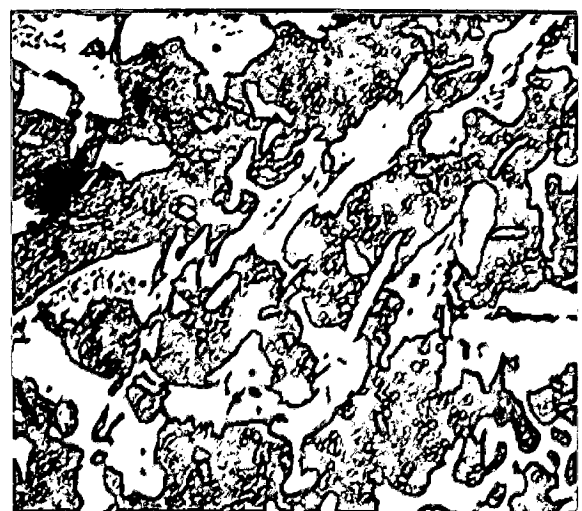
(c)



(d)



(e)



(f)

FIG. 5.16

Fig. 5.17

(a) B<sub>2</sub>, 850°C, 2h, 00  
(x1000)

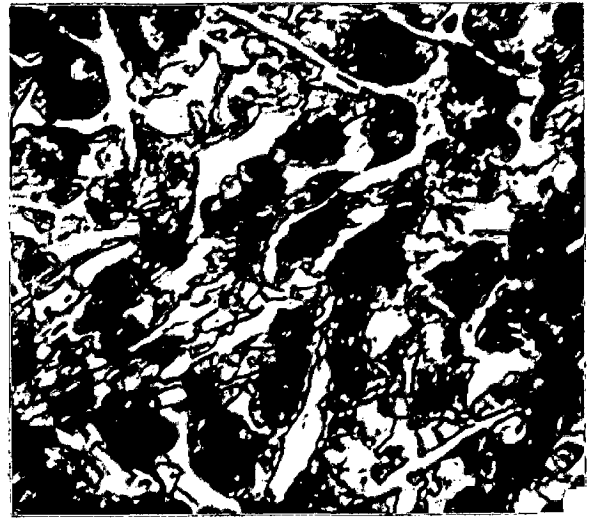
(b) B<sub>2</sub>, 850°C, 2h, 00  
(x200)

(c) B<sub>2</sub>, 850°C, 10h, 00  
(x1000)

(d) B<sub>2</sub>, 850°C, 10h, 00  
(x200)



(a)



(b)



(c)



(d)

FIG. 5.17



Fig. 5.18

(a)  $B_3$ , 850°C, 2h, 00  
(x1000)

(b)  $B_3$ , 850°C, 2h, 00  
(x200)

(c)  $B_3$ , 850°C, 10h, 00  
(x1000)

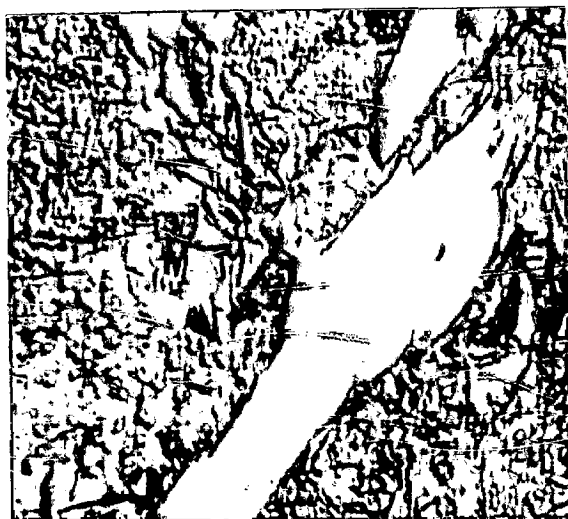
(d)  $B_3$ , 850°C, 10h, 00  
(x200)



(a)



(b)



(c)



(d)

FIG. 5.18

Fig. 5.19

(a)  $B_4$ , 850°C, 2h, 00  
(x1000)

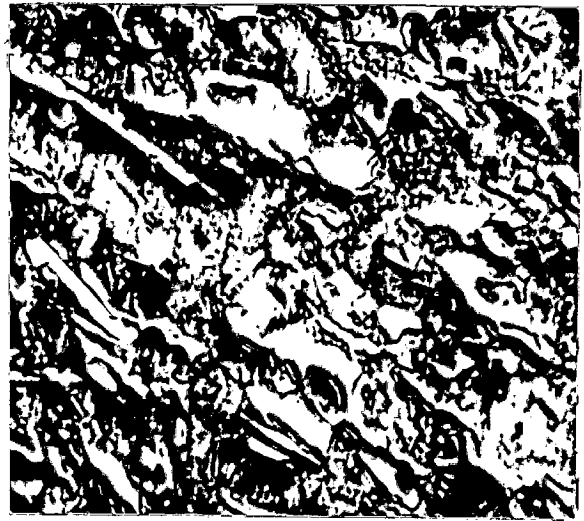
(b)  $B_4$ , 850°C, 2h, 00  
(x200)

(c)  $B_4$ , 850°C, 10h, 00  
(x1000)

(d)  $B_4$ , 850°C, 10h, 00  
(x200)



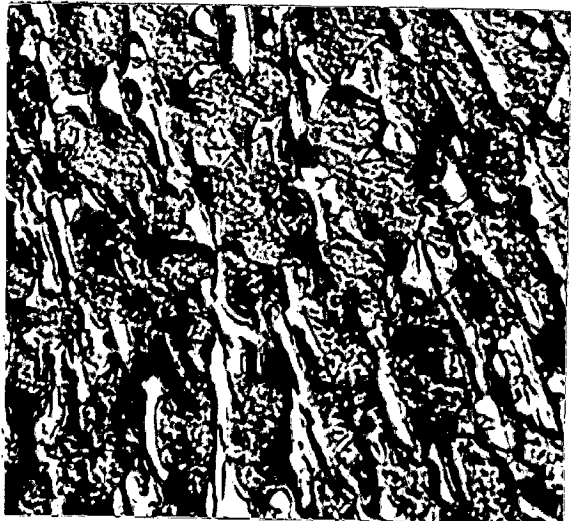
(a)



(b)



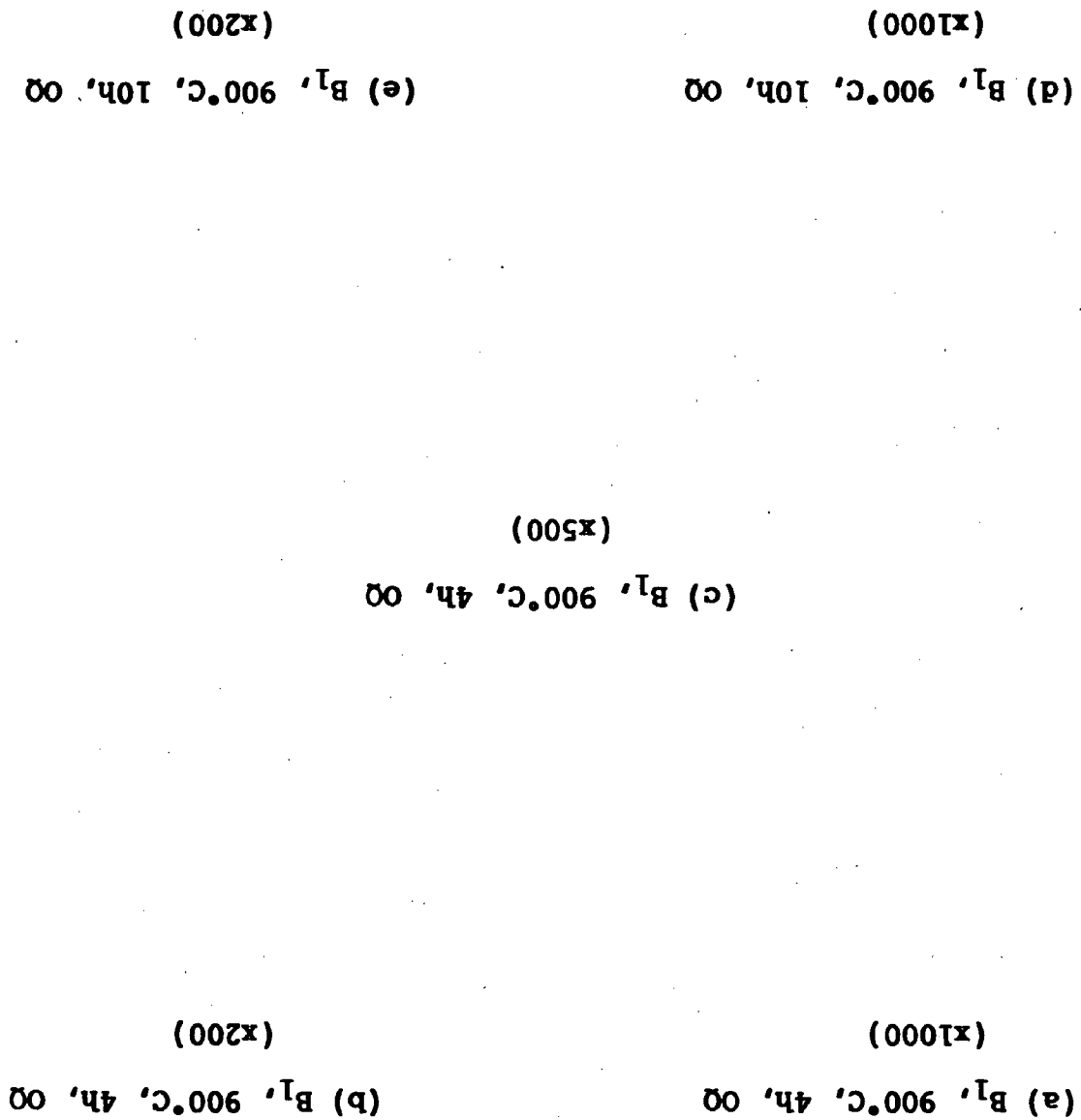
(c)



(d)

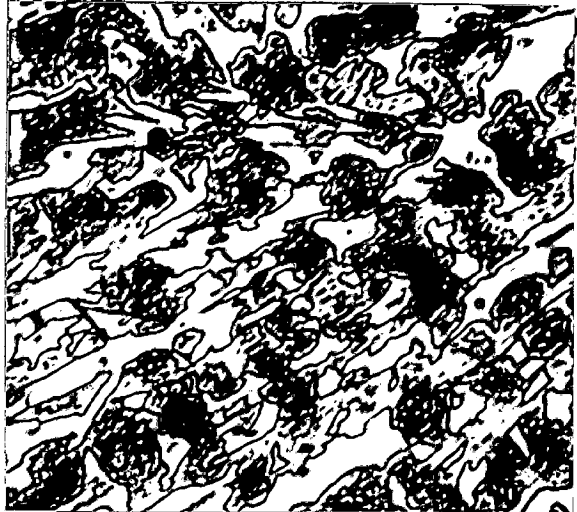
FIG. 5.19

Fig. 5.20





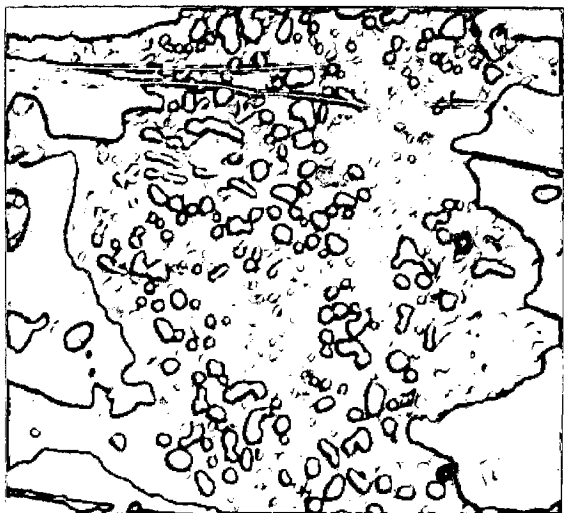
(a)



(b)



(c)



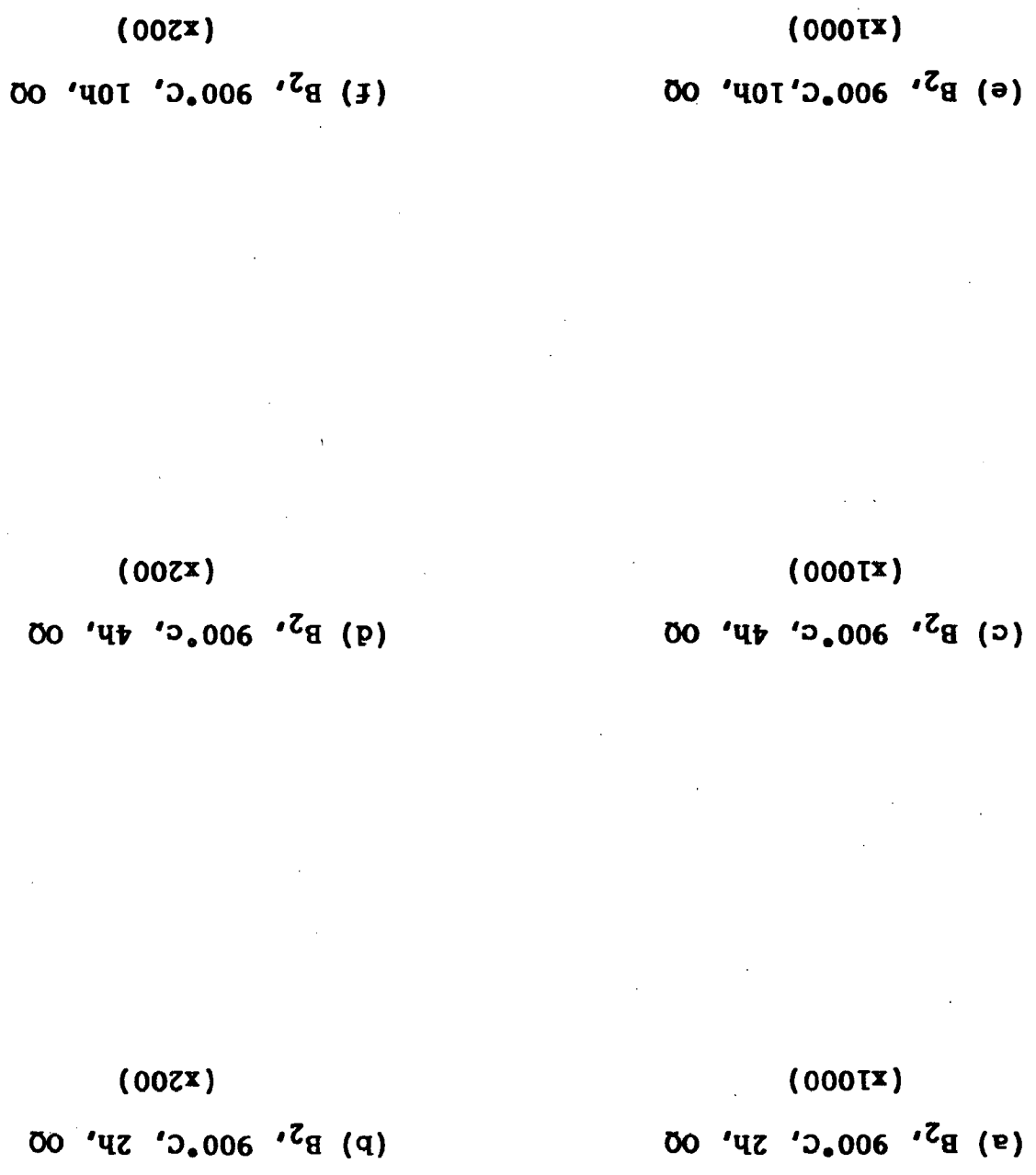
(d)



(e)

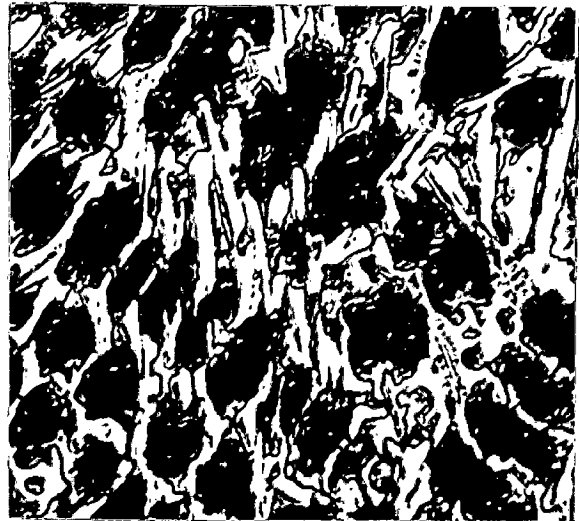
FIG. 5.20

Fig. 5.21





(a)



(b)



(c)



(d)



(e)



(f)

FIG. 5.21



Fig. 5.22

(a)  $B_3$ , 900°C, 4h, OQ  
(x1000)

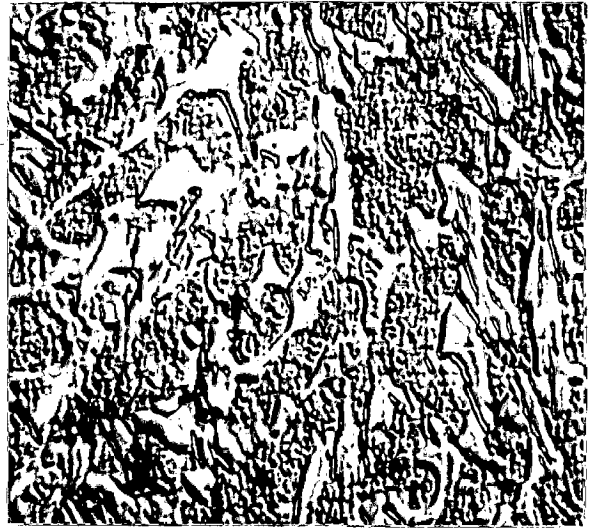
(b)  $B_3$ , 900°C, 4h, OQ  
(x200)

(c)  $B_3$ , 900°C, 10h, OQ  
(x1000)

(d)  $B_3$ , 900°C, 10h, OQ  
(x200)



(a)



(b)



(c)



(d)

FIG. 5.22

Fig. 5.23

(a) B<sub>4</sub>, 900°C, 2h, OQ  
(x1000)

(b) B<sub>4</sub>, 900°C, 2h, OQ  
(x200)

(c) B<sub>4</sub>, 900°C, 4h, OQ  
(x1000)

(d) B<sub>4</sub>, 900°C, 4h, OQ  
(x200)

(e) B<sub>4</sub>, 900°C, 10h, OQ  
(x1000)

(f) B<sub>4</sub>, 900°C, 10h, OQ  
(x200)



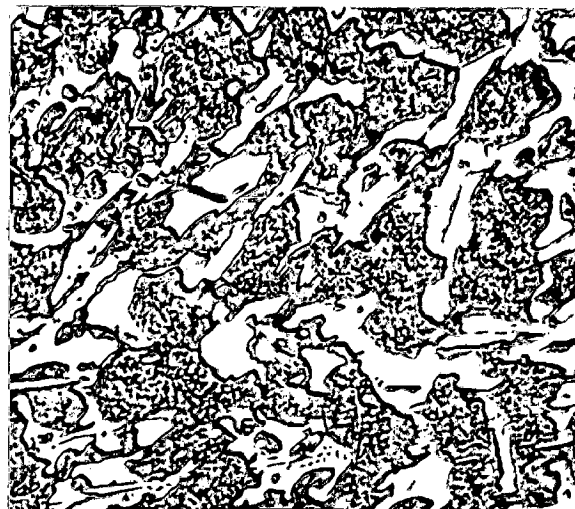
(a)



(b)



(c)



(d)

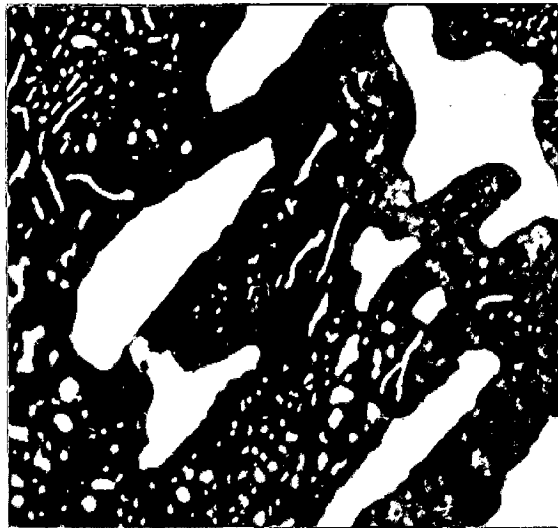


(e)

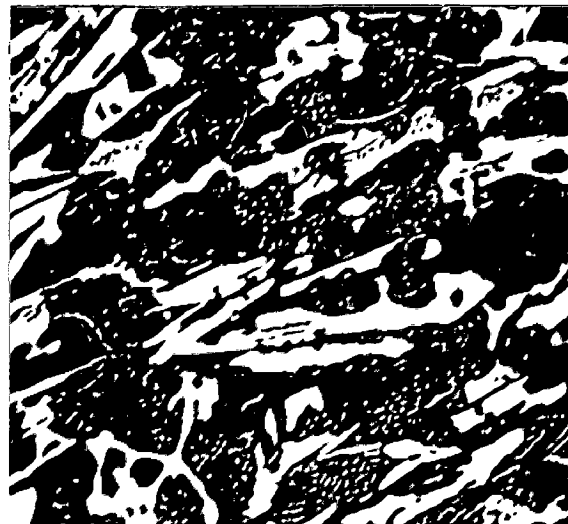


(f)

FIG. 5.23



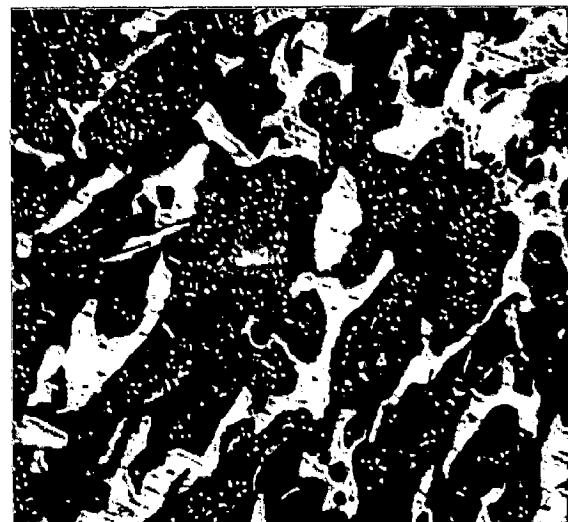
(a)



(b)



(c)



(d)

FIG. 5.24

Fig. 5.24

(a) B<sub>1</sub>, 950°C, 2h, OQ  
(x1000)

(b) B<sub>1</sub>, 950°C, 2h, OQ  
(x200)

(c) B<sub>1</sub>, 950°C, 10h, OQ  
(x1000)

(d) B<sub>1</sub>, 950°C, 10h, OQ  
(x200)

Fig. 5.25

(a) B<sub>2</sub>, 950°C, 2h, OQ  
(x1000)

(b) B<sub>2</sub>, 950°C, 2h, OQ  
(x200)

(c) B<sub>2</sub>, 950°C, 4h, OQ  
(x1000)

(d) B<sub>2</sub>, 950°C, 4h, OQ  
(x200)

(e) B<sub>2</sub>, 950°C, 10h, OQ  
(x1000)

(f) B<sub>2</sub>, 950°C, 10h, OQ  
(x200)



(a)



(b)



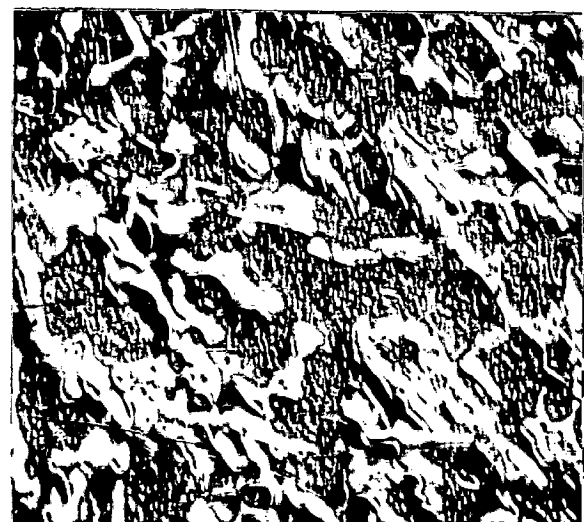
(c)



(d)



(e)



(f)

FIG. 5.25



Fig. 5.26

(a) B<sub>3</sub>, 950°C, 2h, OQ  
(x1000)

(b) B<sub>3</sub>, 950°C, 2h, OQ  
(x200)

(c) B<sub>3</sub>, 950°C, 4h, OQ  
(x1000)

(d) B<sub>3</sub>, 950°C, 4h, OQ  
(x200)

(e) B<sub>3</sub>, 950°C, 10h, OQ  
(x1000)

(f) B<sub>3</sub>, 950°C, 10h, OQ  
(x200)



(a)



(b)



(c)



(d)



(e)



(f)

FIG. 5.26

Fig. 5.27

(a) B<sub>4</sub>, 950°C, 2h, OQ  
(x1000)

(b) B<sub>4</sub>, 950°C, 2h, OQ  
(x200)

(c) B<sub>4</sub>, 950°C, 4h, OQ  
(x1000)

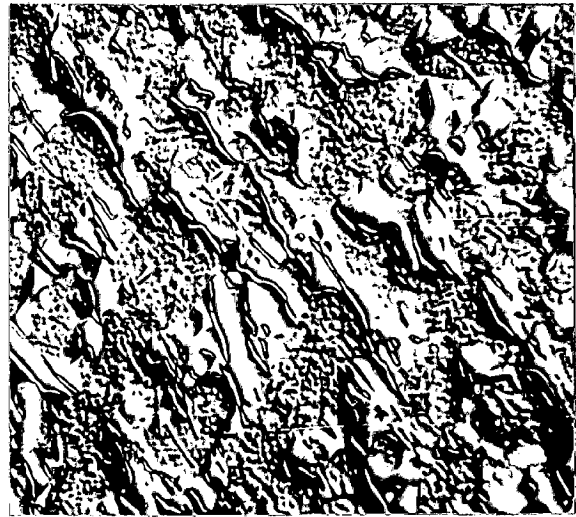
(d) B<sub>4</sub>, 950°C, 4h, OQ  
(x200)

(e) B<sub>4</sub>, 950°C, 10h, OQ  
(x1000)

(f) B<sub>4</sub>, 950°C, 10h, OQ  
(x200)



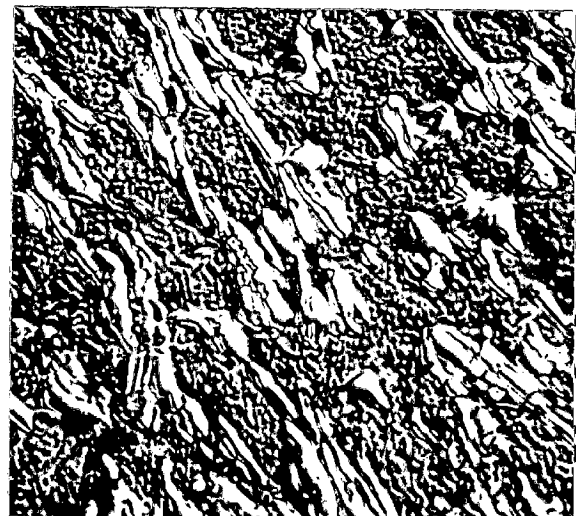
(a)



(b)



(c)



(d)



(e)



(f)

FIG. 5.27

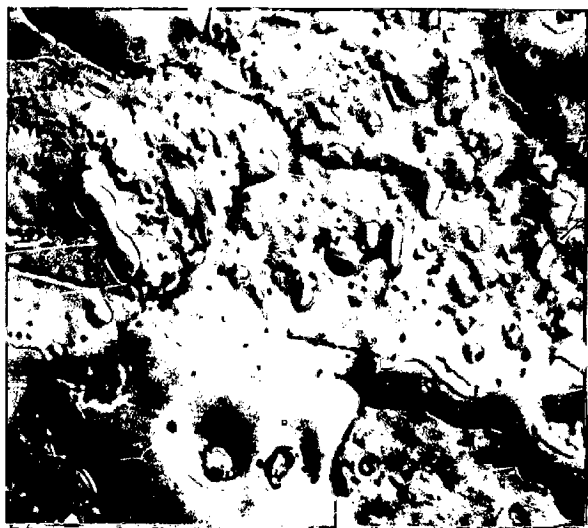
Fig. 5.28

(a) B<sub>1</sub>, 1000°C, 2h, OQ  
(x1000)

(b) B<sub>1</sub>, 1000°C, 2h, OQ  
(x200)

(c) B<sub>1</sub>, 1000°C, 10h, OQ  
(x1000)

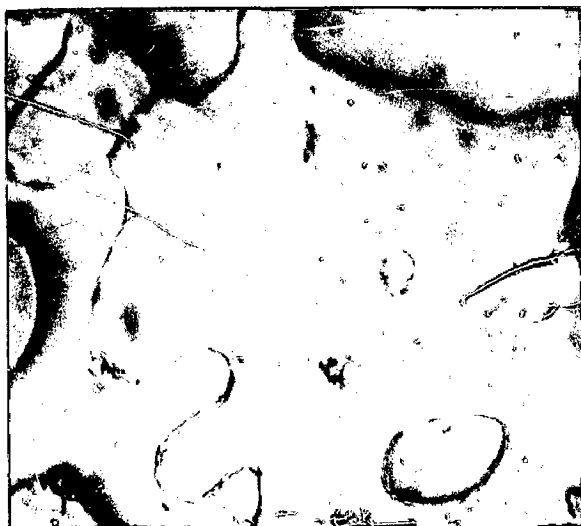
(d) B<sub>1</sub>, 1000°C, 10h, OQ  
(x200)



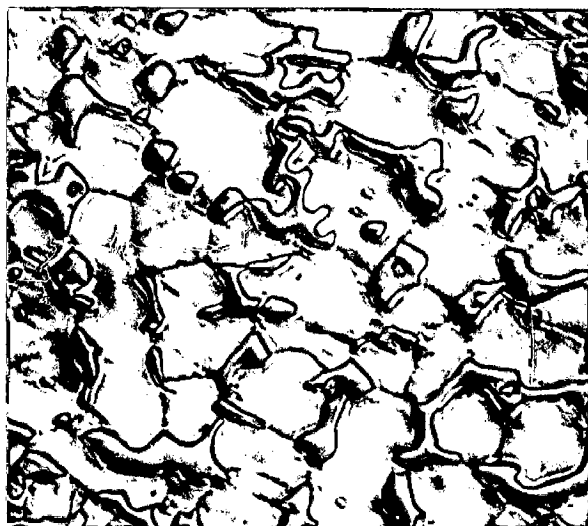
(a)



(b)



(c)



(d)

FIG. 5.28

Fig. 5.29

(a) B<sub>2</sub>, 1000°C, 2h, OQ  
(x1000)

(b) B<sub>2</sub>, 1000°C, 2h, OQ  
(x200)

(c) B<sub>2</sub>, 1000°C, 4h, OQ  
(x1000)

(d) B<sub>2</sub>, 1000°C, 4h, OQ  
(x200)

(e) B<sub>2</sub>, 1000°C, 10h, OQ  
(x1000)

(f) B<sub>2</sub>, 1000°C, 10h, OQ  
(x200)



(a)



(b)



(c)



(d)



(e)



(f)

FIG. 5.29



Fig. 5.30

(a) B<sub>3</sub>, 1000°C, 2h, OQ  
(x1000)

(b) B<sub>3</sub>, 1000°C, 2h, OQ  
(x200)

(c) B<sub>3</sub>, 1000°C, 4h, OQ  
(x1000)

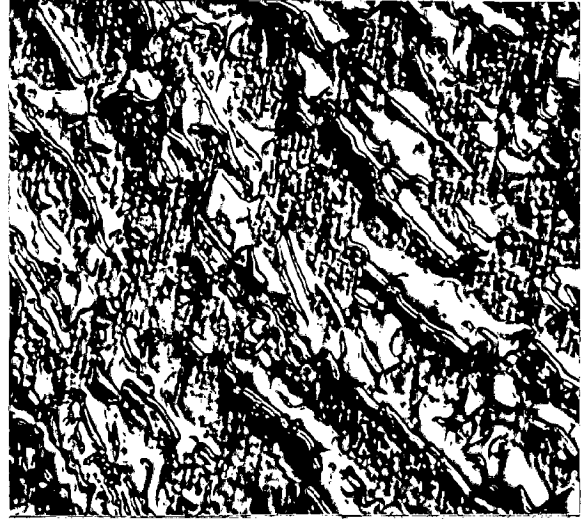
(d) B<sub>3</sub>, 1000°C, 4h, OQ  
(x200)

(e) B<sub>3</sub>, 1000°C, 10h, OQ  
(x1000)

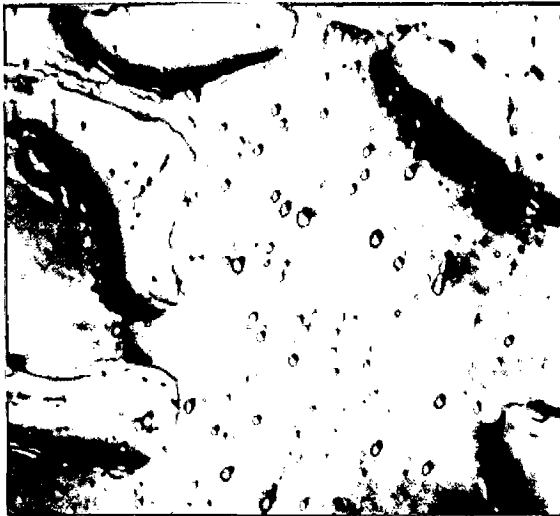
(f) B<sub>3</sub>, 1000°C, 10h, OQ  
(x200)



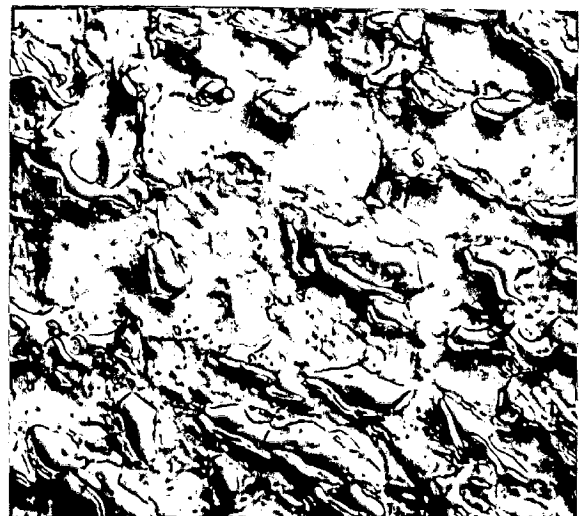
(a)



(b)



(c)



(d)



(e)



(f)

FIG. 5.30

Fig. 5.31

(a) B<sub>4</sub>, 1000°C, 2h, OQ  
(x1000)

(b) B<sub>4</sub>, 1000°C, 2h, OQ  
(x200)

(c) B<sub>4</sub>, 1000°C, 4h, OQ  
(x1000)

(d) B<sub>4</sub>, 1000°C, 4h, OQ  
(x200)

(e) B<sub>4</sub>, 1000°C, 10h, OQ  
(x1000)

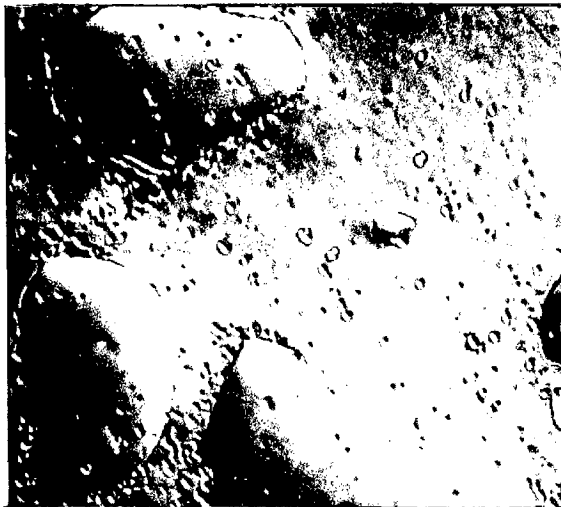
(f) B<sub>4</sub>, 1000°C, 10h, OQ  
(x200)



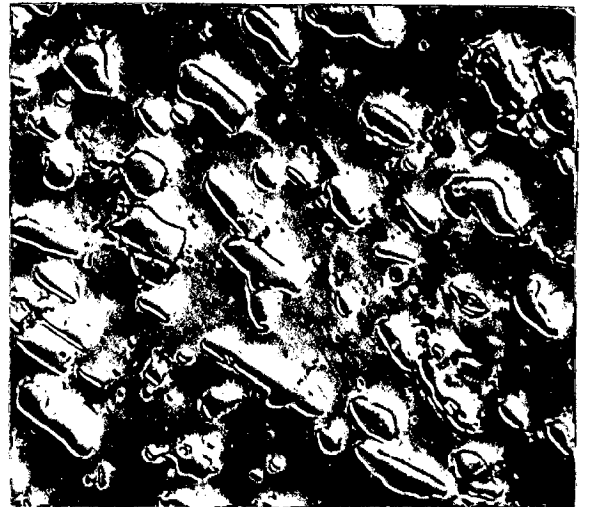
(a)



(b)



(c)



(d)



(e)



(f)

FIG. 5.31

Fig. 5.32

(a) B<sub>1</sub>, 1050°C, 2h, OQ  
(x1000)

(b) B<sub>1</sub>, 1050°C, 2h, OQ  
(x200)

(c) B<sub>1</sub>, 1050°C, 4h, OQ  
(x1000)

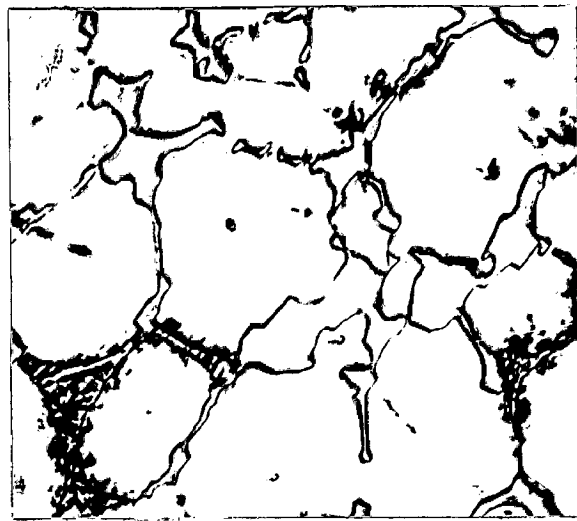
(d) B<sub>1</sub>, 1050°C, 4h, OQ  
(x200)

(e) B<sub>1</sub>, 1050°C, 6h, OQ  
(x1000)

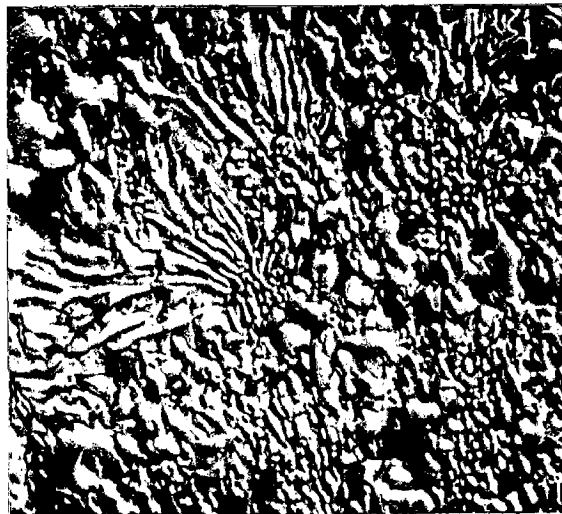
(f) B<sub>1</sub>, 1050°C, 6h, OQ  
(x200)



(a)



(b)



(c)



(d)



(e)



(f)

FIG. 5.32

Fig. 5.32

(g) B<sub>1</sub>, 1050°C, 10h, OQ  
(x1000)

(h) B<sub>1</sub>, 1050°C, 10h, OQ  
(x200)

(i) B<sub>1</sub>, 1050°C, 10h, OQ  
(x1000)

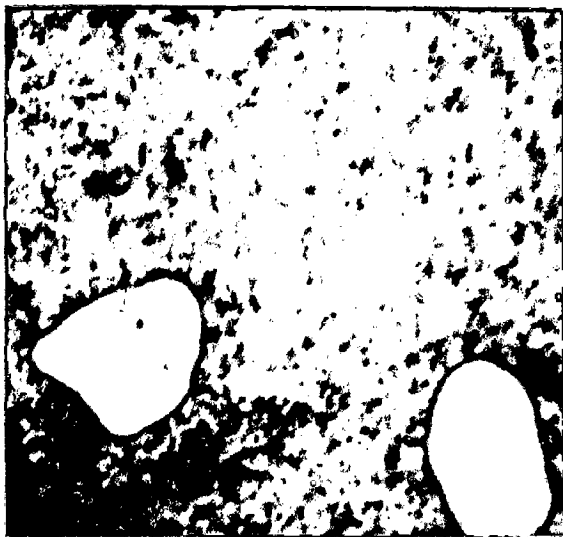
(j) B<sub>1</sub>, 1050°C, 10h, OQ  
(x200)



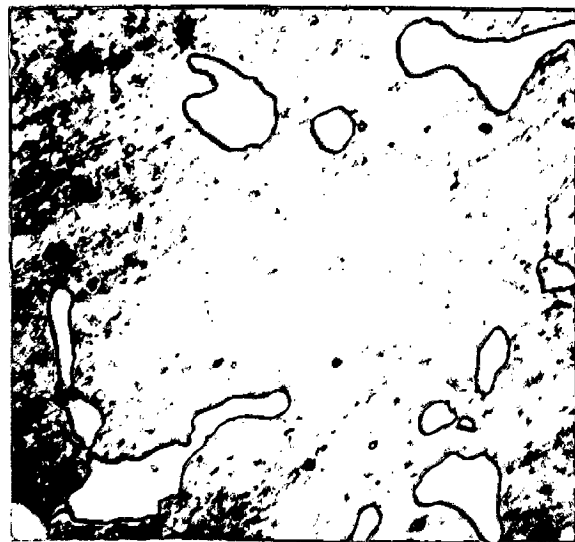
(g)



(h)



(i)



(j)

FIG. 5.32



Fig. 5.33

(a) B<sub>2</sub>, 1050°C, 2h, OQ  
(x1000)

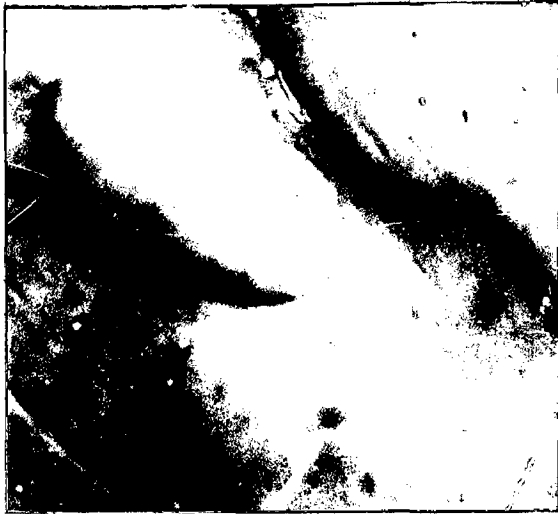
(b) B<sub>2</sub>, 1050°C, 2h, OQ  
(x200)

(c) B<sub>2</sub>, 1050°C, 6h, OQ  
(x1000)

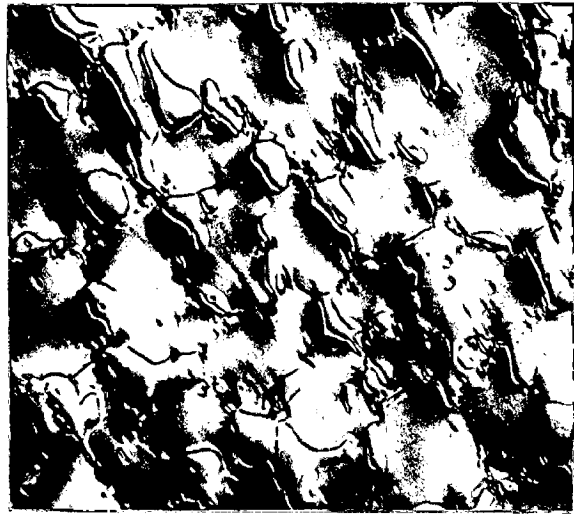
(d) B<sub>2</sub>, 1050°C, 6h, OQ  
(x200)

(e) B<sub>2</sub>, 1050°C, 10h, OQ  
(x1000)

(f) B<sub>2</sub>, 1050°C, 10h, OQ  
(x200)



(a)



(b)



(c)



(d)



(e)



(f)

FIG. 5.33

Fig. 5.34

(a) B<sub>3</sub>, 1050°C, 2h, OQ  
(x1000)

(b) B<sub>3</sub>, 1050°C, 2h, OQ  
(x200)

(c) B<sub>3</sub>, 1050°C, 4h, OQ  
(x1000)

(d) B<sub>3</sub>, 1050°C, 4h, OQ  
(x200)

(e) B<sub>3</sub>, 1050°C, 10h, OQ  
(x1000)

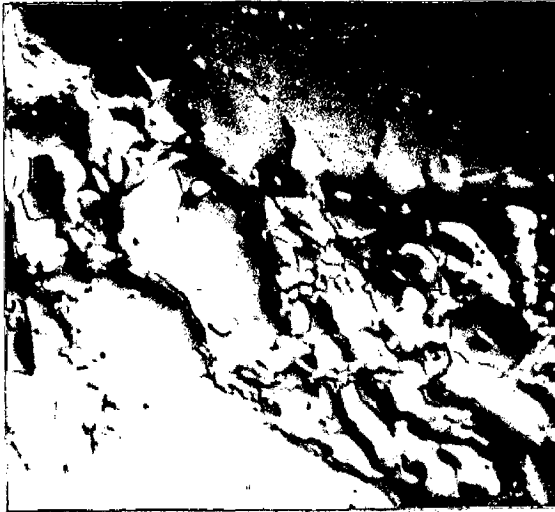
(f) B<sub>3</sub>, 1050°C, 10h, OQ  
(x200)



(a)



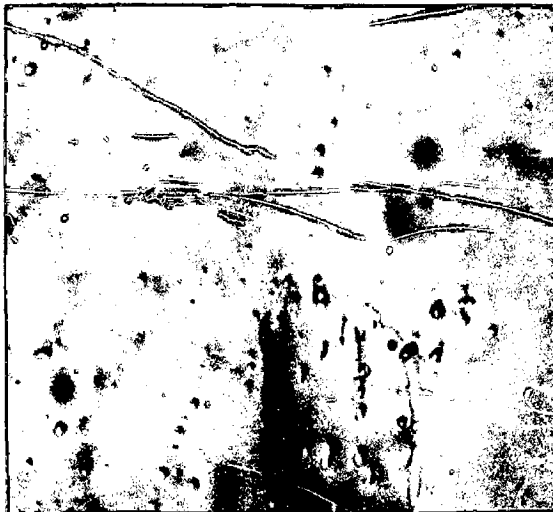
(b)



(c)



(d)



(e)



(f)

FIG. 5.34

Fig. 5.35

(a) B<sub>4</sub>, 1050°C, 2h, OQ  
(x1000)

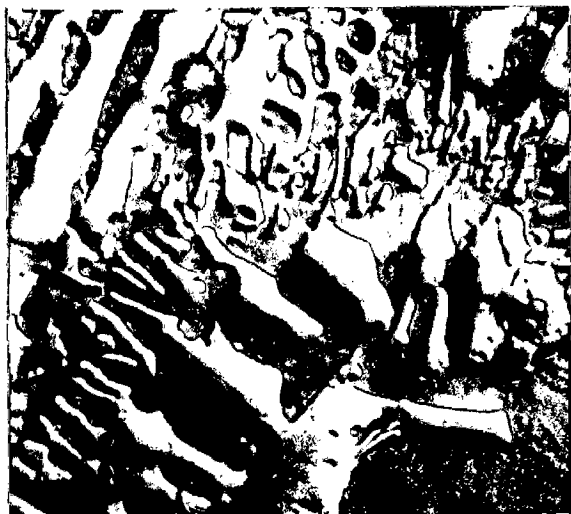
(b) B<sub>4</sub>, 1050°C, 2h, OQ  
(x200)

(c) B<sub>4</sub>, 1050°C, 6h, OQ  
(x1000)

(d) B<sub>4</sub>, 1050°C, 6h, OQ  
(x200)

(e) B<sub>4</sub>, 1050°C, 10h, OQ  
(x1000)

(f) B<sub>4</sub>, 1050°C, 10h, OQ  
(x200)



(a)



(b)



(c)



(d)

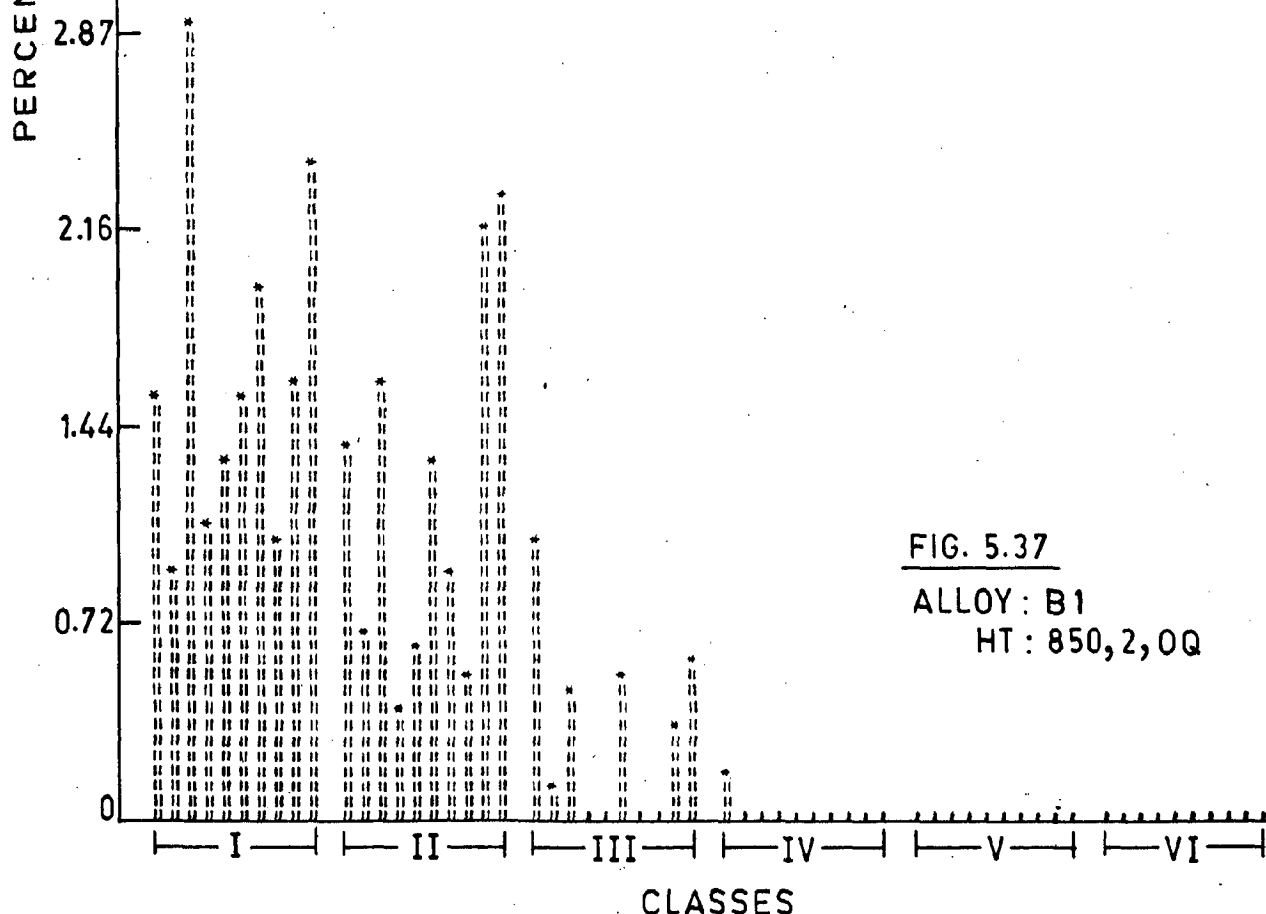
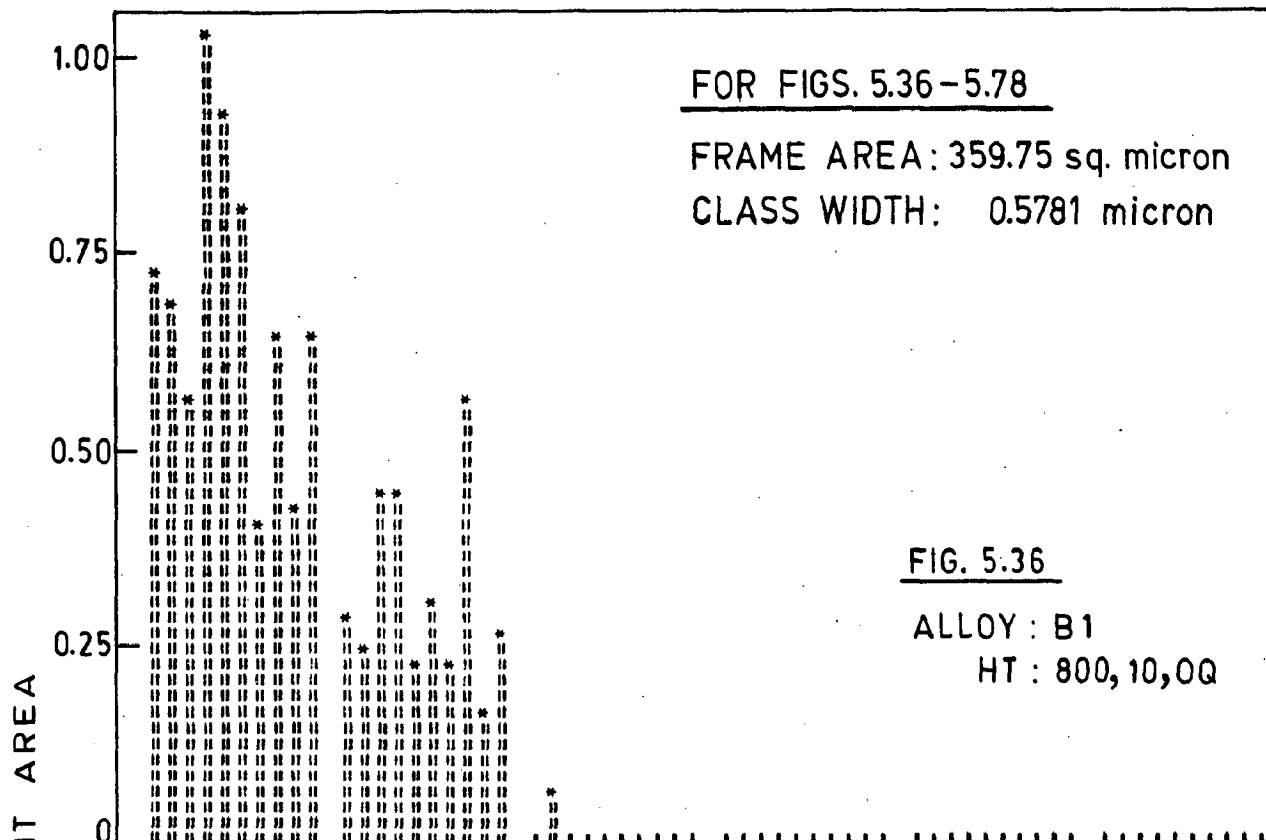


(e)

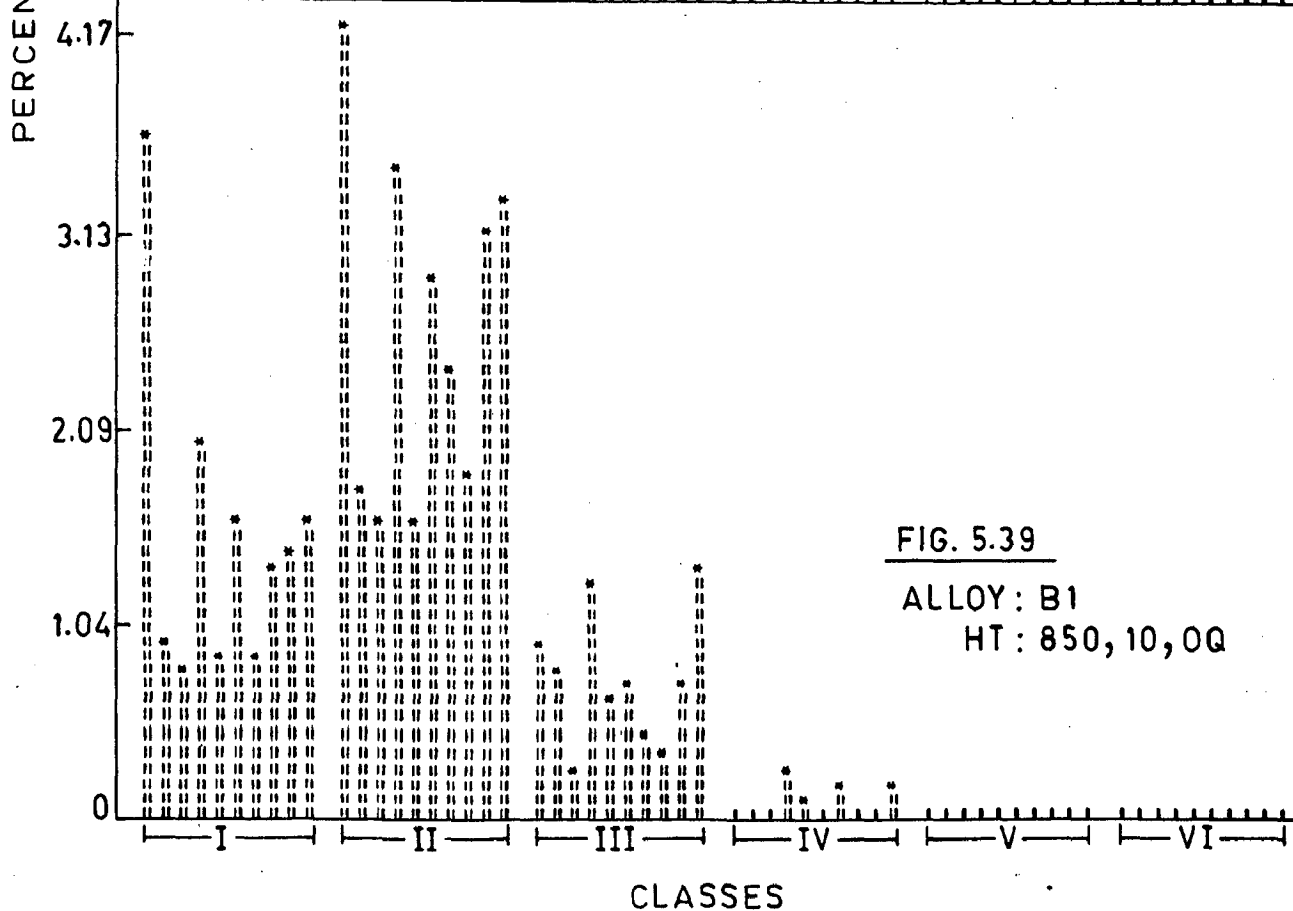
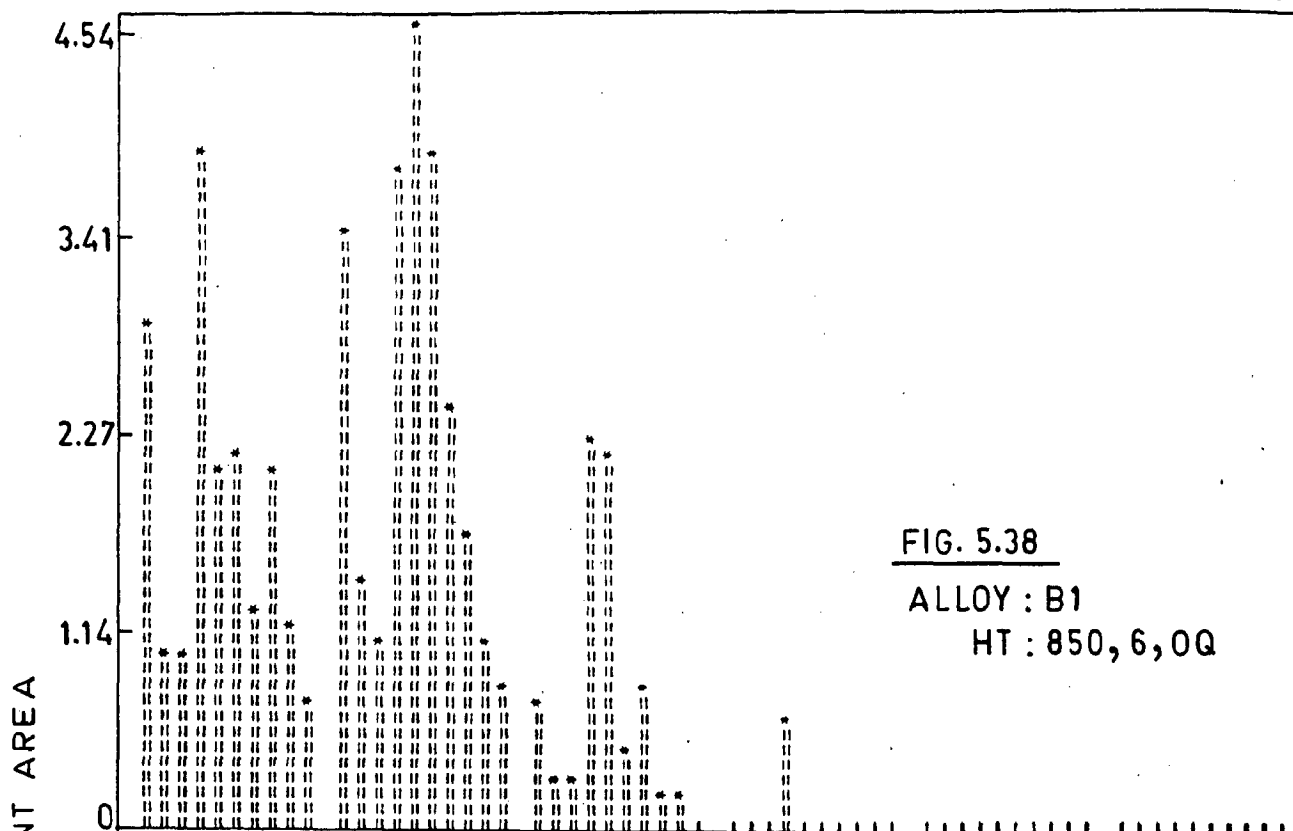


(f)

FIG. 5.35



COMPOSITE HISTOGRAMS DEPICTING CLASS WISE PARTICLE-DISTRIBUTION AT TEN DIFFERENT LOCATIONS.



COMPOSITE HYSTOGRAMS DEPICTING CLASS WISE PARTICLE - DISTRIBUTION AT TEN DIFFERENT LOCATIONS.



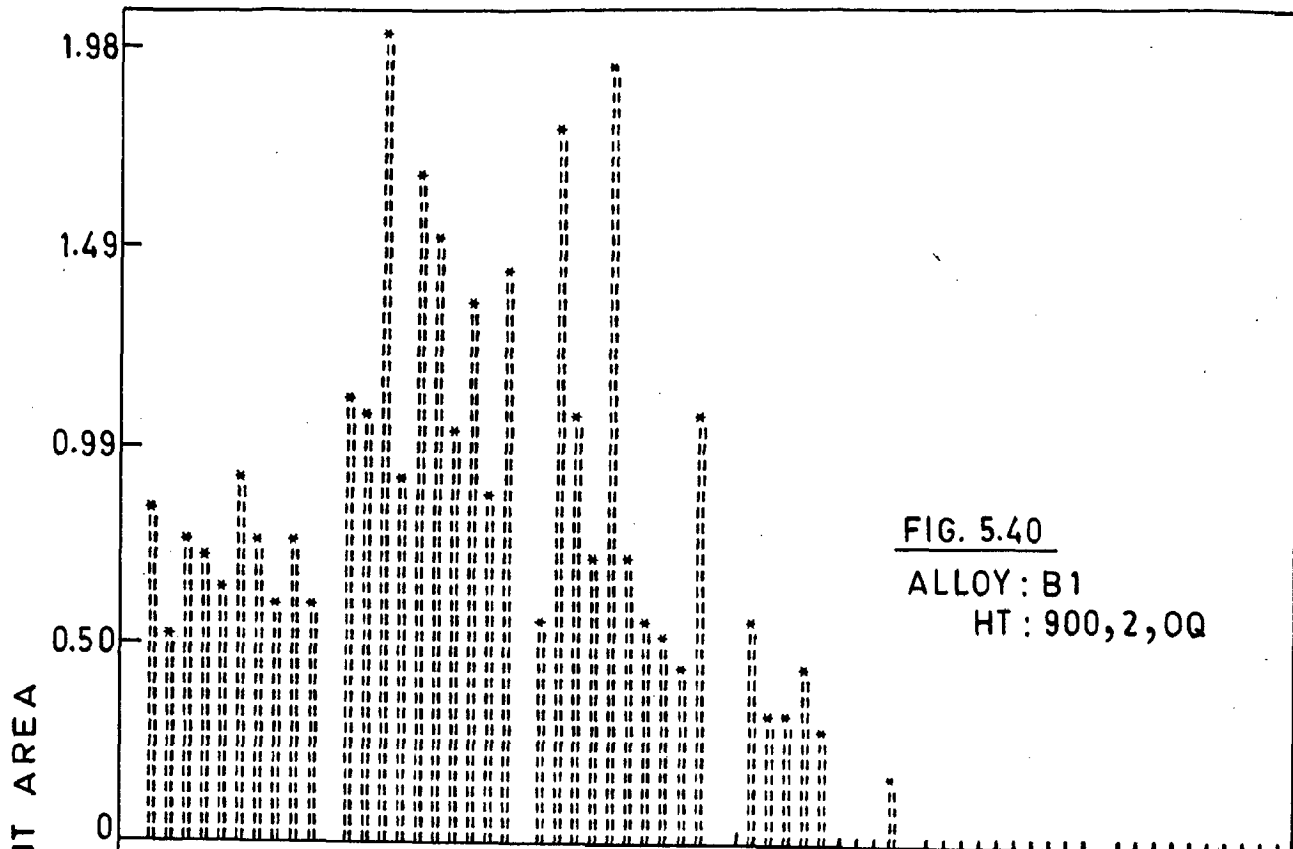


FIG. 5.40  
ALLOY : B1  
HT : 900, 2, OQ

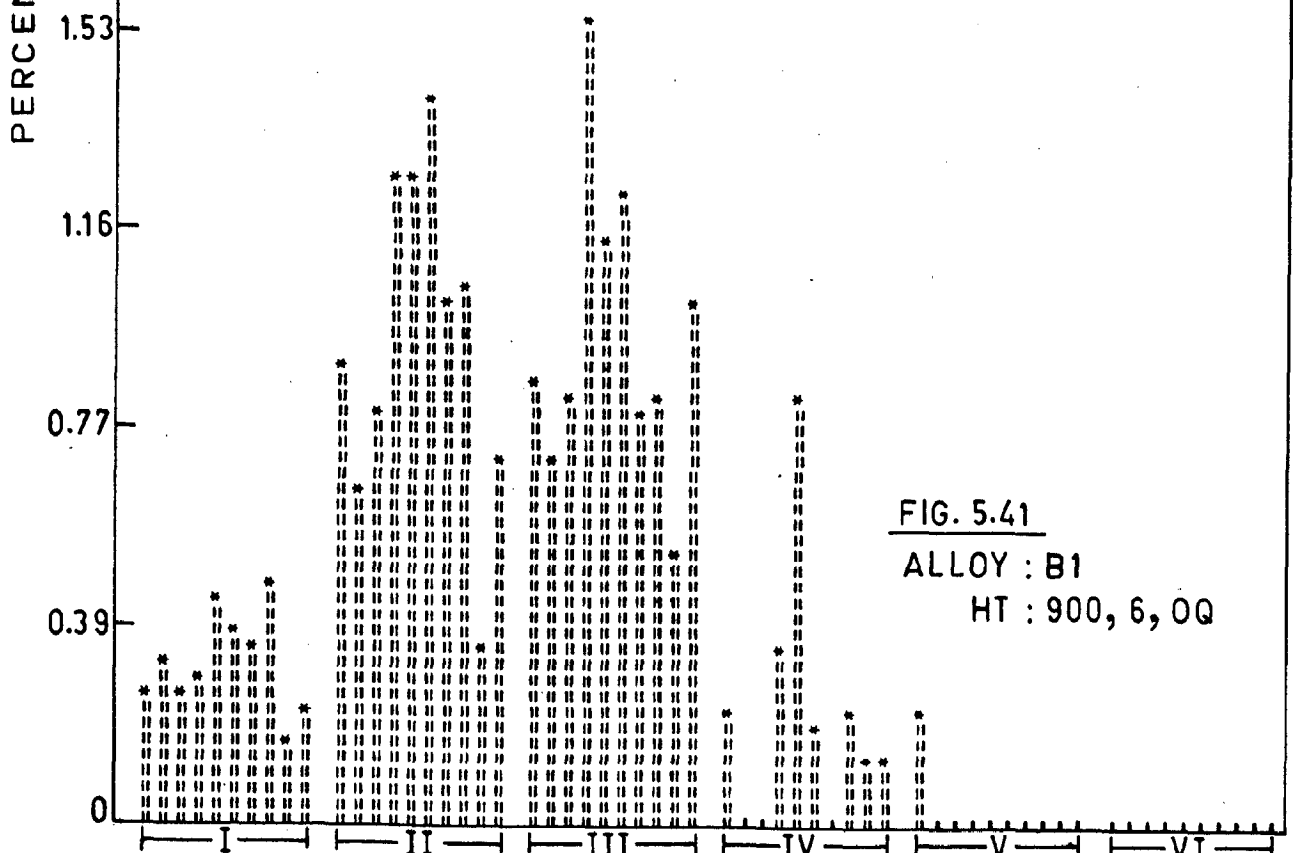
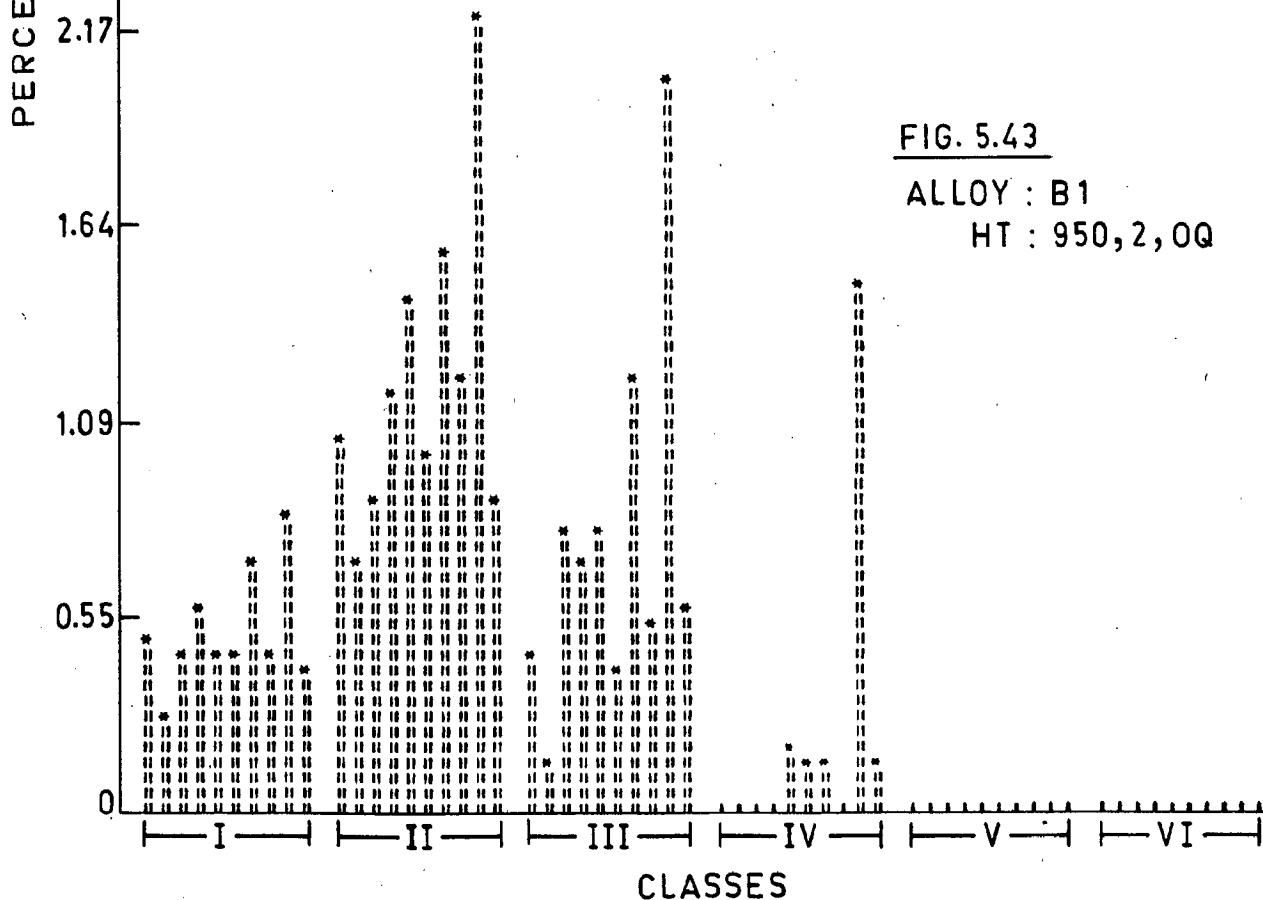
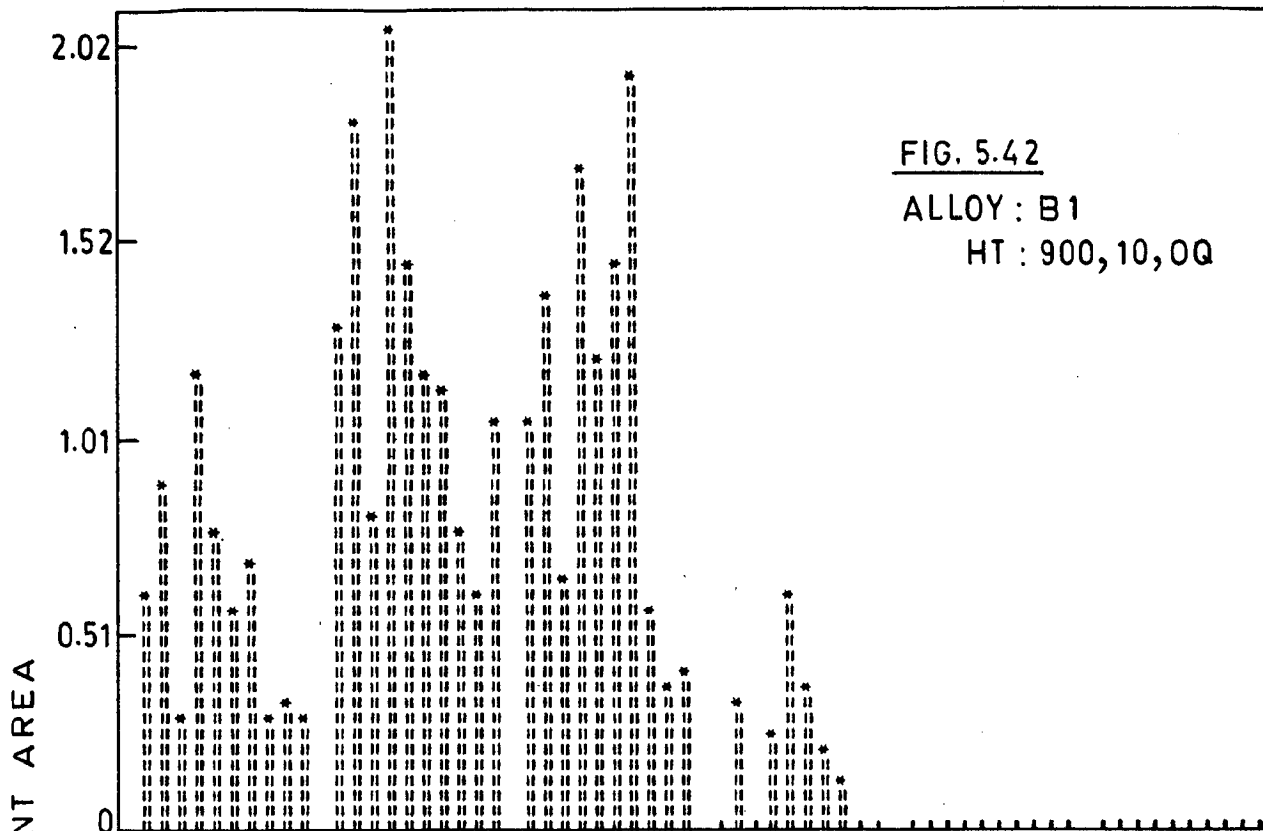
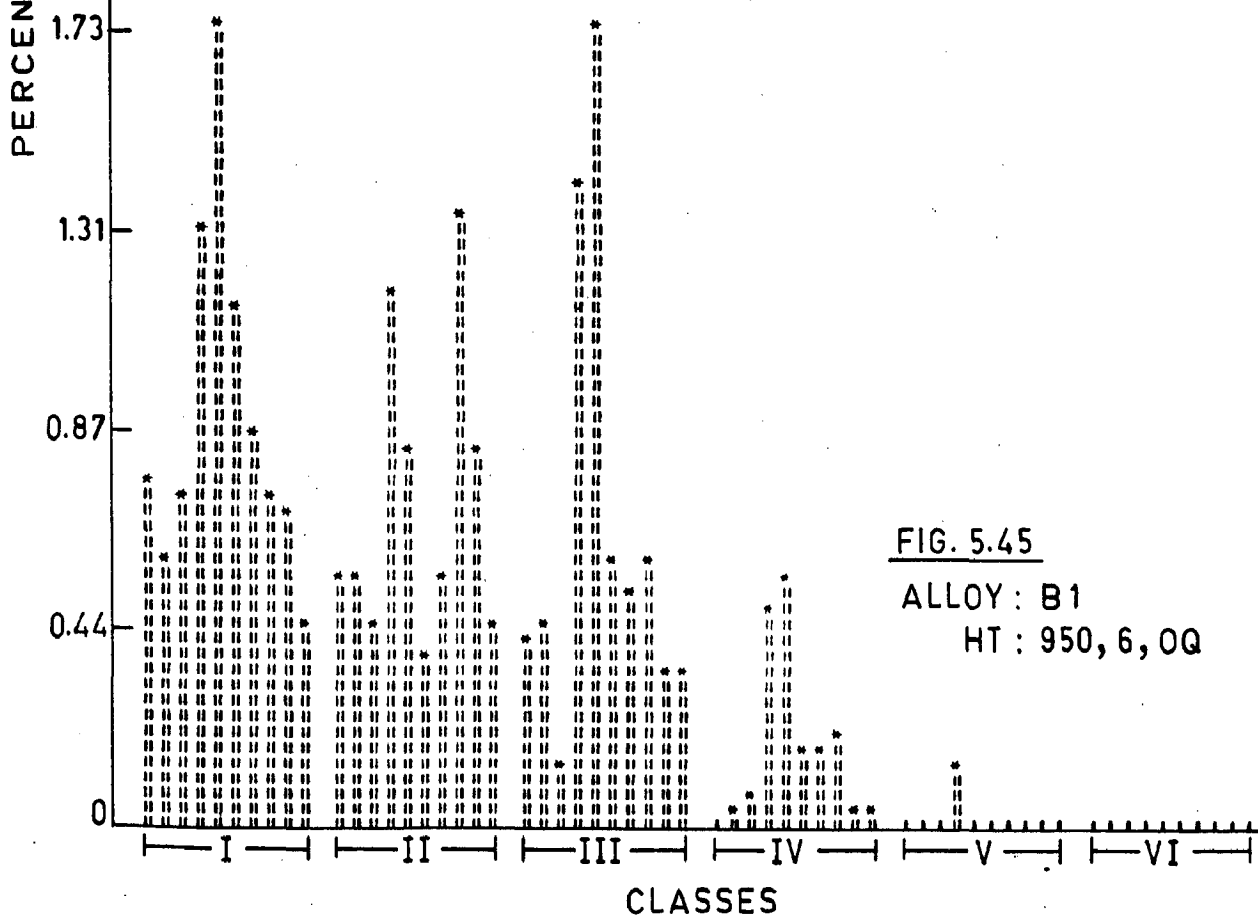
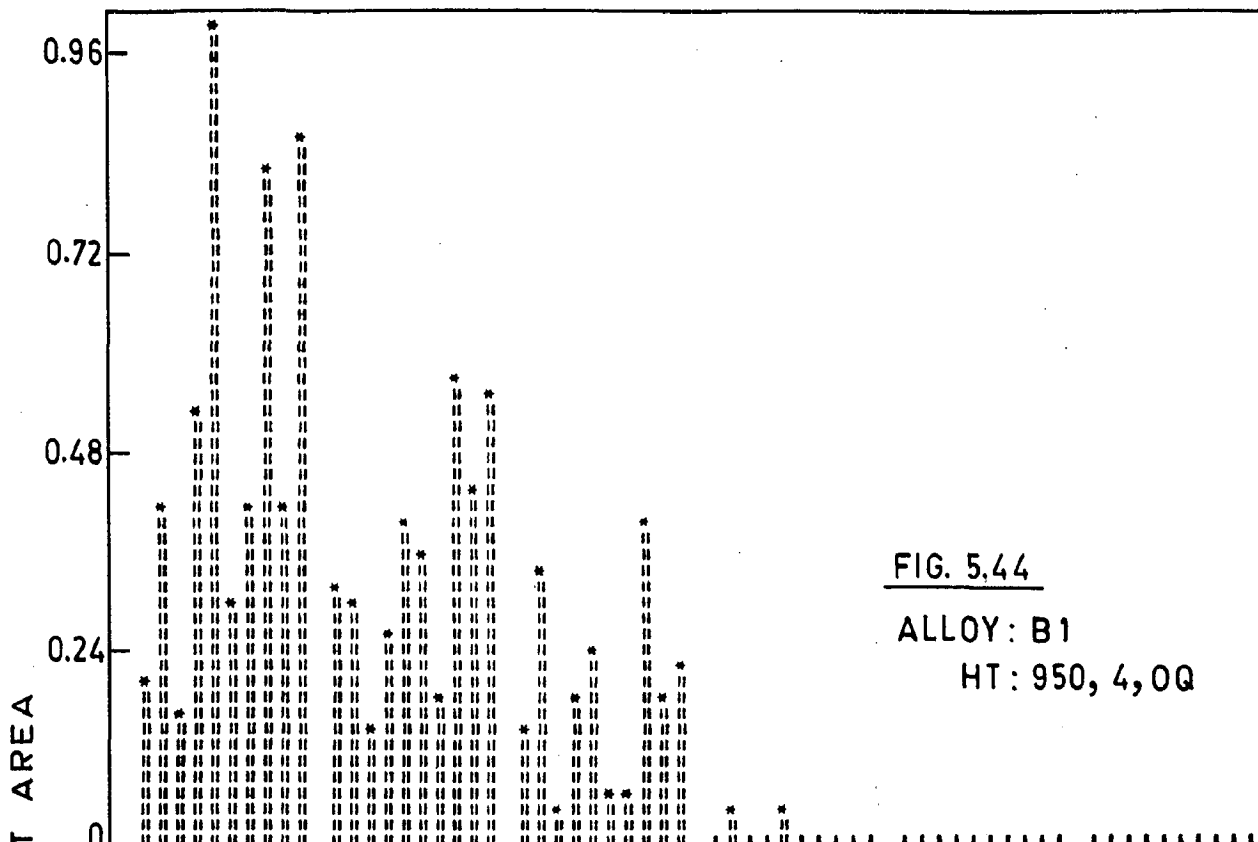


FIG. 5.41  
ALLOY : B1  
HT : 900, 6, OQ

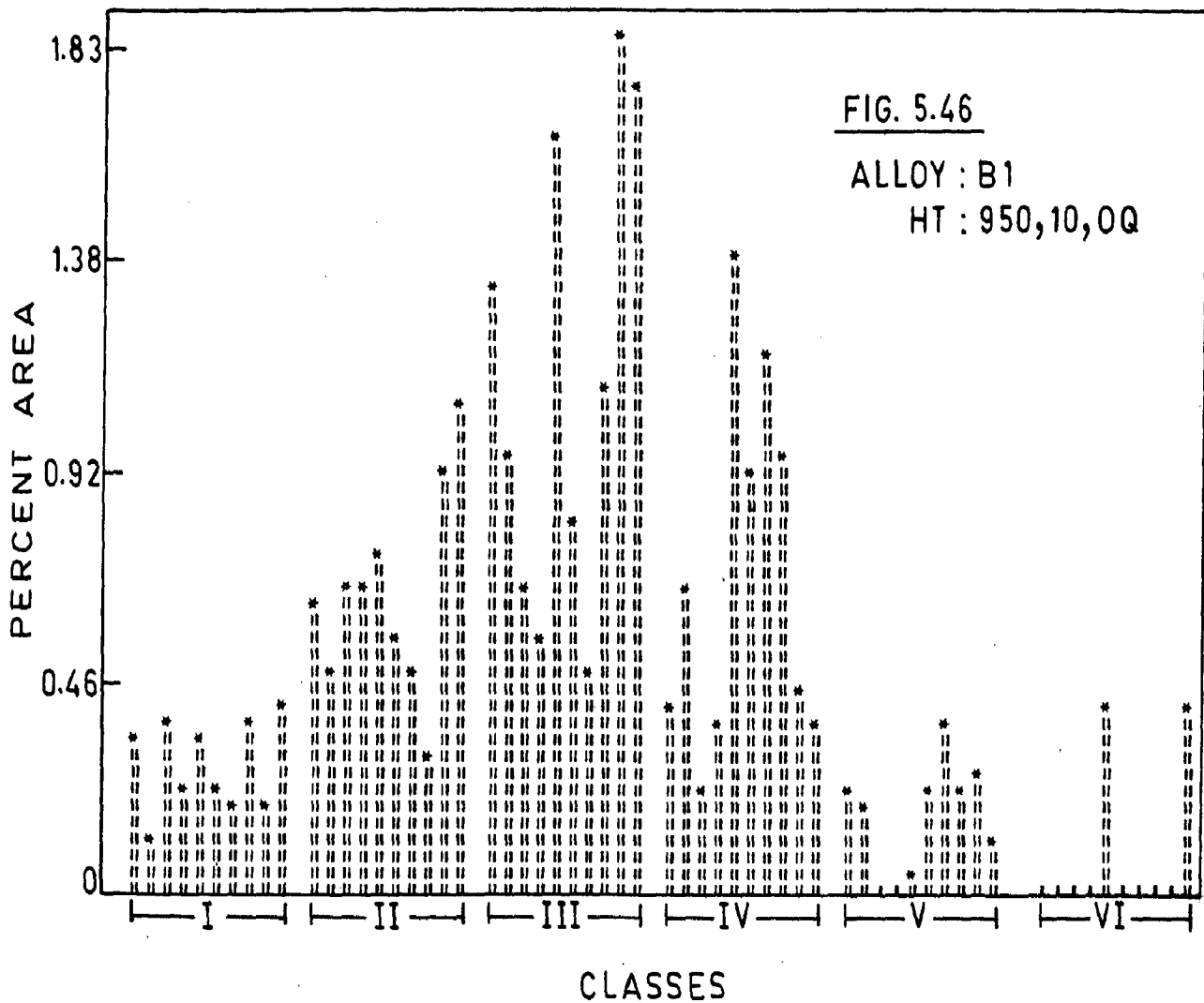
COMPOSITE HISTOGRAMS DEPICTING CLASS WISE PARTICLE-DISTRIBUTION AT TEN DIFFERENT LOCATIONS.



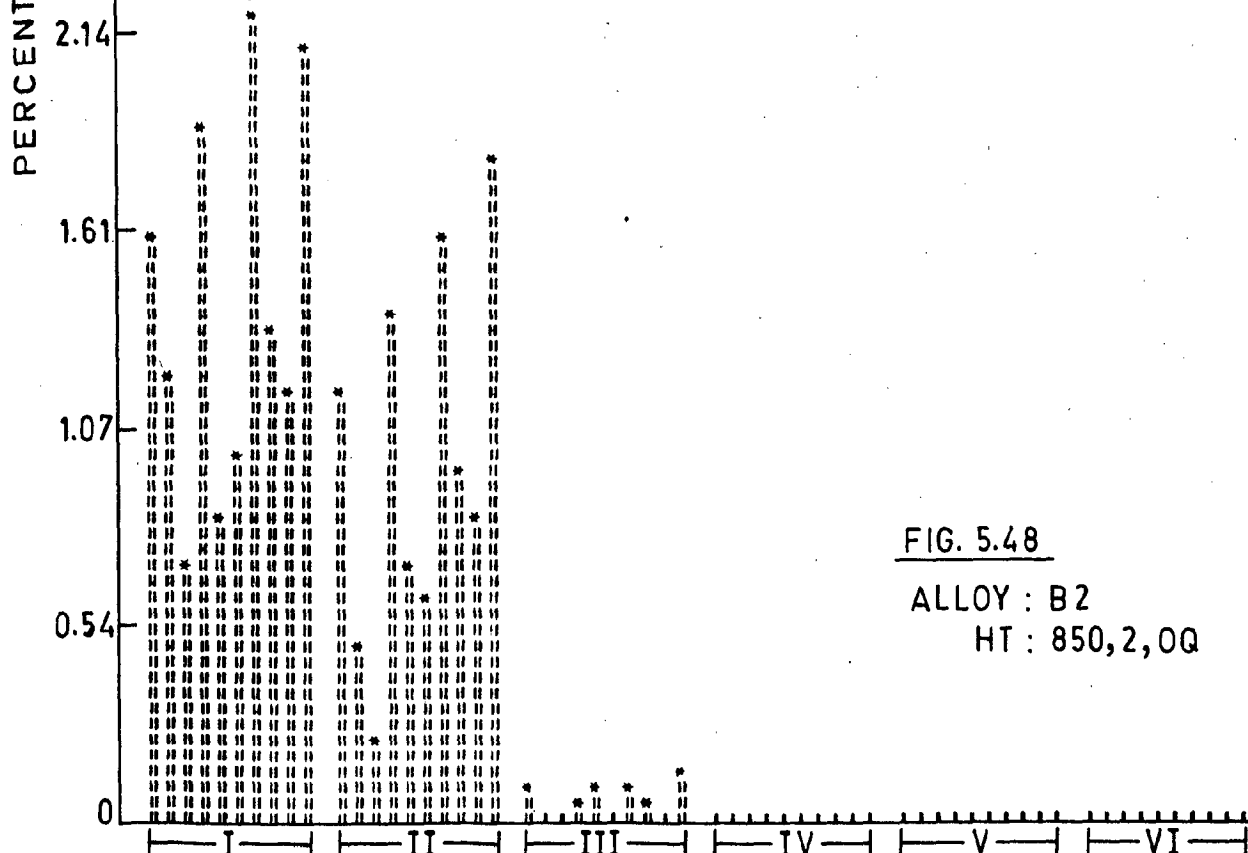
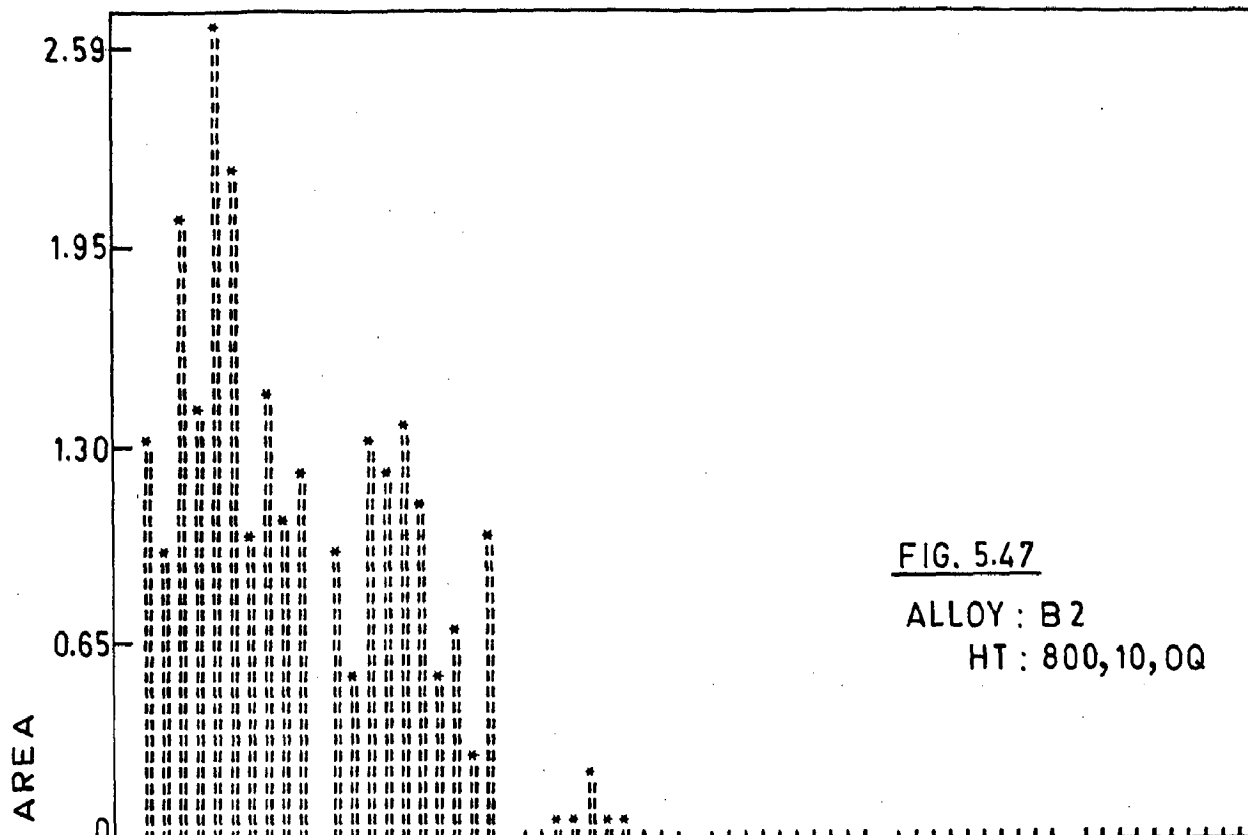
COMPOSITE HISTOGRAMS DEPICTING CLASS WISE PARTICLE-DISTRIBUTION AT TEN DIFFERENT LOCATIONS.



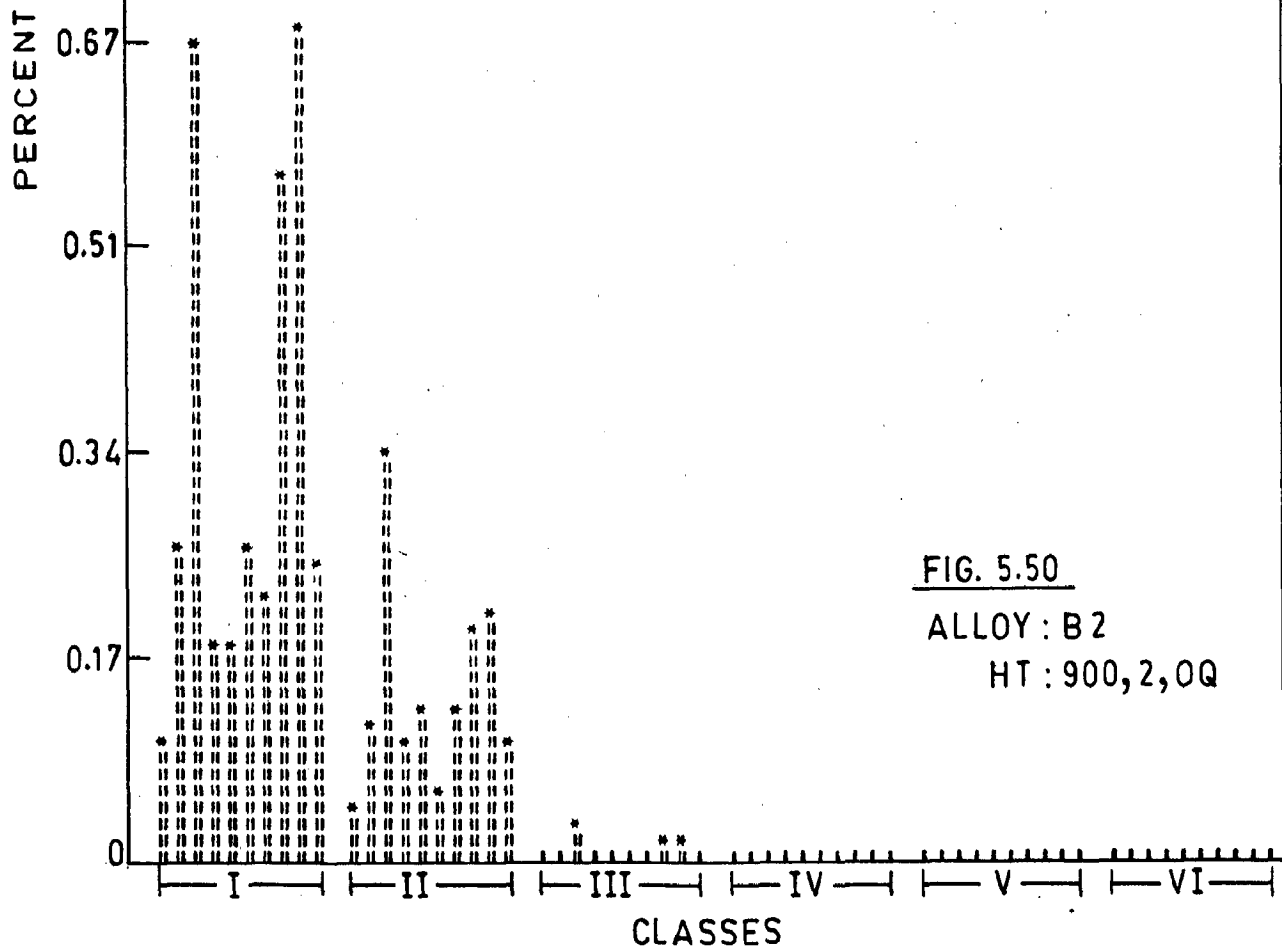
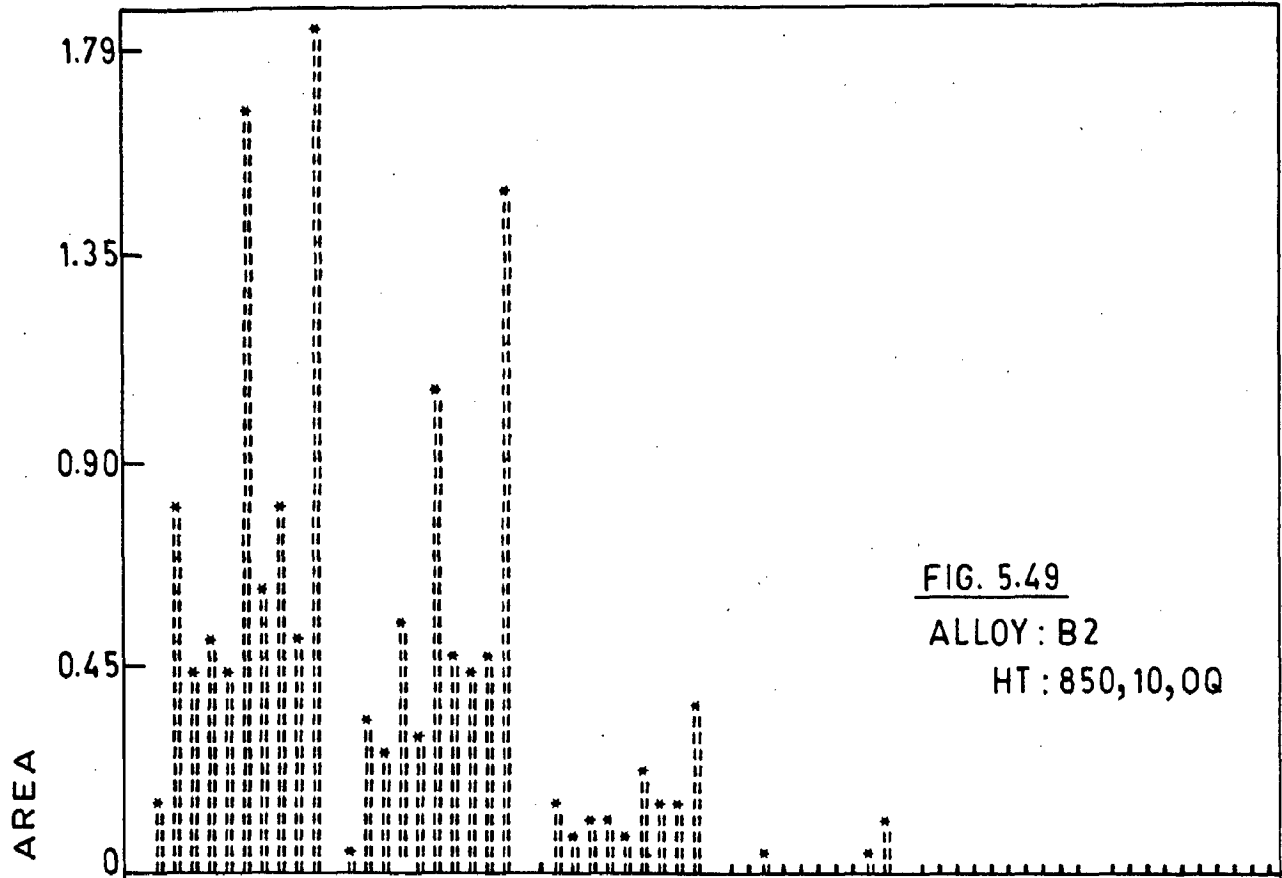
COMPOSITE HISTOGRAMS DEPICTING CLASS WISE PARTICLE-DISTRIBUTION AT TEN DIFFERENT LOCATIONS.



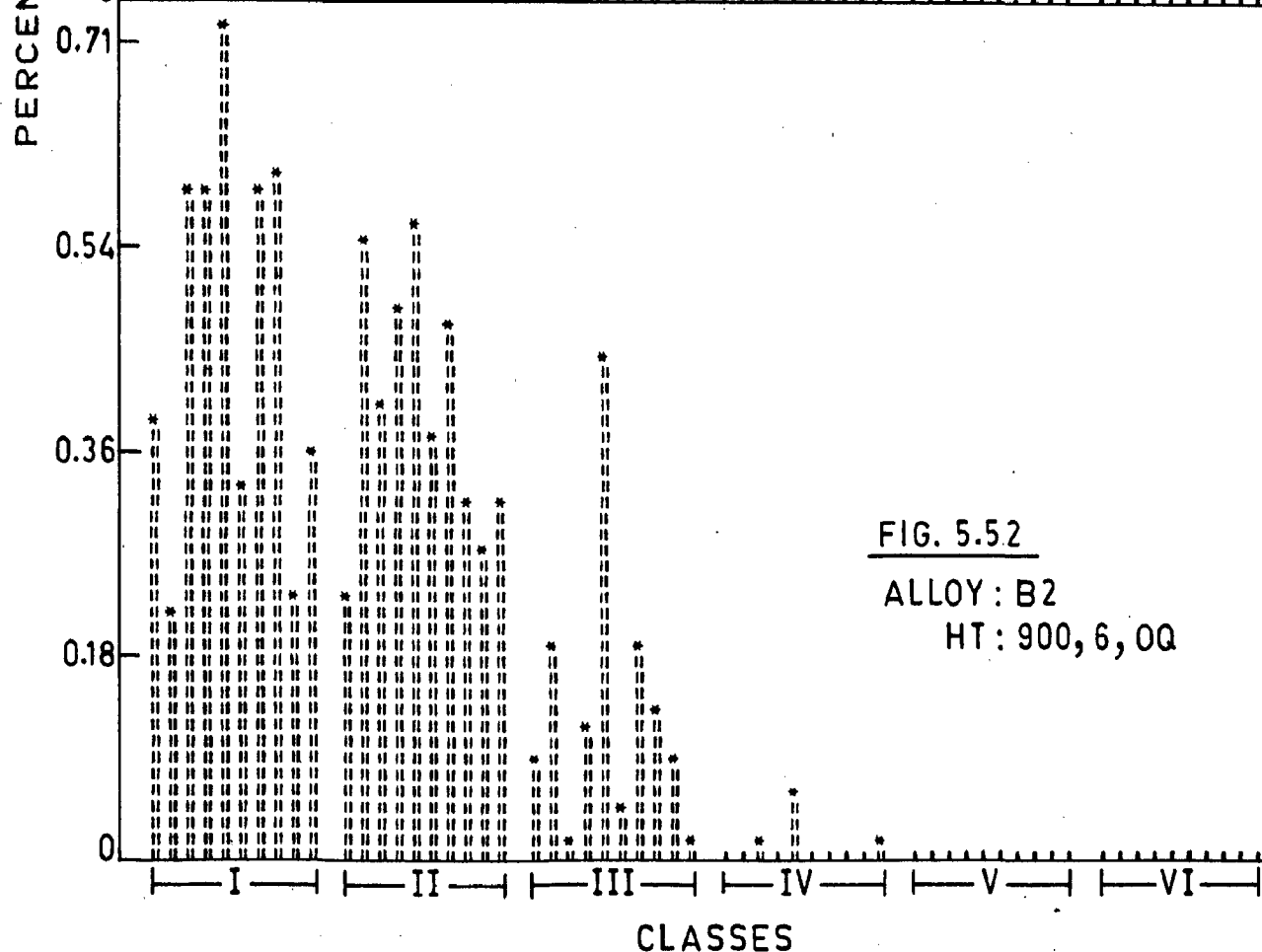
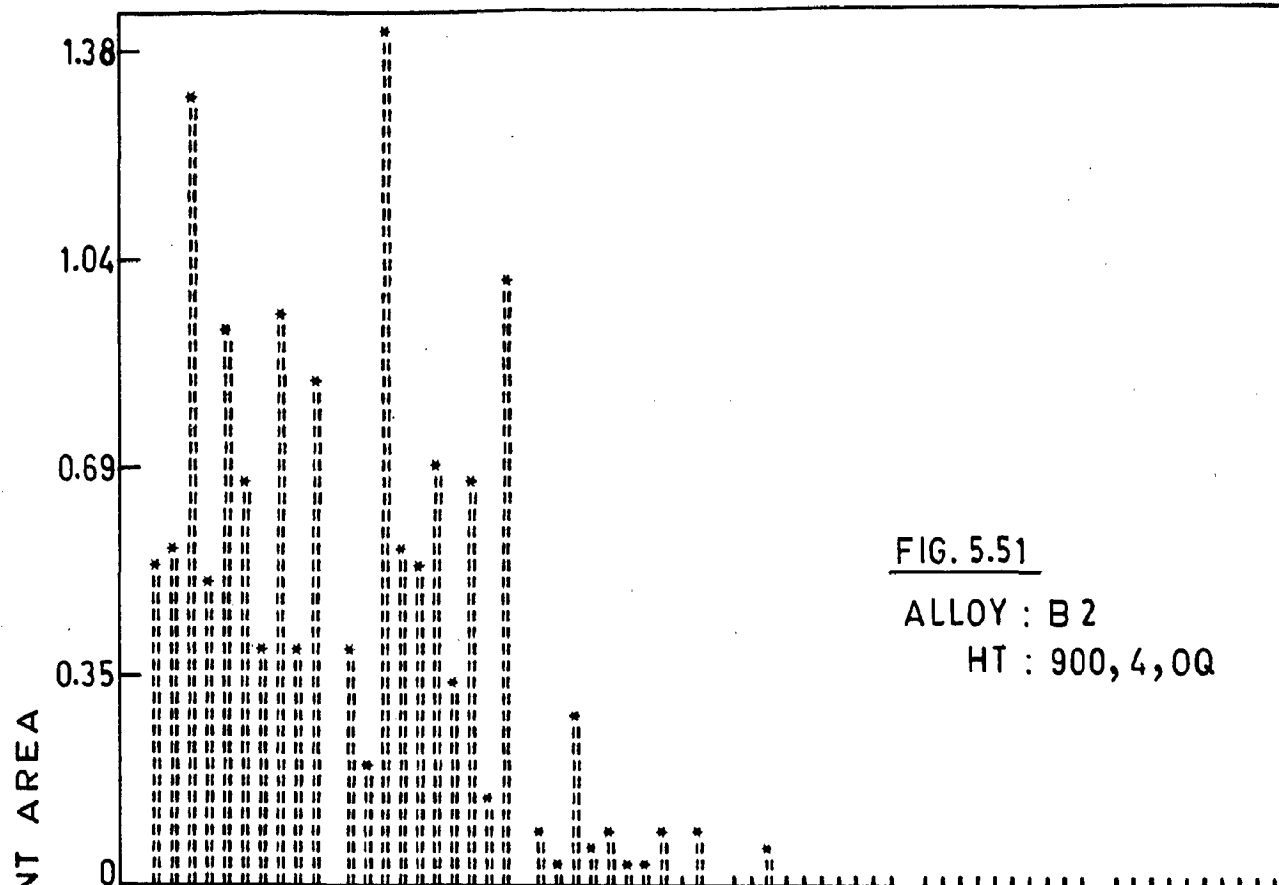
COMPOSITE HYSTOGRAMS DEPICTING CLASS WISE PARTICLE-DISTRIBUTION AT TEN DIFFERENT LOCATIONS.



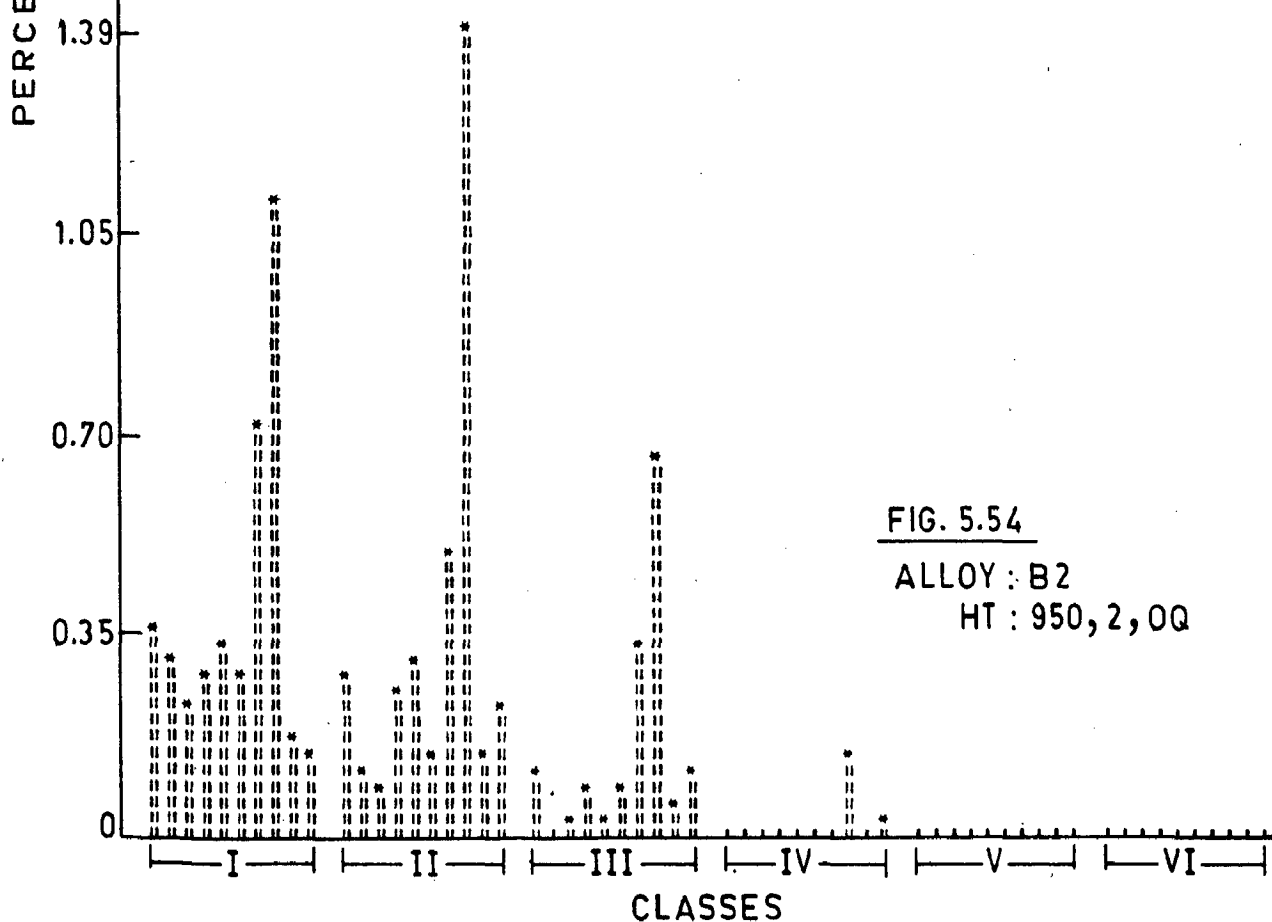
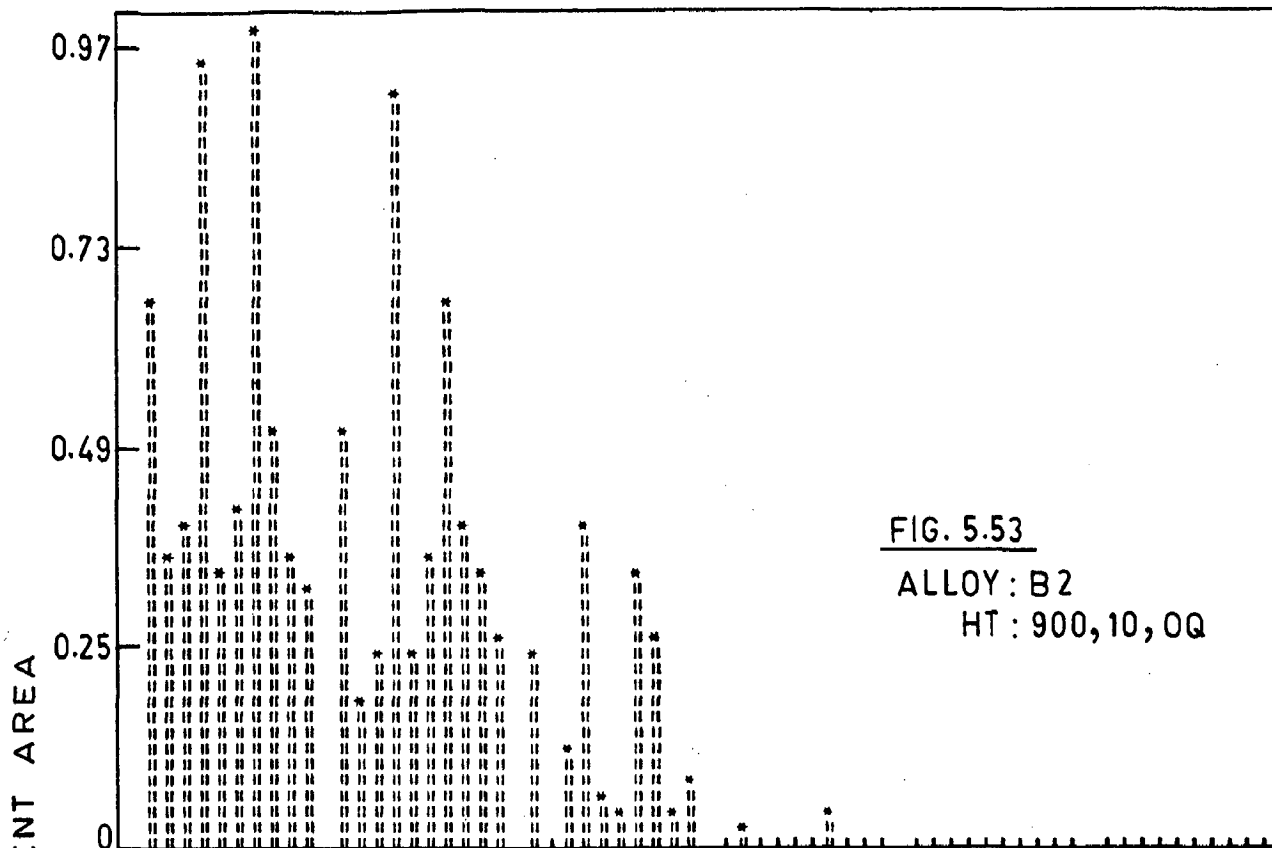
COMPOSITE HISTOGRAMS DEPICTING CLASS WISE PARTICLE - DISTRIBUTION AT TEN DIFFERENT LOCATIONS.



COMPOSITE HYSTOGRAMS DEPICTING CLASS WISE PARTICLE-DISTRIBUTION AT TEN DIFFERENT LOCATIONS.

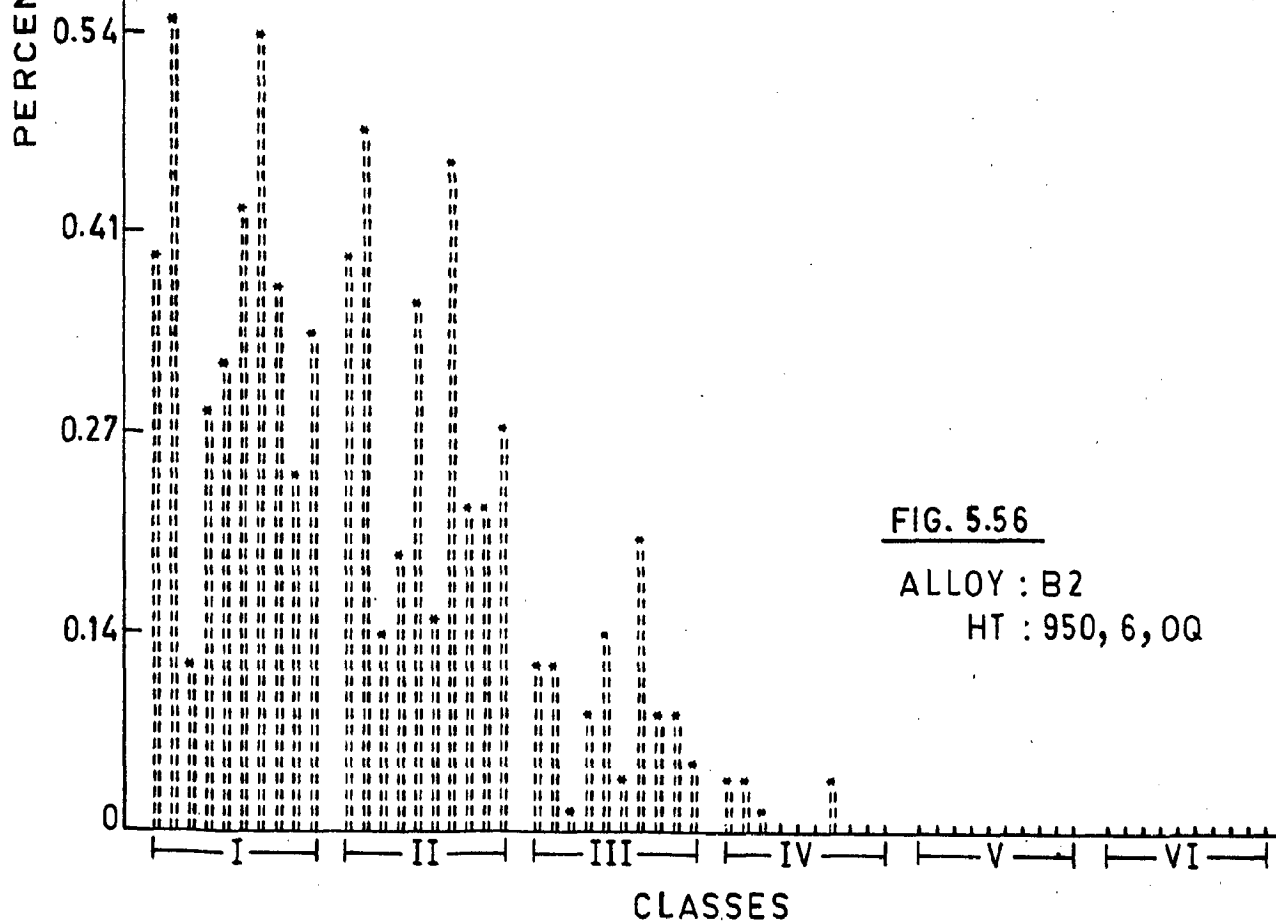
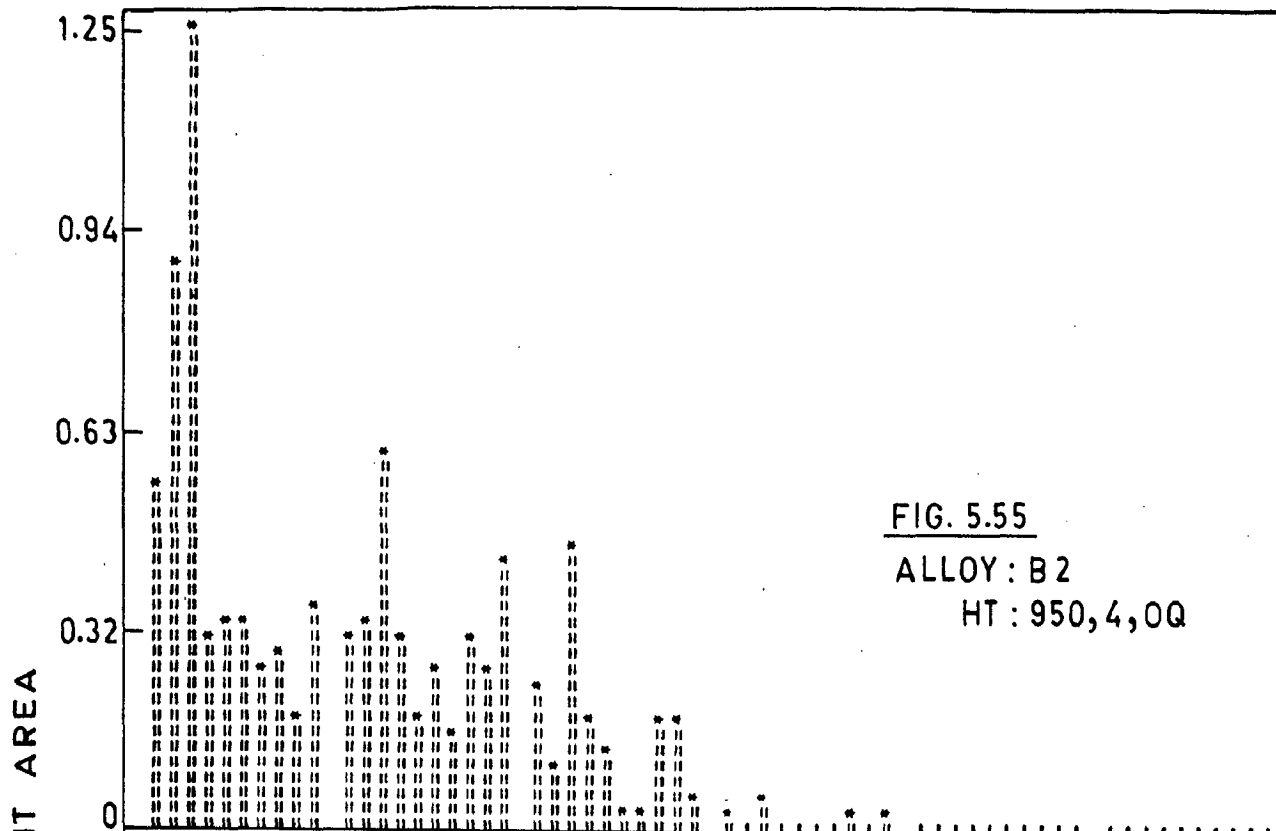


COMPOSITE HISTOGRAMS DEPICTING CLASS WISE PARTICLE - DISTRIBUTION AT TEN DIFFERENT LOCATIONS.

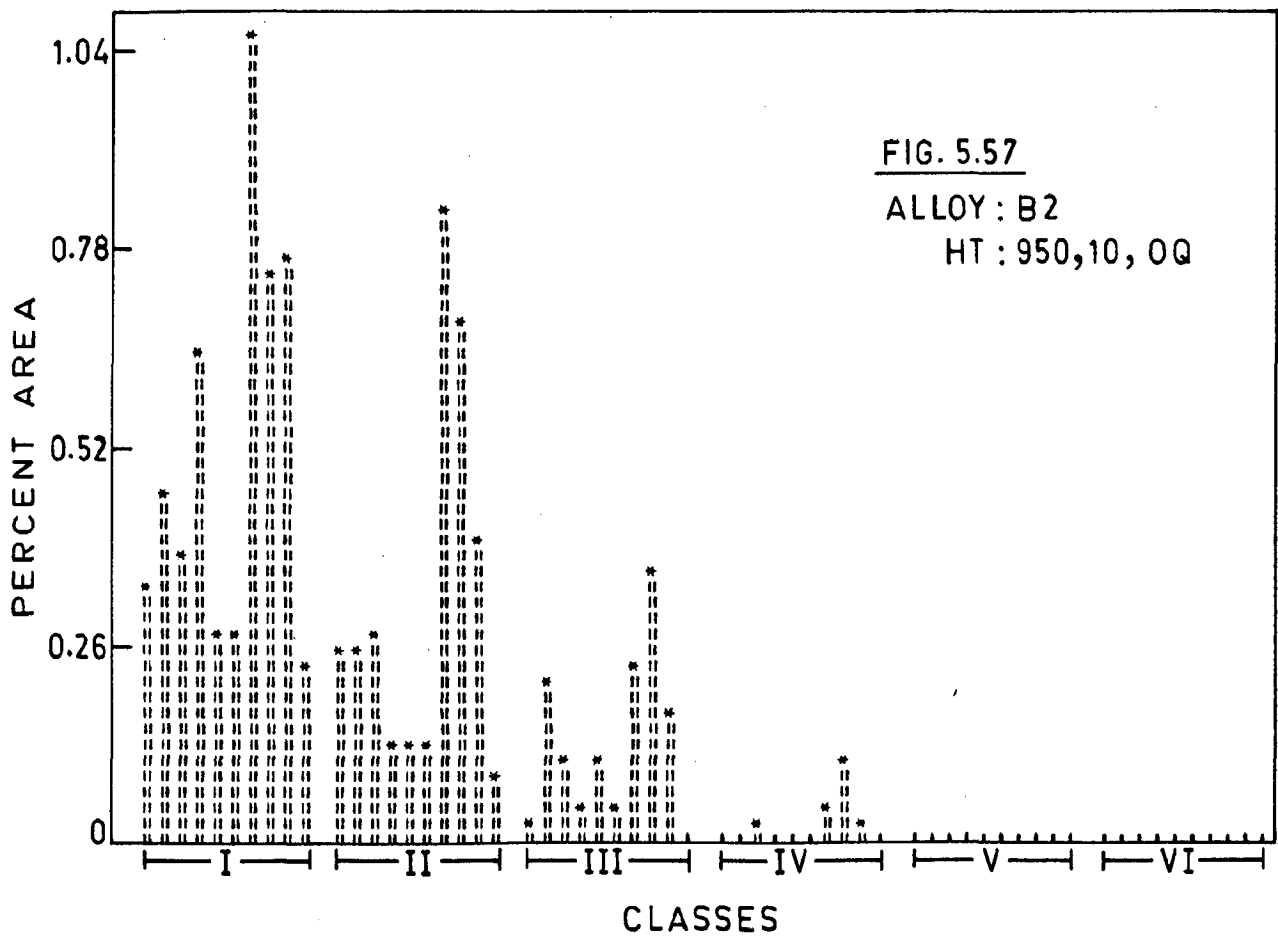


COMPOSITE HISTOGRAMS DEPICTING CLASS WISE PARTICLE-DISTRIBUTION AT TEN DIFFERENT LOCATIONS.

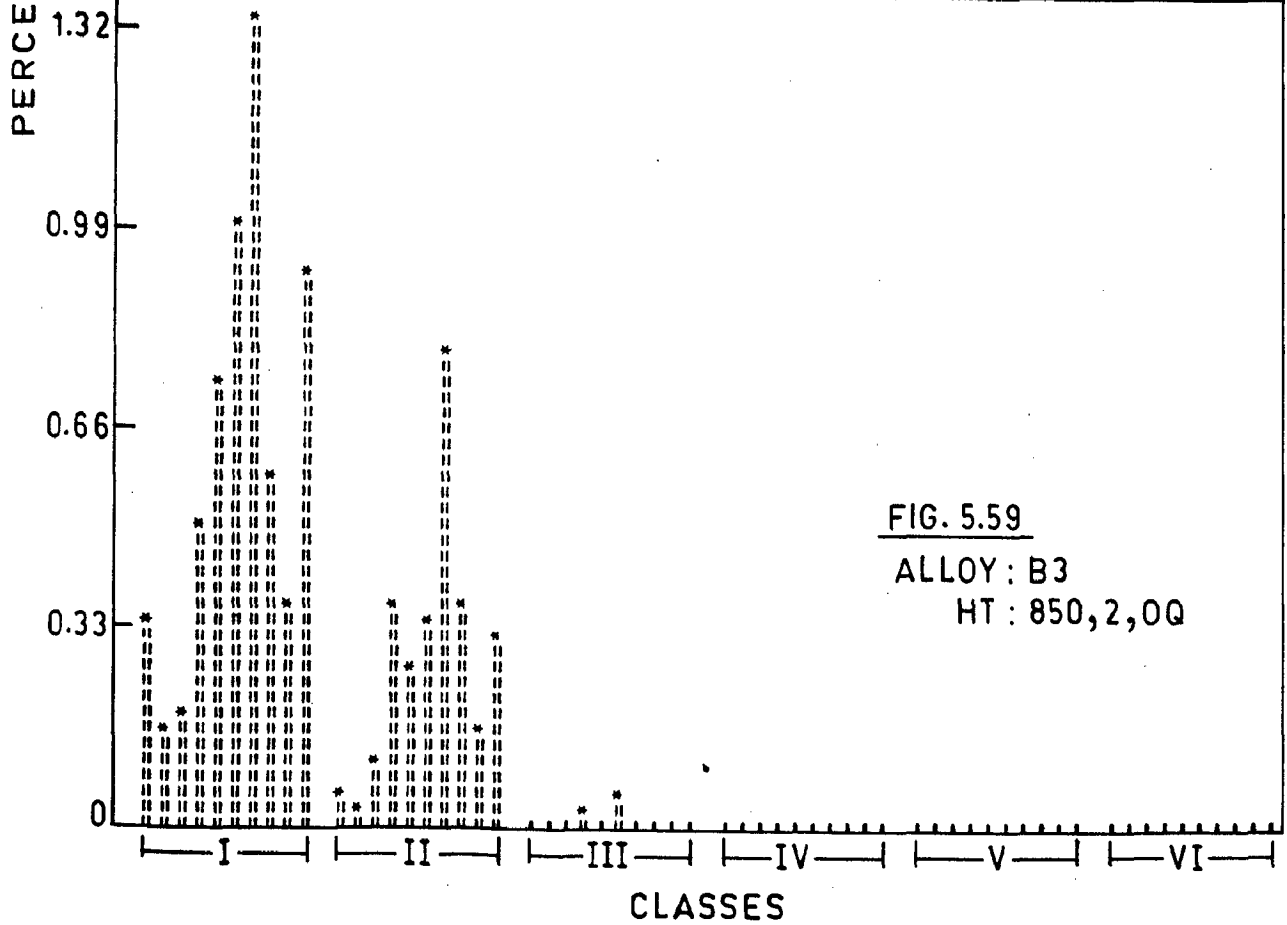
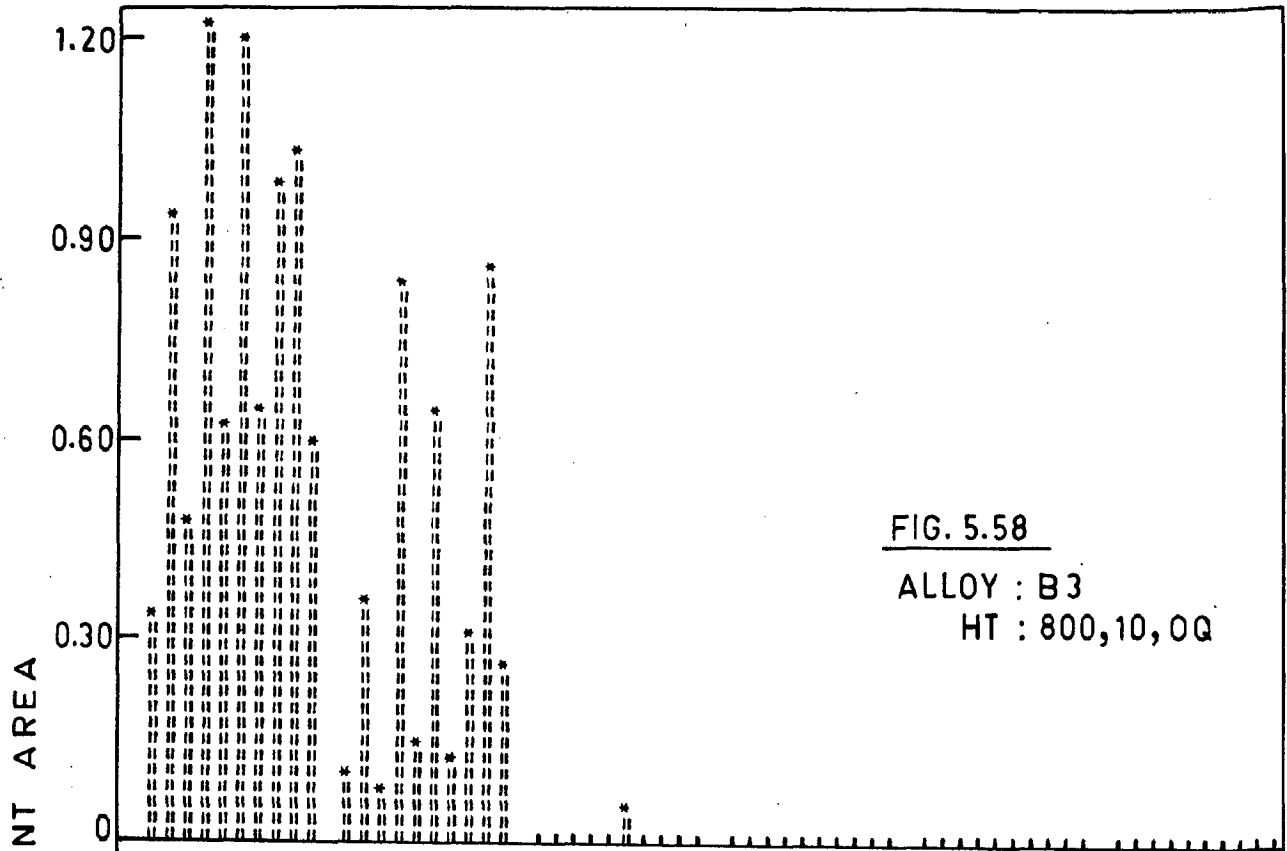




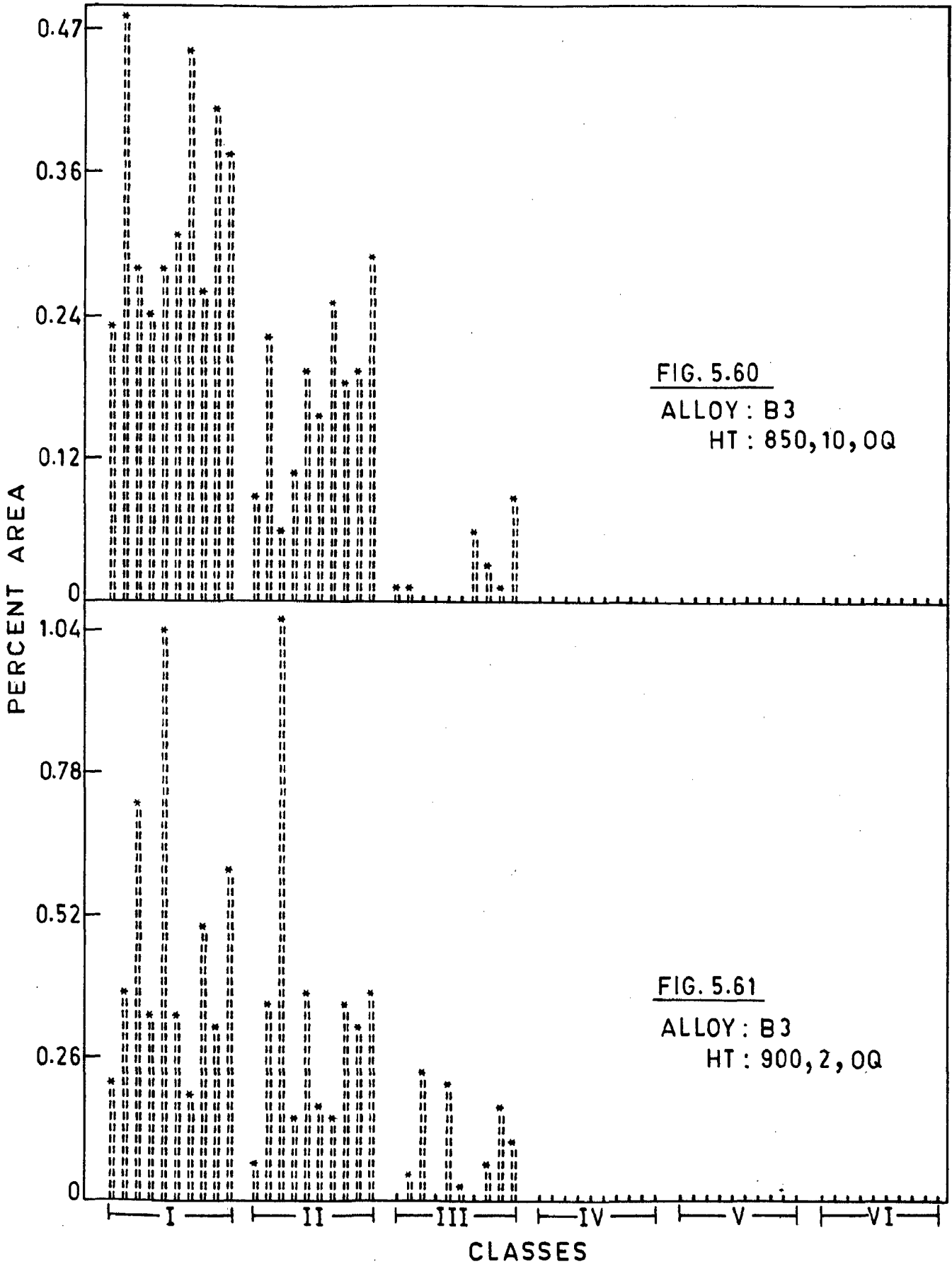
COMPOSITE HYSTOGRAMS DEPICTING CLASS WISE PARTICLE-DISTRIBUTION AT TEN DIFFERENT LOCATIONS.



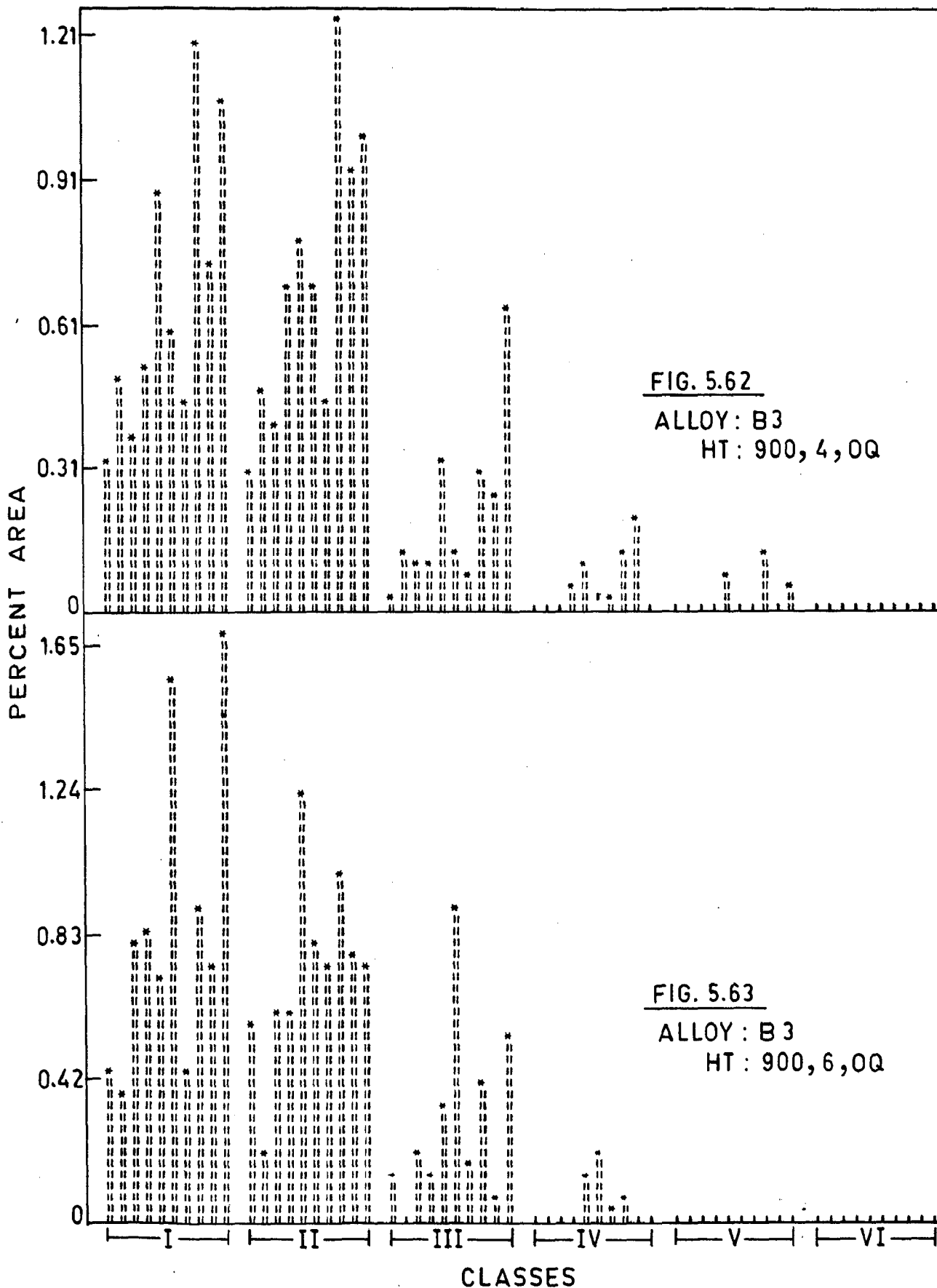
COMPOSITE HYSTOGRAMS DEPICTING CLASS WISE PARTICLE-DISTRIBUTION AT TEN DIFFERENT LOCATIONS.



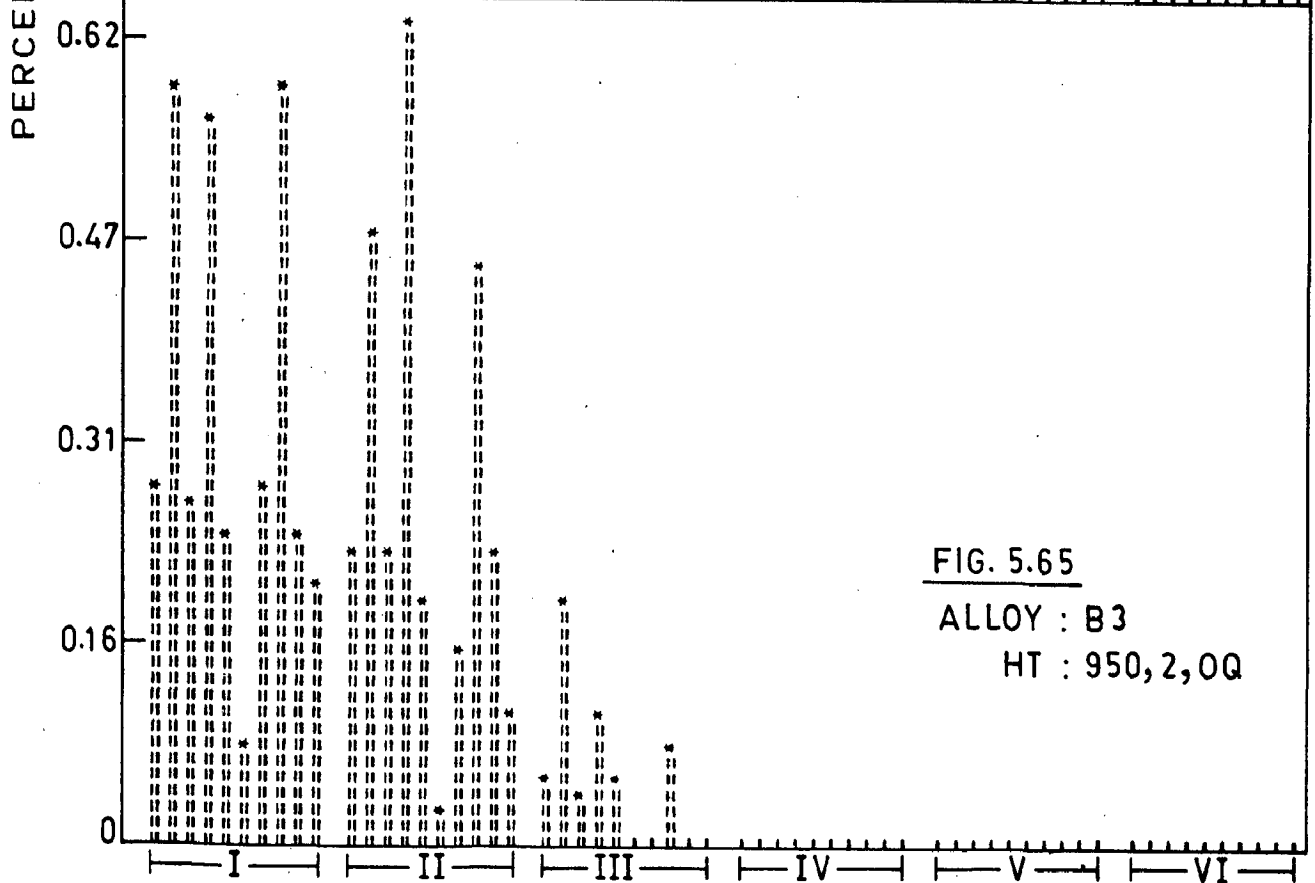
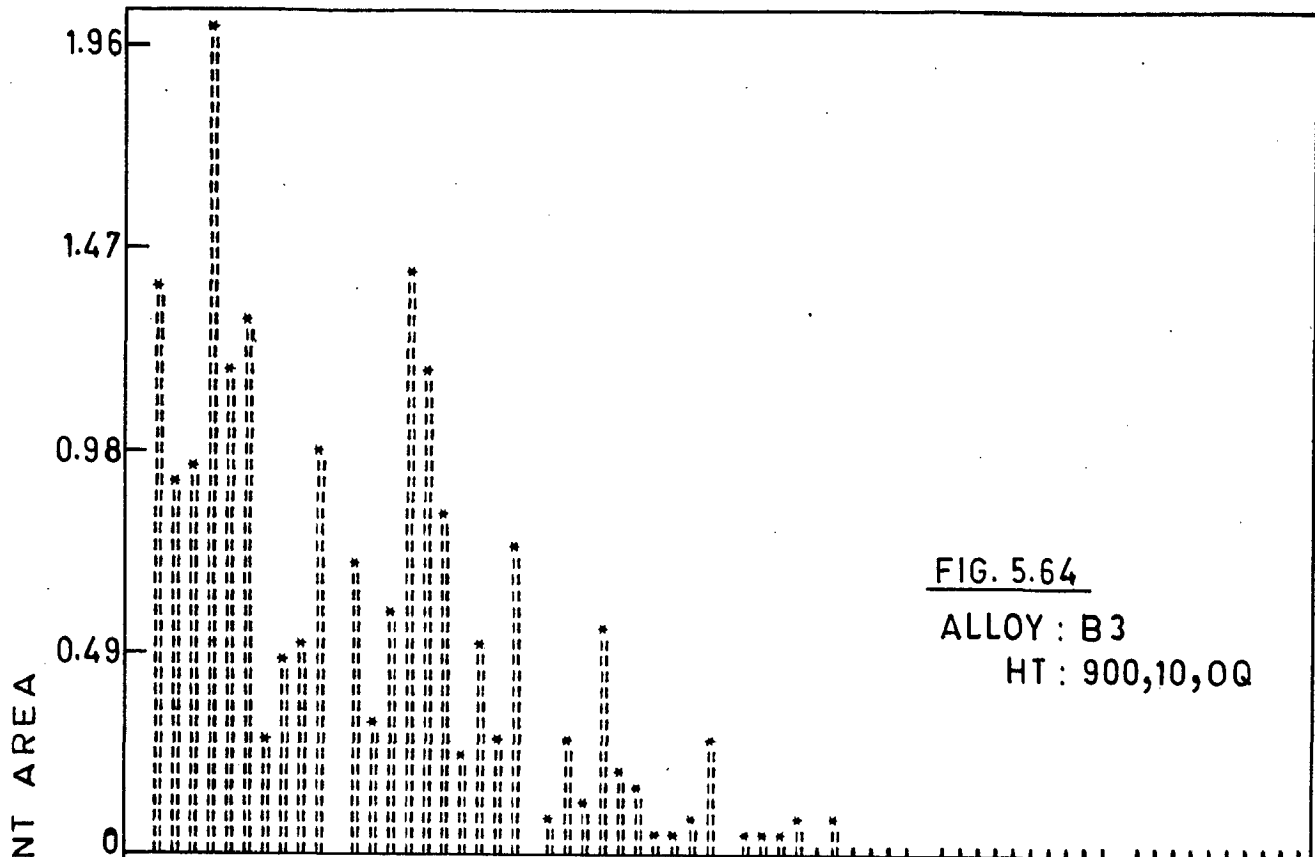
COMPOSITE HISTOGRAMS DEPICTING CLASS WISE PARTICLE-DISTRIBUTION AT TEN DIFFERENT LOCATIONS.



COMPOSITE HISTOGRAMS DEPICTING CLASS WISE PARTICLE - DISTRIBUTION AT TEN DIFFERENT LOCATIONS.

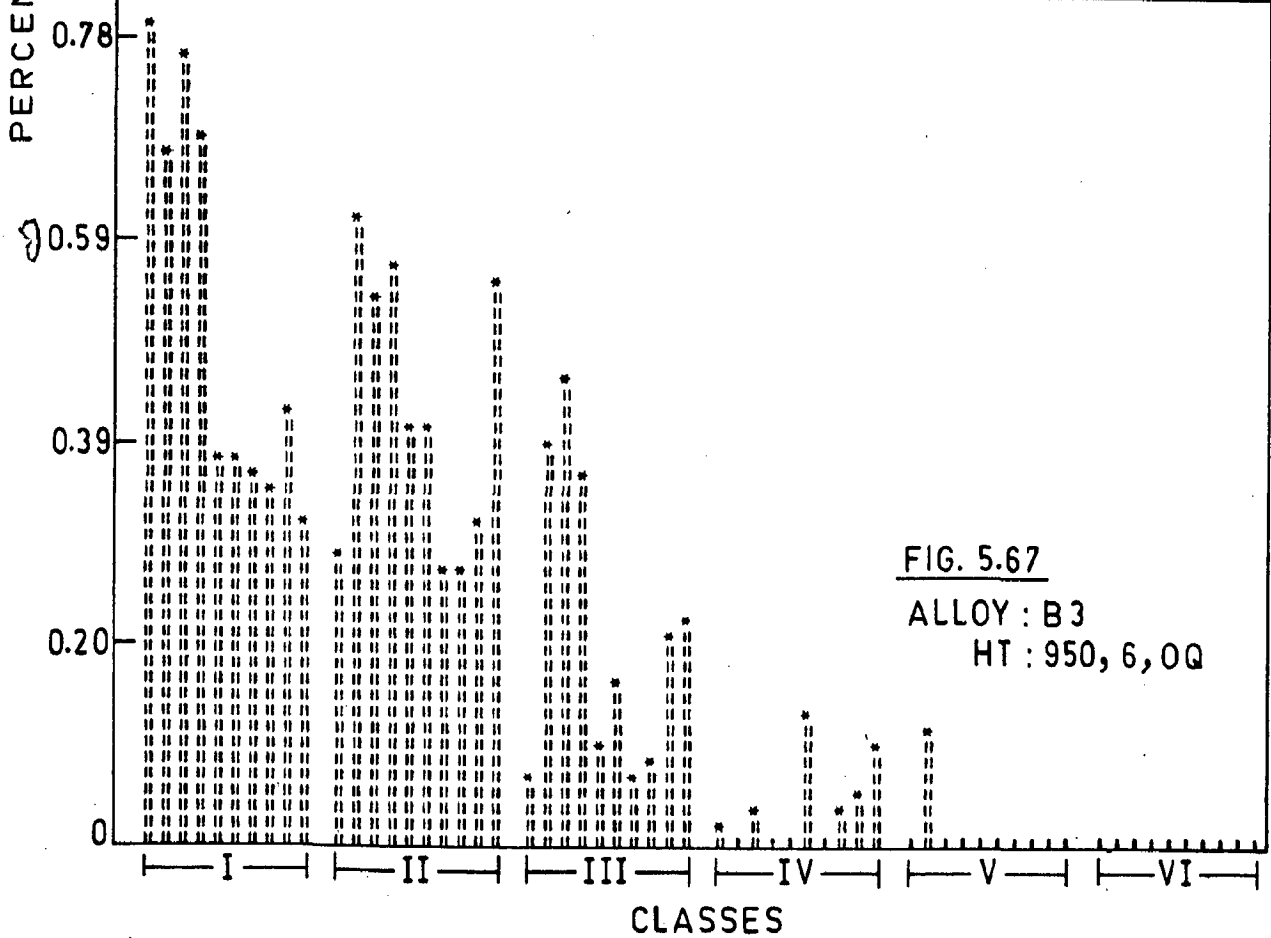
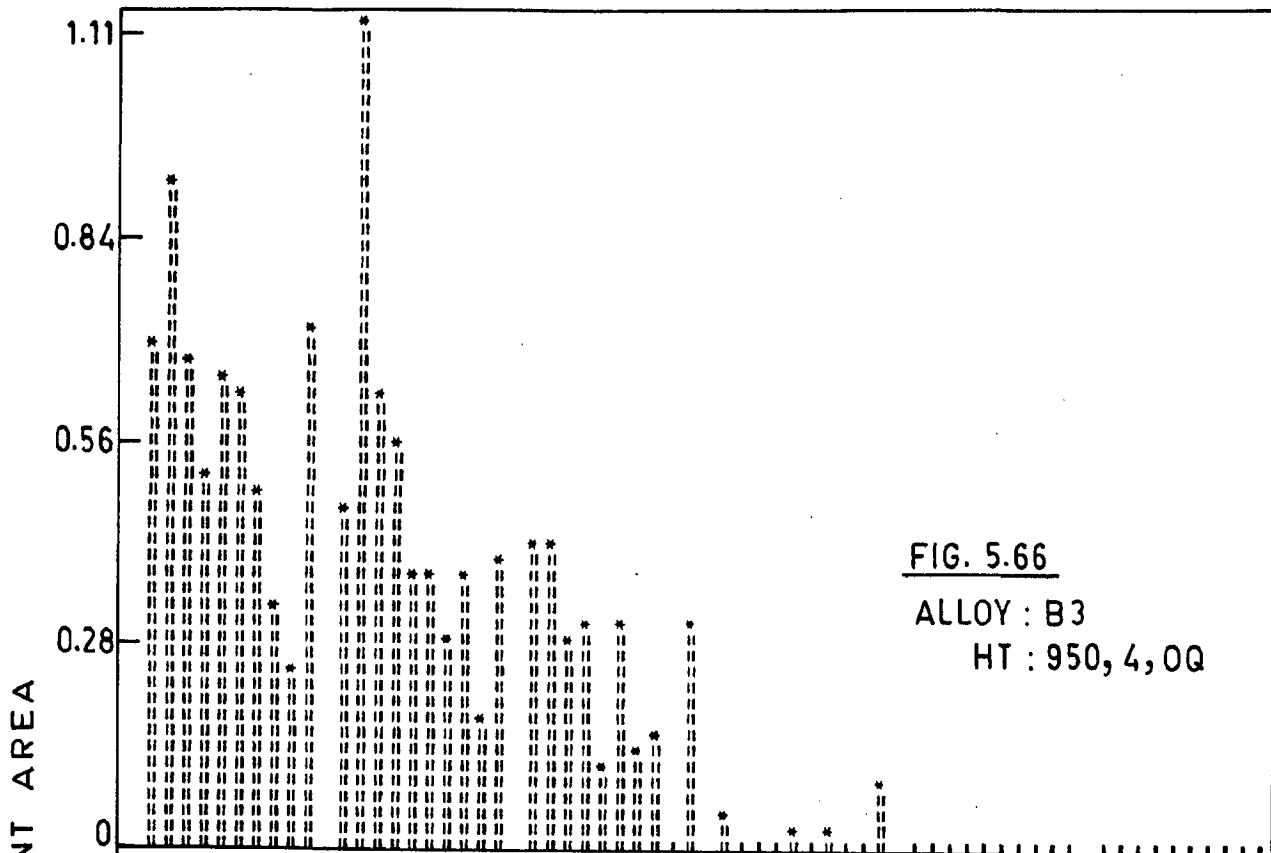


COMPOSITE HISTOGRAMS DEPICTING CLASS WISE PARTICLE-DISTRIBUTION AT TEN DIFFERENT LOCATIONS.

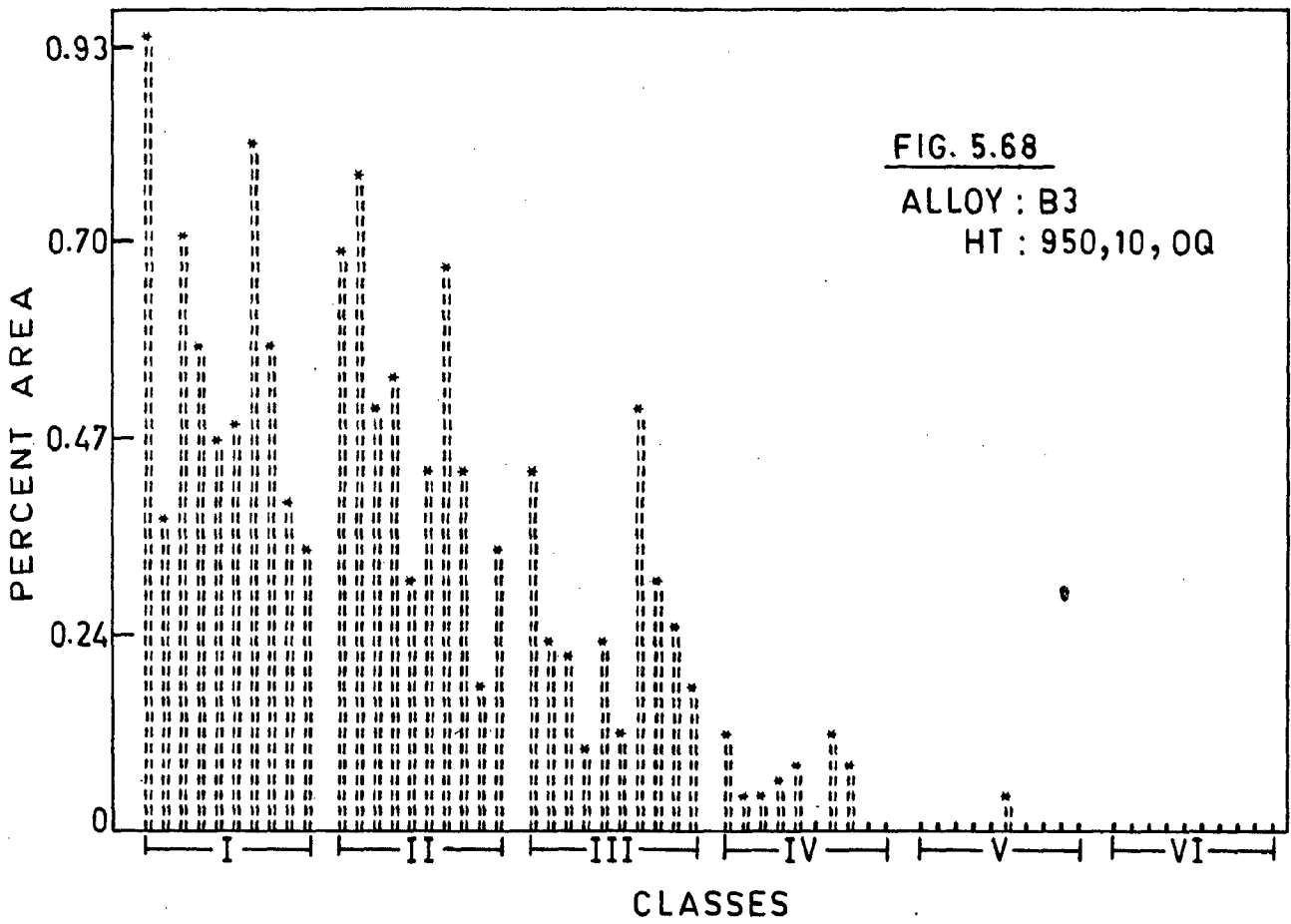


CLASSES

COMPOSITE HISTOGRAMS DEPICTING CLASS WISE PARTICLE-DISTRIBUTION AT TEN DIFFERENT LOCATIONS.

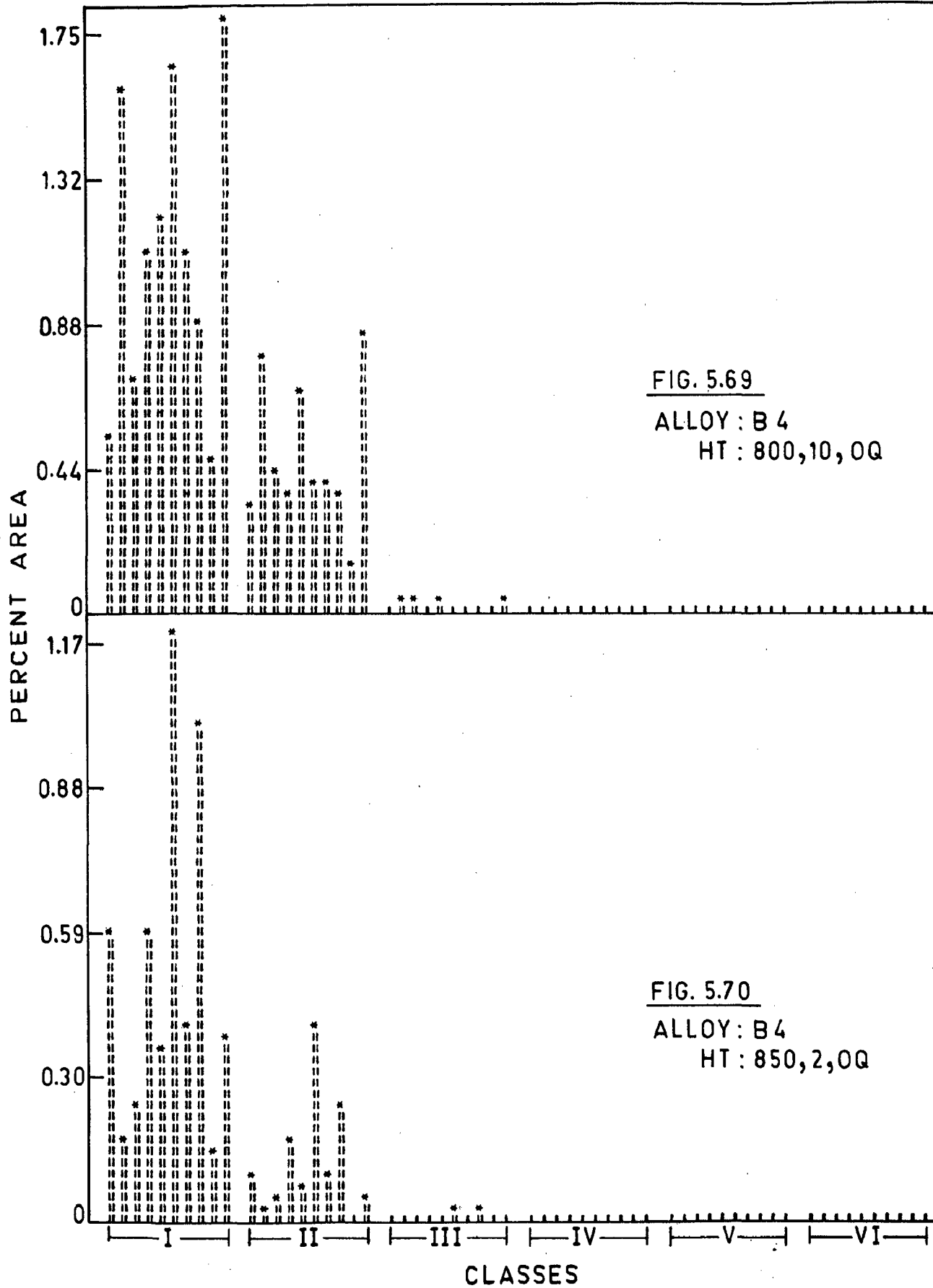


COMPOSITE HYSTOGRAMS DEPICTING CLASS WISE PARTICLE-DISTRIBUTION AT TEN DIFFERENT LOCATIONS.

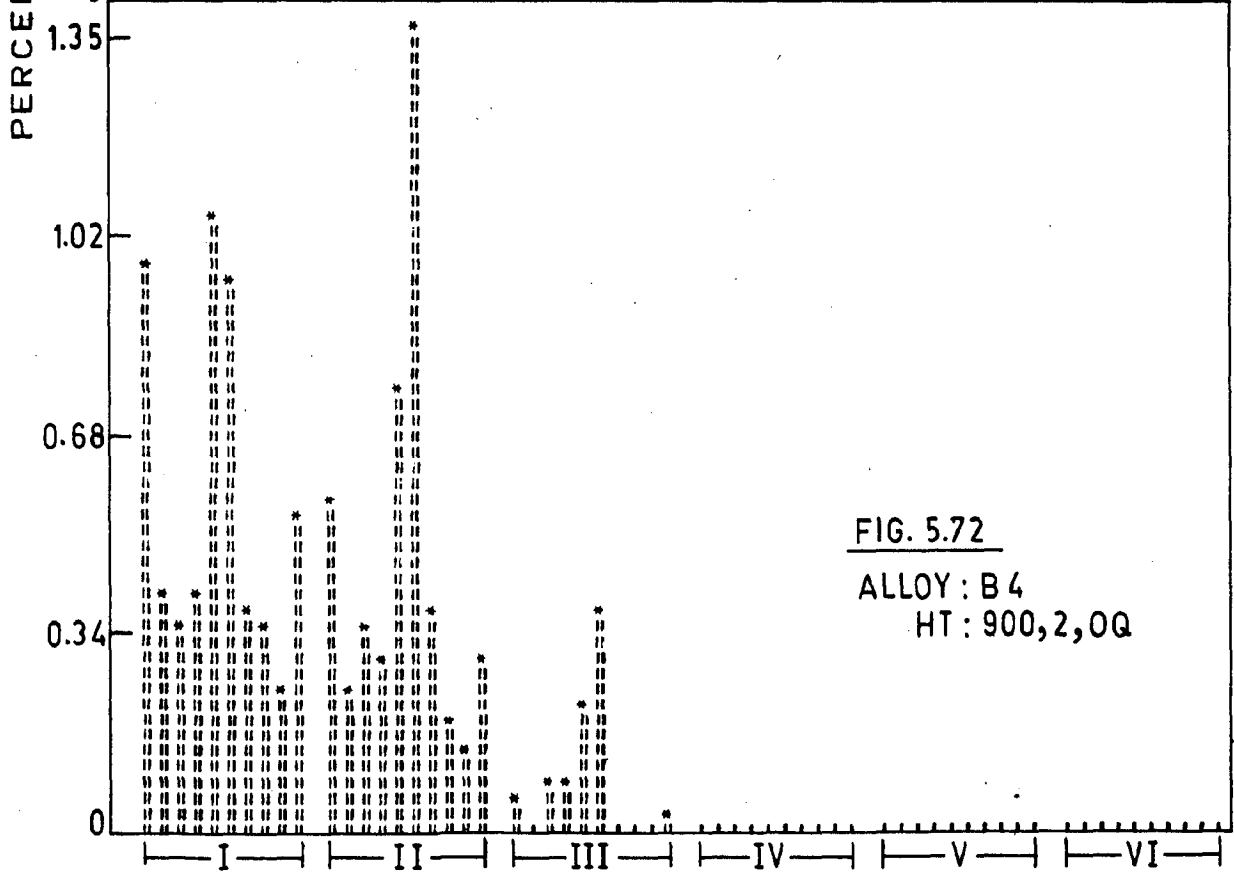
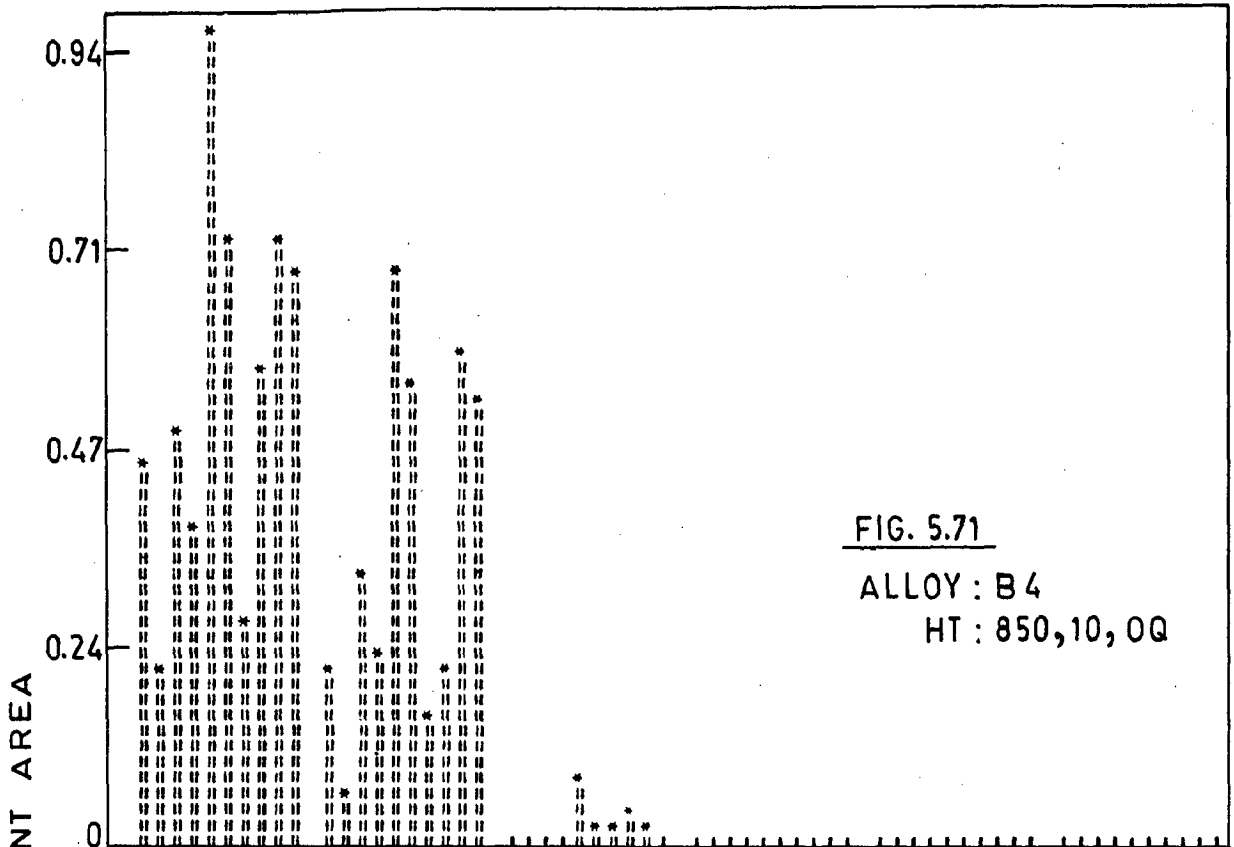


COMPOSITE HYSTOGRAMS DEPICTING CLASS WISE PARTICLE-DISTRIBUTION AT TEN DIFFERENT LOCATIONS.

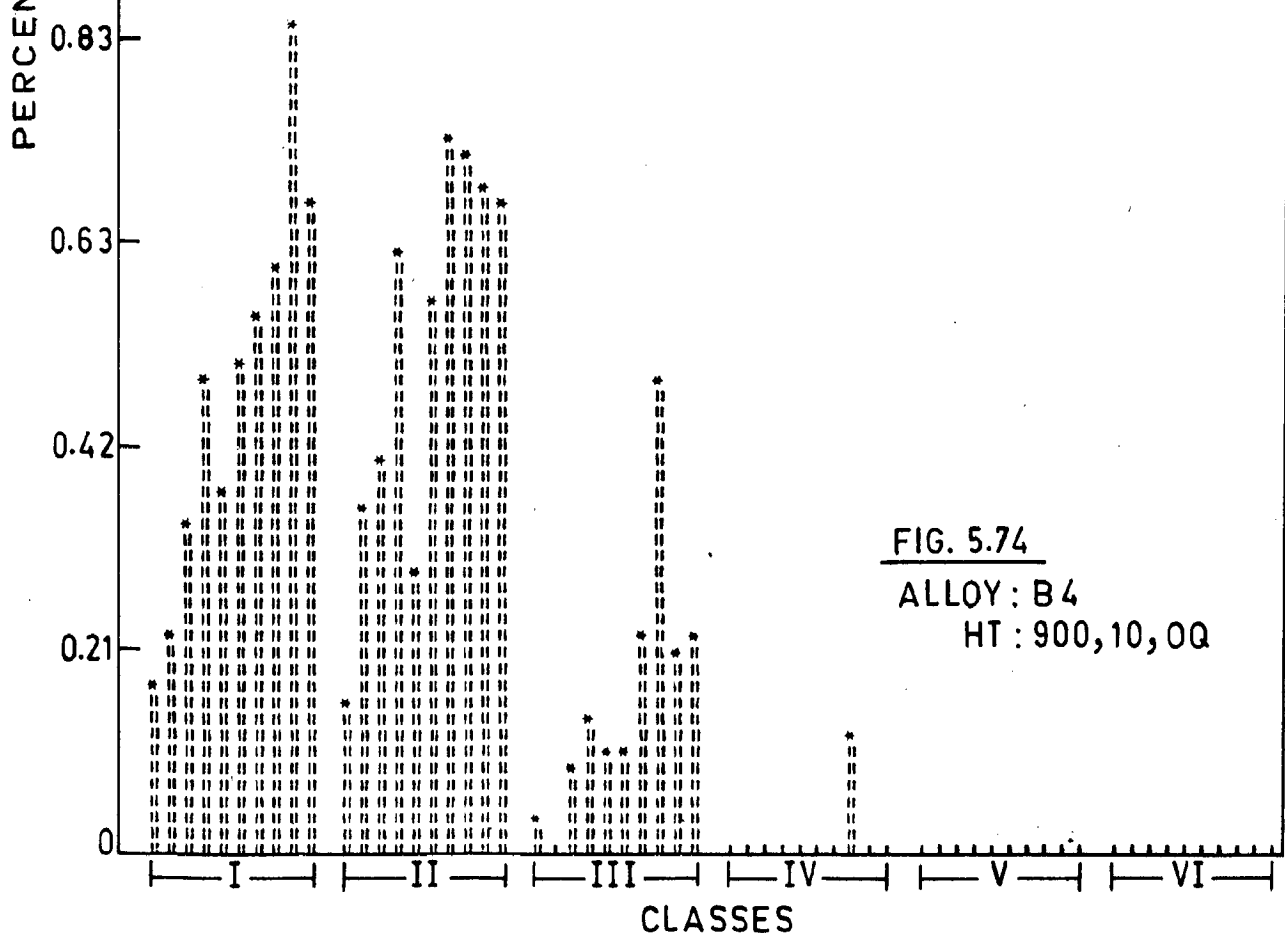
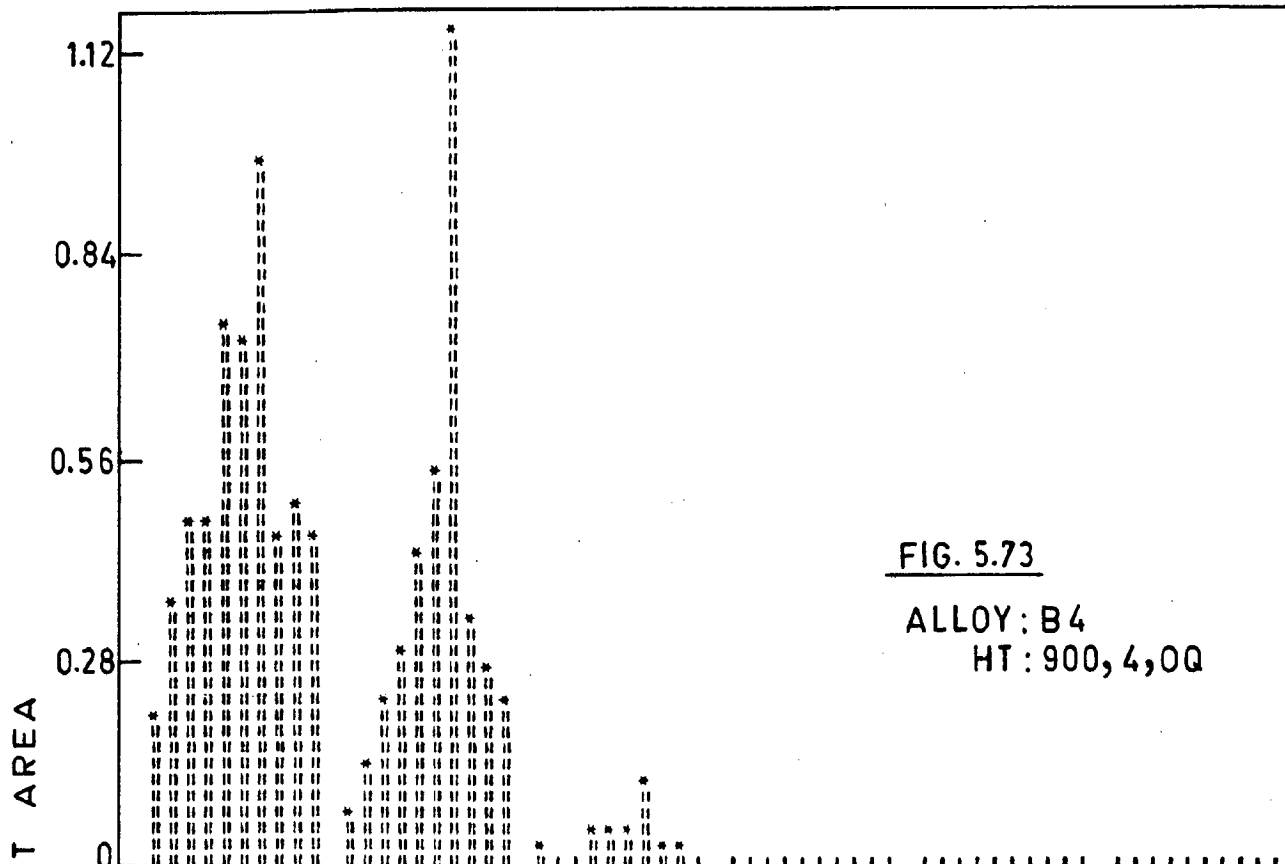




COMPOSITE HISTOGRAMS DEPICTING CLASS WISE PARTICLE-DISTRIBUTION AT TEN DIFFERENT LOCATIONS.



COMPOSITE HISTOGRAMS DEPICTING CLASS WISE PARTICLE-DISTRIBUTION AT TEN DIFFERENT LOCATIONS.



COMPOSITE HYSTOGRAMS DEPICTING CLASS WISE PARTICLE-DISTRIBUTION AT TEN DIFFERENT LOCATIONS.

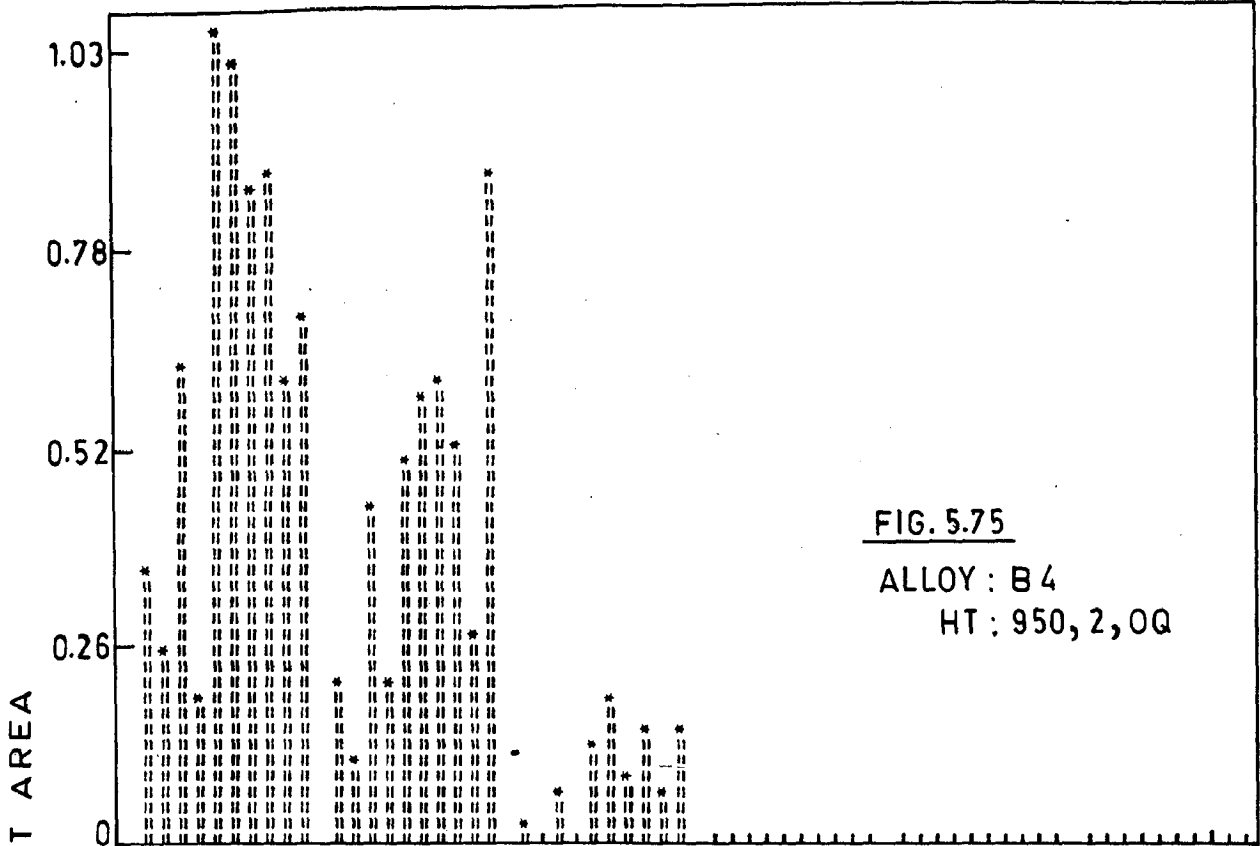


FIG. 5.75

ALLOY : B 4

HT : 950, 2, 0Q

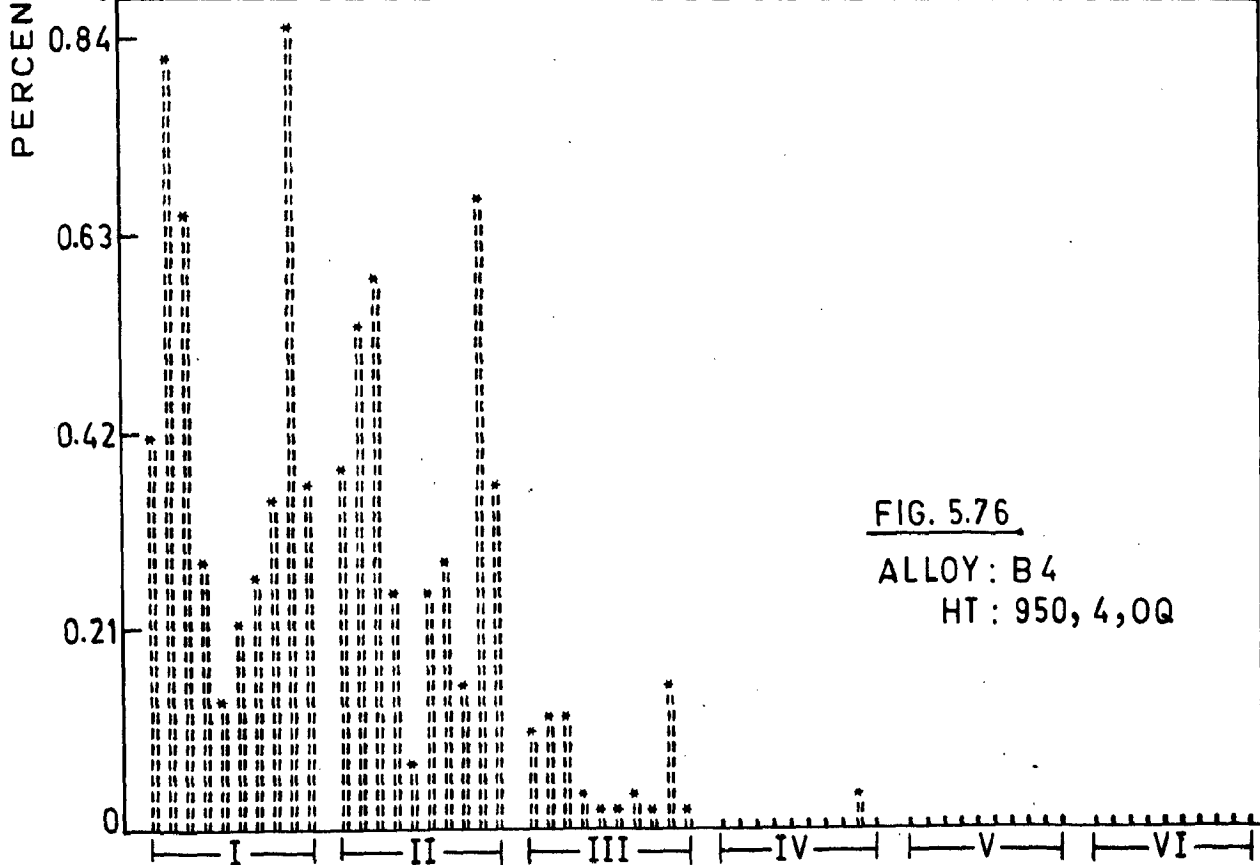


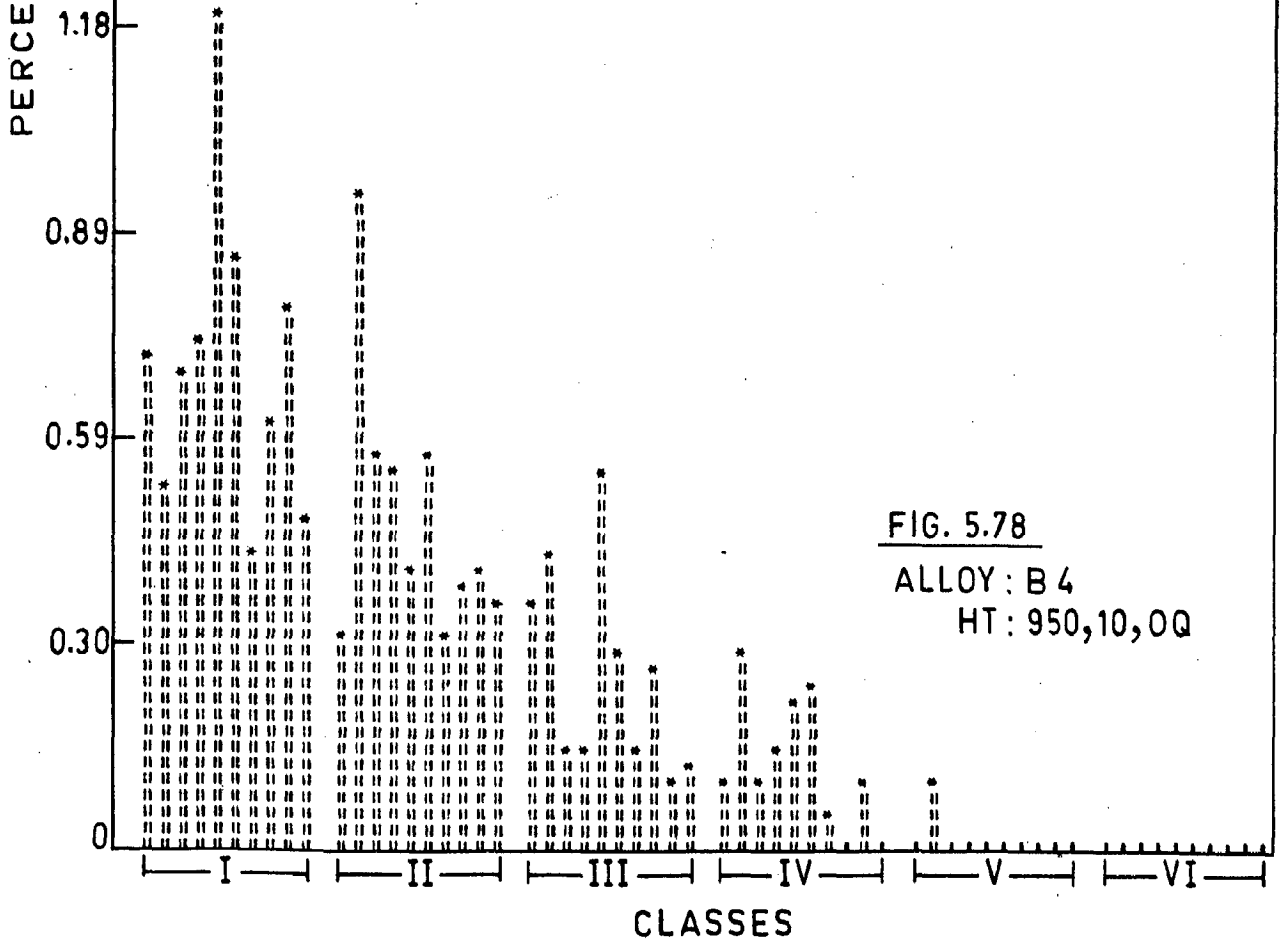
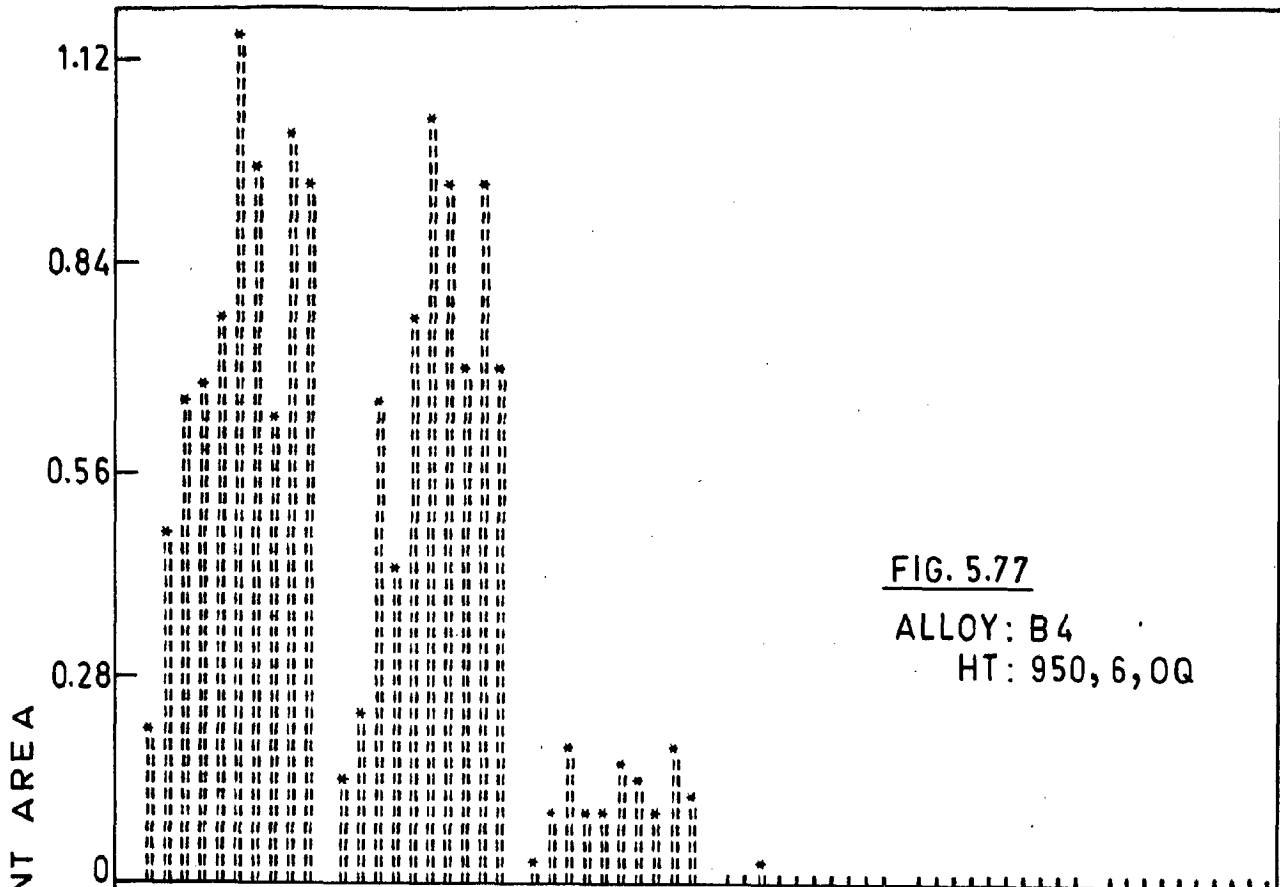
FIG. 5.76

ALLOY : B 4

HT : 950, 4, 0Q

CLASSES

COMPOSITE HYSTOGRAMS DEPICTING CLASS WISE PARTICLE-DISTRIBUTION AT TEN DIFFERENT LOCATIONS.



COMPOSITE HYSTOGRAMS DEPICTING CLASS WISE PARTICLE-DISTRIBUTION AT TEN DIFFERENT LOCATIONS.

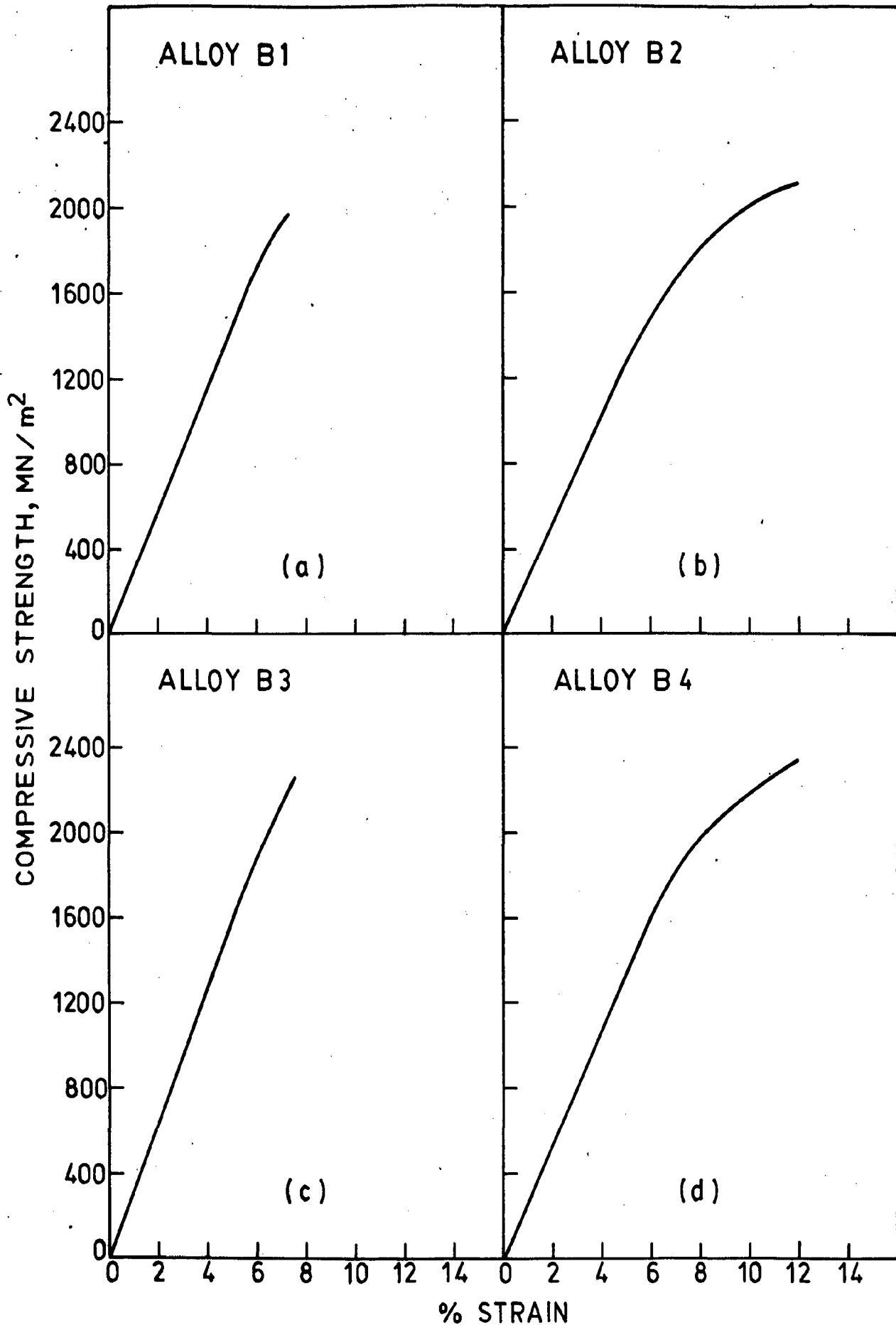


FIG. 5.79 STRESS-STRAIN CURVES UNDER COMPRESSION:  
AS CAST.

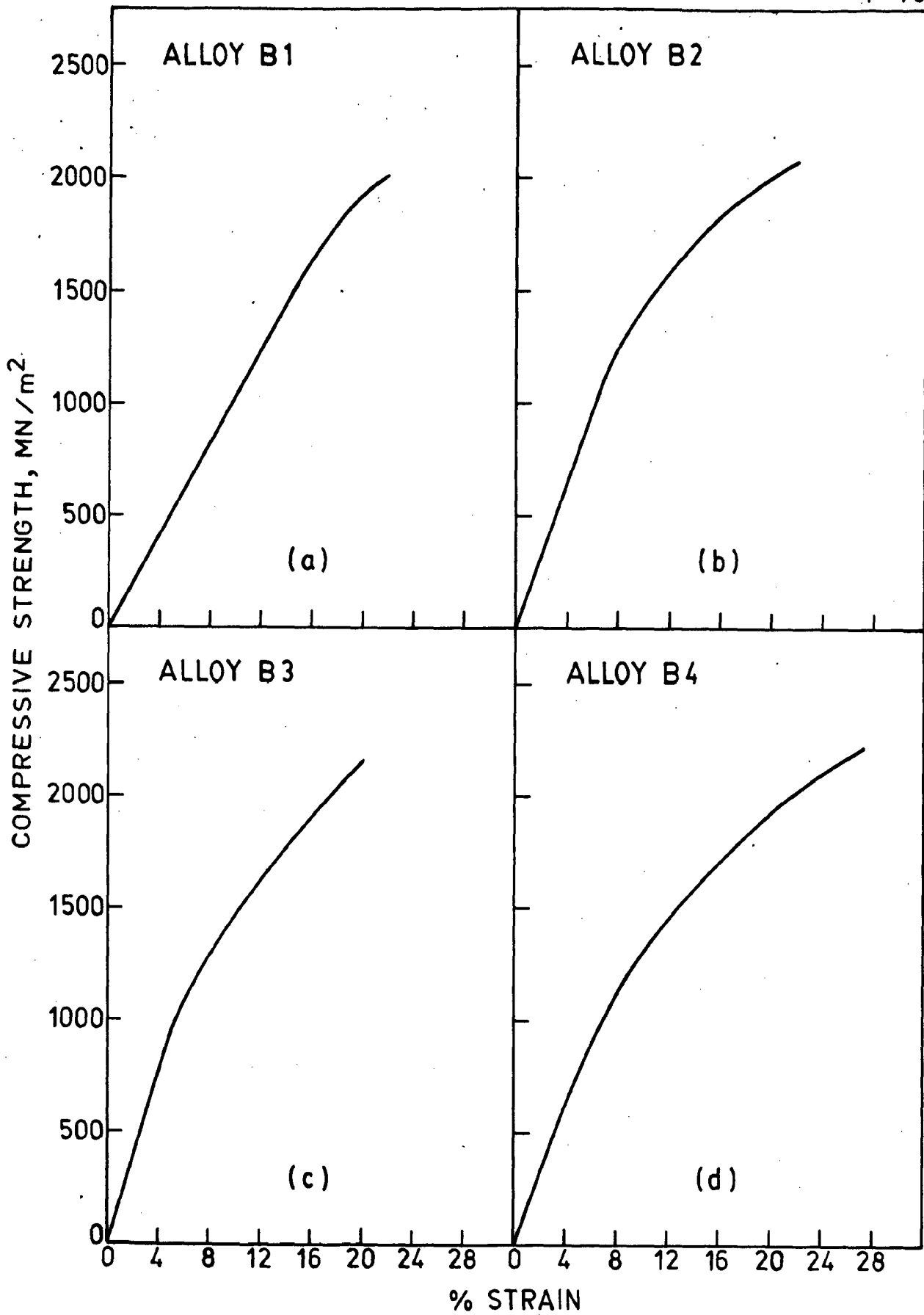


FIG. 5.80 STRESS-STRAIN CURVES UNDER COMPRESSION:  
900, 4, 0Q.

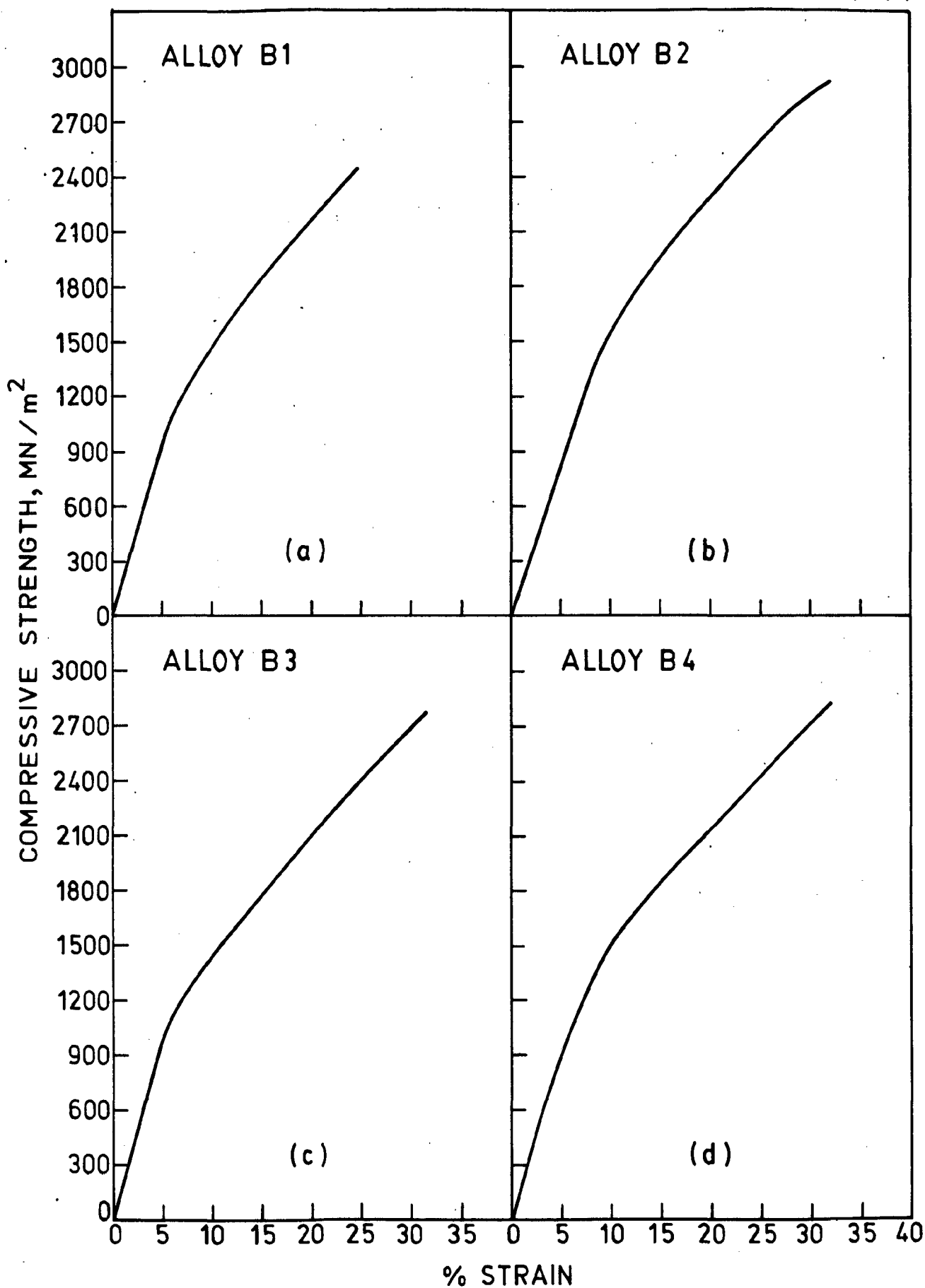


FIG. 5.81 STRESS-STRAIN CURVES UNDER COMPRESSION:  
1000, 10, 0Q.



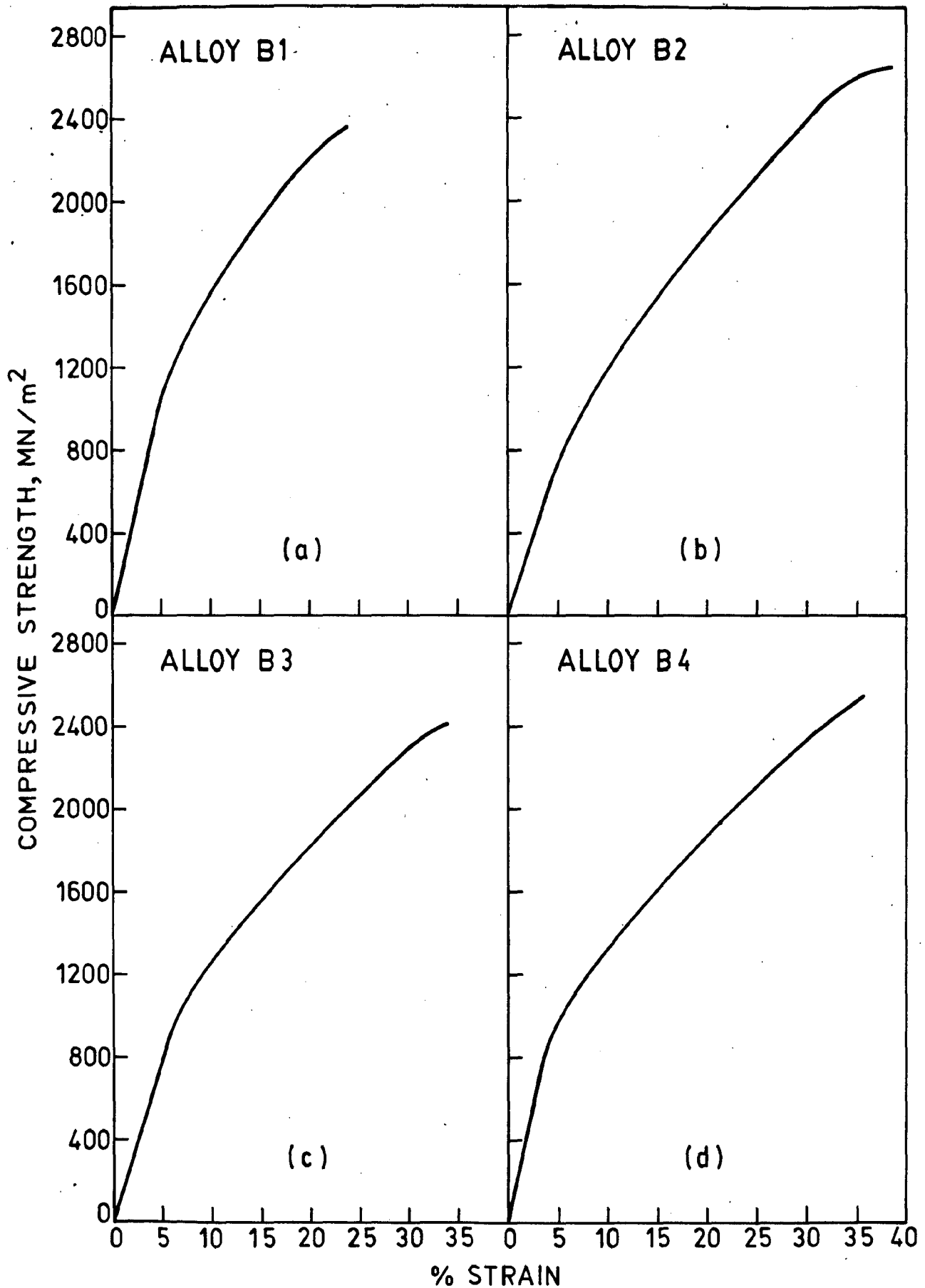


FIG. 5.82 STRESS-STRAIN CURVES UNDER COMPRESSION:  
1050, 4, 0Q.

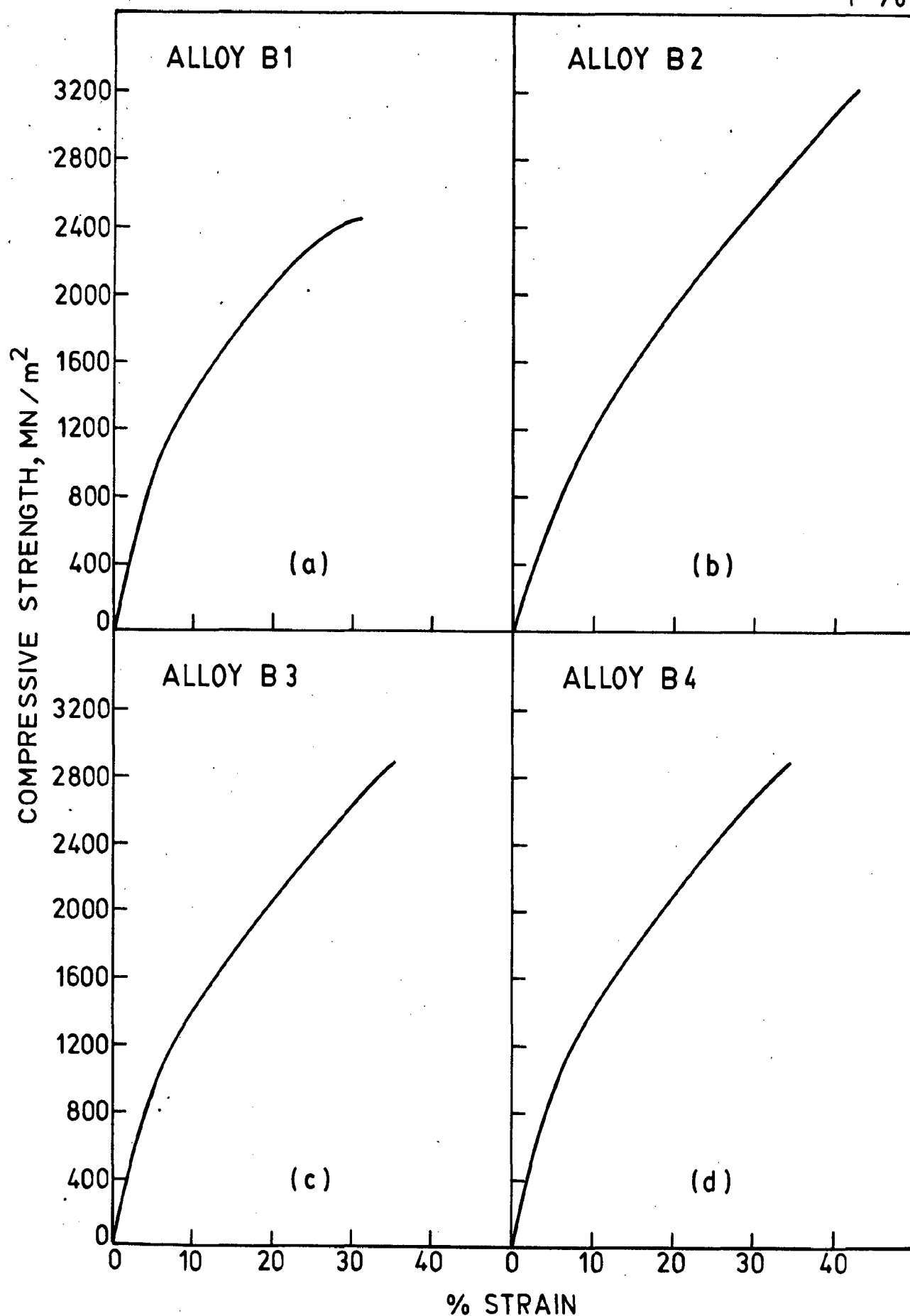


FIG. 5.83 STRESS-STRAIN CURVES UNDER COMPRESSION:  
1050, 10, 0Q.

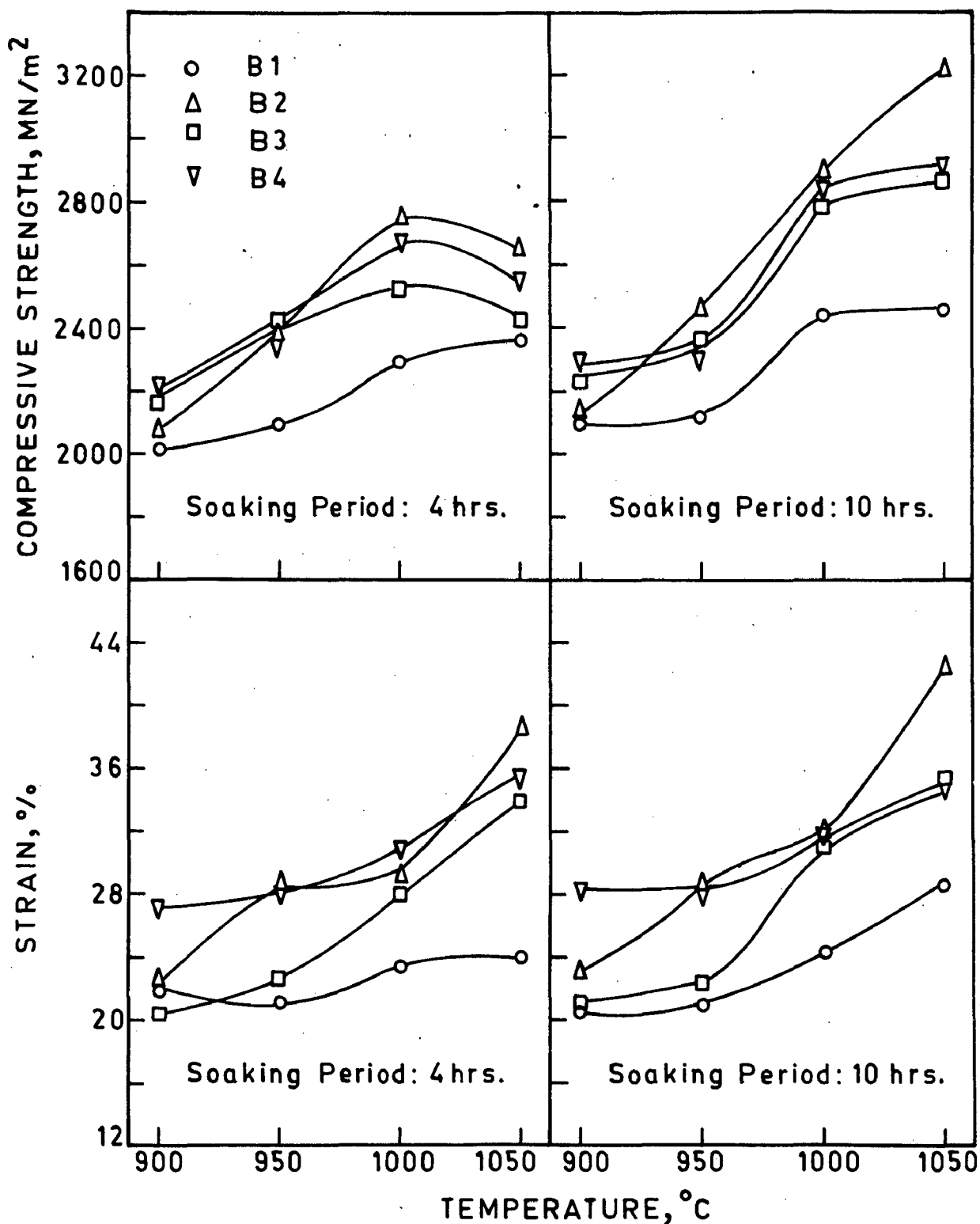


FIG. 5.84 EFFECT OF HEAT TREATING TEMPERATURE ON THE DEFORMATION BEHAVIOUR.

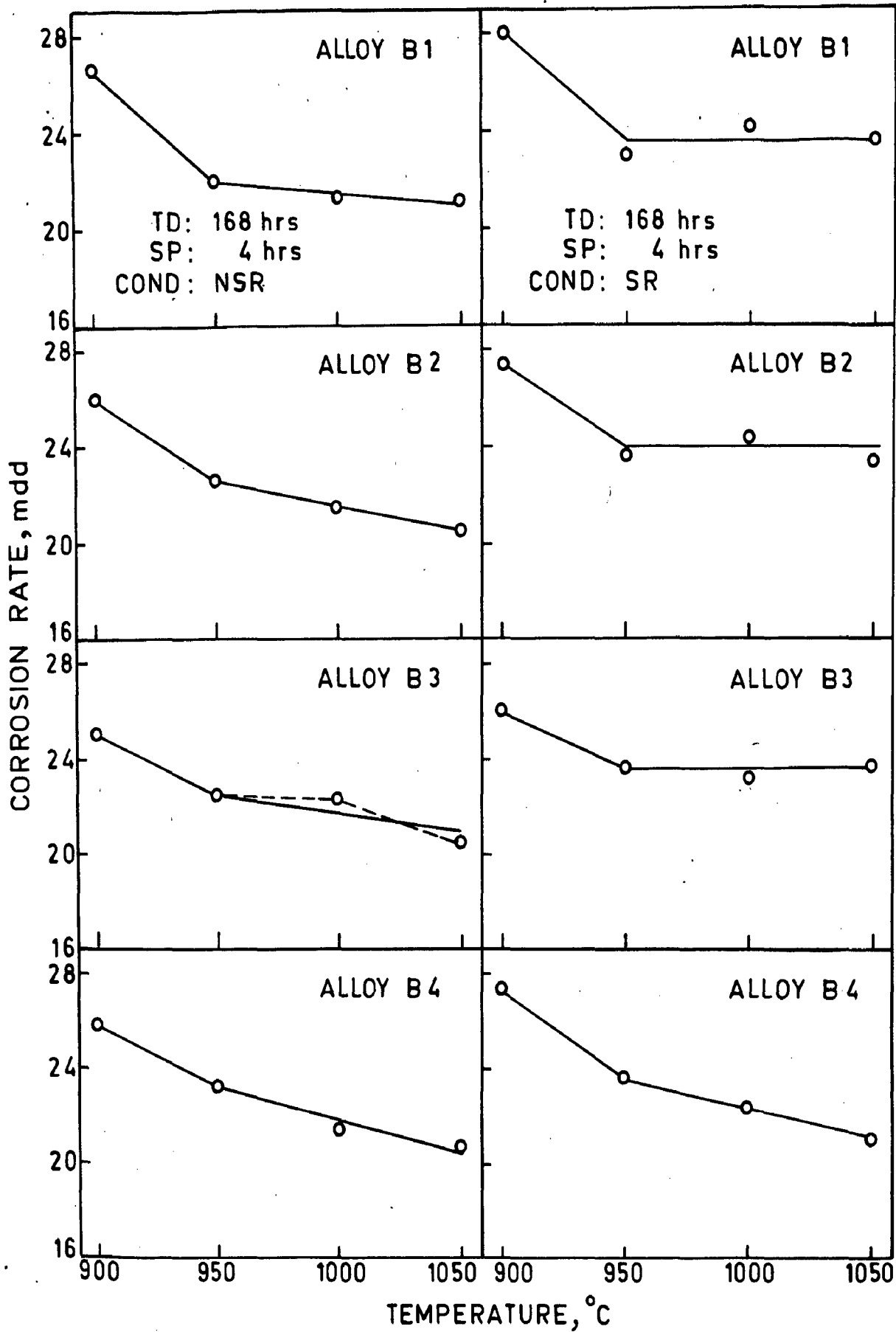


FIG. 5.85 EFFECT OF HEAT-TREATING TEMPERATURE ON CORROSION RATE.

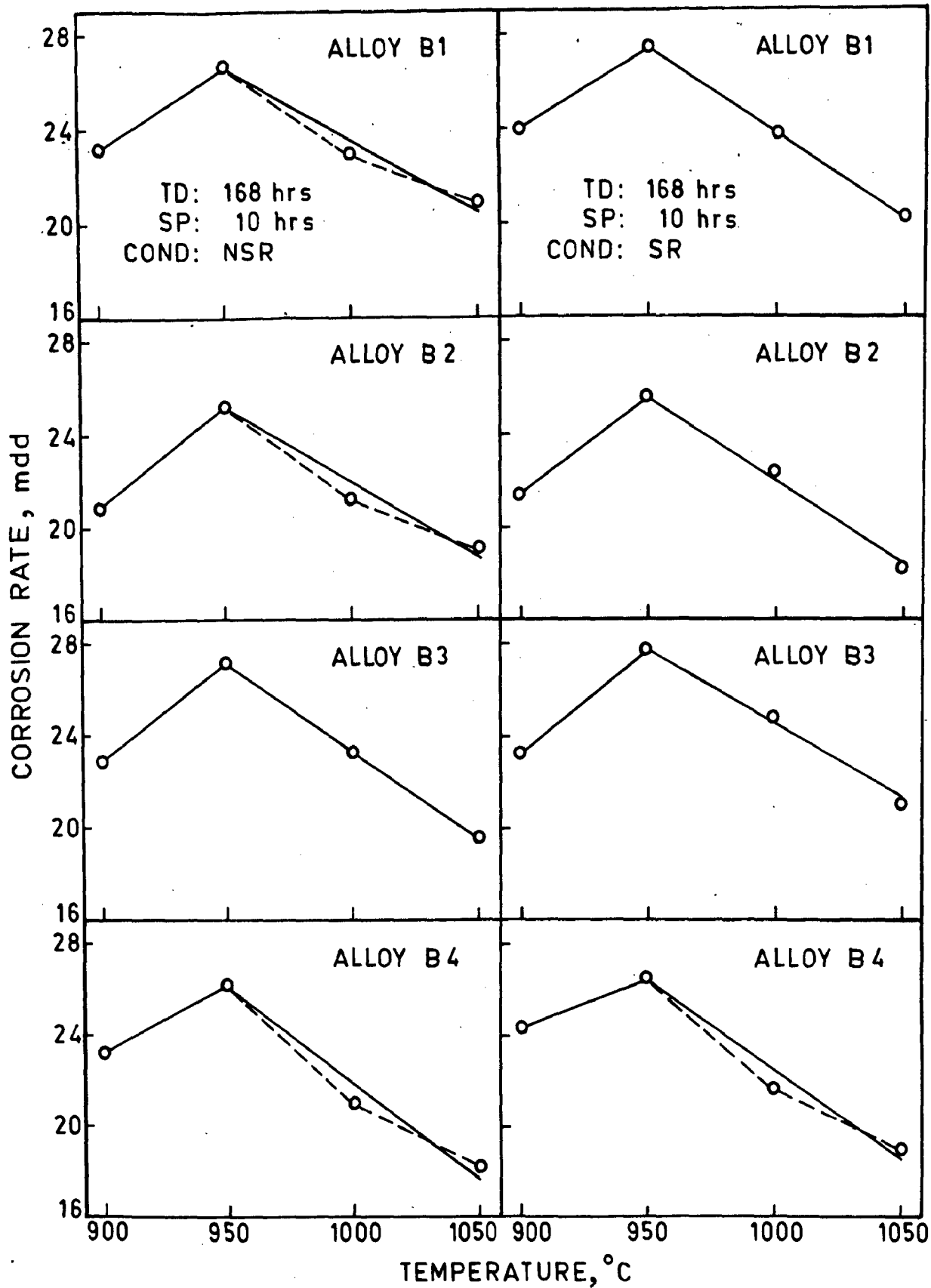


FIG. 5.86 EFFECT OF HEAT-TREATING TEMPERATURE ON CORROSION RATE.

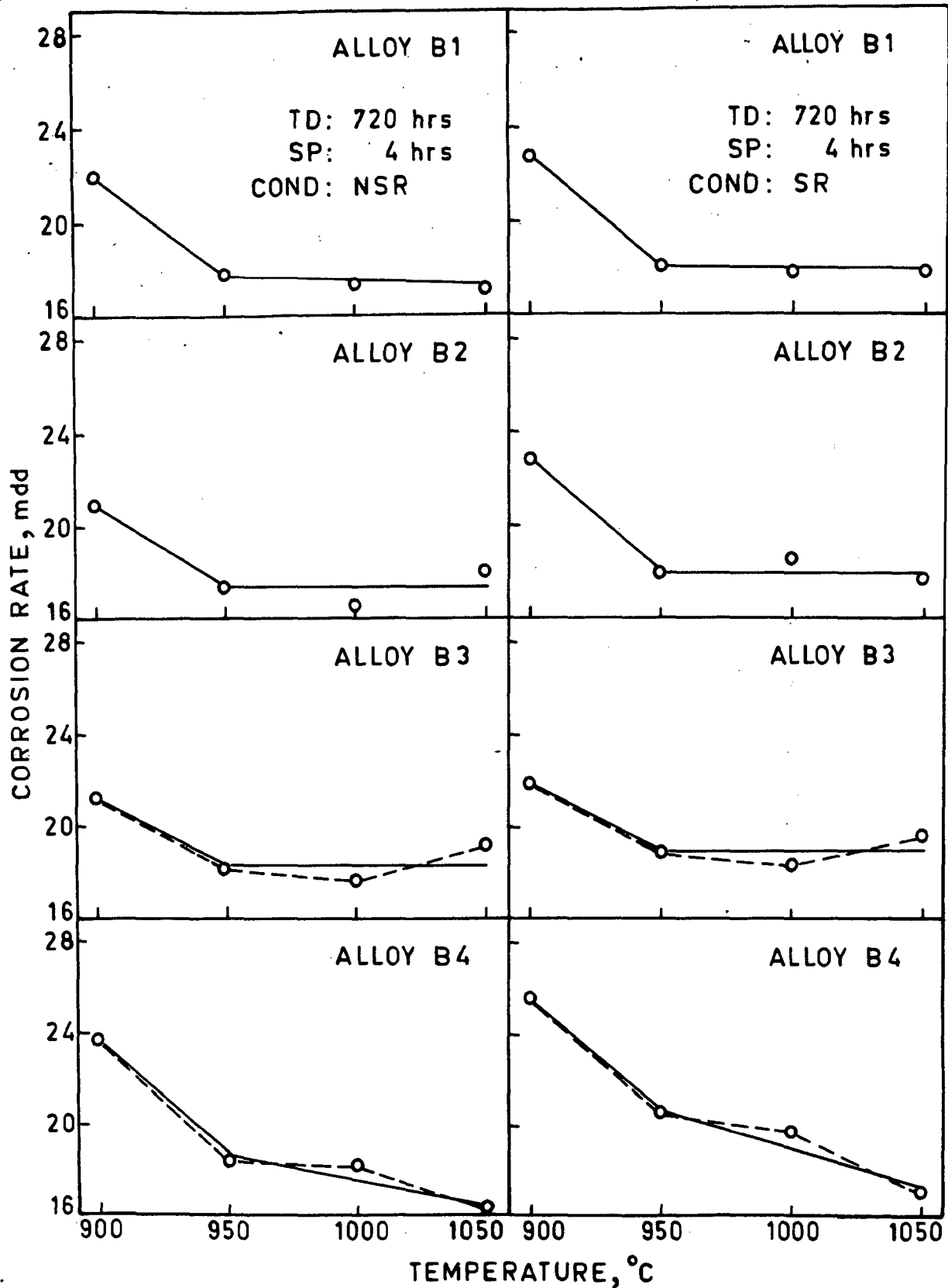


FIG. 5.87 EFFECT OF HEAT-TREATING TEMPERATURE ON CORROSION RATE.

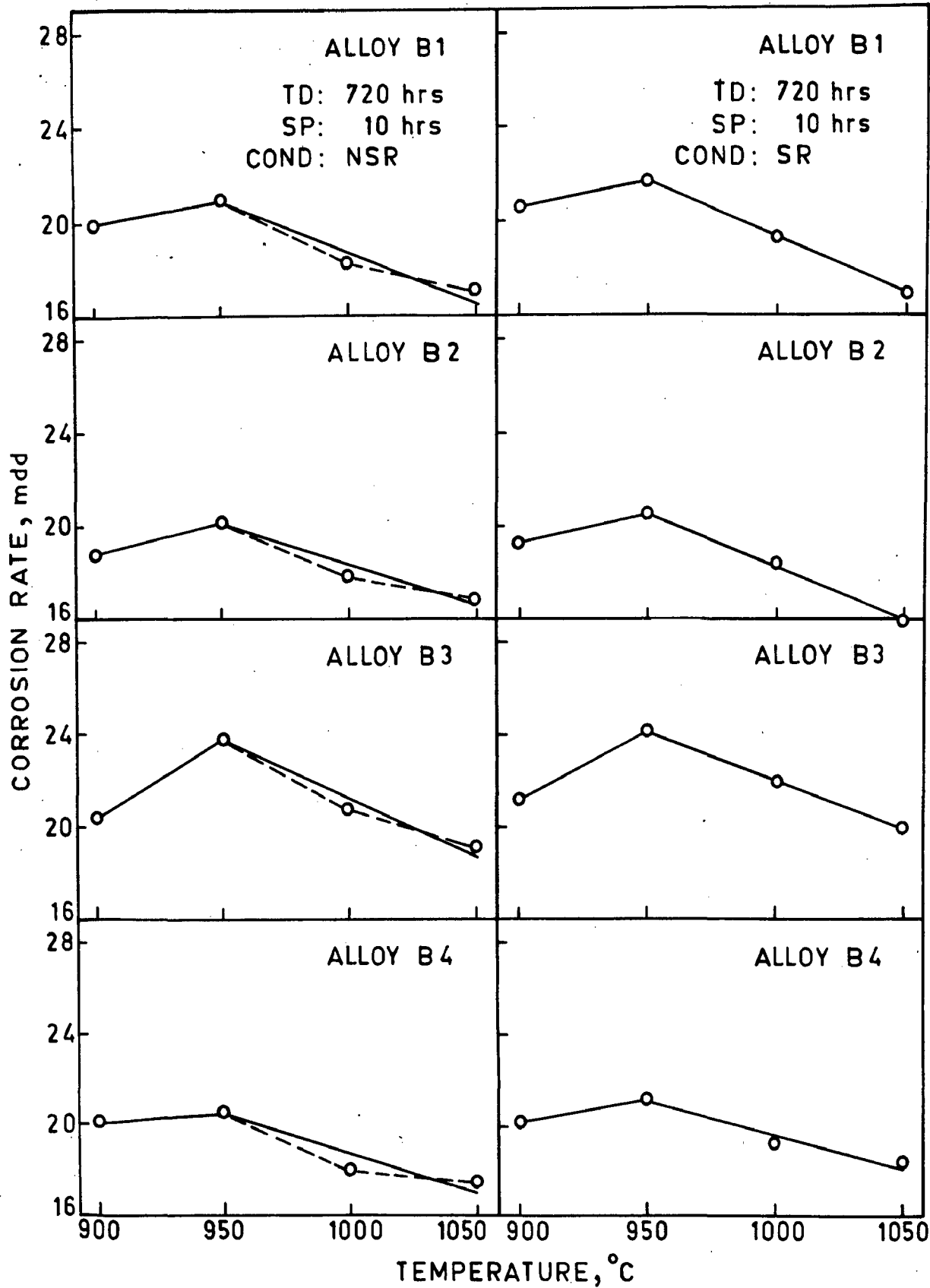


FIG. 5.88 EFFECT OF HEAT-TREATING TEMPERATURE ON CORROSION RATE.

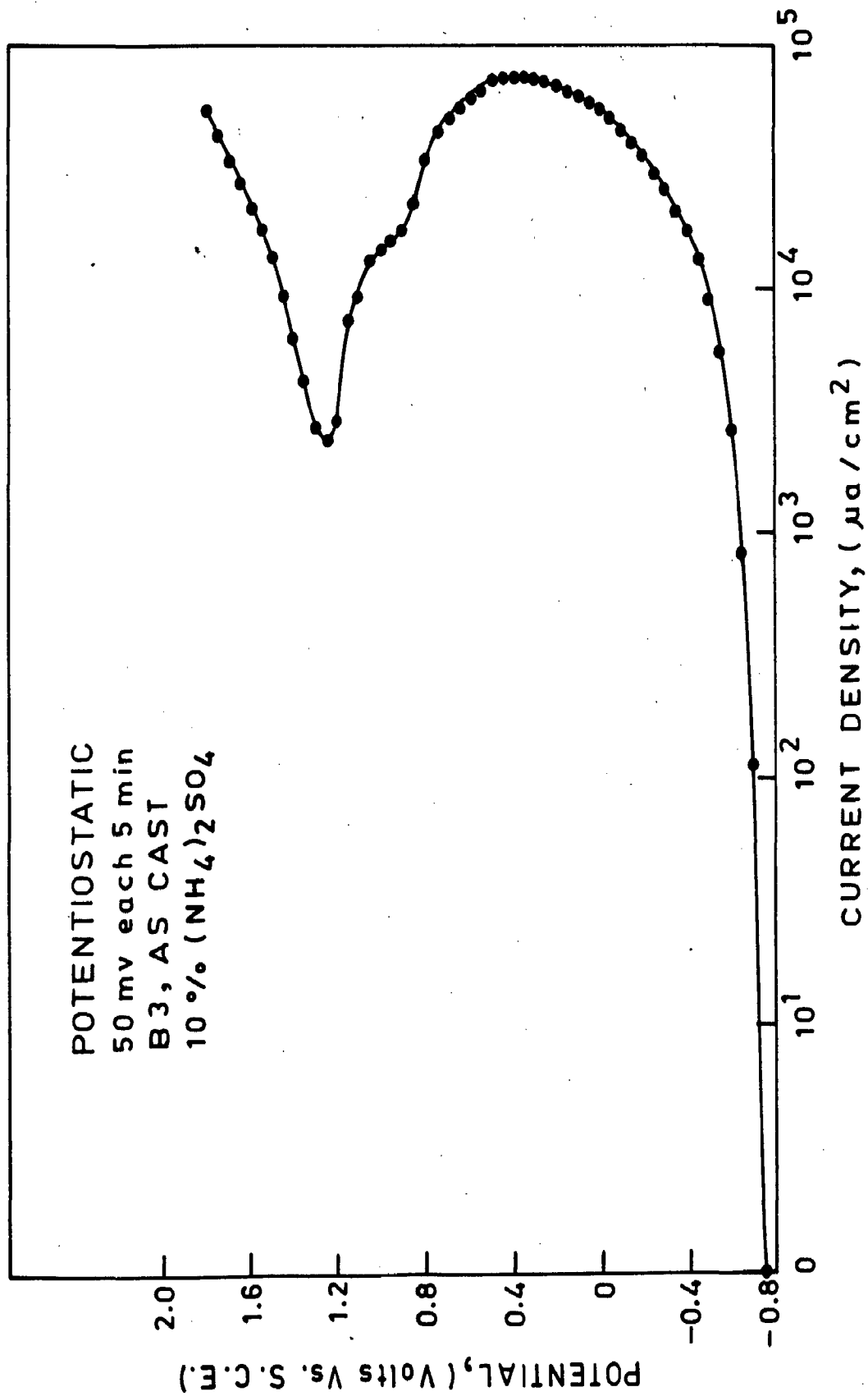


FIG. 5.89 POTENTIOSTATIC ANODIC POLARIZATION CURVE.



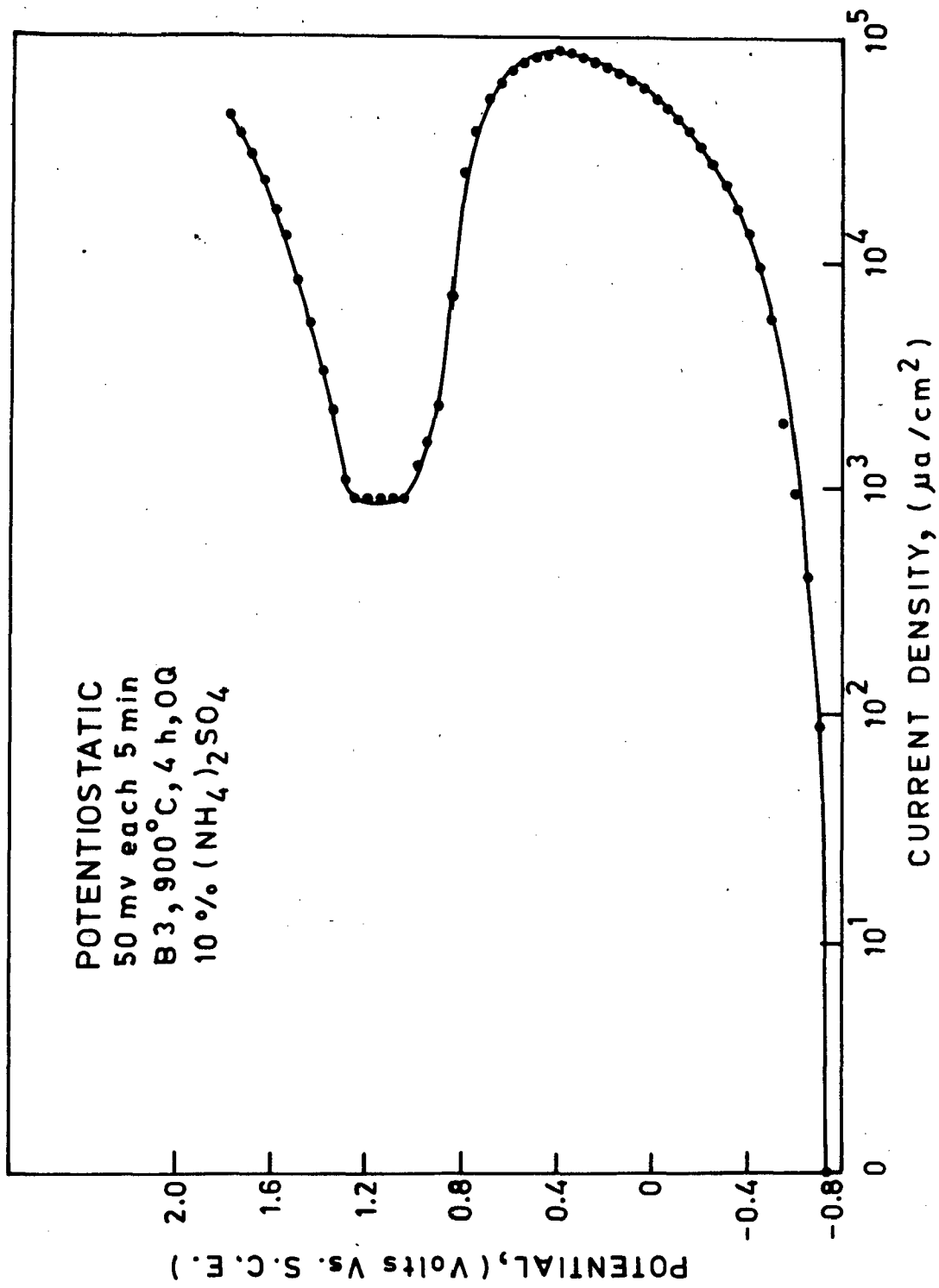


FIG. 5.90 POTENTIOSTATIC ANODIC POLARIZATION CURVE.

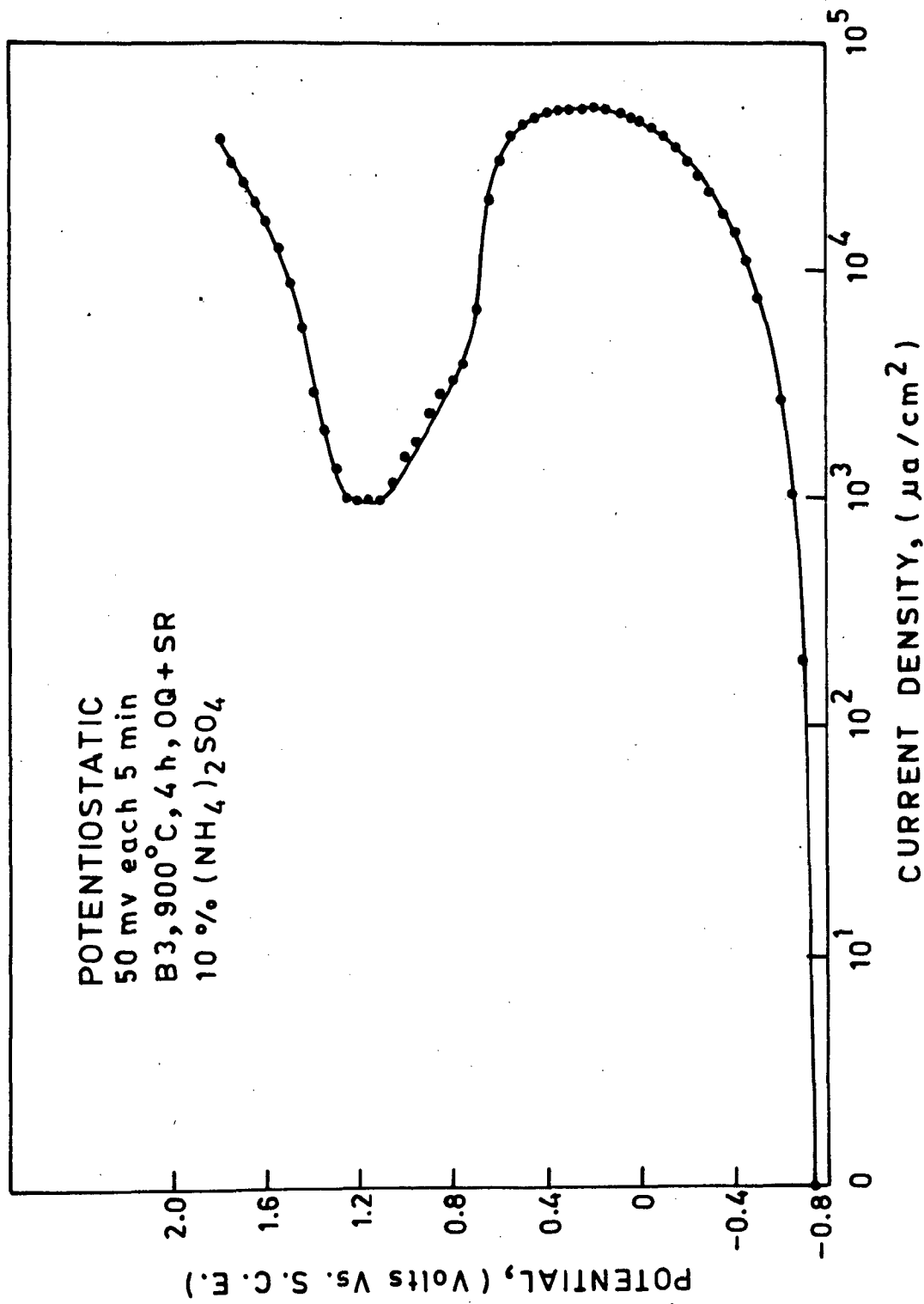


FIG. 5.91 POTENTIOSTATIC ANODIC POLARIZATION CURVE.

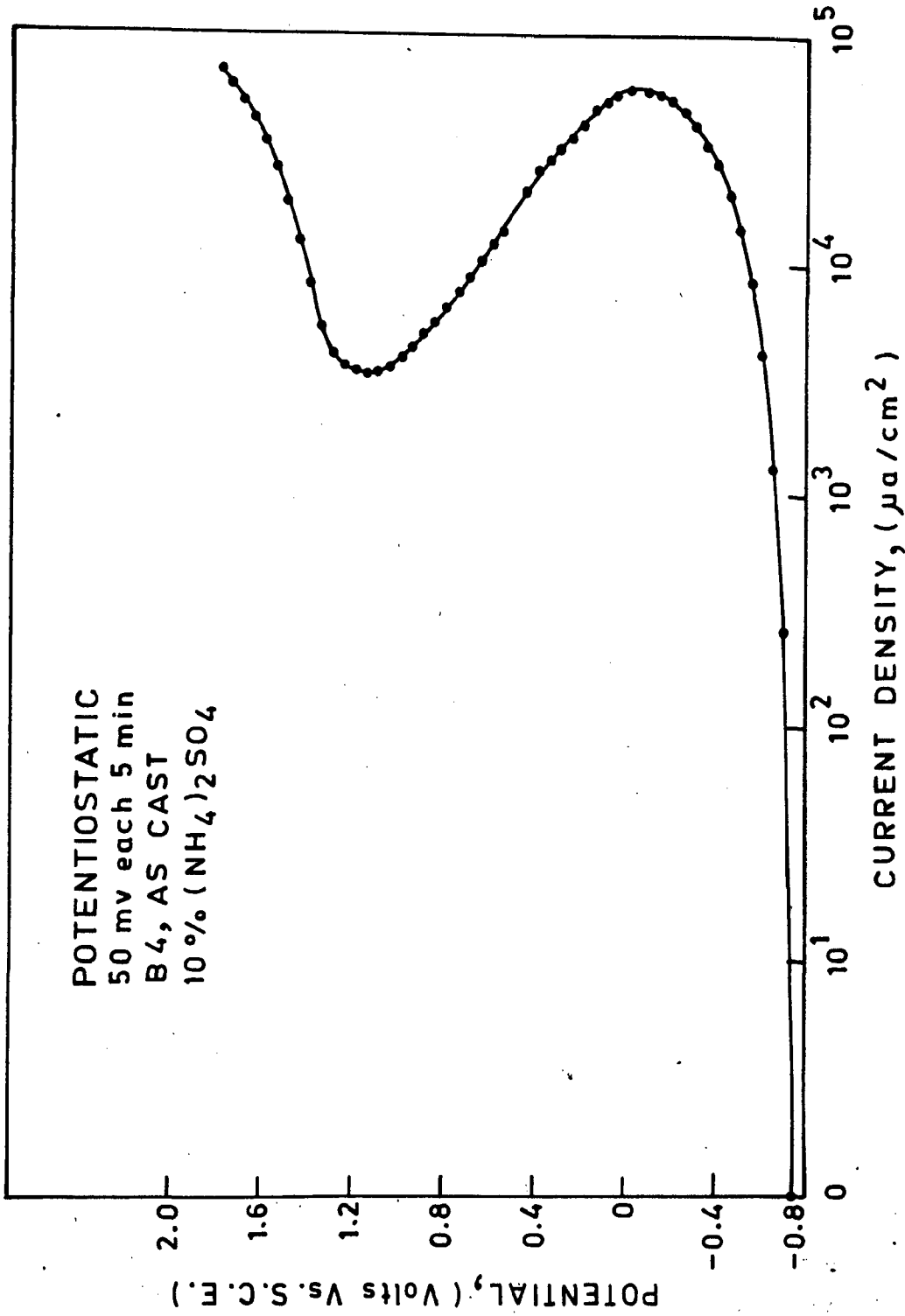


FIG: 5.92 POTENTIOSTATIC ANODIC POLARIZATION CURVE.

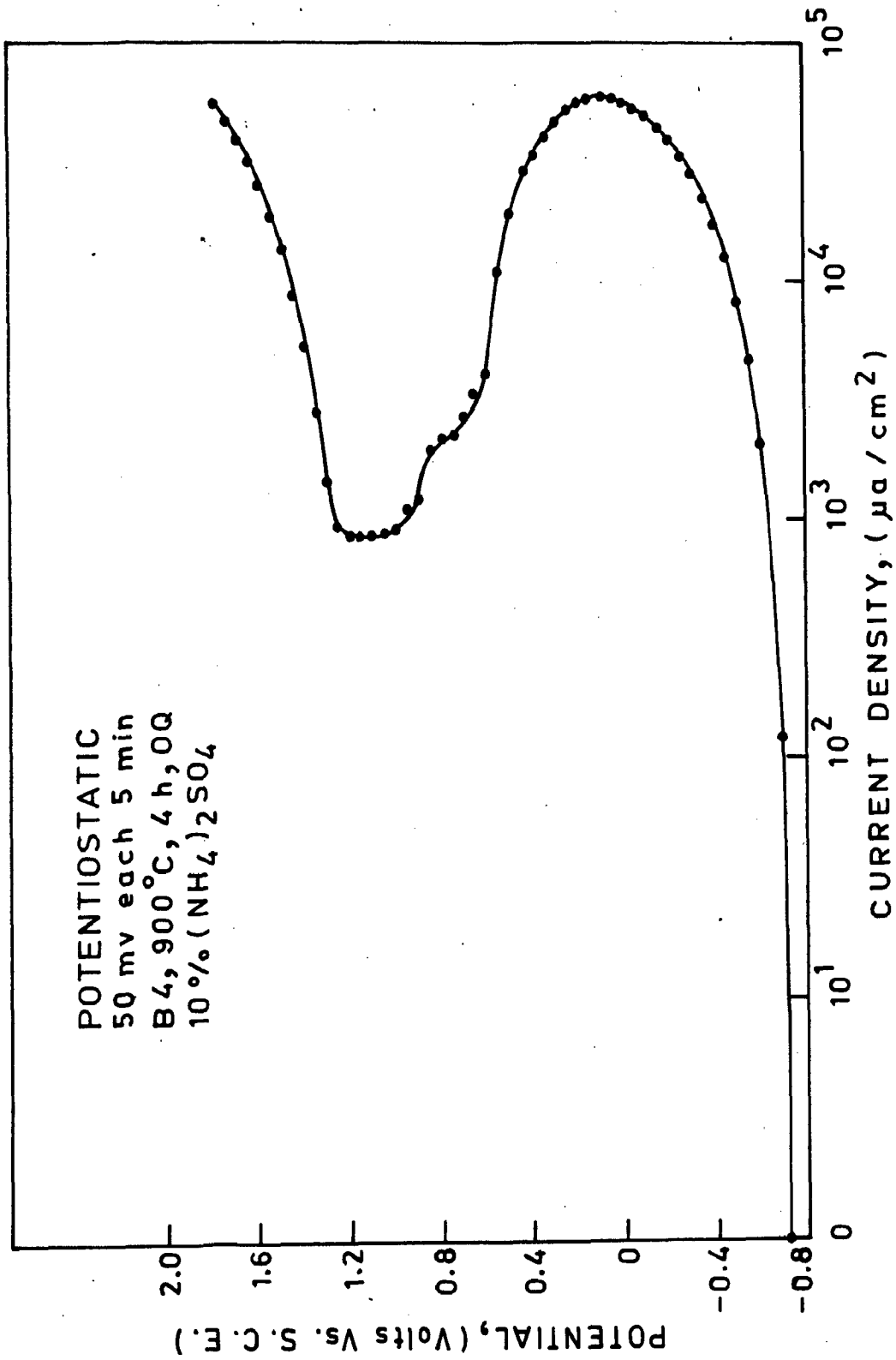


FIG. 5.93 POTENTIOSTATIC ANODIC POLARIZATION CURVE.

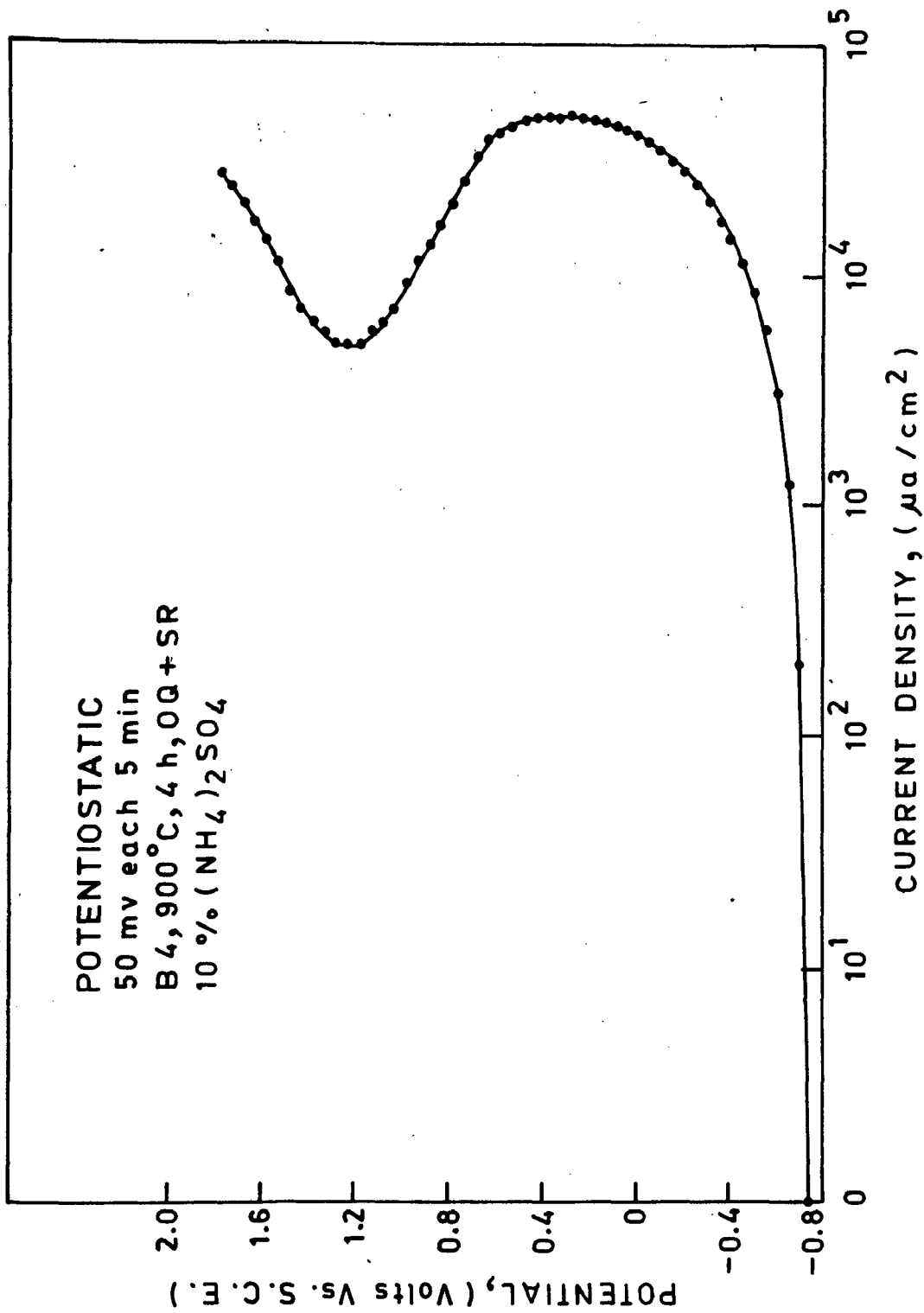


FIG. 5.94 POTENTIOSTATIC ANODIC POLARIZATION CURVE.

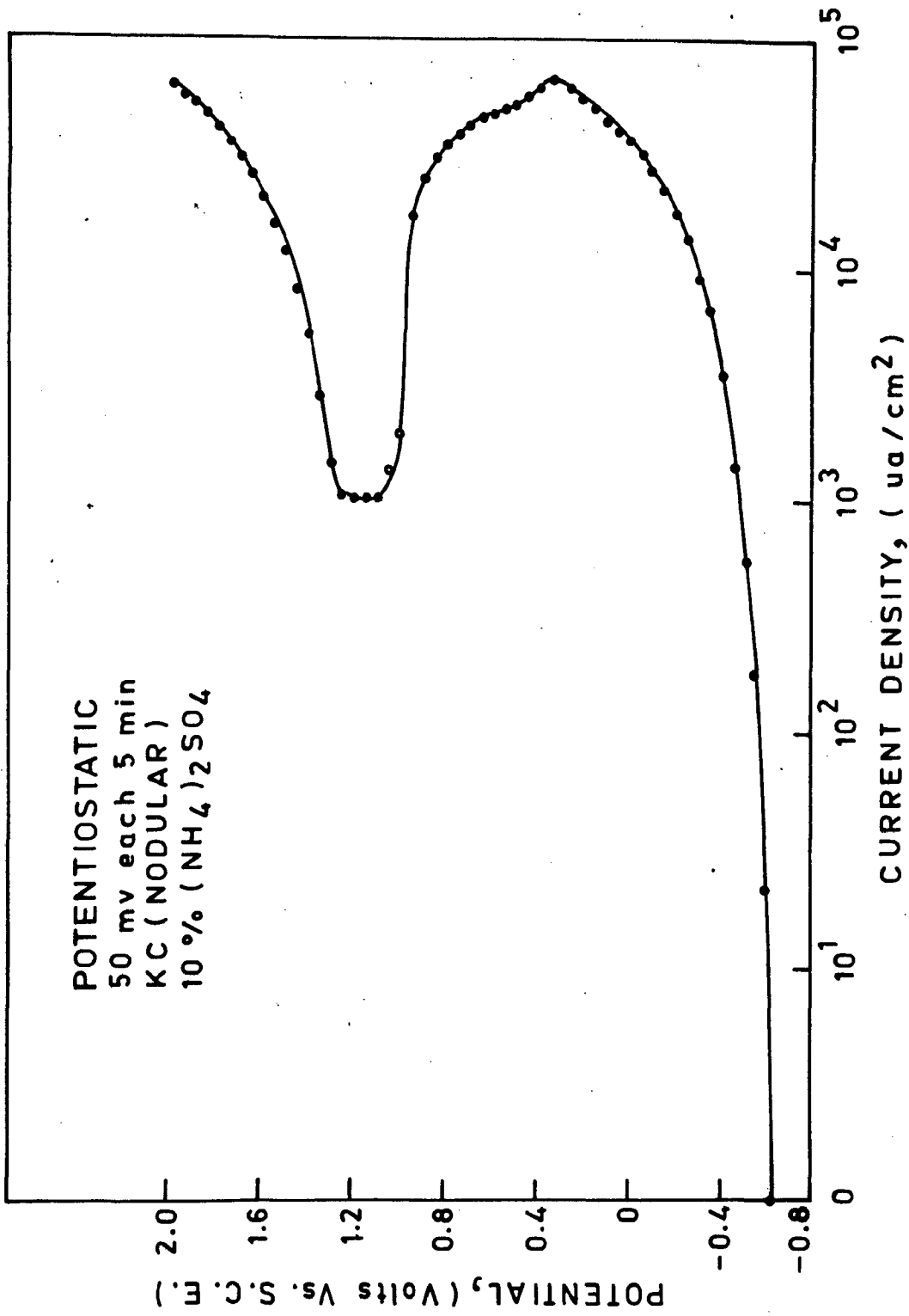


FIG.5.95 POTENTIOSTATIC ANODIC POLARIZATION CURVE.

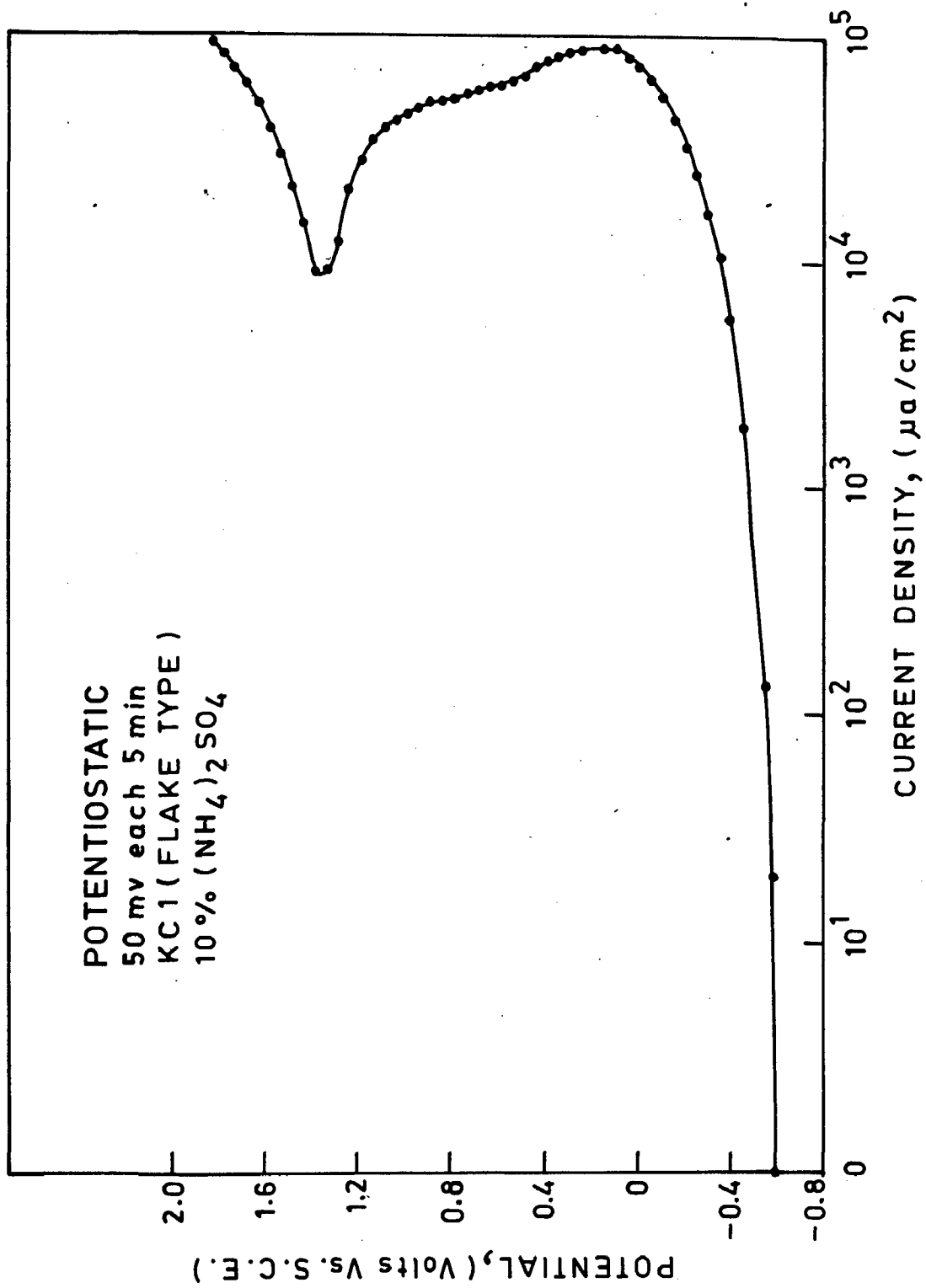


FIG. 5.96 POTENTIOSTATIC ANODIC POLARIZATION CURVE.

Fig. 5.97

(a) KC, As-Cast

168 hrs.

x(160 x 1.0)

(b) KC, As-Cast

168 hrs.

x(640 x 1.0)

(c) KC, As-Cast

168 hrs.

x(640 x 1.0)

(d) KCl, As-Cast

168 hrs.

x(160 x 1.0)

(e) KCl, As-Cast

168 hrs.

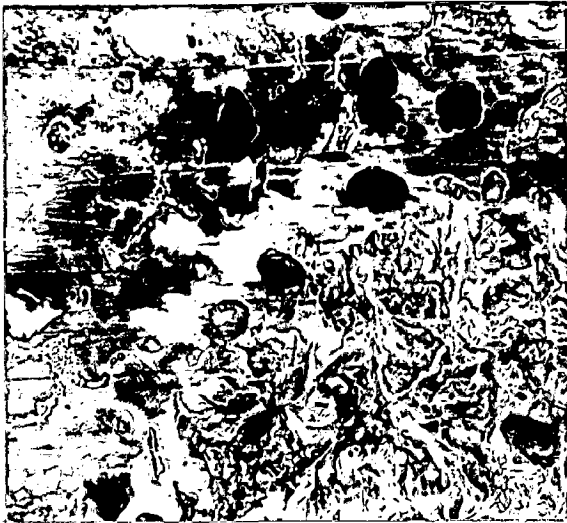
x(640 x 0.95)

(f) KCl, As-Cast

168 hrs.

x(640 x 0.95)





(a)



(b)



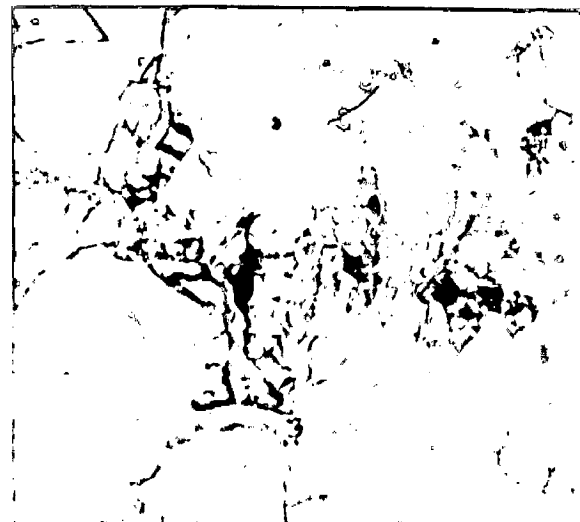
(c)



(d)



(e)



(f)

FIG. 5.97

Fig. 5.98

(a) B<sub>1</sub>, As-Cast  
168 hrs.  
x(640 x 1.0)

(b) B<sub>1</sub>, As-Cast  
168 hrs.  
x(5000 x 1.0)

(c) B<sub>1</sub>, 900°C, 4h, OQ  
720 hrs.  
x(640 x 1.0)

(d) B<sub>1</sub>, 900°C, 4h, OQ + SR  
720 hrs.  
x(640 x 1.0)

(e) B<sub>1</sub>, 950°C, 10h, OQ + SR  
168 hrs.  
x(2500 x 1.1)



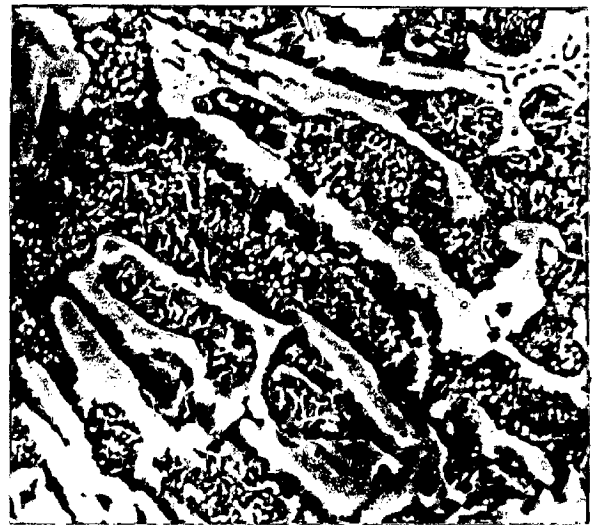
(a)



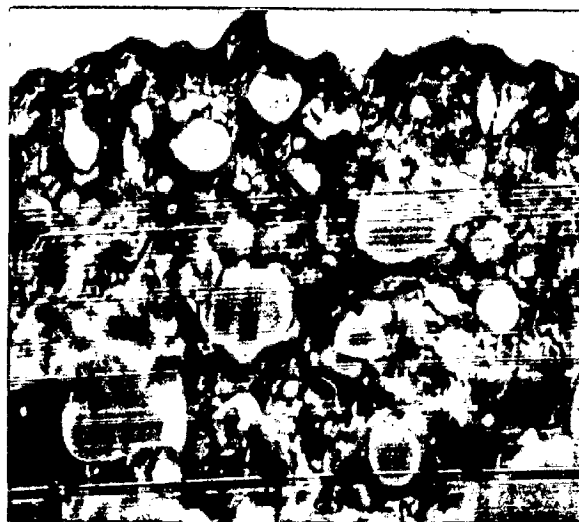
(b)



(c)



(d)



(e)

FIG. 5.98

Fig. 5.99

(a) B<sub>1</sub>, 1000°C, 10h, OQ  
168 hrs.  
x(640 x 1.0)

(b) B<sub>1</sub>, 1000°C, 10h, OQ + SR  
168 hrs.  
x(640 x 1.0)

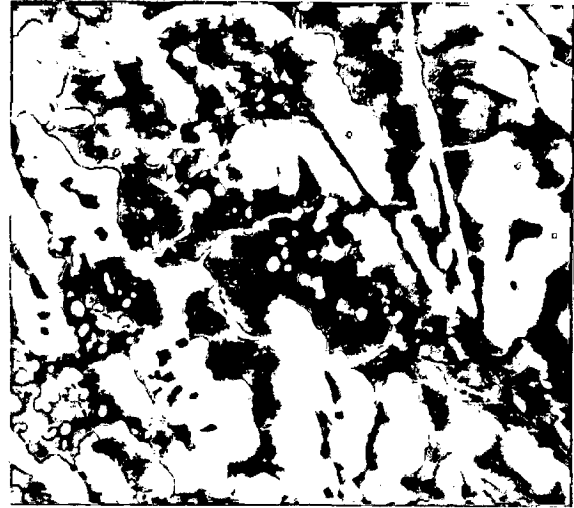
(c) B<sub>1</sub>, 1050°C, 4h, OQ  
720 hrs.  
x(1250 x 1.0)

(d) B<sub>1</sub>, 1050°C, 4h, OQ + SR  
720 hrs.  
x(1250 x 1.0)

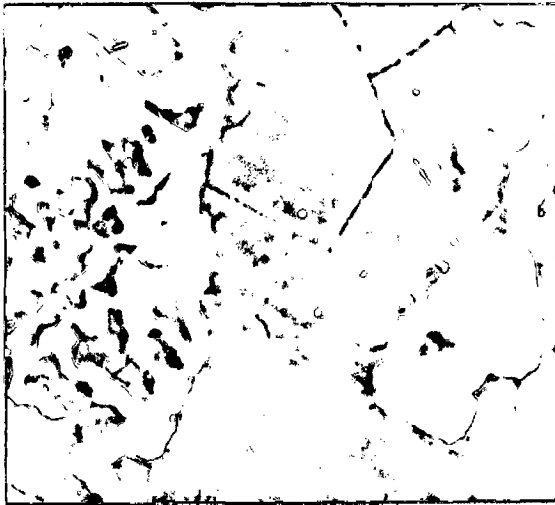
(e) B<sub>1</sub>, 1050°C, 10h, OQ + SR  
720 hrs.  
x(640 x 1.0)



(a)



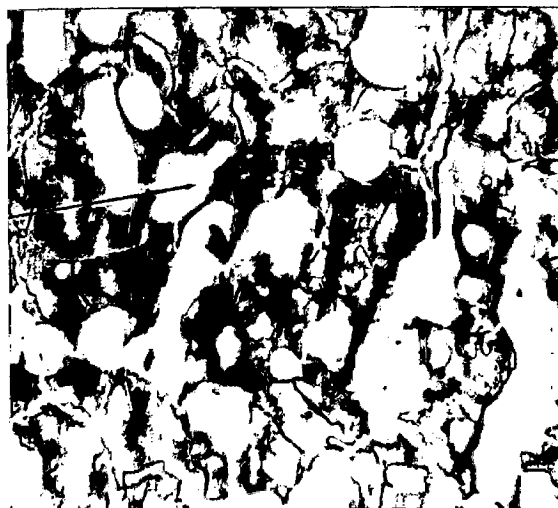
(b)



(c)



(d)



(e)

FIG. 5.99

Fig. 5.100

(a) B<sub>2</sub>, As-Cast

168 hrs.

x(640 x 1.0)

(b) B<sub>2</sub>, 950°C, 4h, OQ

720 hrs.

x(640 x 1.1)

(c) B<sub>2</sub>, 950°C, 10h, OQ

720 hrs.

x(640 x 1.0)

(d) B<sub>2</sub>, 950°C, 10h, OQ + SR

720 hrs.

x(640 x 1.0)

(e) B<sub>2</sub>, 1000°C, 10h, OQ

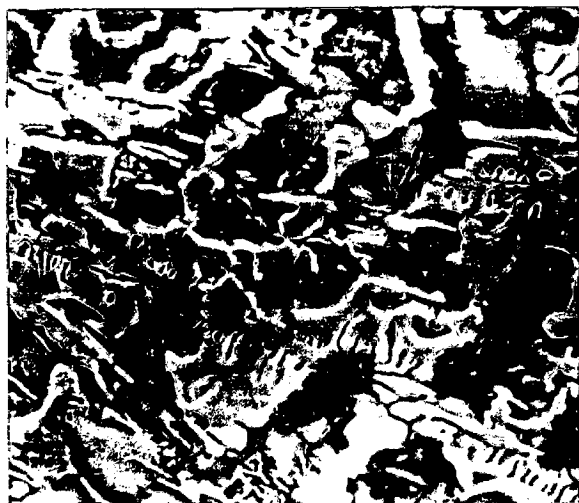
720 hrs.

x(640 x 1.2)

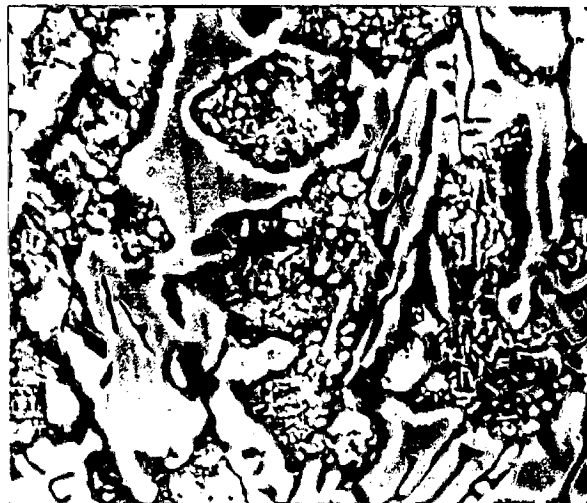
(f) B<sub>2</sub>, 1000°C, 10h, OQ + SR

168 hrs.

x(1250 x 0.95)



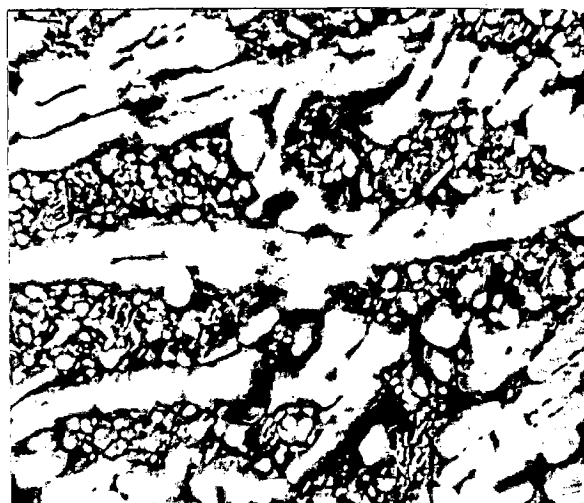
(a)



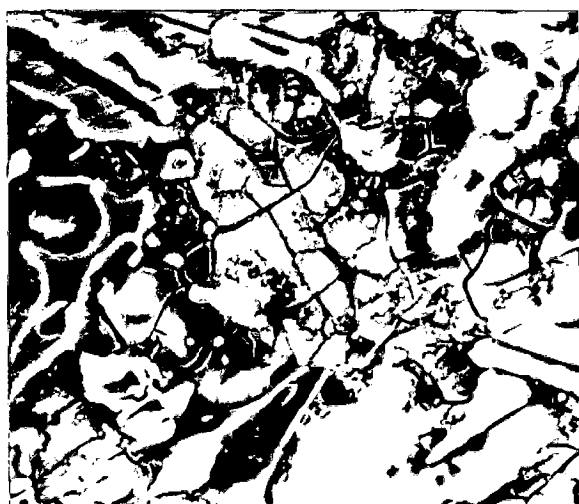
(b)



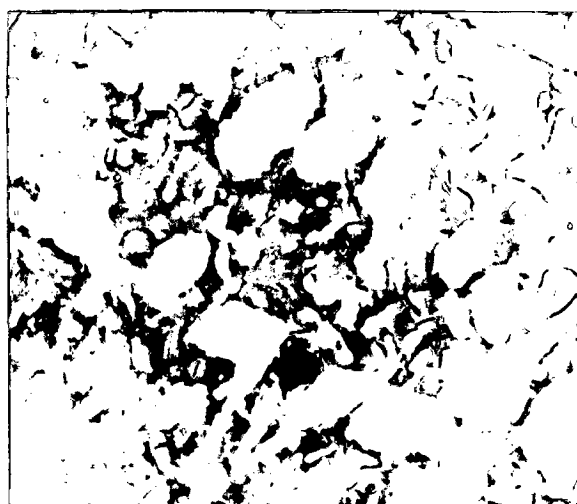
(c)



(d)



(e)



(f)

FIG. 5.100

Fig. 5.101

(a) B<sub>2</sub>, 1050°C, 4h, OQ  
720 hrs.  
x(1250 x 1.0)

(b) B<sub>2</sub>, 1050°C, 4h, OQ + SR  
720 hrs.  
x(1250 x 1.0)

(c) B<sub>2</sub>, 1050°C, 10h, OQ  
720 hrs.  
x(320 x 1.0)

(d) B<sub>2</sub>, 1050°C, 10h, OQ  
720 hrs.  
x(640 x 1.0)

(e) B<sub>2</sub>, 1050°C, 10h, OQ + SR  
720 hrs.  
x(640 x 1.0)

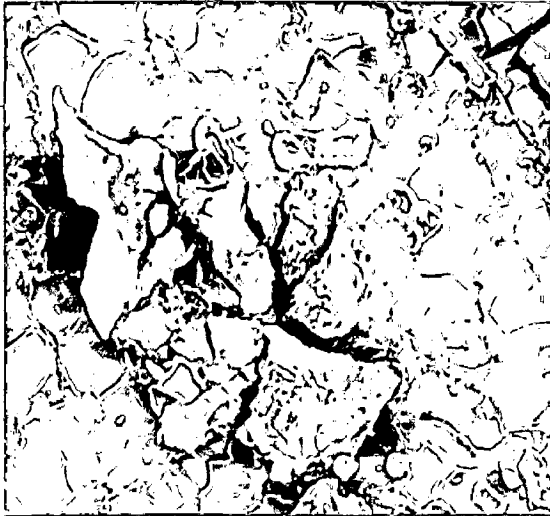




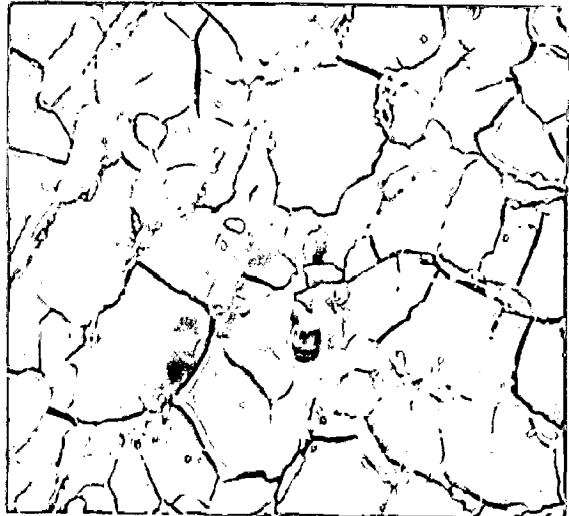
(a)



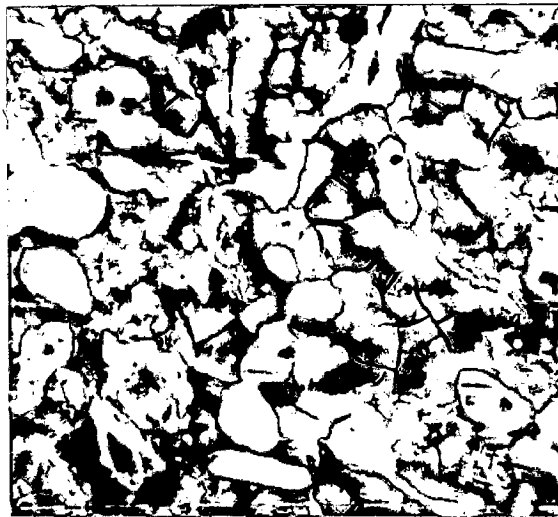
(b)



(c)



(d)



(e)

FIG. 5.101

Fig. 5.102

(a) B<sub>3</sub>, As-Cast

168 hrs.

x(640 x 0.95)

(b) B<sub>3</sub>, 900°C, 4h, OQ

720 hrs.

x(2500 x 1.0)

(c) B<sub>3</sub>, 900°C, 4h, OQ + SR

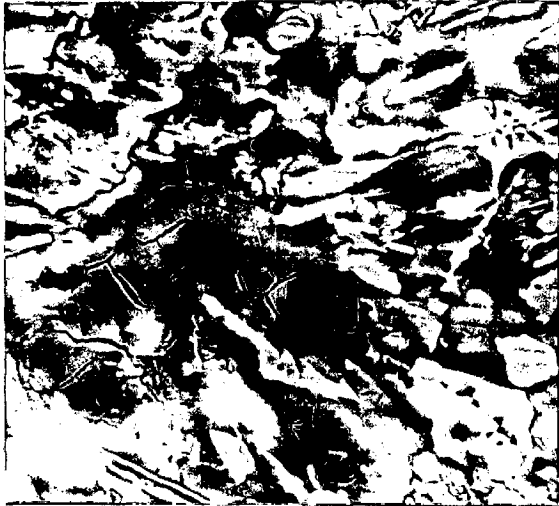
720 hrs.

x(1250 x 0.95)

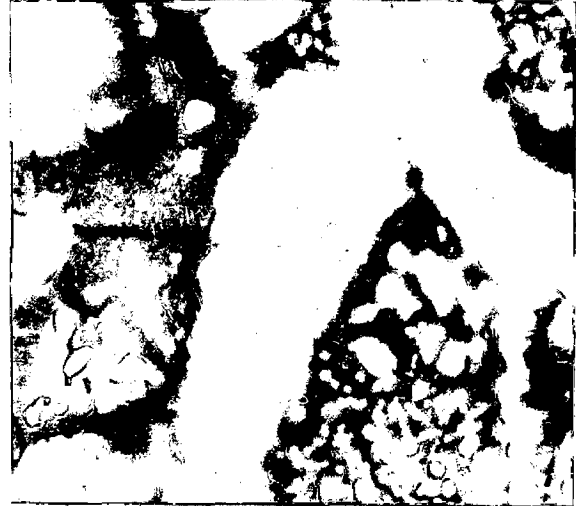
(d) B<sub>3</sub>, 1000°C, 10h, OQ

168 hrs.

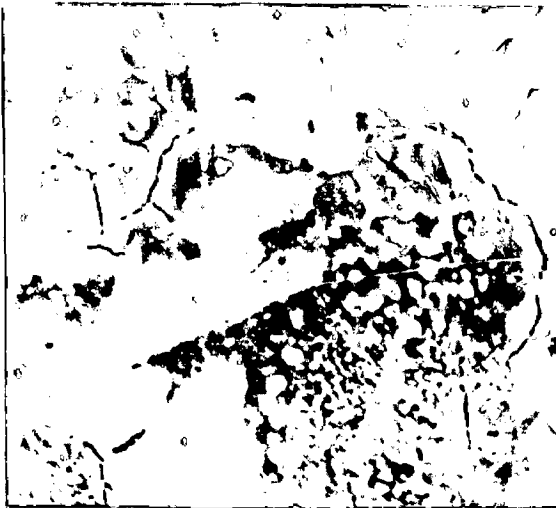
x(1250 x 1.0)



(a)



(b)



(c)



(d)

FIG. 5.102

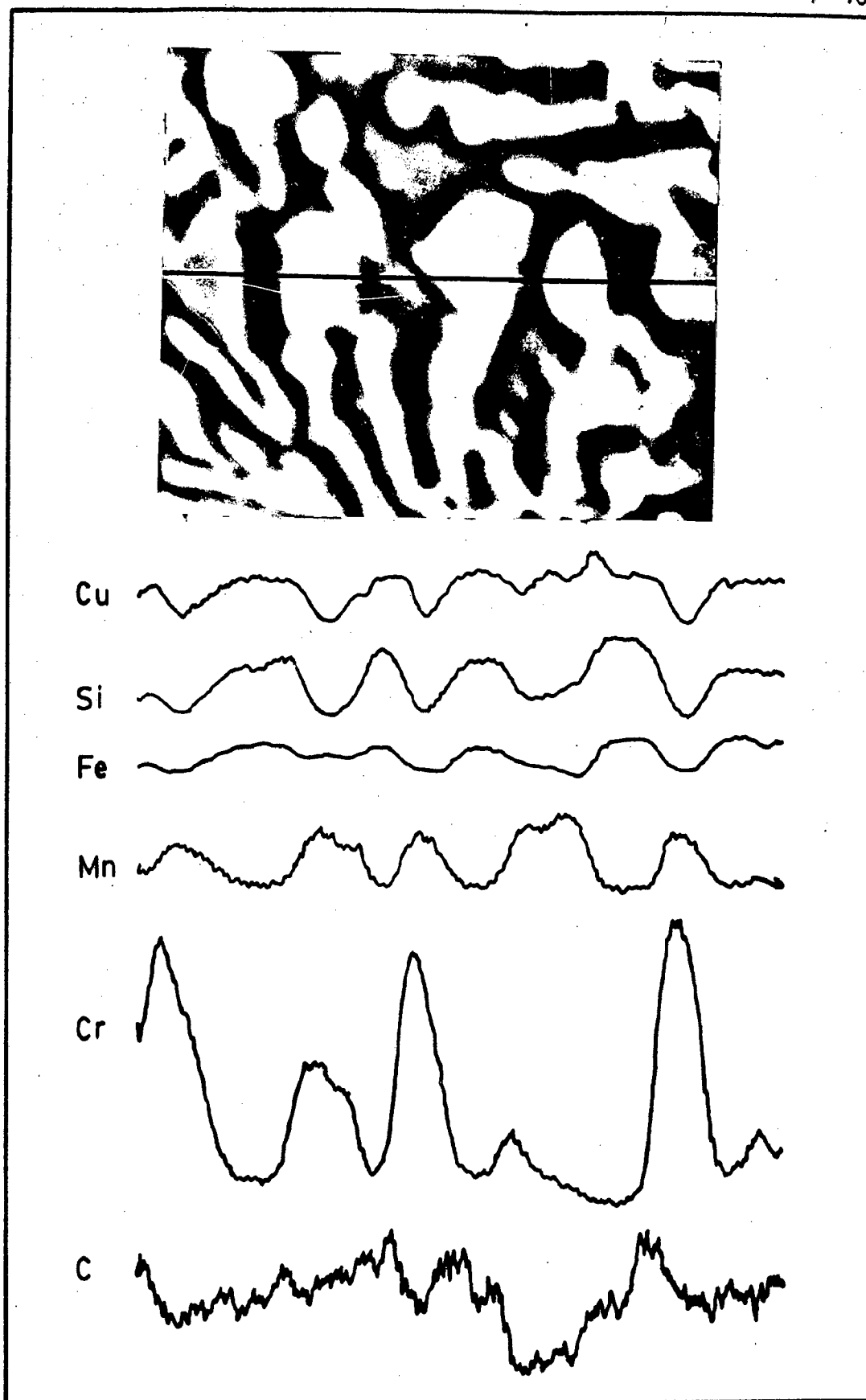
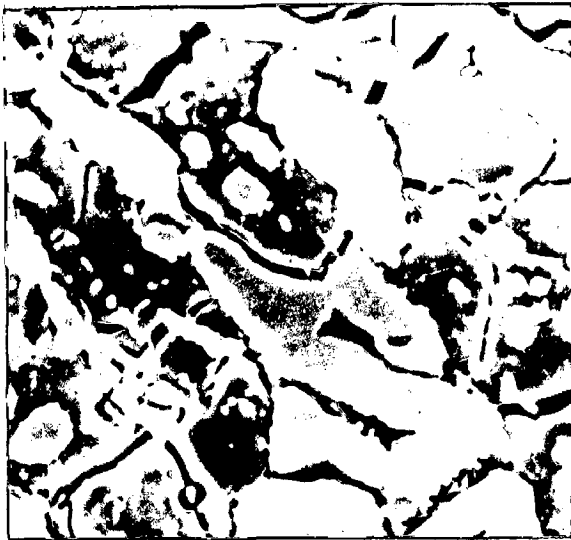


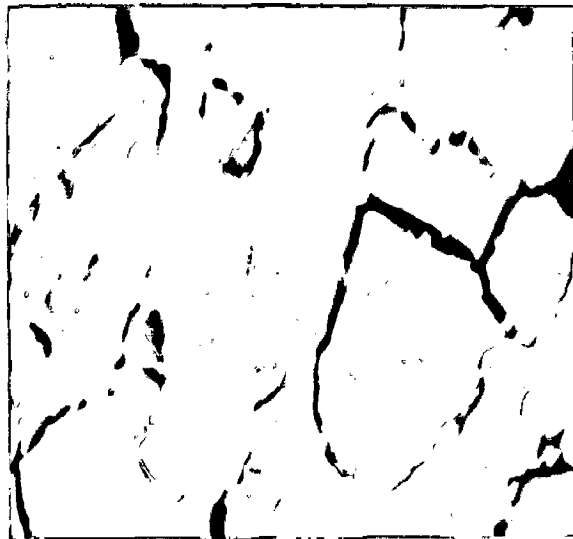
FIG. 5.107 LINE SCANS OF Cu, Si, Fe, Mn, Cr AND C IN NEW PHASE (B1, 1050°C, 4 h, OQ).



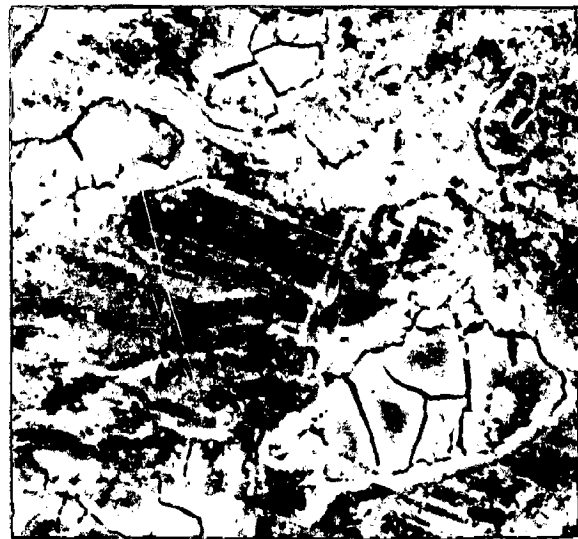
(a)



(b)



(c)



(d)

FIG. 5.105

Fig. 5.105

(a) B<sub>4</sub>, 1000°C, 10h, OQ

168 hrs.

x(1250 x 1.0)

(b) B<sub>4</sub>, 1000°C, 10h, OQ + SR

168 hrs.

x(1250 x 1.0)

(c) B<sub>4</sub>, 1050°C, 10h, OQ

720 hrs.

x(1250 x 1.0)

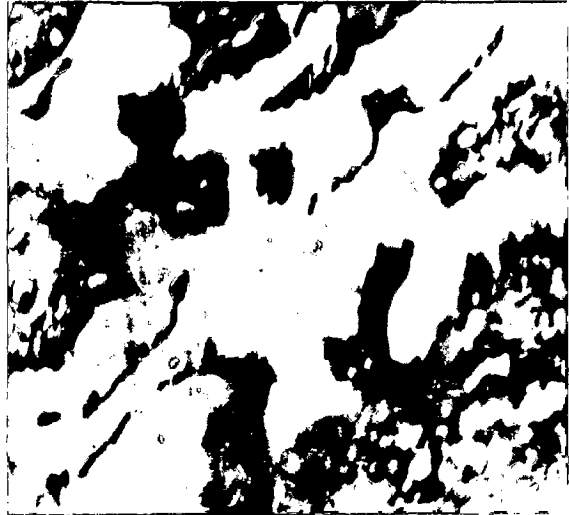
(d) B<sub>4</sub>, 1050°C, 10h, OQ + SR

168 hrs.

x(1250 x 1.0)



(a)



(b)



(c)



(d)

FIG. 5.104

Fig. 5.104

(a) B<sub>4</sub>, As-Cast  
168 hrs.  
x(640 x 1.0)

(b) B<sub>4</sub>, 900°C, 4h, OQ + SR  
720 hrs.  
x(1250 x 1.1)

(c) B<sub>4</sub>, 950°C, 10h, OQ + SR  
168 hrs.  
x(2500 x 1.1)

(d) B<sub>4</sub>, 950°C, 10h, OQ  
168 hrs.  
x(1250 x 1.1)

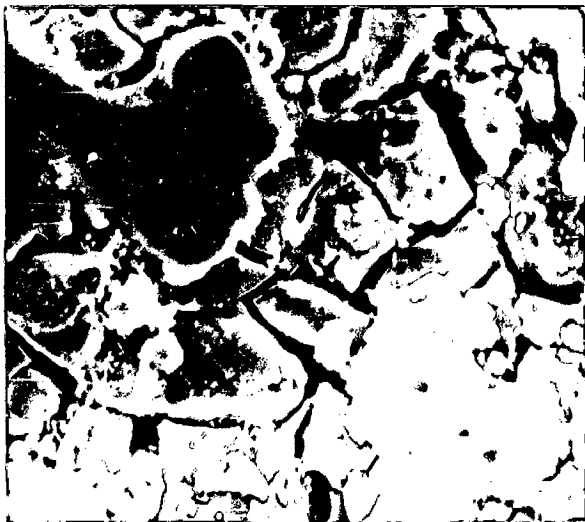




(a)



(b)



(c)



(d)

FIG. 5.103

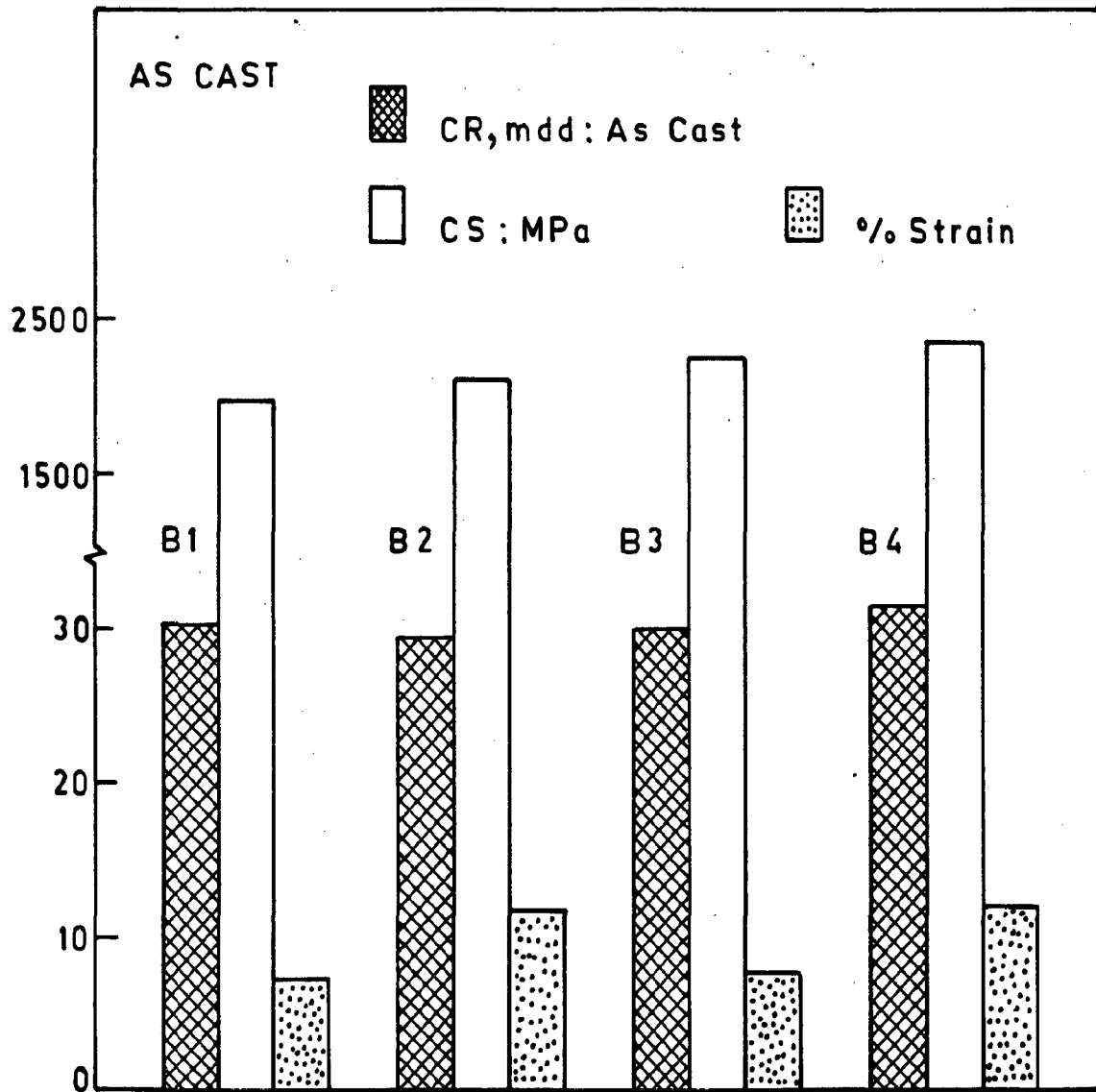


FIG. 5.108 RELATIVE PROPERTIES OF THE EXPERIMENTAL ALLOYS.

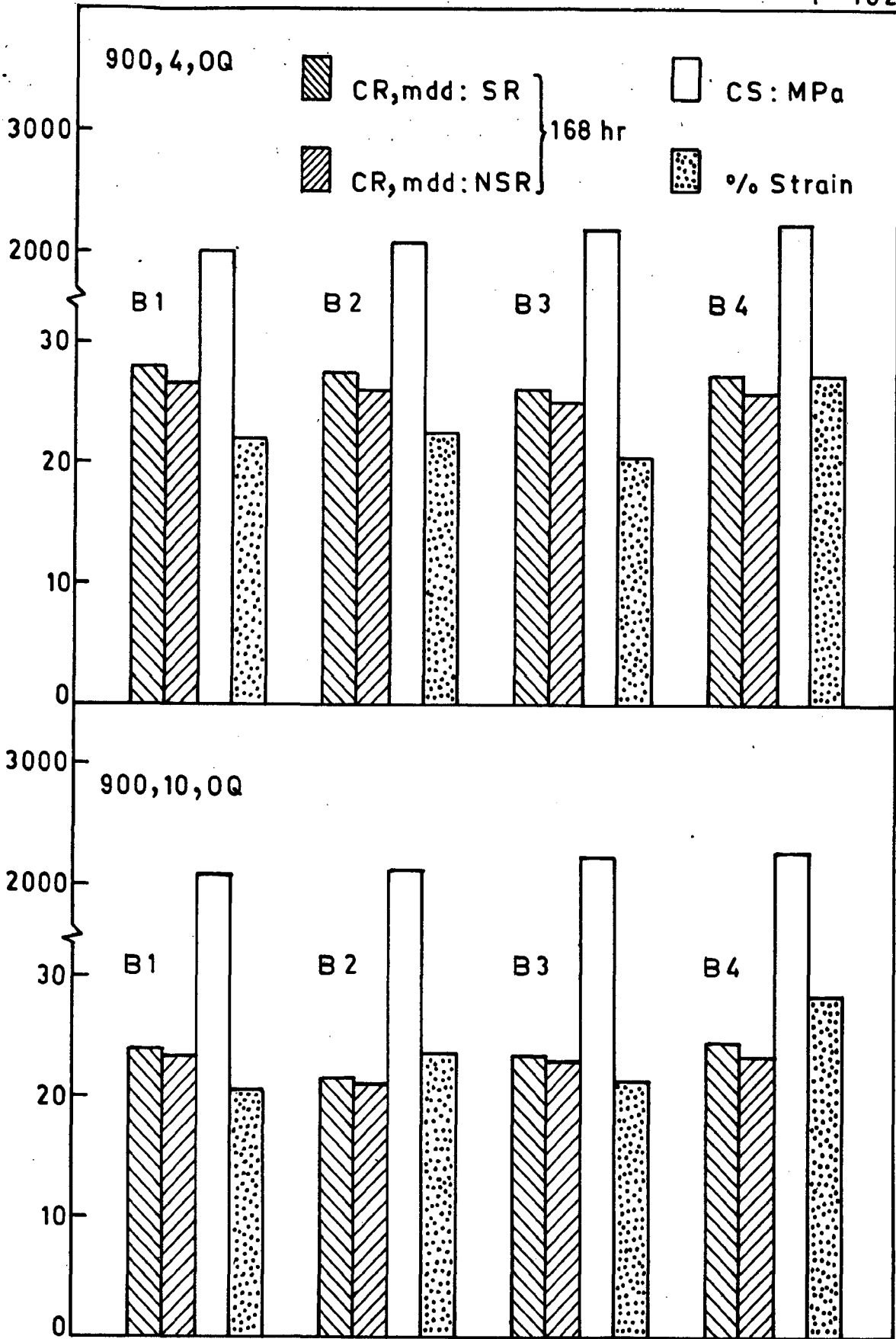


FIG. 5.109 RELATIVE PROPERTIES OF THE EXPERIMENTAL ALLOYS.

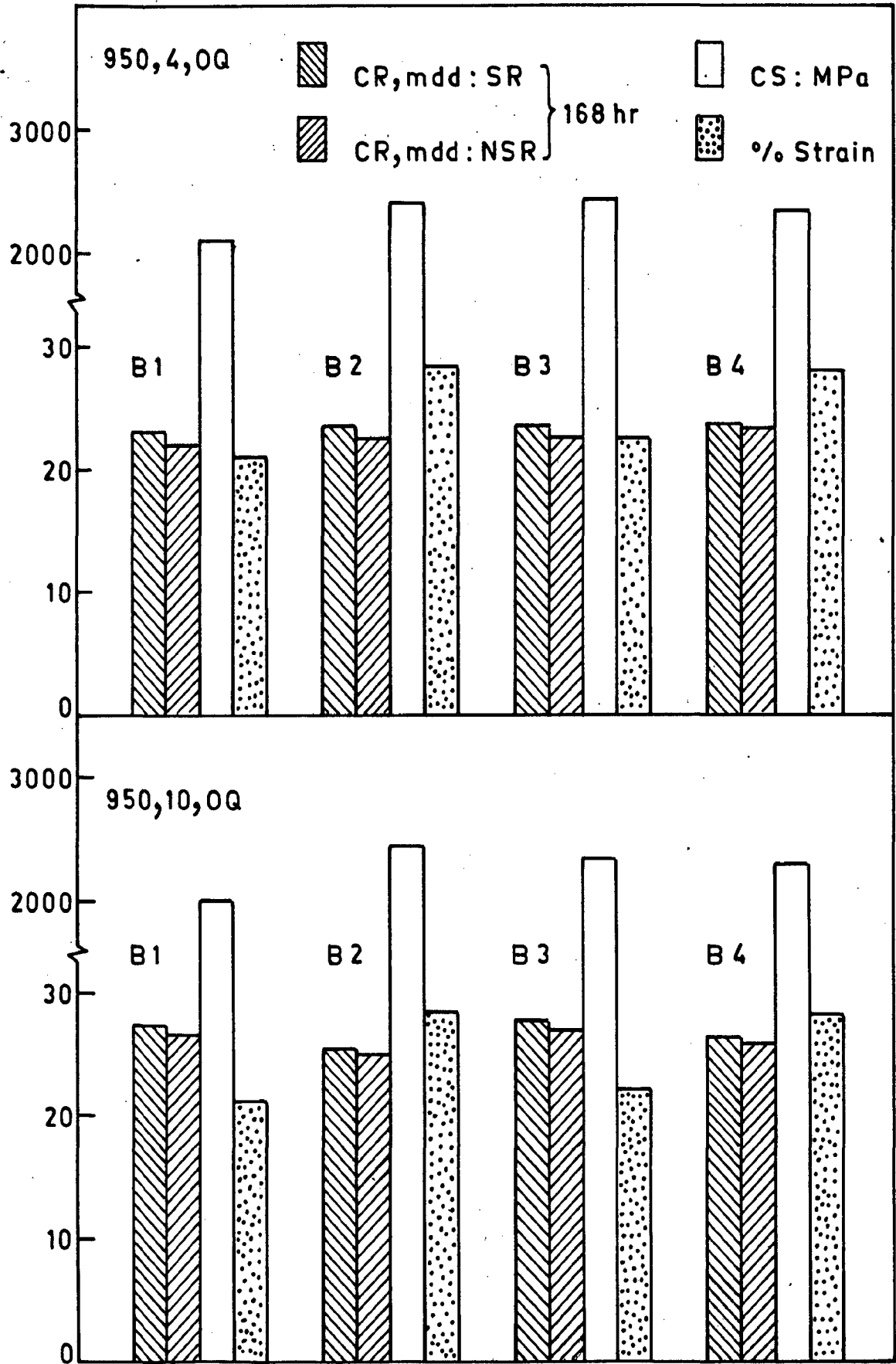


FIG.5.110 RELATIVE PROPERTIES OF THE EXPERIMENTAL ALLOYS.

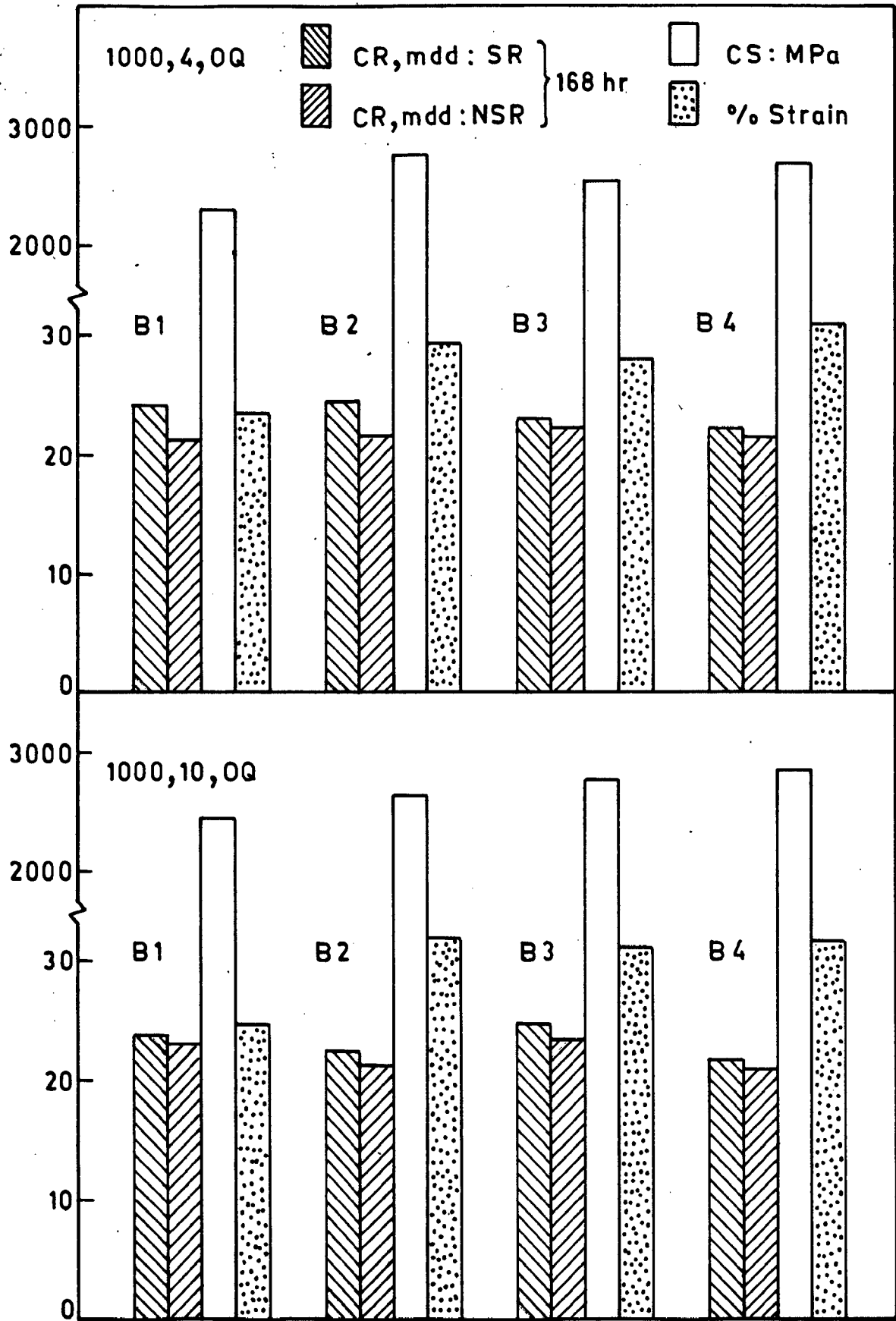


FIG.5.111 RELATIVE PROPERTIES OF THE EXPERIMENTAL ALLOYS.

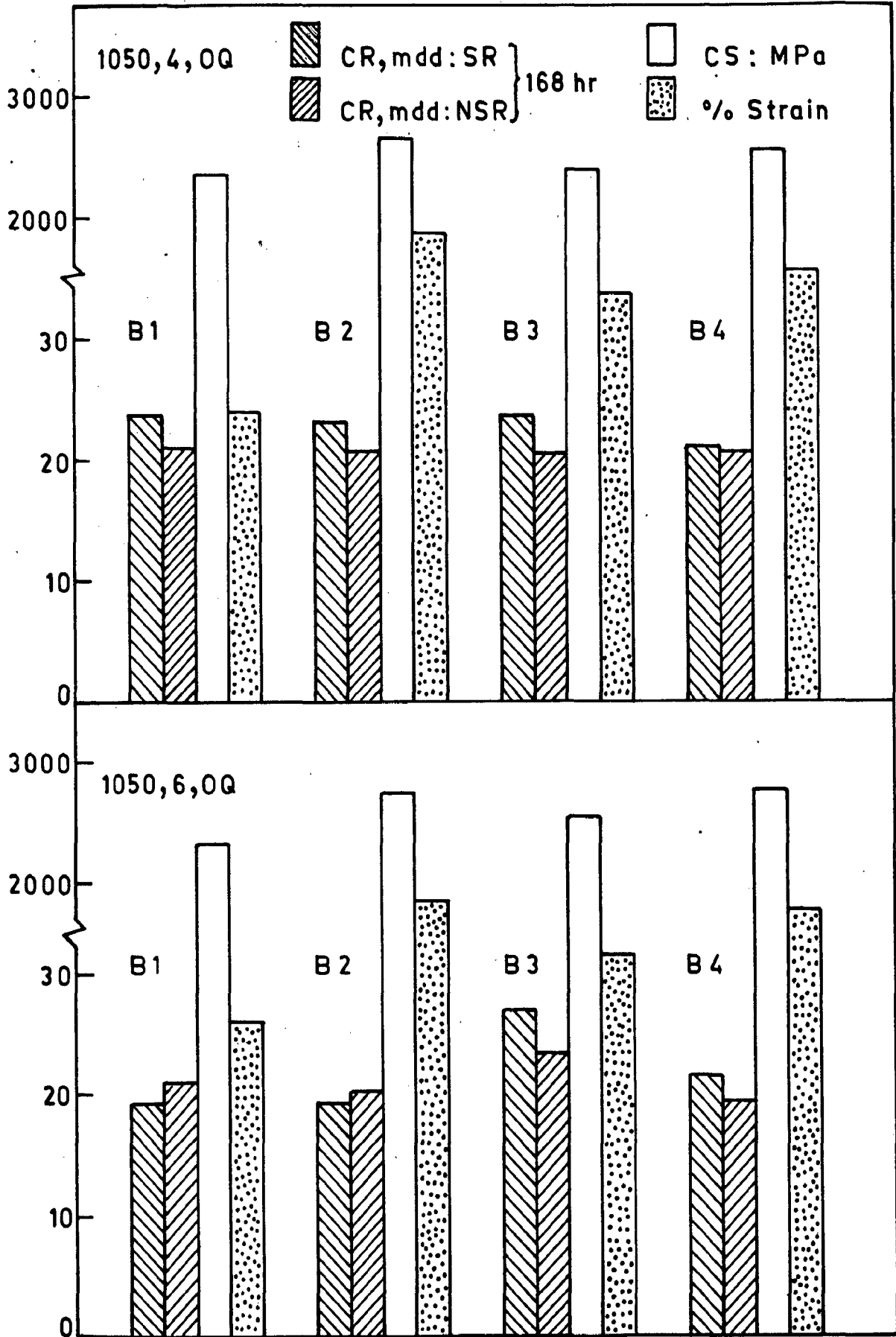


FIG.5.112 RELATIVE PROPERTIES OF THE EXPERIMENTAL ALLOYS.

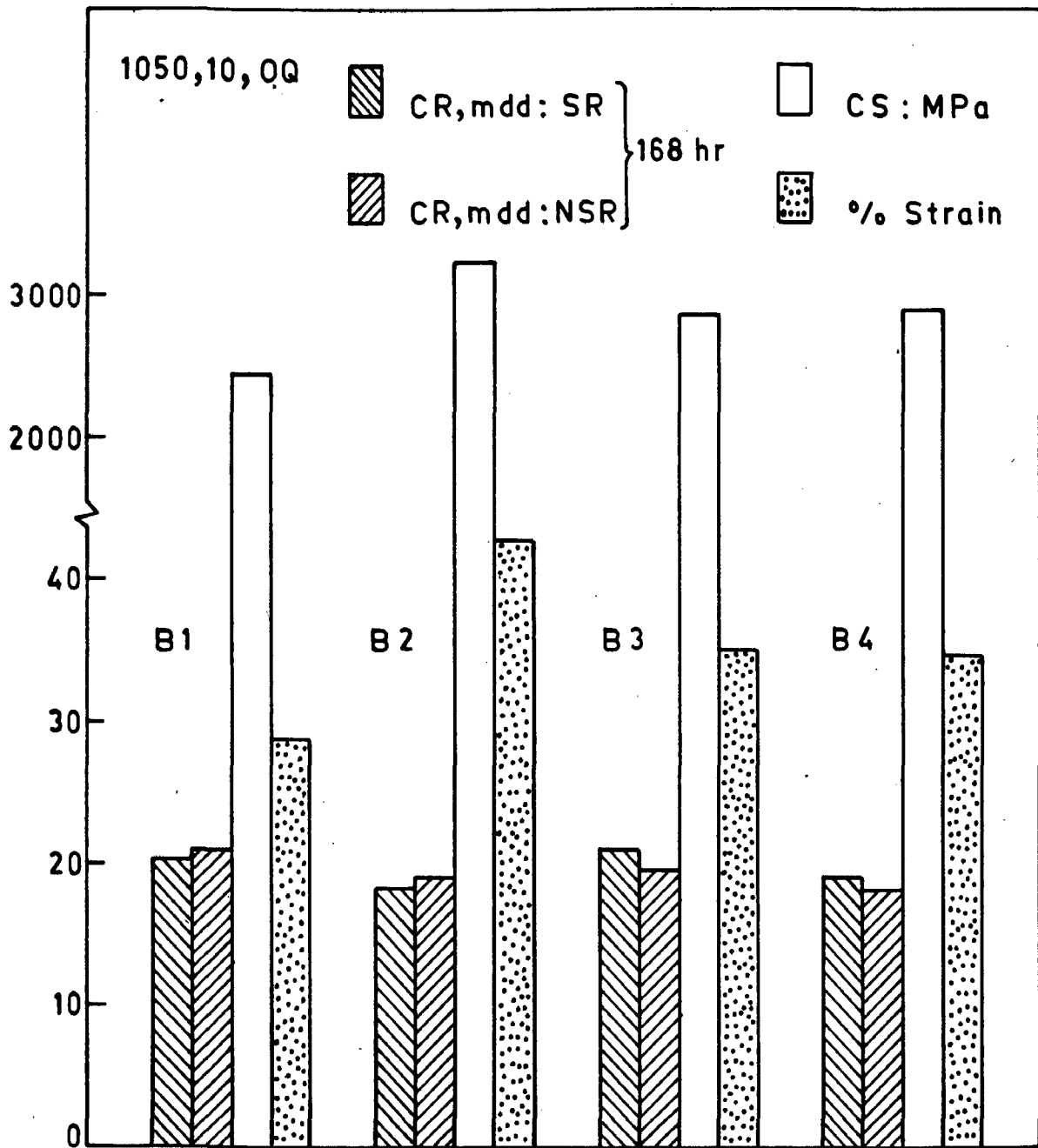


FIG. 5.113 RELATIVE PROPERTIES OF THE EXPERIMENTAL ALLOYS.

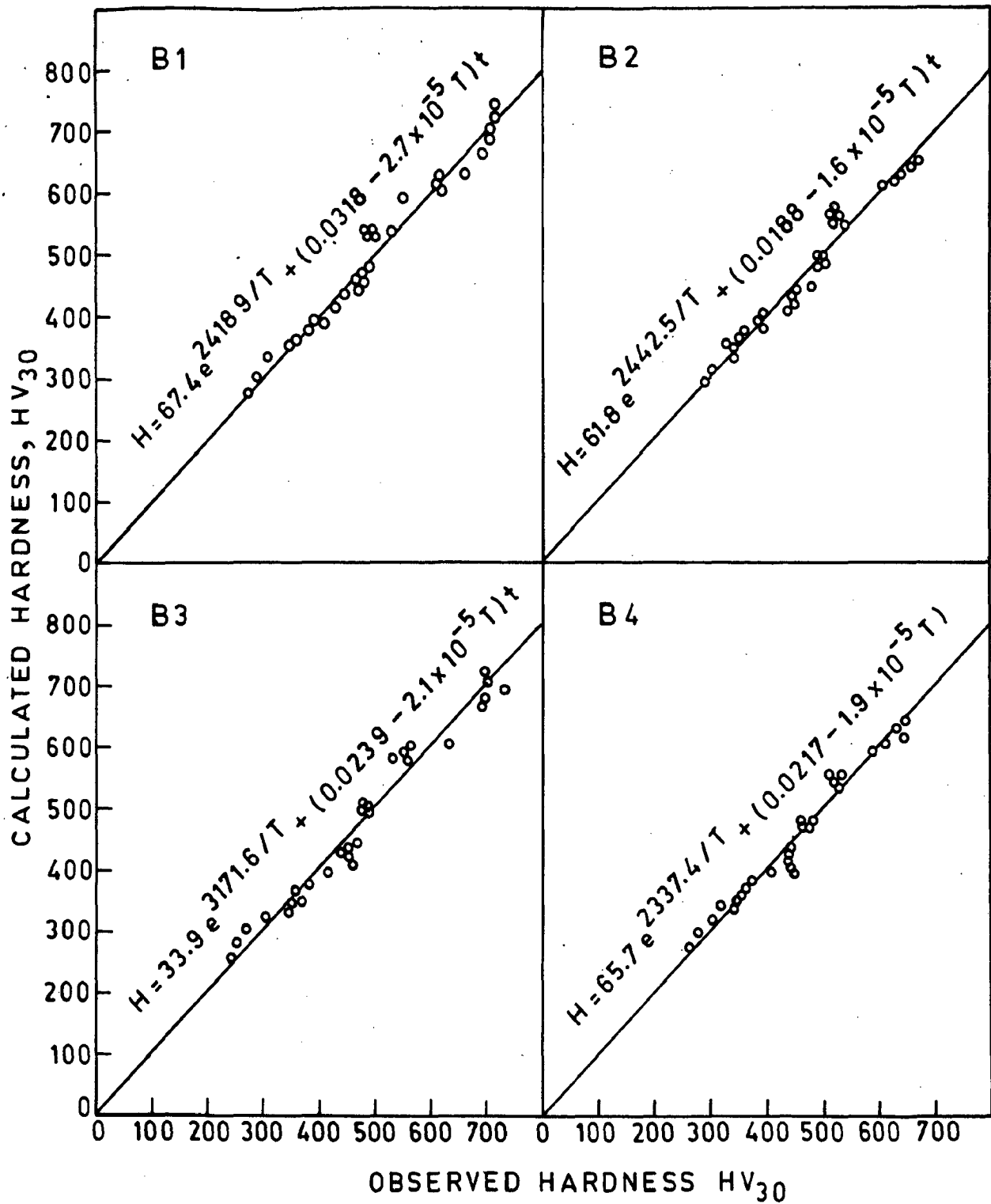


FIG. A-1 CALCULATED Vs. OBSERVED HARDNESS VALUES OF EXPERIMENTAL ALLOYS (Appendix-1).



Fig. 5.103

- (a)  $B_3, 1000^\circ C, 10h, O_2 + SR$   
720 hrs.  
 $\times(1250 \times 1.0)$
- (b)  $B_3, 1050^\circ C, 4h, O_2$   
720 hrs.  
 $\times(640 \times 1.0)$
- (c)  $B_3, 1050^\circ C, 10h, O_2$   
720 hrs.  
 $\times(1250 \times 0.95)$
- (d)  $B_3, 1050^\circ C, 10h, O_2 + SR$   
168 hrs.  
 $\times(2500 \times 1.1)$

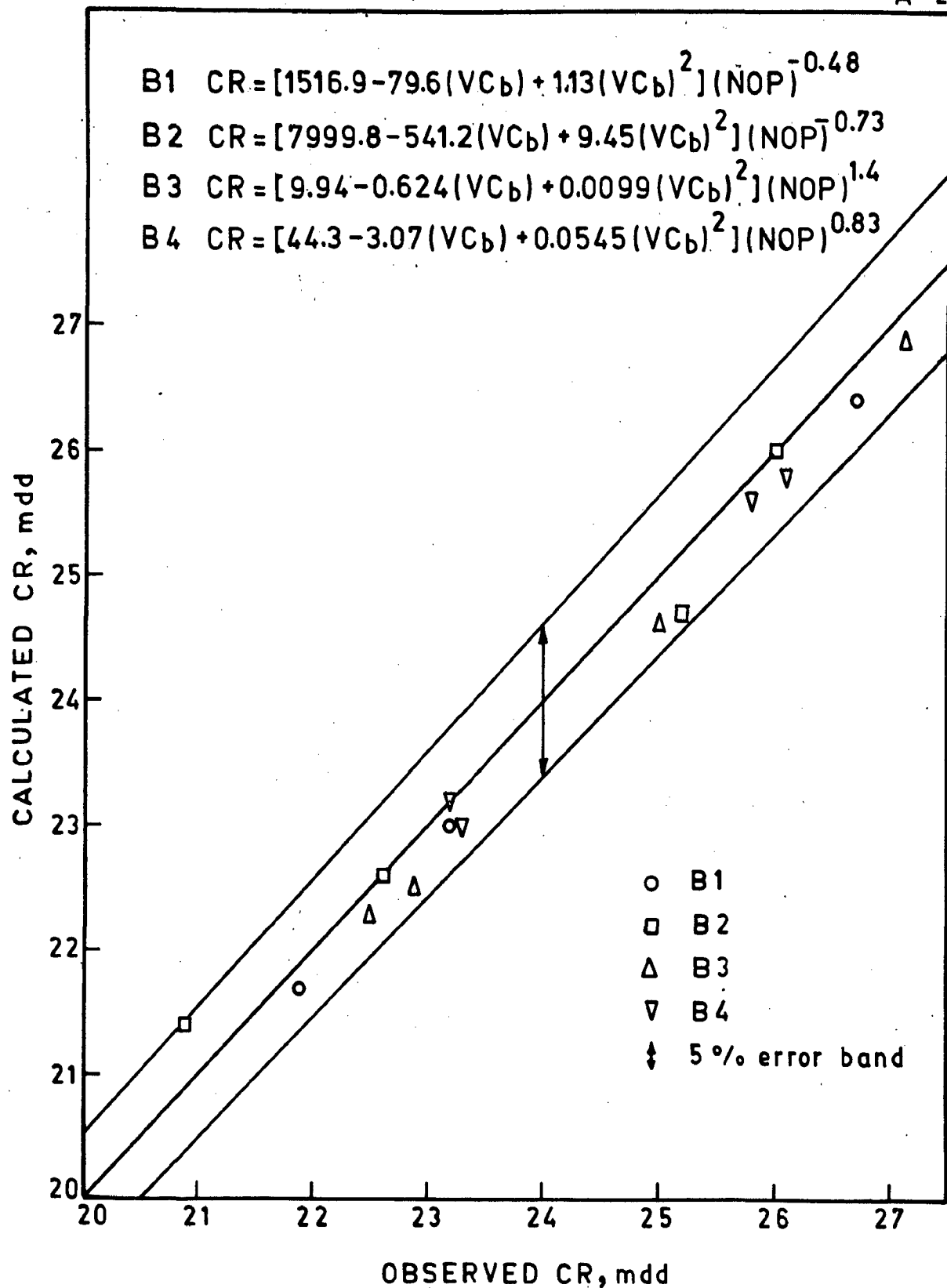


FIG. A-2 CALCULATED Vs. OBSERVED CORROSION RATE VALUES OF EXPERIMENTAL ALLOYS (Appendix-2).